

**PHYTOCHEMICAL AND BIOLOGICAL
STUDIES OF THE EXTRACTS OF
PSEUDUVARIA MONTICOLA AND
*PSEUDUVARIA MACROPHYLLA***

HAIRIN BINTI TAHA

**FACULTY OF SCIENCE
UNIVERSITY OF MALAYA
KUALA LUMPUR**

2016

**PHYTOCHEMICAL AND BIOLOGICAL STUDIES OF
THE EXTRACTS OF *PSEUDUVARIA MONTICOLA* AND
*PSEUDUVARIA MACROPHYLLA***

HAIRIN BINTI TAHA

**THESIS SUBMITTED IN FULFILMENT
OF THE REQUIREMENTS FOR THE DEGREE
OF DOCTOR OF PHILOSOPHY**

**DEPARTMENT OF CHEMISTRY
FACULTY OF SCIENCE
UNIVERSITY OF MALAYA
KUALA LUMPUR**

2016

UNIVERSITY OF MALAYA
ORIGINAL LITERARY WORK DECLARATION

Name of Candidate: **HAIRIN BINTI TAHA**

Registration/Matric No: **SHC 110084**

Name of Degree: **DOCTOR OF PHILOSOPHY (PhD)**

Title of Project Paper/Research Report/Dissertation/Thesis (“this Work”):

**PHYTOCHEMICAL AND BIOLOGICAL STUDIES OF THE EXTRACTS
OF *PSEUDUVARIA MONTICOLA* AND *PSEUDUVARIA MACROPHYLLA*.**

Field of Study: **NATURAL PRODUCTS CHEMISTRY**

I do solemnly and sincerely declare that:

- (1) I am the sole author/writer of this Work;
- (2) This Work is original;
- (3) Any use of any work in which copyright exists was done by way of fair dealing and for permitted purposes and any excerpt or extract from, or reference to or reproduction of any copyright work has been disclosed expressly and sufficiently and the title of the Work and its authorship have been acknowledged in this Work;
- (4) I do not have any actual knowledge nor do I ought reasonably to know that the making of this work constitutes an infringement of any copyright work;
- (5) I hereby assign all and every rights in the copyright to this Work to the University of Malaya (“UM”), who henceforth shall be owner of the copyright in this Work and that any reproduction or use in any form or by any means whatsoever is prohibited without the written consent of UM having been first had and obtained;
- (6) I am fully aware that if in the course of making this Work I have infringed any copyright whether intentionally or otherwise, I may be subject to legal action or any other action as may be determined by UM.

Candidate’s Signature

Date:

Subscribed and solemnly declared before,

Witness’s Signature

Date:

Name:

Designation:

ABSTRACT

The chemical constituents of two *Pseuduvaria* species from the Annonaceae family; *Pseuduvaria monticola* and *Pseuduvaria macrophylla* have been investigated. The extraction of the compounds from the bark and leaves was carried out using *n*-hexane, dichloromethane and methanol followed by chromatographic techniques such as column chromatography (CC), preparative thin layer chromatography (PTLC) and high performance liquid chromatography (HPLC). Structural elucidations of the compounds were established through spectroscopic methods; 1D-NMR (^1H , ^{13}C , DEPT 135), 2D-NMR (COSY, HMQC, HMBC), UV, IR and MS (LC-MS, GC-MS) and comparison from the published data. The leaf essential oils were extracted by Clavenger-type apparatus and analyzed by GC-MS/TOF. A total of 29 chemical constituents (**3**, **39**, **40**, **4**, **41**, **42**, **43**, **14**, **15**, **32**, **44**, **45**, **46**, **47**, **48**, **39**, **10**, **5**, **7**, **16**, **49**, **26**, **50**, **52**, **53**, **54**, **55**) including 2 new compounds (**32**, **51**) were isolated and elucidated from both species. 15 chemical compounds were isolated from the bark and leaves of *Pseuduvaria monticola*. They are four oxoaporphine alkaloids; liriodenine (**3**), lysicamine (**39**), oxoputerine (**40**), ouregidione (**4**), two phenanthrene alkaloids; atherosperminine (**41**) and argentinine (**42**), one sesquiterpene; tau cadinol (**43**), three benzopyran derivatives; oligandrol (**14**), (*6E,10E*) isopolycerasoidol (**15**), (*6E,10E*) isopolycerasoidol methyl ester (a new compound) (**32**), two phenolic acids; caffeic acid (**44**) and chlorogenic acid (**45**), two fatty acids; *n*-hexadecanoic acid (**46**), methyl oleate (**47**) and one sterol; stigmasterol (**48**). From *Pseuduvaria macrophylla*, 14 compounds were isolated from the leaves and bark. They are one new compound; 1,3,5,7-tetramethoxy-2-naphthoic acid (**51**), five oxoaporphine alkaloids; liriodenine (**3**), lysicamine (**39**) atherospermidine (**10**), *N*-methyl ouregidione (**5**) and *O*-methylmoschatoline (**7**), two benzopyran derivatives; polycerasoidol (**16**) and polycerasoidin (**49**), two phenyl propanoids; elimicin (**26**) and elimicin 6-methoxy (**50**), two sterols; β -sitosterol (**52**) and stigmasta-5,22-diene, 3 methoxy (**53**) and two fatty acids; oleic acid (**54**) and *n*-hexadecanoic acid methyl ester (**55**). The major compounds in the leaf essential oils of *Pseuduvaria monticola* were alpha cadinol (**56**) (13.0 %), cis-calamenene (**57**) (6.9 %) and alpha copaene (**25**) (4 %) whereas the major compounds in the leaf essential oils of *Pseuduvaria macrophylla* were caryophyllene oxide (**29**) (29.7 %) and elimicin (**26**) (28 %). In DPPH assay, polycerasoidol (**16**) and (*6E,10E*) isopolycerasoidol (**15**) demonstrated good antioxidant activity (IC_{50} of 18.89 $\mu\text{g/mL}$ and 22.56 $\mu\text{g/mL}$) respectively, compared to quercetin (IC_{50} 7.01 $\mu\text{g/mL}$). Leaf essential oil of *Pseuduvaria macrophylla* exhibited slightly greater antioxidant activity than that of *Pseuduvaria monticola*. In anticancer activity, (*6E, 10E*) isopolycerasoidol (**15**) and (*6E,10E*) isopolycerasoidol methyl ester (**32**) demonstrated cytotoxic effects on MCF-7 and MDA-MB-231 human breast cancer cells (IC_{50} 59 ± 5.1 , 43 ± 2.4 and 76 ± 8.5 , 58 ± 2.6 respectively) and induced apoptosis. In antidiabetic study, the bark methanolic extract of *Pseuduvaria monticola* induced the glucose uptake and insulin secretion of mouse pancreatic β -cell line (NIT-1) and upregulated insulin secretion and downregulated oxidative stress and hyperglycemia in STZ-nicotinamide-induced type 2 diabetic rats whereas the methanol extract of *Pseuduvaria macrophylla* upregulated insulin and C-peptide levels and down-regulated hyperglycemia and oxidative stress in STZ-nicotinamide-induced type 2 diabetic rats.

ABSTRAK

Kajian terhadap sebatian kimia dari dua spesies *Pseuduvaria* (Annonaceae) iaitu *Pseuduvaria monticola* dan *Pseuduvaria macrophylla* telah dijalankan. Pengekstrakan sebatian kimia dari kulit batang pokok dan daun dilakukan dengan pelarut hexana, diklorometana dan metanol, diikuti pelbagai kaedah kromatografi seperti kromatografi turus (CC), kromatografi persiapan lapisan nipis (PTLC) dan kromatografi cecair prestasi tinggi (HPLC). Elusidasi struktur ke atas sebatian dijalankan dengan menggunakan teknik spektroskopi seperti 1D-NMR (^1H , ^{13}C dan DEPT 135), 2D-NMR (COSY, HMQC dan HMBC), UV, IR dan MS (GC-MS dan LC-MS) serta perbandingan data literatur yang telah diterbitkan. Minyak esential dari daun pokok diekstrak menggunakan radas Clavenger dan dianalisa dengan GC-MSTOF. Sejumlah 29 sebatian (**3**, **39**, **40**, **4**, **41**, **42**, **43**, **14**, **15**, **32**, **44**, **45**, **46**, **47**, **48**, **39**, **10**, **5**, **7**, **16**, **49**, **26**, **50**, **52**, **53**, **54**, **55**) termasuk 2 sebatian baru (**32**, **51**) telah dipisahkan dari *Pseuduvaria monticola* dan *Pseuduvaria macrophylla*. 15 sebatian telah diasingkan dari daun dan kulit batang *Pseuduvaria monticola*, terdiri daripada empat oxoaporpina alkaloid; liriodenina (**3**), lysicamina (**39**), oxoputerina (**40**), ouregidiona (**4**) satu sesquiterpena; tau cadinol (**43**), tiga derivatif benzopyran; oligandrol (**14**), (*6E,10E*) isopolycerasoidol (**15**), (*6E,10E*) isopolycerasoidol methyl ester (**32**) (sebatian baru); dua asid fenolik; asid caffeic (**44**) and asid chlorogenic (**45**), dua asid lemak; *n*-hexadecanoic acid (**46**) dan methyl oleate (**47**) dan satu sterol; stigmasterol (**48**). Dari *Pseuduvaria macrophylla* pula, 14 sebatian telah diasingkan iaitu satu sebatian baru; 1,3,5,7-tetramethoxy-2-naphthoic acid (**51**), lima alkaloid oxoaporpina; liriodenina (**3**), lysicamina (**39**) atherospermidina (**10**), *N*-methyl ouregidiona (**5**) and *O*-methylmoschatolina (**7**), dua derivatif benzopyran; polycerasoidol (**16**) and polycerasoidin (**51**), dua fenil propanoid; elimicin (**26**) and elimicin 6-methoxy (**50**), dua sterol; β -sitosterol (**52**) and stigmasta-5,22-diene, 3 methoxy (**53**) dan dua asid lemak; asid oleik (**54**) dan asid *n*-hexadecanoik metil ester (**55**). Sebatian utama dalam daun minyak esential dari pokok *Pseuduvaria monticola* terdiri daripada alfa cadinol (**56**) (13 %), cis calaminin (**57**) (6.9 %) dan alfa copaene (**25**) (4 %). Sebatian utama dalam daun minyak esential dari pokok *Pseuduvaria macrophylla* pula terdiri daripada caryophyllene oxide (**29**) (29.7 %) dan elimicin (**26**) (28 %). Ujian DPPH untuk aktiviti antioksidasi menunjukkan polycerasoidol (**16**) and (*6E,10E*) isopolycerasoidol (**15**) memperlihatkan aktiviti antioksidasi yang agak baik (IC_{50} 18.89 $\mu\text{g/mL}$ dan 22.56 $\mu\text{g/mL}$) di bandingkan dengan quercetin (IC_{50} 7.0 $\mu\text{g/mL}$). Manakala ekstrak daun minyak esential *Pseuduvaria macrophylla* menunjukkan aktiviti antioksidasi yang lebih tinggi dari *Pseuduvaria monticola*. Dalam aktiviti anti kanser pula, sebatian (*6E,10E*) isopolycerasoidol (**15**) and (*6E,10E*) isopolycerasoidol methyl ester (**32**) menunjukkan kesan sitotoksik ke atas sel kanser MCF-7 and MDA-MB-231 (IC_{50} 59 \pm 5.1, 43 \pm 2.4 and 76 \pm 8.5, 58 \pm 2.6) dan merangsang apoptosis. Dalam kajian antidiabetik, ekstrak metanol dari *Pseuduvaria monticola* menunjukkan peningkatan resapan glukos dan rembesan insulin dan penurunan stres oksidatif dan hiperglikemia dalam tikus diabetik induksi STZ Type 2 manakala ekstrak metanol dari *Pseuduvaria macrophylla* menunjukkan peningkatan insulin dan takat C-peptida serta penurunan stres oksidatif dan hiperglikemia dalam tikus diabetik induksi STZ Type 2.

ACKNOWLEDGEMENTS

First and foremost, syukur Alhamdulillah to ALLAH S.W.T the Most Merciful and Compassionate for His Love , Guidance and His Endless Care.

I would like to express my sincere gratitude to my late supervisor, Professor Datuk Dr. A.Hamid A.Hadi. May the Almighty rest his noble soul in Jannah.

I would also like to express my sincerest appreciation to my supervisors, Professor Dr. Hapipah Mohd Ali and Professor Dr.Mustafa Ali Mohd for their continuous support and encouragement.

Many thanks to Dr Aditya and Dr Looi for their collaboration in the antidiabetic and anticancer work which have resulted in two Tier One papers and to all my friends and colleagues, Dr Mehran , Dr Hanita, P.Narrima, Jad, Azie and Afifah.

I would also like to acknowledge UM grants (High Impact Research Grant UM-MOHE UM.C/625/1/HIR/MOHE/09 and PG064-2012) for supporting the study.

This thesis is especially dedicated to my parents, my late daughter Aiman (May your soul rest in Jannah), my family and my sweet children Ayyub, Arham, Afiqah and Awadah.

THANK YOU

TABLE OF CONTENTS

	Page
ABSTRACT	iii
ABSTRAK	iv
ACKNOWLEDGEMENTS	v
TABLE OF CONTENTS	vi
LIST OF SCHEMES	xii
LIST OF FIGURES	xiv
LIST OF TABLES	xxii
ABBREVIATION	xxv
CHAPTER 1: INTRODUCTION	1
CHAPTER 2: LITERATURE REVIEW	7
2.1 Family Annonaceae	7
2.1.1 Annonacea: General appearance and morphology	7
2.1.2 Classification of Annonaceae	8
2.1.3 Medicinal and Economic Importance	9
2.1.4 Genus <i>Pseuduvaria</i>	10
2.1.5 <i>Pseuduvaria monticola</i> : botanical morphology	11
2.1.6 <i>Pseuduvaria macrophylla</i> : botanical morphology	12
2.2 Chemical aspects of <i>Pseuduvaria</i> species	15
2.3 Bioactive compounds from <i>Pseuduvaria</i> species	21
2.4 Alkaloids	22
2.4.1 Classification of alkaloids	23
2.4.2 The isoquinoline alkaloids	25

2.4.3	Simple isoquinoline	26
2.4.4	Aporphine	27
2.4.5	Oxoaporphine and dioxoaporphine alkaloids	27
2.4.6	Phenanthrene alkaloids	28
2.5	Phenolic compounds	29
2.5.1	Phenolic acid	30
2.6	Benzopyran	31
2.7	Essential oils	34
 CHAPTER 3 : EXPERIMENTAL		
3.1	General Experimental and Instrumentation	36
3.1.1	Solvents	36
3.1.2	Ultra violet spectra (UV)	36
3.1.3	Infrared (IR)	36
3.1.4	Optical Rotation (OR)	36
3.1.5	NMR Spectra	36
3.1.6	Column Chromatography (CC)	37
3.1.7	Thin layer chromatography (TLC)	37
3.1.8	High Performance Liquid Chromatography (HPLC)	37
3.1.9	Mass Spectra (MS)	38
3.1.10	GC-TOFMS Analysis	38
3.2	Reagents	39
3.3	Extraction of leaf essential oil	39
3.3.1	% Yield determination	40
3.4	Plant material	41
3.5	Extraction and isolation	42

3.5.1	Hexane extract	43
3.5.2	Acid base extraction of alkaloids	46
3.5.3	Isolation of the alkaloids	46
3.5.4	Isolation of compounds from methanol extract	49
3.6	Physical and Spectral Data of Isolated Compounds from <i>Pseuduvaria monticola</i> and <i>Pseuduvaria macrophylla</i>	53
3.7	Antioxidant activity	60
3.7.1	DPPH Radical Scavenging Activity	60
3.7.2	ORAC Assay	60
3.7.3	Statistical analysis	61
3.8	Cytotoxicity assay	61
3.8.1	Cell culture	62
3.8.2	MTT cell viability assay	62
3.8.3	Flow cytometry	63
3.9	Antidiabetic study	63
3.9.1	<i>In vitro</i> cell line studies	63
3.9.2	MTT cell viability assay	64
3.9.3	Real-time cell proliferation	64
3.9.4	2-NBDG glucose uptake	65
3.9.5	<i>In vitro</i> insulin secretion	65
3.9.6	<i>In vivo</i> acute toxicity study	66
3.9.7	Type 1 diabetes in rats	67
3.9.8	Type 2 diabetes in rats	67
3.9.9	Division of diabetic animals for the study	67
3.9.10	Experimental procedure	68
3.9.11	Glucose tolerance test	68
3.9.12	Assessment of serum insulin and C-peptide levels	69

3.9.13	Assessment of oxidative stress markers	69
3.9.14	Animal models for <i>Pseuduvaria macrophylla</i> study	69
3.9.15	Experimental design	70
3.9.16	Acute toxicity study	70
3.9.17	T2DM (Type 2 Diabetes Mellitus) induction	70
3.9.18	Blood samples	71
3.9.19	Biochemical activity	71
3.9.20	Measurement of oxidative stress markers	71

CHAPTER 4 : RESULTS AND DISCUSSION

4.1	Chemical Constituents of <i>Pseuduvaria Monticola</i>	72
4.2	Structural Elucidation of Compounds from <i>Pseuduvaria Monticola</i>	74
4.2.1	Liriodenine (3)	74
4.2.2	Lysicamine (39)	82
4.2.3	Oxoputerine (40)	90
4.2.4	Ouregidione (4)	98
4.2.5	Atherosperminine (41)	105
4.2.6	Argentinine (42)	112
4.2.7	T-cadinol (43)	117
4.2.8	Oligandrol (14)	119
4.2.9	(6 <i>E</i> ,10 <i>E</i>) Isopolycerasoidol (15)	126
4.2.10	(6 <i>E</i> ,10 <i>E</i>) Isopolycerasoidol methyl ester (32)	134
4.2.11	Caffeic acid (44)	142
4.2.12	Chlorogenic acid (45)	148
4.2.13	<i>N</i> -hexadecanoic acid (46)	156

4.2.14	Methyl oleate (47)	160
4.2.14	Stigmasterol (48)	164
4.3	Chemical constituents of <i>Pseuduvaria macrophylla</i>	169
4.3.1	Liriodenine (3)	171
4.3.2	Lysicamine (39)	172
4.3.3	Atherospermidine (10)	173
4.3.4	<i>N</i> -methylouregidione (5)	180
4.3.5	<i>O</i> -methyloschatoline (7)	187
4.3.6	Polycerasoidol (16)	196
4.3.7	Polycerasoidin (49)	204
4.3.8	Elemicin (26)	211
4.3.9	Elemicin 6- methoxy (50)	218
4.3.10	1, 3, 5, 7-tetramethoxy-2-naphthoic acid (51)	225
4.3.11	β -Sitosterol (52)	232
4.3.12	Stigmasta-5, 22-diene, 3 methoxy (53)	237
4.3.13	Oleic acid (54)	243
4.3.14	Hexadecanoic acid methyl ester (55)	247
4.4	Chemical compounds identified from <i>P. monticola</i> leaf essential oil	252
4.4.1	Chemical compounds identified from <i>P. macrophylla</i> leaf essential oil	255
4.5	Biological activities	
4.5.1	Antioxidant activity	257
4.5.2	Antioxidant activity of leaf essential oils by DPPH assay	257
4.5.3	Antioxidant activity of crude extracts and isolated compounds by DPPH and ORAC assays	258
4.5.2	Anticancer activity	261

4.5.2.1	Cytotoxic effects and apoptosis induction of (6 <i>E</i> ,10 <i>E</i>) isopolycerasoidol and (6 <i>E</i> ,10 <i>E</i>) isopolycerasoidol methyl ester	262
4.5.3	Antidiabetic activity	266
4.5.3.1	<i>In vitro</i> study	267
4.5.3.2	MTT cell viability assay	267
4.5.3.3	Effect of the Pmt extract on 2-NBDG glucose uptake	268
4.5.3.4	Effect of the Pmt extract on insulin secretion	269
4.5.3.5	Acute toxicity study	270
4.5.3.6	Effect of PMt on blood glucose levels of Type 1 and Type 2 diabetic rats	270
4.5.3.7	Oral glucose tolerance test on type 2 diabetic rats	272
4.5.3.8	Effect of PMt extract on Insulin and C-peptide level of type 1 and type 2 diabetic rats	273
4.5.3.9	Effect of PMt on oxidative stress markers of Type 1 and Type 2 diabetic rats	274
4.5.3.10	<i>In vivo</i> antidiabetic study of <i>Pseuduvaria macrophylla</i> methanol extract on streptozotocin-nicotinamide (STZ) induced type 2 diabetic rats	276
4.5.3.11	Overall result	280
CHAPTER 5: CONCLUSION		282
REFERENCES		285
APPENDIX		

LIST OF SCHEMES

	Page	
1	Classification of Annonaceae	8
2	Genera of Annonaceae	9
3.1	Fractionation of crude extracts from the plant sample	42
3.2	Isolation of the compounds from the hexane bark extract of <i>P. monticola</i>	44
3.3	Isolation of the compounds from the hexane leave extract of <i>P. monticola</i>	44
3.4	Isolation of the compounds from the hexane bark extract of <i>P. macrophylla</i>	45
3.5	Isolation of the compounds from the hexane leave extract of <i>P. macrophylla</i>	45
3.6	Isolation of the alkaloids from the bark of <i>P. monticola</i> .	47
3.7	Isolation of the alkaloids from the leaves of <i>P. monticola</i>	47
3.8	Isolation of the alkaloids from the bark of <i>P. macrophylla</i> .	48
3.9	Isolation of the alkaloids from the leaves of <i>P. macrophylla</i>	48
3.10	Extraction of the polar compounds from the bark of <i>P. monticola</i> .	50
3.11	Extraction of the polar compounds from the bark of <i>P. macrophylla</i>	50
4.1	The HMBC and COSY correlations of liriodenine (3)	81
4.2	The HMBC and COSY correlations of lysicamine (39)	89
4.3	The HMBC correlations of atherosperminine (41)	111
4.4	The HMBC correlations of oligandrol (14)	125
4.5	The HMBC correlations of (6E, 10E) isopolycerasoidol (15)	133
4.6	The HMBC correlations of (6E, 10E) isopolycerasoidol methyl ester (32)	141
4.7	The HMBC correlations of chlorogenic acid (45)	155
4.8	The HMBC correlations of atherospermidine (10)	179

4.9	The HMBC correlations of <i>n</i> -methyl ouregidione (5)	186
4.10	The HMBC correlations of <i>o</i> -methylnoschadolone (7)	195
4.11	The HMBC correlations of polycerasoidol (16)	203
4.12	The HMBC correlations of polycerasoidin (49)	210
4.13	The HMBC correlations of elimicin (26)	217
4.14	The HMBC correlations of 1,3,5,7-tetramethoxy-2-naphthoic acid (51)	231

University of Malaya

LIST OF FIGURES

	Page
1.1 Drug discovery process	5
2.1 Bark and leaves of <i>Pseuduvaria monticola</i>	13
2.2 Bark and leaves of <i>Pseuduvaria macrophylla</i>	14
2.3 General structure of simple isoquinoline alkaloids	26
2.4 Basic aporphine skeleton	27
2.5 Biogenetic pathway of oxoaporphine	28
2.6 Basic skeleton of phenantrene alkaloid	29
2.7 Basic structures of benzopyran	31
3.1 Clavenger's Apparatus	40
4.1 LC-MS spectrum of liriodenine (3)	77
4.2 ¹ H NMR spectrum of liriodenine (3)	77
4.3 ¹³ C NMR spectrum of liriodenine (3)	78
4.4 DEPT 135 and ¹³ C NMR spectrum of liriodenine (3)	78
4.5 COSY spectrum of liriodenine (3)	79
4.6 Expanded COSY spectrum of liriodenine (3)	79
4.7 HMQC spectrum of liriodenine (3)	80
4.8 Expanded HMQC spectrum of liriodenine (3)	80
4.9 LC-MS of lysicamine (39)	85
4.10 ¹ H NMR spectrum of lysicamine (39)	85
4.11 ¹³ C NMR spectrum of lysicamine (39)	86
4.12 DEPT 135 spectrum of lysicamine (39)	86
4.13 COSY spectrum of lysicamine (39)	87
4.14 Expanded COSY spectrum of lysicamine (39)	87
4.15 HSQC Spectrum of lysicamine (39)	88
4.16 Expanded HSQC spectrum of lysicamine (39)	88

4.17	LC-MS spectrum of oxoputerine (40)	93
4.18	¹ H NMR spectrum of oxoputerine (40)	93
4.19	Expanded ¹ H NMR of oxoputerine (40) in the aromatic region.	94
4.20	¹³ C NMR spectrum of oxoputerine (40)	94
4.21	DEPT 135/ ¹³ C NMR spectrum of oxoputerine (40)	95
4.22	COSY spectrum of oxoputerine (40)	95
4.23	Expanded COSY spectrum of oxoputerine (40)	96
4.24	HSQC spectrum of oxoputerine (40)	96
4.25	Expanded HSQC spectrum of oxoputerine (40)	97
4.26	HMBC spectrum of oxoputerine (40)	97
4.27	LC-MS spectrum of ouregidione (4)	101
4.28	¹ H-NMR spectrum of ouregidione (4)	101
4.29	¹³ C-NMR spectrum of ouregidione (4)	102
4.30	DEPT 135 spectrum of ouregidione (4)	102
4.31	COSY spectrum of ouregidione (4)	103
4.32	HMQC spectrum of ouregidione (4)	103
4.33	Expanded HMQC spectrum of ouregidione (4)	104
4.34	HMBC correlation of ouregidione (4)	104
4.35	LCMS spectrum of atherosperminine (41)	108
4.36	¹ H-NMR spectrum of atherosperminine (41)	108
4.37	¹³ C-NMR spectrum of atherosperminine (41)	109
4.38	DEPT 135 spectrum of atherosperminine (41)	109
4.39	COSY spectrum of atherosperminine (41)	110
4.40	HMQC spectrum of atherosperminine (41)	110
4.41	HMBC spectrum of atherosperminine (41)	111
4.42	LC-MS spectrum of argentinine (42)	115
4.43	¹ H-NMR spectrum of argentinine (42)	115

4.44	¹³ C-NMR spectrum of argentinine (42)	116
4.45	GC-MS peak of tau cadinol (43)	118
4.46	GC-MS spectrum of tau cadinol (43)	118
4.47	LC-MS of oligandrol (14)	122
4.48	¹ H NMR spectrum of oligandrol (14)	122
4.49	¹³ C-NMR spectrum of oligandrol (14)	123
4.50	DEPT 135 NMR spectrum of oligandrol (14)	123
4.51	COSY spectrum of oligandrol (14)	124
4.52	HMQC spectrum of oligandrol (14)	124
4.53	HMBC spectrum of oligandrol (14)	125
4.54	UV spectra of (6 <i>E</i> ,10 <i>E</i>) isopolycerasoidol (15)	129
4.55	IR spectra of (6 <i>E</i> ,10 <i>E</i>) isopolycerasoidol (15)	129
4.56	LC-MS of (6 <i>E</i> ,10 <i>E</i>) isopolycerasoidol (15)	130
4.57	¹ H NMR of (6 <i>E</i> ,10 <i>E</i>) isopolycerasoidol (15)	130
4.58	¹³ C NMR of (6 <i>E</i> ,10 <i>E</i>) isopolycerasoidol (15)	131
4.59	DEPT 135 of (6 <i>E</i> ,10 <i>E</i>) isopolycerasoidol (15)	131
4.60	COSY spectrum of (6 <i>E</i> ,10 <i>E</i>) isopolycerasoidol (15)	132
4.61	HMQC spectrum of (6 <i>E</i> ,10 <i>E</i>) isopolycerasoidol (15)	132
4.62	HMBC spectrum of (6 <i>E</i> ,10 <i>E</i>) isopolycerasoidol (15)	133
4.63	UV spectra of (6 <i>E</i> ,10 <i>E</i>) isopolycerasoidol methyl ester (32)	137
4.64	IR spectra of (6 <i>E</i> ,10 <i>E</i>) isopolycerasoidol methyl ester (32)	137
4.65	LCMS of (6 <i>E</i> ,10 <i>E</i>) isopolycerasoidol methyl ester (32)	138
4.66	¹ H NMR spectra of (6 <i>E</i> ,10 <i>E</i>) isopolycerasoidol methyl ester (32)	138
4.67	¹³ C NMR spectra of (6 <i>E</i> ,10 <i>E</i>) isopolycerasoidol methyl ester (32)	139
4.68	DEPT-135/ ¹³ C NMR spectra of (6 <i>E</i> ,10 <i>E</i>) isopolycerasoidol methyl ester (32)	139
4.69	COSY spectrum of (6 <i>E</i> ,10 <i>E</i>) isopolycerasoidol methyl ester (32)	140
4.70	HMQC spectrum of (6 <i>E</i> ,10 <i>E</i>) isopolycerasoidol methyl ester (32)	140

4.71	HMBC spectra of (6 <i>E</i> ,10 <i>E</i>) isopolycerasoidol methyl ester (32)	141
4.72	LC-MS spectrum of caffeic acid (44) in negative mode	144
4.73	¹ H NMR spectrum of caffeic acid (44)	144
4.74	¹³ C NMR of caffeic acid (44)	145
4.75	DEPT 135 spectrum of caffeic acid (44)	145
4.76	COSY spectrum of caffeic acid (44)	146
4.77	HMQC spectrum of caffeic acid (44)	146
4.78	HMBC spectrum of caffeic acid (44)	147
4.79	TIC of chlorogenic acid (45) in negative mode	151
4.80	LC-MS spectrum of chlorogenic acid (45) in negative mode	151
4.81	¹ H NMR spectrum of chlorogenic acid (45)	152
4.82	¹³ C NMR spectrum of chlorogenic acid (45)	152
4.83	DEPT 135 NMR spectrum of chlorogenic acid (45)	153
4.84	COSY spectrum of chlorogenic acid (45)	153
4.85	HMQC spectrum of chlorogenic acid (45)	154
4.86	HMBC spectrum of chlorogenic acid (45)	154
4.87	GC-MS spectrum of <i>n</i> -hexadecanoic acid (46)	158
4.88	¹ H-NMR spectrum of <i>n</i> -hexadecanoic acid (46)	158
4.89	¹³ C NMR of <i>n</i> -hexadecanoic acid (46)	159
4.90	DEPT 135 spectrum of of <i>n</i> -hexadecanoic acid (46)	159
4.91	GC-MS spectrum of methyl oleate (47)	162
4.92	¹ H NMR spectrum of methyl oleate (47)	162
4.93	¹³ C NMR and DEPT 135 spectrum of methyl oleate (47)	163
4.94	GC-MS spectrum of stigmasterol (48)	167
4.95	¹ H-NMR spectrum of stigmasterol (48)	167
4.96	¹³ C-NMR spectrum of stigmasterol (48)	168
4.97	DEPT 135 NMR spectrum of stigmasterol (48)	168
4.98	¹ H NMR spectrum of liriodenine (3)	171

4.99	¹ H NMR spectrum of lysicamine (39)	172
4.100	LC-MS spectrum of atherospermidine (10)	176
4.101	¹ H NMR Spectrum of atherospermidine (10)	176
4.102	¹³ C NMR spectrum of atherospermidine (10)	177
4.103	DEPT 135 and ¹³ C NMR spectrum of atherospermidine (10)	177
4.104	Expanded COSY spectrum of atherospermidine (10)	178
4.105	HMQC spectrum of atherospermidine (10)	178
4.106	Expanded HMQC spectrum of atherospermidine (10)	179
4.107	LC-MS Spectrum of <i>n</i> -methyl ouregidione (5)	183
4.108	¹ H NMR Spectrum of <i>n</i> -methyl ouregidione (5)	183
4.109	¹³ C- NMR spectrum of <i>n</i> -methyl ouregidione (5)	184
4.110	DEPT135 NMR spectrum of <i>n</i> -methyl ouregidione (5)	184
4.111	COSY spectrum of <i>n</i> -methyl ouregidione (5)	185
4.112	Expanded COSY spectrum of <i>n</i> -methyl ouregidione (5)	185
4.113	HMQC spectrum of <i>n</i> -methyl ouregidione (5)	186
4.114	LC-MS Spectrum of <i>o</i> -methyloschatoline (7)	190
4.115	¹ H NMR Spectrum of <i>o</i> -methyloschatoline (7)	190
4.116	Expanded ¹ H NMR spectrum of <i>o</i> -methyloschatoline (7)	191
4.117	¹³ C NMR spectrum of <i>o</i> -methyloschatoline (7)	191
4.118	Expanded ¹³ C NMR spectrum of <i>o</i> -methyloschatoline (7)	192
4.119	DEPT 135 spectrum of <i>o</i> -methyloschatoline (7)	192
4.120	COSY spectrum of <i>o</i> -methyloschatoline (7)	193
4.121	Expanded COSY spectrum of <i>o</i> -methyloschatoline (7)	193
4.122	HMQC spectrum of <i>o</i> -methyloschatoline (7)	194
4.123	Expanded HMQC spectrum of <i>o</i> -methyloschatoline (7)	194
4.124	LC-MS spectrum of polycerasoidol (16)	199
4.125	¹ H NMR spectrum of polycerasoidol (16)	199
4.126	¹³ C NMR of polycerasoidol (16)	200

4.127	DEPT 135 NMR spectrum of polycerasoidol (16)	200
4.128	COSY spectrum of polycerasoidol (16)	201
4.129	HMQC spectrum of polycerasoidol (16)	201
4.130	Expanded HMQC spectrum in the aliphatic region	202
4.131	Expanded HMQC spectrum in the aromatic region	202
4.132	HMBC spectrum of polycerasoidol (16)	203
4.133	LC-MS Spectrum of polycerasoidin (49)	207
4.134	¹ H NMR Spectrum of polycerasoidin (49)	207
4.135	¹³ C NMR Spectrum of polycerasoidin (49)	208
4.136	DEPT 135 NMR Spectrum of polycerasoidin (49)	208
4.137	COSY Spectrum of polycerasoidin (49)	209
4.138	HMQC Spectrum of polycerasoidin (49)	209
4.139	HMBC Spectrum of polycerasoidin (49)	210
4.140	LC-MS spectrum of elimicin (26)	214
4.141	¹ H-NMR spectrum of elimicin (26)	214
4.142	¹³ C-NMR spectrum of elimicin (26)	215
4.143	DEPT 135 NMR spectrum of elimicin (26)	215
4.144	COSY NMR spectrum of elimicin (26)	216
4.145	HMQC spectrum of elimicin (26)	216
4.146	HMBC spectrum of elimicin (26)	217
4.147	LC-MS spectrum of elimicin-6-methoxy (50)	221
4.148	GC-MS spectrum of elimicin-6-methoxy (50)	221
4.149	¹ H-NMR spectrum of elimicin-6-methoxy (50)	222
4.150	¹³ C -NMR spectrum of elimicin-6-methoxy (50)	222
4.151	DEPT 135 spectrum of elimicin-6-methoxy (50)	223
4.152	COSY spectrum of elimicin-6-methoxy (50)	223
4.153	HMQC spectrum of elimicin-6-methoxy (50)	224
4.154	HMBC spectrum of elimicin-6-methoxy (50)	224

4.155	LC-MS spectrum of 1,3,5,7-tetramethoxy-2-naphthoic acid (51)	228
4.156	¹ H NMR spectrum of 1,3,5,7-tetramethoxy-2-naphthoic acid (51)	228
4.157	¹³ C NMR spectrum of 1,3,5,7-tetramethoxy-2-naphthoic acid (51)	229
4.158	DEPT 135 spectrum of 1,3,5,7-tetramethoxy-2-naphthoic acid (51)	229
4.159	COSY spectrum of 1,3,5,7-tetramethoxy-2-naphthoic acid (51)	230
4.160	HMQC spectrum of 1,3,5,7-tetramethoxy-2-naphthoic acid (51)	230
4.161	HMBC spectrum of 1,3,5,7-tetramethoxy-2-naphthoic acid (51)	231
4.162	GC-MS spectrum of β-Sitosterol (52)	235
4.163	¹ H-NMR spectrum of β-Sitosterol (52)	235
4.164	¹³ C-NMR spectrum of β-Sitosterol (52)	236
4.165	DEPT 135 spectrum of β-Sitosterol (52)	236
4.166	GC-MS spectrum of stigmasta-5, 22-diene, 3 methoxy (53)	240
4.167	¹ H-NMR spectrum of stigmasta-5,22-diene,3 methoxy (53)	240
4.168	¹³ C-NMR spectrum of stigmasta-5,22-diene,3 methoxy (53)	241
4.169	DEPT 135 spectrum of stigmasta-5,22-diene,3 methoxy (53)	241
4.170	HMQC spectrum of stigmasta-5,22-diene,3 methoxy (53)	242
4.171	GC-MS spectrum of oleic acid (54)	245
4.172	¹ H NMR spectrum of oleic acid (54)	245
4.173	¹³ C NMR spectrum of oleic acid (54)	248
4.174	DEPT 135 NMR spectrum of oleic acid (54)	248
4.175	GCMS spectrum of hexadecanoic acid methyl ester (55)	249
4.176	¹ H NMR spectrum of hexadecanoic acid methyl ester (55)	249
4.177	¹³ C NMR spectrum of hexadecanoic acid methyl ester (55)	250
4.178	DEPT 135 NMR spectrum of hexadecanoic acid methyl ester (55)	250
4.179	TIC chromatogram of <i>Pseuduvaria monticola</i> leaf essential oil by GC-MSTOF	252
4.180	TIC chromatogram from GC-TOFMS analysis of <i>Pseuduvaria macrophylla</i> leaf essential oil	255
4.181	Percentage inhibition of <i>P.monticola</i> and <i>P.macrophylla</i> leaf essential oils at varying concentrations	258

4.182 (A)(B)	Flow cytometry analysis of MCF-7, MDA-MB-231 and MCF-10A cells stained with Annexin V/PI.	264
4.182 (C)	Representative micrograph of MCF-7, MDA-MB-231 and MCF-10A cells stained with senescence-associated β -gal.	265
4.183	Effect of PMt extract on NIT-1 cells	268
4.184	Fluorescence images and glucose uptake of PMt-treated and untreated mouse NIT-1 cells	269
4.185	Effect of PMt on insulin secretion by NIT-1 cell line.	270
4.186	Serum insulin and C-peptide levels in type 1 and type 2 diabetic rats	274
4.187	Serum GSH (a) and MDA (b) levels in type 1 and type 2 diabetic rats	275
4.188	Effects of <i>P. macrophylla</i> extract on body weight in normal and diabetic rats.	277
4.189	Effects of <i>P. macrophylla</i> extract on glucose level in normal and diabetic rats	277
4.190	Effects of <i>P. macrophylla</i> extract on Insulin (A) and C-peptide (B) levels	278
4.191	Effects of <i>P. macrophylla</i> extract on GSH (A) and LPO (B) levels	279
4.192	Summary of antidiabetic results of <i>P. monticola</i>	281
4.193	Summary of antidiabetic results of <i>P. macrophylla</i>	281

LIST OF TABLES

	Page
2.1 Biological Activities of Extracts and Isolated Compounds from <i>Pseuduvaria</i> Species	22
2.2 Some examples of basic alkaloids	25
2.3 General classification of phenolic compounds	30
2.4 Some examples of bioactive naturally occurring compound with benzopyran backbone	33
3.1 Mayer's test indicator on alkaloid content	39
3.2 % Yield of leaf essential oils of <i>P. monticola</i> and <i>P. macrophylla</i>	41
3.3 Yield of crude extracts from <i>Pseuduvaria monticola</i> and <i>Pseuduvaria macrophylla</i>	43
3.4 Yield of isolated compounds from <i>Pseuduvaria monticola</i>	51
3.5 Yield of isolated compounds from <i>Pseuduvaria macrophylla</i>	52
4.1 Chemical Compounds isolated from <i>Pseuduvaria monticola</i>	73
4.2 ¹ H NMR and ¹³ C NMR spectral data of liriodenine (3) at 500MHz in CDCl ₃ (δ in ppm, <i>J</i> in Hz)	76
4.3 ¹ H and ¹³ C NMR (600 MHz) spectral data of lysicamine (39) in CDCl ₃ (δ in ppm, <i>J</i> in Hz)	84
4.4 ¹ H and ¹³ C NMR (600 MHz) spectral data of oxoputerine (40) in CDCl ₃ (δ in ppm, <i>J</i> in Hz)	92
4.5 ¹ H and ¹³ C NMR spectral data of ouregidione (4) at 500MHz in CDCl ₃ (δ in ppm, <i>J</i> in Hz)	100
4.6 ¹ H and ¹³ C NMR spectral data of atherosperminine (41) at 400MHz in CDCl ₃ (δ in ppm, <i>J</i> in Hz)	107
4.7 ¹ H and ¹³ C NMR spectral data of argentinine (42) at 400MHz in CDCl ₃ (δ in ppm, <i>J</i> in Hz)	114
4.8 ¹ H and ¹³ C NMR spectral data of oligandrol (14) at 500MHz in CDCl ₃ (δ in ppm, <i>J</i> in Hz)	121
4.9 ¹ H and ¹³ C NMR spectral data of (6 <i>E</i> , 10 <i>E</i>) isopolycerasoidol (15) at 500MHz in CDCl ₃ (δ in ppm, <i>J</i> in Hz)	128

4.10	¹ H and ¹³ C NMR spectral data of (6 <i>E</i> , 10 <i>E</i>) isopolycerasoidol methyl ester (32) at 500MHz in CDCl ₃ (δ in ppm, <i>J</i> in Hz)	136
4.11	¹ H and ¹³ C NMR (500 MHz) spectral data of caffeic acid (44) in CDOD ₃ (δ in ppm, <i>J</i> in Hz)	143
4.12	¹ H and ¹³ C NMR (500 MHz) spectral data of chlorogenic acid (45) in CDOD ₃ (δ in ppm, <i>J</i> in Hz)	150
4.13	¹ H and ¹³ C NMR (500 MHz) spectral data of <i>n</i> -hexadecanoic acid (46) in CDCL ₃ (δ in ppm, <i>J</i> in Hz)	157
4.14	¹ H and ¹³ C NMR (500 MHz) spectral data of methyl oleate (47) in CDCL ₃ (δ in ppm, <i>J</i> in Hz)	161
4.15	¹ H and ¹³ C NMR (500 MHz) spectral data of stigmasterol (48) in CDCl ₃ (δ in ppm, <i>J</i> in Hz)	166
4.16	Compounds isolated from the bark of <i>Pseuduvaria macrophylla</i>	170
4.17	¹ H NMR and ¹³ C NMR (500 MHz) spectral data of atherospermidine (10) in CDCl ₃ (δ in ppm, <i>J</i> in Hz)	175
4.18	¹ H and ¹³ C NMR spectral data of <i>N</i> -methyl ouregidione (5) at 500MHz in CDCl ₃ (δ in ppm, <i>J</i> in Hz)	182
4.19	¹ HNMR and ¹³ CNMR spectral data of o-methylmoschatoline (7) at 500MHz in CDCl ₃	189
4.20	¹ HNMR and ¹³ CNMR spectral data of polycerasoidol (16) at 500MHz in CDCl ₃ (δ in ppm, <i>J</i> in Hz)	198
4.21	¹ HNMR and ¹³ CNMR spectral data of polycerasoidin (49) at 500MHz in CDCl ₃ (δ in ppm, <i>J</i> in Hz)	206
4.22	¹ H and ¹³ C NMR (500 MHz) spectral data of elimicin (26) in CDCl ₃ (δ in ppm, <i>J</i> in Hz)	213
4.23	¹ H and ¹³ C NMR (500 MHz) spectral data of elimicin 6-methoxy (50) in CDCl ₃ (δ in ppm, <i>J</i> in Hz)	220

4.24	¹ H and ¹³ C NMR (500 MHz) spectral data of 1,3,5,7-tetramethoxy-2-naphthoic acid (51) in CDCl ₃ (δ in ppm, <i>J</i> in Hz)	227
4.25	¹ H and ¹³ C NMR (500 MHz) spectral data of β-Sitosterol (52) in CDCl ₃ (δ in ppm, <i>J</i> in Hz)	234
4.26	¹ H and ¹³ C NMR (500 MHz) spectral data of stigmasta-5,22-diene,3-methoxy (53) in CDCl ₃ (δ in ppm, <i>J</i> in Hz)	239
4.27	¹ H and ¹³ C NMR (500 MHz) spectral data of oleic acid (54) in CDCl ₃ (δ in ppm, <i>J</i> in Hz)	244
4.28	¹ H and ¹³ C NMR (500 MHz) spectral data of hexadecanoic acid methyl ester (55) in CDCl ₃ (δ in ppm, <i>J</i> in Hz)	248
4.29	Chemical compounds identified from the leaf essential oil of <i>Pseuduvaria monticola</i> by GC-MSTOF.	253
4.30	Chemical compounds of <i>Pseuduvaria macrophylla</i> leaf essential oil	256
4.31	DPPH radical scavenging activity of <i>P. monticola</i> and <i>P. macrophylla</i> extracts	259
4.32	DPPH and ORAC assays of isolated compounds from <i>Pseuduvaria monticola</i> .	259
4.33	DPPH and ORAC assays of isolated compounds from <i>Pseuduvaria macrophylla</i>	260
4.34	Cytotoxic effects of (6 <i>E</i> ,10 <i>E</i>) isopolycerasoidol and isopolycerasoidol methyl ester on MCF-7, MDA-MB-231 and MCF-10A breast cell lines (IC ₅₀).	262
4.35	Effects of PMt on fasting blood glucose level of type 1 diabetic rats	271
4.36	Effects of PMm on fasting blood glucose level of type 2 diabetic rats	272
4.37	Effects of PMt on fasting blood glucose level of type 2 diabetic rats after glucose load.	273

ABBREVIATION

α	Alpha
β	Beta
CC	Column Chromatography
TLC	Thin Layer Chromatography
PTLC	Preparative Thin Layer Chromatography
CDCl_3	Deuterated chloroform
CHCl_3	Chloroform
CD_3OH	Deuterated methanol
CH_2CL_2	Dichloromethane
$\text{MeOH}/\text{CH}_3\text{OH}$	Methanol
CH_3COCH_3	Acetone
HCl	Hydrochloric acid
NH_3	Ammonia
CH_3	Methyl group
C_6H_{12}	Hexane
COSY	H-H Correlation Spectroscopy
δ	Delta value (chemical shift) in ppm
br	Broad
d	Doublet
dd	Doublet of doublet
dt	Doublet of triplet
ESI	Electrospray Ionization
FT-NMR	Fourier Transform NMR
g	Gram
GCMS	Gas Chromatogram-Mass Spectrometry
LCMS	Liquid Chromatography Mass Spectroscopy
HREIMS	High Resolution Electron Impact Mass Spectroscopy
ESI	Electrospray Ionization
HMBC	Heteronuclear Multiple Bond Correlation
HMQC	Heteronuclear Multiple Quantum Correlation
HSQC	Heteronuclear Single Quantum Correlation

DEPT	Distortionless Enhancement by Polarization Transfer
OD	Optical Density
m/z	Mass per charge
Hz	Hertz
IR	Infrared
<i>J</i>	Coupling Constant (Hz)
λ_{max}	Maximum wavelength
m	Metre
m/z	Mass to charge ratio
MHz	Mega Hertz
MS	Mass Spectrum
ml	Mililiter
mg/ml ⁻¹	Microgram per millilitre
nm	Nanometer
NMR	Nuclear Magnetic Resonance
NOE	Nuclear Overhauser Effect
OCH ₃	Methoxyl group
OCH ₂ O	Methylenedioxy group
OH	Hydroxyl group
¹ H	Proton
¹³ C	13-Carbon
ppm	Parts per million
1D NMR	One dimensional Nuclear Magnetic Resonance
2D NMR	Two-dimensional Nuclear Magnetic Resonance
UV	Ultraviolet
IC ₅₀	Inhibitory concentration at 50%
OH	Hydroxyl
S	singlet
HPLC	High Performance liquid Chromatography
COSY	¹ H- ¹ H Correlation Spectroscopy

CHAPTER 1: INTRODUCTION

Malaysia ranks the 12th largest in the world in term of biodiversity. More than 60% of the woods from the tropical forest are processed and commercially exported to other countries for the timber industry. Apart from being the main source for timber industry, Malaysian tropical forest too is rich with all kinds of plants and flora with medicinal properties which have long been utilized by the local people and traditional practitioners. The vast variety of flora and fauna provides a great opportunity in discovering potential new lead compounds for medicinal and drug discovery purposes (Jantan, 2010). For example, ginger species (*Zingiberaceae* rhizomes) or locally known as 'halia' commonly used in foods and supplements by the locals were found to demonstrate anti-tumor promoter activity (Vimala *et al.*, 1999).

Plants and their by-products have long been used as source of medicines and poisons since ancient times. Plants have variety of chemical constituents called 'phytochemicals' with protective and disease preventive properties. The term 'phytochemicals' refer to chemical substances produced naturally in plants that demonstrate various biological activities such as antioxidant, antimicrobial, antifungal, anti-inflammatory, anti-malarial and anticancer activities (Tan *et al.*, 2010).

These phytochemicals include alkaloids, polyphenols, isoflavones, flavonoid and terpenoids which are clinically proven to be of pharmacologically importance which may help in the treatment of many diseases such as cancer, cardiovascular disease, diabetes, degenerative diseases and HIV infection (Asres *et al.*, 2005). Vegetables, fruits, herbs and seeds are some of the plants that contain phytochemicals that are rich in phenolic compounds such as flavanoids, phenolic acids, anthraquinones and coumarins (Young *et al.*, 2005).

The search for new drugs to treat human ailments is never-ending as new diseases emerge globally and as the number of drug-resistance cases increases (Koehn & Carter, 2005). As a result, research in natural products and drug discovery continues to expand with the latest development of technology in separation methods, spectroscopic techniques and instruments and advanced bioassays including hyphenated technique. Over the years, there have been significant findings and evidence in the pharmaceutical industry that naturally-occurring compounds derived from higher plants have the potential to be developed as modern therapeutic drugs.

Approximately, about 25% of the drugs used in the world today originate from higher plants and among them were taxol, morphine, quinine caffeine, atropine, and reserpine (Rates, 2001). And there are more than 127 potential natural-product- derived drugs currently undergoing clinical trials throughout the world (Prajna *et al.*, 2013).

The pursuit for new lead compounds from plant-derived medicines or organisms for the development of conventional drugs or vaccines is becoming more commercialized in the modern medicine throughout the world due to increasing needs and demand for medicinal drugs. For example, the production of Tamiflu (influenza drug) has increased in volume by demands in the past year following repeating occurrence of pandemic flu throughout the world (Abbot, 2005).

Chemical compounds from natural products still continue to serve as valuable sources for new therapeutic agents especially with the profound understanding of the biological significance and mechanism of actions of the active compounds. As more diseases become prevalent and the trend for drug resistance and side-effects increases, there is the need to discover new medicinal drugs from natural origin with specific targets and the least side-effects. On the other hand, synthetic drugs tend to show rapid onset of action with more side-effects in comparison to naturally occurring drugs (Topliss *et al.*, 2002).

There are two types of metabolites produced by the plants; primary and secondary metabolites. The primary metabolites are made during active cell growth which include polysaccharide, protein, fatty acids and lipids, while secondary metabolites are the production of unique biosynthetic pathways from the primary metabolites.

Secondary metabolites are bioactive compounds synthesized in certain plant species or in specific parts of the plant as a defence mechanism against herbivores and predators in order to survive in their surroundings. They are not ubiquitous and their occurrences are limited. They also do not participate in the biosynthesis of primary metabolites. In the past years, previous secondary metabolites with unknown biological activities have been extensively investigated as a source of medicinal agents where these phytochemicals were further investigated *in vitro* and *in vivo* (Balaabirami & Patharajan, 2012).

Secondary metabolites may also function as metal transporting agents, as symbiotic agents between the plant host and microbes, as sexual hormones and as differentiation effectors (Demain & Fang, 2000; Kosuta *et al.*, 2008). They are not ubiquitous and their occurrences are limited. They also do not participate in the biosynthesis of primary metabolites.

Secondary metabolites are not required for the vital growth of the plant and therefore they are not biosynthesized in a higher concentration and usually their presence in plants are affected or induced in response to the surrounding factors, conditions and stress such as the climate, the soil condition, herbivores, etc. (Christophersen, 1995; Figueiredo *et al.*, 2008). They are grouped according to their structures, biosynthetic pathways and the type of plants which produce them.

In the process of drug discovery, random screenings of various compounds in natural products are preliminary tested *in vitro* or *in vivo* where subsequently, only compounds that show significant biological activities and selectivity will proceed to the next level of

identification, evaluation and clinical trials (Harvey, 2010; Harvey *et al.*, 2010) Figure 1.1 shows the general flow for the drug discovery process.

There are several approaches in the selection of plants that may contain bioactive compounds. One of them is through ethno medical reports based on the traditional medicinal information of the plant which may contribute to higher chances of discovering potential lead drug (Gyllenhaal *et al.*, 2012).

In the bioassay-guided fractionation approach, the crude extracts of the selective plants are screened first and this is followed by bioassay-guided isolation where every stage of fractionation and isolation is guided by bioassays (Guerro-Analco *et al.*, 2010; Phillipson *et al.*, 2002). The active chemical compounds are then isolated from the bioactive fractions and the structures of the active compounds are further determined and identified by structural elucidation using chromatographic and spectroscopic methods such as NMR, 2D NMR, UV, IR and MS.

Another method is through chemotaxonomical approaches that utilize the previous information of a certain group of plants with specific chemical compounds to establish the compounds in another plant in the same taxonomic group (Heinrichs *et al.*, 2000).

Dereplication is a process where recurrence of similar or known compounds is avoided by differentiating between known and unknown compounds. This is done through the use of high throughput screening (HTS) and by applying hyphenated techniques such as the liquid chromatography–electrospray ionization–mass spectrophotometry (LC/ESI/MS), liquid chromatography-photoiodide array detection (LC/PDA) and liquid-chromatography-nuclear magnetic resonance (LC/NMR) chromatography where known compounds are identified in a shorter time without the need for extensive purifications compared to the traditional method (Lang *et al.*, 2008; Wolfender *et al.*, 2010).

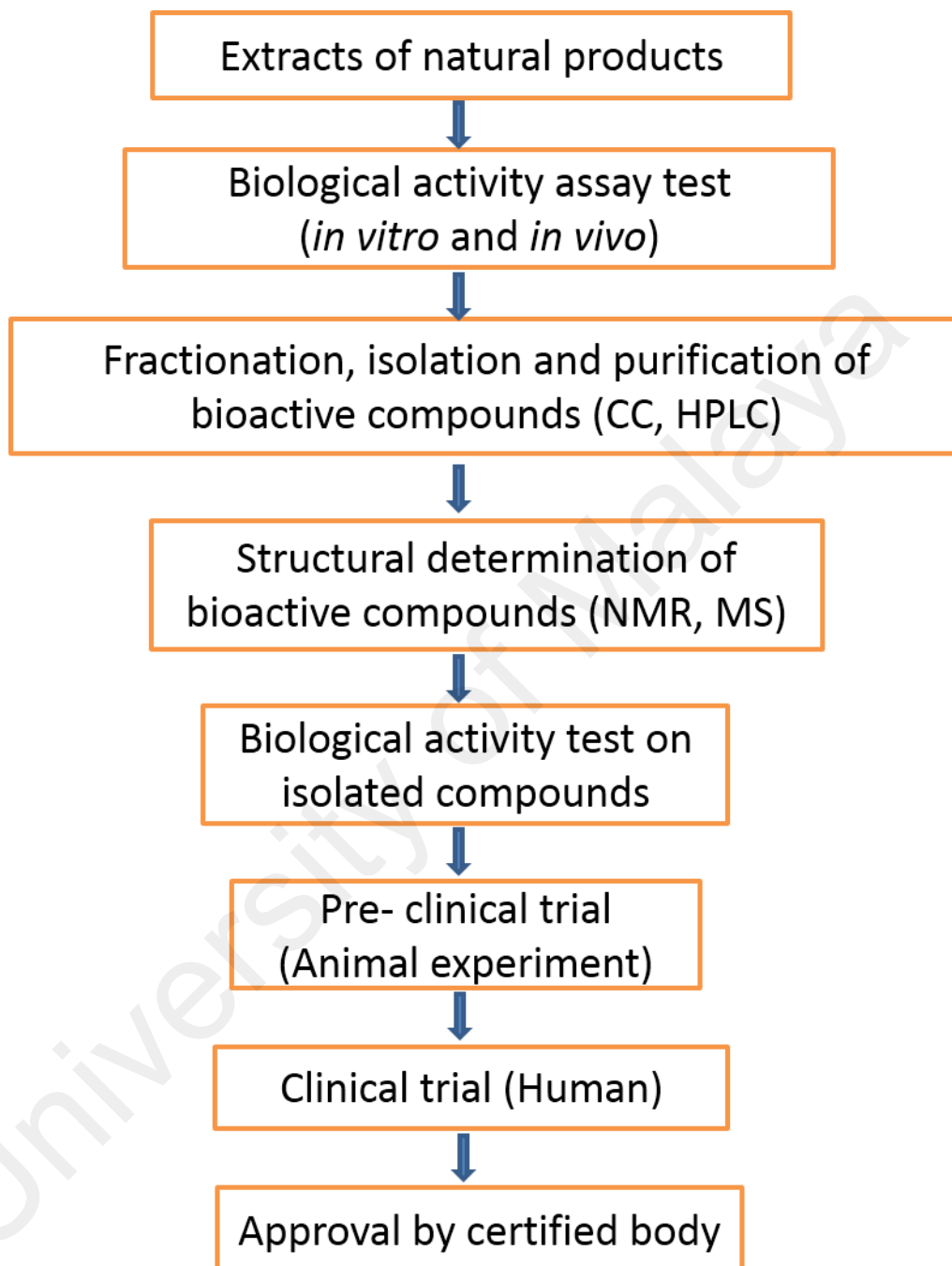


Fig. 1.1: Drug discovery process

The objectives of this study are:

1. To extract the essential oils from the leaves of two *Pseuduvaria* species by hydrodistillation using Clevenger's apparatus and analyze the leaf essential oils by GC-MS.
2. To extract and isolate the chemical constituents from the leaves and bark of *Pseuduvaria monticola* and *Pseuduvaria macrophylla* using various chromatographic methods (CC, PTLC, HPLC)
3. To determine the structures of pure compounds particularly new compounds by spectroscopic methods such as NMR, UV, IR and MS.
4. To evaluate the antidiabetic, anticancer and antioxidant activities of the crude extracts and isolated compounds.

CHAPTER 2: LITERATURE REVIEW

2.1 Family Annonaceae

The family Annonaceae is very diverse and one of the largest family of the flowering plants (Angiosperma) which consists of approximately 128 genera and over 3,000 species (Xu & Ronse, 2010).

In Malaysia, there are 38 genera, 198 native and 5 cultivated species including 17 varieties of Annonaceae plants and they are abundantly found in the lowland forests mostly below 2,000 feet (J.Sinclair, 1955). The members of the Annonaceae family are made up of small trees, shrubs and woody climbers that be found mainly in the tropical and subtropical regions (Couvreur *et al.*, 2011).

The Annonaceous plants are well known as folk medicines for the treatment of fever, coughing, diarrhea, stomachache, constipation and minor ailments (Savithramma *et al.*, 2011). There are numerous scientific reports on the bioactive compounds isolated from the family that exhibit potent biological activities such as cytotoxic, antitumor, antimalarial, antibacterial, antifungal, antiplatelet aggregation and immunosuppressive activities which justify the medicinal properties of the plants (De Lima *et al.*, 2008).

The Annonaceae family also serve as important sources for timber and fragrances such as perfumes and soaps. The Annonaceae plants have been known to be rich in alkaloids especially the isoquinoline alkaloids where they are found mainly in most parts of the plants (Nishiyama *et al.*, 2004, Rasamizafy *et al.*, 1987).

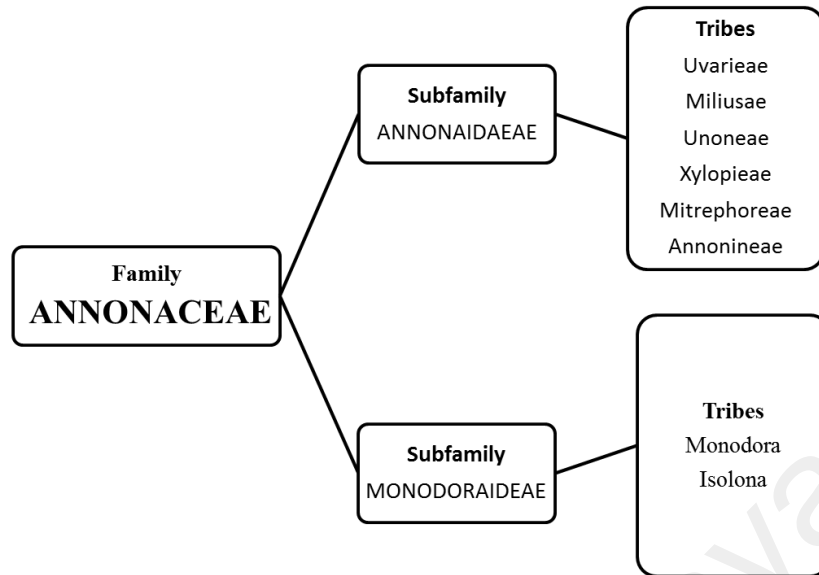
2.1.1 General Appearance and Morphology

The Annonaceae family consists of trees and shrubs and can be divided into climbing and non-climbing. The plants in the Annonaceae family are generally monopodial trees with resinuous or sourly aromatic tissues such as barks and leaves. The leaves are always simple, membraneous, alternate and entire without stipulates. The bark is generally smooth and entire, pale grey or buff to brown. The flowers are solitary and scented, mostly trimerous with free carpels and seeds with ruminant endosperm. Fruiting carpels are sessile or stipitate, usually in an aggregate of berries; appear like a bunch of small bananas, which acquired the common Malay name, 'pisang-pisang' or 'mempisang' (Van Heusden, 1994).

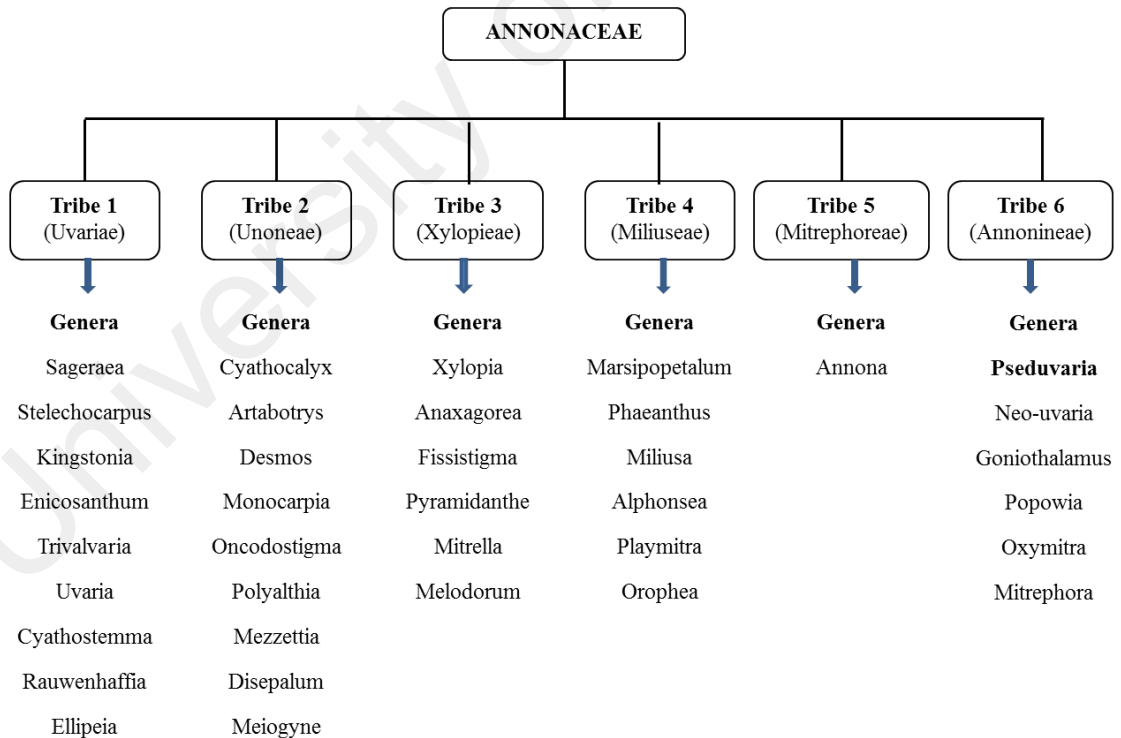
2.1.2 Classification of Annonaceae

The Annonaceae family belongs to the Angiosperma (flowering plants) group and the Dicotyledonae class. The dicotyledons are herbs, shrubs or trees the seeds of which have two cotyledons. It belongs to the order of the Ranales.

In general, the Annonaceae family can be divided into two subfamilies: Monodoroideae (carpels united into a one-celled ovary, with parietal placentation) and Annonoideae (free carpels) (Scheme 1). These subfamilies are further divided into tribes and each tribe consist of several genera. The classification of the genera is based on the characteristics of petals and fruits (Scheme 2).



Scheme 1: Classification of Annonaceae



Scheme 2: Genera of Annonaceae

2.1.3 Medicinal and Economic Importance

The Annonaceous plants are well known as folk medicines for the treatment of fever, coughing, diarrhea, stomach ache and minor ailments (Suleiman *et al.*, 2008). There are numerous reports on the bioactive compounds isolated from the plants in the family which justify the medicinal properties of the plants (Prachayasittikul *et al.*, 2009; Taha *et al.*, 2013).

In fact, the broad pharmacological activities exhibited by the plants provide the bio-source for the pharmaceutical industry (Aminimoghadamfarouj *et al.*, 2011). Various types of compounds including alkaloids, flavonoids, and acetogenins have been extracted from the seeds and other parts of these plants. *Asimicin*, an acetogenin isolated from *Asimina triloba* demonstrated insecticidal activity (Rieser *et al.*, 1991).

The plants of the Annonaceae family also serve as a main source of commercial timber supplies and commercial products. A study showed that high tannin content in *Acacia mangium* bark provide a new source of polyflavanoid material that can replace commercial adhesive in plywood industry (Hoong *et al.*, 2011).)

The Annonaceae family is also economically and nutritionally important as a source of edible fruits; the pawpaw (*Asimina*), cherimoya (*Annona cherimola*), sweetsop, soursop and custard apple. Cherimoya pulp, besides being tasty, is high in antioxidant and cytotoxic properties due to its high total phenols contents (Barreca *et al.*, 2011). Flowers of some plants in the Annonaceae family are used in perfumery and the seed oils are used in soap production and edible oils. For example; *Cananga Odorata* from the species of kenanga is known for its perfume oil, Ylang Ylang or Macassar oil which is used as the main ingredient for a branded perfume (Buchbauer, 2004).

2.1.4 Genus *Pseuduvaria*

Pseuduvaria is a rainforest plant species that belongs to the family Annonaceae. Plants in this genus are in the major group of flowering plants (Angiosperms) that are made up of shrubs and trees usually found in the rainforest population. It was reported that the *Pseuduvaria* species originated from Sundaland in the late Miocene and later migrated to the other part of the region (Su & Saunders, 2009).

The *Pseuduvaria* species are mostly distributed throughout South East Asia including Malaysia, Thailand, Burma, Indonesia, Australia and Papua New Guinea. In Australia, the species are mostly found in the northeastern part of Queensland, Australia. Currently, there are about 52 *Pseuduvaria* species that were classified and documented but only a few have been investigated chemically and biologically (Su *et al.*, 2008).

The species are known to contain mostly alkaloids due to its aromatic nature including phenolic compounds, terpenoids and benzopyran derivatives. There are currently eight *Pseuduvaria* species documented in Peninsular Malaysia (Latiff, 2015). In Malaysia, *Pseuduvaria* species are used by the locals to treat fever and stomachache but it is not well documented. In Thailand, the root of *Pseuduvaria setosa* has been traditionally used to treat cough, fever and stomach ailments (Wirasathien *et al.*, 2006).

2.1.5 *Pseuduvaria monticola*: botanical morphology

Pseuduvaria monticola is a tree of 5-7 m high with slender and dark colored young twigs (Figure 2.1). The leaves are simple and alternate, membraneous and papery with lanceolate shape (spear shaped). The fruits are small which look like a bunch of berries consist of a group of fleshy carpels that is attached on a torus. The bark is fibrous and aromatic, smooth and grey to brown in color. The flowers are bisexual and inflorescences which are arranged in axillary fascicles solitary, paired or clustered and

they are characterized by a cyclic perianth of three trimerous whorls, an androecium of several stamens and a gynoecium of free carpels on a flat or conical receptacle.

2.1.6 *Pseuduvaria macrophylla*: botanical morphology

The tree is about 5-10 m high with slender and dark colored young twigs. The leaves are large and elongated, membranous and oblong where the apex and the base are acute and narrowed (Figure 2.2). The flowers are usually unisexual, resembling three sepals and two whorls of three petals. The inner petals are longer than the outer petals, and purple-reddish in color. The fruits are small which look like a bunch of berries consist of a group of fleshy carpels that is attached on a torus. The bark is fibrous and aromatic, smooth and grey to brown in color. *Pseuduvaria macrophylla* can be found throughout Malaysia including Pulau Tioman and Taman Negara (Latiff, 2015).



Figure 2.1: Bark (A) and leaves (B) of *Pseuduvaria monticola*



Figure 2.2: Bark (A), flower (B), fruit and leaves (C) of *Pseuduvaria macrophylla*

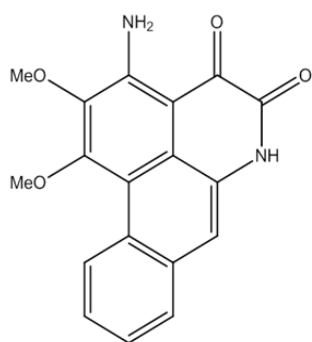
2.2 Chemical aspects of *Pseuduvaria* species

Previous phytochemical investigation on *Pseuduvaria* species led to the isolation of a number of chemical constituents including alkaloids, terpenoids, benzopyran derivatives and leaf essential oils. Literature reviews indicated that only a small number of species in the genus *Pseuduvaria* have been investigated for its chemical compounds and biological activities. Most studies have emphasized the isolation of alkaloids from the species.

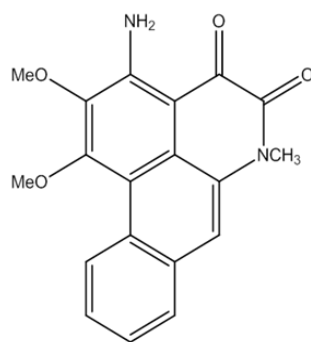
Some of the alkaloids commonly found in the *Pseuduvaria* species were mostly aporphine alkaloids. Recent phytochemical investigation on the stem bark of *Pseuduvaria rugosa* revealed two new dioxoaporphine alkaloids with an amino moiety; *Pseuduvarine* A (**1**) (3-amino-1,2-dimethoxy-4,5-dioxoaporphine) and *Pseuduvarine* B (**2**) (N-methyl-3-amino-1,2-dimethoxy-4,5-dioxoaporphine). The rest of the oxoaporphine alkaloids were liriodenine (**3**), ouregidione (**4**), N-methylouregidione (**5**) and 1,2,3-trimethoxy-5-oxonoraporphine (**6**) (Taha *et al.*, 2011; Uadkla *et al.*, 2013).

Two aporphinoid alkaloids; O-methylmoschatoline (**7**) and N-Methylouregidione (**5**) were isolated from the stem bark of *Pseuduvaria macrophylla* that were collected in the forest in Taman Negara, Pahang, Malaysia (Mahmood *et al.*, 1986).

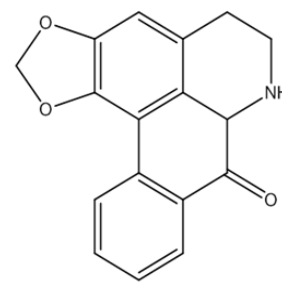
Since that, there was no further report or experimental data on the isolation of other chemical constituents from *Pseuduvaria macrophylla* until the time this study was commenced.



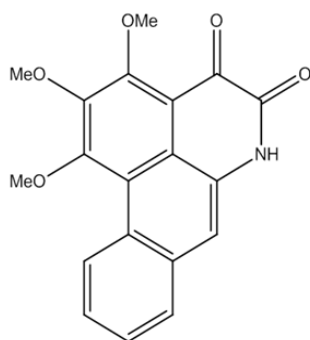
1



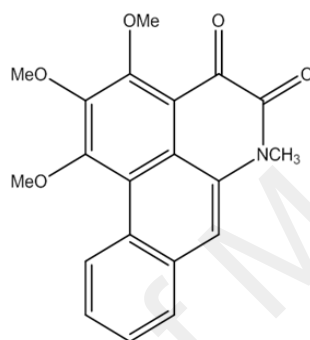
2



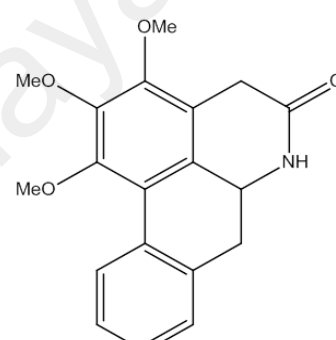
3



4

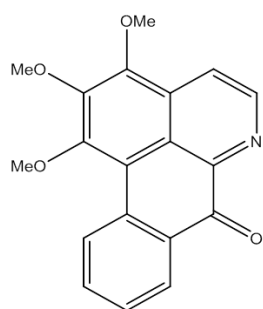


5

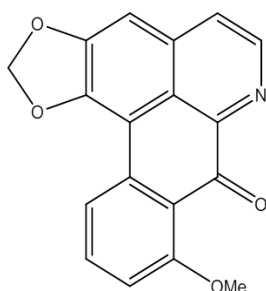


6

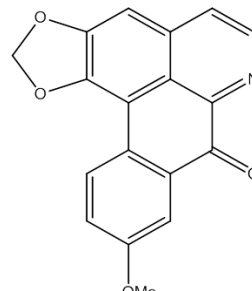
Pseuduvaria setosa (King) J. Sinclair is another species of *Pseuduvaria* genus that has been investigated. In Malaysia, the fruits of *Pseuduvaria setosa* are normally consumed by fruit bats as one of their main diets during the fruiting season (Robert Hodgkinson, 2004). Two dioxoaporphine alkaloids were isolated; ouregidione (**4**), *N*-methylouregidione (**5**) along with two oxoaporphine alkaloids, liriodenine (**3**) and oxostephanine (**8**) from the aerial part of *Pseuduvaria setosa* (King) J. Sinclair (Wirasathien *et al.*, 2006).



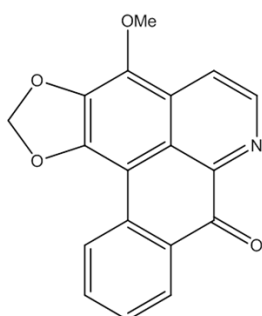
7



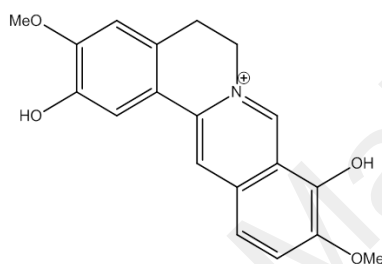
8



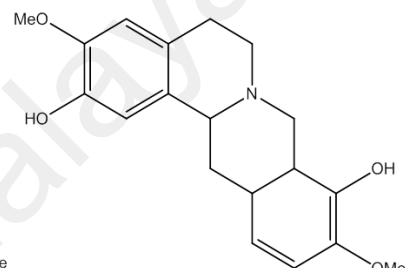
9



10



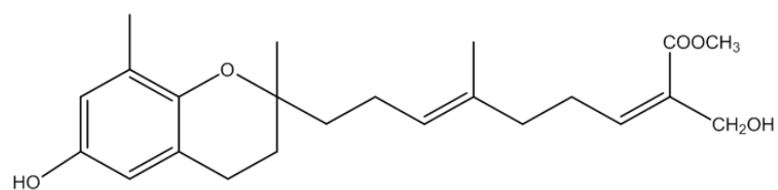
11



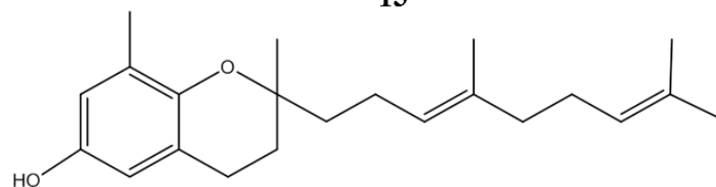
12

Phytochemical investigation on the stem bark of *Pseuduvaria indochnesis* (Shou-Ming *et al.*, 1988) has led to the isolation and characterization of three known oxoaporphine alkaloids, liriodenine (**3**), oxoanolobine (**9**) atherospermidine (**10**) and two protoberberine alkaloids, dehydroscoulerine (**11**) and scoulerine (**12**).

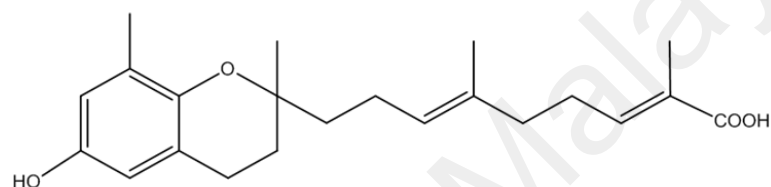
Another recent study reported on a new benzopyran derivative, pseudindochin (**13**) and three known compounds from the same chemical group (benzopyran derivatives), oligandrol (**14**), (6*E*,10*E*) isopolycerasoidol (**15**) and polycerasoidol (**16**) from the ethanol extract of twigs and leaves of *Pseuduvaria indochnensis* Merr. (Zhao *et al.*, 2014).



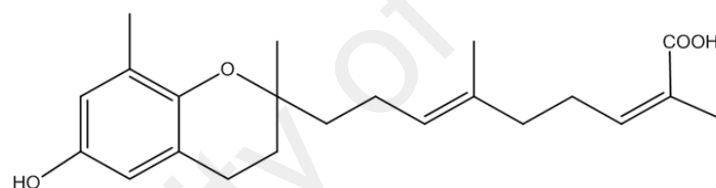
13



14

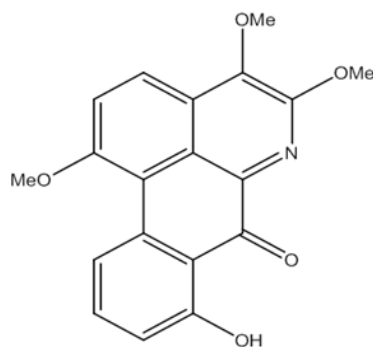


15



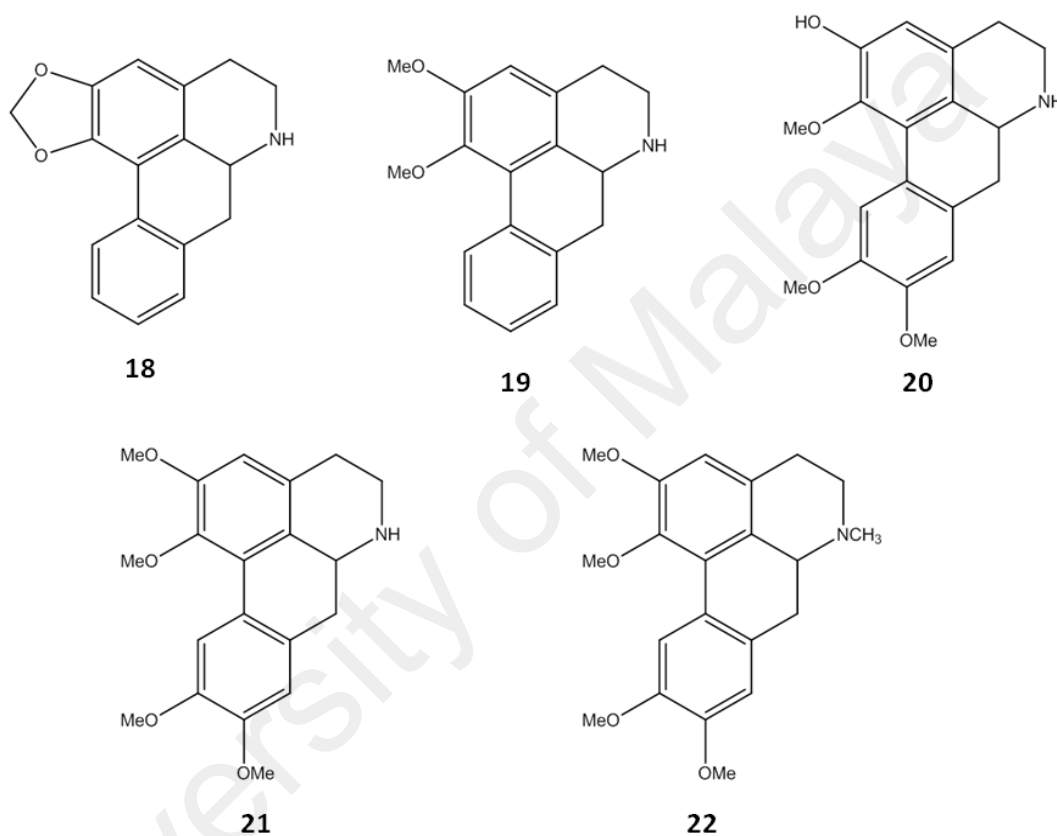
16

Two more aporphine alkaloids isolated from *Pseuduvaria trimera* (Craib) were ouregidione (**4**) and 8-hydroxy-1,4,5-trimethoxy-7-oxoaporphine or 8-hydroxyartabonatine C (**17**) which was a new compound (Sesang *et al.*, 2014).

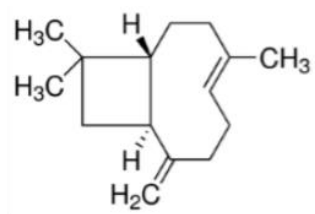


17

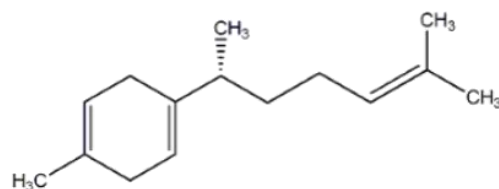
The alkaloids found from two *Pseuduvaria* species in Australia, *Pseuduvaria cf. grandifolia* and *Pseuduvaria cf. dolichonema* were liriodenine (**3**), anonaine (**18**) and nornuciferine (**19**) and glaucine (**20**), 2-hydroxy-1,9,10- trimethoxynoraporphine (**21**) and norglaucine (**22**), respectively (Johns *et al.*, 1970).



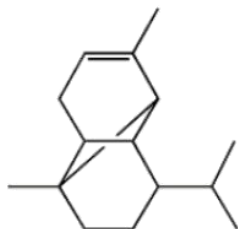
A GC-MS analysis on the leaf essential oils of *Pseuduvaria* species from Australia was reported. The species investigated were *Pseuduvaria mulgraveana* var. *mulgraveana*, *Pseuduvaria mulgraveana* var. *glabrescens*, *Pseuduvaria hylandii*, *Pseuduvaria villosa*, and *Pseuduvaria froggattii* (Brophy *et al.*, 2007). These species are mainly found in the wet tropics of northeastern Queensland (Jessup, 1987). The major compounds present in the leaf oils were β -caryophyllene (**23**), α -curcumene (**24**), α -copaene (**25**), elimicin (**26**), methyl eugenol (**27**), spathulenol (**28**) and caryophyllene oxide (**29**).



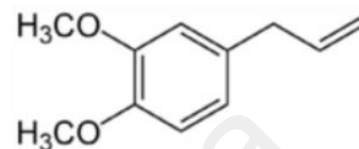
23



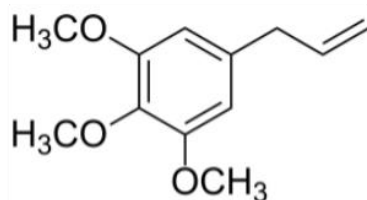
24



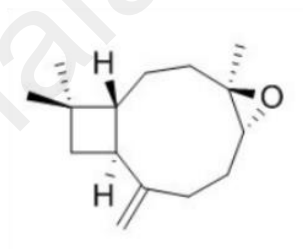
25



26

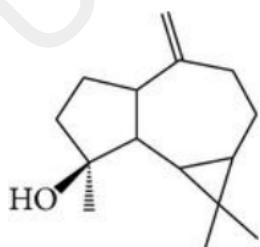


27

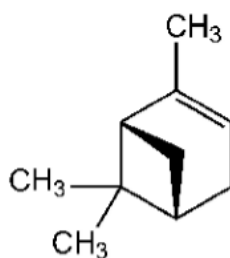


28

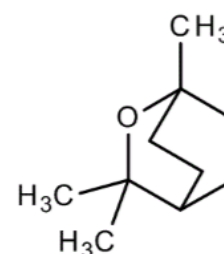
In *Pseuduvaria indochinensis*, sesquiterpenes and monoterpenes made up the whole composition of the leaf essential oil. The major constituents were α -copaene (**25**) (26.5%), α -pinene (**30**) (7.6%) and 1,8 cineole (**31**) (5.7%) (Dai *et al.*, 2014).



29



30



31

In summary, the majority of alkaloids isolated from the *Pseuduvaria* species were of aporphine type alkaloids. Liriodenine (**1**) can be regarded as the chemical bio-marker for *Pseuduvaria* species because it was frequently isolated as one of the major compounds.

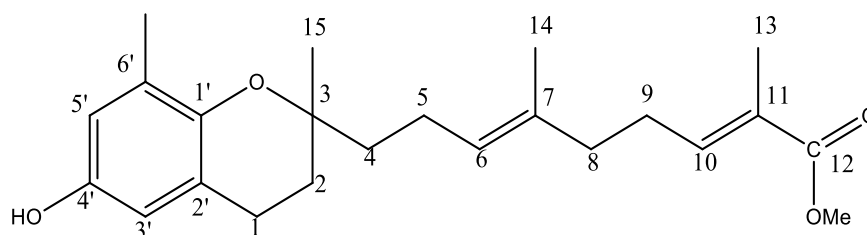
2.3 Bioactive compounds from *Pseuduvaria* species

There were not many reports or data on the pharmacological activities of *Pseuduvaria* species even though the plants have history of medicinal values. However, in the past years, several studies have demonstrated that crude extracts and chemical compounds isolated from *Pseuduvaria* species display wide range of biological activities. In Thailand, the roots of *Pseuduvaria macrophylla* were used by the locals as medicinal concoction to treat stomach ailment (Sesang *et al.*, 2014).

Polar extracts of *Pseuduvaria* species were found to exhibit anticancer, antibacterial, antioxidant and antidiabetic activities. Total phenolic content in the previous study indicated the presence of phenolic compounds and flavonoids in the polar extracts that may contribute to the antioxidant and antidiabetic activities (Chu, 2014). On the other hand, the hexane and crude alkaloid extracts have shown significant *in vitro* anti cancer activity. The list of the reported biological investigations that were carried out on *Pseuduvaria* species until present is listed in Table 2.1 below;

Table 2.1: Biological Activities of Extracts and Isolated Compounds from *Pseuduvaria* Species

Pseuduvaria Species	Extracts /Compounds	Biological activities
<i>P. rugosa</i>	<i>Pseuduvarine</i> A (1), <i>Pseuduvarine</i> B (2) , ouregidione (4) , <i>N</i> -methyl ouregidione (5) , liriodenine (3) , oxostephanine (8), 1,2,3-trimethoxy-5-oxonorporphine (6)	Anticancer (Hairin <i>et al.</i> , 2011; Uadkla <i>et al.</i> , 2013).
<i>P. setosa</i>	<i>N</i> -methyl ouregidione (5), ouregidione (4), liriodenine (3), oxostephanine (8)	Anticancer, Antituberculosis Antimalarial (Wirasathien <i>et al.</i> , 2006).
<i>P. trimera</i>	8-hydroxy-1,4,5-trimethoxy-7-oxoaporphine (16), ouregidione (4)	Anticancer (Sesang <i>et al.</i> , 2014).
<i>P. macrophylla</i>	Ethanol extract	Anticancer, Antibacterial, Antioxidant (Chu, 2014; Othman <i>et al.</i> , 2011)
	Methanol extract	Antidiabetic (Arya <i>et al.</i> , 2014)
<i>P. monticola</i>	Methanol extract	Antidiabetic (Taha <i>et al.</i> , 2014)
	(6 <i>E</i> ,10 <i>E</i>) isopolycerasoidol (15), (6 <i>E</i> ,10 <i>E</i>) isopolycerasoidol methyl ester (32)	Anticancer (Taha <i>et al.</i> , 2015)



2.4 Alkaloids

Alkaloids are heterocyclic nitrogenous compounds found in 20% of plant species and have been regarded as toxic principles which are part of the plant defense mechanism against herbivores and pathogens (Mithofer & Boland, 2012). Other microorganisms such as bacteria, fungi and insects also produce alkaloids. Originally, the name alkaloids derived from the Arabian word *al-qali* from which soda was isolated (Massotte & Kieffer, 1998).

Alkaloids applied to compounds which contain nitrogen as part of the heterocyclic system which comprises the largest class of secondary plant substances. These compounds are grouped according to the presence of nitrogen atom in their structures. Alkaloids are considered as by-products of plant metabolism during the process of growth, metabolism and reproduction by series of chemical reactions. Some scientists also regard alkaloids as nitrogen storage reservoir for protein synthesis. Insects use plant alkaloids as source of sex pheromones such as the pyrrolizidine alkaloids (McNeil & Delisle, 1989).

Throughout the history, alkaloids from plant extracts have been utilized by human beings as medicinal concoction and poisons in their daily life (Tan & Vanitha, 2004). Traditionally, ancient community use plant alkaloid extracts to treat minor ailments such as fever and headache but since the discovery of more new alkaloids and their derivatives, a broad range of diseases are now treatable and curable (Asano *et al.*, 2000).

In plants and micro organisms, alkaloids are present in the form of salts. In order to extract the alkaloids, the plants need to be treated with a strong base to release the nitrogen-containing compounds, and then re-extract with acid. This process is called acid-base extraction. Alkaloids are largely distributed in the families of Rutaceae, Solanaceae, Paveraceae, Rubiaceae, Apocynaceae and Annonaceae. In the Annonaceae family, most of the alkaloids belong to the isoquinoline type.

2.4.1 Classification of alkaloids

Alkaloids are classified into three groups based on their biogenesis;

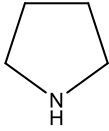
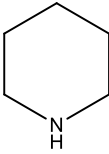
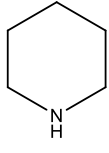
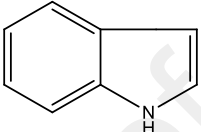
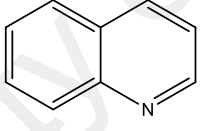
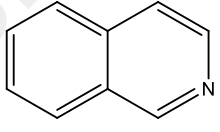
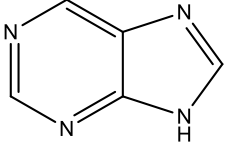
a) The true alkaloids : Nitrogen containing compounds derived from an amino acid in a heterocyclic system and normally occurs as soluble salts such as malates, citrates, titrates and benzoates. E.g. Atropine.

b) The protoalkaloids: They are simple amines, derived from amino acids or biogenetic amines with no heterocyclic system or nitrogen atom is not part of a heterocyclic ring. They exist in nature by the biogenetic amine and their methylated derivatives. E.g. Mescaline.

c) The pseudo alkaloids: They do not derived from amino acids but have all the characteristics of true alkaloids. They have nitrogen in the heterocyclic ring but the carbon skeletons derived from monoterpenes, diterpenes, triterpene, sterols and acetate derived, aliphatic polyketo acids. E.g. Paravallarine.

Table 2.2 showed a general chemical classification of alkaloids based on the type of carbon skeleton and heterocyclic system.

Table 2.2: Some examples of basic alkaloid skeletons

Type of Alkaloids	Basic skeleton	Examples
Pyrollidine		Piriferine (Saifah <i>et al.</i> , 1988).
Piperidine		Piperdardine (De Araujo-Junior <i>et al.</i> , 1997).
Pyridine		Cerpegin (Adibatti <i>et al.</i> , 1991).
Indole		Harman (Kusurkar <i>et al.</i> , 2003)
Quinoline		Transtorine (Al-Khalil <i>et al.</i> , 1998)
Isoquinoline		Crispine A (Zhang <i>et al.</i> , 2002).
Purine		Caffeine (Ashihara & Crozier, 2001).

2.4.2 The isoquinoline alkaloids

Alkaloids with isoquinoline skeleton derived structures represent the major type of alkaloids found in Annonaceae. Isoquinolines form one of the largest groups of plant alkaloids which include a number of important pharmaceutical agents such as codeine,

morphine, emetine and tubocurarine. Isoquinoline alkaloids are most frequently found in the Annonaceae family. All isoquinoline alkaloids derived from benzyloisoquinoline with an isoquinoline basic skeleton. Isoquinoline alkaloids can be divided into several classes depending on the origin of their biogenesis; simple isoquinoline, benzyloisoquinoline, bisbenzyloisoquinoline, protoberberine, aporphine, oxoaporphine, phenanthrene and miscellaneous isoquinoline type alkaloids.

The most common type of alkaloids in the Annonaceae family are those belonging to the four subgroups; benzyloisoquinolines, bisbenzyloisoquinolines, protoberberines and aporphinoids.

2.4.3 Simple isoquinoline

Simple isoquinolines contain one aromatic ring with no other cyclic structure except a methylenedioxy substituent at carbon C-6 and C-7. The nitrogen function in the ring B is often tertiary and N-methylated, can also be secondary, N-formylated, N-acetylated, N-ethylated or oxidised to the imine stage.

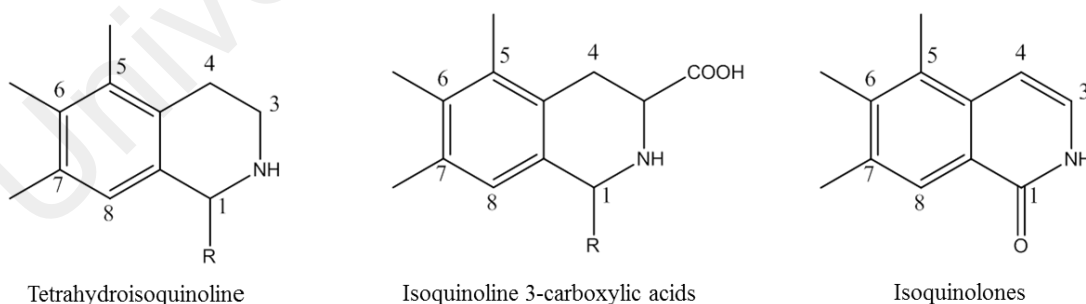


Fig.2.3: General structure of simple isoquinoline alkaloids

2.4.4 Aporphine

The aporphine alkaloid (Fig. 2.4) has a twisted biphenyl system consisting of 4 ring structures; A, B, C and D. The nitrogen atom in the B ring can be secondary, tertiary or quaternary. Figure shows the basic skeleton of aporphine alkaloid. The most common occurrence of the aporphine alkaloid is the oxygenated type, where the carbon position at C-1 and C-2 are always oxygenated, and either substituted with hydroxyl, methoxyl or methylenedioxy.

In few cases, a hydroxyl or methyl function group is located at C-7. Plants from the families of Annonaceae and Lauraceae are very rich in the aporphine alkaloids with broad range of biological activities (Montenegro *et al.*, 2003; Stevigny *et al.*, 2002).

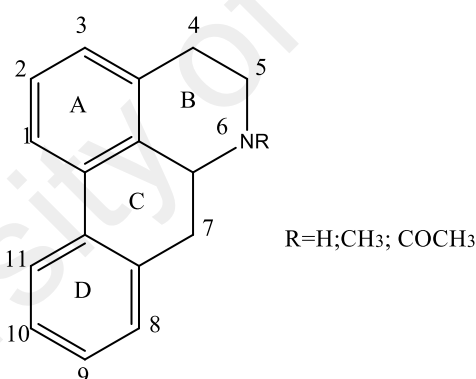


Fig.2.4: Basic aporphine skeleton

2.4.5 Oxoaporphine and dioxoaporphine alkaloids

An aporphine with an aromatic isoquinoline ring and a conjugated ketone group at C-7 give a structure called oxoaporphine. Oxoaporphine are formed by multiple oxidation and dehydrogenation of an aporphine through the intermediacy of dehydroaporphines and didehydroaporphines. Figure 2.5 shows the biogenetic pathway to an oxopaorphine. C-7

oxygenated aporphines are the major 7-substituted aporphines isolated from Annonaceae. The oxoaporphine alkaloids usually possess an intense yellow or orange because of the highly conjugated system. Liriodenine (**1**) is widely encountered in almost all the genera of Annonaceae family.

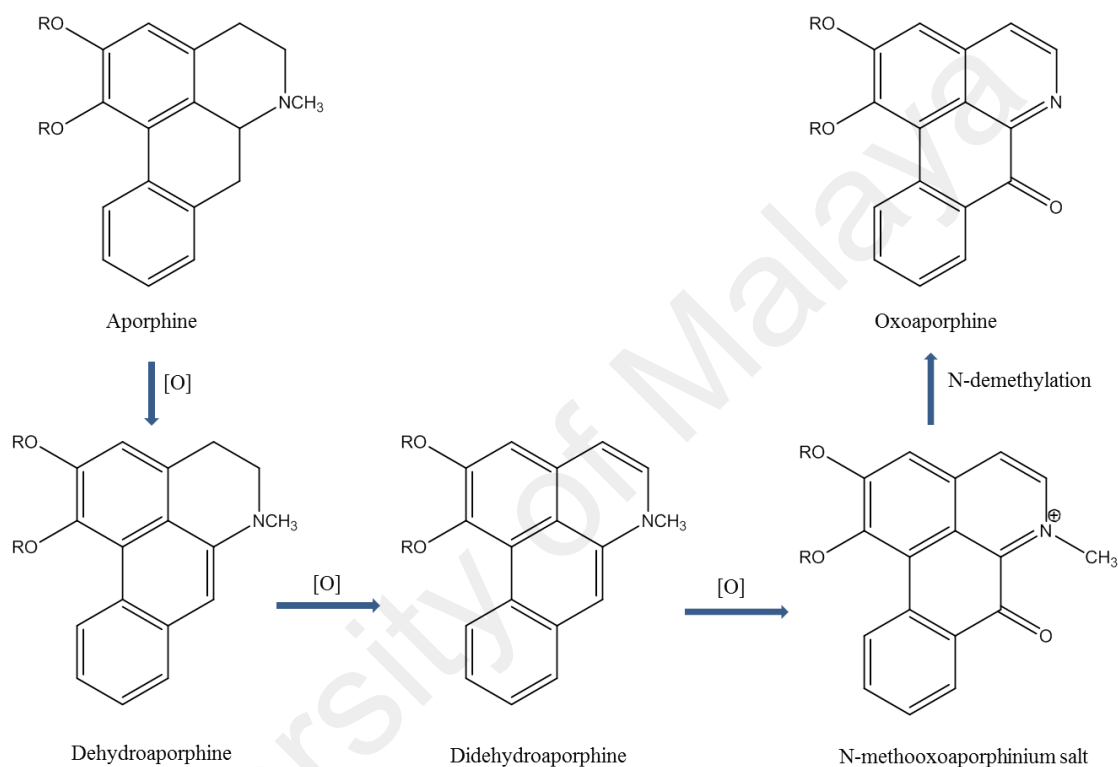


Fig. 2.5: Biogenetic pathway of oxoaporphine

2.4.6 Phenanthrene alkaloids

Phenanthrene alkaloids are widely distributed in Annonaceae, Menispermaceae, Ranunculaceae, Fumariaceae, Lauraceae and Aristolochiaceae families and normally found closely together with aporphine alkaloids because they are biogenetically related (Estevez *et al.*, 1990). The skeleton structure of phenanthrene alkaloids is indicated by an opening in ring B (Figure 2.6) and it does not have a nitrogen heterocycle.

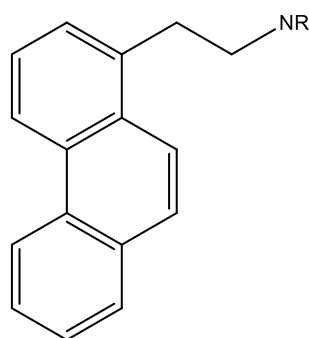


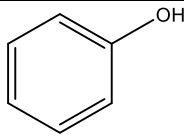
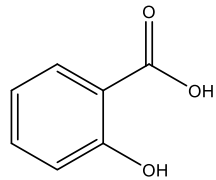
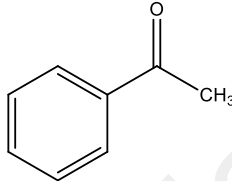
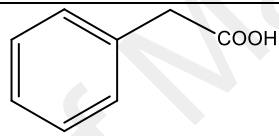
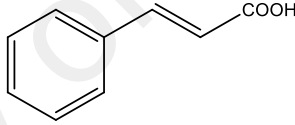
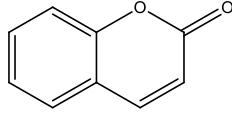
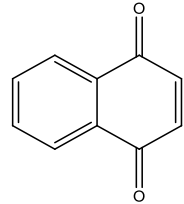
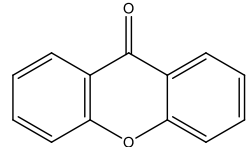
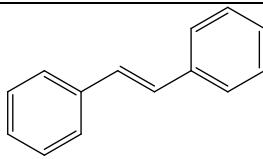
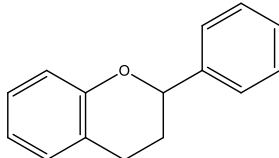
Fig. 2.6: Basic skeleton of phenanthrene alkaloid.

2.5 Phenolic compounds

Phenolic compounds are secondary plant metabolites widely distributed among all classes of plants which are produced as part of the defense mechanism against pathogens. They are important in the growth and reproduction of plants. Phenolic compounds include simple phenols, phenolic acids, flavonoids, coumarins, benzoic and cinnamic acids and etc. More than 8,000 phenolic compounds were identified from various plant species with significant biological activities such as antidiabetic, anti cancer, antioxidant, anti-Alzheimer and etc (Pandey & Rizvi, 2009).

In general, phenolic compounds have one or more hydroxyl groups attached to the aromatic ring and can be classified into two groups; simple phenolic compounds and polyphenolic compounds, according to the number and arrangement of the carbon atoms (Crozier *et al.*, 2009). Table 2.3 illustrates the general classification of phenolic compounds.

Table 2.3: General classification of phenolic compounds

Skeleton	Classification	Basic structure	Examples
C6	Phenol		Pyrogallol, hydroquinone
C6-C1	Hydroxybenzoic acids		Gallic, salicylic
C6-C2	Acetophenones		2-Hydroxyacetophenone
C6-C2	Phenylacetic acid		p-Hydroxyphenylacetic
C6-C3	Hydrocinnamic acids		Caffeic acid, ferulic acid
C6-C3	Coumarins		Umbelliferone, aesculetin
C6-C4	Naphthoquinones		Juglone, plumbagin
C6-C1-C6	Xanthones		Mangiferin
C6-C2-C6	Stilbenes		Resveratrol
C6-C3-C6	Flavanoids		Quercetin, cyanidin

The term 'phenolic acids' in general, describes phenols that contain one carboxylic acid group. They are also known as hydroxybenzoates. They exist in most plants as secondary metabolites particularly in dried fruits and they play a significant role as antioxidants most importantly due their ability to reduce oxidative stress in chronic diseases. Phenolic acids comprise of two distinctive carbon frameworks: the hydroxycinnamic and hydroxybenzoic structures. The numbers and positions of the hydroxyl groups on the aromatic ring make the difference, although the basic skeleton remains the same. Caffeic, p-coumaric, vanillic, and ferulic acids are among the naturally occurring phenolic acids present in nearly all plants.

2.6 Benzopyran

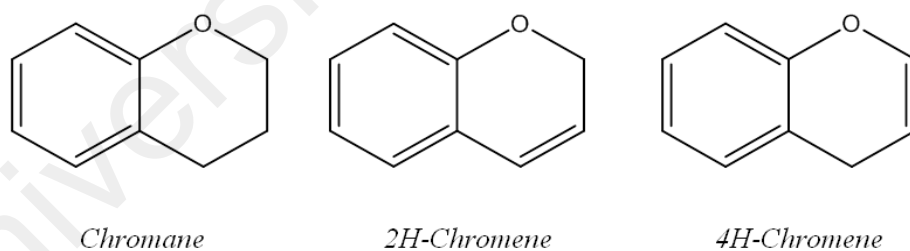


Fig. 2.7: Basic structures of benzopyran

Bioactive compounds with benzopyran structures as the basic backbone have been frequently isolated from the natural resources and reported in the literature for their broad spectrum of pharmacological activities such as anti cancer, antitumor, anti oxidant,

antifungal, anti bacterial, anti-HIV, TNF- α inhibitor, anti-inflammatory, anticonvulsant and many others (Keri *et al.*, 2014).

Benzopyran was also known as chromene according to IUPAC nomenclature. Benzopyrans derived from the combination of a pyran ring and a benzene ring in a heterocyclic ring system.

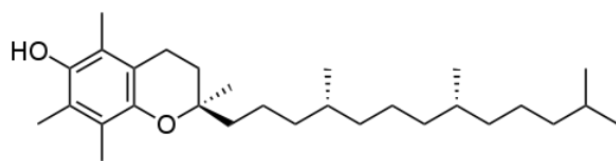
The basic general structures of benzopyrans are shown in Figure 2.7. They are classified into two classes, 1-benzopyran and 2-benzopyran, based on the position of the oxygen atom in the ring.

Chemical compounds such as alkaloids, tocopherols, flavanoids and anthocyanins from natural products with chromane ring have always been a subject of extensive studies due to their remarkable biological activities. Vitamin E is a perfect example for naturally occurring benzopyran derivative with significant antioxidant activity.

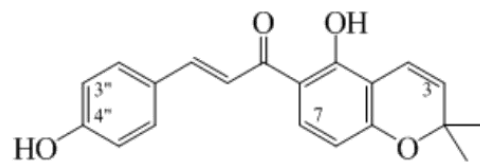
There were more than 4,000 analogs based on benzopyran structures or having benzopyran moieties reported from the natural product literature (Newman *et al.*, 2014). In fact, benzopyran-based structures were among the biologically active heterocyclic scaffolds to be selected as privileged structure for the design and construction of natural and natural product-like libraries due to its wide range of biological activities and its lipophilic nature to penetrate cell membrane (Lee & Gong, 2012; Nicolau *et al.*, 2000). Examples of bioactive compounds with benzopyran backbone are shown in Table 2.4.

Table 2.4: Some examples of bioactive naturally occurring compound with benzopyran backbone

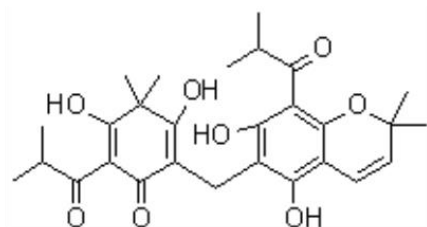
Compounds	Biological activity	Plant sources
Vitamin E (33)	Antioxidant (Fryer, 1992)	In most plants particularly seeds
Polycerasoidol (16)	Antioxidant (Hostettmann & Marston, 2002)	<i>Polyalthia cerasoides</i>
4-Hydroxylonchocarpin (34)	Anticancer (Kuetze <i>et al.</i> , 2011)	<i>Dorstenia</i> genus
Uliginosin B (35)	Antinociceptive, antidepressant (Stein <i>et al.</i> , 2012; Stoltz <i>et al.</i> , 2014).	<i>Hypericum polyanthemum</i>
Suksdorfin (36)	Anti-HIV (Zhao, H <i>et al.</i> , 1997)	<i>Lomatium suksdorfii</i>
Demethoxyencecalin (37) Demethylencecalin (38)	Antimicrobial (Satoh <i>et al.</i> , 1996)	<i>Helianthus annuus</i>



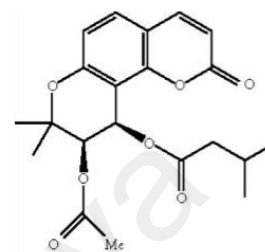
33



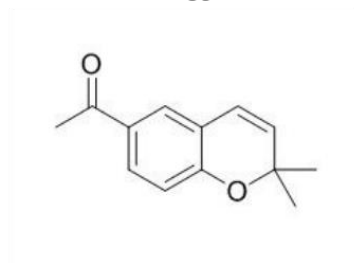
34



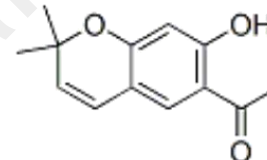
35



36



37



38

2.7 Essential oils

Essential oils are odorous secondary metabolites produced from various parts of the plant. These oils give out distinctive and unique aromas associated with the plant species and their phytochemicals. They are soluble in alcohol and fats, but only slightly soluble in water. They are oxidized when exposed to light and air.

Essential oils are also called volatile oils, since they evaporate when exposed to heat. Usually, the total essential oil content in plants is generally very low (<1 %). Most essential oils consist of complex mixture of chemical compounds and the combination of the compounds and types of functional group usually determine their biological activities (Holley & Patel, 2005).

The composition of the essential oils can differ according to the season, time of day, growing conditions, genetic make-up of the plant and also influenced by the method of extraction (Lahlou, 2004). SFME and solvent-free microwave extraction tend to yield more chemical constituents compared to conventional methods (Lucchesi *et al.*, 2004). Essential oils have been widely used as flavoring agents in foods since ancient time as well as therapeutic agents and have displayed variety of biological activities such as antifungal, antioxidant and antimicrobial (Bakkali *et al.*, 2008).

For example, essential oils from the aromatic basil leaves are often used in foods and commercial products, and traditionally used as a medicinal plant in treating various symptoms, and have been scientifically proven as natural antioxidants (Lee *et al.*, 2005). Essential oils from rosemary extract *Rosmarinus officinalis* L. demonstrated the highest antimicrobial activity against *S. aureus* (Santoyo *et al.*, 2005).

CHAPTER 3: EXPERIMENTAL

3.1 General Experimental and Instrumentation

3.1.1 Solvents

All solvents used such as hexane, dichloromethane and methanol for extraction, column separation and fractionation are of analytical grade (AR). Solvents such as acetonitrile, methanol and water were of HPLC and LC-MS grade for HPLC and LC-TOFMS analysis. Hexane and ethyl acetate solvent for GC-MS analysis were of GC grade.

3.1.2 Ultra Violet Spectra (UV)

Ultra violet spectra were obtained in methanol on a Shimadzu UV-250 uv-visible spectrophotometer and the wavelength which the spectrum was recorded is 190-500nm.

3.1.3 Infrared Spectra (IR)

The infrared spectra were recorded on a Perkin Elmer FTIR (model 1600) spectrophotometer. Solvent used for dilution the sample is CHCl_3 .

3.1.4 Optical Rotation (OR)

The optical rotation was obtained on Jasco DIP-1000 Digital polarimeter with tungsten lamp at 25°C.

3.1.5 NMR Spectra

NMR spectra and data analysis were obtained using JEOL FT NMR, JEOL ECA 500 MHz and Bruker 400 and 600 MHz with deuterated chloroform (CDCl_3), deuterated methanol (CD_3OD) and deuterated acetone ($\text{C}_3\text{D}_6\text{O}$) used as solvents. Chemical shifts were reported in ppm and coupling constants were measured in Hertz (Hz).

3.1.6 Column Chromatography (CC)

Separation and fractionation of the crude extracts were conducted using chromatographic columns packed with Silica Gel 60F (230-400 mesh) Merck 9385 with ratio 30:1 for the crude samples.

3.1.7 Thin Layer Chromatography (TLC)

Aluminium supported silica gel 60 F254 TLC sheets were used to monitor the separated compounds in each fraction after column chromatography. The compounds were visualized under UV light (254 nm and 365 nm).

3.1.8 High Performance Liquid Chromatography (HPLC)

HPLC analysis of the methanol extract were performed by preparative reverse phase HPLC using Waters Nova-Pak C18 column (25 x 100 mm, particle size 6 μ m) using acetonitrile and water with 0.1% formic acid as the eluents.

HPLC chromatograms were monitored at 250-400 nm. HPLC fractionation of the methanol fraction (sample concentration is 500 mg/mL) was conducted on a 150 x 3.9 mm i.d Nova Pak C18 RP (Waters) prep column, using solvent A (Acetonitrile in 0.1% FA) and solvent B (Water in 0.1% FA), with a gradient flow of 10% to 100% acetonitrile in 90 minutes at a flow rate of 12 mL/min.

All samples were first centrifuged to remove any sediment and filtered with 0.45 μ m nylon membrane filter (Phenomenex) before injecting 2 mL of methanol fraction into preparative HPLC. Collected fractions were dried using speed vacuum concentrator at 40°C (miVac Quattro concentrator).

3.1.9 Mass Spectra (MS)

Mass spectra were analyzed on liquid chromatography mass spectrometry (LC-MSQTOF, AB Sciex Triple TOF 4600) coupled to UHPLC system (Symbiosis Pico, Holland) with Waters X- Bridge RP C-18 column (2.1 mm id x 50 mm, particle size 2.5 μ m). The complete scans of the mass spectra were recorded from 50 m/z to 1000 m/z. The data was processed by Analyst Software (v1.5.1).

3.1.10 GC-TOFMS Analysis

Gas chromatography time of flight mass spectrometry (GC-TOFMS) analysis of the crude extract was carried out on a Pegasus HT GC-TOFMS 7890A (LECO, USA) system. Separation was conducted on an RXI-5 MS column (30 m \times 0.32 mm \times 0.25 μ m), with helium as the carrier gas (flow rate of 1.0 mL/min). The injection volume was 1 μ L in a split mode (10:1).

The column temperature was initially held at 40°C for 5 minutes and then increased to 260°C at a rate of 10°C/min, then maintained at 260°C for 10 minutes. The temperatures of the injector and detector were 250°C and 280°C, respectively.

Mass acquisition was performed in the range of 40–550 atomic mass units (a. m. u) using electron impact ionization at 70 eV. The chemical constituents in the sample were identified by a spectral database matching against the library of National Institute of Standards and Technology (NIST21 and NIST Wiley) and Adam's library.

3.2 Reagents

Mayer's and Dragendorff's reagents were used to detect the presence of alkaloids and heterocyclic nitrogen compounds.

a. Mayer's reagent (Potassium mercury iodide)

A solution of mercury (II) chloride (1.4g) in distilled water (60 mL) was mixed into a solution of potassium iodide (5.0g) in distilled water (10 mL). The mixture was then made up to 150 mL with distilled water. The level of alkaloid content is indicated by the formation of white precipitate as indicated by Table 3.1 below;

Table 3.1: Mayer's test indicator on alkaloid content

Observation	Indicator	<i>P. monticola</i>	<i>P. macrophylla</i>
No reaction or clear	- (Not present)		
Weak precipitate	+ or ++ (Low to medium)	++ (medium)	++ (medium)
White precipitate	+++ (High)		
Strong and deep precipitate	++++ (Very high)		

b. Dragendorff's reagent (Potassium bismuth iodide)

(Solution A)- Bismuth (III) nitrate (0.85 g) in a mixture of glacial acid (10mL) and distilled water (40 mL).

(Solution B)- Potassium iodide (8.0 g) in distilled water (20 mL)

Stock solution: A mixture of equal volumes of solution A and solution B. The stock solution (20 mL) was diluted in a mixture of acetic acid (20 mL) and distilled water (60 mL).

Test: Positive result is indicated by the formation of orange or yellow spots.

3.3 Extraction of leaf essential oil

The essential oil from the leaves of the two plant species was extracted through hydrodistillation method using the Clevenger's apparatus (Figure 3.1) (Wang & Yang, 2009). This is the most common procedure of extracting essential oils. Approximately about 100 g of the leaves is boiled in 250 mL distilled water in a Clevenger's apparatus for 8 hours. The essential oils were collected and dried over anhydrous Na_2SO_4 and kept in the freezer in capped vials. The essential oils are then subjected to GC-MSTOF analysis and tested for antioxidant activity.

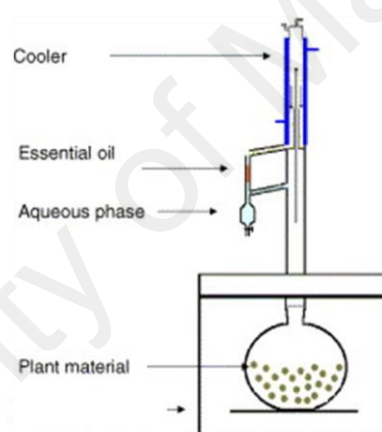


Fig. 3.1: Clavenger's Apparatus

% Yield determination

The percentage yield was calculated based on the dried weight of plant sample

$$\frac{\text{Oil collected (g)}}{\text{Weight of dry sample (g)}} \times 100\% = \% \text{ yield}$$

Table 3.2: % Yield of leaf essential oils of *P.monticola* and *P.macrophylla*

Leaf samples	% Yield of leaf essential oil
<i>Pseuduvaria monticola</i>	0.40 %
<i>Pseuduvaria macrophylla</i>	0.25 %

3.4 Plant Material

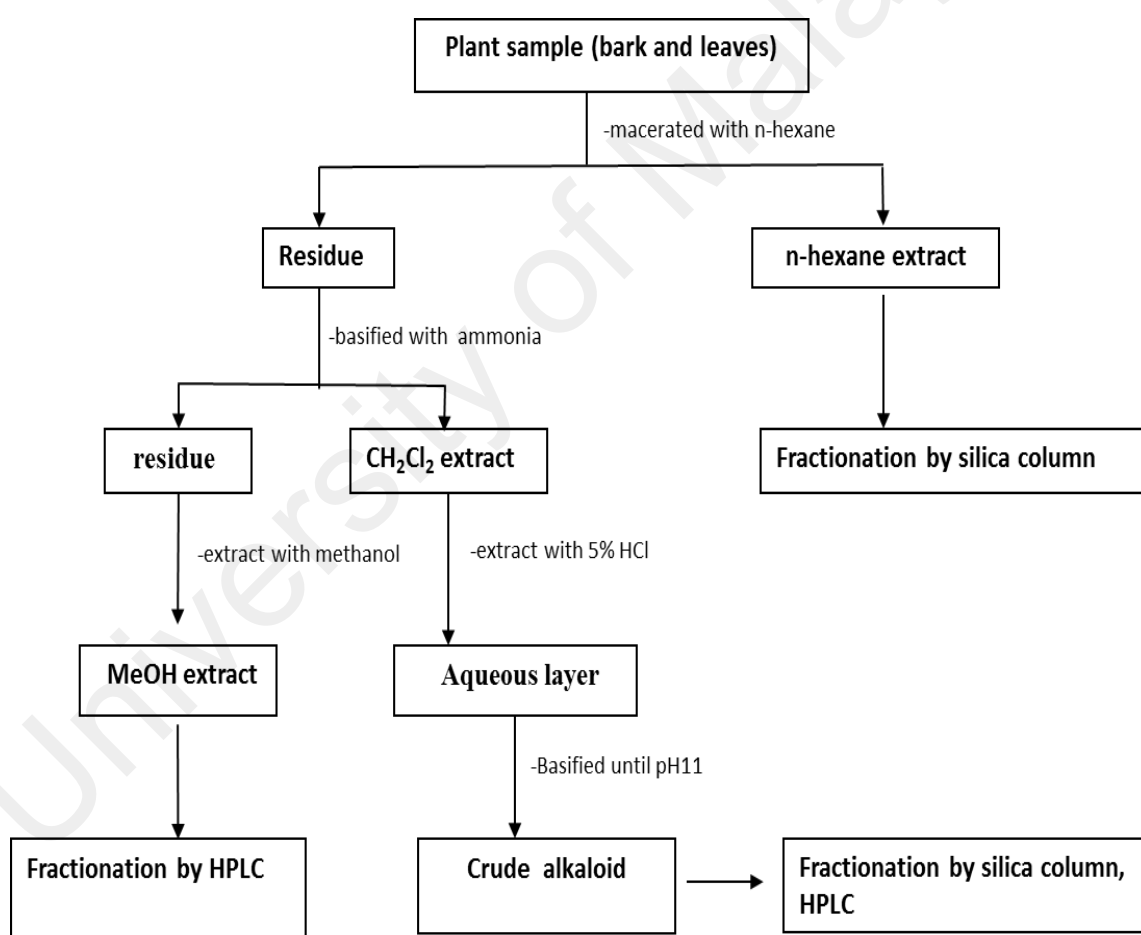
- I. *Pseuduvaria monticola* was collected from the national park located at Cameron Highland Montane forest, Pahang, Malaysia in October, 2011. The plant was botanically identified and classified by the phytochemical group of the Department of Chemistry, Faculty of Science, University of Malaya. Voucher specimen (**HIR 0009**) was deposited at the herbarium, Chemistry Department of the University of Malaya.

- II. *Pseuduvaria macrophylla* was collected from the Jerantut Forest Park, Jerantut, Pahang, Malaysia in March 1986. The plant identified by L.E. Teo (Herbarium group of Phytolab) from the Department of Chemistry, University of Malaya. A voucher specimen (**KL 3886**) was deposited at the herbarium, Chemistry Department, University of Malaya.

Note: At the time of the collection, fresh sample of *P.macrophylla* could not be obtained due to its scarcity and the late supervisor decided to use the specimen from the herbarium in order to compare the two species claimed to share the same phylogeny.

3.5 Extraction and isolation

The plant extraction was carried out by cold percolation, starting with n-hexane to obtain hexane extract, then dichloromethane followed by acid base extraction to retrieve alkaloid compounds and finally with methanol to extract the polar compounds (Scheme 3.1). Table 3.3 tabulates the final yields of the crude extracts from the bark and leaves of *Pseuduvaria monticola* and *Pseuduvaria macrophylla*.



Scheme 3.1: Fractionation of crude extracts from the plant sample

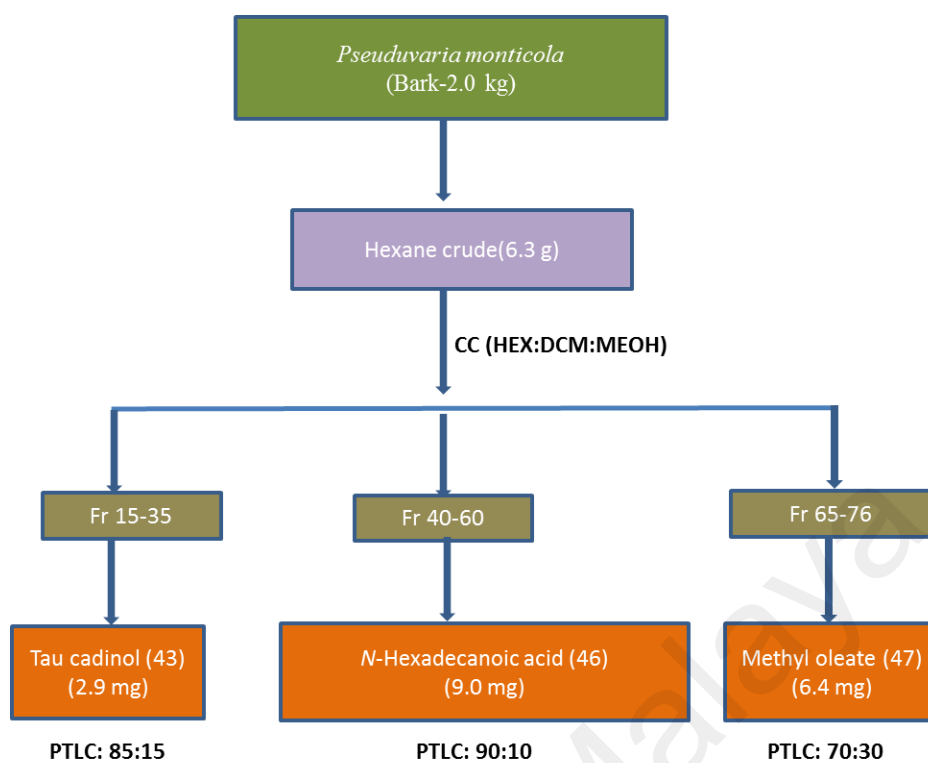
Table 3.3: Yield of crude extracts from *Pseuduvaria monticola* and *Pseuduvaria macrophylla*

Species	Part of plant	Weight of crudes (g)		% yield
<i>Pseuduvaria monticola</i> (HIR 0009)	Leaves (1.8 kg)	n-hexane	5.9	0.32
		alkaloid	4.3	0.24
	Bark (2.0 kg)	n-hexane	6.3	0.32
		alkaloid	5.3	0.27
		methanol	12.0	0.60
<i>Pseuduvaria macrophylla</i> (KL 3886)	Leaves (1.8 kg)	n-hexane	5.7	0.32
		alkaloid	4.5	0.25
	Bark (2.0 kg)	n-hexane	6.0	0.30
		alkaloid	5.6	0.28
		methanol	11.5	0.58

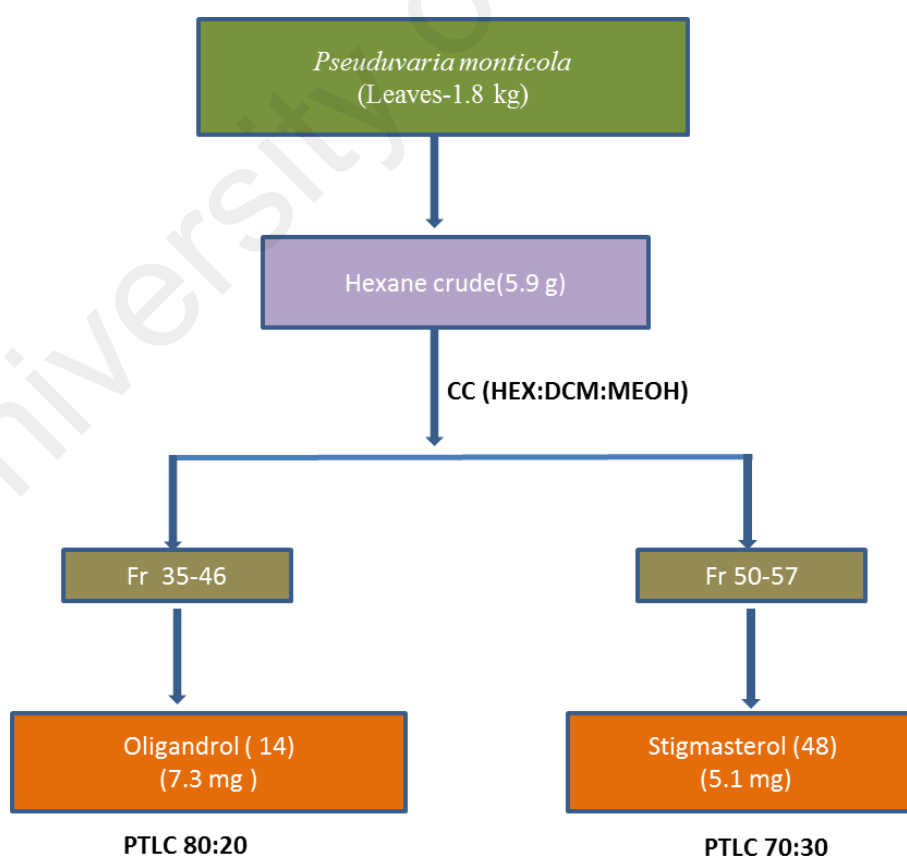
3.5.1 Hexane extract

The leaves and barks were first defatted in n-hexane for 48 hours. Then the extract was dried on the rotary evaporator to yield hexane extract which was subjected to a silica gel column chromatography (230-400 mesh) using solvents (n-hexane/DCM/MeOH) in increasing polarity for the separation of compounds.

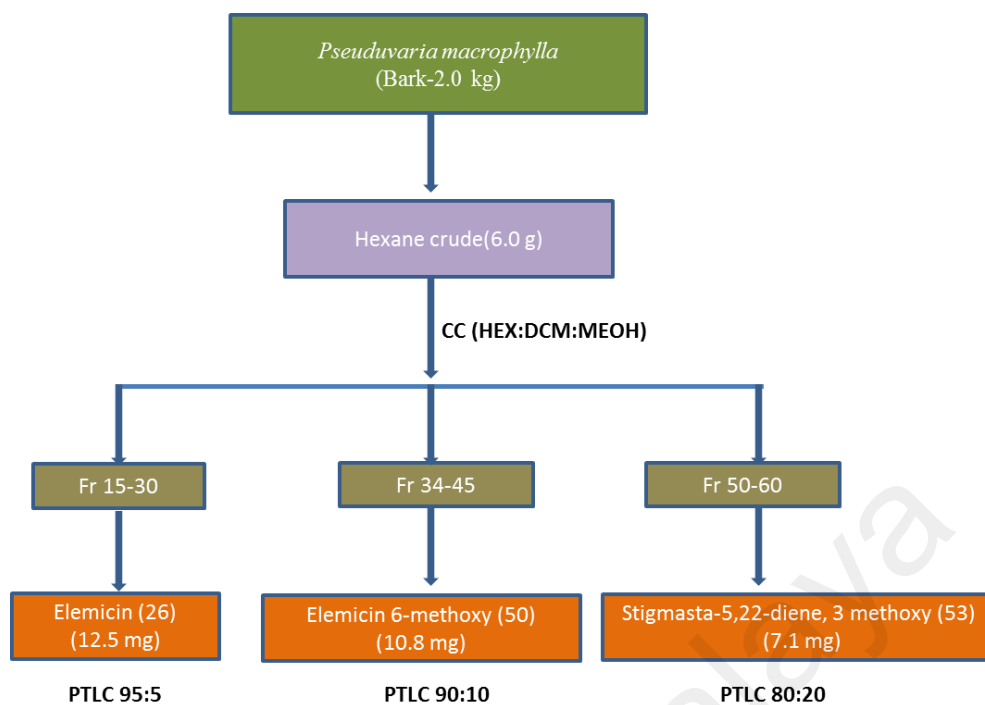
Each fraction collected (200 mL) was monitored by TLC and pooled together for similar fractions, and further purified by PTLC using n-hexane/dichloromethane as the solvent system. The isolation and purification processes are shown in Scheme 3.2 and 3.3 for *Pseuduvaria monticola* and Scheme 3.4 and 3.5 for *Pseuduvaria macrophylla*, respectively.



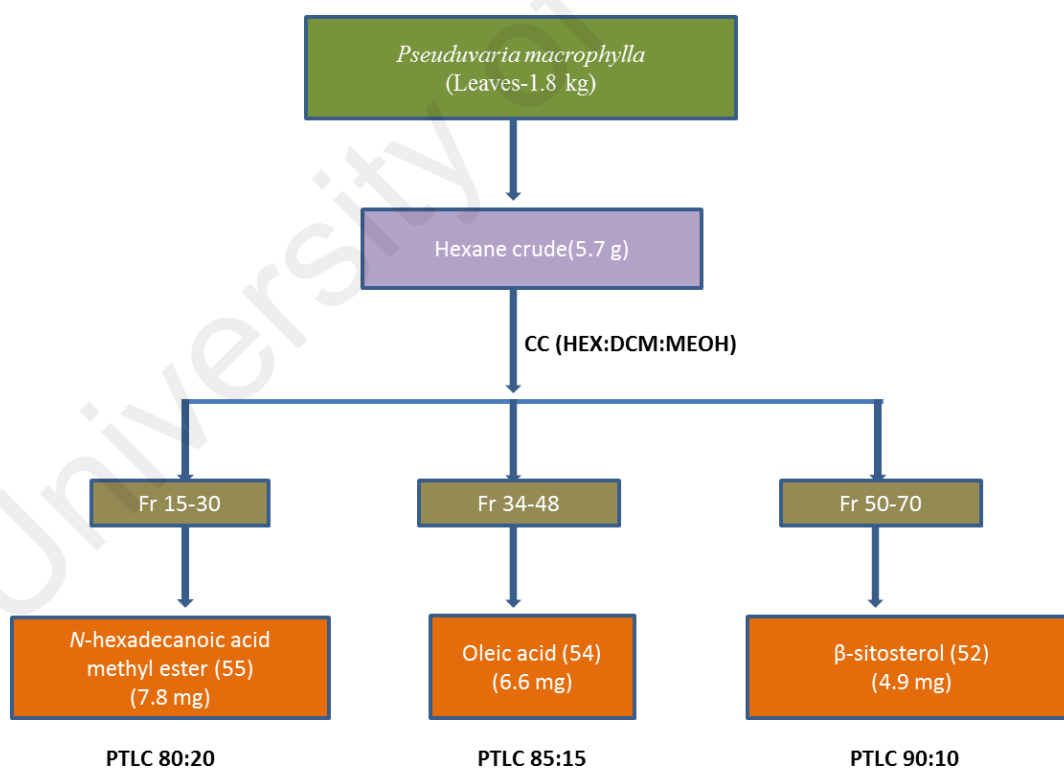
Scheme 3.2: Isolation of the compounds from the hexane bark extract of *P. monticola*



Scheme 3.3: Isolation of the compounds from the hexane leaf extract of *P. monticola*



Scheme 3.4: Isolation of the compounds from the hexane bark extract of *P. macrophylla*



Scheme 3.5: Isolation of the compounds from the the hexane leave extract of *P. macrophylla*

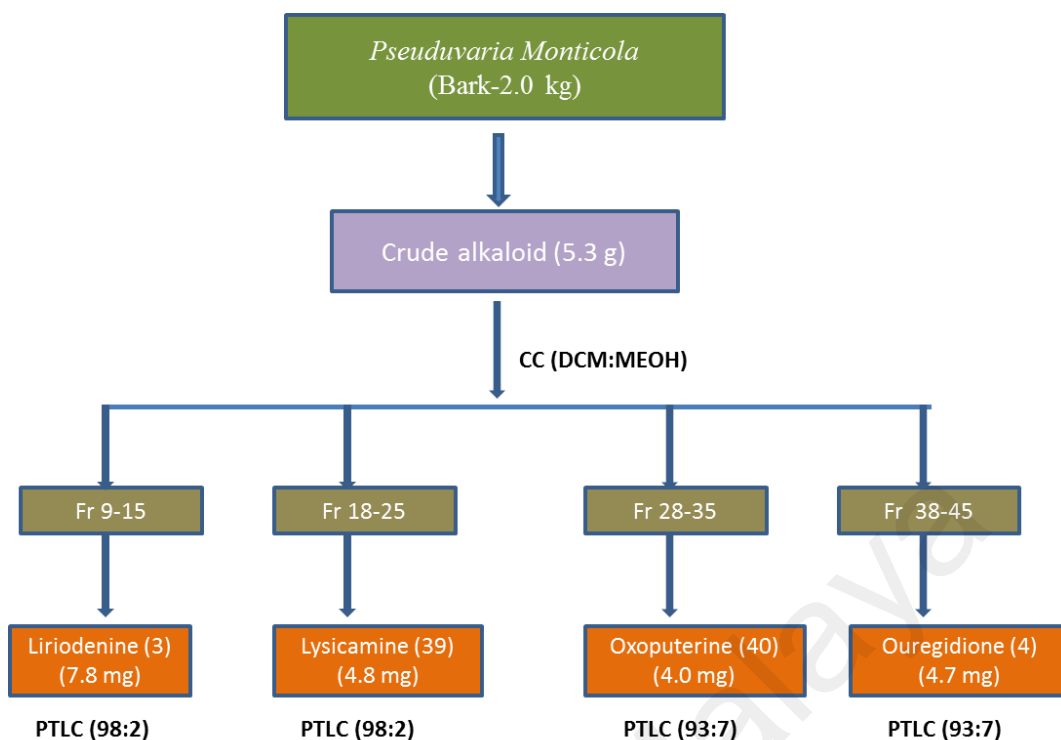
3.5.2 Acid base extraction of alkaloids

The plant residue was left to dry and then moistened with 10% of ammonia solution (NH_4OH) and soaked overnight to release the nitrogen-containing compounds from their salt forms. Then the sample was re-extracted successively with dichloromethane (CH_2Cl_2). The dichloromethane crude extract was dissolved in CH_2Cl_2 and re-extracted with 5% hydrochloric acid (HCl) until a negative Mayer test result was obtained.

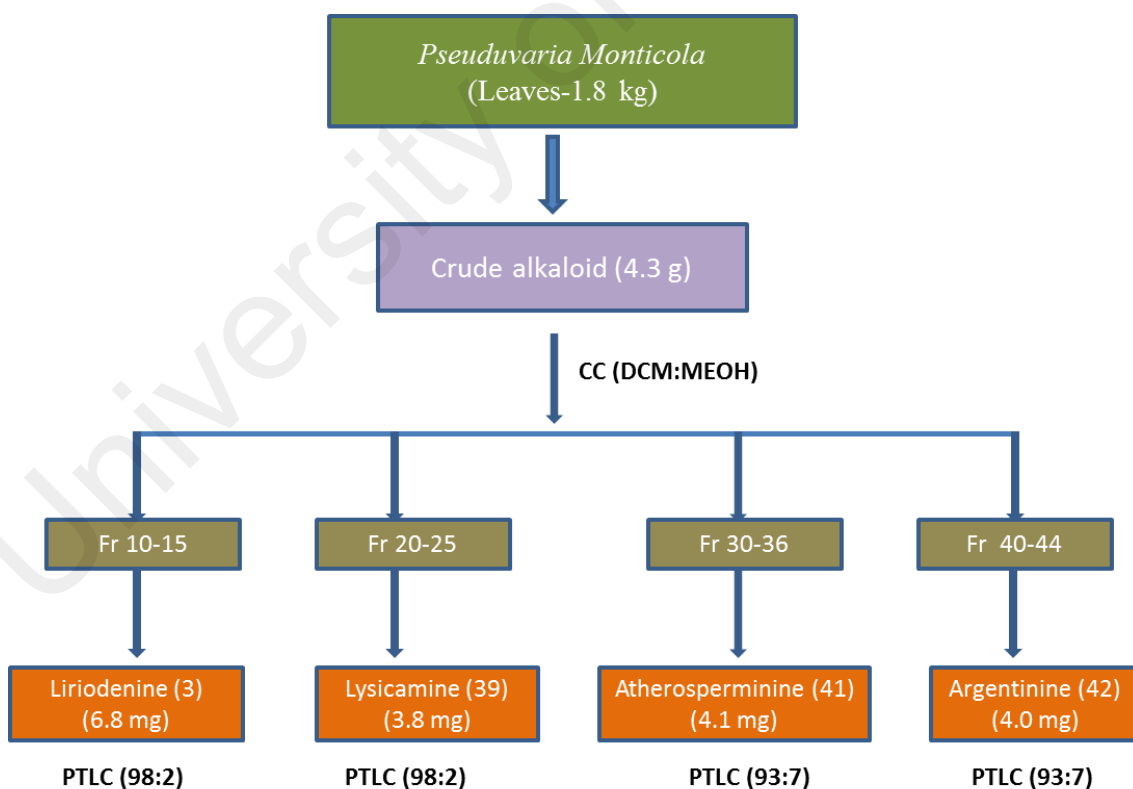
The extract was then basified with 25% NH_3 solution until pH indicator reach 11 and again re-extracted with CH_2Cl_2 until Mayer test showed negative. The CH_2Cl_2 extract was filtered, evaporated and dried with sodium sulfate anhydrous to yield crude alkaloid extract. The remnant of the residues were soaked with MeOH (90%) for 3 days, followed by extraction and evaporation to yield crude methanol extract. The overall extraction procedure was shown in Scheme 3.1.

3.5.3 Isolation of the alkaloids

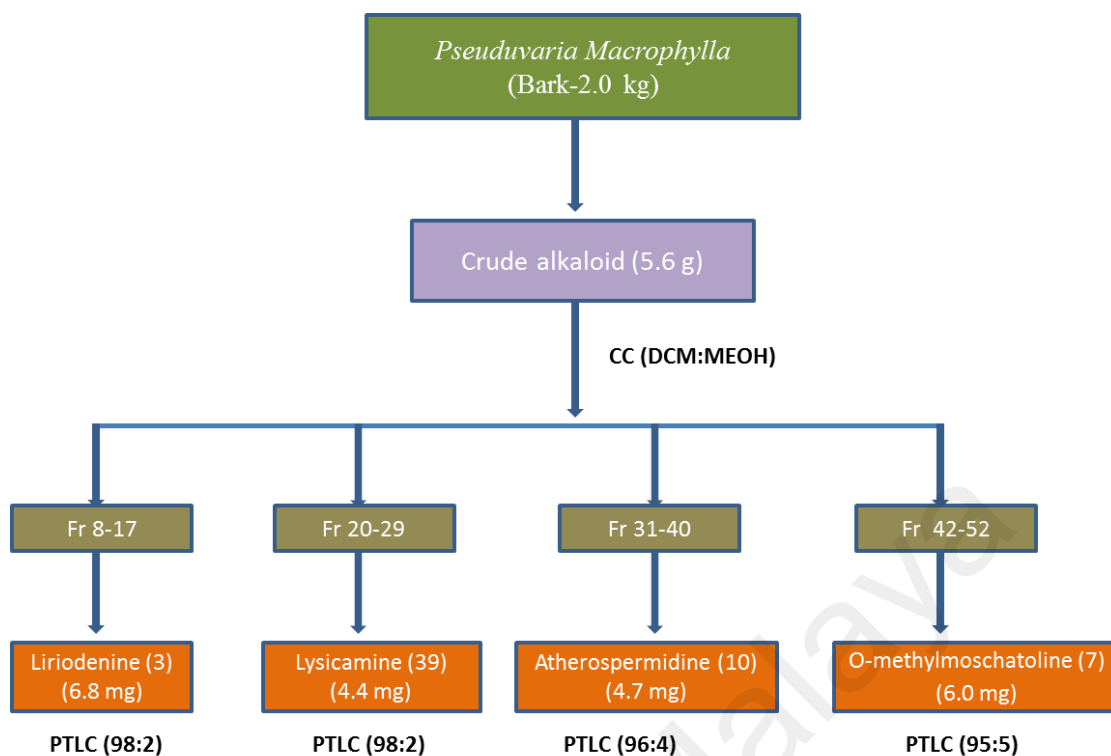
The crude alkaloid extract was introduced to column chromatography over a column of silica gel using dichloromethane/methanol as a solvent system with ratio 100:0-0:100. The ratio of the solvents were (100:0, 99:1; 98:2, 96:4, 93:7, 90:10, 85:15, 80:10 and 50:50). Each fraction collected was then monitored by TLC and visualized under the UV light at wavelength 254 nm and 366 nm. Fractions with similar TLC profiles were combined for further chromatographic analysis. The spots on TLC sheets were sprayed with Dragendorff's reagent to detect and confirm the presence of alkaloids. The alkaloids were isolated by extensive column chromatography and purified by PTLC with a solvent system of $\text{CH}_2\text{Cl}_2/\text{MeOH}$. The isolation and purification procedure were summarized in the flow diagram shown in Scheme 3.6 and 3.7 for *P. monticola* and Scheme 3.8 and 3.9 for *P. macrophylla*.



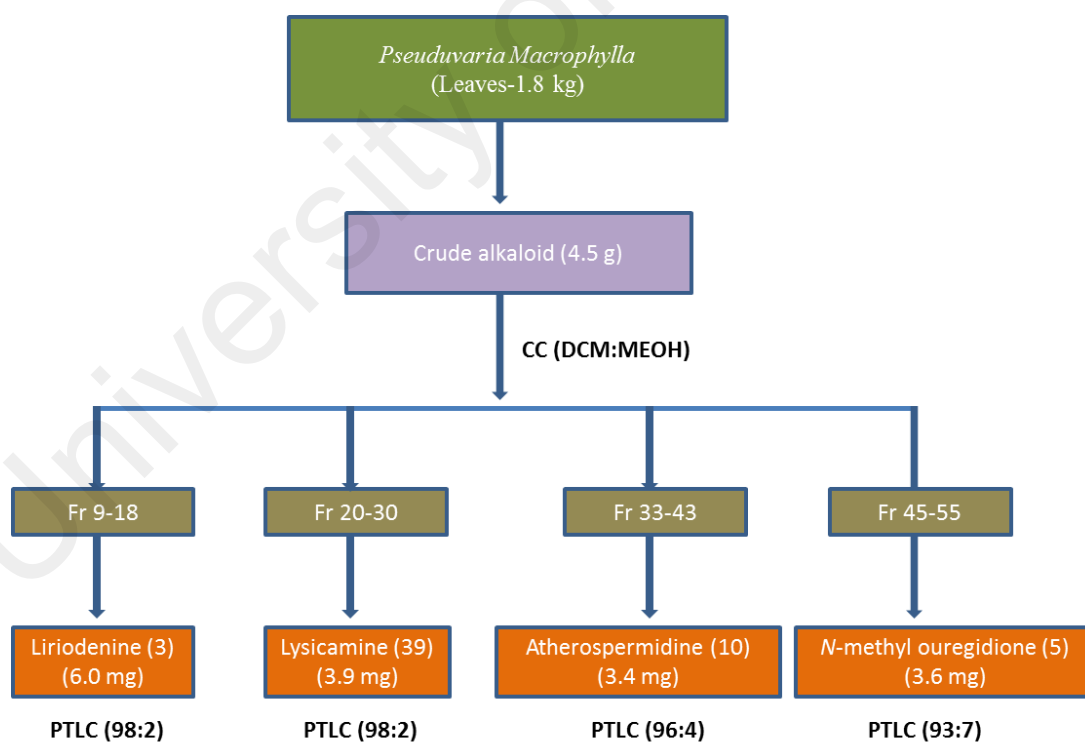
Scheme 3.6: Isolation of the alkaloids from the bark of *P. monticola*.



Scheme 3.7: Isolation of the alkaloids from the leaves of *P. monticola*.



Scheme 3.8: Isolation of the alkaloids from the bark of *P. macrophylla*.

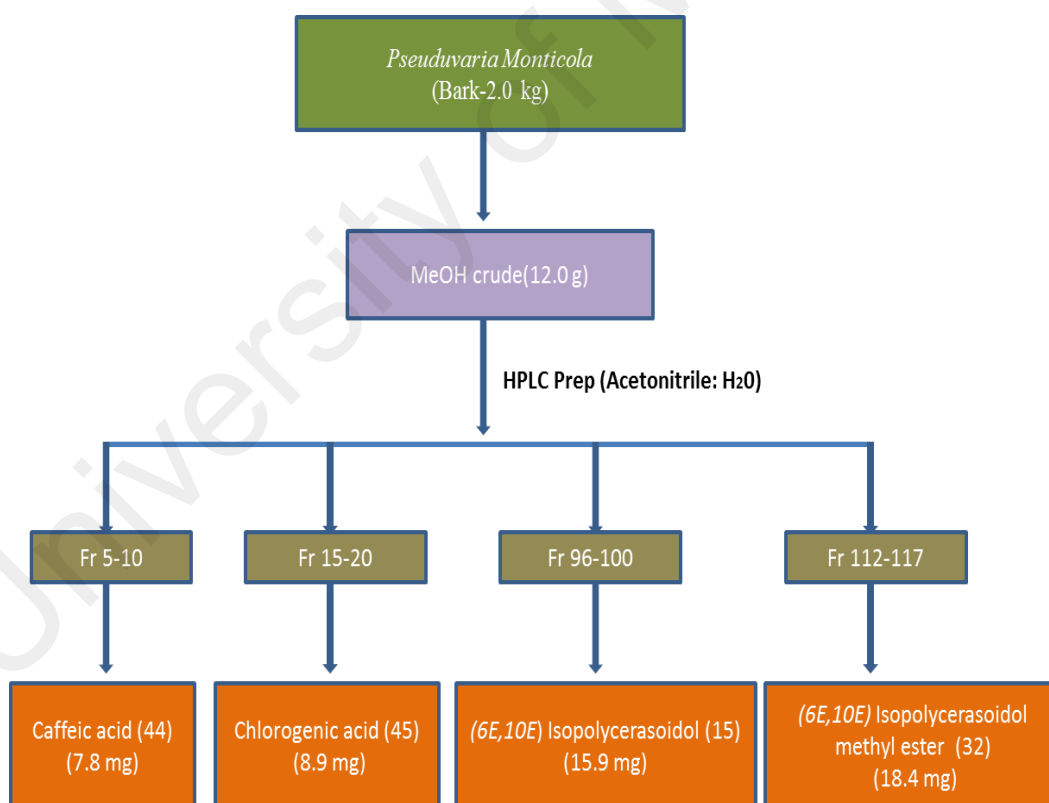


Scheme 3.9: Isolation of the alkaloids from the leaves of *P. macrophylla*.

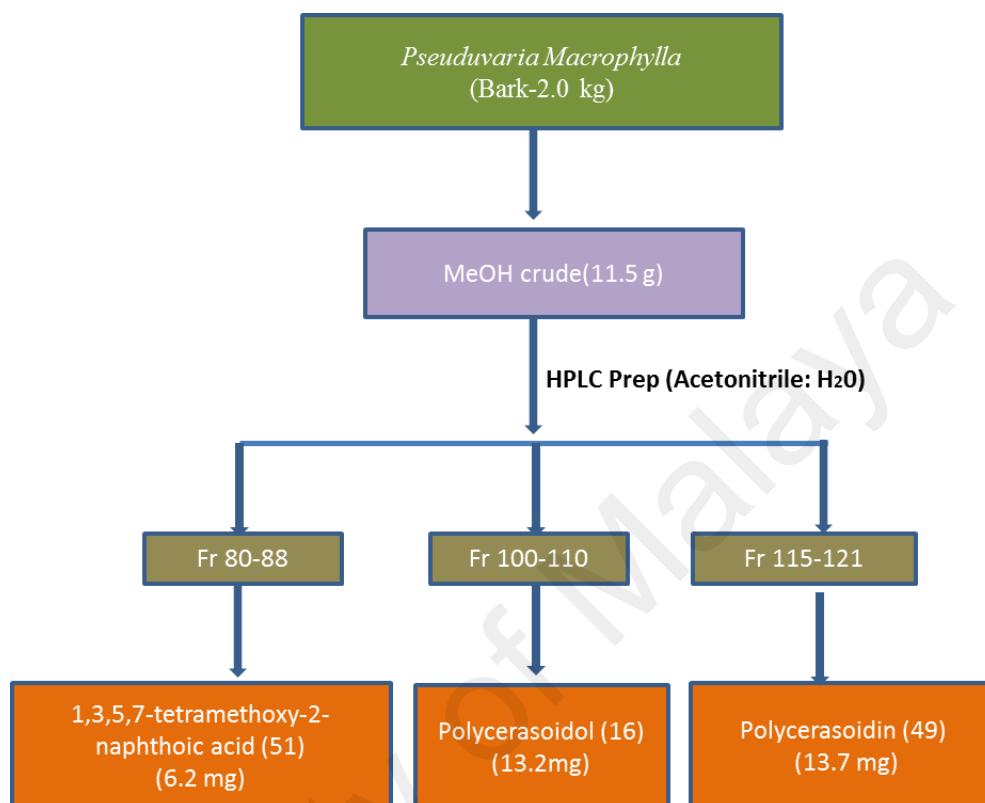
3.5.4 Isolation of Compounds from methanol extract

The methanol extract (2 mL) was first filtered and centrifuged to remove any sediment prior to HPLC preparative analysis. Fractions of isolated compounds from the peaks detected by UV at 250 and 350 nm were collected in tubes (10 mL) and dried in a centrifugal evaporator. Then each tube was carefully analyzed by TLC and pooled together to get pure compounds (Scheme 3.10 and 3.11).

The yield of pure compounds isolated from *P. monticola* and *P. macrophylla* are shown in Tables 3.4 and 3.5.



Scheme 3.10: Isolation of the polar compounds from the bark of *P. monticola*.



Scheme 3.11: Isolation of the polar compounds from the bark of *P. macrophylla*.

Table 3.4: Yield of isolated compounds isolated from *Pseuduvaria monticola*

No	Compounds	Yield (mg)	% Yield
1	Liriodenine (3)		
	Bark	7.8	0.15
	Leave	6.8	0.16
2	Lysicamine (39)		
	Bark	4.8	0.10
	Leave	3.8	0.09
3	Oxoputerine (40)	4.0	0.08
4	Ouregidione (4)	4.7	0.09
5	Atherosperminine (41)	4.1	0.10
6	Argentinine (42)	4.0	0.09
7	Tau cadinol (43)	2.9	0.05
8	Oligandrol (14)	7.3	0.12
9	(6 <i>E</i> ,10 <i>E</i>) isopolycerasoidol (15)	15.9	0.13
10	(6 <i>E</i> ,10 <i>E</i>)isopolycerasoidol methyl ester (32)	18.4	0.15
11	Caffeic acid (44)	7.8	0.07
12	Chlorogenic acid (45)	8.9	0.07
13	<i>N</i> -hexadecanoic acid (46)	9.0	0.14
14	Methyl oleate (47)	6.4	0.10
15	Stigmasterol (48)	5.1	0.09

Table 3.5: Yield of isolated compounds isolated from *Pseuduvaria macrophylla*

No	Compounds	Yield (mg)	% Yield
1	Liriodenine (3)		
	Bark	6.8	0.12
	Leave	6.0	0.13
2	Lysicamine (39)		
	Bark	4.4	0.08
	Leave	3.9	0.08
3	Atherospermidine (10)		
	Bark	4.7	0.08
	Leave	3.4	0.08
4	<i>N</i> -methyl ouregidione (5)	3.6	0.08
5	O-methylmoschatoline (7)	6.0	0.11
6	Polycerasoidol (16)	13.2	0.12
7	Polycerasoidin (49)	13.7	0.12
8	Elemicin (26)	12.5	0.21
9	Elemicin 6-methoxy (50)	10.8	0.18
10	1,3,5,7-tetramethoxy-2-naphthoic acid (51)	0.05	
11	β -sitosterol (52)	4.9	0.09
12	Stigmasta-5,22-diene,3 methoxy (53)	7.1	0.12
13	Oleic acid (54)	6.6	0.12
14	<i>N</i> -hexadecanoic acid methyl ester (55)	7.8	0.14

3.6 Physical and Spectral Data of Isolated Compounds from *Pseuduvaria monticola* and *Pseuduvaria macrophylla*.

Liriodenine (3)	: yellow needles
Molecular formula	: C ₁₇ H ₉ NO ₃
UV λ_{\max} (MeOH), nm	: 255, 276, 327, 400
IR ν_{\max} (CHCl ₃), cm ⁻¹	: 1700, 1450, 1360, 1261
Mass spectrum, m/z	: 276 [M + H] ⁺
¹ H NMR (CDCl ₃), ppm	: See Table 4.2
¹³ C NMR (CDCl ₃), ppm	: See Table 4.2

Lysicamine (39)	: yellow amorphous solid
Molecular formula	: C ₁₈ H ₁₃ NO ₃
UV λ_{\max} (MeOH), nm	: 210, 237, 270, 395
IR ν_{\max} (CHCl ₃), cm ⁻¹	: 1668
Mass spectrum, m/z	: 292 [M + H] ⁺
¹ H NMR (CDCl ₃), ppm	: See Table 4.3
¹³ C NMR (CDCl ₃), ppm	: See Table 4.3

Oxoputerine (40)	: yellow amorphous solid
Molecular formula	: C ₁₈ H ₁₁ NO ₄
UV λ_{\max} (MeOH), nm	: 230, 276, 320
IR ν_{\max} (CHCl ₃), cm ⁻¹	: 1665, 1042
Mass spectrum, m/z	: 306 [M + H] ⁺
¹ H NMR (CDCl ₃), ppm	: See Table 4.4
¹³ C NMR (CDCl ₃), ppm	: See Table 4.4

Atherospermidine (10) : yellow amorphous solid
Molecular formula : C₁₈H₁₁NO₄
UV λ_{\max} (MeOH), nm : 312, 383, 440
IR ν_{\max} (CHCl₃), cm⁻¹ : 1737, 1051, 948
Mass spectrum, m/z : 306 [M + H]⁺
¹H NMR (CDCl₃), ppm : See Table 4.17
¹³C NMR (CDCl₃), ppm : See Table 4.17

Atherosperminine (41) : yellow amorphous solid
Molecular formula : C₂₀H₂₃NO₂
UV λ_{\max} (MeOH), nm : 280, 300
IR ν_{\max} (CHCl₃), cm⁻¹ : 2850, 1581
Mass spectrum, m/z : 310 [M + H]⁺
¹H NMR (CDCl₃), ppm : See figure 4.6
¹³C NMR (CDCl₃), ppm : See figure 4.6

Argentinine (42) : brown amorphous solid
Molecular formula : C₁₉H₂₁NO₂
UV λ_{\max} (MeOH), nm : 225, 245
IR ν_{\max} (CHCl₃), cm⁻¹ : 3398
Mass spectrum, m/z : 296[M + H]⁺
¹H NMR (CDCl₃), ppm : See Table 4.7
¹³C NMR (CDCl₃), ppm : See Table 4.7

Ouregidione (4) : orange amorphous solid
Molecular formula : C₁₉H₁₅NO₅
UV λ_{\max} (MeOH), nm : 215, 229, 480
IR ν_{\max} (CHCl₃), cm⁻¹ : 1733, 1667, 1455
Mass spectrum, m/z : 338[M + H]⁺
¹H NMR (CDCl₃), ppm : See Table 4.5
¹³C NMR (CDCl₃), ppm : See Table 4.5

<i>N</i>-methyl ouregidione (5)	: orange amorphous solid
Molecular formula	: C ₂₀ H ₁₂ NO ₅
UV λ_{\max} (MeOH), nm	: 212,242,300
IR ν_{\max} (CHCl ₃), cm ⁻¹	: 1715, 1602
Mass spectrum, m/z	: 352[M + H] ⁺
¹ H NMR (CDCl ₃), ppm	: See Table 4.18
¹³ C NMR (CDCl ₃), ppm	: See Table 4.18

O-methymoschatoline (7)	: yellow amorphous solid
Molecular formula	: C ₁₉ H ₁₅ NO ₄
UV λ_{\max} (MeOH), nm	: 270,316,430
IR ν_{\max} (CHCl ₃), cm ⁻¹	: 1665
Mass spectrum, m/z	: 322 [M + H] ⁺
¹ H NMR (CDCl ₃), ppm	: See Table 4.19
¹³ C NMR (CDCl ₃), ppm	: See Table 4.19

Oligandrol (14)	: yellow oil
Molecular formula	: C ₂₂ H ₃₂ O ₂
UV λ_{\max} (MeOH), nm	: 225,295
IR ν_{\max} (CHCl ₃), cm ⁻¹	: 3475, 1734, 1645
Mass spectrum, m/z	: 329 [M + H] ⁺
¹ H NMR (CDCl ₃), ppm	: See Table 4.8
¹³ C NMR (CDCl ₃), ppm	: See Table 4.8

Polycerasoidin (49)	: yellow oil
Molecular formula	: C ₂₃ H ₃₂ O ₄
UV λ_{\max} (MeOH), nm	: 208,292
IR ν_{\max} (CHCl ₃), cm ⁻¹	: 1689
Mass spectrum, m/z	: 373 [M + H] ⁺
¹ H NMR (CDCl ₃), ppm	: See Table 4.21
¹³ C NMR (CDCl ₃), ppm	: See Table 4.21

Polycerasoidol (16) : yellow oil
Molecular formula : C₂₂H₃₀O₄
UV λ_{max} (MeOH), nm : 230,298
IR ν_{max} (CHCl₃), cm⁻¹ : 3371, 1692
Mass spectrum, m/z : 359 [M + H]⁺
¹H NMR (CDCl₃), ppm : See Table 4.20
¹³C NMR (CDCl₃), ppm : See Table 4.20

(6E,10E) isopolycerasoidol (15) : yellow oil
Molecular formula : C₂₂H₃₀O₄
UV λ_{max} (MeOH), nm : 211,296
IR ν_{max} (CHCl₃), cm⁻¹ : 3357, 1693
Mass spectrum, m/z : 359 [M + H]⁺
¹H NMR (CDCl₃), ppm : See Table 4.9
¹³C NMR (CDCl₃), ppm : See Table 4.9

(6E,10E) isopolycerasoidol methyl ester (32) : yellow oil
Molecular formula : C₂₃H₃₂O₄
UV λ_{max} (MeOH), nm : 211,296
IR ν_{max} (CHCl₃), cm⁻¹ : 3357, 1693
Mass spectrum, m/z : 373[M + H]⁺
¹H NMR (CDCl₃), ppm : See Table 4.10
¹³C NMR (CDCl₃), ppm : See Table 4.10

Caffeic acid (44) : brownish amorphous solid
Molecular formula : C₉H₈O₄
UV λ_{max} (MeOH), nm : 290, 320
IR ν_{max} (CHCl₃), cm⁻¹ : 3430, 1700
Mass spectrum, m/z : 179 [M - H]⁻
¹H NMR (CDCl₃), ppm : See Table 4.11
¹³C NMR (CDCl₃), ppm : See Table 4.11

Chlorogenic acid (45) : light brown amorphous solid
Molecular formula : C₁₆H₁₈O₉
UV λ_{max} (MeOH), nm : 250, 30
IR ν_{max} (CHCl₃), cm⁻¹ : 3395, 1650, 1590
Mass spectrum, m/z : 353[M - H]⁻
¹H NMR (CDCl₃), ppm : See Table 4.12
¹³C NMR (CDCl₃), ppm : See Table 4.12

Elemicin (26) : colorless oil
Molecular formula : C₁₂H₁₆O
UV λ_{max} (MeOH), nm : 265
IR ν_{max} (CHCl₃), cm⁻¹ : 3076, 1636, 1514
Mass spectrum, m/z : 209 [M + H]⁺
¹H NMR (CDCl₃), ppm : See Table 4.23
¹³C NMR (CDCl₃), ppm : See Table 4.23

Elemicin 6-methoxy (50) : colourless oil
Molecular formula : C₁₃H₁₆O₃
UV λ_{max} (MeOH), nm : 278, 239
IR ν_{max} (CHCl₃), cm⁻¹ : 1636, 1592
Mass spectrum, m/z : 238 [M]⁺
¹H NMR (CDCl₃), ppm : See Table 4.23
¹³C NMR (CDCl₃), ppm : See Table 4.23

1,3,5,7-tetramethoxy-2-naphthoic acid (51) : white amorphous solid
Molecular formula : C₁₅H₁₆O₆
UV λ_{max} (MeOH), nm : 250, 300
IR ν_{max} (CHCl₃), cm⁻¹ : 1721
Mass spectrum, m/z : 293[M + H]⁺
¹H NMR (CDCl₃), ppm : See Table 4.24
¹³C NMR (CDCl₃), ppm : See Table 4.24

Tau cadinol (43) : colorless oil
Molecular formula : C₅H₂₆O
UV λ_{\max} (MeOH), nm : 191,200
IR ν_{\max} (CHCl₃), cm⁻¹ : 3368
Mass spectrum, m/z : 222 [M]⁺
¹H NMR (CDCl₃), ppm : not available
¹³C NMR (CDCl₃), ppm : not available

β -Sitosterol (52) : white amorphous solid
Molecular formula : C₂₉H₅₀O
UV λ_{\max} (MeOH), nm : 250 , 300
IR ν_{\max} (CHCl₃), cm⁻¹ : 3400, 1645
Mass spectrum, m/z : 414 [M]⁺
¹H NMR (CDCl₃), ppm : See Table 4.25
¹³C NMR (CDCl₃), ppm : See Table 4.25

Stigmasterol (48) : white amorphous solid
Molecular formula : C₂₉H₄₈O
UV λ_{\max} (MeOH), nm : 250, 300
IR ν_{\max} (CHCl₃), cm⁻¹ : 3400, 1645
Mass spectrum [M]⁺ : 412 [M]⁺
¹H NMR (CDCl₃), ppm : See Table 4.15
¹³C NMR (CDCl₃), ppm : See Table 4.15

Stigmasta-5,22-diene,3 methoxy (53) : white amorphous solid
Molecular formula : C₃₀H₅₀O
UV λ_{\max} (MeOH), nm : 282
IR ν_{\max} (CHCl₃), cm⁻¹ : 1618, 1676
Mass spectrum [M]⁺ : 426 [M]⁺
¹H NMR (CDCl₃), ppm : See Table 4.26
¹³C NMR (CDCl₃), ppm : See Table 4.26

<i>N</i>-hexadecanoic acid (46)	: light yellow oil
Molecular formula	: C ₁₆ H ₃₂ O ₂
UV λ _{max} (MeOH), nm	: 232
IR ν _{max} (CHCl ₃), cm ⁻¹	: 3500, 1702
Mass spectrum [M] ⁺	: 256 [M] ⁺
¹ H NMR (CDCl ₃), ppm	: See Table 4.13
¹³ C NMR (CDCl ₃), ppm	: See Table 4.13

Hexadecanoic acid methyl ester (55)	: yellow oil
Molecular formula	: C ₁₇ H ₃₄ O ₂
UV λ _{max} (MeOH), nm	: 230
IR ν _{max} (CHCl ₃), cm ⁻¹	: 1732, 1661
Mass spectrum [M] ⁺	: 270 [M] ⁺
¹ H NMR (CDCl ₃), ppm	: See Table 4.28
¹³ C NMR (CDCl ₃), ppm	: See Table 4.28

Methyl oleate (47)	: pale yellow oil
Molecular formula	: C ₁₉ H ₃₆ O ₂
UV λ _{max} (MeOH), nm	: nil
IR ν _{max} (CHCl ₃), cm ⁻¹	: 2925, 1730
Mass spectrum [M] ⁺	: 296 [M] ⁺
¹ H NMR (CDCl ₃), ppm	: See Table 4.14
¹³ C NMR (CDCl ₃), ppm	: See Table 4.14

Oleic acid (54)	: pale yellow oil
Molecular formula	: C ₁₈ H ₃₄ O ₂
UV λ _{max} (MeOH), nm	: 280
IR ν _{max} (CHCl ₃), cm ⁻¹	: 3432, 1704
Mass spectrum [M] ⁺	: 264 [M-18] ⁺
¹ H NMR (CDCl ₃), ppm	: See Table 4.27
¹³ C NMR (CDCl ₃), ppm	: See Table 4.27

3.7 Antioxidant activity

3.7.1 DPPH Radical Scavenging Activity

The DPPH radical scavenging assay is commonly used to determine antioxidant activity of extracts or compounds. When treated with substances or samples that are hydrogen atom donors, the DPPH radical is converted into a stable DPPH radical, indicated by a color change from purple to yellow. The DPPH assay was performed according to previously published method with modifications (Arya *et al.*, 2012). Briefly, 1.00 mg/mL of tested compounds in methanol were prepared by dissolving 1.00 mg of compound in 1.00 mL methanol.

The scavenging activity was tested by mixing 1250 μL of 60 μM DPPH solution with 250 μL of each sample at different concentrations (250 $\mu\text{g/mL}$, 125 $\mu\text{g/mL}$, 62.50 $\mu\text{g/mL}$, 31.25 $\mu\text{g/mL}$, 15.63 $\mu\text{g/mL}$, 3.13 $\mu\text{g/mL}$). Quercetin was used as the positive standard reference and methanol as the negative control. After 30 min of incubation, the absorbance at 517 nm was measured with ELISA reader (Sunrise, Switzerland). The percentage of scavenging of DPPH was calculated using the following equation:

$$\% \text{ Inhibition} = [(AB-AA)/AB] \times 100$$

where AB; absorption of blank sample; AA : absorption of tested samples. Tests were carried out in triplicate.

3.7.2 ORAC Assay

The ORAC assay is based upon the inhibition of the peroxy-radical-induced oxidation initiated by thermal decomposition of [2, 2' -azobis (2-amidino-propane) dihydrochloride (AAPH)]. ORAC assay was carried out based on previous procedure with slight modification. Briefly, samples were dissolved with PBS at concentrations of 800 $\mu\text{g/mL}$ and further diluted to 160 $\mu\text{g/mL}$, and serial dilutions for the Trolox standards were prepared accordingly.

ORAC assay was performed in a 96-well black microplate with 25 μL of samples/standard/positive control and 150 μL of fluorescence sodium salt solution, followed by 25 μL of AAPH solution after 45 min incubation at 37 $^{\circ}\text{C}$ (200 μL total well volume). The positive control was quercetin and the negative control was blank solvent/PBS.

Finally, the fluorescence was measured with an excitation wavelength of 485 nm and an emission wavelength of 535 nm using Plate ChameleonTM V Multilabel Counter (Hidex, Turku, Finland). Data were collected every 2 min for a duration of 2 hour. The quantification of the antioxidant activity was based on the calculation of the area under the curve (AUC). The results were expressed as μM of Trolox Equivalents (TE) per 100 $\mu\text{g}/\text{mL}$ of sample.

3.7.3 Statistical analysis

Results were expressed as mean \pm standard deviation (SD) of three separate determinations. Analysis of variance (ANOVA) was performed using Graph Pad Prism 5 software. Statistical significance was defined when $P < 0.05$.

3.8 Cytotoxicity Assay

The anti-proliferative and cytotoxic effects of *Pseuduvaria monticola* methanol extract, and two benzopyran derivatives, isopolycerasoidol (**15**) and isopolycerasoidol methyl ester (**32**) were evaluated on MCF-7 and MDA-MB-231 human breast cancer cells, and human breast normal epithelial cell-line (MCF-10A) using MTT assays. To confirm that isopolycerasoidol (**15**) and isopolycerasoidol methyl ester (**32**) induced apoptosis in MCF-7 and MDA-MB-231 cells, the cells were stained with Annexin V/propidium iodide (PI) and flow cytometry analysis was performed.

3.8.1 Cell culture

Human breast cancer cell-lines; MCF-7 and MDA-MB-231 and MCF-10A, human normal breast epithelial cell-lines were purchased from American Type Culture Collection (ATCC, Manassas, VA). Cells were grown in Dulbecco's Modified Eagle Medium (DMEM, Life Technologies, Inc, Rockville, MD) supplemented with 10% heat-inactivated fetal bovine serum (FBS, Sigma-Aldrich, St. Louis, MO), 1% penicillin and streptomycin. Cells were cultured in tissue culture flasks (Corning, USA) at 37°C in a humidified atmosphere with 5% CO₂. For experimental purposes, cells in exponential growth phase (approximately 70-80% confluency) were used.

3.8.2 MTT cell viability assay

The cytotoxic effect on cancer cells was determined by MTT assay (Mohammadjavad Paydar *et al.*, 2013). 1.0×10^4 cells were seeded into a 96-well plate and incubated overnight at 37 °C in 5% CO₂. After 24 hours, the cells were treated with a two-fold dilution series of six concentrations of PMT, isopolycerasoidol and isopolycerasoidol methyl ester and incubated for a further 72 hours. MTT solution (4,5-dimethylthiazol-2-yl-2,5-diphenyltetrazoliumbromide; 2 mg/ml final concentration) was added and after 2 hours the formazan crystal was dissolved in DMSO. The plate was read at 570 nm in absorbance using Tecan M200 Pro microplate reader (Hidex, Turku, Finland).

The percentage of viable cells was calculated as the ratio of the absorbance of compound-treated cells to the absorbance of DMSO-treated control cells (Looi *et al.*, 2011; Mohammadjavad Paydar *et al.*, 2013). IC₅₀ was defined as the concentration of the extract that cause a 50% percent reduction of the absorbance of treated cells compared to DMSO-treated control cells. The experiments were done in triplicate.

3.8.3 Flow cytometry

Apoptosis-mediated cell death of tumor cell was examined by a double staining method using FITC-labeled Annexin V/PI apoptosis detection kit (BD Bioscience, San Jose, CA) according to the manufacturer's instructions. Briefly, cells were treated for 24 hours and then harvested, washed in cold phosphate-buffered saline (PBS) twice, stained with fluorescein isothiocyanate (FITC)-conjugated Annexin V and PI dyes. The externalization of phosphatidylserine and the permeability to PI were evaluated by FACS Calibur flowcytometer (BD Bioscience, San Jose, CA). Data from 10,000 gated events per sample were collected. Cells in early stages of apoptosis were positively stained using Annexin V, whereas cells in late apoptosis were positively stained with both Annexin V and PI.

3.9 Antidiabetic study

The aim of the study was to evaluate the hypoglycaemic and antidiabetic activities of the bark methanolic extract of *Pseuduvaria monticola* (PMt) using *in vitro* screening models ; cytotoxicity, 2-NBDG glucose uptake , insulin secretion and *in vivo* models ; Type 1 and Type 2 streptozotocin (STZ) induced diabetes in rats to study its mechanism of action.

3.9.1 *In vitro* cell line studies

Cell culture

Mouse pancreatic β -cell line (NIT-1) was purchased from American Type Culture Collection (ATCC, Manassas, VA). Cells were grown in Dulbecco's Modified Eagle Medium (DMEM, Life Technologies, Inc, Rockville, MD) supplemented with 10% heat-inactivated fetal bovine serum (FBS, Sigma-Aldrich, St. Louis, MO), 1% penicillin and streptomycin. Cells were cultured in tissue culture flasks (Corning, USA) and were kept in incubator at 37°C in a humidified atmosphere with 5% CO₂. For experimental

purposes, cells in exponential growth phase (approximately 70-80% confluency) were used.

3.9.2 MTT cell viability assay

The influence of the extract on NIT-1 cells was determined by MTT assay, 48 h after treatment. On the first day, 1.0×10^4 cells were seeded into a 96-well plate and the plate was incubated overnight at 37 °C in 5% CO₂. The cells were treated with a two-fold dilution series of six concentrations of the methanolic extract of *P. monticola* bark on the next day, and they were incubated at 37 °C in 5% CO₂ for 48 h. MTT solution (4,5-dimethylthiazol-2-yl-2,5-diphenyltetrazoliumbromide) was then added at 2 mg/mL and after 2 hours of incubation at 37 °C in 5% CO₂, the formazan crystals were dissolved in DMSO (Mohammadjavad Paydar *et al.*, 2013).

The plate was then read at 570 nm absorbance in Chameleon multitechnology microplate reader (Hidex, Turku, Finland). The viability percentage of the cells was calculated as the ratio of the absorbance of PMt-treated cells to the absorbance of DMSO-treated control cells (Looi CY *et al.*, 2011). IC₅₀ was defined as the concentration of the extract that caused a 50% percent reduction of the absorbance of treated cells compared to DMSO-treated control cells. The experiment was carried out in triplicate.

3.9.3 Real-time cell proliferation

In vitro proliferation of PMt-treated and untreated cells was surveyed using an xCELLigence Real-Time Cellular Analysis (RTCA) system (Roche, Mannheim, Germany). On the first day, 1.0×10^4 cells were seeded in each well of a 16X E-plate background measurement, which was done by adding 100 μ L of the appropriate medium to the wells. The RTCA system monitored the proliferation of cells every 5 min for about 20 hours. During the log growth phase, the cells were treated with different concentrations

(3.125, 6.25, 12.5, 25, 50, 100 and 200 µg/ml) of PMt or left untreated and monitored continuously for another 72 hour.

3.9.4 2-NBDG glucose uptake

The effect of the extract on the uptake of fluorescent hexose 2-NBDG (a glucose analog) by NIT-1 cells was investigated as previously described (Loiza *et al.*, 2003; Arya *et al.*, 2012). In brief, 1.0×10^4 cells were seeded in a 96-well plate and incubated overnight at 37°C in 5% CO₂. The medium was then discarded and the cells were washed twice with phosphate-buffered saline (PBS).

Next, 100 µL of glucose-free DMEM media supplemented with L-glutamine and 15% (v/v) FBS was added to each well and the cells were incubated for 60 min at 37 °C in 5% CO₂. Then the conditioning medium was replaced with basal medium containing 1 mM 2-NBDG (Invitrogen, Carlsbad, CA, USA) in the presence or absence of the extract.

The cells were incubated for 30 min at 37 °C in 5% CO₂ to permit endocytosis of the 2-NBDG, with the selected concentration being the minimum concentration capable of producing an adequate signal-to-noise ratio.

The 2-NBDG containing medium was then removed, the cells washed with PBS, and stained with the nucleic dye Hoechst 33342 for another 30 min. The plates were then evaluated using the ArrayScan High Content Screening (HCS) system (Cellomics Inc., Pittsburgh, PA, USA) and analyzed with Target Activation BioApplication software (Cellomics Inc.).

3.9.5 *In vitro* insulin secretion

The NIT-1 cells (1.0×10^4 cells/mL) were seeded in a 24-well plate and incubated overnight at 37 °C in 5% CO₂. The next day, the cells were washed twice with glucose-

free Krebs/HEPES Ringer solution (115 mM NaCl, 24 mM NaHCO₃, 5 mM KCl, 1 mM MgCl₂, 2.5 mM CaCl₂, 25 mM HEPES [pH 7.4]) and pre-incubated at 37 °C in 5% CO₂ for 30 min with the glucose-free Krebs/HEPES Ringer solution. The cells were then incubated for 1 h in Krebs/HEPES Ringer solution containing 1 mg/mL bovine serum albumin and 6.25, 12.5, 25, or 50 µg/mL of glucose in the presence or absence of the extract. An aliquot of the supernatant was collected for ELISA. The amount of insulin released was measured with a Mouse Insulin ELISA kit (Merckodia, Uppsala, Sweden) according to the manufacturer protocol. Results (in pmol) are expressed as the means ±SD of three independent experiments.

3.9.6 *In vivo* acute toxicity study

Acute toxicity test was conducted as per the guidelines of the Organization for Economic Co-operation and Development (OECD). Healthy adult Sprague Dawley rats of either sex were used. The rats were fasted overnight, divided into 6 groups (n = 6), and orally fed with PMm at doses 100, 200, 400, 800, and 2000 mg/kg body weight (bw), PMt was dissolved in distilled water and fed to the animals; the control groups were given distilled water alone.

All the group rats were observed for 1 h continuously and then every 1 h for 4 h and finally after every 24 h up to 14 days for any physical signs of toxicity such as writhing, gasping, palpitation, and decreased respiratory rate or for any lethality. The animal experiments were carried out according to the guidelines of animal experimentation approved by the Animal Care and Use Committee at the University of Malaya (Ethics Number: PM/27/2014/MMJA[R]).

3.9.7 Type 1 diabetes in rats

Type 1 diabetes in rats was induced in normal male rats. Rats were fasted for 15 hours (overnight period), thereafter, injected intraperitoneally with 65 mg/kg bw of freshly prepared STZ ((Sigma-Aldrich, St. Louis, MO, USA)) in 0.1 M citrate buffer (pH 4.5) in a volume of 1 mL/kg bw. To these STZ-injected rats, 20% glucose solution was given for 12 h to prevent hypoglycemic mortality, which might cause due to STZ injection. Diabetes was confirmed in rats by measuring the blood glucose levels, determined at 96 h after the STZ administration. Rats with fasting blood glucose level of 19–24 mmol/L were considered with type 1 diabetes and used for the study.

3.9.8 Type 2 diabetes in rats

Type 2 diabetes in rats was induced in normal male rats. Rats were fasted for 15 hours (overnight period) and administered with nicotinamide intraperitoneally at dose (210 mg/kg). After 15 minutes, 55 mg/kg bw of freshly prepared STZ in 0.1 M citrate buffer (pH 4.5) in a volume of 1 mL/kg bw was injected. Diabetes was confirmed in rats by measuring the blood glucose levels, determined at 96 h after the STZ-nicotinamide administration. Rats with fasting blood glucose level of 11–14 mmol/L were considered with type 2 diabetes and subsequently used for the study.

3.9.9 Division of diabetic animals for the study

For the study, Type 1 and Type 2 diabetic rats were divided into 2 segments:

The Type 1 segment consisted of the following groups:

Group 1: normal control rats

Group 2: type 1 diabetic control rats

Group 3: type 1 diabetic rats treated with 6 U/kg of insulin (standard positive)

Group 4: diabetic rats treated with 200 mg/kg of PMt

Group 5: diabetic rats treated with 400 mg/kg of PMt.

The Type 2 segment was divided into the following groups:

Group 1: normal control rats

Group 2: type 2 diabetic control rats

Group 3: type 2 diabetic rats treated with 50 mg/kg of glibenclamide (standard positive)

Group 4: diabetic rats treated with 200 mg/kg of PMt

Group 5: diabetic rats treated with 400 mg/kg of PMt.

Rats in each groups were injected and fed with the respective doses of PMt and standard drug once daily every morning for 45 days; administration was based on volume (2 mL/200 g bw), PMt was completely dissolved in distilled water and filtered before administration.

3.9.10 Experimental procedure

Fasting blood glucose in all the group rats were measured on every eleventh day of administration by a glucose oxidase-peroxidase enzymatic method using a standardized glucometer (Accu-Check Performa, Roche Diagnostic Germany) by tail snipping method; changes in body weight, food intake, and water intake were recorded daily.

After 45 days treatment period, all groups were fasted for 12 h and then anesthetized using pentobarbital; the blood was collected into heparinized tubes and centrifuged at 2000 rpm for 10 min and the serum was collected and stored at -80°C until analysis for biochemical parameters, oxidative stress markers and pro-inflammatory cytokines levels.

3.9.11 Glucose tolerance test

Oral glucose tolerance test (OGTT) was evaluated in those group segments that had demonstrated the highest glycemic control in the Type 1 and Type 2 diabetic rat models to determine the effectiveness of PMt. PMt (200 or 400 mg/kg) was administered to

overnight-fasted rats in 2 mL/200 g bw doses. Fasting blood glucose concentrations were measured before the respective PMt administrations, following which oral glucose (3 g/kg) was administered and blood glucose levels were measured at 30, 60, 90, and 120 min, respectively.

3.9.12 Assessment of serum insulin and C-peptide levels

Serum insulin and C-peptide levels were determined by using ELISAKit (eBioscience, San Diego, CA, USA) according to the manufacturer protocol. In addition, the whole body weight, food and water intake were measured on daily basis in all the group rats including type 1 and type 2 diabetic rats.

3.9.13 Assessment of oxidative stress markers

Serum was used to determine the GSH and MDA levels following the method described in published literature (Aslan *et al.*, 2007).

3.9.14 Animal models for *Pseudovaria macrophylla* study

33 Sprague Dawley (SD) male rats (250-300g) were obtained from the Experimental Animal House, Faculty of Medicine, University of Malaya. The animal experiments were carried out according to the guidelines of animal experimentation approved by the Animal Care and Use Committee at the University of Malaya (Ethics Number: PM/27/2014/MMJA[R]).

3.9.15 Experimental design

The experimental animals were divided randomly into five groups (6 rats per group).

Groups	Condition
Group 1 (Normal control, NC)	Rats fed with normal water.
Group 2 (Diabetic Control, DC)	STZ-Nicotinamide induced diabetic rats
Group 3 (PMA)	STZ-Nicotinamide induced diabetic rats, treated with 200 mg/kg extract.
Group 4, (PMb)	STZ-Nicotinamide induced diabetic rats, treated with 400 mg/kg extract.
Group 5 (Positive control, PC)	STZ-Nicotinamide induced diabetic rats, treated with glibenclamide (2.5 mg/kg)

3.9.16 Acute toxicity study

The rats were fasted overnight and orally administered with doses of 500, 1,000 and 3,000 mg/kg body weight on the next day. The control group was given only distilled water. All experimental rats were observed during the first 2 hours and further monitored until 72 hours for signs of abnormalities in behavioral, neurological and anatomical changes. The study was done according to the guidelines of the Organization for Economic Co-Operation and Development (OECD).

3.9.17 T2DM (Type 2 Diabetes Mellitus) induction

T2DM was induced in overnight-fasted rats by a single intraperitoneal injection of 60 mg/kg streptozotocin (Sigma Aldrich, Germany), followed by 120 mg/kg of nicotinamide (Sigma Aldrich, Germany) , injected intraperitoneally, after 15 min. Blood glucose levels were then measured after 72 hours to confirm Type 2 diabetes in rats.

3.9.18 Blood samples

After 45 days of treatment, rats were anesthetized and blood samples collected from the inner canthus of the eye using capillary tubes. Then the blood samples were centrifuged for 10 minutes at 4000 rpm to get the serum and plasma.

3.9.19 Biochemical activity

The fasting blood glucose levels (measured by portable glucometer, Acu-Check Nano Perfoma) and body weights of all rats in the groups were measured on day 0, 14, 21, 28 and 45. Serum insulin levels were measured by enzyme linked immunosorbent assay kits (Elisa kit, Chemical Item Number 589501) and C-peptide levels were measured using RAT EIA Kit K4757. All tests were done accordingly to manufacturer's instructions.

3.9.20 Measurement of oxidative stress markers

Glutathione reductase (GSH) and lipid peroxidation (LPO) levels in the serum of diabetic rats were measured using GSH and LPO assay kits (Cayman Chemical, USA, Item Number 703002, 705003) and tests were performed according to the manufacturer's instructions.

CHAPTER 4: RESULTS AND DISCUSSION

Two *Pseuduvaria* species from the family of Annonaceae collected from the Malaysian forest; *Pseuduvaria monticola* J.Sinclair and *Pseuduvaria macrophylla* (Oliv.) Merr, were investigated for their chemical constituents and biological activities.

The compounds were isolated using various chromatographic methods such as column chromatography (CC) and preparative thin layer chromatography (PTLC) and high performance liquid chromatography (HPLC).

The structural elucidations of the isolated compounds was achieved by the application of numerous spectroscopic techniques (NMR, IR, MS and UV) and also by comparison with published literature data.

4.1 Chemical constituents of *Pseuduvaria monticola*

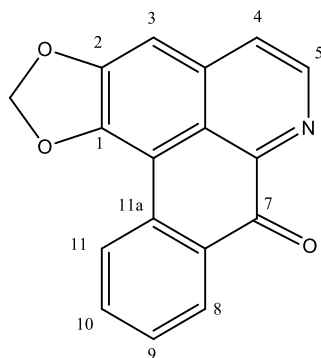
Phytochemical analysis on the leaves and bark of *Pseuduvaria monticola* resulted in the isolation of fifteen chemical compounds: four oxoapophine alkaloids; liriodenine (**3**), lysicamine (**39**), oxoputerine (**40**), ouregidione (**4**), two phenanthrene alkaloids; atherosperminine (**41**) and argentinine (**42**), one sesquiterpene; tau cadinol (**43**) three benzopyran derivatives; oligandrol (**14**), (6*E*,10*E*) isopolycerasoidol (**15**), (6*E*,10*E*) isopolycerasoidol methyl ester (a new derivative) (**32**), two phenolic acids; caffeic acid (**44**) and chlorogenic acid (**45**), two fatty acids; hexadecanoic acid (**46**) and methyl oleate (**47**) and one sterol; stigmasterol (**48**). All the compounds were listed in Table 4.1.

Table 4.1: Chemical compounds isolated from *Pseuduvaria monticola*

No	Compounds	Classification of compounds	Parts of plant
1	Liriodenine (3)	Oxoaporphine	Leave/Bark
2	Lysicamine (39)	Oxoaporphine	Leave/Bark
3	Oxoputerine (40)	Oxoaporphine	Bark
4	Ouregidione (4)	Oxoaporphine	Bark
5	Atherosperminine (41)	Phenanthrene alkaloid	Leave
6	Argentinine (42)	Phenanthrene alkaloid	Leave
7	Tau cadinol (43)	Sesquiterpene	Leave
8	Oligandrol (14)	Benzopyran derivative	Bark
9	(6E,10E) Isopolycerasoidol (15)	Benzopyran derivative	Leave/Bark
10	(6E,10E)isopolycerasoidol methyl ester (32)	Benzopyran derivative	Leave/Bark
11	Caffeic acid (44)	Phenolic acids	Bark
12	Chlorogenic acid (45)	Phenolic acids	Bark
13	N-hexadecanoic acid (46)	Fatty acid	Bark
14	Methyl oleate (47)	Fatty acid	Bark
15	Stigmasterol (48)	Sterol	Leave

4.2 Structural Elucidation of Compounds from *Pseuduvaria monticola*

4.2.1 Liriodenine (3)



3

Alkaloid liriodenine (**3**) was isolated as yellow needles, with melting point 275-276 °C (272 °C, Buchanan & Dickey, 1960). The intense yellow fluorescence was consistent with the presence of a chromophore moiety. The UV spectrum showed absorptions at λ_{\max} 255, 276, 327 and 400 nm, typical of an oxoaporphine skeleton with highly conjugated system. The IR band at 1700 cm^{-1} indicated the presence of a conjugated carbonyl function and absorption bands at 1450, 1360 and 1261 cm^{-1} indicated C-O stretching vibrations of methylenedioxy group. The molecular formula was determined as $\text{C}_{17}\text{H}_9\text{NO}_3$ based on the HREIMS spectrum in positive mode at m/z 276.0673 $[\text{M}+\text{H}]^+$ (Figure 4.1).

The ^1H NMR spectra (Figure 4.2) showed seven aromatic protons in the aromatic region; two doublets at δ 8.56 ($J=7.8$ Hz) and 8.62 ($J=8.0$ Hz) were assigned to H-8 and H-11, respectively. Two set of doublet of triplet signals at δ 7.57 ($J=7.5, 1.8$ Hz) and δ 7.74 ($J=7.5, 1.8$ Hz) were assigned to H-9 and H-10 respectively, and H-4 and H-5 peaks at δ 7.75 and 8.88 as doublet ($J=5.2$ Hz), respectively. The methylene proton resonated as a singlet at δ 7.22 (1H) was assigned to H-3. Another signal of two protons was observed

at δ 7.16 which belong to a methylenedioxy group attached at C-1 and C-2. The COSY spectrum (Figure 4.4 and 4.5) showed the correlations of vicinal protons between H-5/H-6, H-7/H-8/ H-9/H-10 and H-11/H-12 indicating of unsubstituted ring D.

The ^{13}C -NMR and DEPT 135 spectrum (Figure 4.3 and 4.4) showed presence of seventeen carbons consisting of one methylenedioxy, seven methines and nine quaternary carbons. The signal at very low field at δ 182.5 ppm indicated the presence of the carbonyl group assigned to C-7.

The methylenedioxy carbon peak was observed at δ 102.4 and this was confirmed by correlation between methylenedioxy carbon peak and methylene proton at δ 6.36 in the HMQC spectrum (Figure 4.7 and 4.8). The COSY spectrum (Figure 4.5 and 4.6) and HMBC spectrum (Scheme 4.1) confirmed the complete assignments of the protons and carbons. Table 4.2 summarizes the ^1H and ^{13}C NMR of the compound.

Finally, all spectroscopic evidence confirmed the structure as liriodenine (**3**) which was also previously isolated from other *Pseuduvaria* species (Taha *et al.*, 2011).

Table 4.2: ^1H NMR (500 MHz) and ^{13}C NMR (125 MHz) spectral data of liriodenine (**3**) in CDCl_3 (δ in ppm, J in Hz)

Position	^1H -NMR (δ ppm)	^{13}C -NMR (δ ppm)	^{13}C -NMR (δ ppm) (Nordin <i>et al.</i> , 2015)
1	-	148.1	147.9
1a	-	106.4	107.1
1b	-	122.7	122.6
2	-	151.8	151.7
3	7.16 (1H, <i>s</i>)	103.3	103.4
3a	-	145.0	144.4
4	7.75 (1H, <i>d</i> , $J=5.2$)	124.4	124.6
5	8.88 (1H, <i>d</i> , $J=5.2$)	145.0	144.9
6a	-	135.8	135.4
7	-	182.7	181.2
7a	-	131.4	130.8
8	8.56 (1H, <i>d</i> , $J=7.8$)	128.6	127.9
9	7.57 (1H, <i>dt</i> , $J=7.5, 1.8$)	128.9	128.6
10	7.74 (1H, <i>dt</i> , $J=7.5, 1.8$)	134.0	134.2
11	8.62 (1H, <i>d</i> , $J=8.0$)	127.4	127.0
11a	-	133.1	132.5
-CH ₂ O ₂ -	6.36 (2H, <i>s</i>)	102.4	103.3

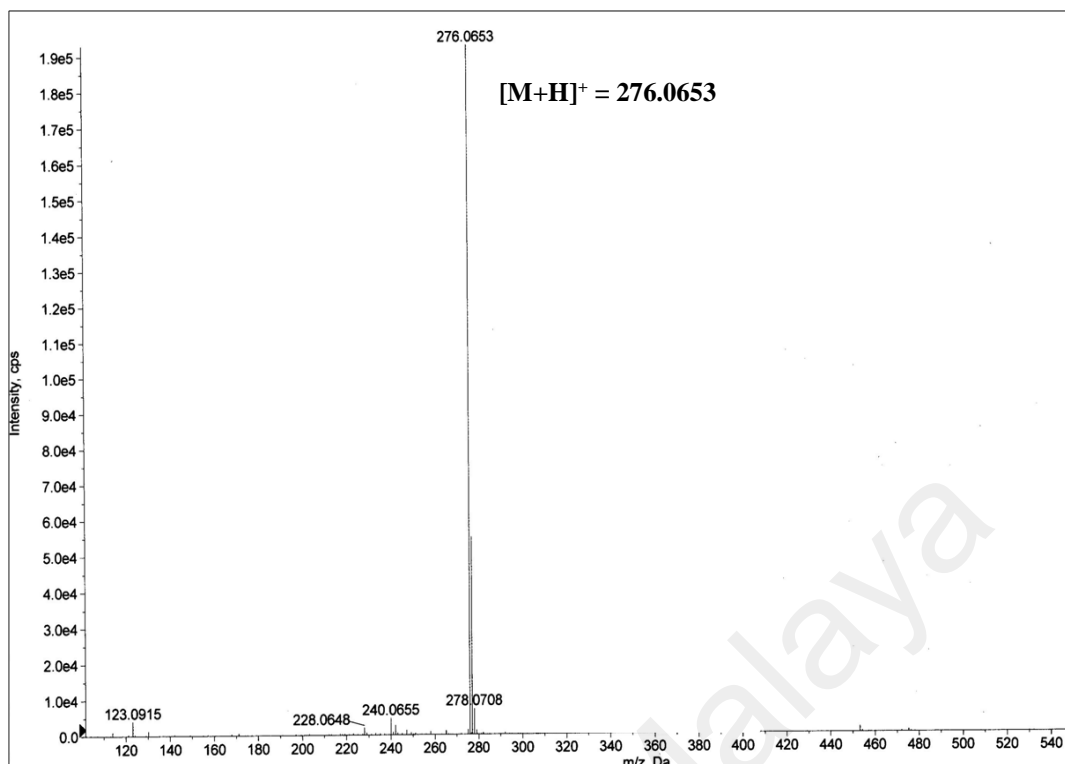


Fig 4.1: LC-MS spectrum of liriodenine (3)

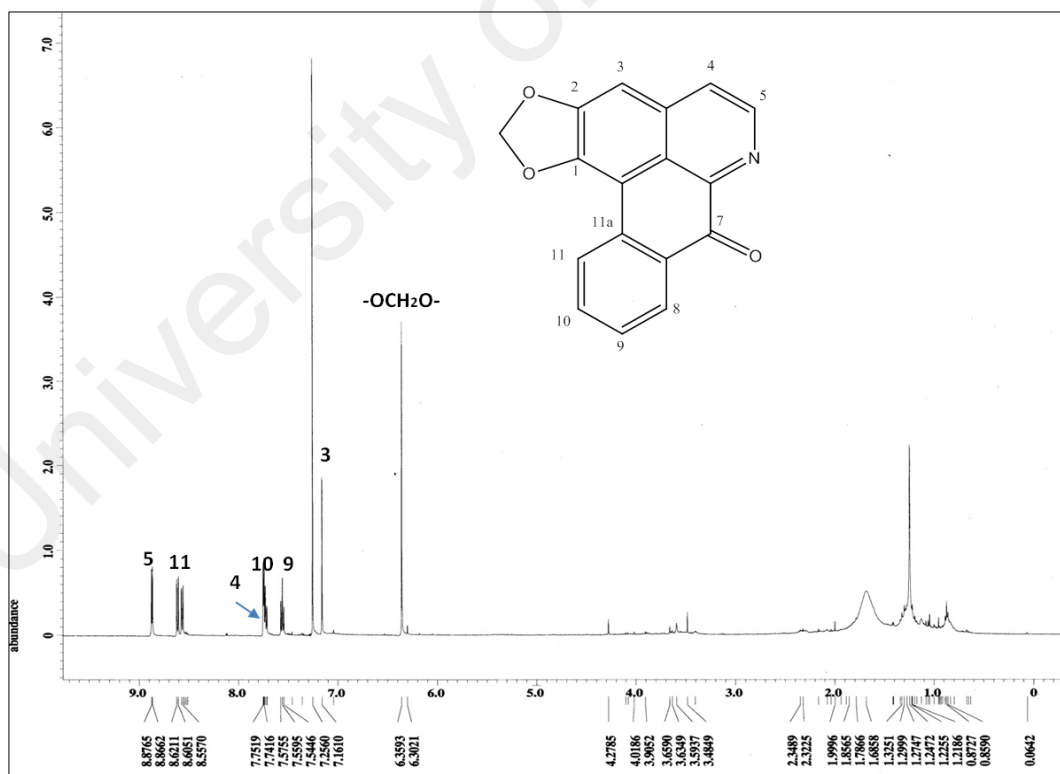


Fig 4.2: ^1H NMR spectrum of liriodenine (3)

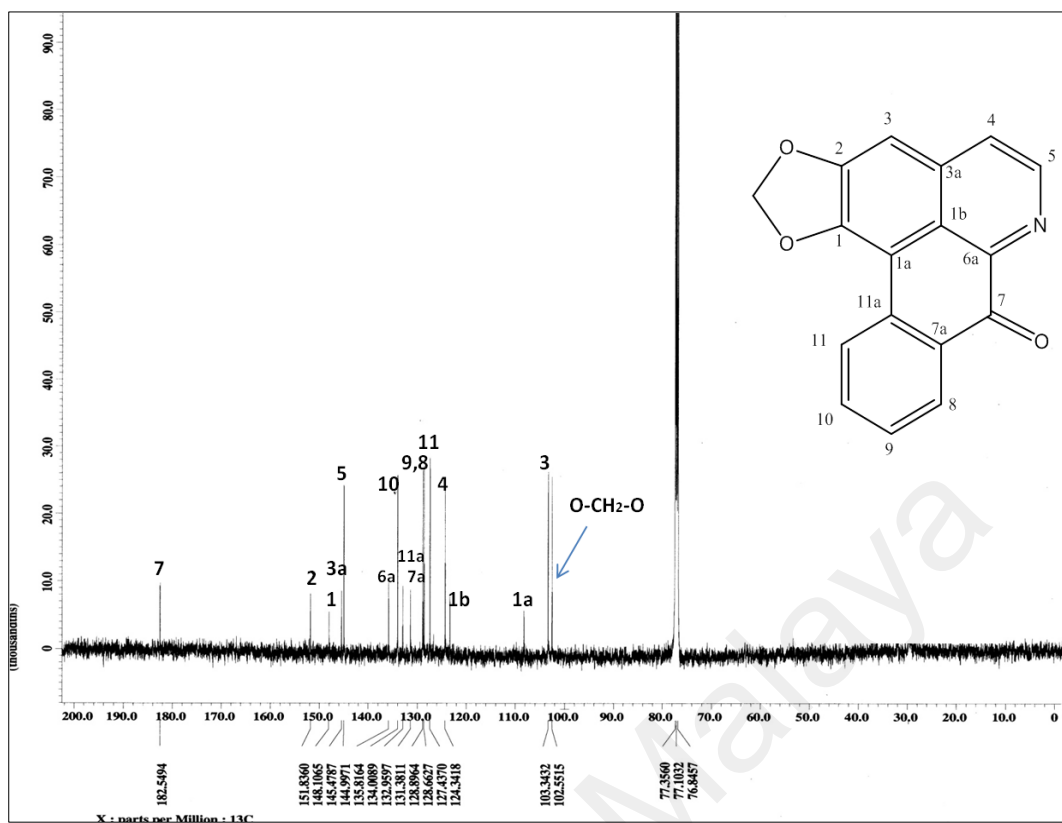


Fig 4.3: ^{13}C NMR spectrum of liriodenine (3)

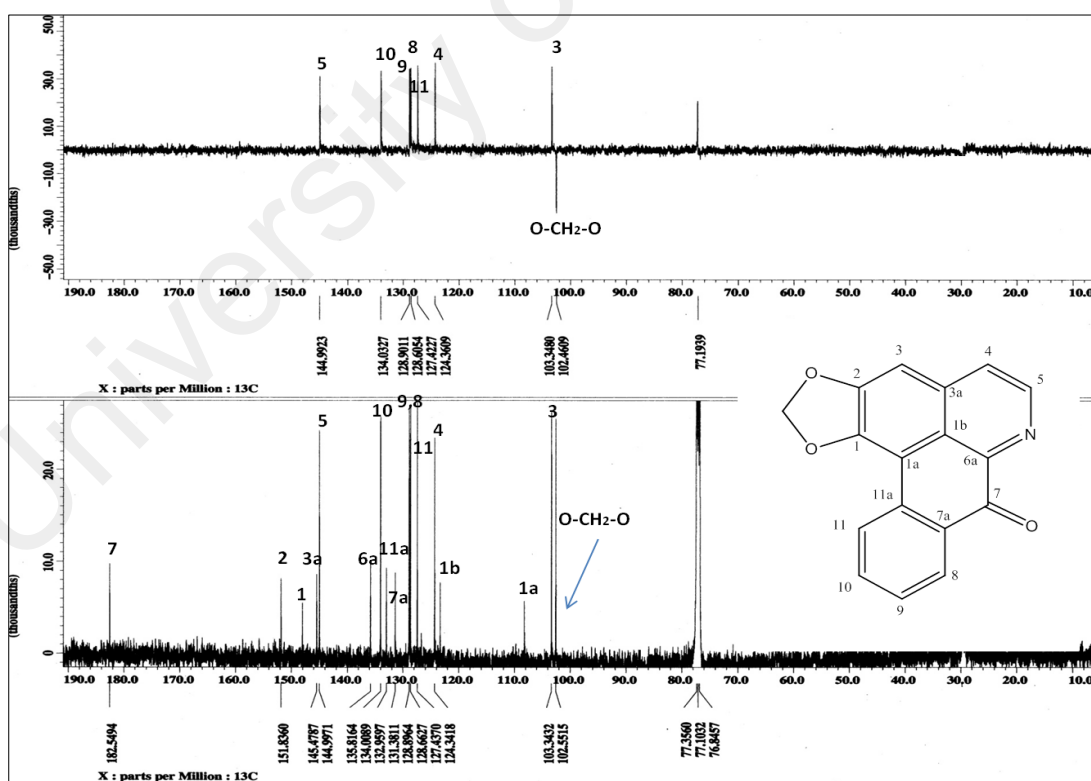


Fig 4.4: DEPT 135 and ^{13}C NMR spectrum of liriodenine (3)

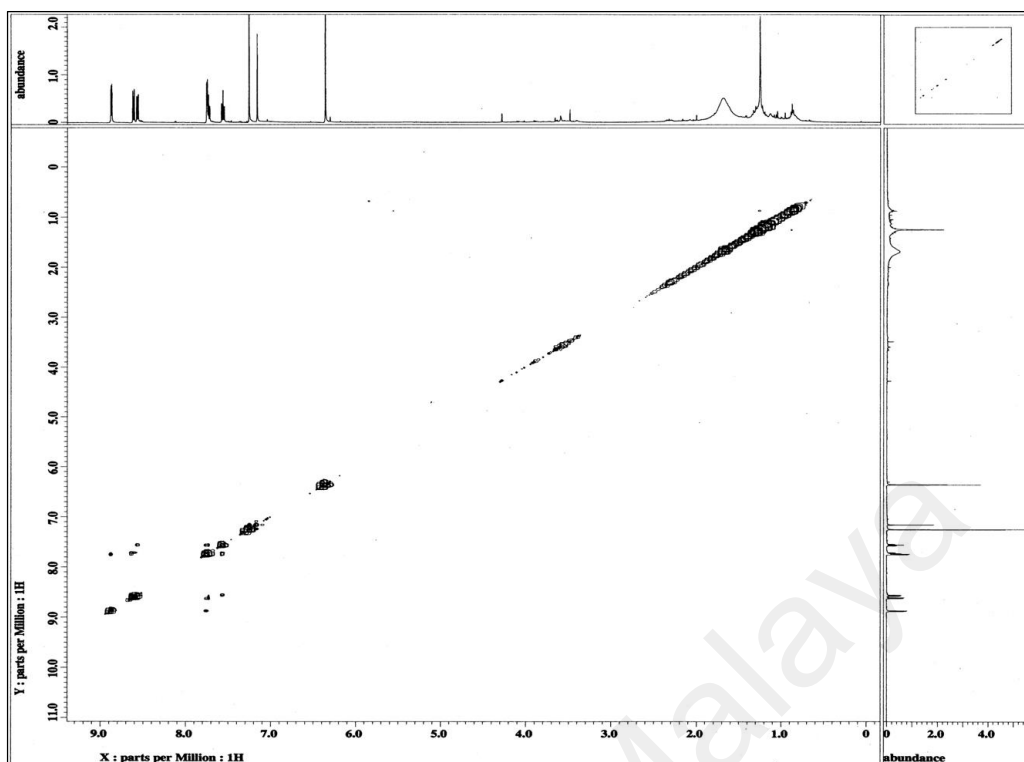


Fig 4.5: COSY spectrum of liriodenine (3)

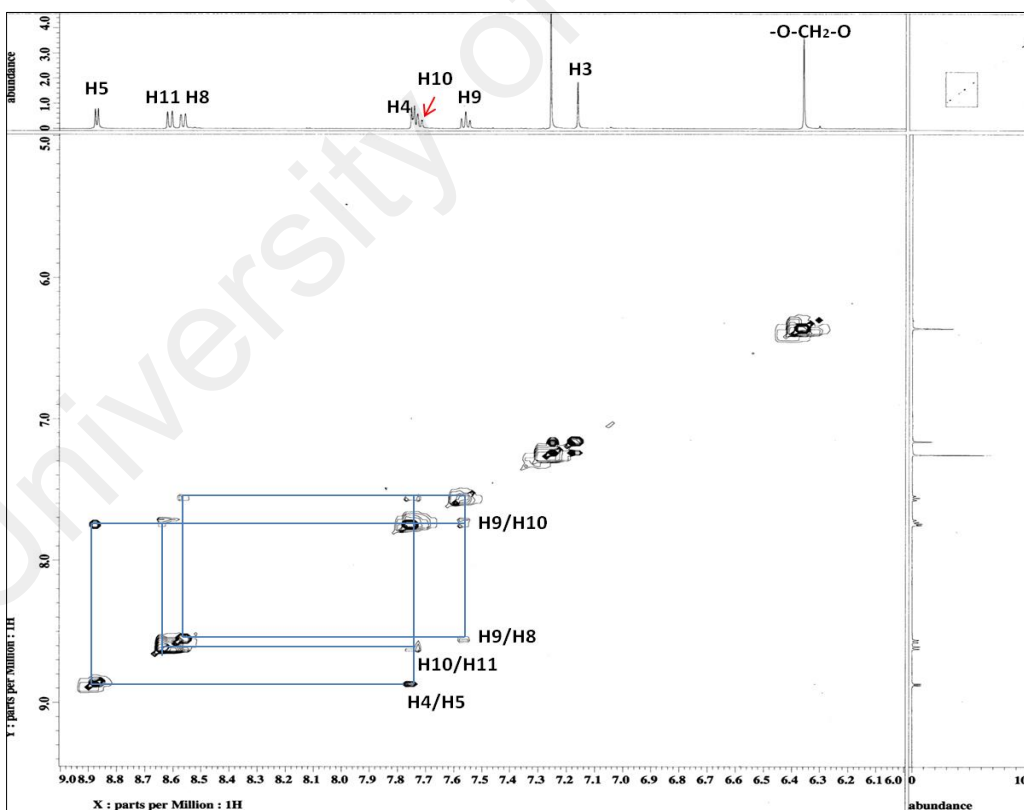


Fig 4.6: Expanded COSY spectrum of liriodenine (3)

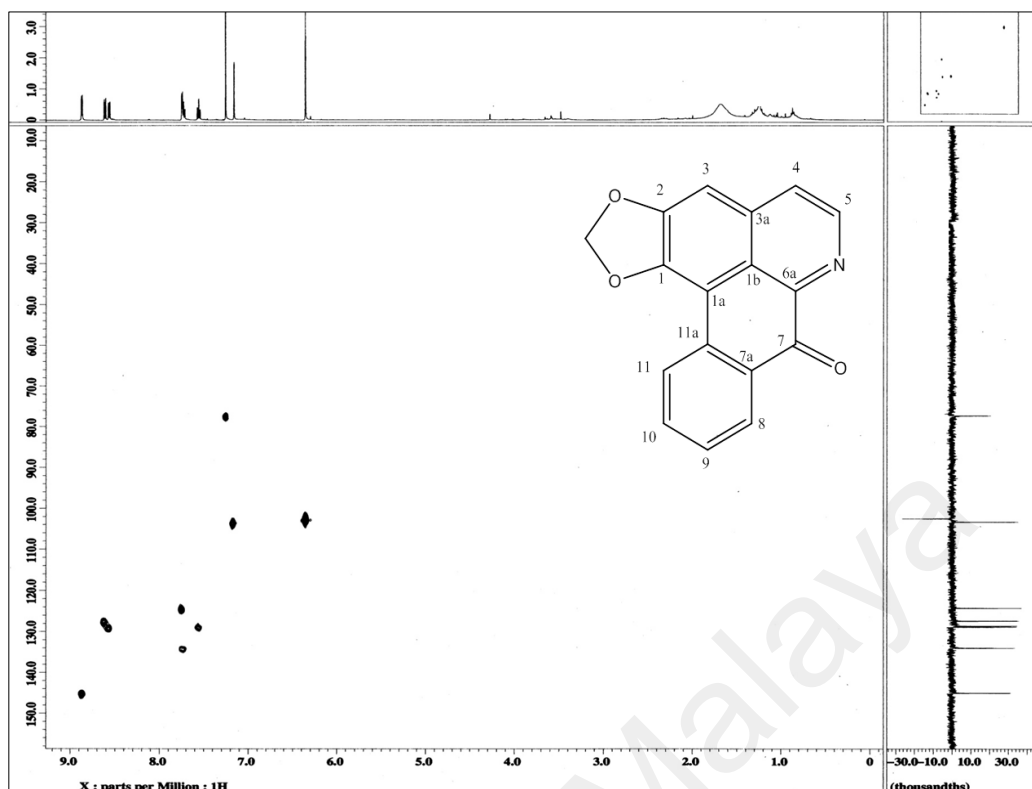


Fig 4.7: HMQC spectrum of liriodenine (3)

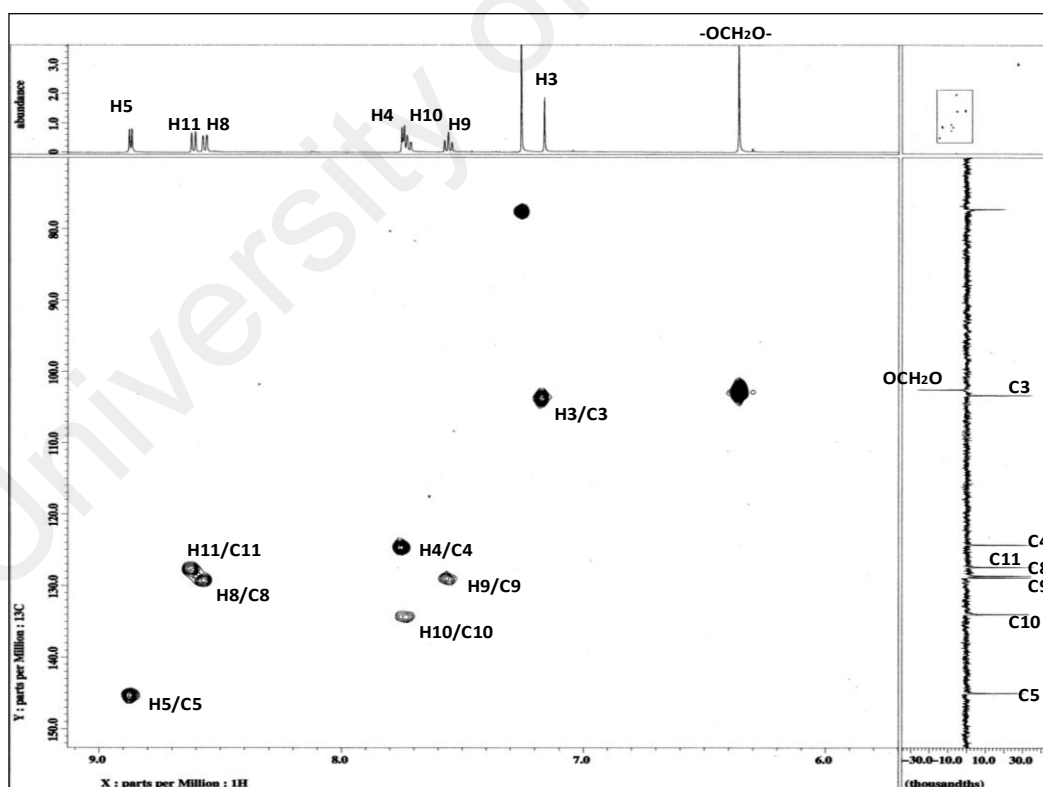
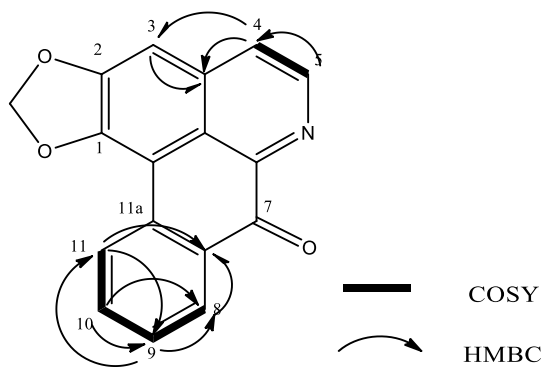


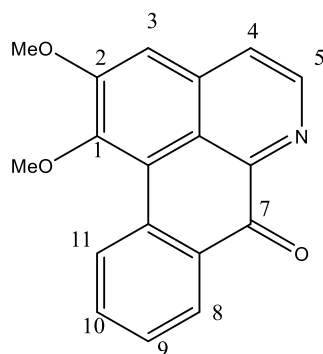
Fig 4.8: Expanded HMQC spectrum of liriodenine (3)



Scheme 4.1: The HMBC and COSY correlations of liriodenine (3)

University of Malaya

4.2.2 Lysicamine (39)



39

Alkaloid lysicamine (**39**) was isolated as a yellow amorphous solid and gave positive result to Dragendorff's test. The UV spectrum showed intense absorption bands at 210, 237, 270 and 395 nm which indicate a highly conjugated oxoaporphine system. The IR spectrum showed a conjugated carbonyl peak at 1668 cm^{-1} . The HREIMS (Figure 4.9) showed a molecular ion peak at $m/z\ 292.0969\ [M+H]^+$ corresponding to a molecular formula $C_{18}H_{13}O_3N$.

The $^1\text{H NMR}$ spectrum (Figure 4.10) revealed the characteristic of an AB doublet-doublet of H-4 and H-5 at $\delta\ 7.76$ and $\delta\ 8.86$ ($J=5.1\text{ Hz}$), respectively. The appearance of a singlet at $\delta\ 7.17$ belongs to H-3, suggesting that the C-1 and C-2 are substituted with two methoxyl groups at $\delta\ 3.96$ and 4.04 , respectively, since there was no signal of methylenedioxy peak. Two aromatic protons were observed at $\delta\ 7.53$ (1H, *dt*, $J=7.5, 1.7\text{ Hz}$) and $\delta\ 7.71$ (1H, *dt*, $J=7.5, 1.7\text{ Hz}$) which was assignable to H-10 and H-9, respectively.

A very downfield signal at $\delta\ 9.13$ (1H, *dd*, $J=8.0, 1.8\text{ Hz}$) was assigned to H-11. It is deshielded by the benzene ring induced field and also by the occurrence of hydrogen

bonding with the oxygen of the methoxyl group at C-1. A doublet of doublet was also observed at δ 8.53 (1H, *dd*, $J=7.9, 1.8$ Hz) which belongs to H-8 that was deshielded from the neighbouring carbonyl at C-7.

The correlations of vicinal protons at H-8/H-9, H-9/H-10 and H-10/H-11 in the COSY spectrum (Figures 4.14 and 4.15) confirmed that ring D was unsubstituted. Table 4.3 summarizes the ^1H - and ^{13}C NMR of the compound.

The ^{13}C and DEPT 135 NMR spectra (Figures 4.11 and 4.12) exhibited a total of eighteen carbons consisting of two methoxy, one carbonyl, seven methines and eight quaternary carbons. The DEPT 135 spectrum also confirmed the absence of any methylene signals.

Further analysis of HSQC (Figures 4.15 and 4.16) and HMBC (Scheme 4.2) confirmed the compound as lysicamine (**3**) which is a 1, 2 dimethoxyoxoaporphine. Lysicamine (**39**) was isolated for the first time from *Pseuduvaria monticola* in this study.

Table 4.3: ^1H NMR (600 MHz) and ^{13}C NMR (150 MHz) spectral data of lysicamine (**39**) in CDCl_3 (δ in ppm, J in Hz)

Position	^1H -NMR (δ ppm)	^{13}C -NMR (δ ppm)	^{13}C -NMR (δ ppm) (Omar <i>et al.</i> , 2013)
1	-	152.1	151.0
1a	-	119.4	118.8
1b	-	122.5	121.2
2	-	156.9	155.8
3	7.17 (1H, <i>s</i>)	106.5	105.4
3a	-	136.2	135.5
4	7.75 (1H, <i>d</i> , $J=5.1$)	123.6	122.6
5	8.86 (1H, <i>d</i> , $J=5.1$)	145.1	144.0
6a	-	145.7	144.3
7	-	182.1	181.7
7a	-	130.8	133.3
8	8.53 (1H, <i>dd</i> , $J=7.9, 1.8$)	128.9	127.8
9	7.71 (1H, <i>dt</i> , $J=7.5, 1.7$)	128.8	127.9
10	7.53 (1H, <i>dt</i> , $J=7.5, 1.7$)	134.3	133.4
11	9.13 (1H, <i>dd</i> , $J=8.0, 1.8$)	128.5	127.4
11a	-	135.5	134.1
OCH ₃ -1	3.96 (3H, <i>s</i>)	60.7	59.7
OCH ₃ -2	4.04 (3H, <i>s</i>)	56.2	55.2

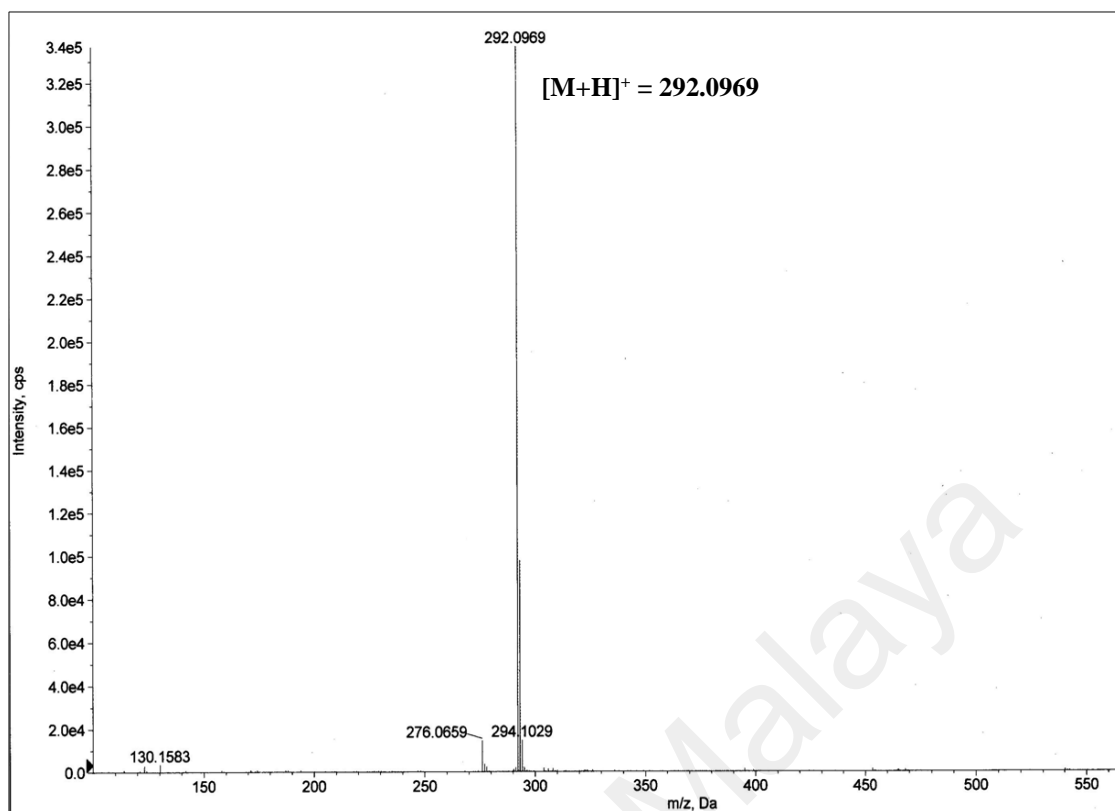


Fig 4.9: LC-MS of lycicamine (**39**)

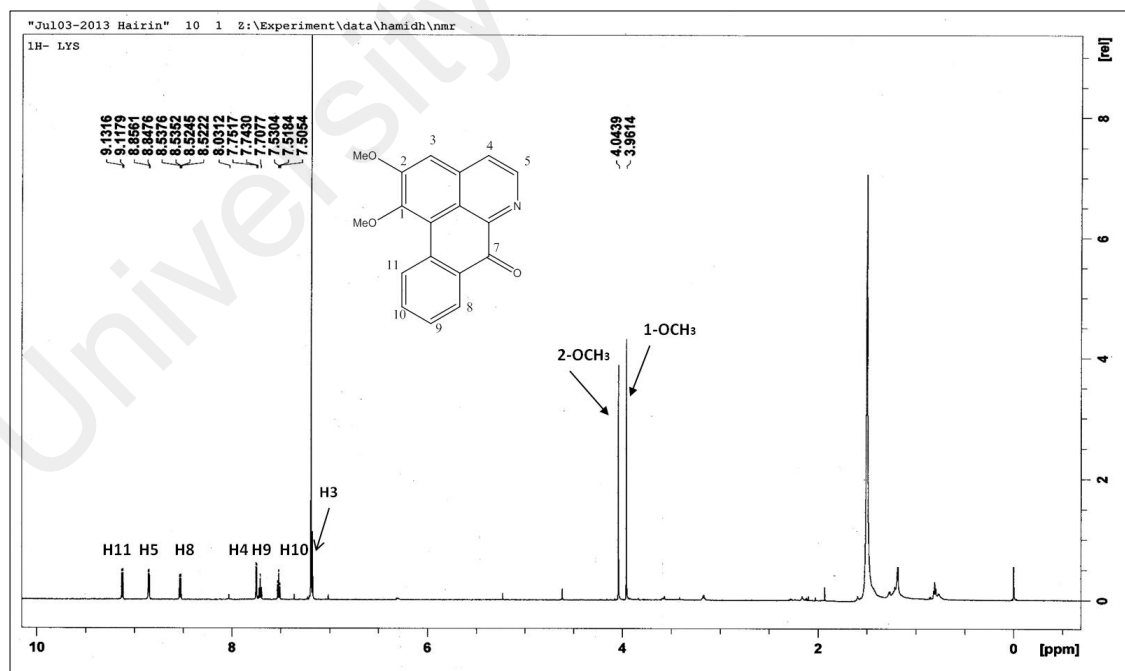


Fig 4.10: ¹H NMR spectrum of lycicamine (**39**)

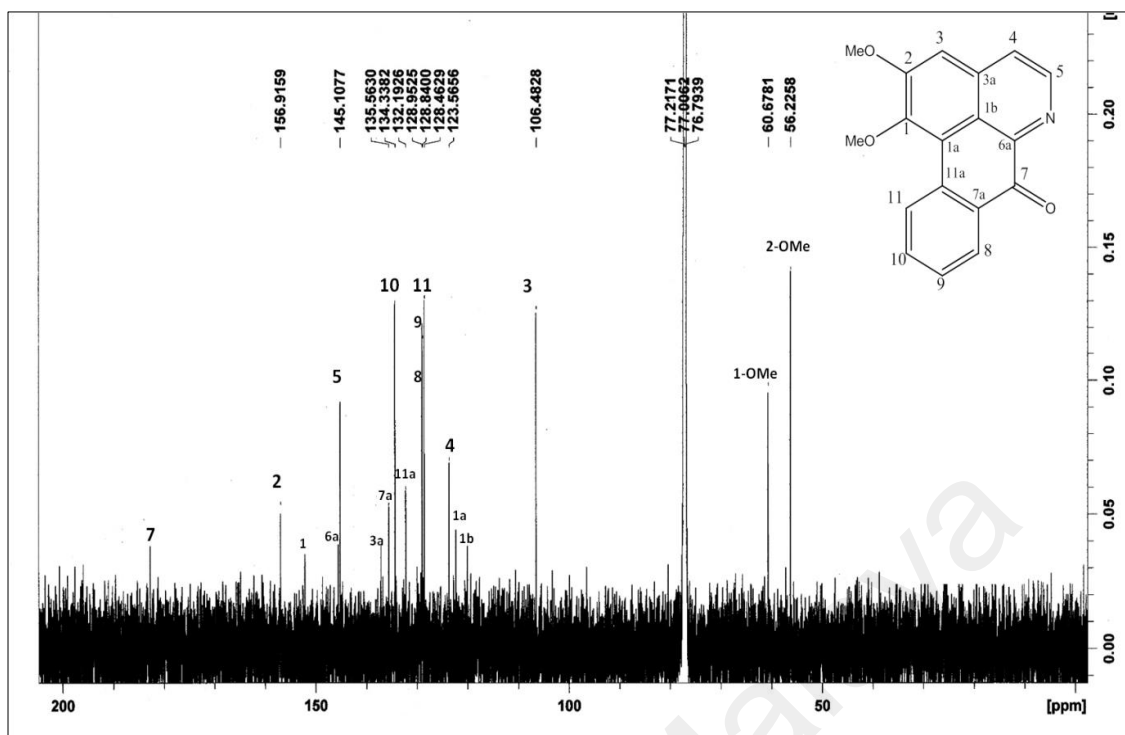


Fig 4.11: ^{13}C NMR spectrum of lysicamine (39)

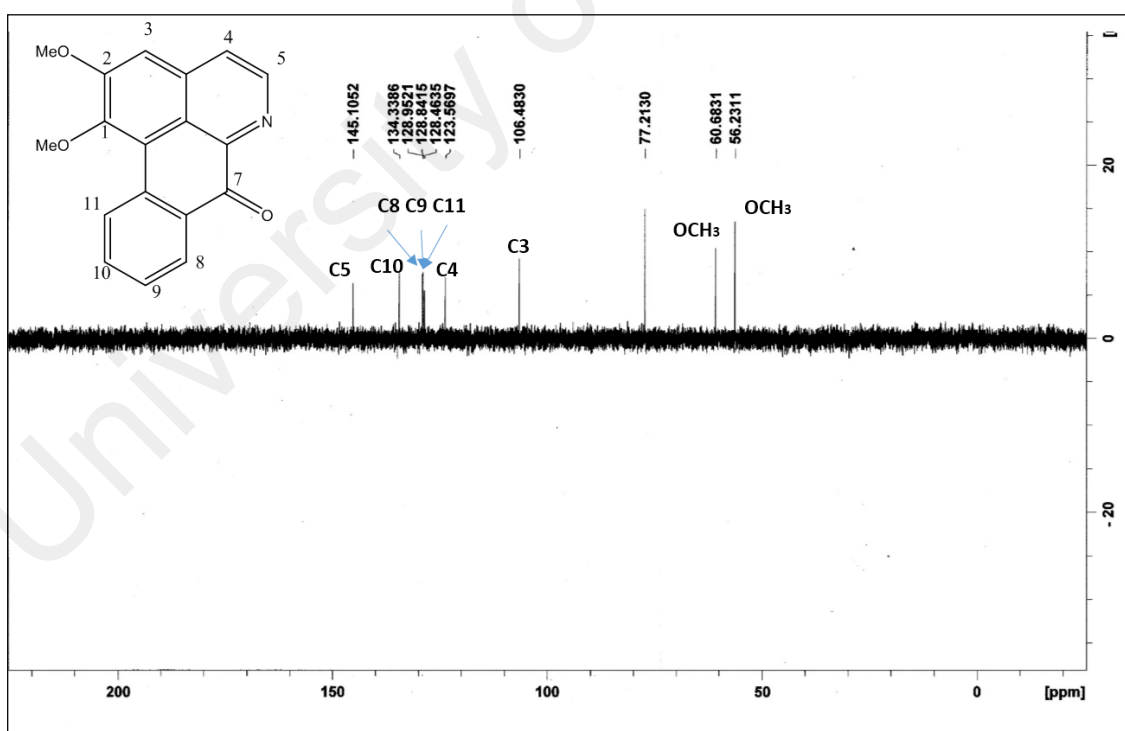


Fig 4.12: DEPT 135 spectrum of lysicamine (39)

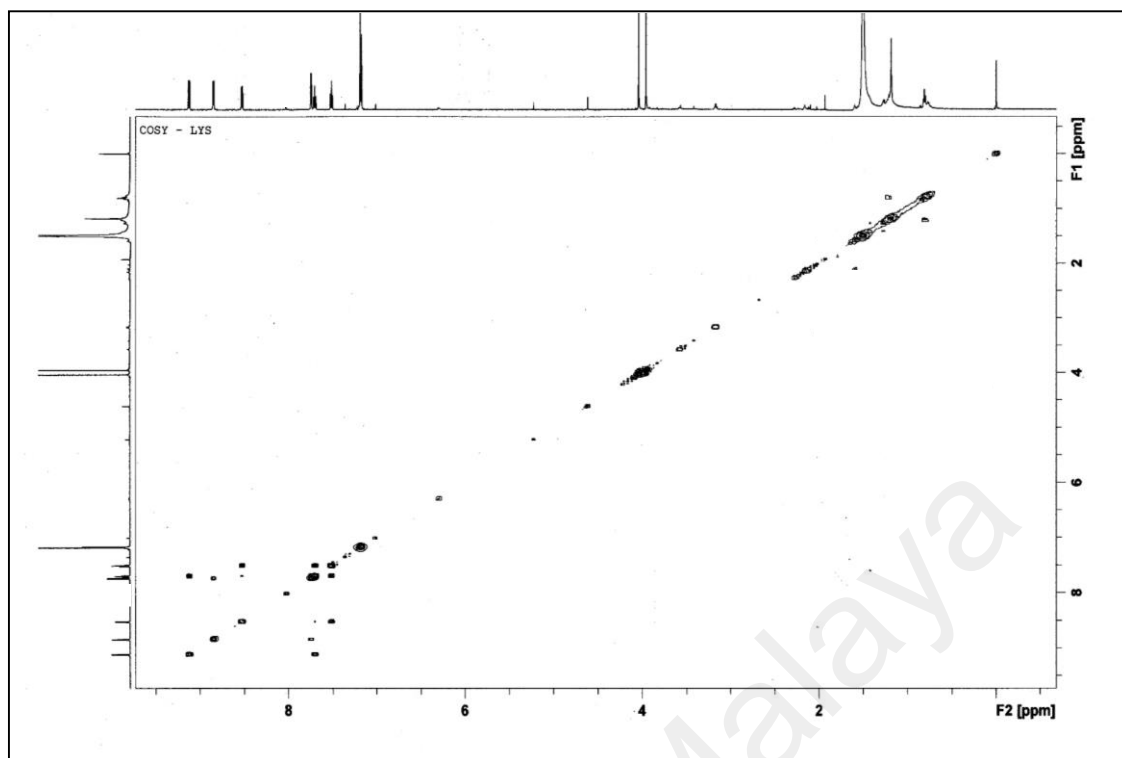


Fig 4.13: COSY spectrum of lysicamine (39)

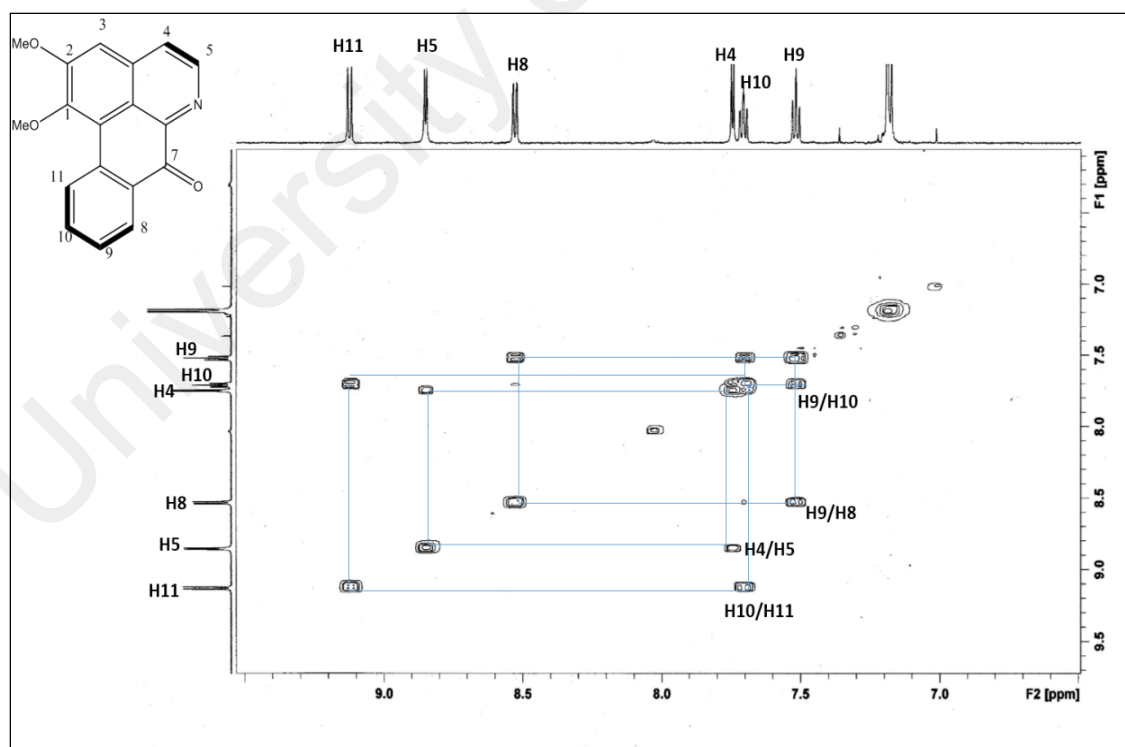


Fig 4.14: Expanded COSY spectrum of lysicamine (39)

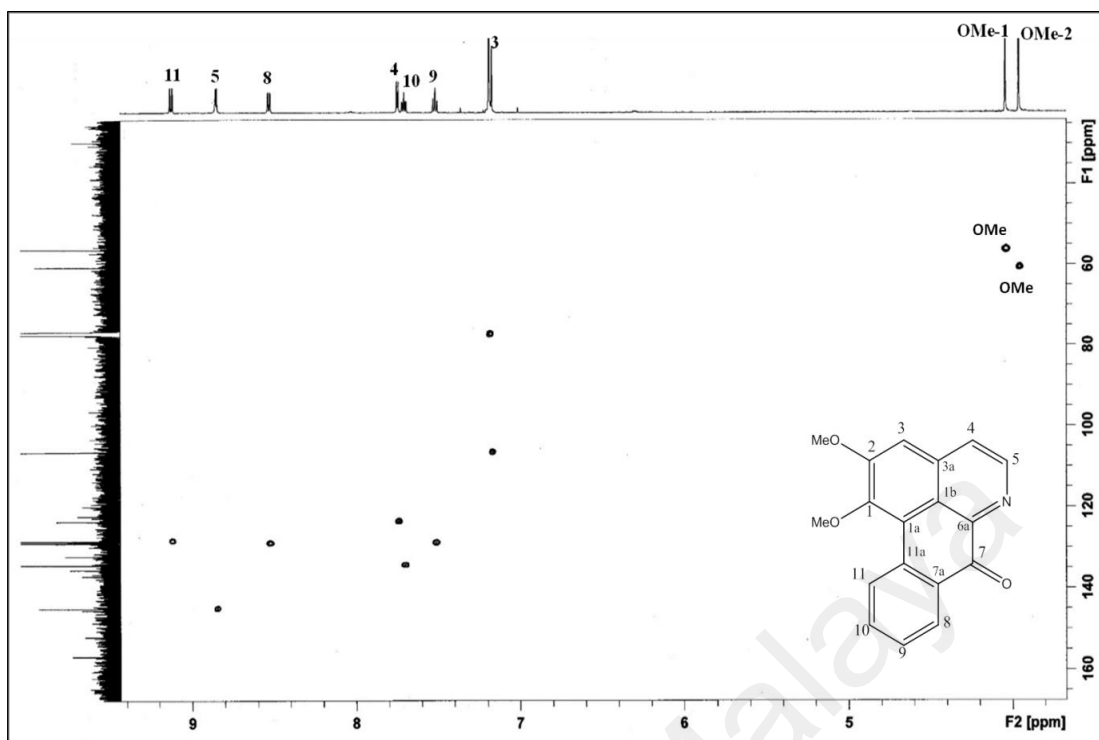


Fig 4.15: HSQC spectrum of lysicamine (39)

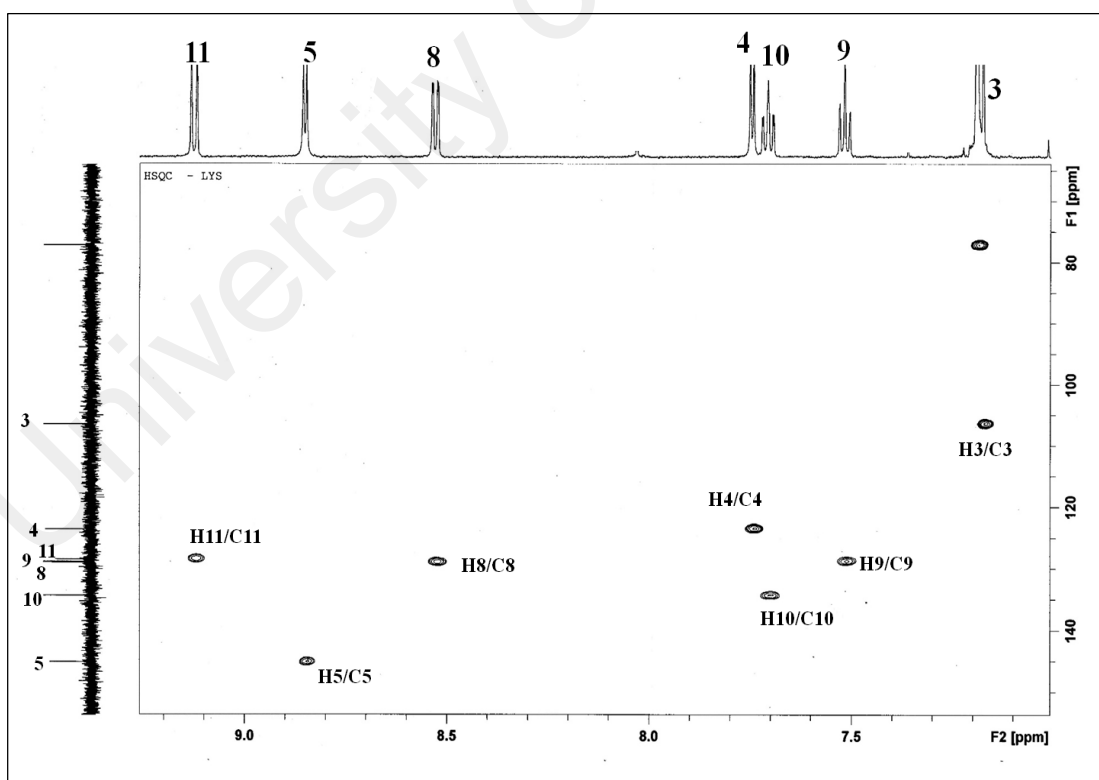
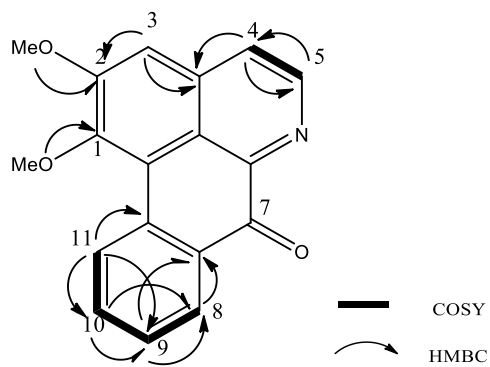


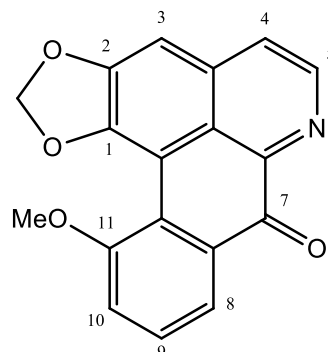
Fig 4.16: Expanded HSQC spectrum of lysicamine (39)



Scheme 4.2: The HMBC and COSY correlations of lysicamine (**39**)

University of Malaya

4.2.3 Oxoputerine (40)



40

Oxoputerine (**40**), an alkaloid was isolated as yellow amorphous solid and gave positive result to Dragendorff's test. The UV spectrum band showed absorption at 230, 276 and 320 nm. The IR spectrum exhibited a strong peak at 1665 cm^{-1} attributed to a carbonyl function and an absorption band at 1042 cm^{-1} which indicates a characteristic of the C-O stretching vibrations of a methylenedioxy group. The HREIMS (Figure 4.17) showed a molecular ion peak at 306.0755 [M+H]^+ suggesting a molecular formula of $\text{C}_{18}\text{H}_{11}\text{O}_4\text{N}$. The elimination of a methyl group at $m/z\ 291\text{ [M-15]}^+$ suggests that ring D is monosubstituted.

The $^1\text{H NMR}$ spectrum (Figure 4.18 and 4.19) displayed the characteristic of AB doublet doublet of H-4 and H-5 at $\delta\ 7.74\ (d, J=5.2\ \text{Hz})$ and $\delta\ 8.88\ (d, J=5.2\ \text{Hz})$. The proton at C-5 was the most highly deshielded due to the neighbouring nitrogen atom. A proton singlet at $\delta\ 7.22$ indicates that C-3 in ring A is not substituted.

Two aromatic protons resonated at $\delta\ 7.13\ (1\text{H}, dd, J=7.5, 1.8\ \text{Hz})$ and $\delta\ 7.70\ (1\text{H}, d, J=8.2\ \text{Hz})$ were assigned for H-10 and H-9, respectively. Another aromatic proton at $\delta\ 8.35\ (1\text{H},$

dd, $J=7.5, 1.8$) were assigned to H-8. COSY spectrum (Figure 4.22 and 4.23) further confirmed the correlations of H-8/H-9, H-9/ H-10 and H4/H-5. A singlet at δ 6.37 (2H) indicates of a methylenedioxy group of an oxoaporphine at C-1 and C-2. A methoxy singlet can be observed at δ 4.07 (3H).

The ^{13}C and DEPT 135 NMR (Figure 4.20 and 4.21) spectra showed a total of eighteen carbon signals consisting of six methines, one methoxy, one methylenedioxy and ten quaternary carbons. One carbon signal assigned for methoxy group was observed at δ 56.4 ppm corresponding to C-11. This is further supported by the correlation of methoxy peak with C-11 in the HMBC spectrum (Figure 4.26). The HSQC correlations of the compound were shown in Figure 4.24 and 4.25 that showed all the complete proton to carbon assignments. Table 4.4 summarizes the ^1H and ^{13}C NMR of the compound.

Based on the combined analysis of 2D spectra and comparison with reported literature values, the compound was deduced as oxoputerine (**40**). This compound was also isolated for the first time from *Pseuduvaria monticola* in this study.

Table 4.4: ^1H NMR (600 MHz) and ^{13}C NMR (150 MHz) spectral data of oxoputerine (**40**) in CDCl_3 (δ in ppm, J in Hz).

Position	^1H -NMR (δ ppm)	^{13}C -NMR (δ ppm)	^{13}C -NMR (δ ppm) (De Fatima <i>et al.</i> , 2015)
1	-	147.7	147.7
1a	-	122.2	121.9
1b	-	121.0	121.6
2	-	151.8	151.9
3	7.22 (1H, <i>s</i>)	103.2	102.1
3a	-	135.4	135.2
4	7.74 (1H, <i>d</i> , $J=5.2$)	123.4	123.3
5	8.88 (1H, <i>d</i> , $J=5.2$)	144.8	144.0
6a	-	147.5	144.3
7	-	181.7	182.0
7a	-	135.3	133.2
8	8.35 (1H, <i>dd</i> , $J=7.5, 1.8$)	119.8	120.2
9	7.70 (1H, <i>d</i> , $J=8.2$)	134.8	129.5
10	7.13 (1H, <i>dd</i> , $J=7.5, 1.8$)	112.4	115.1
11-OMe	-	156.2	156.0
11a	-	120.3	123.1
CH_2O_2	6.37 (2H, <i>s</i>)	102.2	101.8
OCH_3	4.07 (3H, <i>s</i>)	56.6	57.0

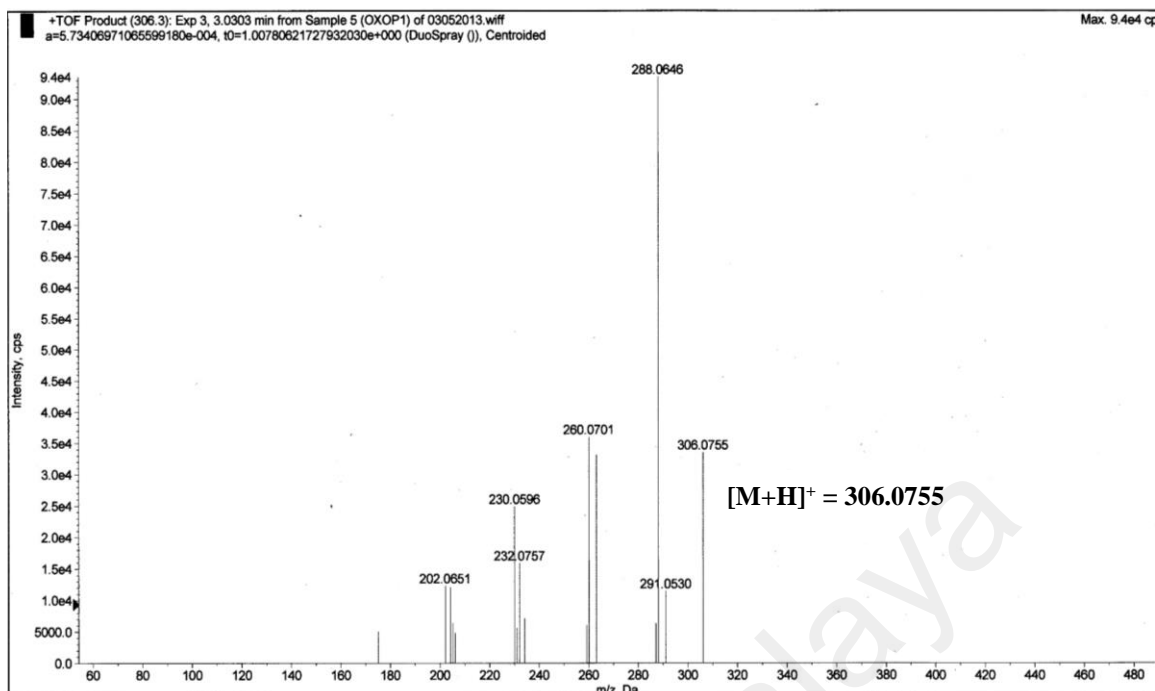


Fig 4.17: LC-MS spectrum of oxoputerine (40)

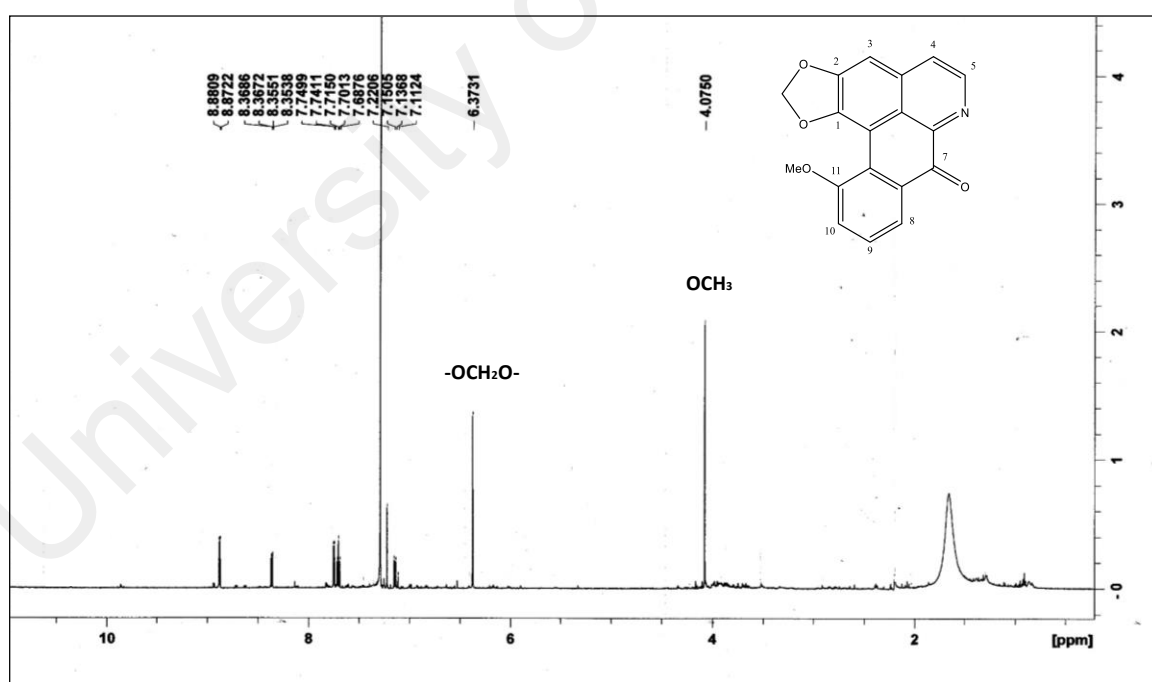


Fig 4.18: ¹H NMR spectrum of oxoputerine (40)

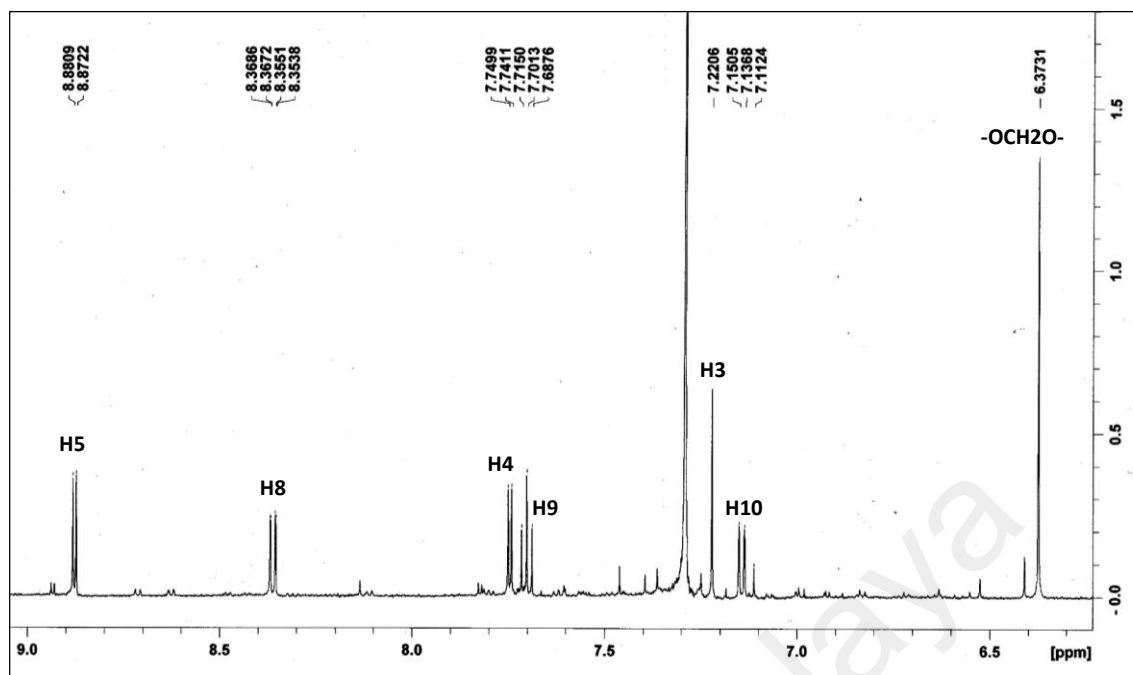


Fig 4.19: Expanded ^1H NMR of oxoputerine (**40**) in the aromatic region.

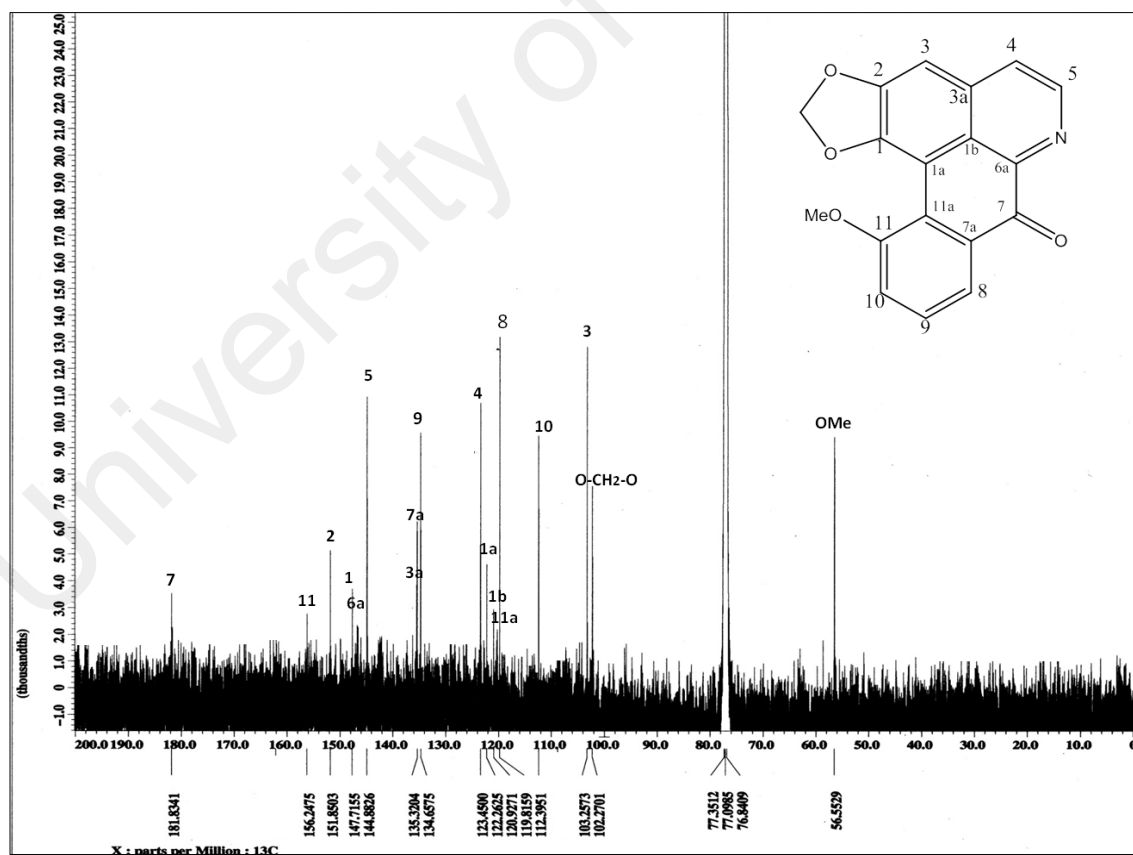


Fig. 4.20: ^{13}C NMR spectrum of oxoputerine (**40**)

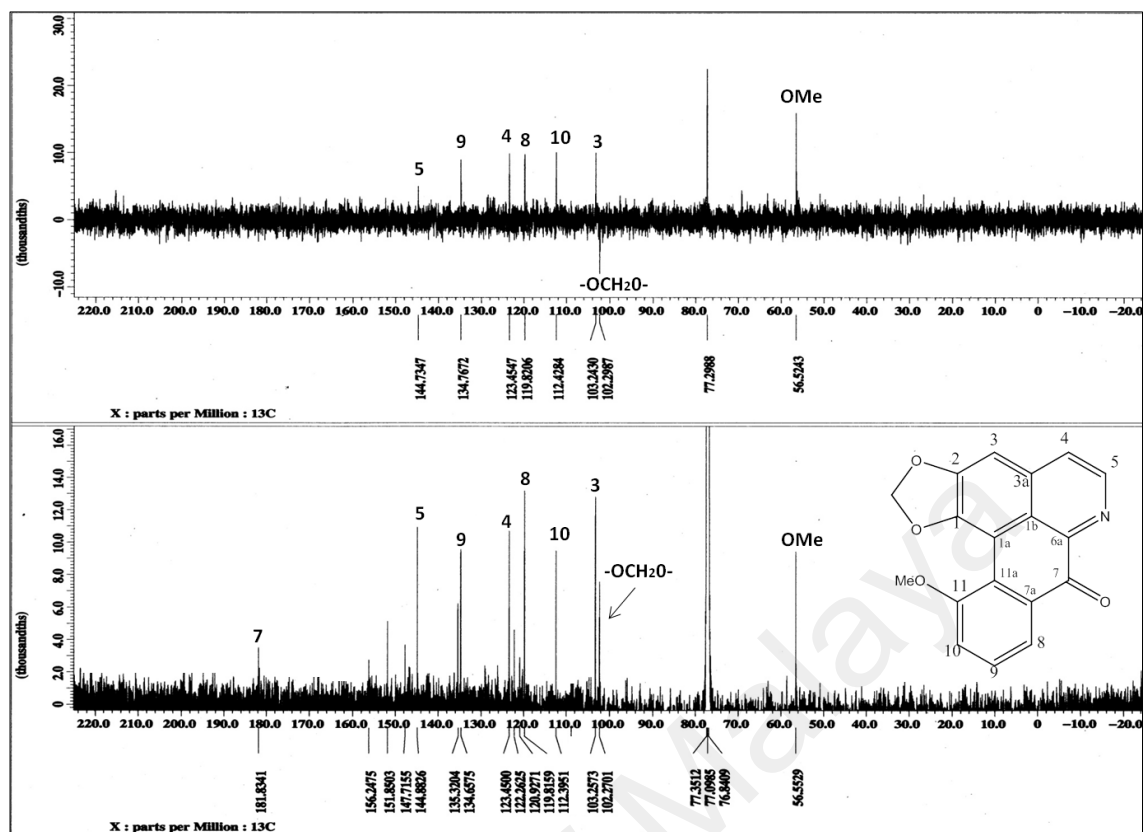


Fig. 4.21: DEPT 135 / ^{13}C NMR spectrum of oxoputerine (40)

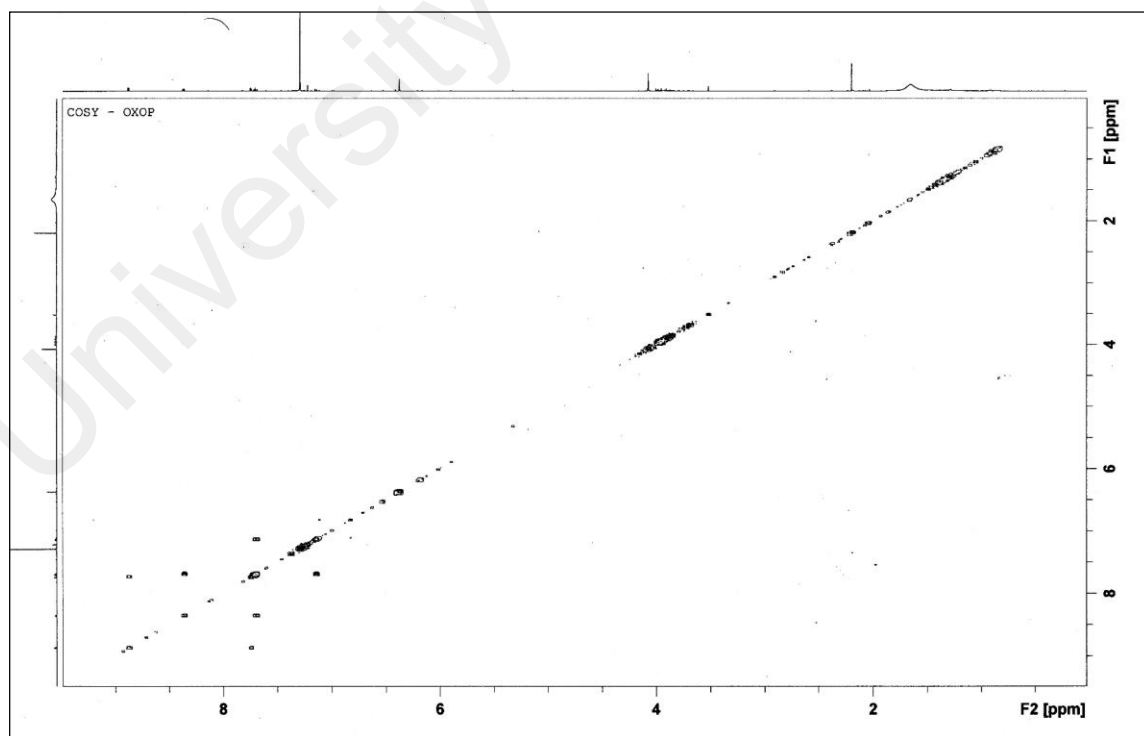


Fig 4.22: COSY spectrum of oxoputerine (40)

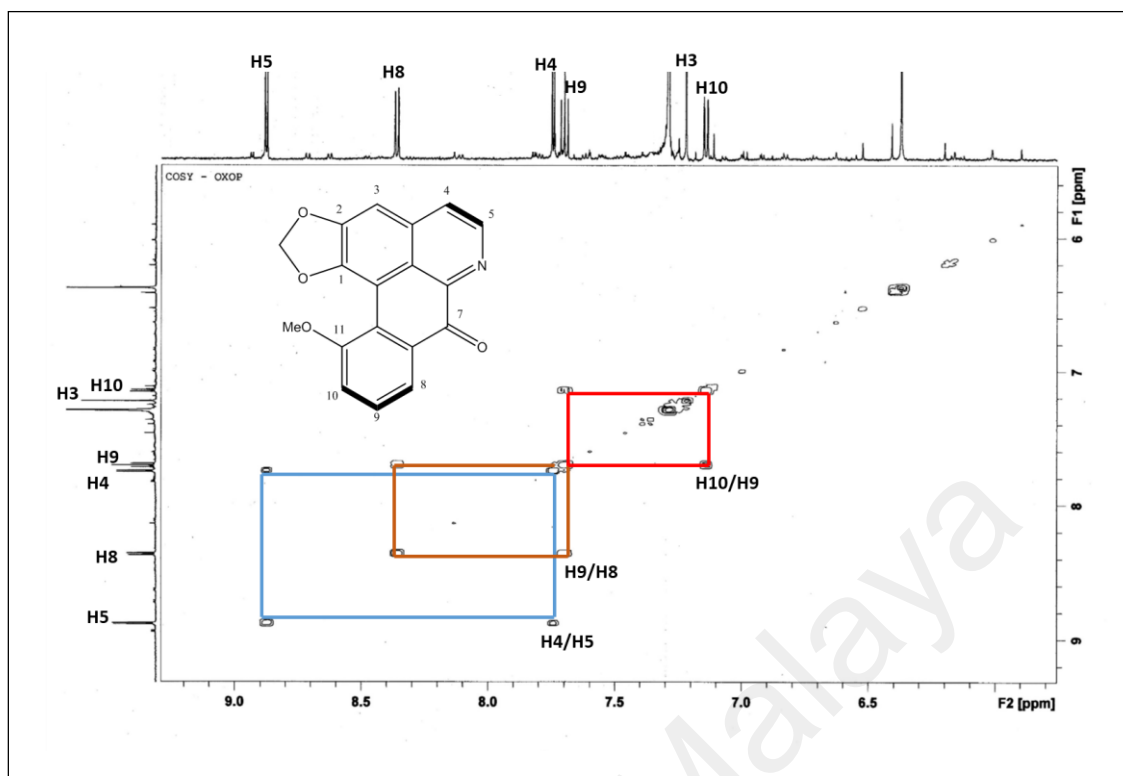


Fig 4.23: Expanded COSY spectrum of oxopterine (40)

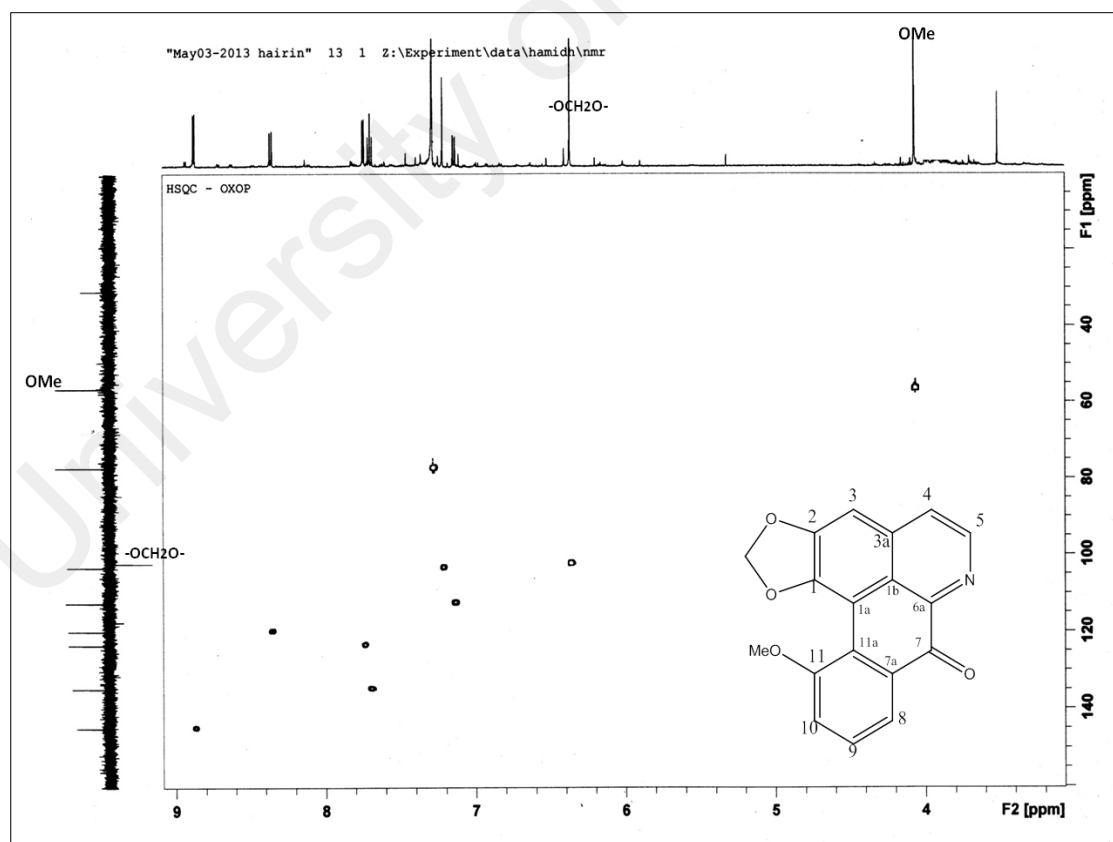


Fig 4.24: HSQC spectrum of oxopterine (40)

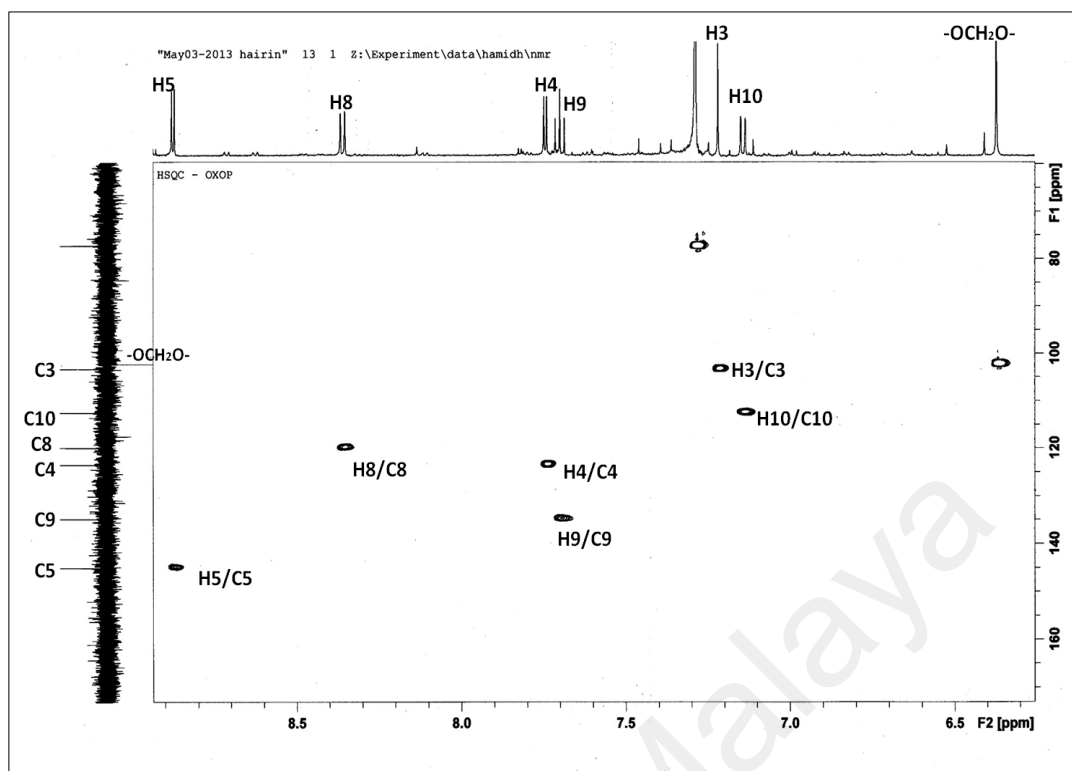


Fig 4.25: Expanded HSQC spectrum of oxopterine (40)

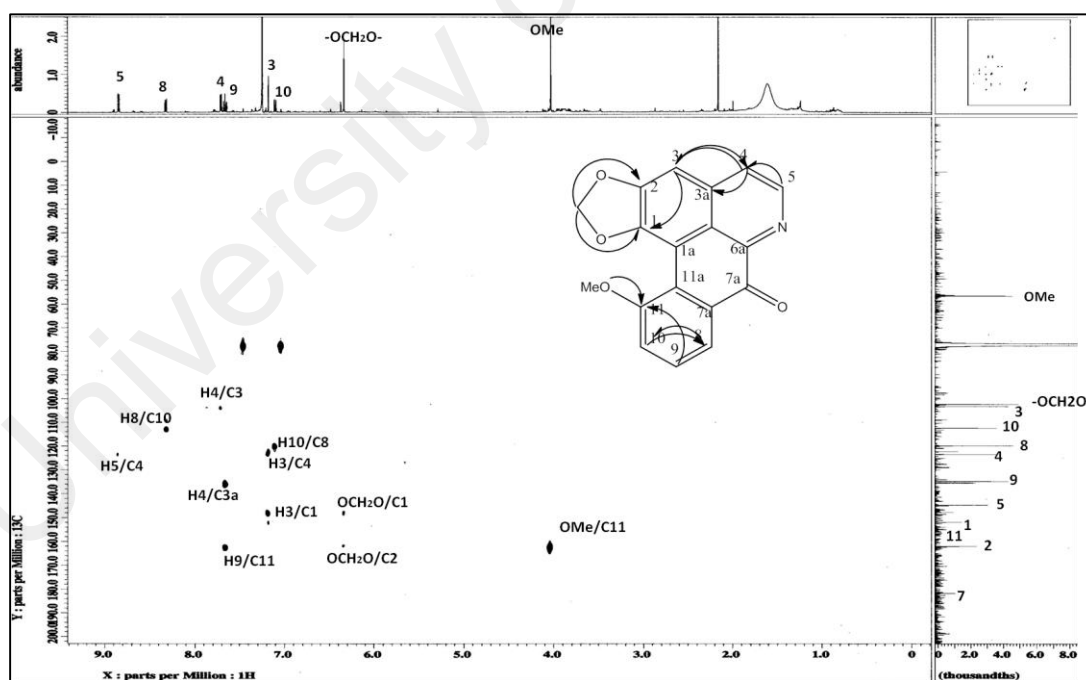
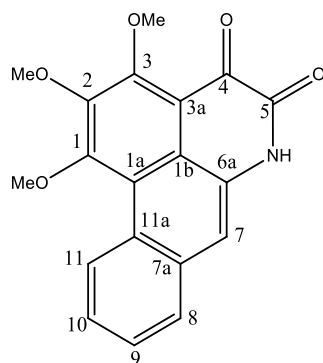


Fig 4.26: HMBC spectrum of oxopterine (40)

4.2.4 Ouregidione (4)



4

Alkaloid ouregidione (**4**) was isolated as orange amorphous solid. The UV spectrum exhibits maximum absorptions at 210, 228 and 480 nm indicating a highly conjugated system. The IR spectrum showed a conjugated ketone at 1733 cm^{-1} and 1455 cm^{-1} (aromatic moiety). The absorption band at 3582 cm^{-1} indicates the presence of NH functional group. On acidification with sulfuric acid, the compound turned reddish in colour indicating a weakly basic compound. The HREIMS (Figure 4.27) showed molecular ion peak at $m/z\ 338.1022\ [M+H]^+$ corresponding to the molecular formula of $C_{19}H_{15}NO_5$.

The ^1H NMR spectrum (Figure 4.28) showed three methoxy peaks at $\delta\ 4.15$, 4.09 and 4.01 (3H) assigned to C-3, C-2 and C1, respectively. Five aromatic protons were observed in the aromatic region. The proton signal for H-11 at $\delta\ 9.41$ (1H, $d, J= 8.6$ Hz) is more deshielded due to the anisotropic effect (deshielding effect) caused by ring A. Another peak appeared as one proton doublet at $\delta\ 7.95$ (1H, $d, J=8$ Hz) was assigned for H-8. Two aromatic protons at $\delta\ 7.56$ (1H, $dt, J=7.5, 1.8$ Hz) and $\delta\ 7.62$ (1H, $dt, J=7.6, 1.8$ Hz) correspond to H-9 and H-10, respectively. The peak at $\delta\ 7.86$ (1H) belongs to proton at C-7. The COSY spectrum (Figure 4.34 and 4.35) confirmed the correlation of aromatic

signals between H-8/H-9, H-9/H-10 and H-10/H-11 on ring D which clearly showed unsubstituted aromatic ring D.

Combined analysis of ^{13}C NMR and DEPT 135 spectrum (Figure 4.29 and 4.30) revealed a total of nineteen carbon signals attributed to three methoxyl groups, five methines and eleven quaternary carbons. The three carbon peaks for methoxy were observed at δ 61.1, 60.9 and 60.6 corresponding to C-3, C-2 and C-1 respectively. The peaks for two carbonyl groups at the most downfield can be observed at δ 160 ppm and δ 179 ppm, assigned for C-4 and C-5, respectively. The HMQC spectrum (Figure 4.32 and 4.33) showed all the correlations for the protons and the carbons. Table 4.5 summarizes the ^1H - and ^{13}C NMR of the compound.

Based on COSY (Figure 4.31), HMQC and HMBC correlations (Figure 4.34), the compound was confirmed as ouregidione (**4**) which had been previously isolated from *Pseuduvaria setosa* and *Pseuduvaria rugosa* (Taha *et al.*, 2011).

Table 4.5: ^1H NMR (500 MHz) and ^{13}C NMR (125 MHz) spectral data of ouregidione (**4**) in CDCl_3 (δ in ppm, J in Hz)

Position	^1H -NMR (δ ppm)	^{13}C -NMR (δ ppm)	^{13}C -NMR (δ ppm) (Sesang <i>et al.</i> , 2014)
1	-	158.1	158.6
1a	-	116.3	116.3
1b	-	119.9	120.3
2	-	147.8	147.5
3	-	160.3	160.4
3a	-	117.5	117.6
4	-	179.25	178.4
5	-	157.2	157.6
6a	-	128.9	128.3
7	7.85 (1H, <i>s</i>)	114.5	115.0
7a	-	130.3	131.2
8	7.95 (1H, <i>d</i> , $J=8.5$)	128.7	128.5
9	7.56 (1H, <i>dt</i> , $J=7.5,1.8$)	126.3	127.6
10	7.62 (1H, <i>dt</i> $J=7.6,1.8$)	127.1	127.4
11	9.41 (1H, <i>d</i> , $J=8.6$)	125.7	126.2
11a	-	127.6	127.2
1-OMe	4.08 (3H, <i>s</i>)	61.1	62.0
2-OMe	4.09 (3H, <i>s</i>)	60.9	61.7
3-OMe	4.15 (3H, <i>s</i>)	60.6	61.1

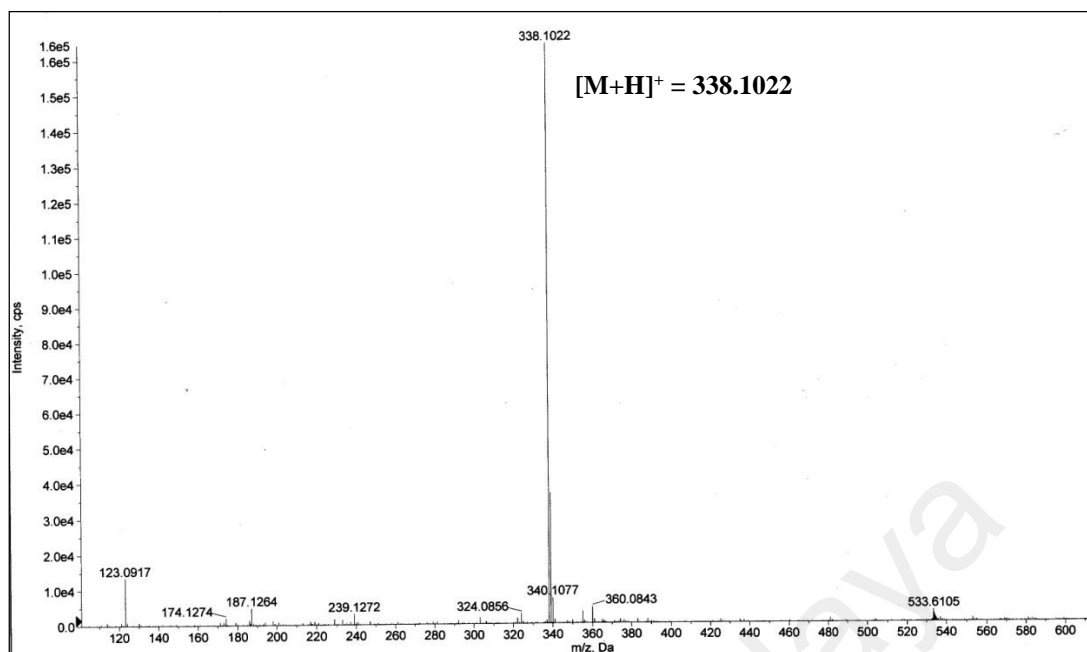


Fig. 4.27: LC-MS spectrum of ouregidione (4)

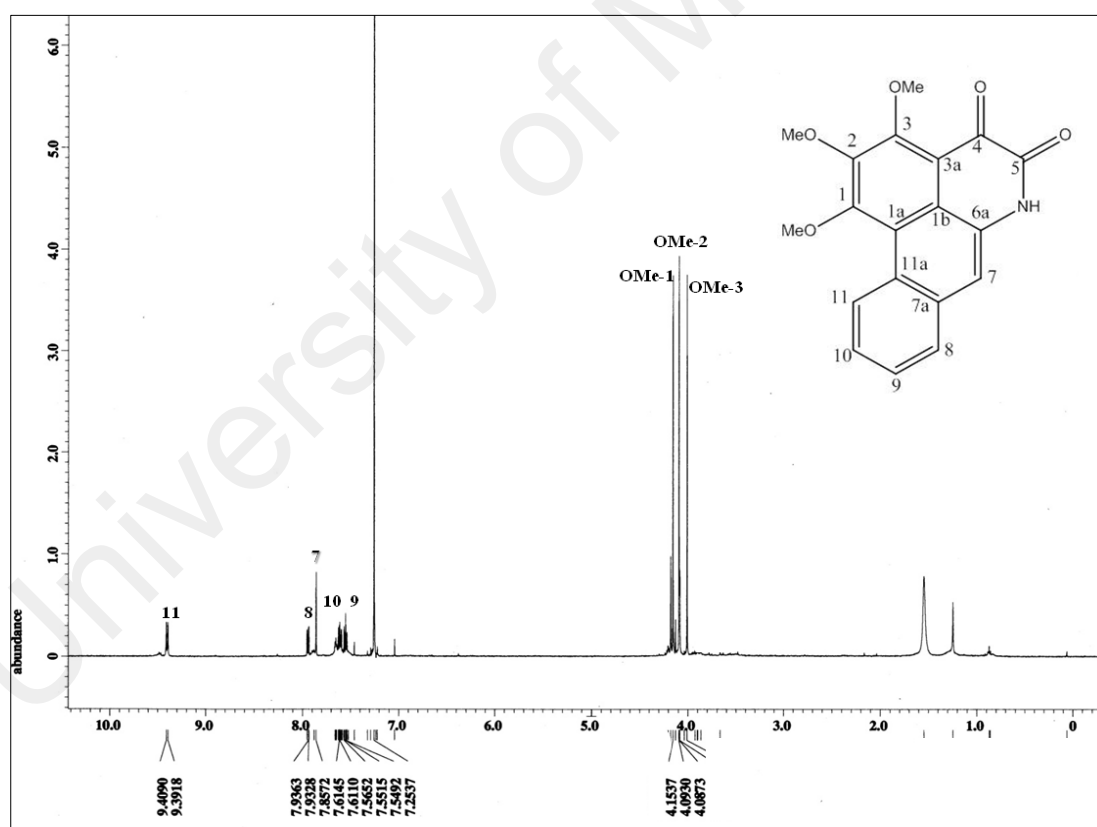


Fig. 4.28: ^1H NMR spectrum of ouregidione (4)

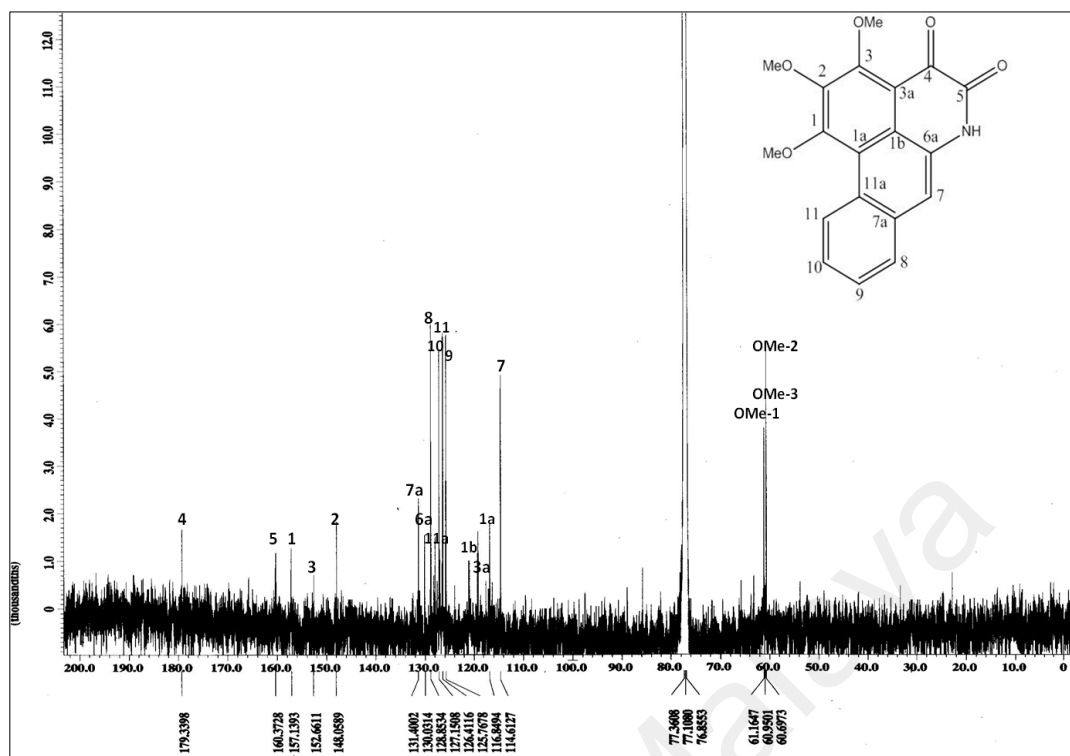


Fig. 4.29: ^{13}C NMR spectrum of ouregidione (4)

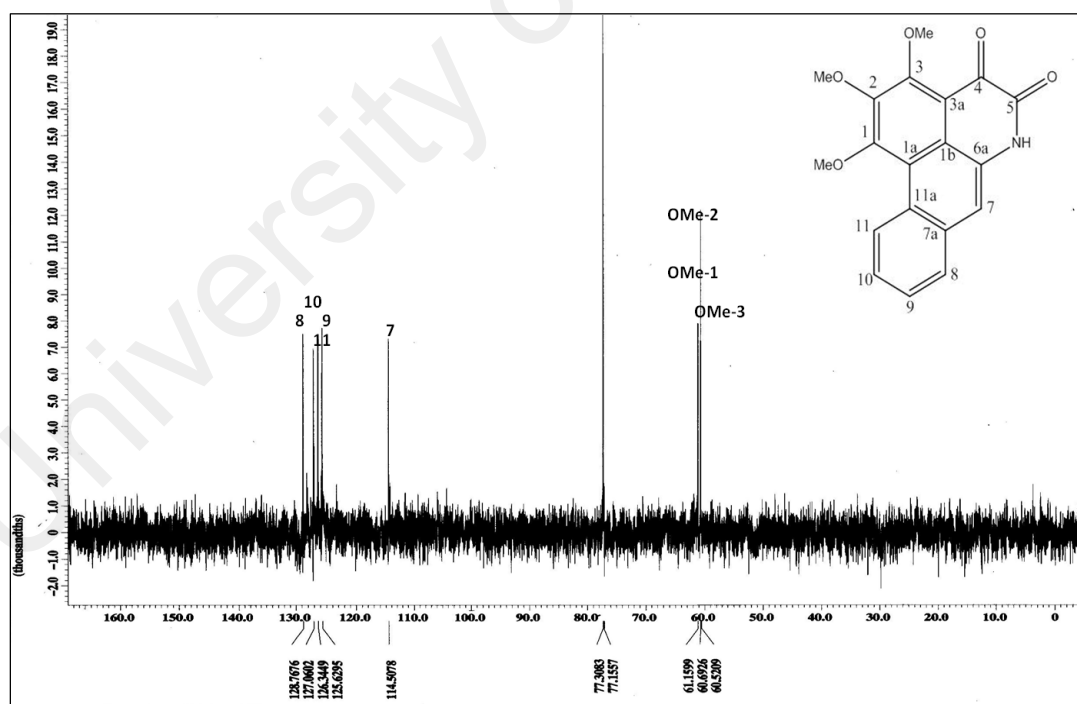


Fig. 4.30: DEPT 135 spectrum of ouregidione (4)

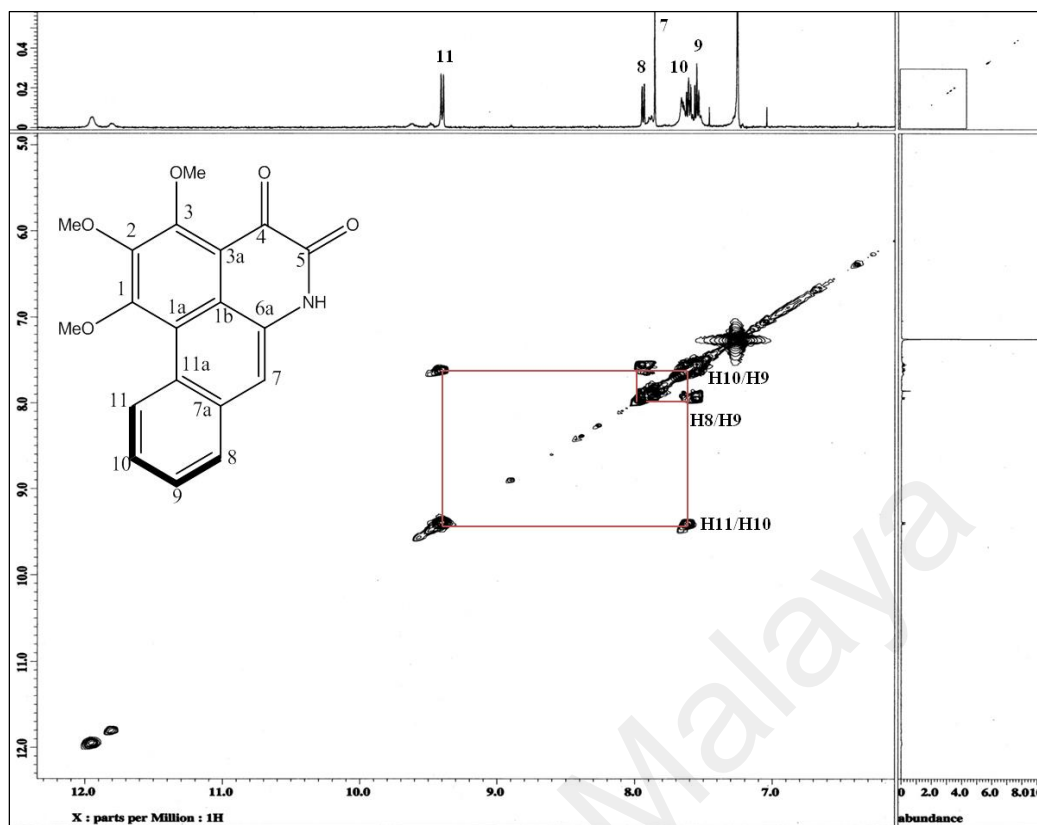


Fig. 4.31: Expanded COSY spectrum of ouregidione (4)

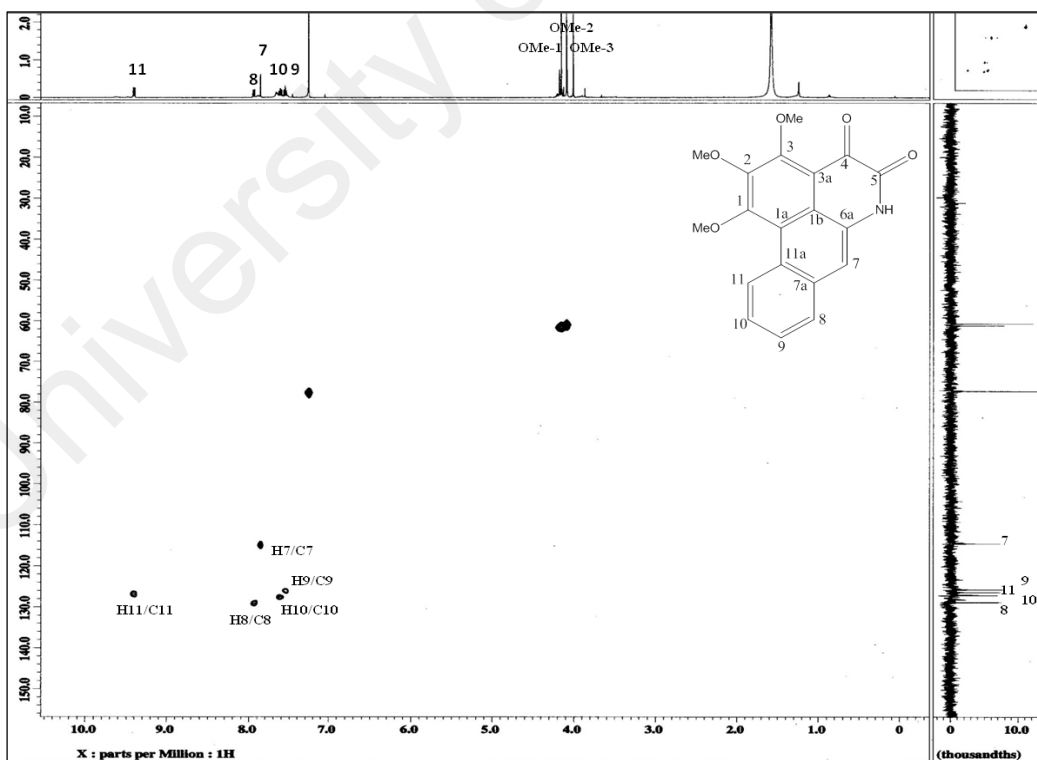


Fig. 4.32: HMQC spectrum of ouregidione (4)

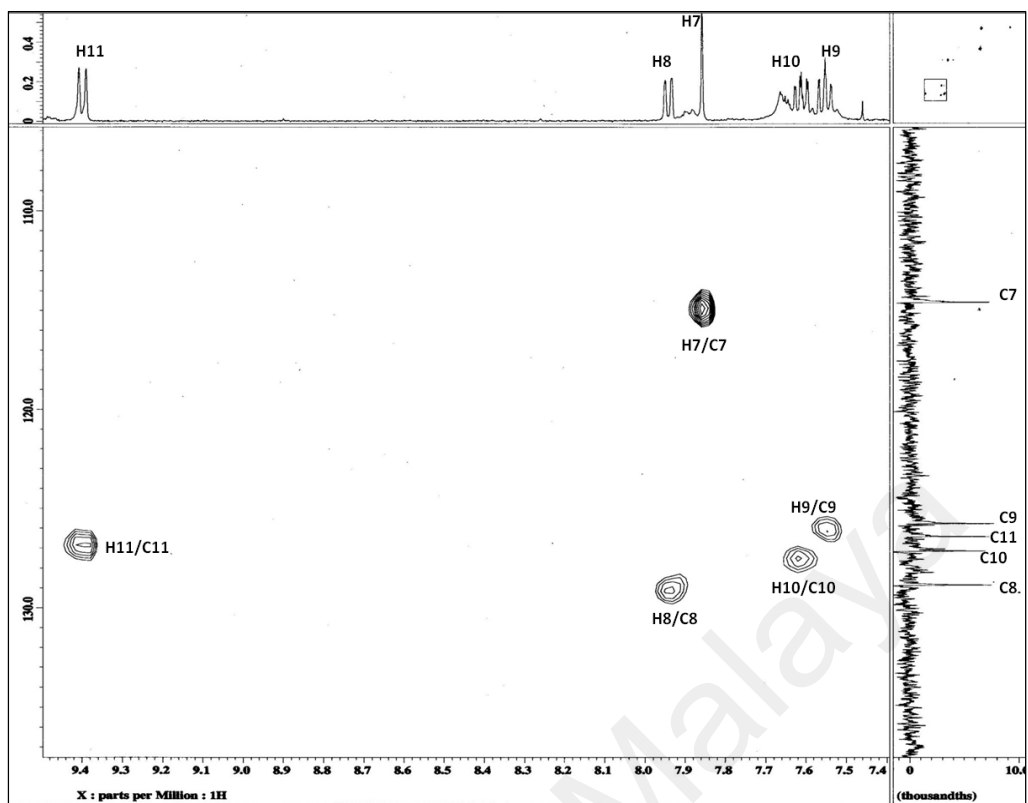


Fig. 4.33: Expanded HMQC spectrum of ouregidione (4)

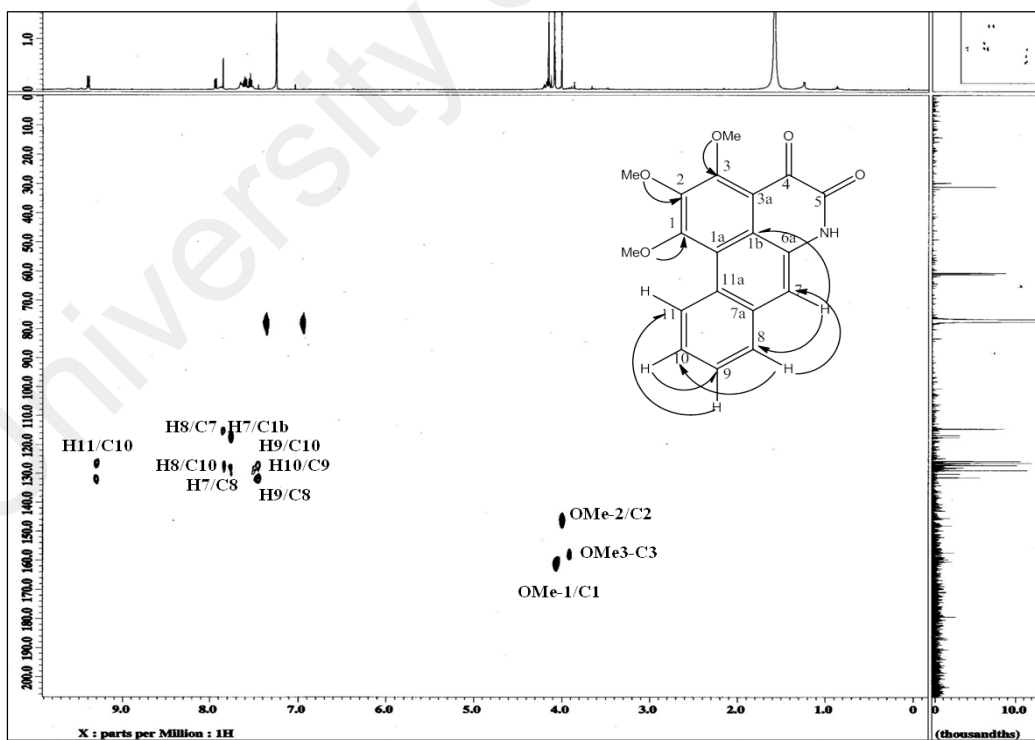
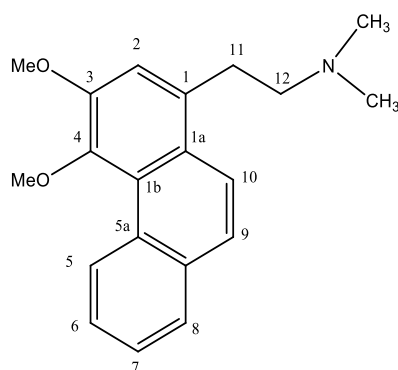


Fig. 4.34: HMBC correlation of ouregidione (4)

4.2.5 Atherosperminine (41)



41

Atherosperminine (**41**), an alkaloid was obtained as yellow amorphous solid. The UV spectrum exhibited absorption bands at 280 and 300 nm, typical of a phenanthrene alkaloid skeleton. The IR spectrum showed the absorption at 2850 and 1581 cm^{-1} indicating the presence of aromatic ring in the structure. The HREIMS (Figure 4.35) exhibited a molecular ion peak at m/z 310.1052 $[\text{M}+\text{H}]^+$ which correlated to the molecular formula of $\text{C}_{20}\text{H}_{23}\text{NO}_2$.

The ^1H NMR (Figure 4.36) exhibited two methoxyl signals which appeared as a singlet at δ 4.02 and δ 3.90 attached C-3 and C-4. One distinctive proton singlet corresponding to the N,N-dimethyl group was observed at δ 2.50. Two sets of doublets aromatic were observed at 7.84 (d , $J = 9.0$ Hz, H-10) and 7.65 (d , $J = 9.2$ Hz, H-9). One proton singlet was observed at 7.25 confirming that C-3 is substituted. The low field signals of three methoxy groups at 4.02 and 3.90 suggest that C-3 and C-4 are substituted by methoxyl group. A very downfield chemical shift was observed at 9.65 attributed to H-5 which was deshielded. The aromatic protons corresponding to H-6, H-7 and H-8 were observed at δ 7.71 (m), 7.60 (m) and 7.68 (dd , $J=9.6, 1.7$ Hz) respectively confirming that ring D was

not substituted. Finally, the aliphatic protons gave two sets of multiplets signals at δ 3.39 and δ 2.82 assigned to H-11 and H-12, respectively which were typical for phenantrene alkaloids.

The ^{13}C NMR and DEPT 135 spectra (Figure 4.37 and 4.38) showed twenty carbon signals consisting of two *N*-methyls, two methoxyl groups, two methylenes, seven methines and seven quaternary carbons. The chemical shift of the methoxyl group appeared at δ 59.9 and δ 56.7, assigned for C-3 and C-4-, respectively, whereas the *N*-CH₃ appeared at δ 44.9 ppm. Table 4.6 summarizes the ^1H - and ^{13}C NMR of the compound.

Combined analysis of COSY and HMQC (Figure 4.39 and 4.40) allowed the complete assignment of the protons and the carbons. In the HMBC spectrum (Figure 4.41 and Scheme 4.3), long range heteronuclear correlation between *N*-CH₃ and carbon at C-12 showed that *N*-CH₃ is not in the cyclic form.

Finally, comparison of the observed spectroscopic data with the literature values, confirmed the compound as atherosperminine (**41**) which was isolated for the first time from *Pseuduvaria monticola*.

Table 4.6: ^1H NMR (400 MHz) and ^{13}C NMR (100 MHz) spectral data of atherosperminine (**41**) in CDCl_3 (δ in ppm, J in Hz)

Position	^1H -NMR (δ ppm)	^{13}C -NMR (δ ppm)	^{13}C -NMR (δ ppm) (Wu <i>et al.</i> , 1990)
1	-	130.1	130.2
1a	-	126.0	126.2
1b	-	125.3	125.3
2	7.25 (1H, <i>s</i>)	114.9	114.8
3	-	150.9	150.9
4	-	146.2	146.0
5	9.65 (1H, <i>d</i> , $J=9.16$)	128.2	128.2
5a	-	132.0	132.9
6	7.60-7.71 (1H, <i>m</i>)	126.7	126.6
7	7.60-7.71 (1H, <i>m</i>)	125.7	125.8
8	7.68, (1H, <i>dd</i> , $J=9.6, 1.7$)	128.2	128.2
8a	-	132.8	133.3
9	7.65 (2H, <i>d</i> , $J=9.2$)	126.7	126.6
10	7.84 (2H, <i>d</i> , $J=9.0$)	122.1	122.5
11	3.39 (2H, <i>m</i>)	31.8	32.6
12	2.82 (2H, <i>m</i>)	60.5	61.1
3-OCH ₃	4.01 (3H, <i>s</i>)	59.9	56.7
4-OCH ₃	3.90 (3H, <i>s</i>)	56.7	59.9
N (-CH ₃) ₂	2.50 (3H, <i>s</i>)	44.9	45.6

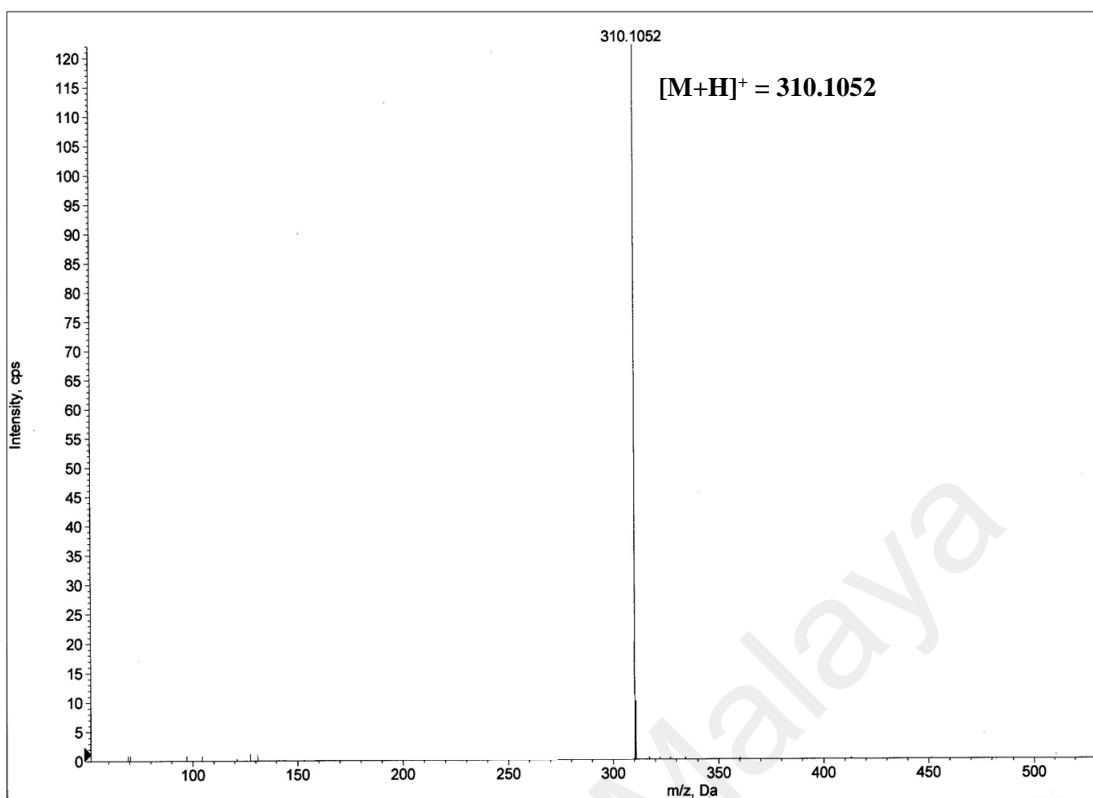


Fig. 4.35: LC-MS spectrum of atherosperminine (**41**)

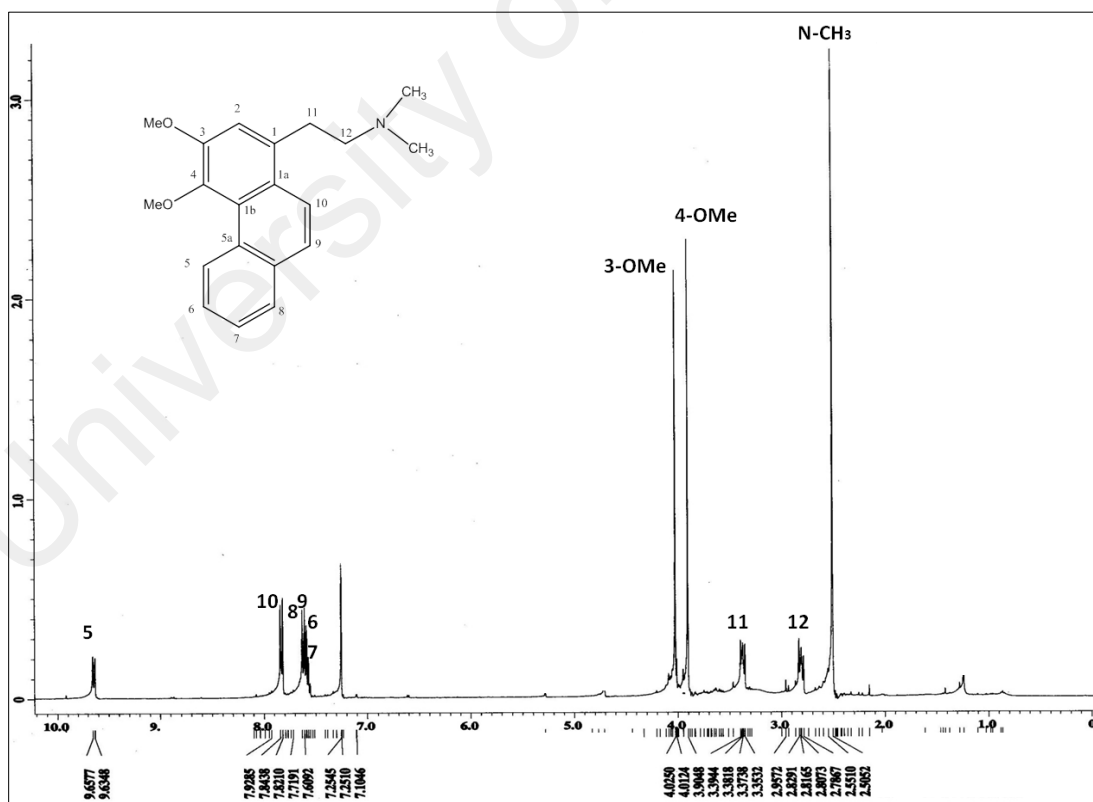


Fig. 4.36: ^1H NMR spectrum of atherosperminine (**41**)

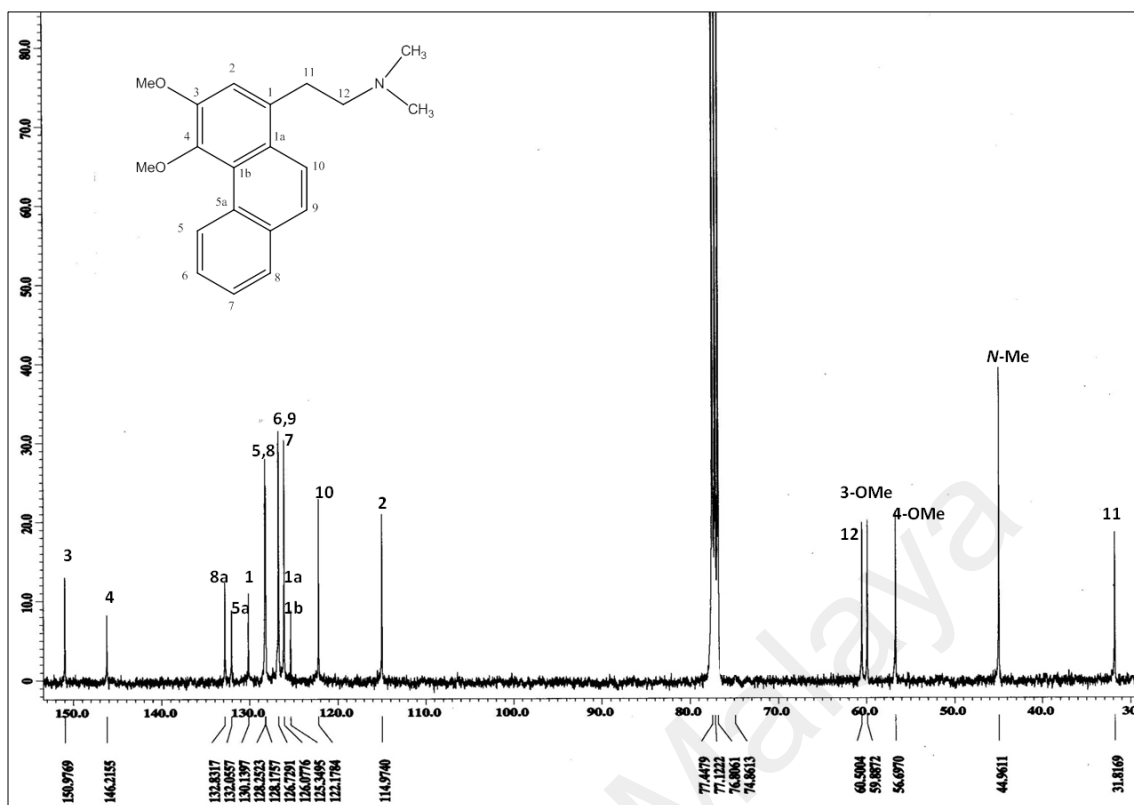


Fig. 4.37: ^{13}C NMR spectrum of atherosperminine (41)

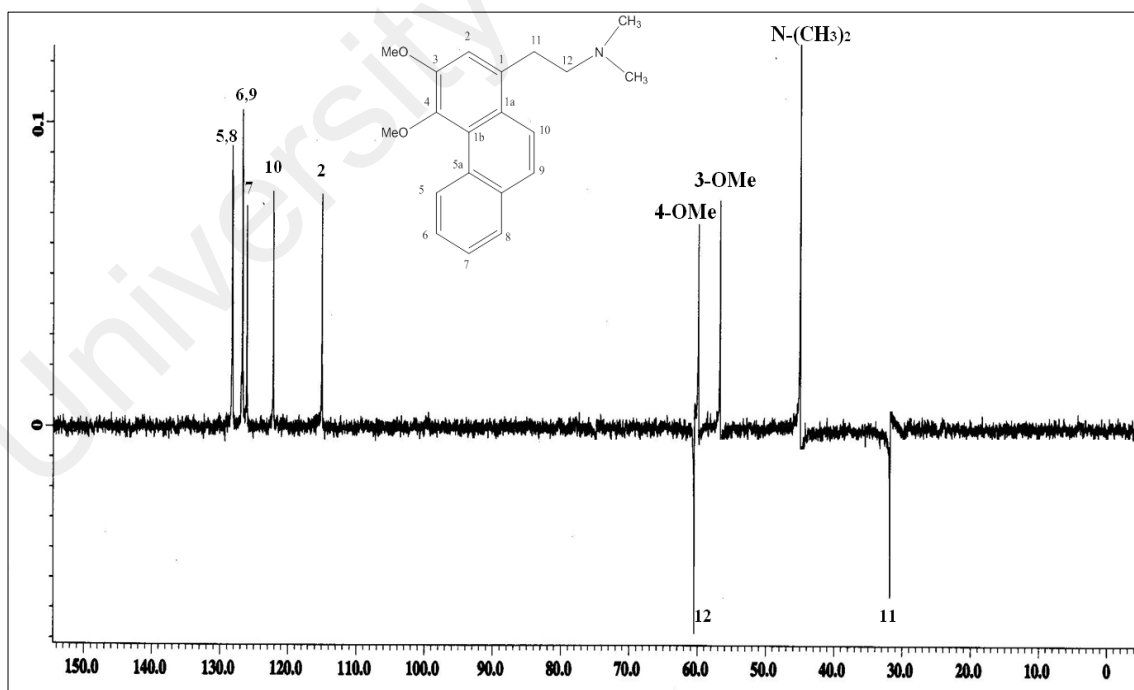


Fig. 4.38: DEPT 135 spectrum of atherosperminine (41)

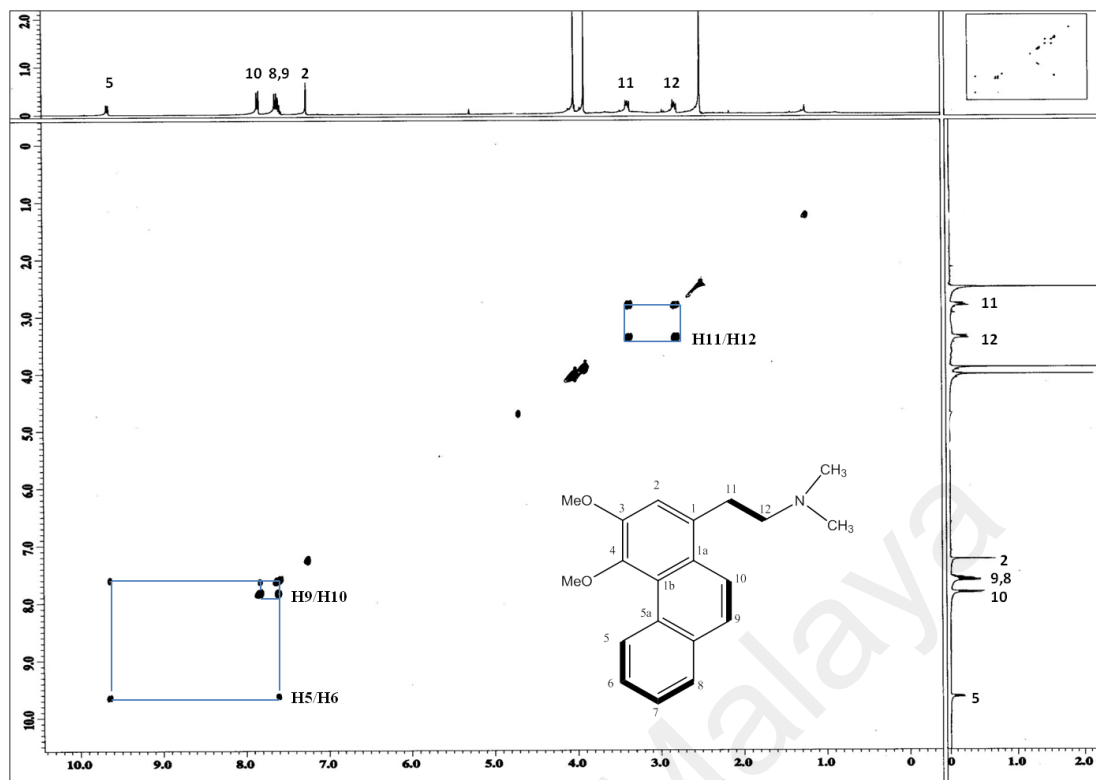


Fig. 4.39: COSY spectrum of atherosperminine (41)

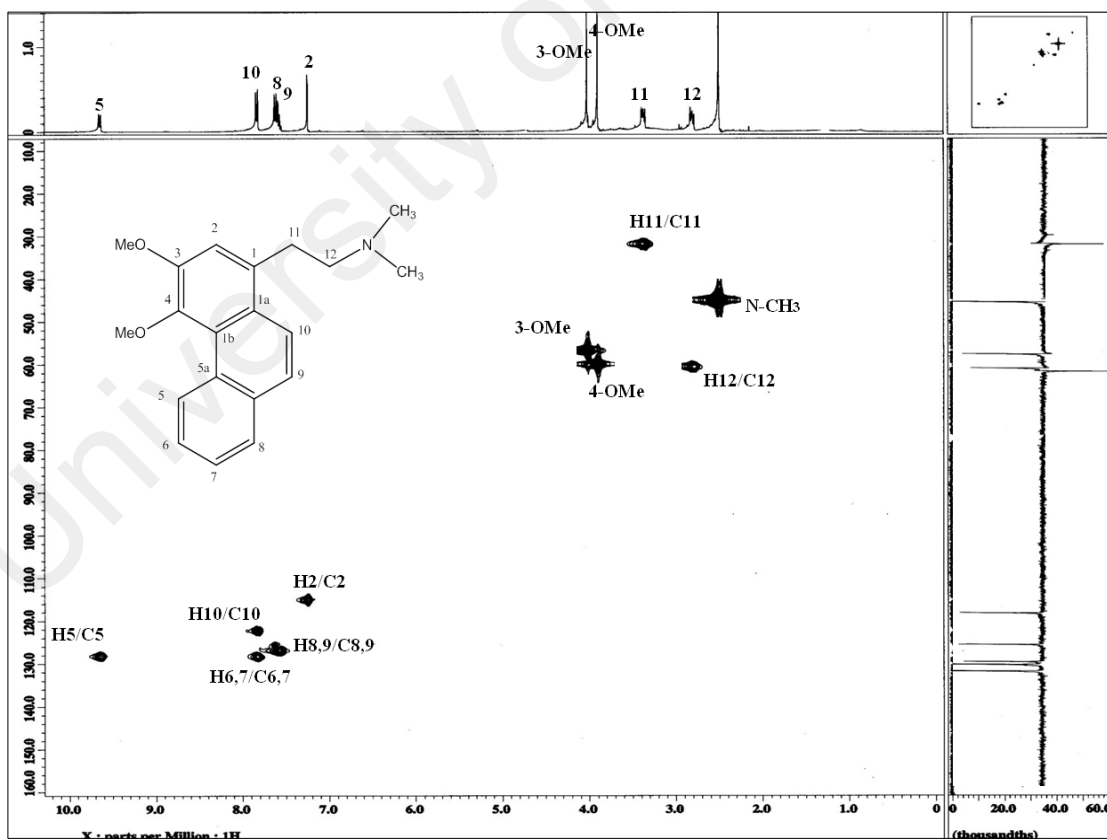


Fig. 4.40: HMQC spectrum of atherosperminine (41)

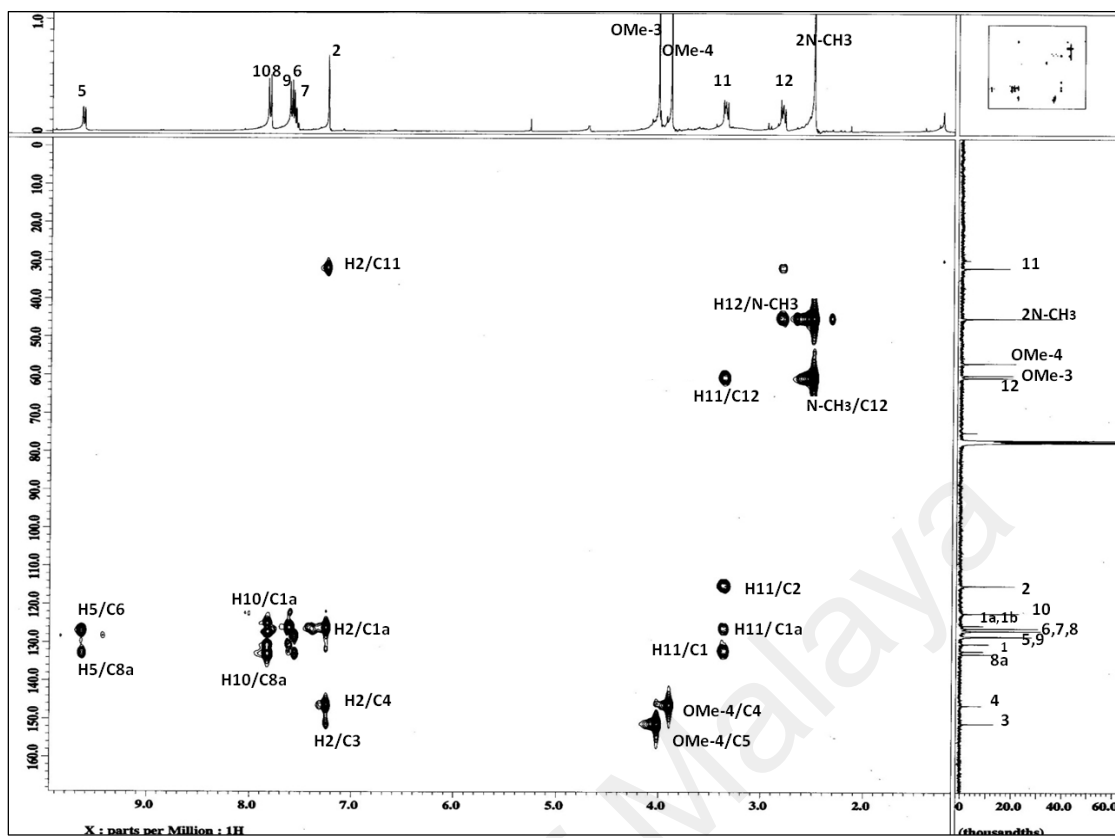
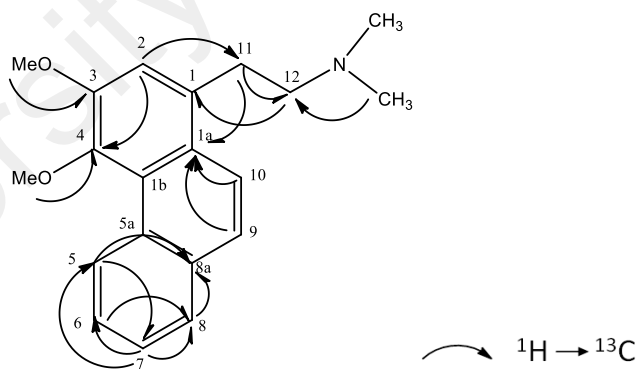
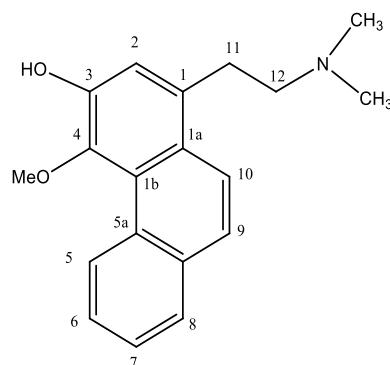


Fig. 4.41: HMBC spectrum of atherosperminine (**41**)



Scheme 4.3: The HMBC correlations of atherosperminine (**41**)

4.2.6 Argentinine (42)



(42)

Alkaloid argentinine (**42**) was obtained as brown amorphous solid. The UV spectrum exhibited absorption bands at 225 and 245 nm. The IR spectrum showed a broad absorption band at 3398 cm^{-1} for hydroxyl group (OH) and 2852 cm^{-1} for C-H stretching. The HREIMS (Figure 4.42) exhibited a molecular ion peak at m/z 296.1280 $[M+H]^+$ corresponding to the molecular formula of $C_{19}H_{21}NO_2$.

The ^1H NMR and ^{13}C NMR (Figure 4.43 and 4.44) of this compound was quite similar to that of atherosperminine (**41**) except that there was only one methoxy signal at δ 3.84 (3H) instead of two. One proton singlet (6H) was observed at δ 2.44 assigned for two *N*-methyl groups. Two set of doublets aromatic as an AB system were observed at δ 7.88 (1H, *d*, $J = 9.04$ Hz) and δ 7.63 (1H, *d*, $J = 9.28$ Hz) which corresponded to H-10 and H-9, respectively. One proton singlet was observed at δ 7.23 confirming that C-3 is substituted. The most downfield chemical shift was observed at δ 9.40 (1H, *d*, $J = 7.8$ Hz) attributed to H-5. The aromatic protons corresponding to H-6, H-7 and H-8 were observed at δ 7.61 (*m*), 7.63 (*m*) and 7.86 (*dd*, $J = 9.60, 1.70$ Hz) respectively. Two sets of multiplets signals at δ 3.26 and δ 2.67 were assigned to H-11 and H-12, respectively. The ^{13}C NMR

showed a total signals for nineteen carbons comprising of three methyls, two methylenes, five methines and nine quaternary carbons. The peak for methoxy group appeared at δ 58.8, and the *N*-methyl group can be observed at δ 43.3. Table 4.7 summarizes the ^1H - and ^{13}C NMR of the compound.

Finally, comparison of all spectroscopic data with published literature, confirmed the compound as argentinine (**42**) which isolated for the first time from *Pseuduvaria monticola*.

University of Malaya

Table 4.7: ^1H NMR (400 MHz) and ^{13}C NMR (100MHz) spectral data of argentinine (**42**) in CDCl_3 (δ in ppm, J in Hz)

Position	^1H NMR (δ ppm)	^{13}C NMR (δ ppm)	^{13}C NMR (δ ppm) (Castedo <i>et al.</i> ,1991)
1	-	129.1	130.1
1a	-	126.9	126.2
1b	-	124.6	125.0
2	7.23 (1H, <i>s</i>)	114.2	114.5
3	-	147.8	148.9
4	-	144.8	145.0
5	9.40 (1H, <i>d</i> , $J=7.8$)	127.2	128.2
5a	-	132.9	132.8
6	7.61-7.63 (1H, <i>m</i>)	126.1	126.6
7	7.61-7.63 (1H, <i>m</i>)	126.8	126.9
8	7.86(1H, <i>m</i>)	128.7	128.8
8a	-	132.9	133.0
9	7.61 (2H, <i>d</i> , $J=9.3$)	127.1	126.8
10	7.88 (2H, <i>d</i> , $J=9.3$)	122.1	122.5
11	3.29 (2H, <i>m</i>)	26.9	27.6
12	2.72 (2H, <i>m</i>)	58.6	57.1
4-OCH ₃	3.84 (3H, <i>s</i>)	60.2	60.5
N (-CH ₃) ₂	2.44 (6H, <i>s</i>)	43.3	44.2

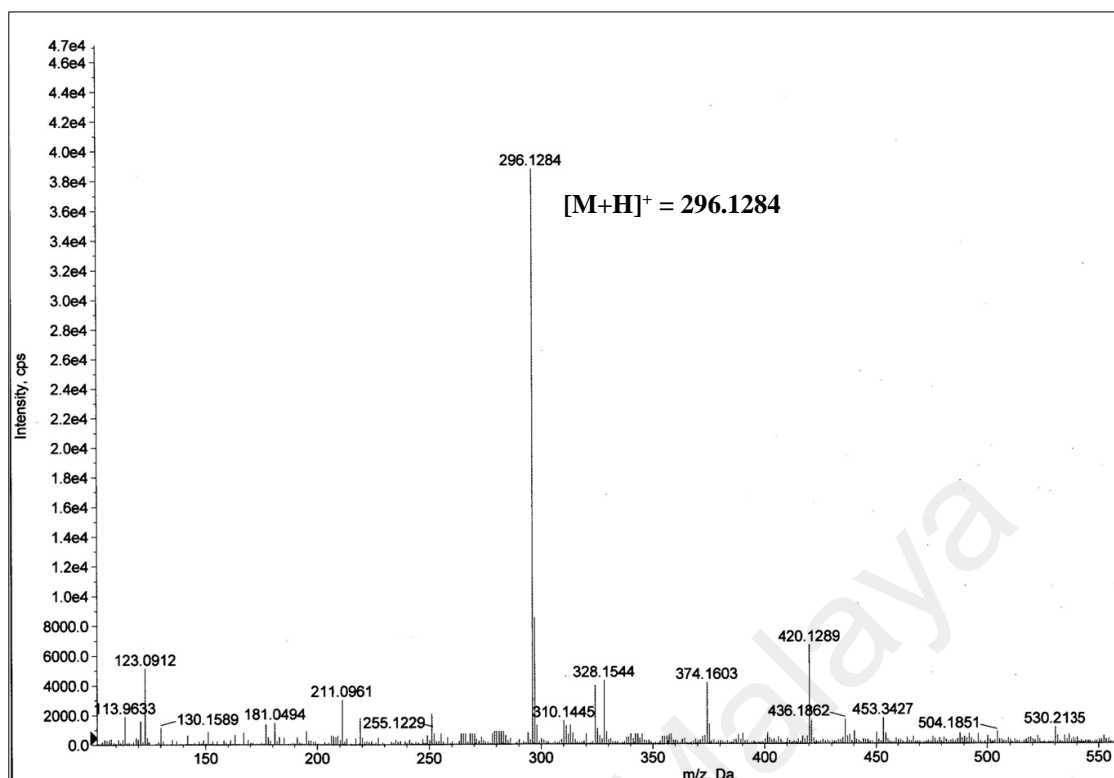


Fig. 4.42: LC-MS spectrum of argentinine (42)

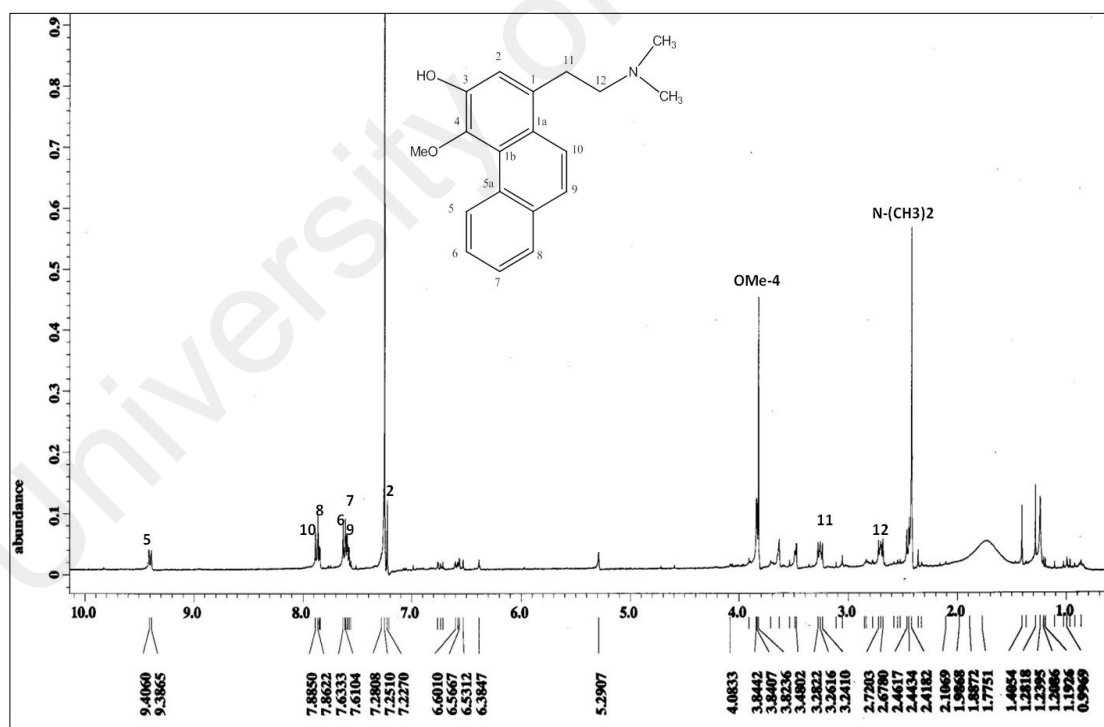


Fig. 4.43: ^1H NMR spectrum of argentinine (42)

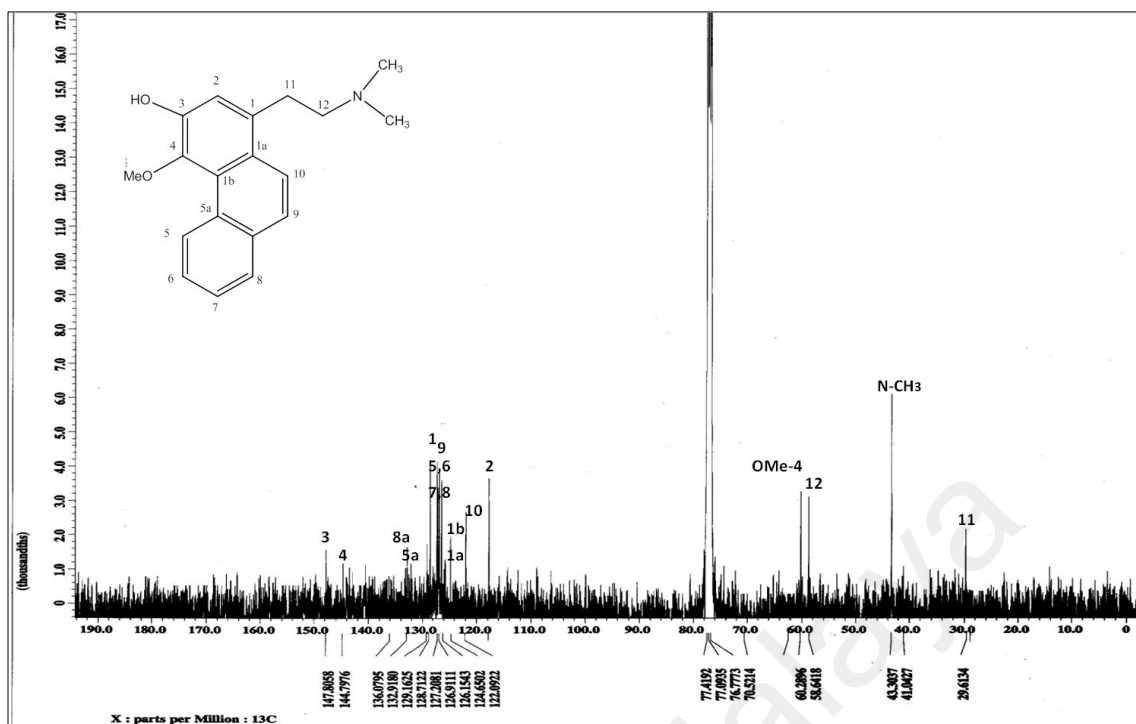
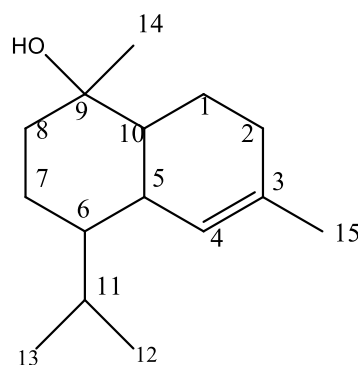


Fig. 4.44: ^{13}C NMR spectrum of argentinine (42)

4.2.7 Tau Cadinol (43)



43

Tau cadinol (**43**), a sesquiterpene was isolated as colorless oil. The UV spectrum showed absorption peaks at 200 and 191 nm. The IR spectrum revealed absorption peak at 3368 cm^{-1} corresponding to hydroxyl group. A complete NMR spectrum could not be obtained because of insufficient sample amount (< 3 mg) and due to its volatility. Therefore, GC-MSTOF was used to identify the compound.

In the GC-MS spectrum (Figure 4.45 and 4.46), the peak showed $[\text{M}-18]^+$ at 204 due to the elimination of water (H_2O) which gave the molecular weight as 222 corresponding to the molecular formula $\text{C}_{15}\text{H}_{26}\text{O}$. When the compound was injected into GC-MSTOF using insert (1 μL), the compound was matched to the NIST library spectrum (SI = 87 %) of tau cadinol (**43**), a sesquiterpene which was first isolated from *Pseuduvaria monticola*.

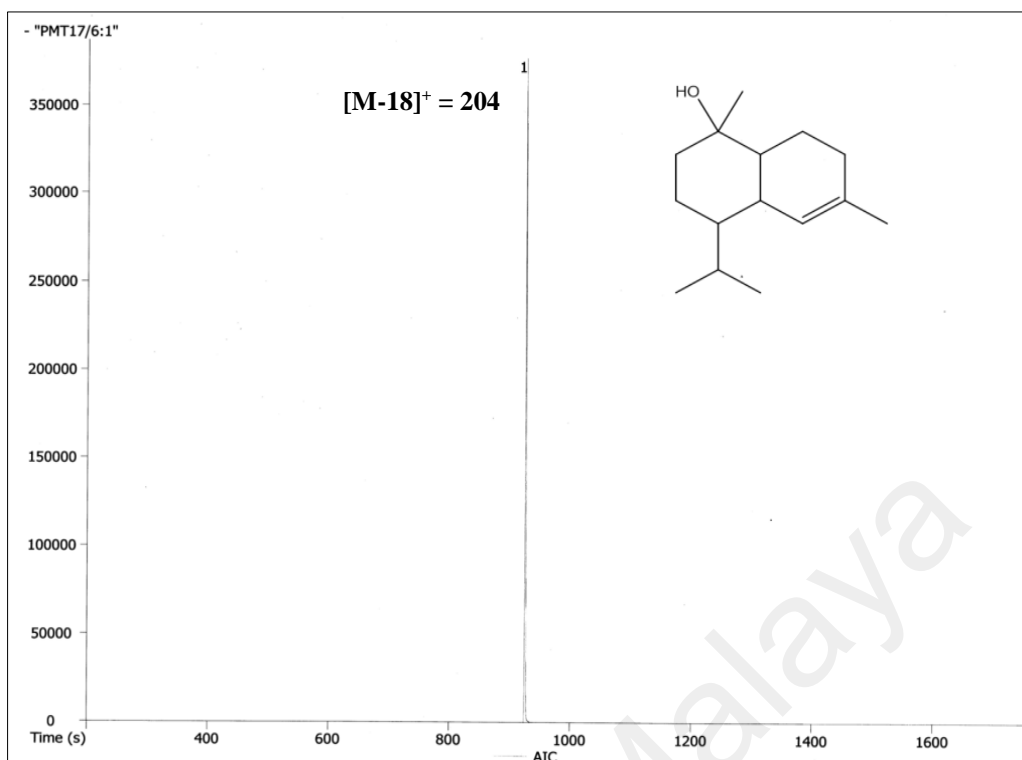


Fig. 4.45: GC-MS peak of tau cadinol (**43**)

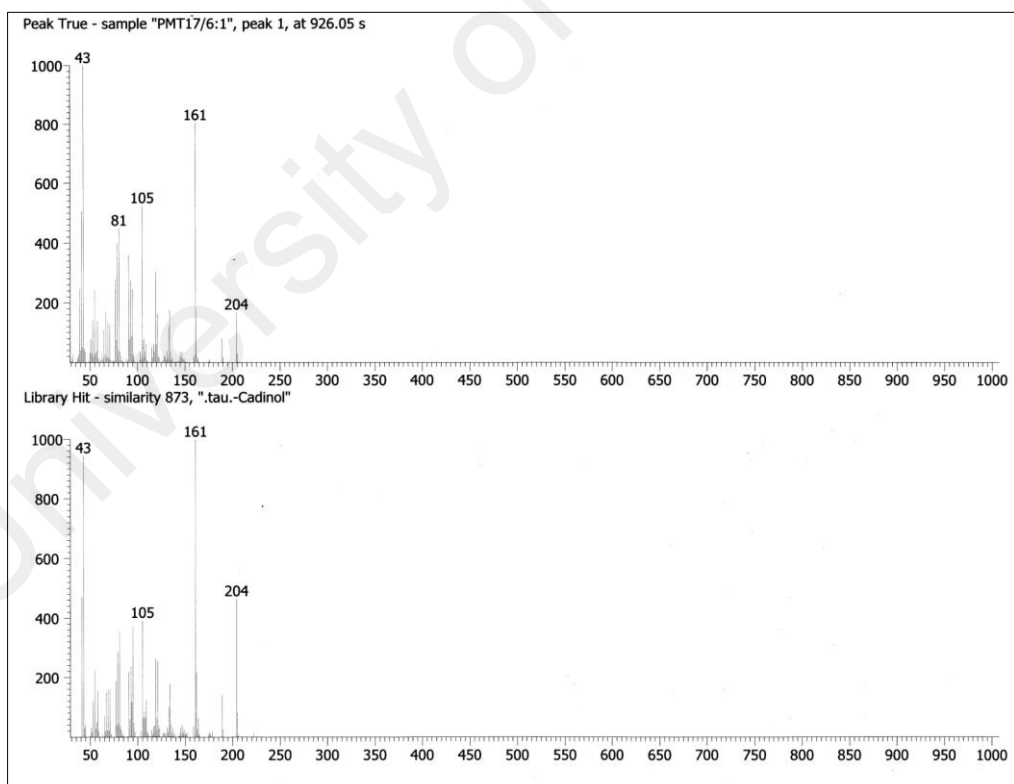
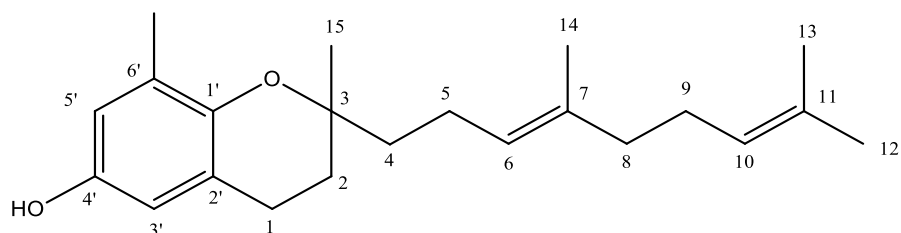


Fig. 4.46: GC-MS spectrum of tau cadinol (**43**)

4.2.8 Oligandrol (14)



14

Oligandrol (**14**), a benzopyran derivative was obtained as yellow oil. The UV spectrum showed absorption band at 295 nm. The IR spectrum suggested the presence of absorption bands for hydroxyl (3475 cm^{-1}), olefin (1645 cm^{-1}) and aromatic ring (1734 cm^{-1}). The molecular formula of this compound was established as $\text{C}_{22}\text{H}_{32}\text{O}_2$ from the molecular ion peak $[\text{M}+\text{H}]^+$ at m/z 329.2338 (Figure 4.47).

The ^1H NMR spectrum (Figure 4.48) revealed five tertiary methyls at δ_{H} 1.25, 1.58, 1.59, 1.89 and 2.13 in the aliphatic region. In the aromatic region, two olefinic methines were observed at δ_{H} 6.04 (*t*, $J=7.0, 1.2\text{ Hz}$, 1H) and δ_{H} 5.35 (*t*, $J=7.0, 1.2\text{ Hz}$, 1H) assigned for H-6 and H-10, respectively. Two meta-coupled aromatic protons were observed at δ_{H} 6.37 (*d*, $J=2.8\text{ Hz}$, 1H) and δ_{H} 6.47 (*d*, $J=2.8\text{ Hz}$, 1H) assigned for H-5' and H-3', respectively.

Both analysis of ^{13}C NMR and DEPT 135 spectra (Figure 4.49 ad 4.50) revealed 22 carbon signals attributed to five methyls, six methylenes, four methines and seven quaternary carbons. One quaternary carbon peak at δ 76.85 represented C-3 which was bonded to oxygen. The ^1H - ^1H COSY spectrum (Figure 4.51) showed connectivity between H-1 and H-2, H-4, H-5 and H-6 and H-8, H-9 and H-10. The HMQC spectrum (Figure 4.52) showed all the correlations of protons and carbons in the compound.

The HMBC correlations (Figure 4.53 and Scheme 4.4) from H-2, H-4 and H-5 to C-3 confirmed the attachment of the prenylated chain to the chroman ring at C-3. Table 4.8 summarizes the ^1H and ^{13}C NMR of the compound.

Based on the spectroscopic data and comparison with published literature, the compound was established as oligandrol (**14**) which was also discovered from *Pseuduvaria indochinensis* Merr. (Zhao *et al.*, 2014) and first time isolated from *Pseuduvaria monticola*.

University of Malaya

Table 4.8: ^1H NMR (500 MHz) and ^{13}C NMR (125 MHz) spectral data of oligandrol (**14**) in CDCl_3 (δ in ppm, J in Hz)

Position	^1H -NMR (δ ppm)	^{13}C -NMR (δ ppm)	^{13}C -NMR (δ ppm) (Banfield <i>et al.</i> , 1994)
1	2.68 (2H, <i>m</i>)	22.2	23.1
2	1.75 (2H, <i>m</i>)	31.4	31.5
3	-	76.8	83.3
4	1.49-1.58 (2H, <i>m</i>)	39.6	39.5
5	2.02-2.11 (2H, <i>m</i>)	22.1	22.9
6	5.35 (1H, <i>t</i> , $J=7.0, 1.2$)	125.1	124.7
7	-	134.4	134.5
8	2.05-2.10 (2H, <i>m</i>)	39.0	39.1
9	2.59 (2H, <i>m</i>)	28.2	27.4
10	6.04 (1H, <i>t</i> , $J=7.0, 1.2$)	146.3	146.5
11	-	127.3	128.0
12	1.59 (3H, <i>s</i>)	22.9	23.1
13	1.89 (3H, <i>s</i>)	19.3	18.9
CH ₃ -14	1.60 (3H, <i>s</i>)	15.8	16.1
CH ₃ -15	1.25 (3H, <i>s</i>)	24.1	25.0
1'	-	146.0	146.2
2'	-	121.3	121.3
3'	6.38 (1H, <i>d</i> , $J=2.5$)	112.7	112.5
4'	-	147.8	147.8
5'	6.47 (1H, <i>d</i> , $J=2.5$)	115.7	115.3
6'	-	126.9	126.4
CH ₃ -6'	2.11 (3H, <i>s</i>)	16.1	16.0

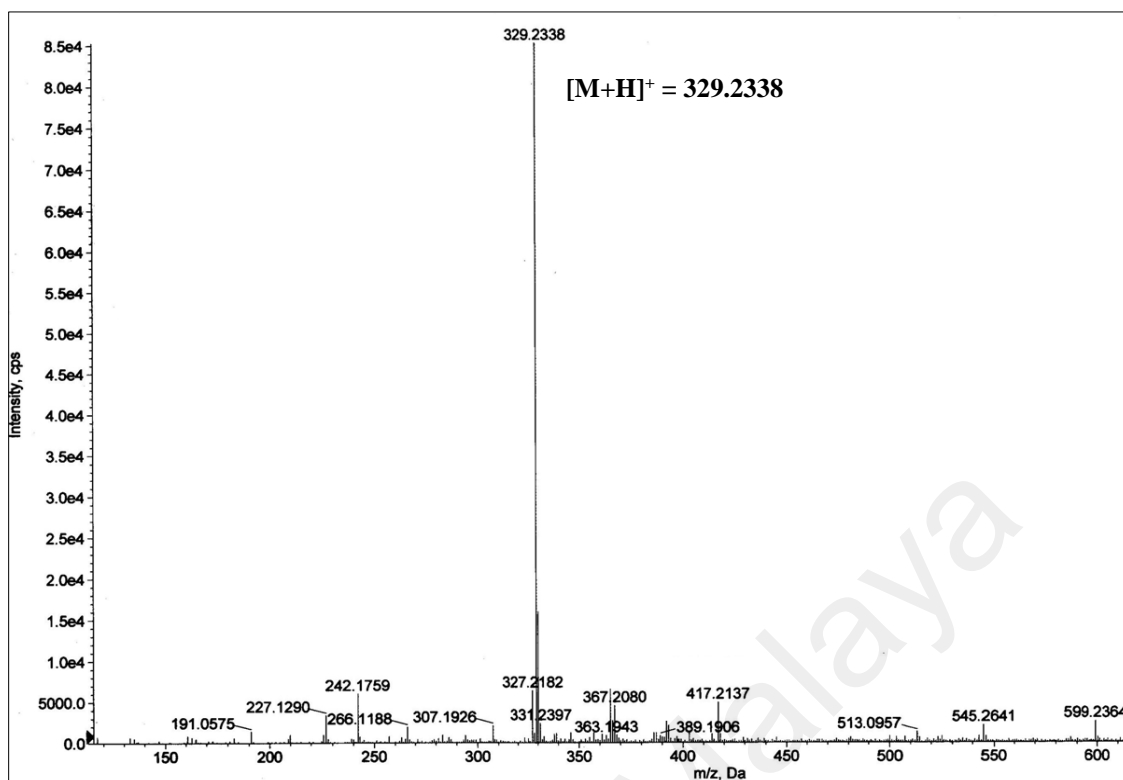


Fig. 4.47: LC-MS of oligandrol (**14**)

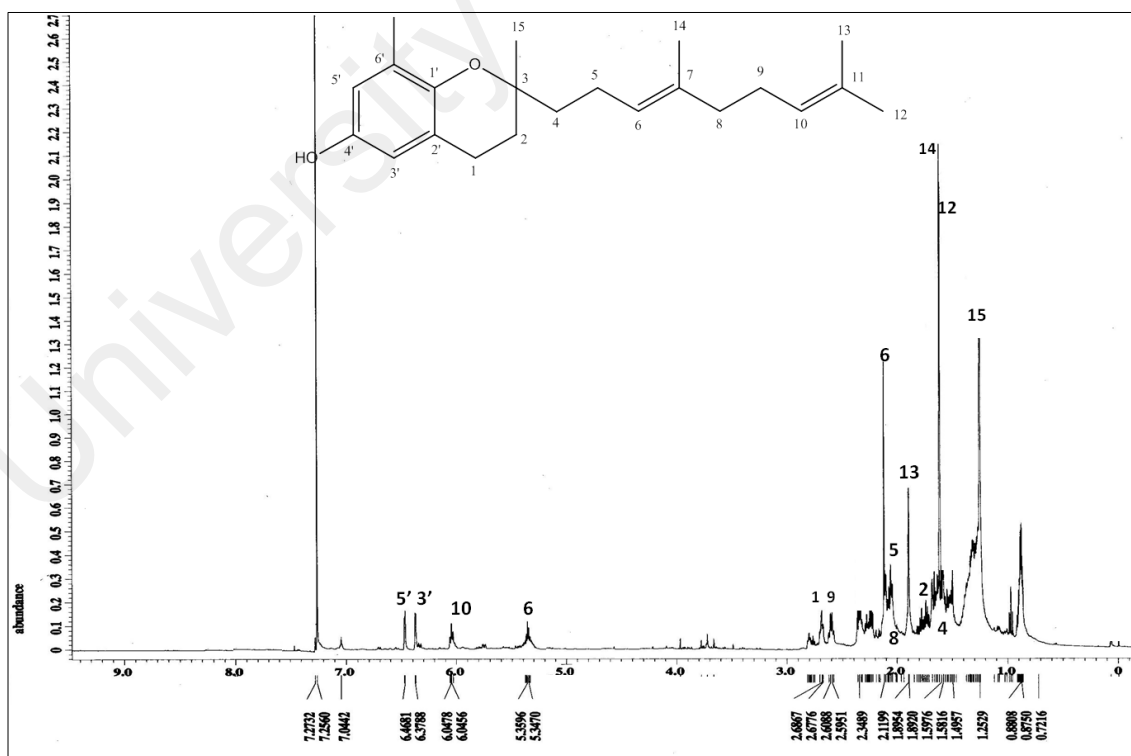


Fig. 4.48: ^1H NMR spectrum of oligandrol (**14**)

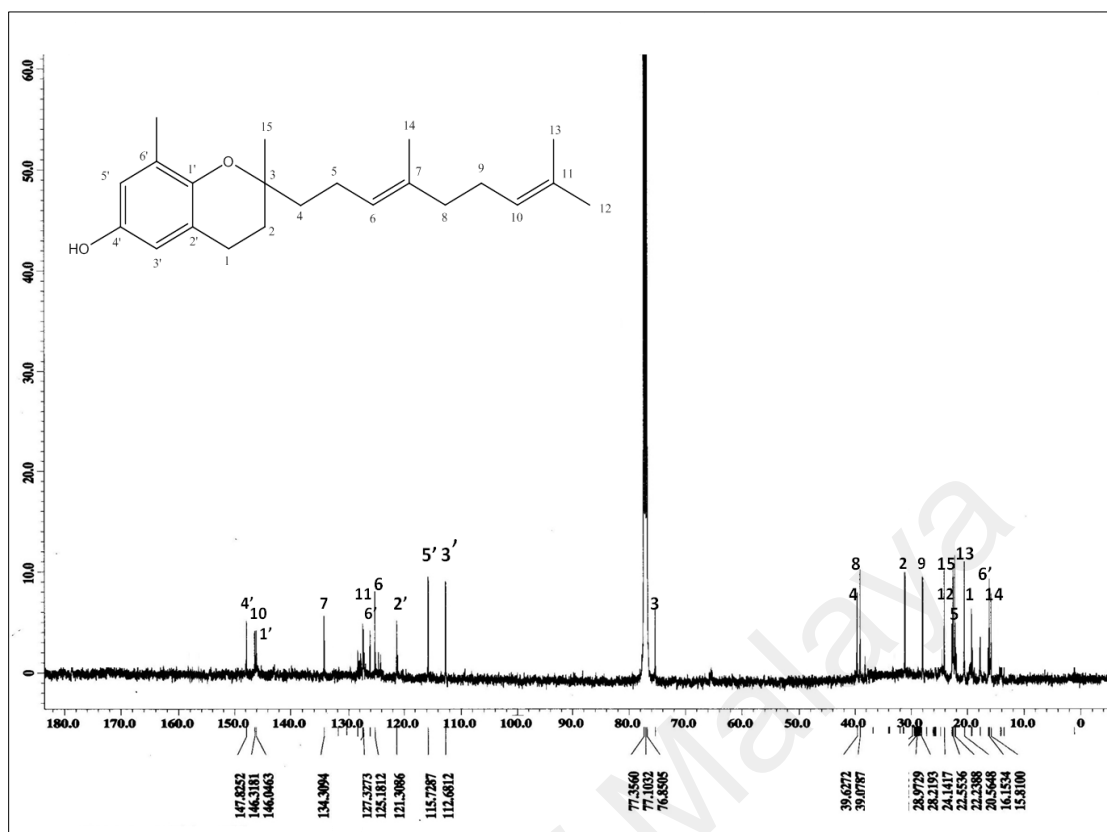


Fig. 4.49: ^{13}C NMR spectrum of oligandrol (14)

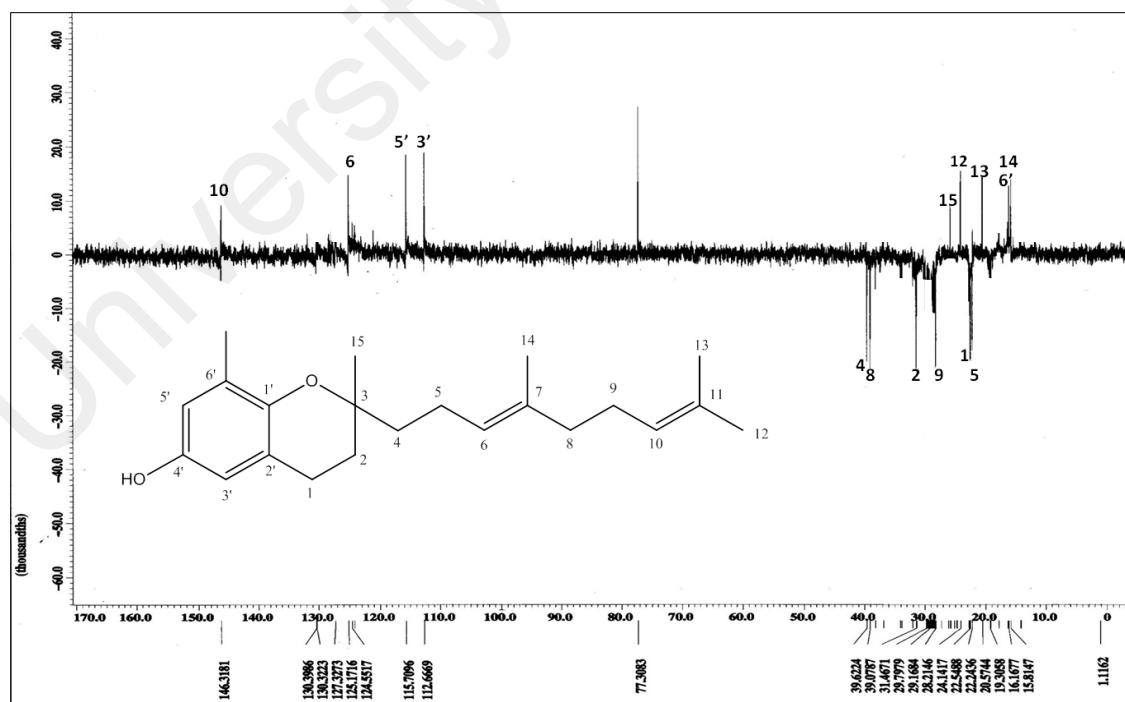


Fig. 4.50: DEPT 135 NMR spectrum of oligandrol (14)

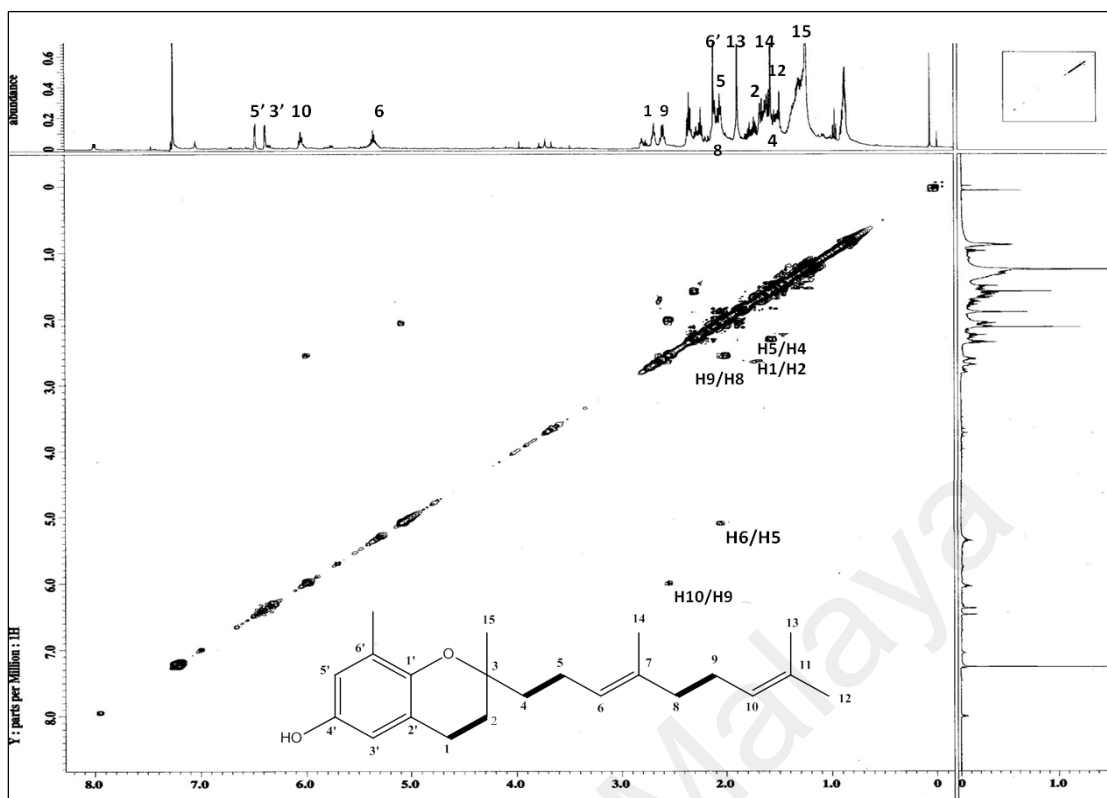


Fig. 4.51: COSY spectrum of oligandrol (14)

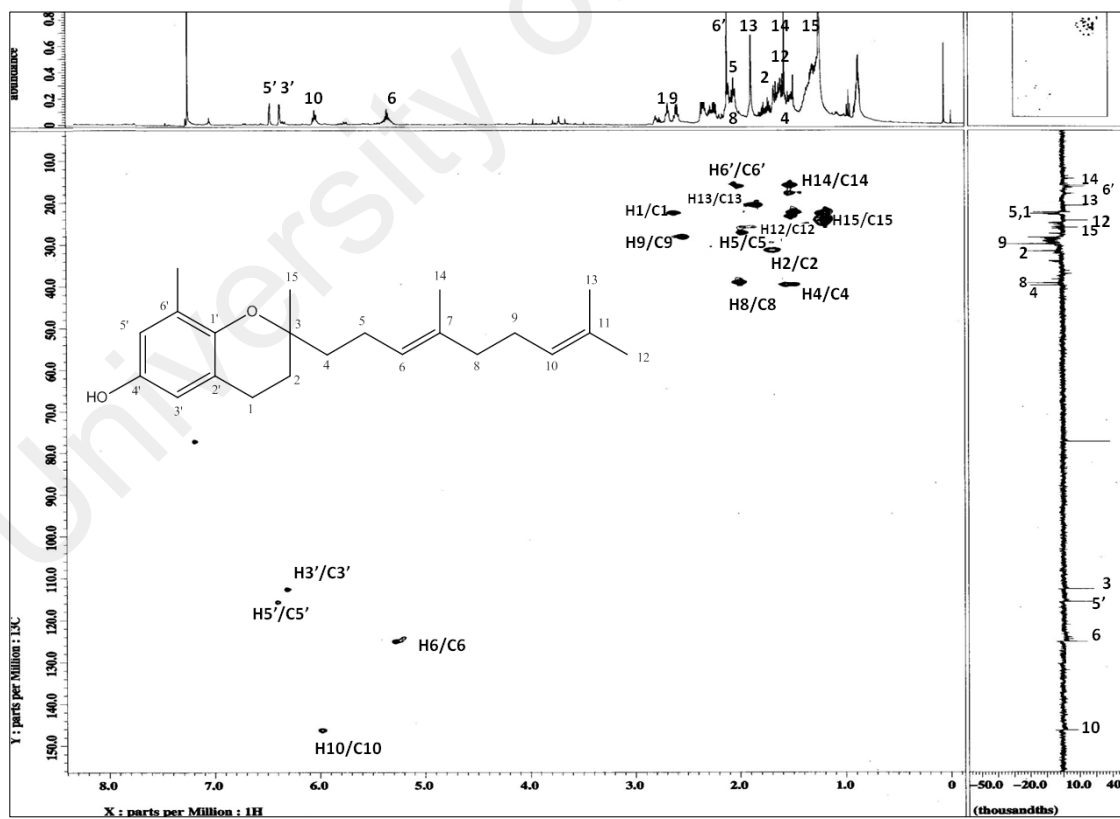


Fig. 4.52: HMQC spectrum of oligandrol (14)

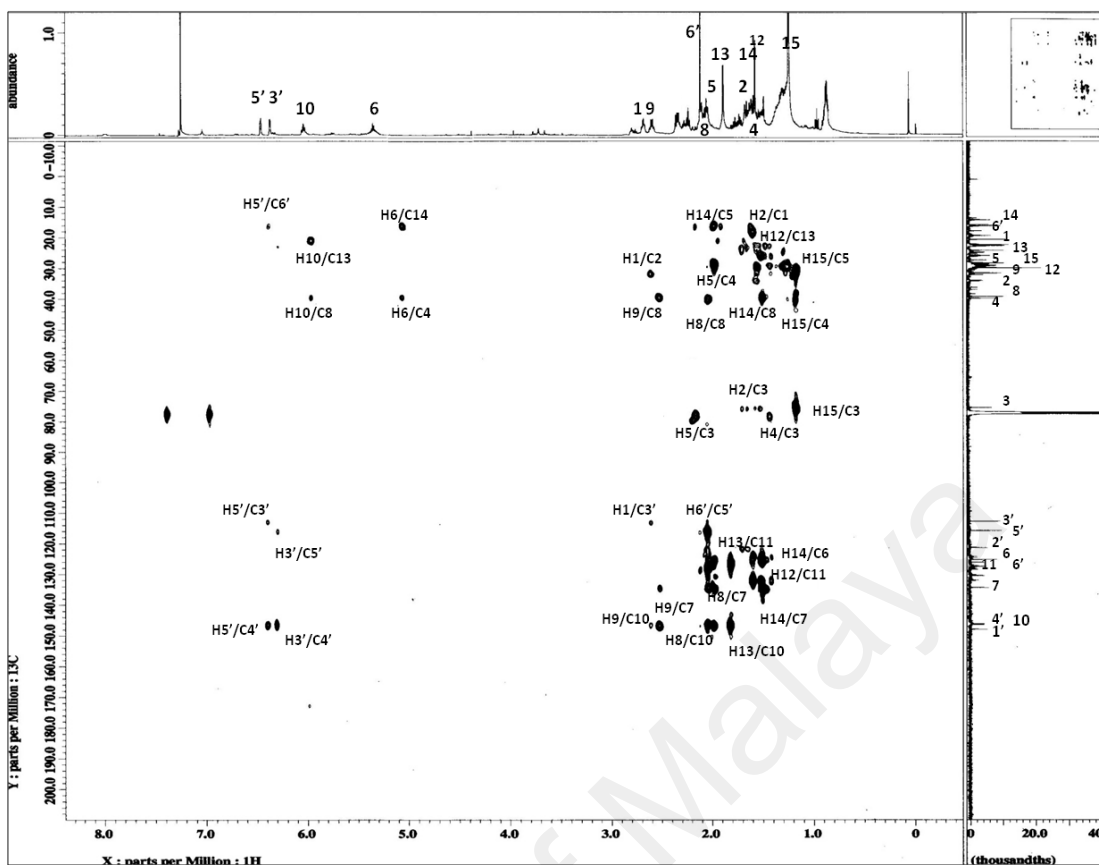
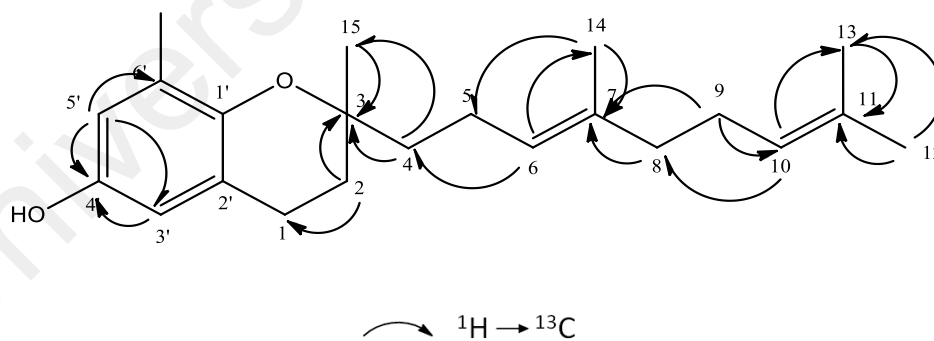
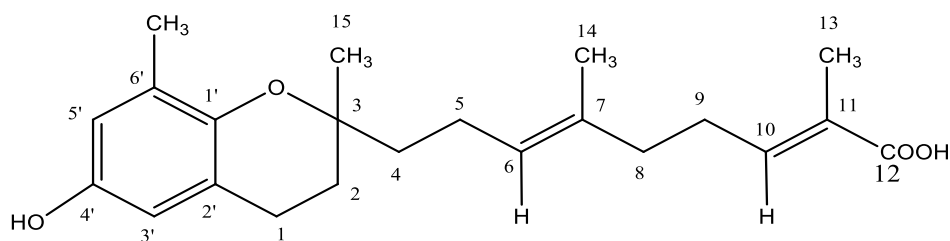


Fig. 4.53: HMBC spectrum of oligandrol (14)



Scheme 4.4: The HMBC correlations of oligandrol (14)

4.2.9 (6*E*,10*E*) isopolycerasoidol (**15**)



15

(6*E*, 10*E*) isopolycerasoidol (**15**) was isolated as yellow oil and showed $[\alpha]_D^{25}$ MeOH - 11.11° (*c* 0.5). The UV spectrum (Figure 4.54) showed absorption bands at 211 and 296 nm typical for an aromatic compound. The IR spectrum (Figure 4.55) showed the absorptions bands for hydroxyl group (3357 cm^{-1}) and the carbonyl group (1693 cm^{-1}). The HREIMS spectrum (Figure 4.56) displayed a molecular ion peak $[\text{M}+\text{H}]^+$ at m/z 359.2057 corresponding to the molecular formula of $\text{C}_{22}\text{H}_{30}\text{O}_4$. The fragment ions at m/z 137 ($\text{C}_8\text{H}_9\text{O}_2$) and m/z 177 ($\text{C}_{11}\text{H}_{13}\text{O}_2$) showed the break down of chroman subunit that did not have a methoxy group in the aromatic ring.

The ^1H NMR spectrum (Figure 4.57) showed meta coupled proton signals at δ 6.34 (2H, $J=2.5$ Hz, H-3') and δ 6.44 (2H, $J=2.5$ Hz, H-5') typical of an AB system, which was apparent from their coupling constant. Four tertiary methyls were observed at δ 1.89, 1.58, 1.25 and 2.12 (3H). Table 4.9 summarizes the ^1H - and ^{13}C NMR of the compound.

The ^{13}C -NMR and DEPT 135 spectra (Figure 4.58 and 4.59) revealed a total of 22 carbon signals attributed to four methyls, six methylenes, four methines and eight quaternary carbons. The most downfield peak at δ 172.7 indicated the carbonyl atom of the carboxylic acid.

The COSY spectrum (Figure 4.60) displayed correlations between H-1/H-2, H-4/H-5, H-5/H-6, H-8/H-9 and H-9/H-10. The HMQC spectrum (Figure 4.61) clearly showed the direct connections of the assigned carbons and protons in the structure. In the HMBC spectrum (Figure 4.62), the crosspeaks between H-3'/C-4' and H-5'/C-4' confirmed the presence of a hydroxyl group at C-4', and the crosspeaks between CH₃-13/C-12 and H-10/C-12 confirmed the position of the carboxylic acid at the terminal chain.

On the basis of 2D NMR and MS analysis, and comparison with the data of a known structure, the compound was established as (6*E*,10*E*) isopolycerasoidol (**15**) (Gonzalez *et al.*, 1995) which was also found in *Pseuduvaria indochinensis* Merr. (Zhao *et al.*, 2014).

Table 4.9: ^1H NMR (500MHz) and ^{13}C NMR (125 MHz) spectral data of (6*E*, 10*E*) isopolycerasoidol (**15**) in CDCl_3 (δ in ppm, *J* in Hz)

Position	^1H -NMR (δ ppm)	^{13}C -NMR(δ ppm)	^{13}C -NMR (δ ppm) (Gonzales <i>et al.</i> , 1996)
1	2.69 (2H, <i>m</i>)	22.5	22.6
2	1.74 (2H, <i>m</i>)	31.5	31.4
3	-	76.8	76.8
4	1.55-1.61 (2H, <i>m</i>)	39.5	39.7
5	2.03-2.11 (2H, <i>m</i>)	22.2	22.2
6	5.14 (1H, <i>t</i> , <i>J</i> =7.0,1.2)	125.1	125.1
7	-	134.4	134.4
8	2.04-2.10 (2H, <i>m</i>)	39.1	39.2
9	2.56 (2H, <i>m</i>)	28.2	28.1
10	6.05 (1H, <i>t</i> , <i>J</i> =7.0,1.2)	146.1	143.3
11	-	127.4	127.4
12	-	172.7	168.6
13	1.89 (3H, <i>s</i>)	20.6	20.7
14	1.58 (3H, <i>s</i>)	15.8	15.8
15	1.25 (3H, <i>s</i>)	24.0	24.1
1'	-	145.9	145.9
2'	-	121.2	121.3
3'	6.34 (1H, <i>d</i> , <i>J</i> =2.5)	112.7	112.7
4'	-	147.9	147.9
5'	6.44 (1H, <i>d</i> , <i>J</i> =2.5)	115.7	115.7
6'	-	126.6	126.9
CH ₃ -6'	2.12 (3H, <i>s</i>)	16.1	16.2

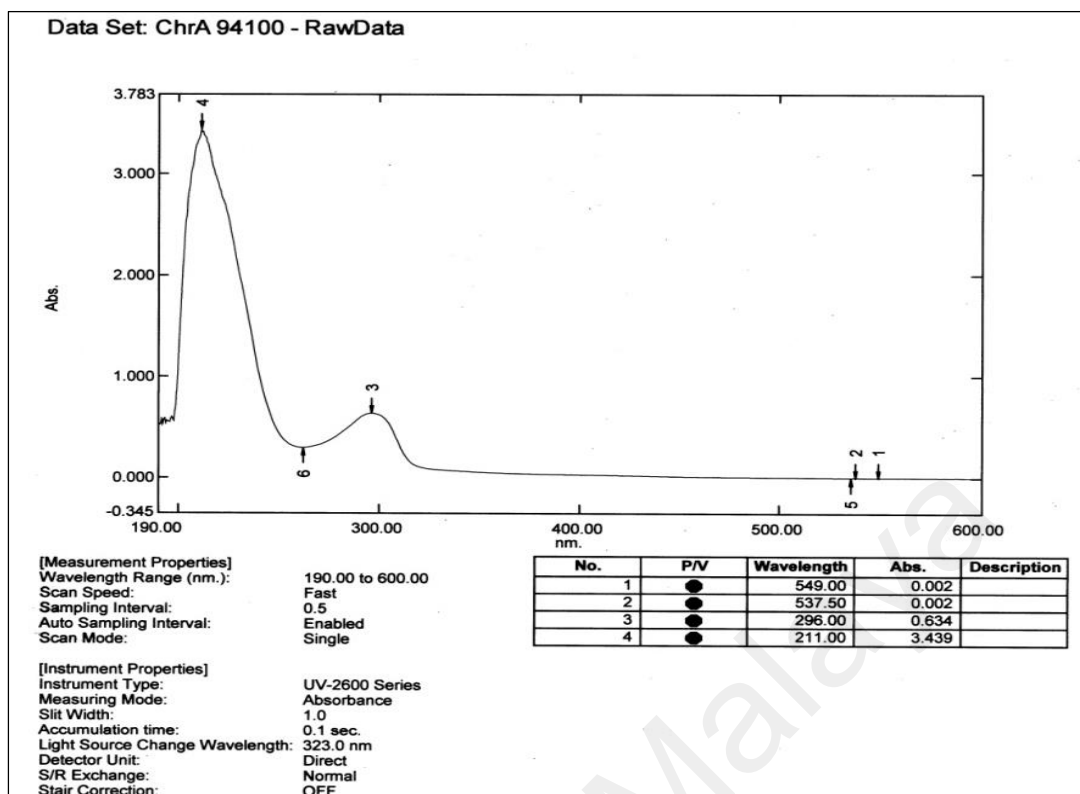


Fig.4.54: UV spectrum of (6E, 10E) isopolycerasoidol (15)

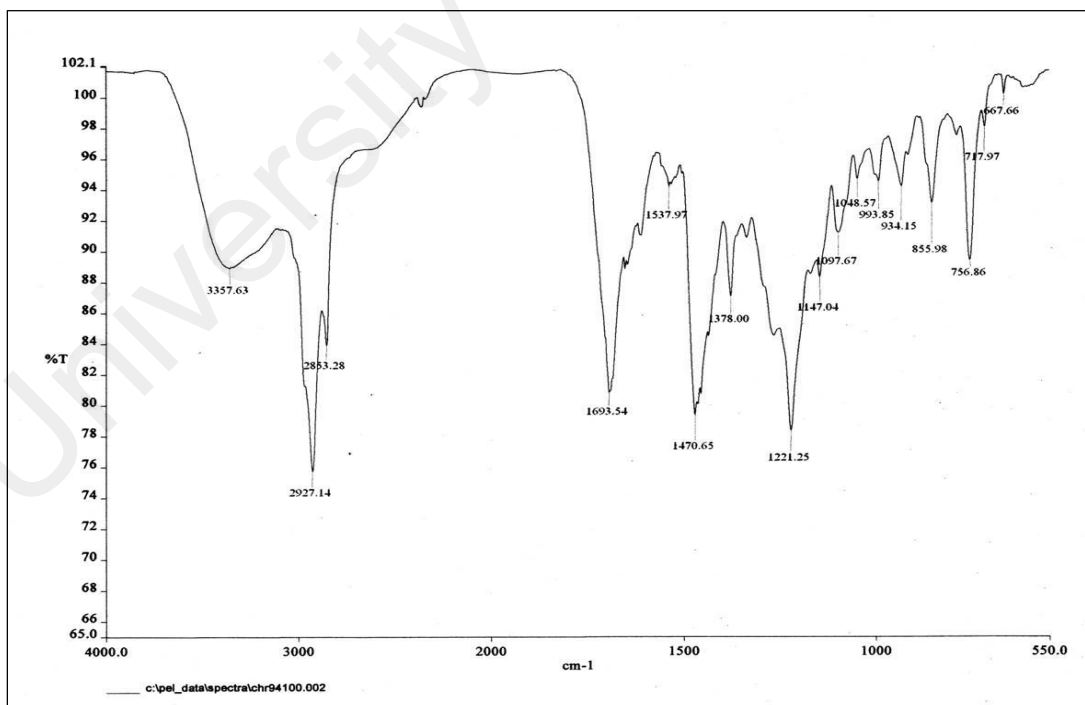


Fig.4.55: IR spectrum of (6E, 10E) isopolycerasoidol (15)

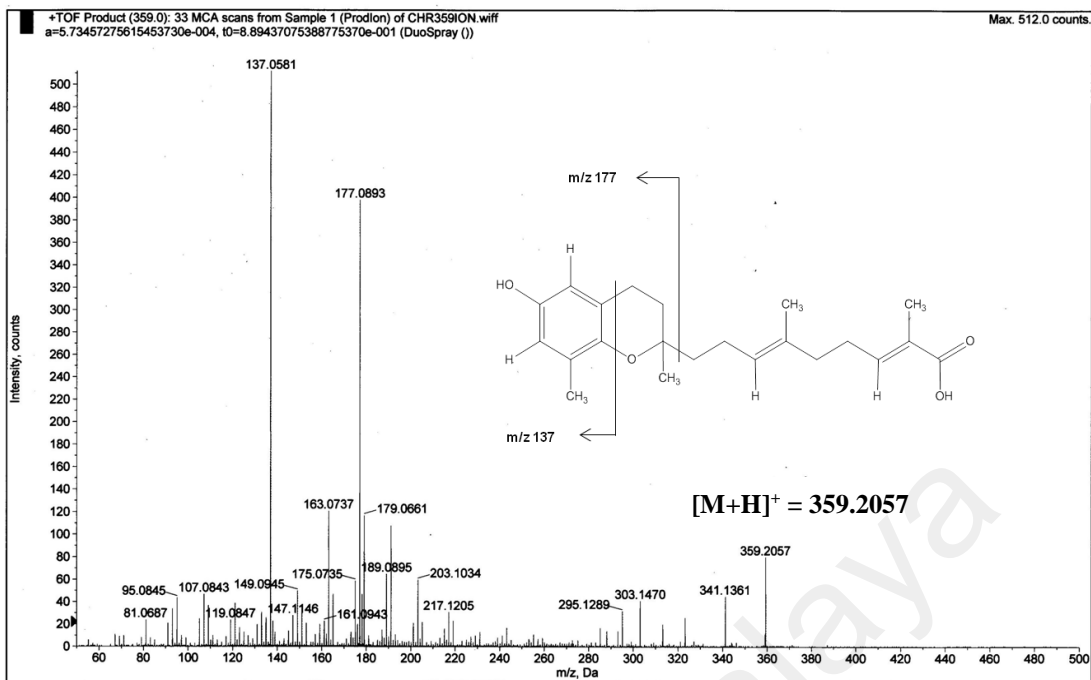


Fig.4.56: LC-MS of (6*E*, 10*E*) isopolycerasoidol (**15**)

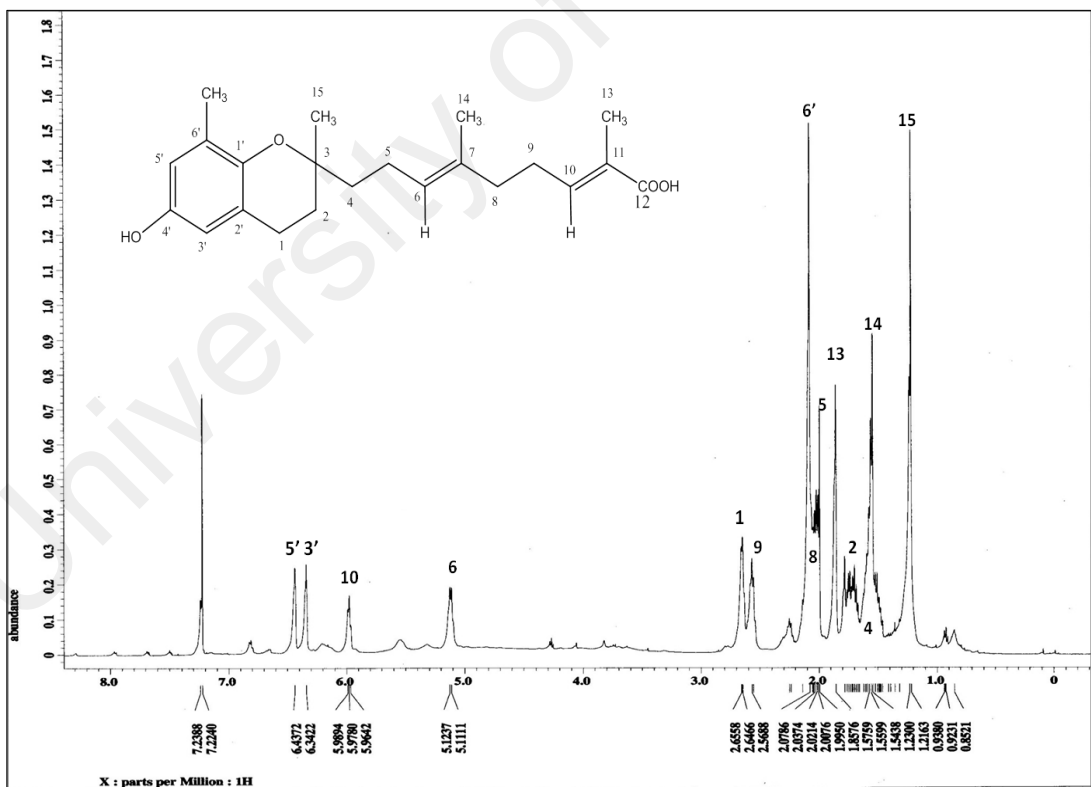


Fig.4.57: ^1H NMR of (6*E*, 10*E*) isopolycerasoidol (**15**)

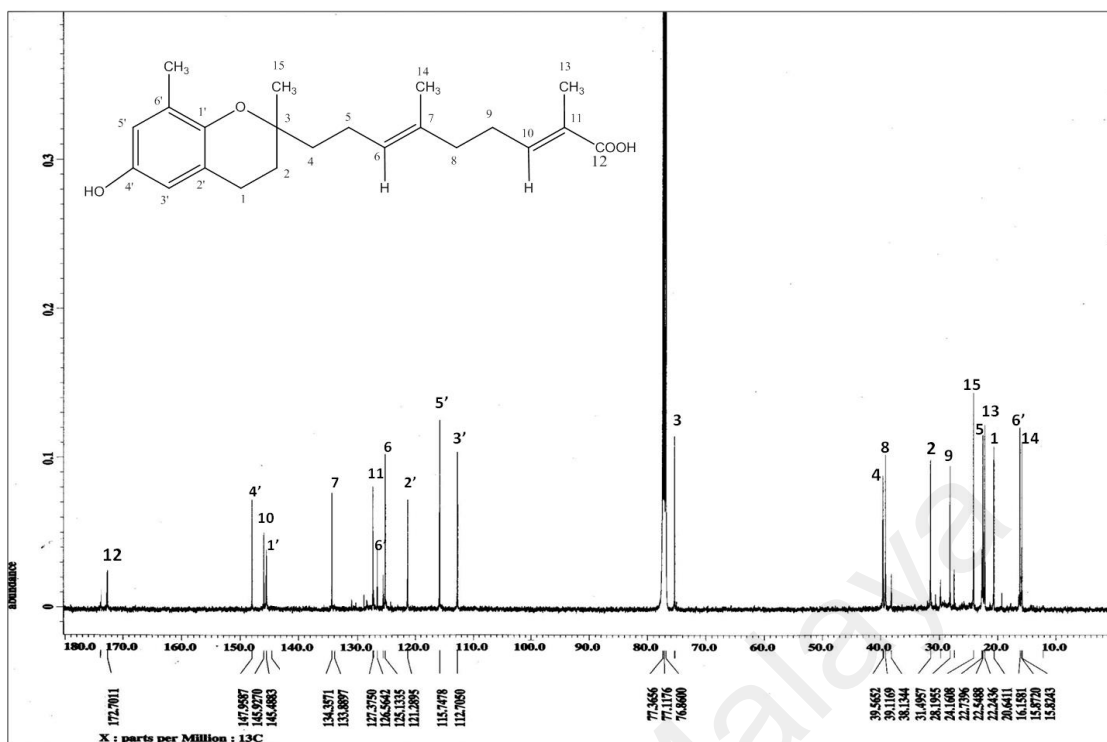


Fig.4.58: ¹³C NMR of (6*E*, 10*E*) isopolycerasoidol (15)

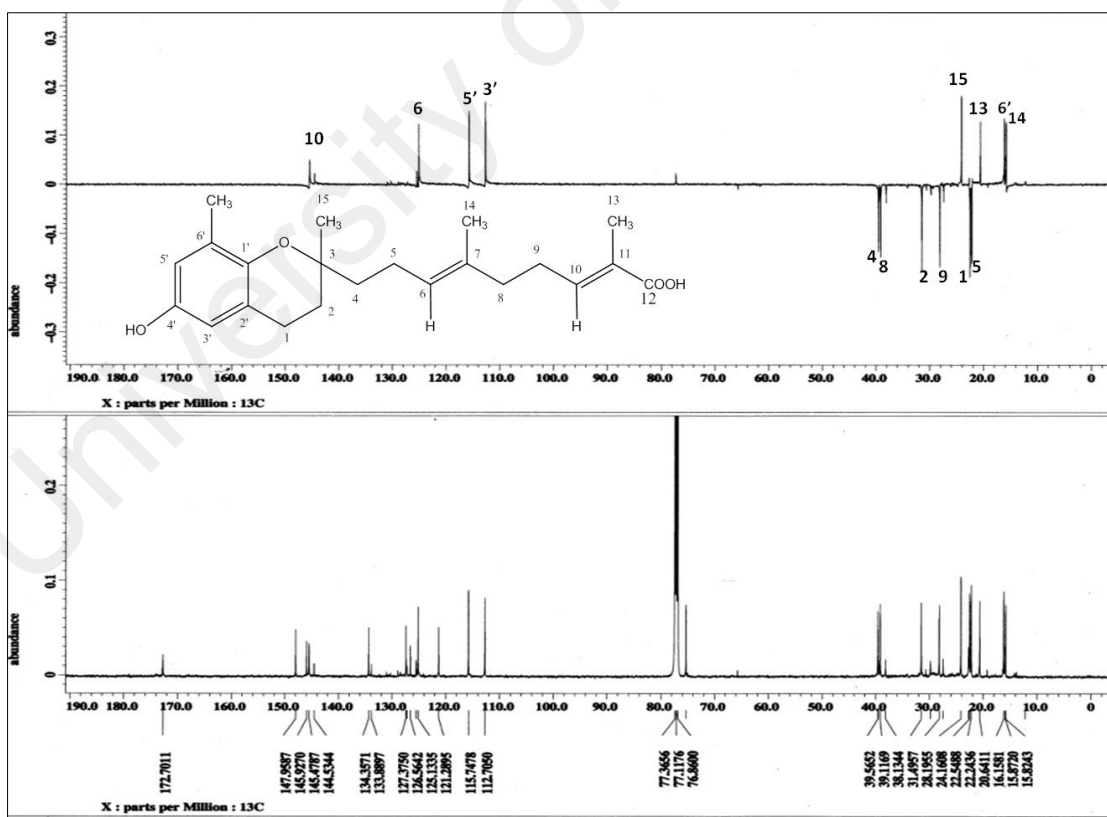


Fig.4.59: DEPT 135 of (6*E*, 10*E*) isopolycerasoidol (15)

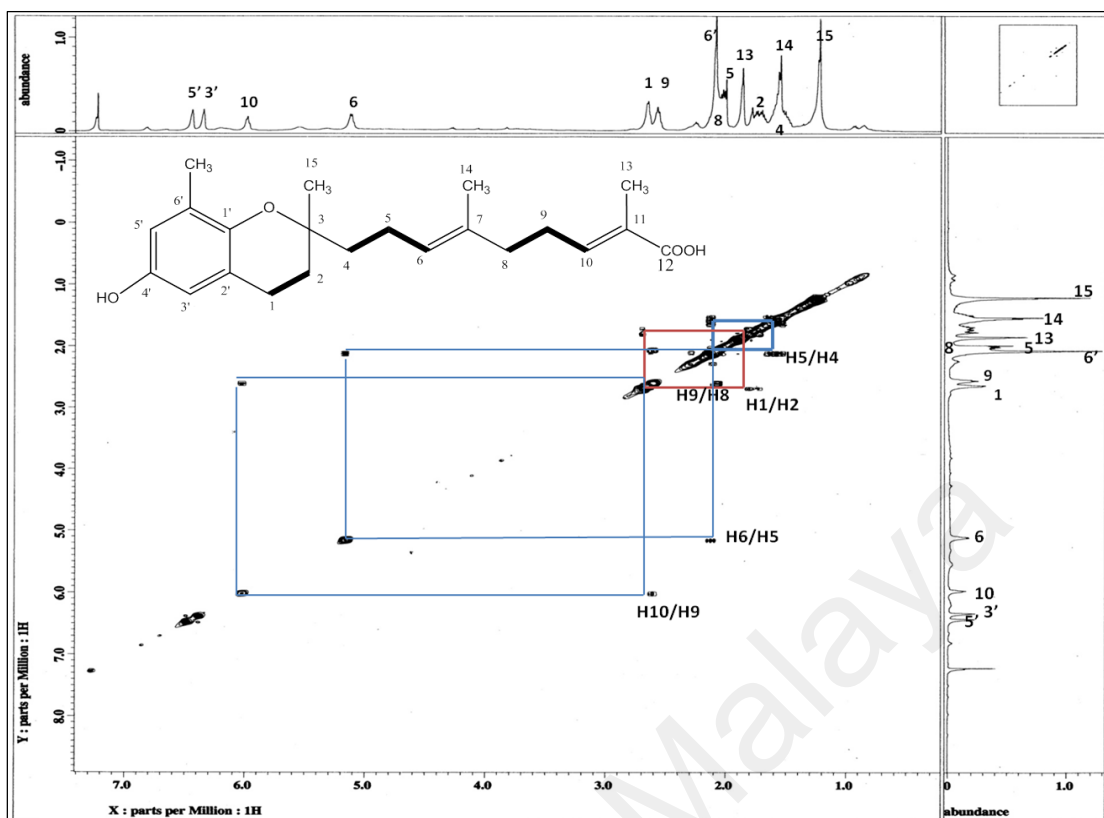


Fig. 4.60: COSY spectrum of (6E, 10E) isopolycerasoidol (15)

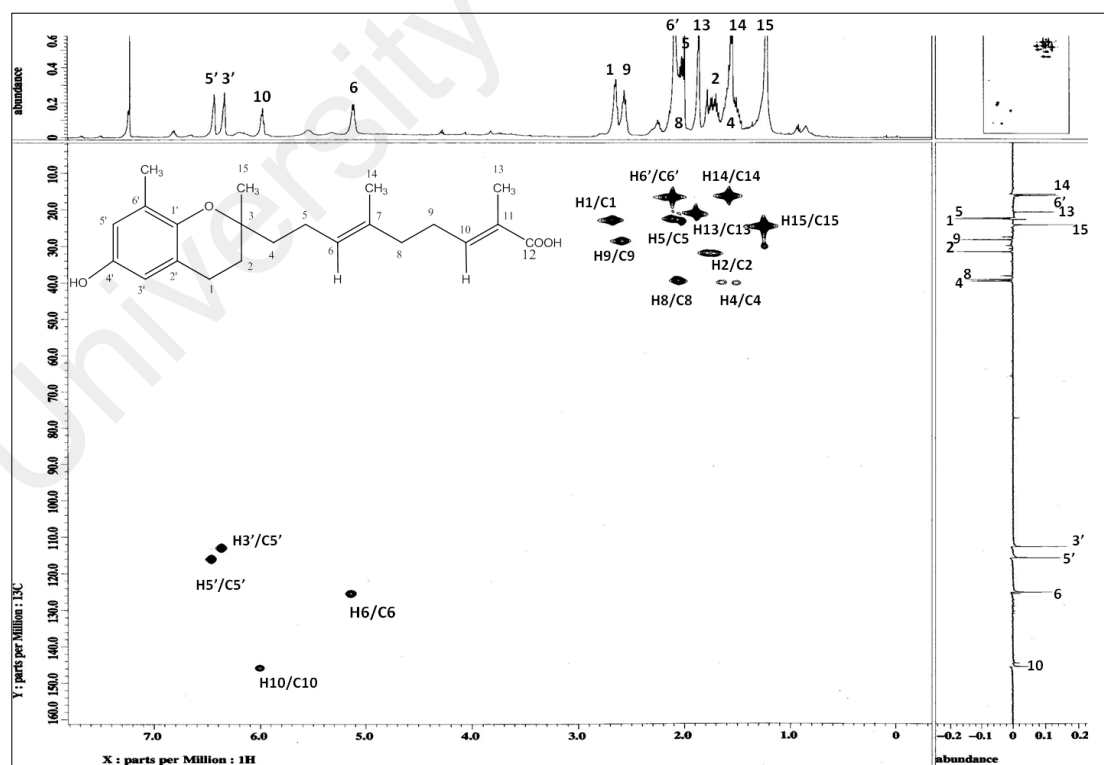


Fig. 4.61: HMQC spectrum of (6E, 10E) isopolycerasoidol (15)

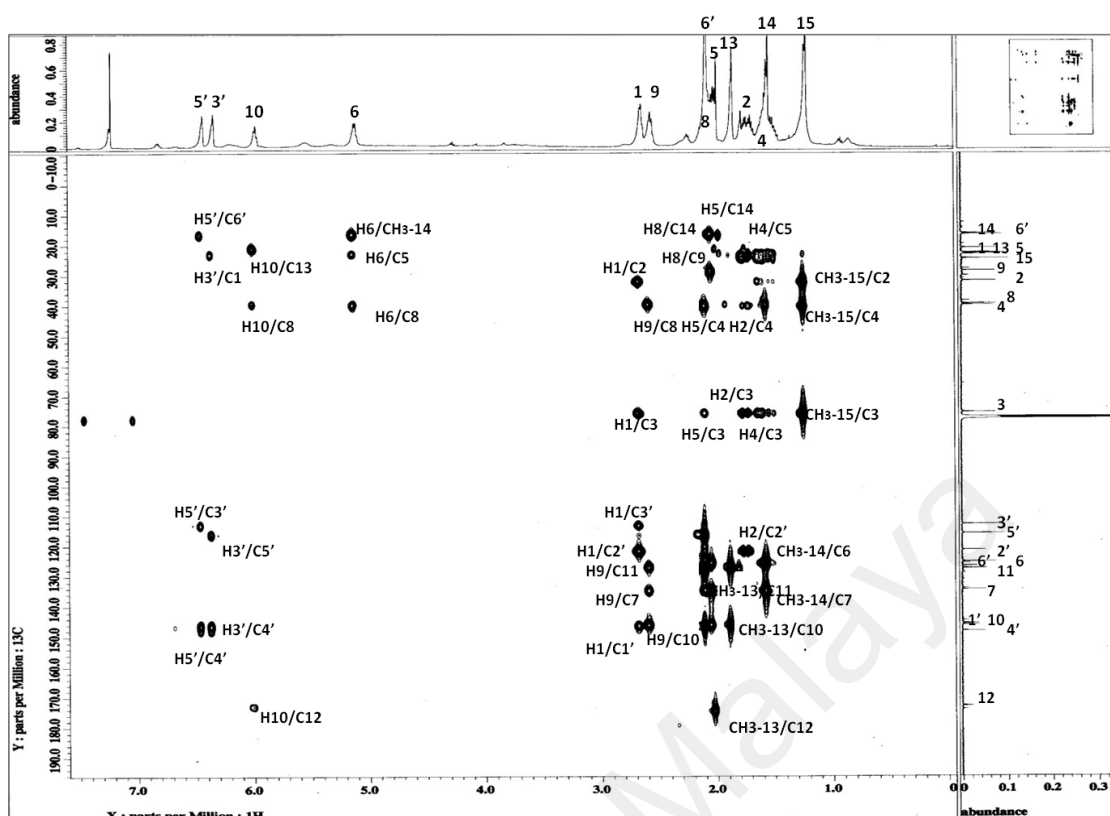
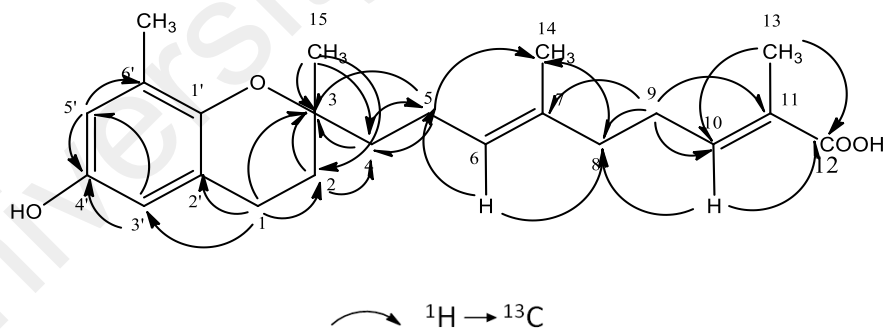
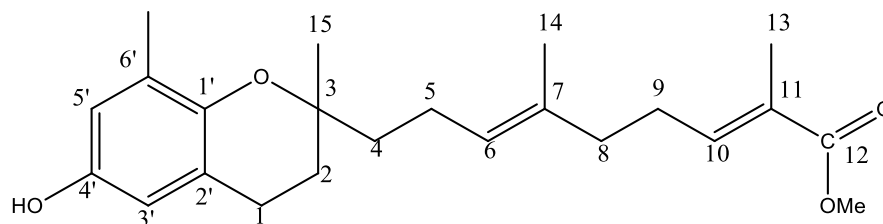


Fig. 4.62: HMBC spectrum of (6*E*, 10*E*) isopolycerasoidol (**15**)



Scheme 4.5: The HMBC correlations of (6*E*, 10*E*) isopolycerasoidol (**15**)

4.2.10 (6*E*,10*E*) isopolycerasoidol methyl ester (32)



32

(6*E*, 10*E*) isopolycerasoidol methyl ester (**32**) was isolated as yellow oil and showed $[\alpha]_D^{25}$ MeOH - 12.5° (*c* 0.5). The IR and UV spectra (Figure 4.63 and 4.64) showed similar pattern of absorption bands to that of (6*E*, 10*E*) isopolycerasoidol (**15**). The HREIMS spectrum (Figure 4.65) revealed a molecular ion peak $[M+H]^+$ at *m/z* 373.2164 corresponding to the molecular formula of C₂₃H₃₂O₄.

The molecular formula of this compound was more by 15 amu than that of (6*E*, 10*E*) isopolycerasoidol (**15**) which could be attributed to the presence of a methoxy group. The fragment ion peaks at *m/z* 137(C₈H₉O₂) and *m/z* 177(C₁₁H₁₃O₂) again suggest a partial subunit of a benzopyran with a hydroxyl group. It can be deduced that the methoxy group is not attached to the chromane nucleus.

The ¹H NMR spectrum (Figure 4.66) also showed similar assignments to those of (6*E*, 10*E*) isopolycerasoidol (**15**) except for an additional presence of a methoxy peak indicated by signals at δ_H 3.72 (3H, *s*) which could suggest the position of the methoxy group either in the aromatic ring or as an ester functionality. The assignments of meta coupled protons (δ 6.34 and 6.44, *d*, *J*=2.5 Hz) indicate a substituted benzene ring. While the ¹³C NMR spectrum (Figure 4.67) showed a methoxy peak at δ_C 51.3 which bring the total carbons to 23. The DEPT 135 spectrum (Figure 4.68) showed carbon signals for one

methoxy group, four methyls, four methines and six methylenes. Table 4.10 summarizes the ^1H and ^{13}C NMR of the compound.

The crosspeak observed in the HMQC spectrum (Figure 4.70) further confirmed the presence of the methoxy group. In the COSY spectrum (Figure 4.69), the allyl protons at H-6 and H-10 showed crosspeaks with H-4, H-5, H-8 and H-9, thus confirming the prenylated side chain in this compound. The HMBC (Figure 4.71) correlations between H-2, H-4 and H-15 to C-3 confirmed the isoprenyl side chain at C-3 linking to the benzopyran ring.

Looking at the basic skeleton, this compound was first thought as a known compound, polycerasoidin (**50**) (Gonzalez *et al.*, 1995). However, the position of the methoxyl group was finally determined by the long-range correlations in the HMBC spectrum (Scheme 4.6).

The HMBC correlations between $\text{OCH}_3/\text{C-12}$ and $\text{CH}_3/\text{C-13}$ helped to determine the assignment of the methoxy group at C-12 which was adjacent to the carbonyl function, thus confirming the methyl esterification in the structure. In fact, the carbonyl peak at δ 168.6 was slightly less deshielded due to the electron-donating effect of the methoxy group.

Finally, based on all spectroscopic data, the compound is proposed to be (*6E,10E*) isopolycerasoidol methyl ester (**32**), which is a new benzopyran derivative that was not reported before and first discovered from *Pseuduvaria monticola*. This compound was not a product of esterification or artifact since it was also detected in the hexane extract.

Table 4.10: ^1H NMR (500 MHz) and ^{13}C NMR (125 MHz) spectral data of (6*E*, 10*E*) isopolycerasoidol methyl ester (**32**) in CDCl_3 (δ in ppm, *J* in Hz)

Position	^1H NMR (δ ppm)	^{13}C NMR (δ ppm)
1	2.69 (2H, <i>m</i>)	22.6
2	1.79 (2H, <i>m</i>)	31.4
3	-	76.8
4	1.54-1.63 (2H, <i>m</i>)	39.7
5	2.02-2.11 (2H, <i>m</i>)	22.2
6	5.16 (1H, <i>t</i> , <i>J</i> =7.0,1.2)	125.1
7	-	134.4
8	2.04-2.10 (2H, <i>m</i>)	39.2
9	2.55 (2H, <i>m</i>)	28.1
10	5.92 (1H, <i>t</i> , <i>J</i> =7.0, 1.2)	143.3
11	-	127.4
12	-	168.6
13	1.87 (3H, <i>s</i>)	20.7
14	1.59 (3H, <i>s</i>)	15.8
15	1.25 (3H, <i>s</i>)	24.1
1'	-	145.9
2'	-	121.3
3'	6.38 (1H, <i>d</i> , <i>J</i> =2.5)	112.7
4'	-	147.9
5'	6.48 (1H, <i>d</i> , <i>J</i> =2.5)	115.7
6'	-	126.9
CH ₃ -6'	2.12 (3H, <i>s</i>)	16.2
COOCH ₃ -12	3.72 (3H, <i>s</i>)	51.3

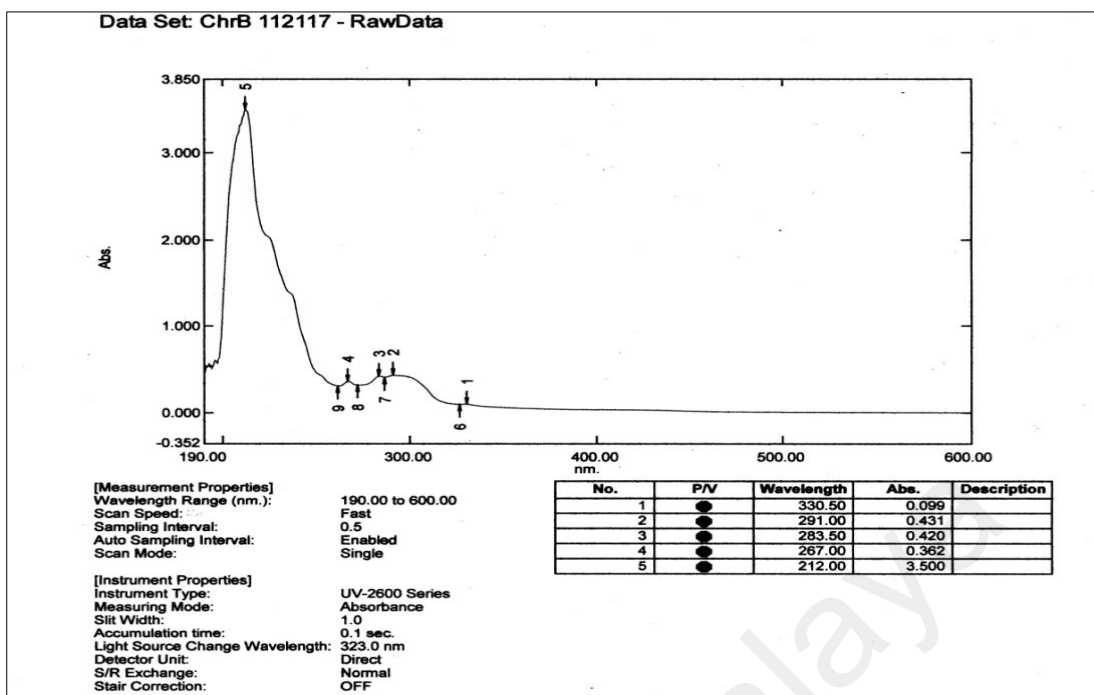


Fig.4.63: UV spectrum of (6E, 10E) isopolycerasoidol methyl ester (32)

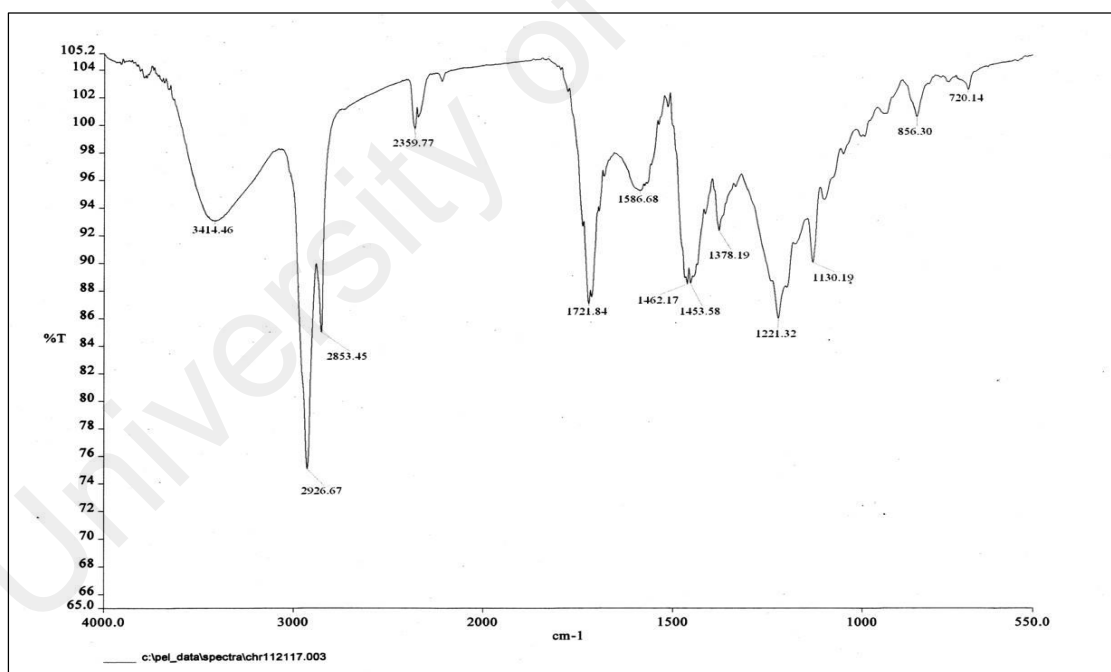


Fig. 4.64: IR spectrum of (6E, 10E) isopolycerasoidol methyl ester (32)

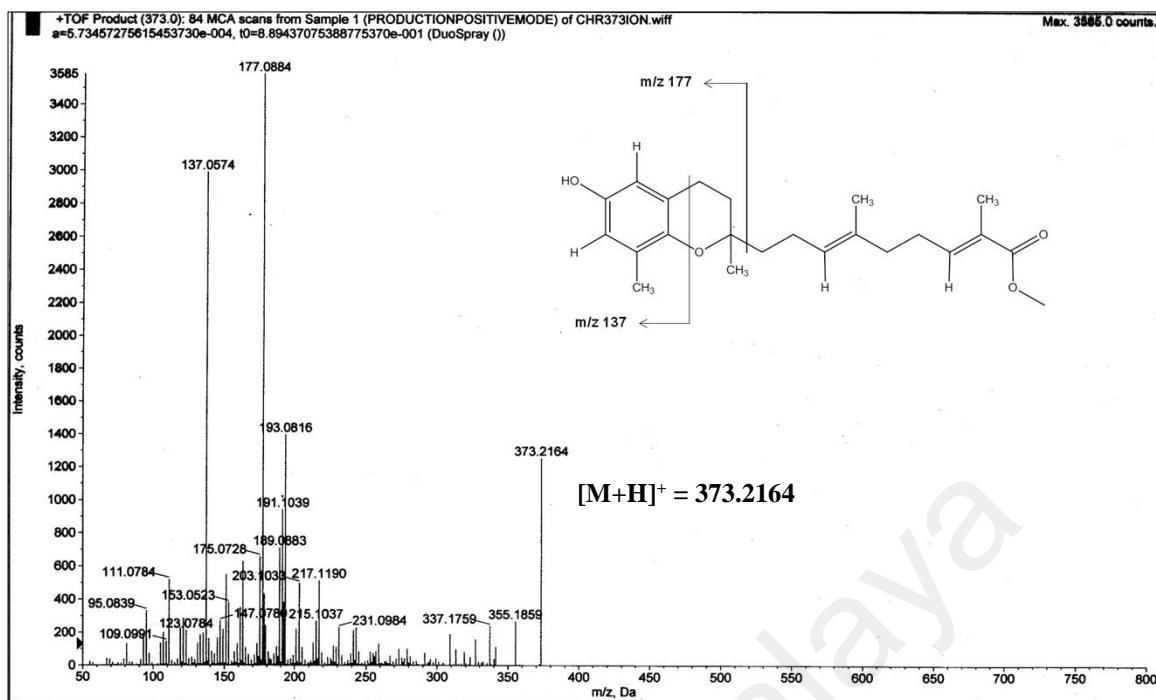


Fig. 4.65: LC-MS of (6*E*, 10*E*) isopolycerasoidol methyl ester (**32**)

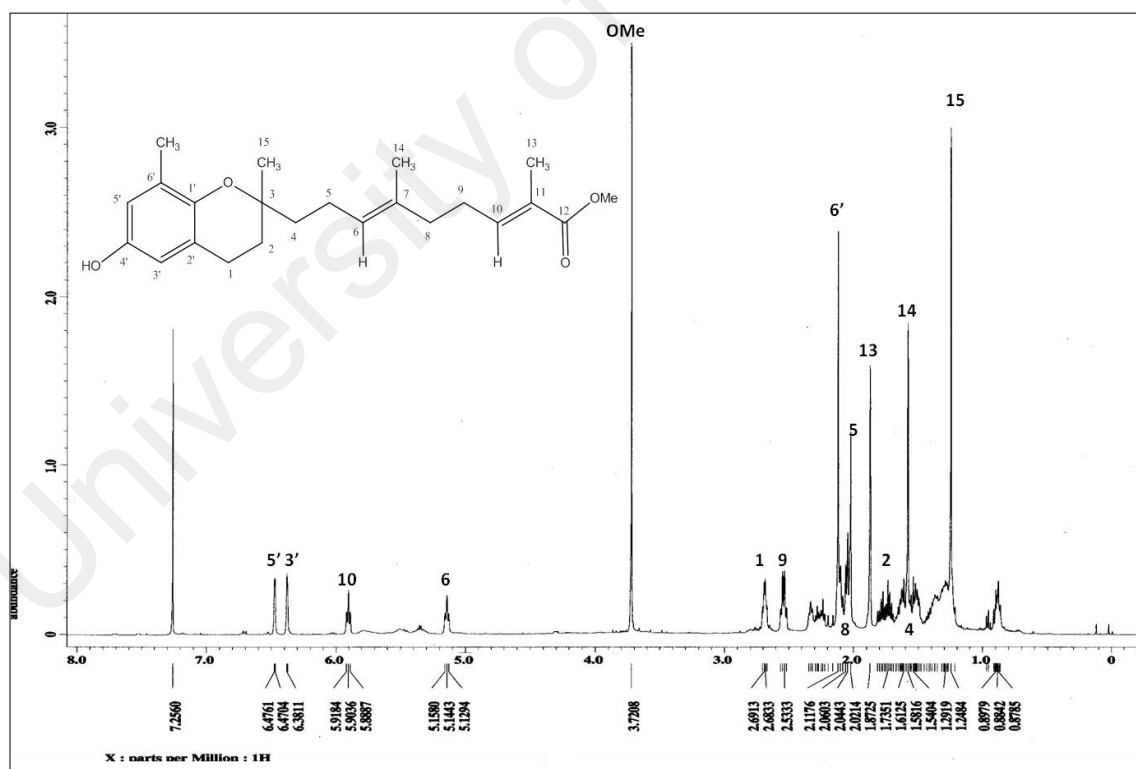


Fig. 4.66: ¹H NMR spectra of (6*E*, 10*E*) isopolycerasoidol methyl ester (**32**)

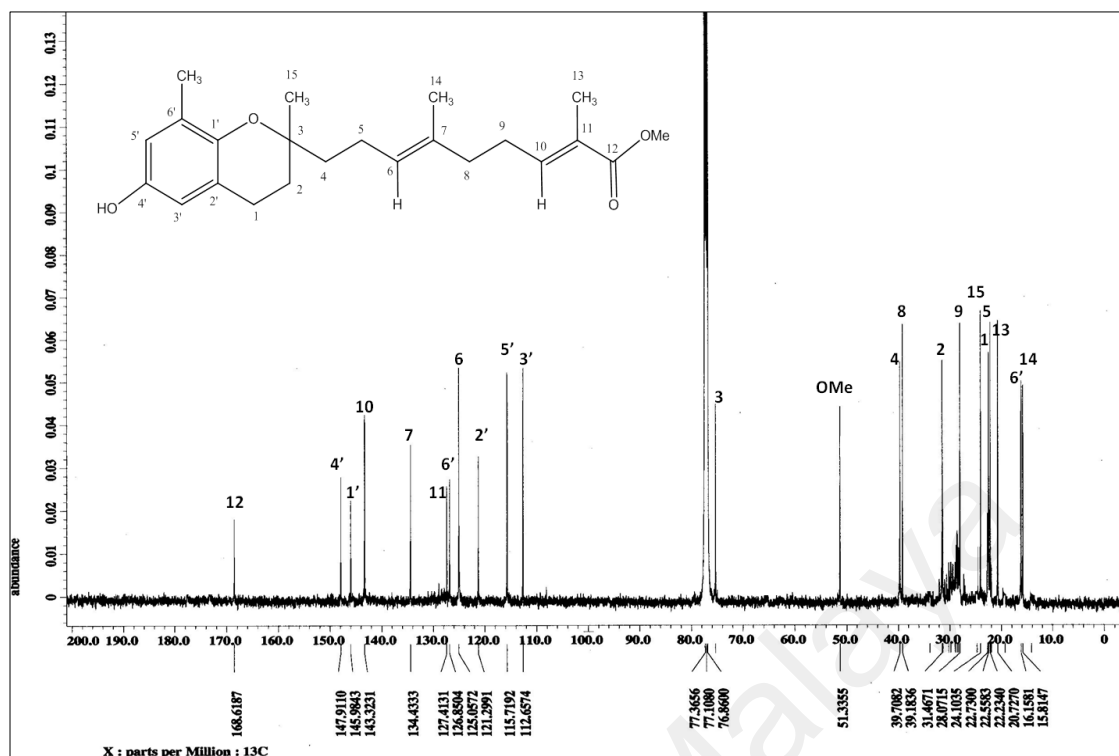


Fig. 4.67: ¹³C NMR spectra of (6*E*, 10*E*) isopolycerasoidol methyl ester (32)

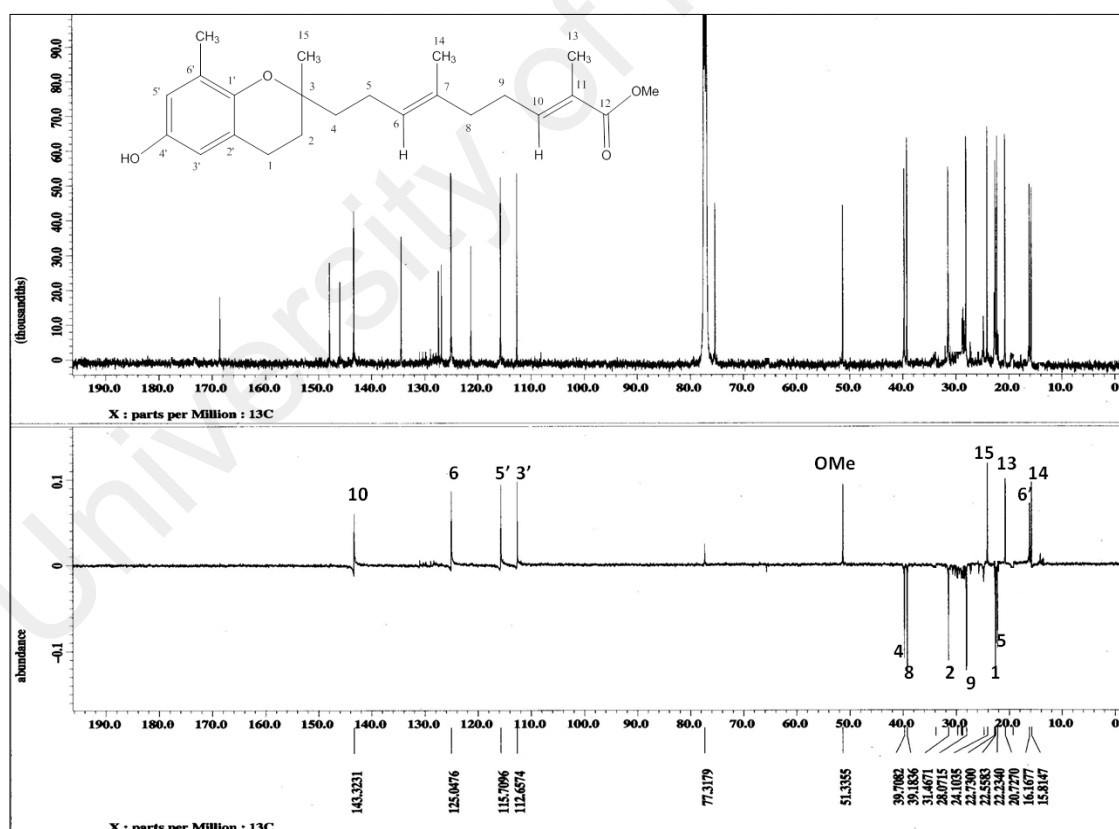


Fig.4.68: DEPT 135 spectrum of (6*E*, 10*E*) isopolycerasoidol methyl ester (32)

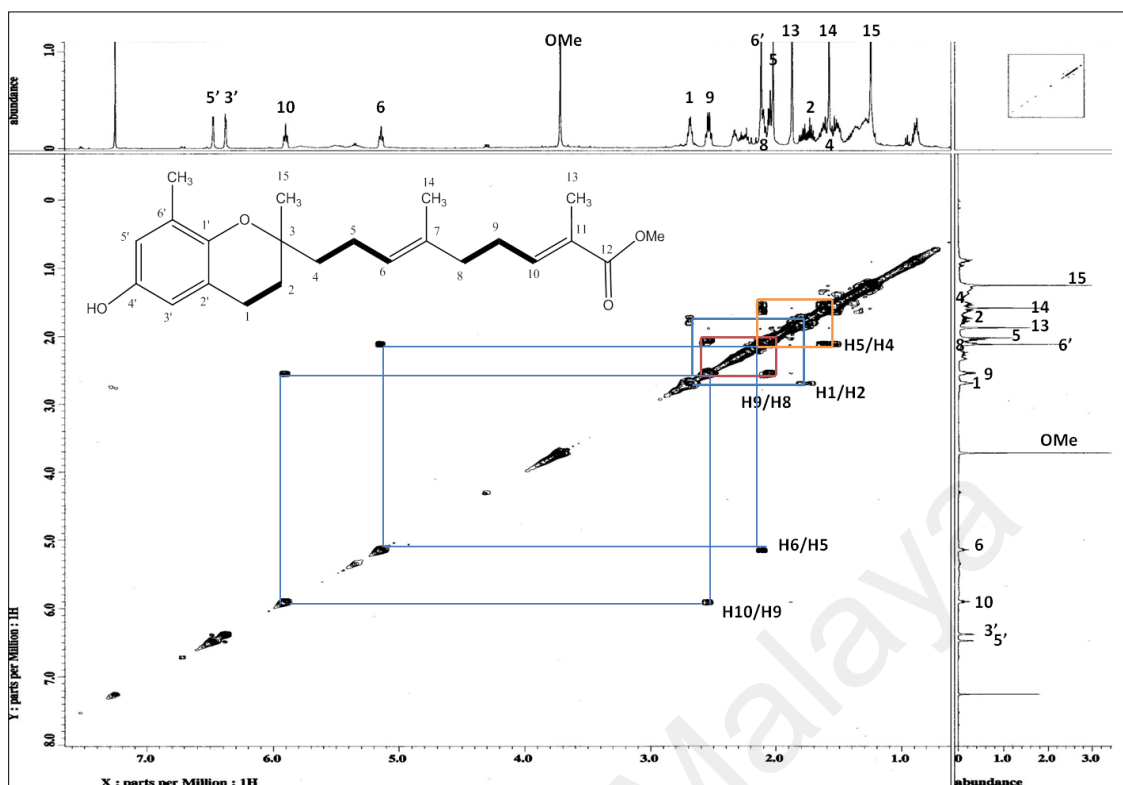


Fig. 4.69: COSY spectrum of (6*E*, 10*E*) isopolycerasoidol methyl ester (32)

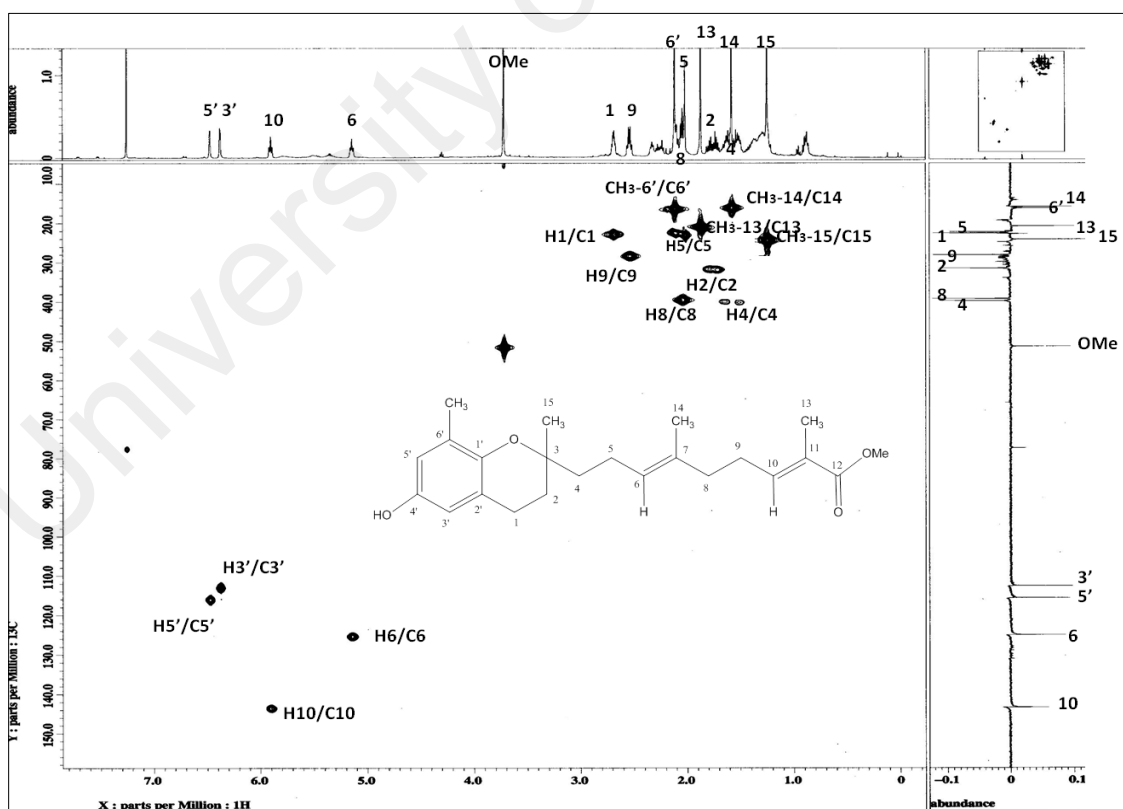


Fig. 4.70: HMBC spectrum of (6*E*, 10*E*) isopolycerasoidol methyl ester (32)

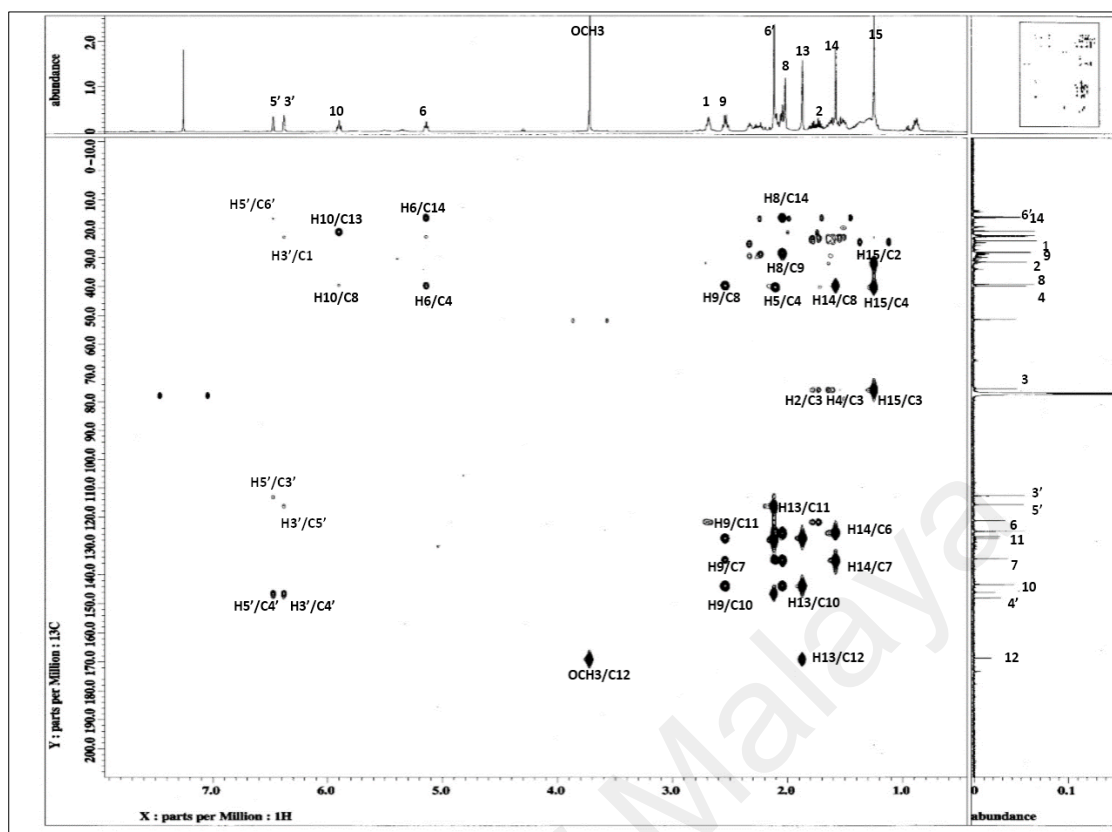
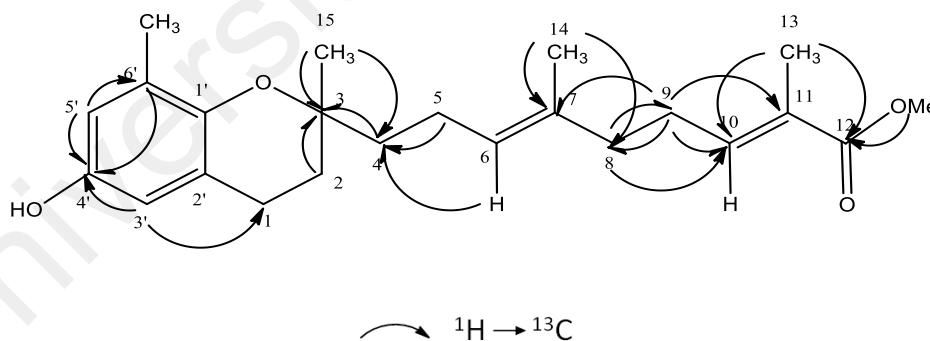
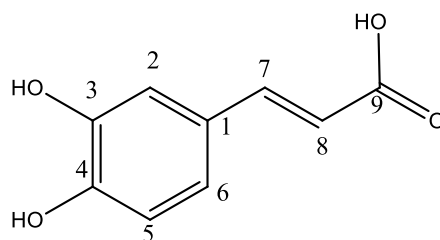


Fig. 4.71: HMBC spectra of (6*E*, 10*E*) isopolycerasoidol methyl ester (**32**)



Scheme 4.6: The HMBC correlations of (6*E*, 10*E*) isopolycerasoidol methyl ester (**32**)

4.2.11 Caffeic acid (44)



44

Caffeic acid (**42**), a phenolic acid was afforded as brownish amorphous solid. The UV spectrum showed absorption peak at 290 and 320 nm. The IR spectrum showed a strong broad peak at 3430 cm^{-1} indicating the presence of a hydroxyl group. The carbonyl group was observed at 1700 cm^{-1} . The HREIMS spectrum (Figure 4.73) in negative mode revealed a molecular ion peak at $m/z\ 179.0294\ [M-H]^-$ corresponding to a molecular formula $C_9H_8O_4$. A base fragment ion peak at $m/z\ 135$ indicates the caffeate (CO_2H) moiety (Catarino *et al.*, 2015).

The 1H NMR spectrum (Figure 4.74) showed chemical shifts at 6.22 ($d, J= 16.0\text{ Hz}$ and 7.53 ($d, J= 16.0\text{ Hz}$) corresponding to H-8 and H-7 respectively. A sharp singlet at $\delta\ 7.02$ (1H) is assigned to H-3. Two proton doublets in ortho couple positions were observed at $\delta\ 6.77\ (J=8.0\text{ Hz})$ and $\delta\ 6.91\ (J=8.0\text{ Hz})$ assigned to H-5 and H-6, respectively. Table 4.11 summarizes the 1H and ^{13}C NMR of the compound.

The ^{13}C and DEPT 135 NMR (Figure 4.75 and 4.76) displayed nine carbon signals consisting of one carbonyl, five methines and three quaternary carbons. The presence of carboxylic functional group is observed at $\delta\ 169.7$. The COSY spectrum (Figure 4.76) showed the proton-proton correlations between H-5 and H-6, and H-7 and H-8. The

assignments of the specific protons and carbons in the compound are shown in the HMQC spectrum (Figure 4.77).

Based on the COSY, HMQC and HMBC spectrum (Figure 4.78), the compound is identified as caffeic acid (**42**) which was isolated for the first time from *Pseuduvaria monticola*.

Table 4.11: ^1H NMR (500 MHz) and ^{13}C NMR (125MHz) spectral data of caffeic acid (**44**) in CDOD_3 (δ in ppm, J in Hz)

Position	^1H NMR(δ ppm)	^{13}C NMR(δ ppm)	^{13}C NMR (Xing <i>et al.</i> , 2012)
1	-	126.5	126.6
2	7.02 (1H, <i>s</i>)	113.8	113.9
3	-	145.5	145.6
4	-	148.1	148.3
5	6.77 (1H, <i>d</i> , $J=8.0$)	115.2	115.4
6	6.91 (1H, <i>d</i> , $J=8.0$)	121.5	121.7
7	7.53 (1H, <i>d</i> , $J=16.0$)	145.7	145.6
8	6.22 (1H, <i>d</i> , $J=16.0$)	114.2	114.3
9	-	169.7	169.9

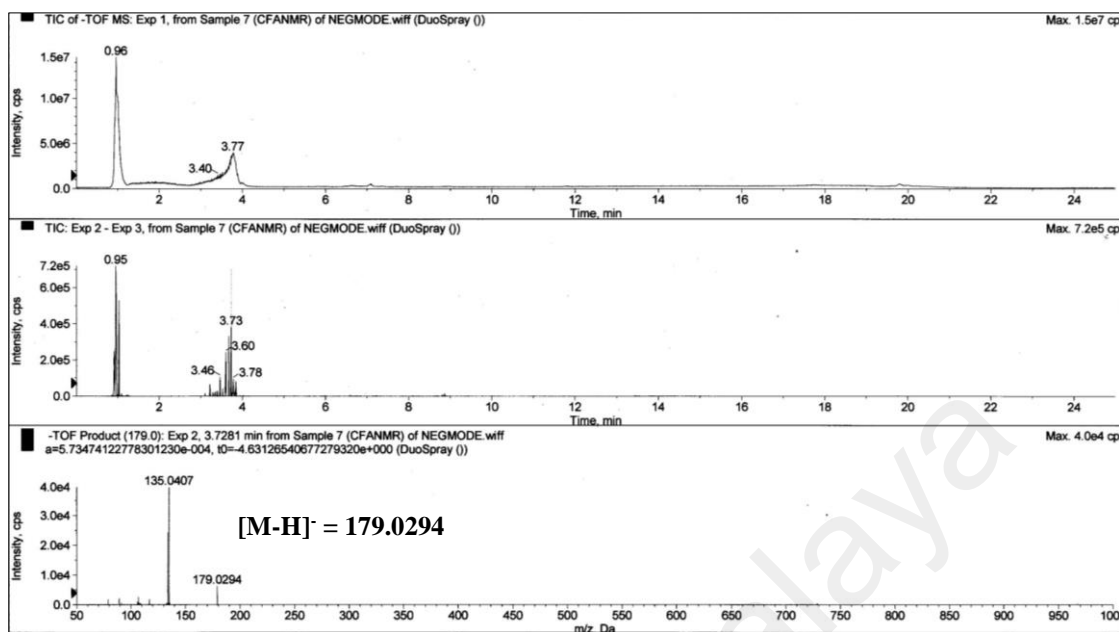


Fig 4.72: TIC and LC-MS spectrum of caffeic acid (**44**) in negative mode

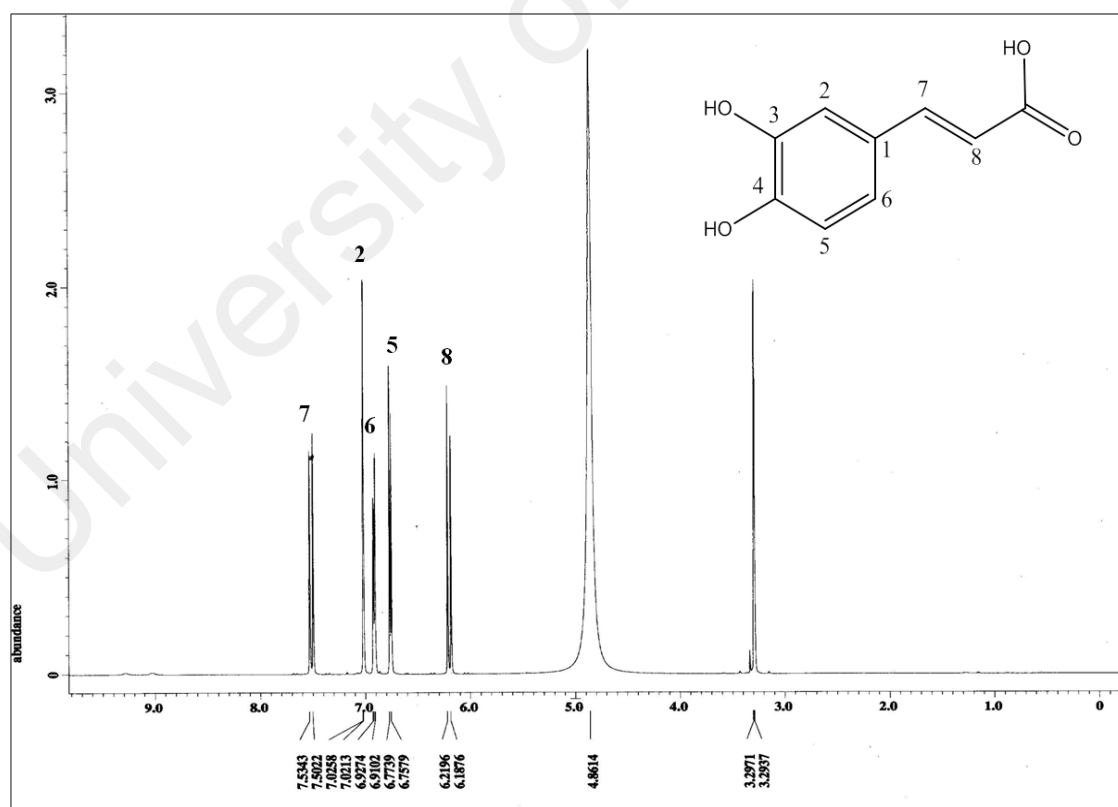


Fig 4.73: ^1H NMR spectrum of caffeic acid (**44**)

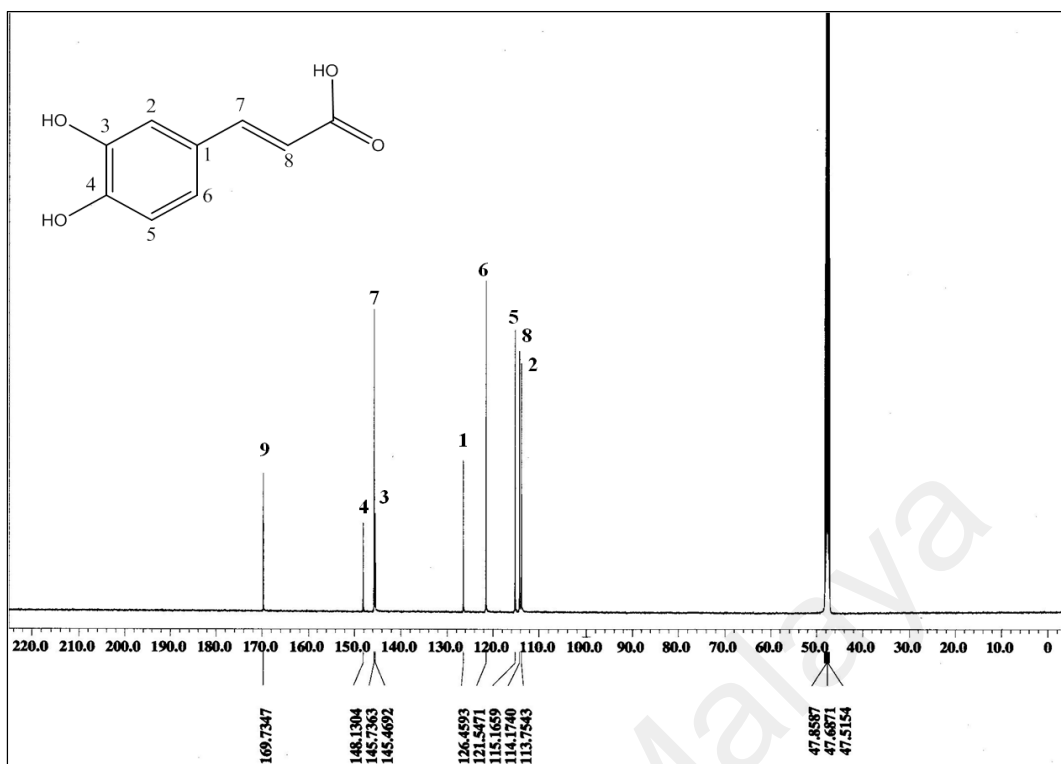


Fig 4.74: ^{13}C NMR of caffeic acid (44)

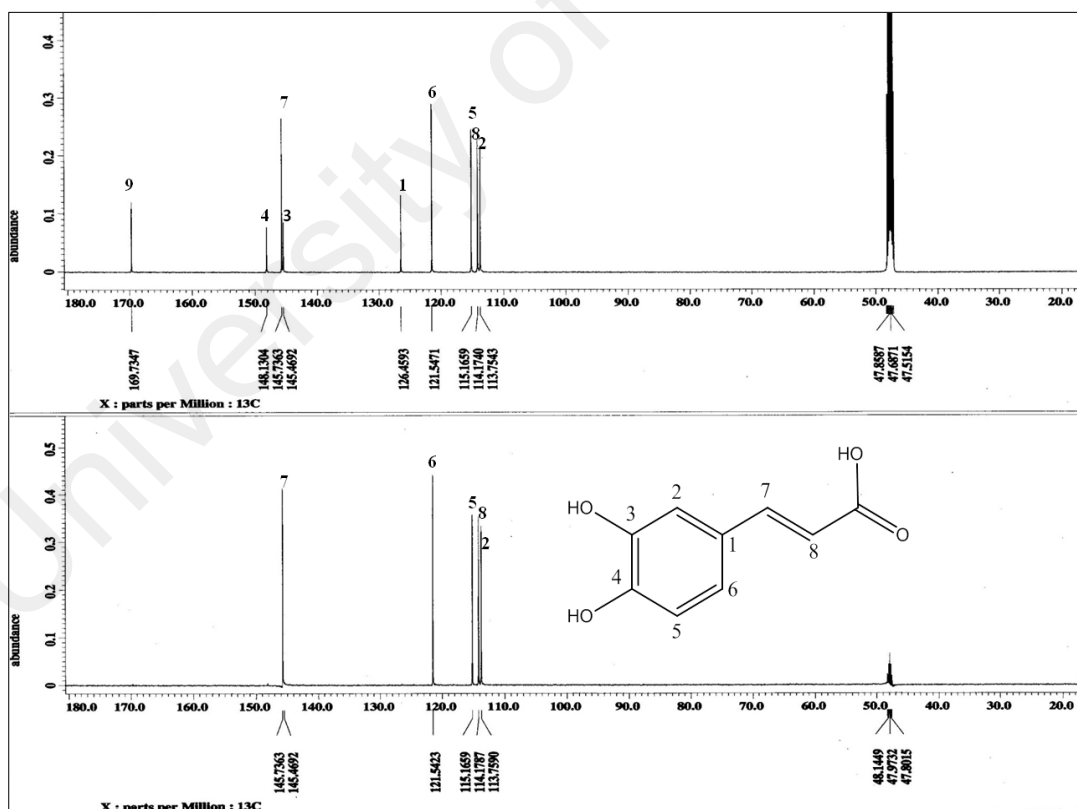


Fig. 4.75: DEPT 135 spectrum of caffeic acid (44)

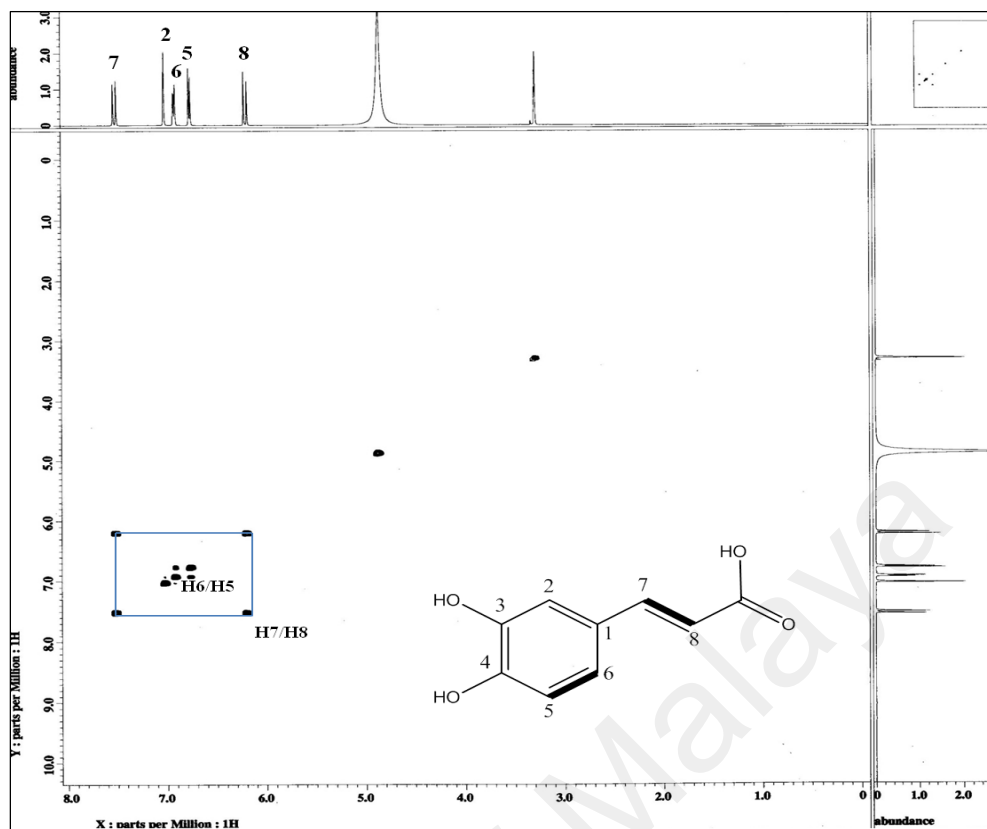


Fig. 4.76: COSY spectrum of caffeic acid (44)

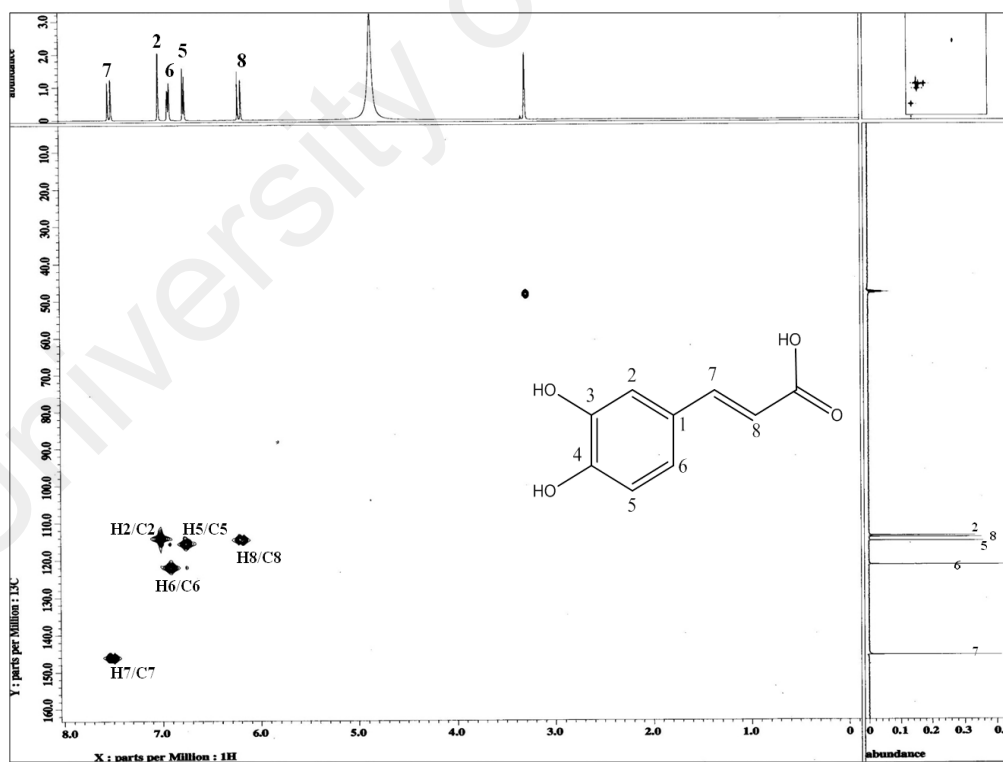


Fig. 4.77: HMQC spectrum of caffeic acid (44)

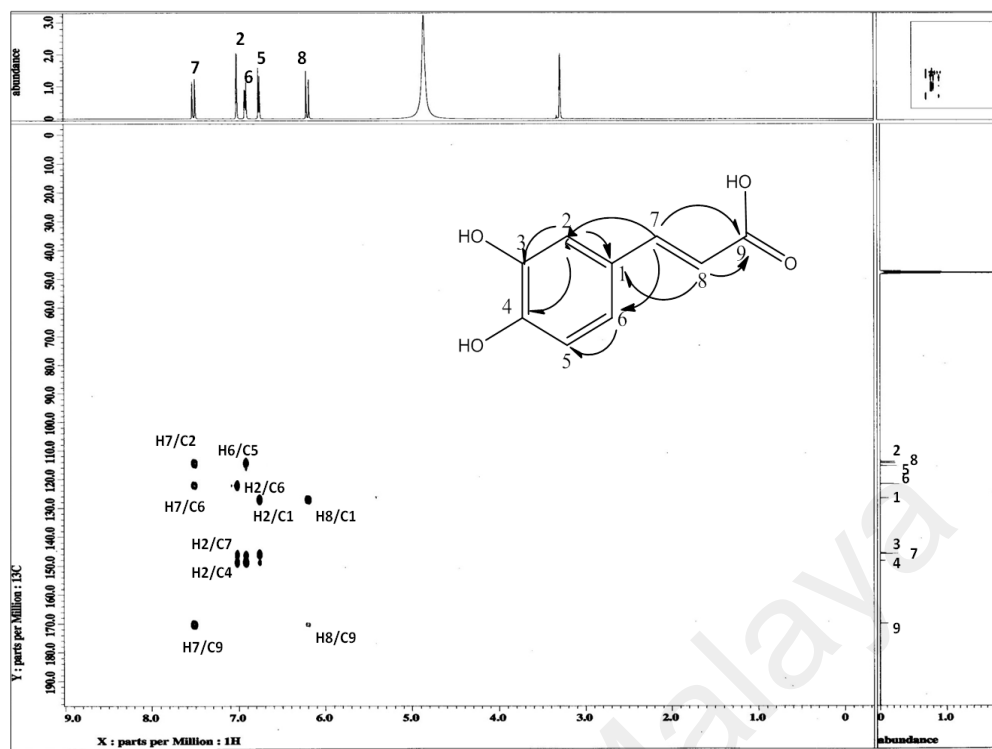
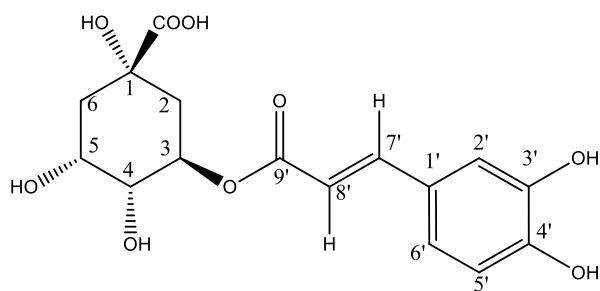


Fig. 4.78: HMBC spectrum of caffeic acid (44)

4.2.12 Chlorogenic acid (45)



45

Chlorogenic acid (**45**) was isolated as light brown amorphous solid. The UV spectrum showed absorption at 250 and 320 nm. The IR spectrum showed broad absorption band of a hydroxyl group at 3395 cm^{-1} , a carbonyl peak at 1650 cm^{-1} and aromatic ring at 1590 cm^{-1} . The intensity of the compound in the sub fraction can be observed from the LCMS-TIC chromatogram (Figure 4.79).

The HREIMS (Figure 4.80) in the negative mode showed a molecular ion peak at 353.0870 $[M-H]^-$ corresponding to the molecular formula $C_{16}H_{18}O_9$. Another significant fragment ion peak m/z 191 represent a quinic acid $[M-H-162]$ suggesting caffeoylquinic acid moiety in the structure.

The ^1H NMR (Figure 4.81) showed three aromatic protons of the caffeoyl group at δ 7.06 (d , $J=2.0$), δ 6.80 (dd , $J=8.0\text{ Hz}$) and δ 6.97 (dd , $J=8.0$) assigned for H-2', H-5' and H-6' respectively. Two methylene protons in multiplet were observed at δ 2.05-2.25 ascribed for H-2 and H-6. Two olefinic protons at δ 7.56 (d , $J=16.0\text{ Hz}$) and δ 6.27 (d , $J=16.0\text{ Hz}$) were assigned for H-7' and H-8' respectively.

COSY spectrum (Figure 4.85) revealed the correlation of cross peaks between H-2 and H-3, H-3 and H-4, H-4 and H-5, H-5' and H-6', and H-7' and H-8'. Table 4.12 summarizes the ^1H and ^{13}C NMR of the compound.

The ^{13}C NMR and DEPT 135 (Figure 4.82 and 4.83) showed a total sixteen carbon signals comprising of carboxylic group (δ 175.8), ester carbonyl (δ 167.3), seven methines, two methylenes and five quaternary carbons.

The HMQC (Figure 4.85) and HMBC spectrum (Figure 4.86 and Scheme 4.7) confirmed all the assigned protons and carbons in the structure. Finally, comparison with the published spectroscopic data, the structure was identified as chlorogenic acid (**45**), a phenolic acid which was isolated for the first time from *Pseuduvaria monticola*.

Table 4.12: ¹H NMR (500 MHz) and ¹³C NMR (125 MHz) spectral data of chlorogenic acid (**45**) in CDOD₃ (δ in ppm, *J* in Hz)

Position	¹ H-NMR (δ ppm)	¹³ C-NMR(δ ppm)	¹³ C-NMR(δ ppm) (Hyun Min & Choi, 2010)
1	-	74.7	74.5
2	2.05, <i>m</i>	36.8	36.2
3	4.18, <i>dd</i> , <i>J</i> =3.2, 5.4	69.9	68.9
4	3.73, <i>dd</i> , <i>J</i> =3.0, 8.5	72.1	71.1
5	5.33, <i>dt</i> , <i>J</i> =4.4, 9.2	70.6	70.3
6	2.25, <i>m</i>	37.4	37.2
1'	-	126.4	125.5
2'	7.06, <i>d</i> , <i>J</i> =2.0	113.7	114.3
3'	-	145.4	145.1
4'	-	148.1	148.4
5'	6.80, <i>dd</i> , <i>J</i> =8.0	115.1	115.8
6'	6.97, <i>dd</i> , <i>J</i> =8.0	121.5	121.4
7'	7.56, <i>d</i> , <i>J</i> =16.0 Hz	145.6	145.6
8'	6.27, <i>d</i> , <i>J</i> =16.0 Hz	113.8	114.0
9'	-	167.2	165.9
COOH	-	175.7	175.0

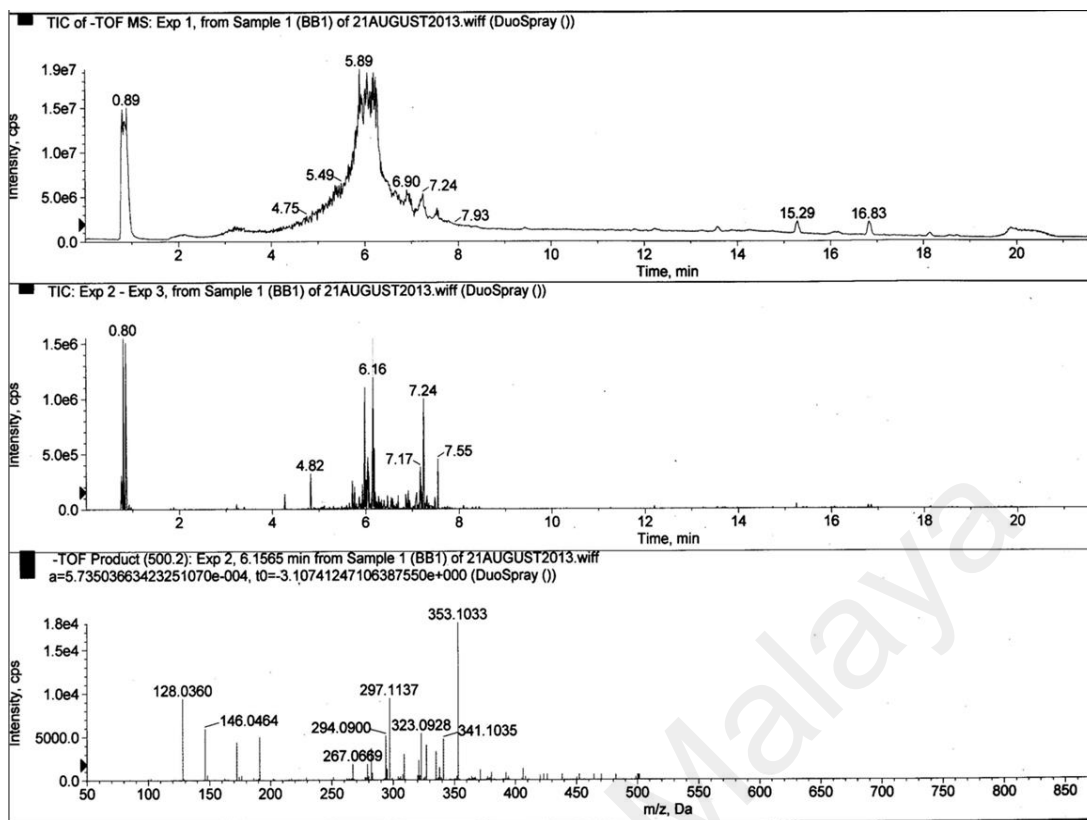


Fig. 4.79: TIC of chlorogenic acid (45) in negative mode

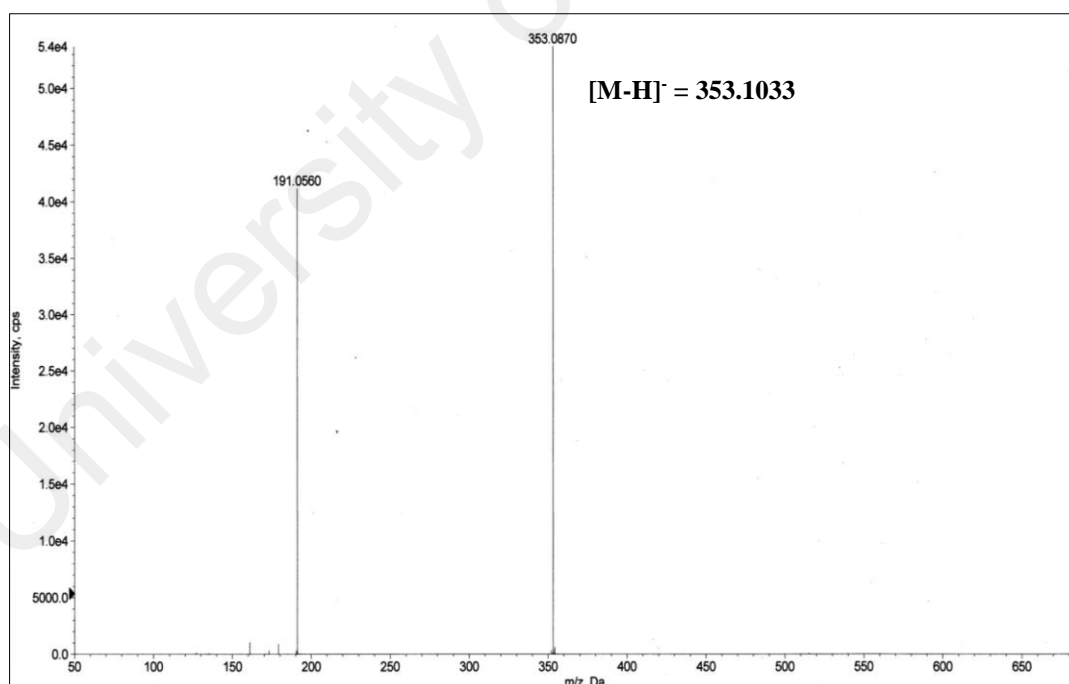


Fig. 4.80 : LC-MS spectrum of chlorogenic acid (45) in negative mode

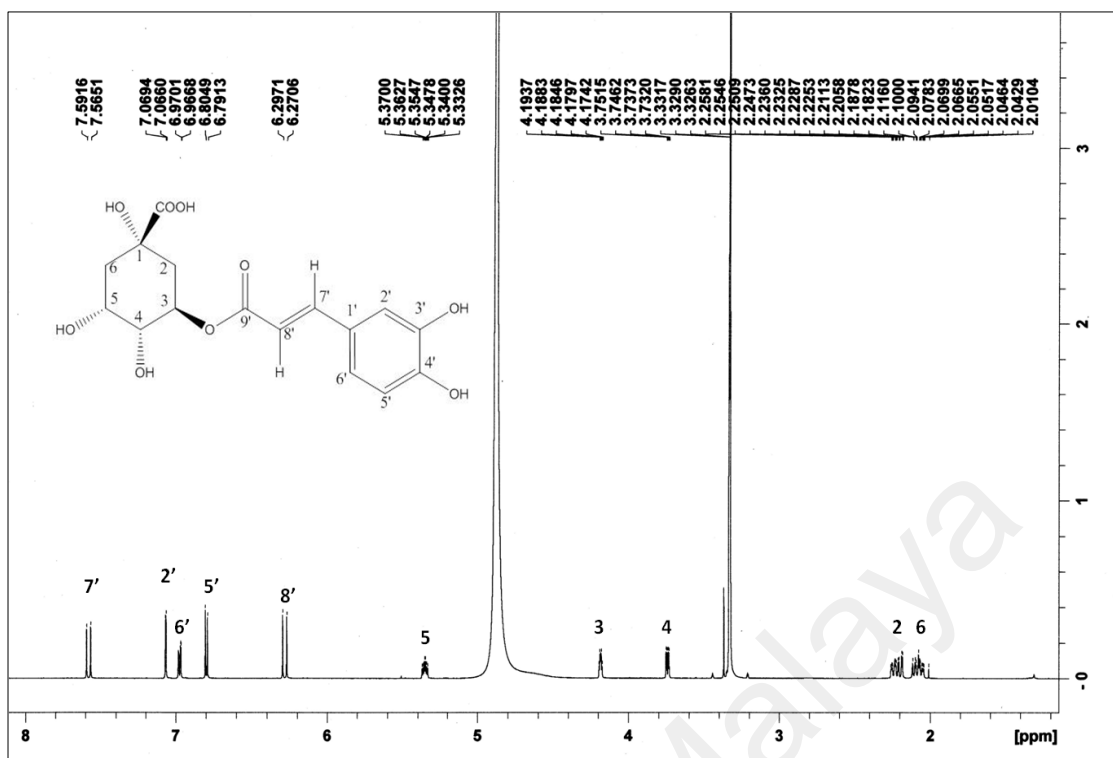


Fig. 4.81: ^1H NMR spectrum of chlorogenic acid (45)

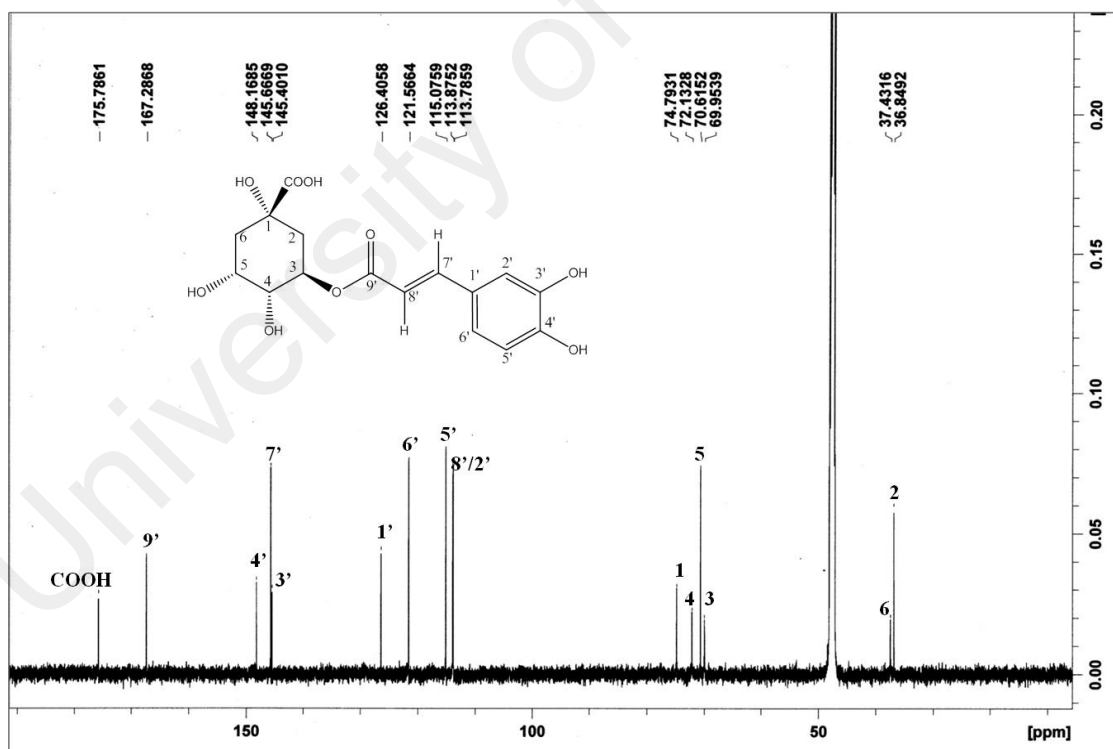


Fig.4.82: ^{13}C NMR spectrum of chlorogenic acid (45)

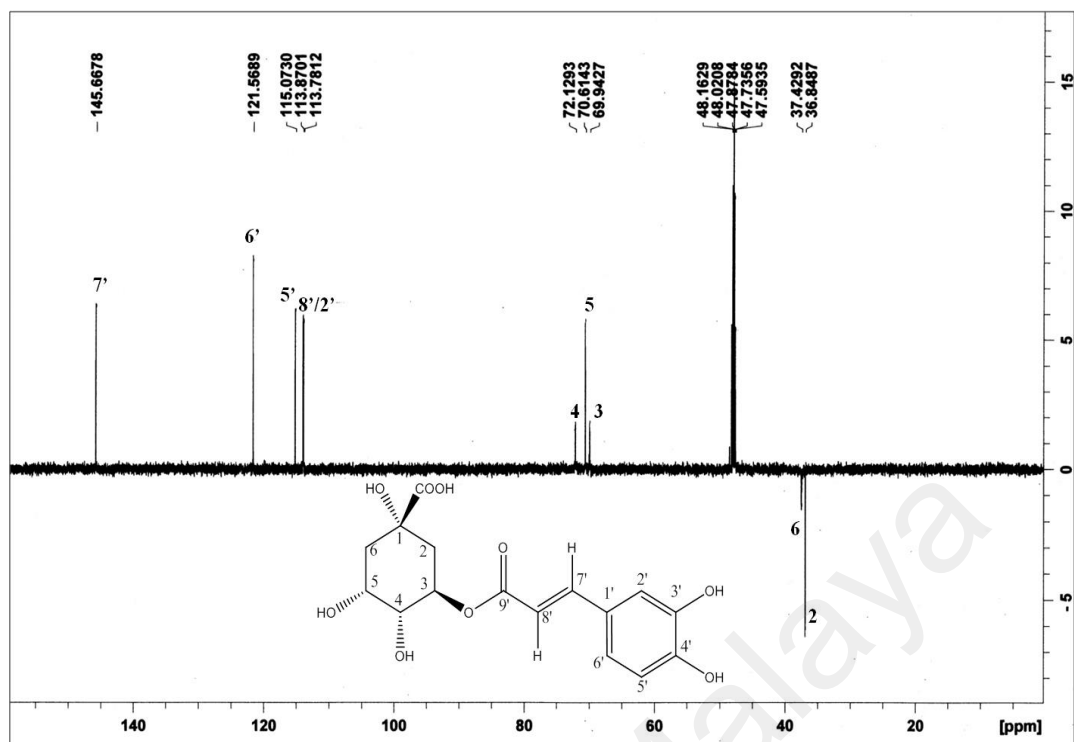


Fig. 4.83: DEPT 135 NMR spectrum of chlorogenic acid (45)

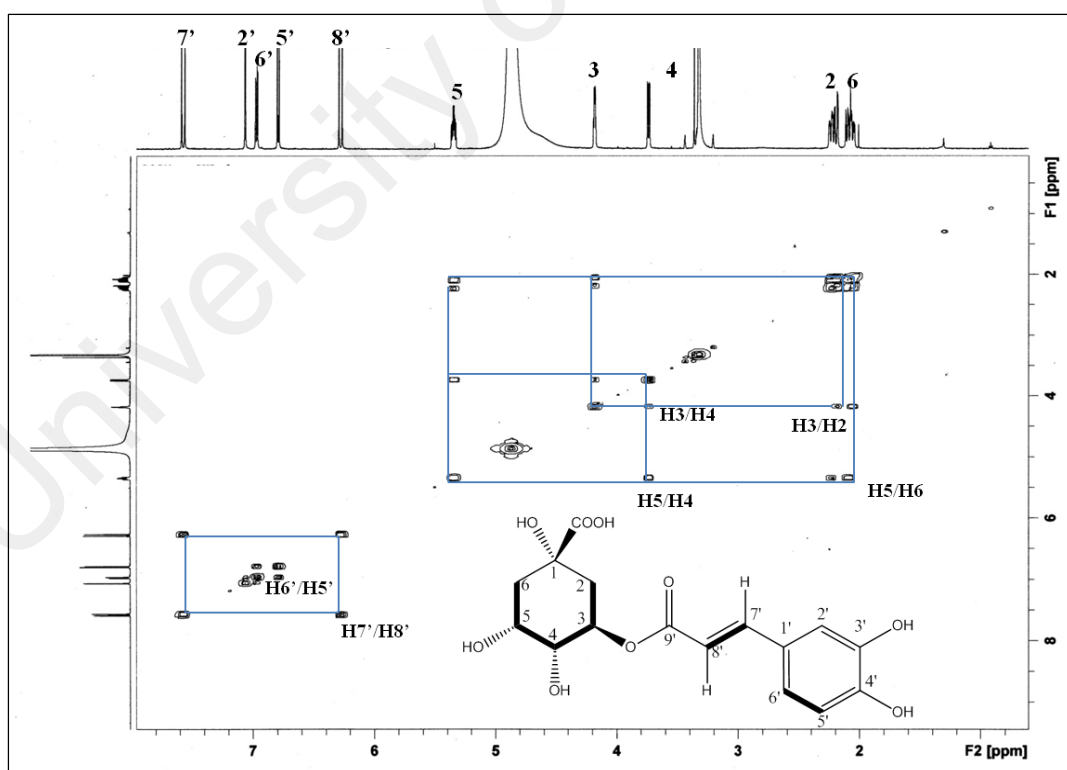


Fig. 4.84: COSY spectrum of chlorogenic acid (45)

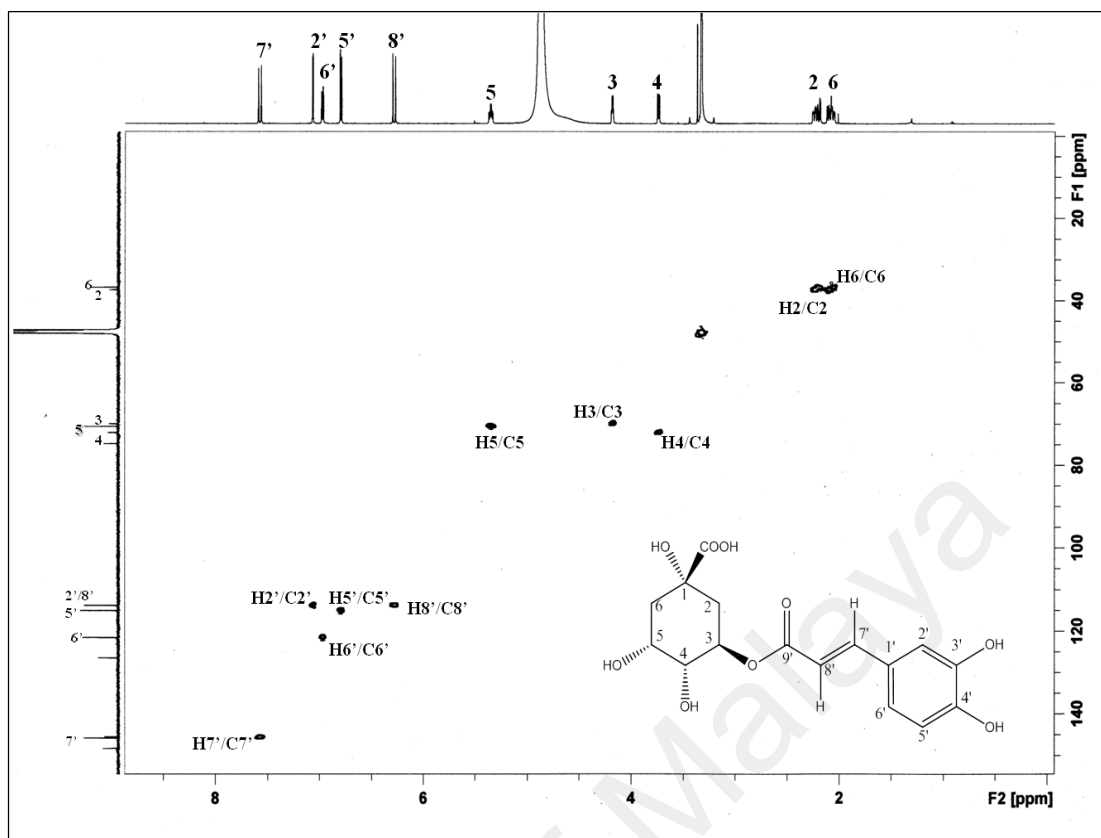


Fig. 4.85: HMBC spectrum of chlorogenic acid (45)

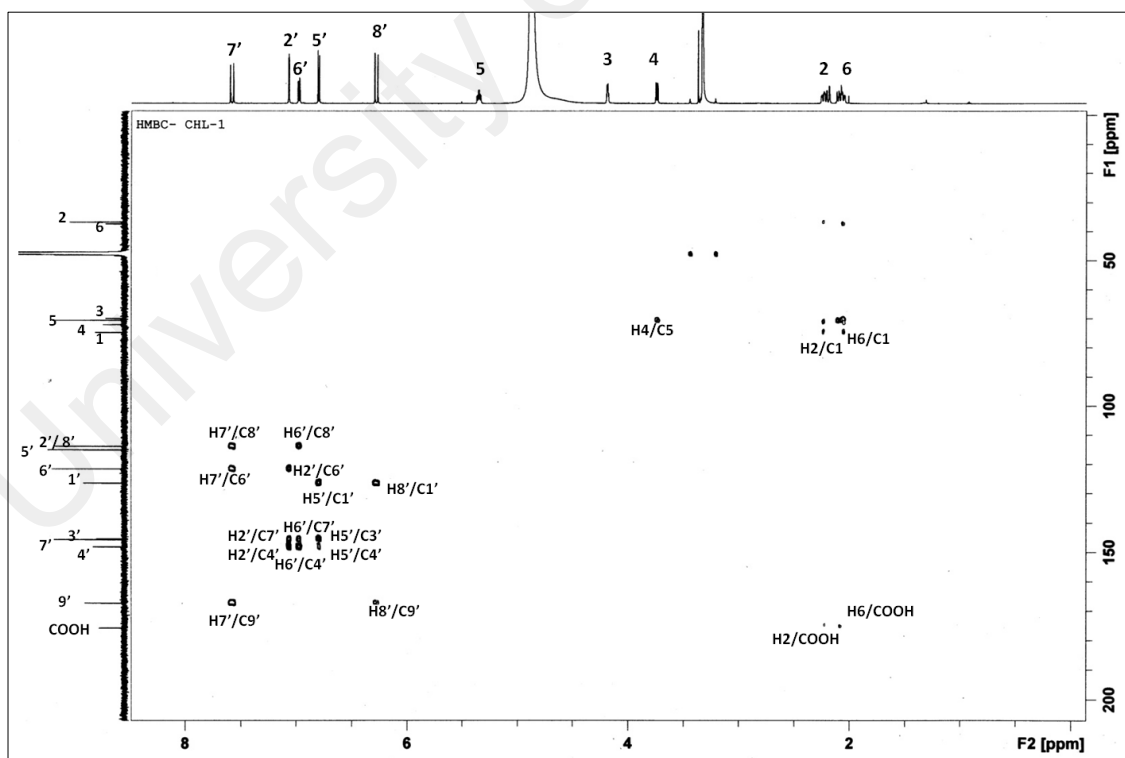
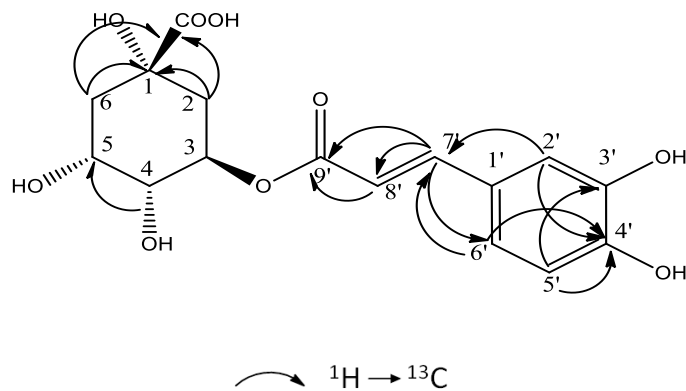


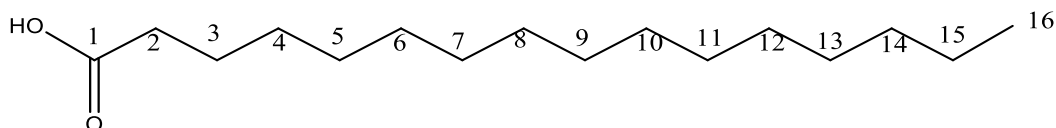
Fig. 4.86: HMBC spectrum of chlorogenic acid (45)



Scheme 4.7: The HMBC correlations of chlorogenic acid (**45**)

University of Malaya

4.2.13 *N*-hexadecanoic acid (**46**)



46

N-hexadecanoic acid (**46**), a fatty acid was isolated as light yellow oil. The UV spectrum showed absorption peak at 232 nm indicating the absence of a conjugated olefinic. The IR spectrum showed broad absorption band at 3500 cm^{-1} and 1702 cm^{-1} for hydroxyl group and carbonyl function, respectively. The GC-MS spectrum (Figure 4.87) gave a molecular ion peak at 256 [M]^+ corresponding to a molecular formula $\text{C}_{16}\text{H}_{32}\text{O}_2$, and this matched the NIST library for *n*-hexadecanoic acid (SI=93%) or palmitic acid.

The ^1H NMR spectrum (Figure 4.88) showed overlapping proton signals for methines and a terminal methyl proton at δ 0.84. Peak resonated at δ 2.27 assigned for H-2 indicate methylene proton next to the carboxylic group. The ^{13}C and DEPT 135 NMR (Figure 4.89 and 4.90) exhibited sixteen carbon signals. The carbon peak at δ 174.4 was assigned for the carbonyl function of the carboxylic acid. One methyl carbon signal was observed at δ 14.19. Table 4.13 summarizes the ^1H and ^{13}C NMR of the compound.

Finally, all relevant data confirmed the compound as *N*-hexadecanoic acid (**45**) which is a major compound in the hexane extract.

Table 4.13: ^1H NMR (500 MHz) and ^{13}C NMR (125 MHz) spectral data of *n*-hexadecanoic acid (**46**) in CDCl_3 (δ in ppm, *J* in Hz)

Position	^1H -NMR (δ ppm)	^{13}C -NMR(δ ppm)	^{13}C -NMR(δ ppm) (Joshi <i>et al.</i> , 2009)
1	-	174.6	173.0
2	2.27 (2H, <i>m</i>)	34.0	33.9
3	1.51 (2H, <i>m</i>)	29.1	29.1
4	1.29 (2H, <i>m</i>)	29.2	29.2
5	1.26 (2H, <i>m</i>)	29.3	29.3
6	1.29 (2H, <i>m</i>)	29.3	29.3
7	1.26 (2H, <i>m</i>)	29.4	29.4
8	1.29 (2H, <i>m</i>)	29.4	29.4
9	1.26 (2H, <i>m</i>)	29.4	29.4
10	1.29 (2H, <i>m</i>)	29.5	29.5
11	1.26 (2H, <i>m</i>)	29.5	29.5
12	1.29 (2H, <i>m</i>)	29.6	29.6
13	1.269 (2H, <i>m</i>)	29.6	29.6
14	1.29 (2H, <i>m</i>)	32.0	31.9
15	1.34 (2H, <i>m</i>)	22.7	22.7
16	0.87 (3H, <i>t</i>)	14.0	14.1

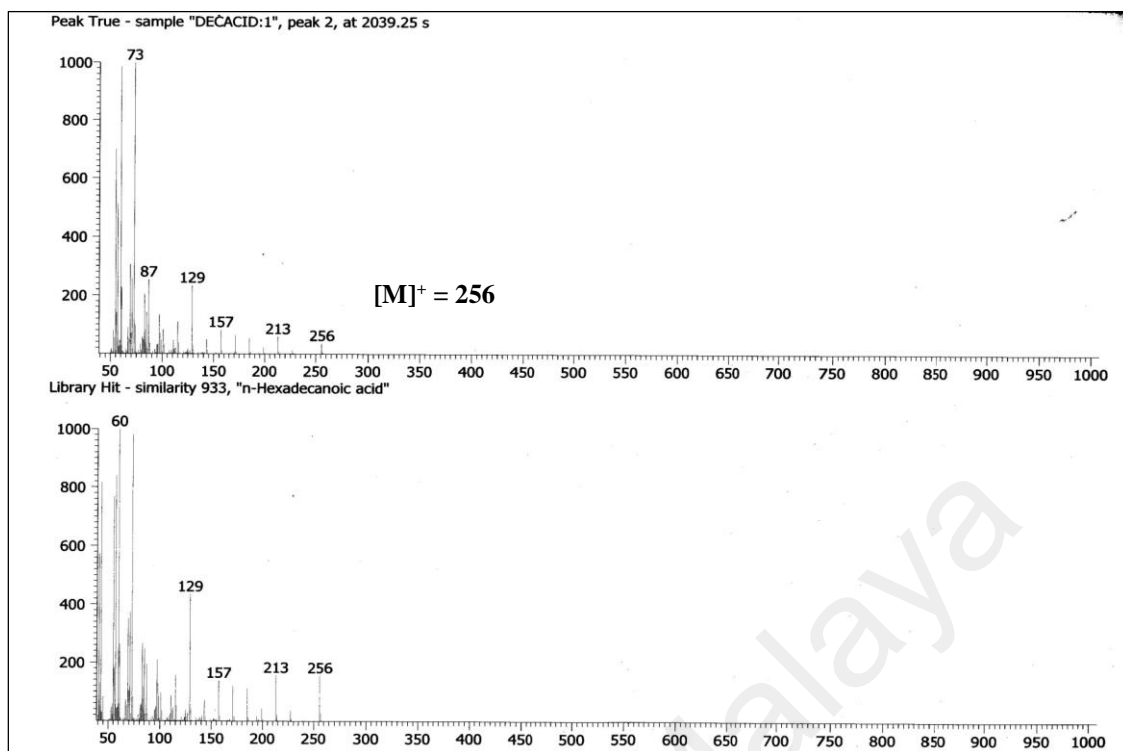


Fig. 4.87: GC-MS spectrum of *N*-hexadecanoic acid (46)

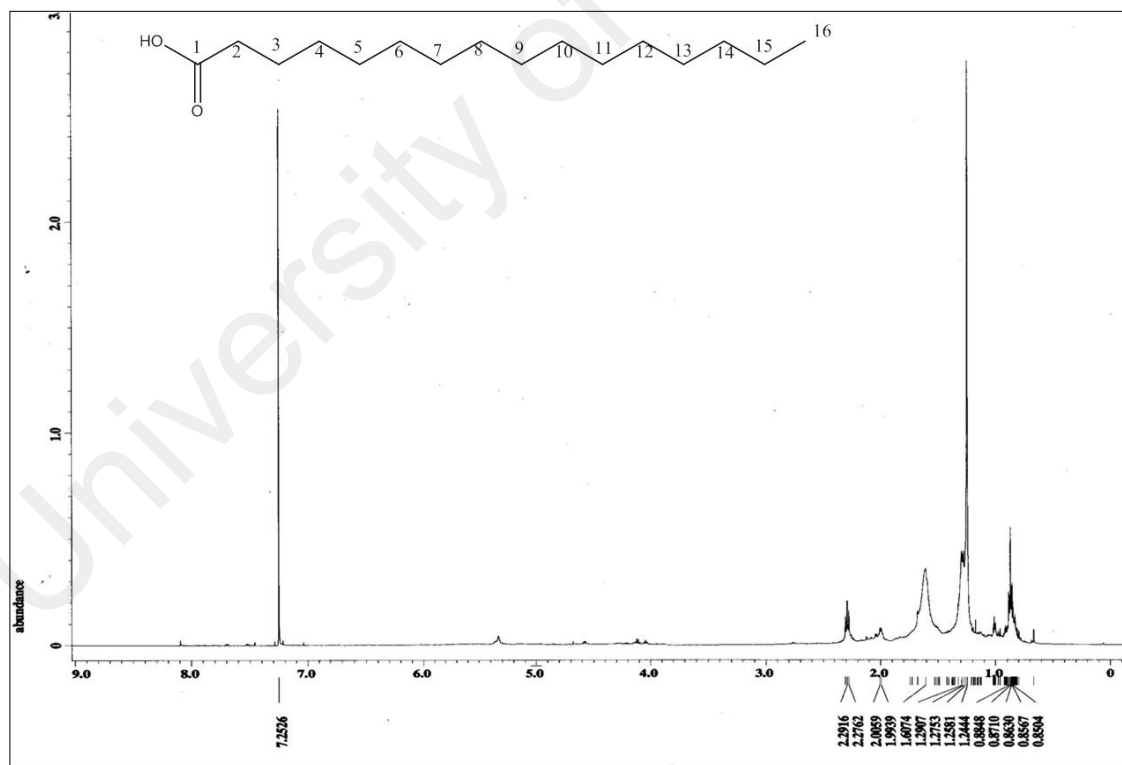


Fig. 4.88: ^1H -NMR spectrum of *N*-hexadecanoic acid (46)

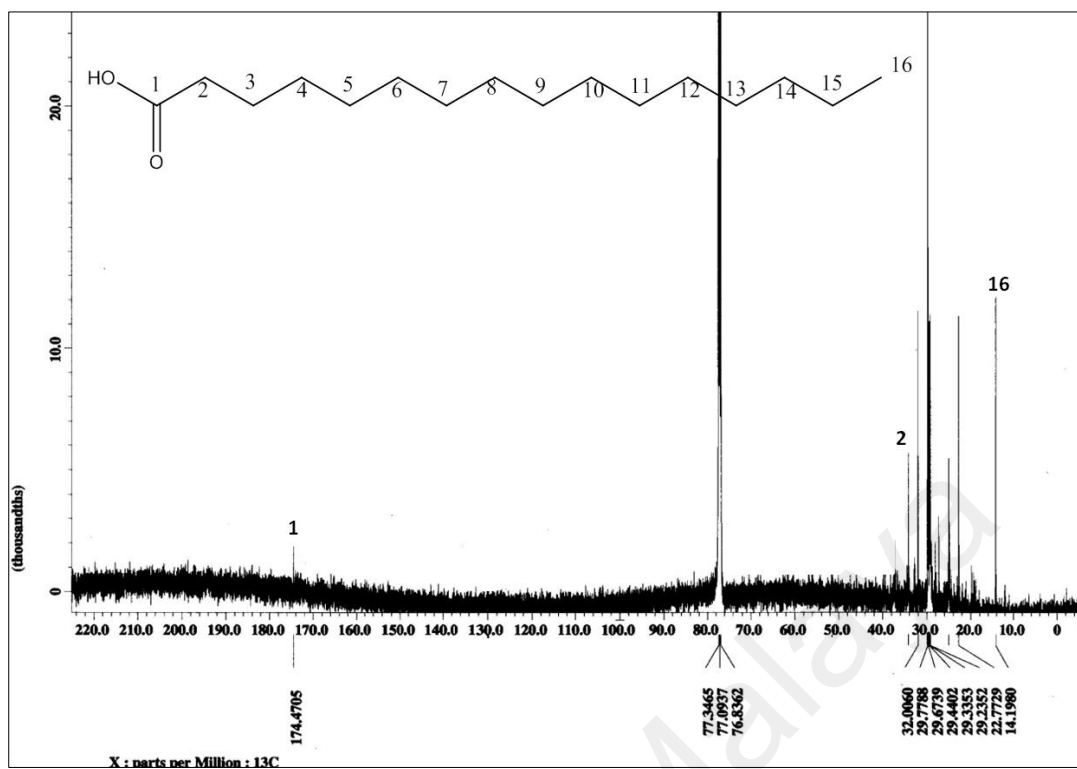


Fig. 4.89 : ^{13}C NMR of *N*-hexadecanoic acid (46)

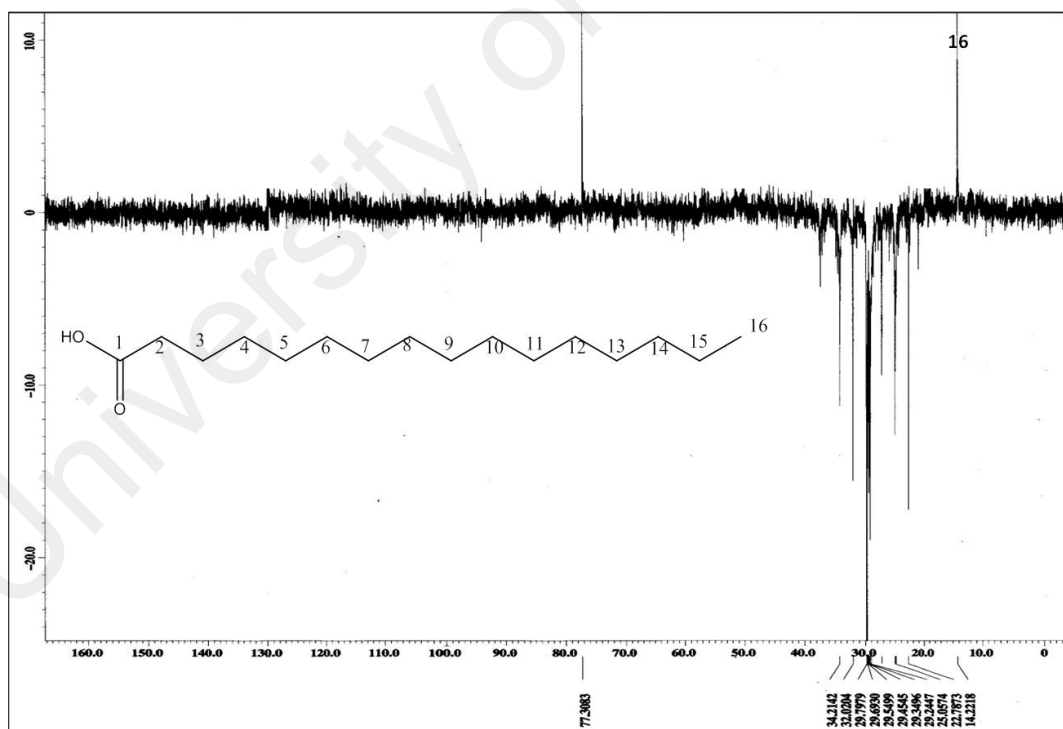
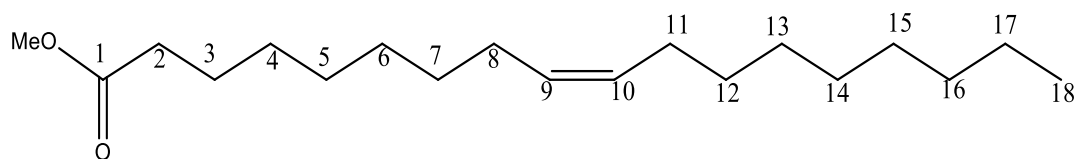


Fig. 4.90 : DEPT 135 spectrum of *N*-hexadecanoic acid (46)

4.2.14 Methyl oleate (47)



47

Methyl oleate (**47**) was afforded as pale yellow oil from the hexane extract. The IR spectrum showed absorption bands at 2925 cm^{-1} of aliphatic -CH stretching and carbonyl group at 1730 cm^{-1} . The GC-MS spectrum (Figure 4.91) showed molecular ion peak at $[M]^+$ 296 corresponding to the molecular formula of $C_{19}H_{36}O_2$.

The ^1H NMR spectrum (Figure 4.92) showed two olefinic protons as multiplet at δ 5.34 ($J=6.0\text{ Hz}$), 15 methylene signals and a methyl group at δ 0.87 (9H, *d*, $J=6.5\text{ Hz}$) in the aliphatic region. The ^{13}C and DEPT 135 spectrum (Figure 4.93) showed a total of nineteen carbon signals comprising of one methyl carbon peak at δ 14.22, two methine carbons at δ 130.32 and δ 130.12, a carbonyl group at δ 179.10 and the rest of fifteen methylene carbons. Table 4.14 summarizes the ^1H - and ^{13}C NMR of the compound.

Based on the spectroscopic data and matching by NIST library (SI=95%), the compound was identified as methyl oleate or 9-octadecanoic acid methyl ester (**47**).

Table 4.14: ^1H NMR (500 MHz) and ^{13}C NMR (125 MHz) spectral data of methyl oleate (**47**) in CDCl_3 (δ in ppm, J in Hz)

Position	^1H -NMR (δ ppm)	^{13}C -NMR(δ ppm)	^{13}C -NMR(δ ppm) (Pinheiro <i>et al.</i> , 2009)
1	-	178.6	179.8
2	2.33 (2H, <i>t</i> , $J= 1.7$, 7.3)	33.90	34.1
3	1.63 (2H, <i>m</i>)	24.7	24.7
4	1.28 (2H, <i>m</i>)	29.1	29.1
5	1.29 (2H, <i>m</i>)	29.2	29.2
6	1.29 (2H, <i>m</i>)	29.3	29.3
7	1.29 (2H, <i>m</i>)	29.6	29.7
8	2.04(2H, <i>m</i>)	27.1	27.3
9	5.33 (1H, <i>m</i>)	129.8	129.7
10	5.35 (1H, <i>m</i>)	130.1	130.0
11	2.76 (2H, <i>t</i> , $J=6.0$)	24.7	24.7
12	1.28 (2H, <i>m</i>)	29.2	29.2
13	1.28 (2H, <i>m</i>)	29.3	29.3
14	2.05(2H, <i>m</i>)	27.3	27.4
15	1.28 (2H, <i>m</i>)	29.6	29.7
16	1.28 (2H, <i>m</i>)	32.1	32.0
17	1.28 (2H, <i>m</i>)	22.8	22.8
18	0.87 (3H, <i>t</i> , $J=1.7$, 6.9)	14.2	14.2
OMe	-	51.4	51.5

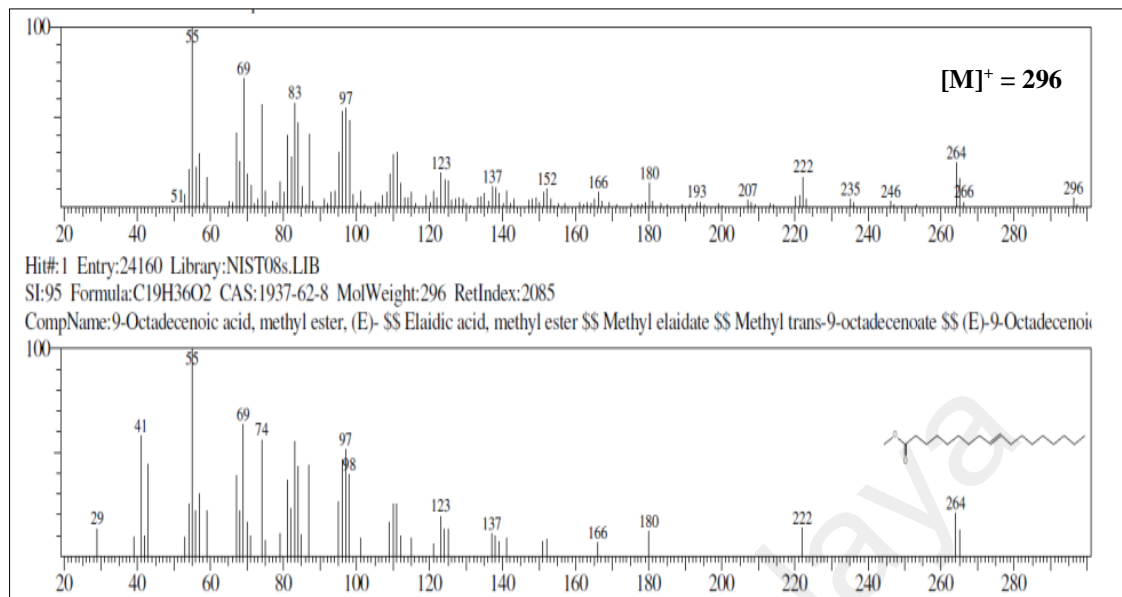


Fig. 4.91: GC-MS spectrum of methyl oleate (47)

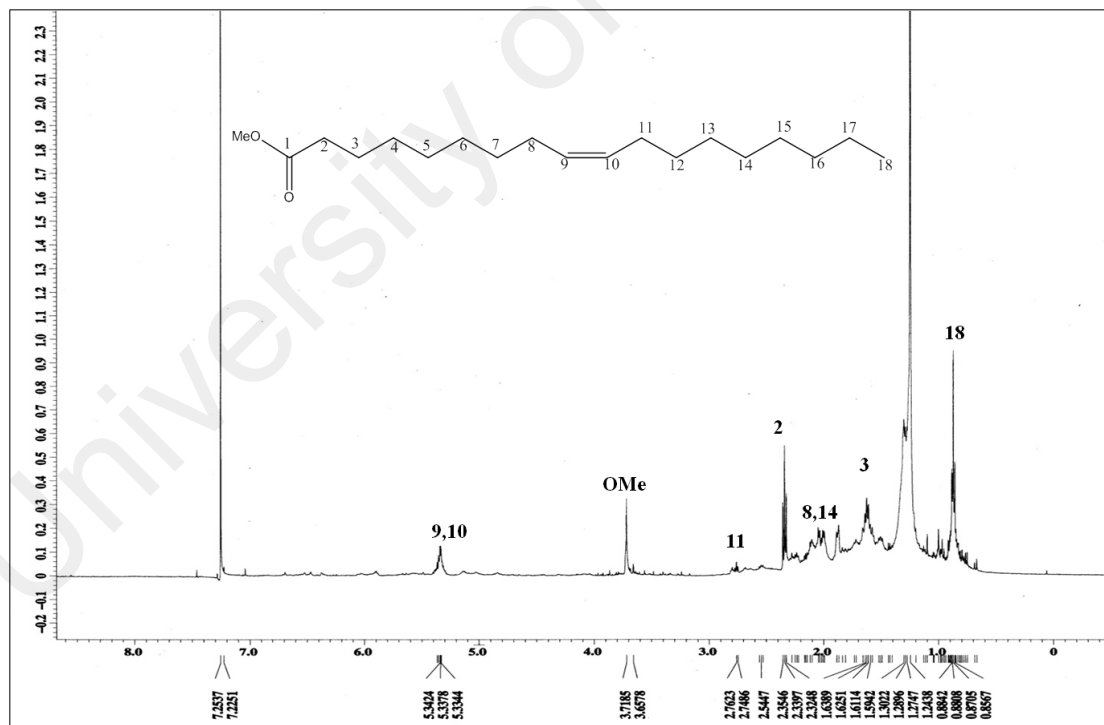


Fig. 4.92: ¹H NMR spectrum of methyl oleate (47)

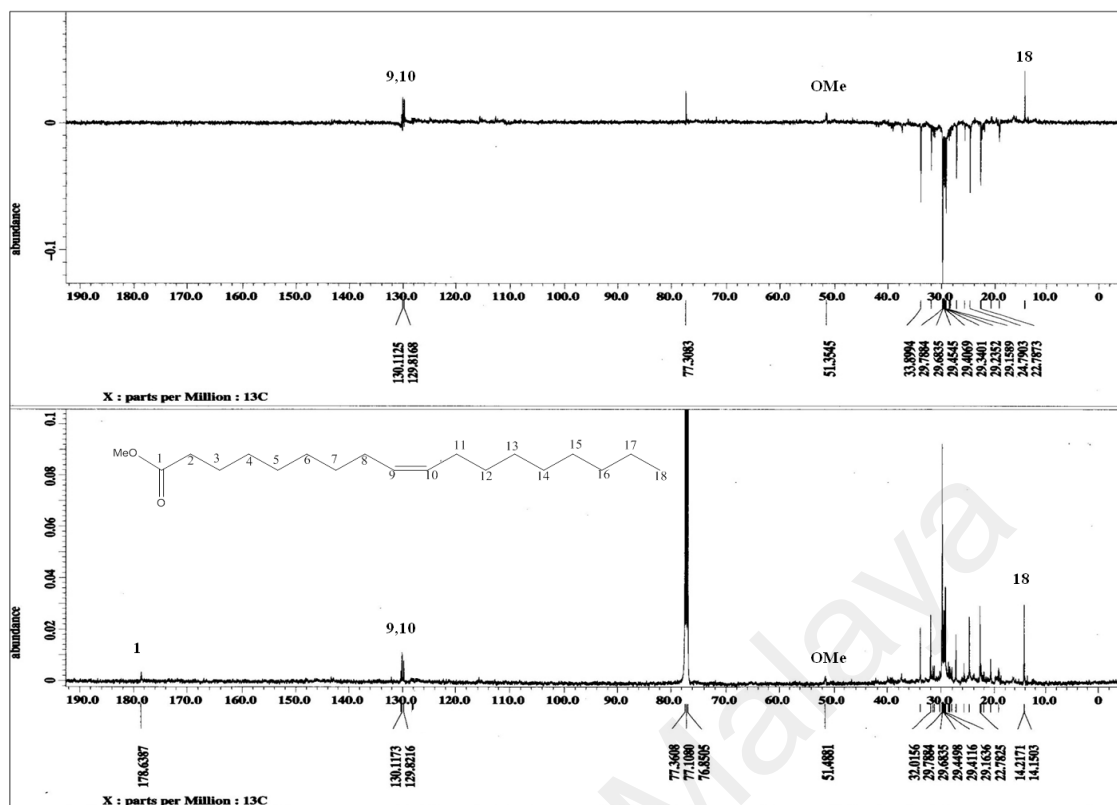
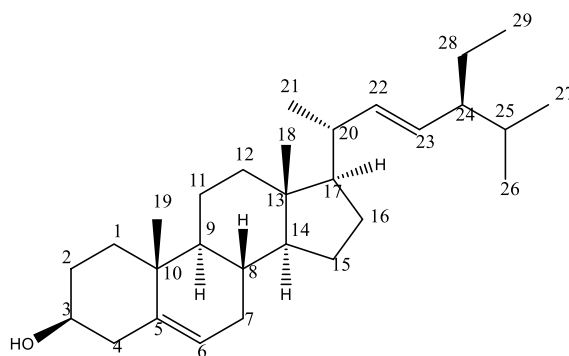


Fig. 4.93: ^{13}C NMR and DEPT 135 spectrum of methyl oleate (47)

4.2.15 Stigmasterol (48)



48

Stigmasterol (**48**) was isolated as white amorphous solid. The GC-MS spectrum (Figure 4.94) gave a molecular ion peak at m/z 412 corresponding to a molecular formula of $C_{29}H_{50}O$. The UV spectrum showed absorption bands at λ_{max} 300 and 250 nm. The IR spectrum showed a broad peak at 3432 cm^{-1} indicating the presence of a hydroxyl group.

The ^1H NMR spectrum (Figure 4.95) showed two doublet of doublet peaks at δ 5.09 (1H, *dd*, $J=8.4\text{ Hz}$) and 4.96 (1H, *dd*, $J=8.4\text{ Hz}$) were assigned to H-22 and H-23 respectively. Two multiplet peaks at δ 5.36 (1H, *m*) and δ 3.52 (1H, *m*) were assigned to H-6 and H-3, respectively. The presence of six methyl signals were observed at δ 0.71 (3H, H-18), 1.01 (3H, H-19), 0.98 (3H, H-21), 0.82 (3H, H-26), 0.80 (3H, H-27) and 0.81 (3H, H-29).

The ^{13}C and DEPT 135 spectra (Figure 4.96 and 4.97) gave a total carbon signal of 29 carbons. The peaks at δ 42.2, 39.7, 37.3, 31.9, 31.7, 28.8, 25.4, 24.4 and 21.1 were assigned to methylene groups of C-4, C-12, C-1, C-7, C-2, C-16, C-28, C-15 and C-11, respectively. Four downfield signals for olefinic carbons were observed at δ 140.8, 138.3, 129.2, and 121.8 were assigned for C-5, C-22, C-23 and C-6, respectively. The peak at

δ 71.8 showed the presence of a hydromethine carbon in the compound. The NMR spectral data are tabulated in Table 4.15.

Based on the spectroscopic data and comparison with literature values, also matching data with NIST library (SI > 80%), the compound was identified as stigmasterol (**48**). Although this compound is a very common sterol found in most plants, it is still worth reporting here for documentation purposes.

University of Malaya

Table 4.15: ^1H NMR (500 MHz) and ^{13}C NMR (125 MHz) spectral data of stigmasterol (**48**) in CDCl_3 (δ in ppm, J in Hz)

Position	^1H -NMR (δ ppm)	^{13}C -NMR (δ ppm)	^{13}C -NMR (δ ppm) (Pateh <i>et al.</i> , 2009)
1	1.81	37.3	37.2
2	1.79	31.7	31.6
3	3.52, <i>m</i>	71.8	71.8
4	2.27	42.3	42.3
5	-	140.8	140.7
6	5.36, <i>m</i>	121.7	121.7
7	1.93	31.9	31.9
8	1.45	31.9	31.9
9	0.92	51.2	51.2
10	-	36.5	36.5
11	1.50	21.1	21.1
12	1.95	39.7	39.7
13	-	42.3	42.2
14	1.00	56.9	56.8
15	1.54	24.4	24.3
16	1.65	28.4	28.5
17	1.12	56.1	56.1
18	0.70 (3H, <i>s</i>)	12.1	12.0
19	1.01, <i>s</i>	21.2	21.2
20	2.00	40.5	40.5
21	1.02, <i>d</i> ,7.5	21.2	21.2
22	5.11	138.3	138.2
23	5.00	129.2	129.2
24	1.52	51.2	51.2
25	1.53	31.9	31.9
26	0.79, (3H, <i>d</i>), $J=6.5$)	21.2	21.1
27	0.85 (3H, <i>d</i>), $J=6.5$)	19.0	19.1
28	1.43	25.4	25.4
29	0.80 (3H, <i>t</i>), $J=7.5$)	12.3	12.2

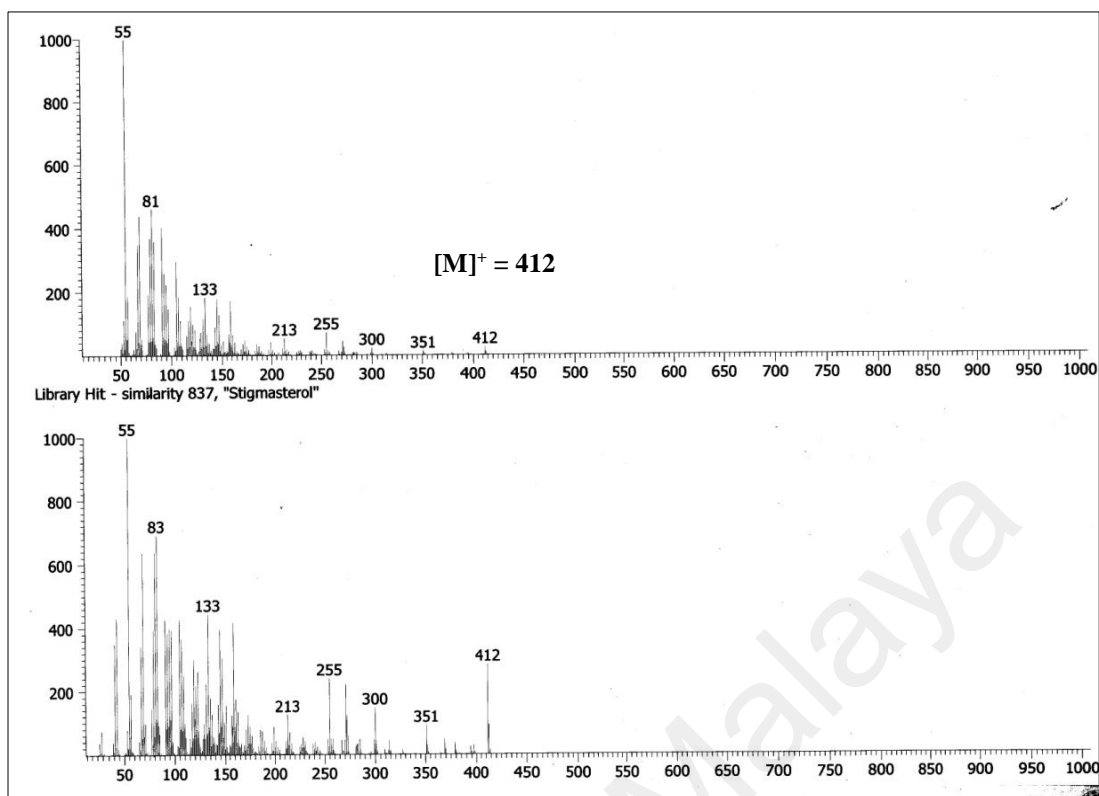


Fig. 4.94: GC-MS spectrum of stigmasterol (48)

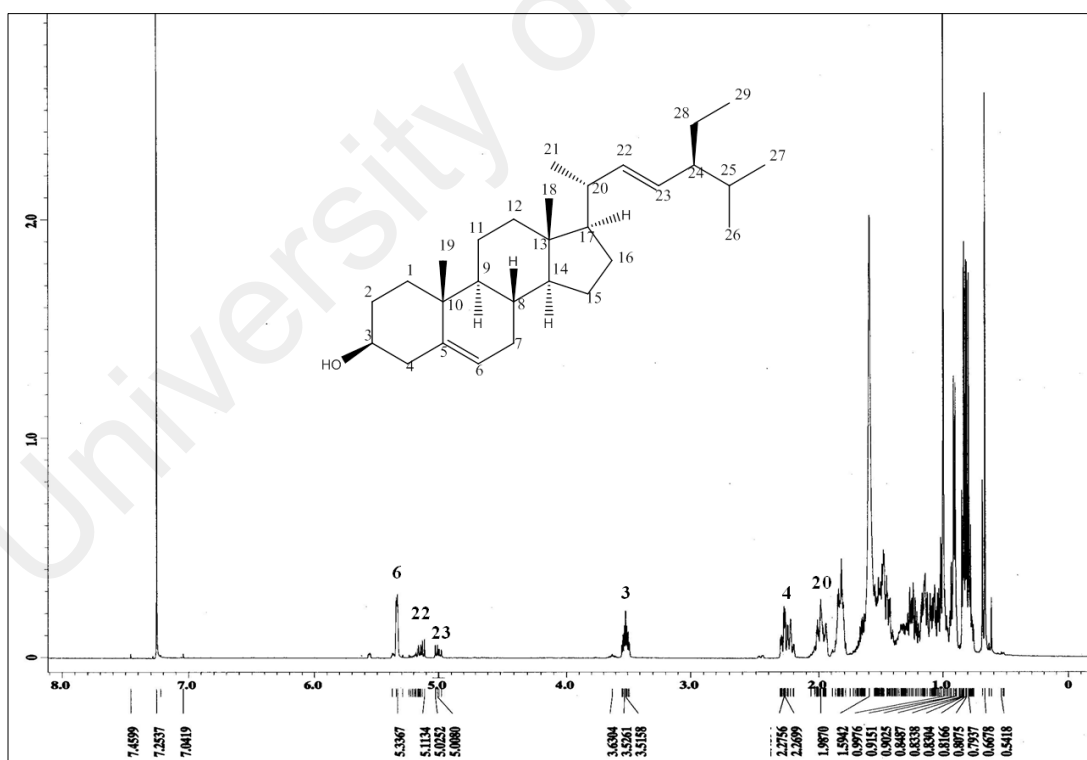


Fig. 4.95: ¹H NMR spectrum of stigmasterol (48)

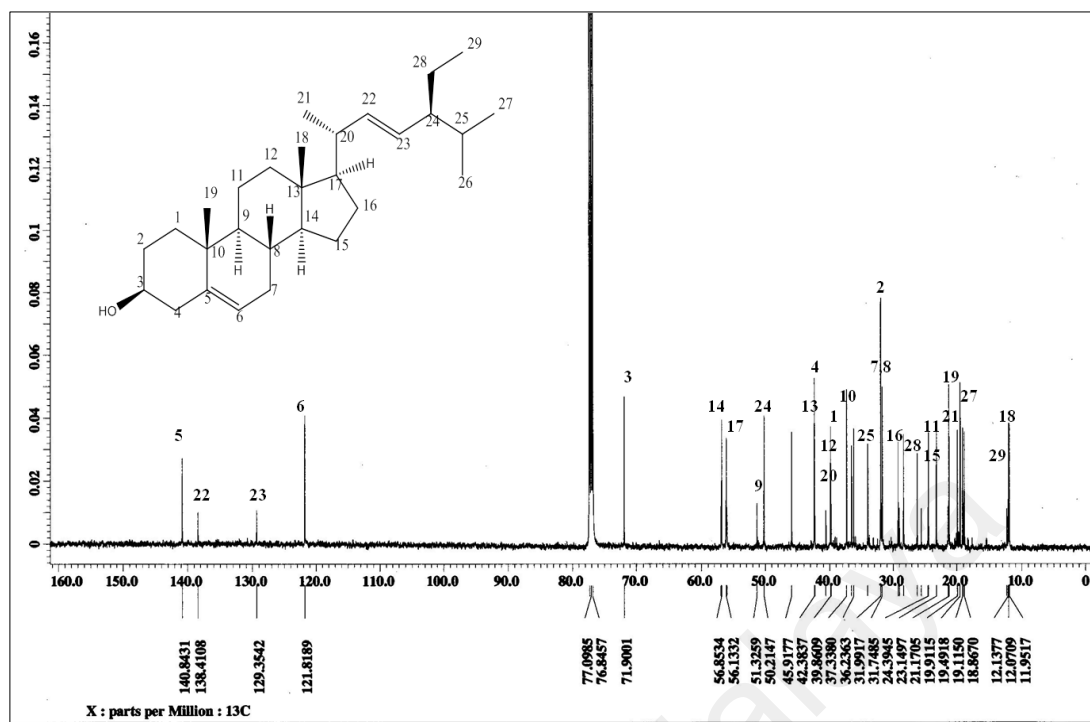


Fig. 4.96: ^{13}C NMR spectrum of stigmasterol (48)

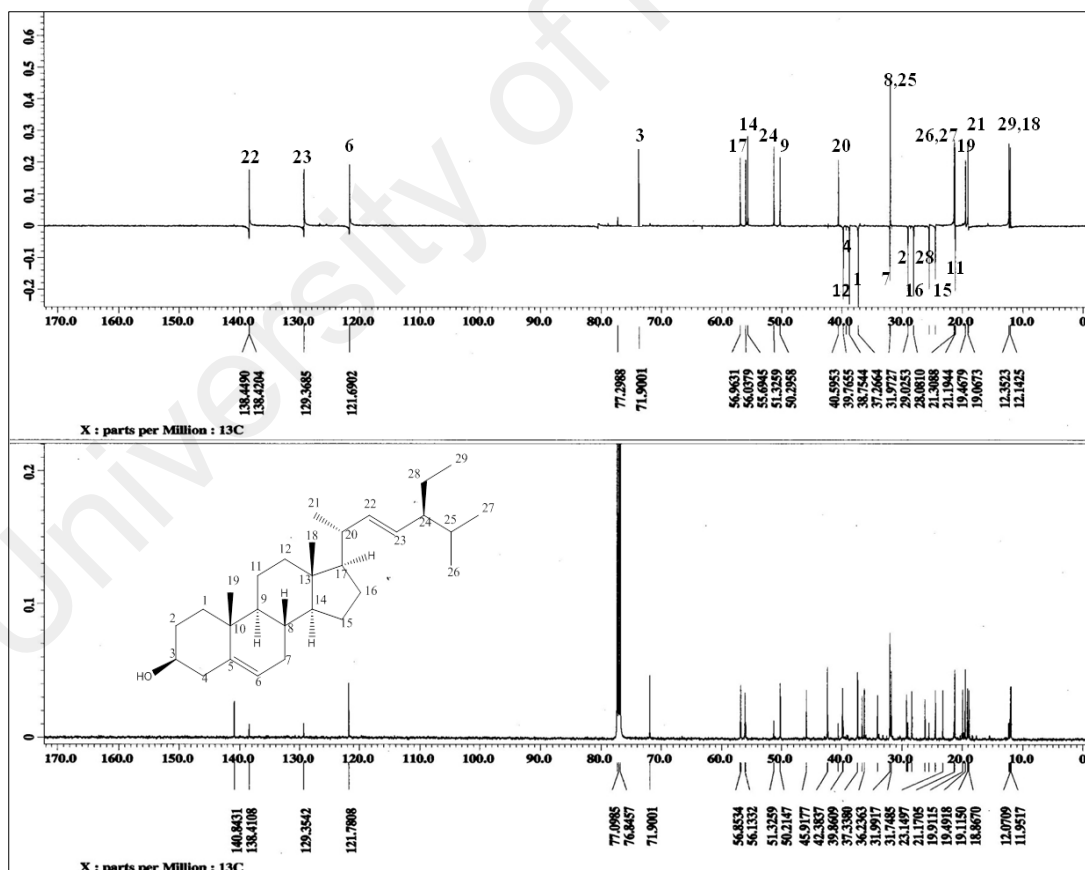


Fig. 4.97: DEPT 135 NMR spectrum of stigmasterol (48)

4.3 Chemical constituents of *Pseuduvaria macrophylla*

Phytochemical analysis on the leaves and bark of *Pseuduvaria macrophylla* resulted in the isolation of fourteen compounds; one new compound; 1,3,5,7-tetramethoxy-2-naphthoic acid (**51**), five oxoaporphine alkaloids; liriodenine (**3**), lysicamine (**39**) atherospermidine (**10**), *N*-methyl ouregidione (**5**) and *O*-methylmoschatoline (**7**), two benzopyran derivatives; polycerasoidol (**16**) and polycerasoidin (**49**), two phenyl propanoids; elimicin (**26**) and elimicin 6-methoxy (**50**), two sterols; β -sitosterol (**52**) and stigmasta-5,22-diene, 3 methoxy (**53**) and two fatty acids; oleic acid (**54**) and hexadecanoic acid methyl ester (**55**). All compounds were listed in Table 4.16.

University of Malaya

Table 4.16: Compounds isolated from the bark of *Pseuduvaria macrophylla*

No	Compounds	Classification of compounds	Parts of plant
1	Liriodenine (3)	Oxoaporphine	Leave/Bark
2	Lysicamine (39)	Oxoaporphine	Leave/Bark
3	Atherospermidine (10)	Oxoaporphine	Leave/Bark
4	<i>N</i> -methyl ouregidione (5)	Oxoaporphine	Leave
5	O-methylmoschatoline (7)	Oxoaporphine	Bark
6	Polycerasoidol (16)	Benzopyran derivative	Leave/Bark
7	Polycerasoidin (49)	Benzopyran derivative	Leave/Bark
8	Elemicin (26)	Phenylpropanoid	Bark
9	Elemicin 6-methoxy (50)	Phenylpropanoid	Bark
10	1,3,5,7-tetramethoxy-2-naphthoic acid (51)	Naphthoic acid derivative	Bark
11	β -sitosterol (52)	Sterol	Bark
12	Stigmasta-5,22-diene, 3 methoxy (53)	Sterol	Bark
13	Oleic acid (54)	Fatty acids	Bark
14	Hexadecanoic acid methyl ester (55)	Fatty acid	Leave/Bark

4.3.1 Liriodenine (3)

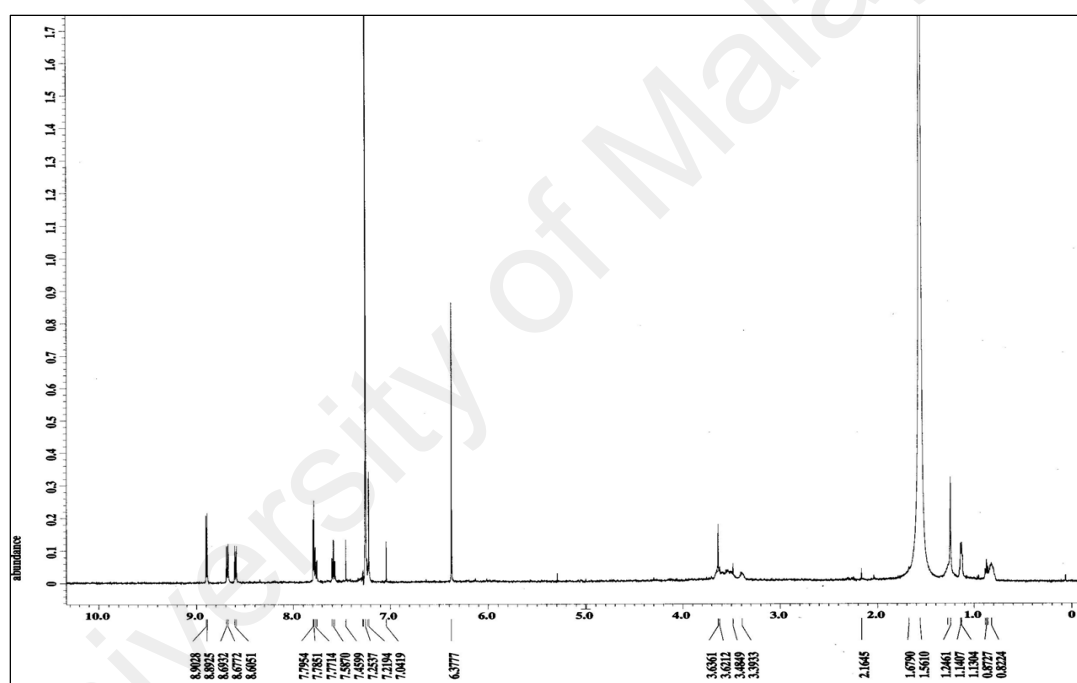
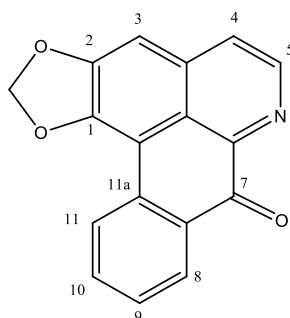
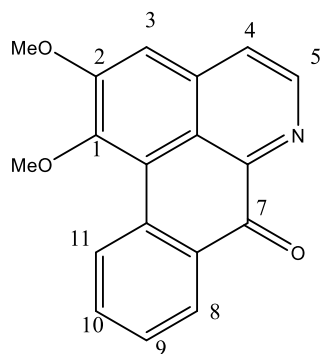


Fig. 4.98: ¹H NMR spectrum of liriodenine (3)

Alkaloid liriodenine (3) was isolated as yellow needles, showed positive result to Dragendorff's test. The ¹H NMR spectrum (Figure 4.98) resembled liriodenine (3) which was isolated from *P. monticola*.

4.3.2 Lysicamine (39)



39

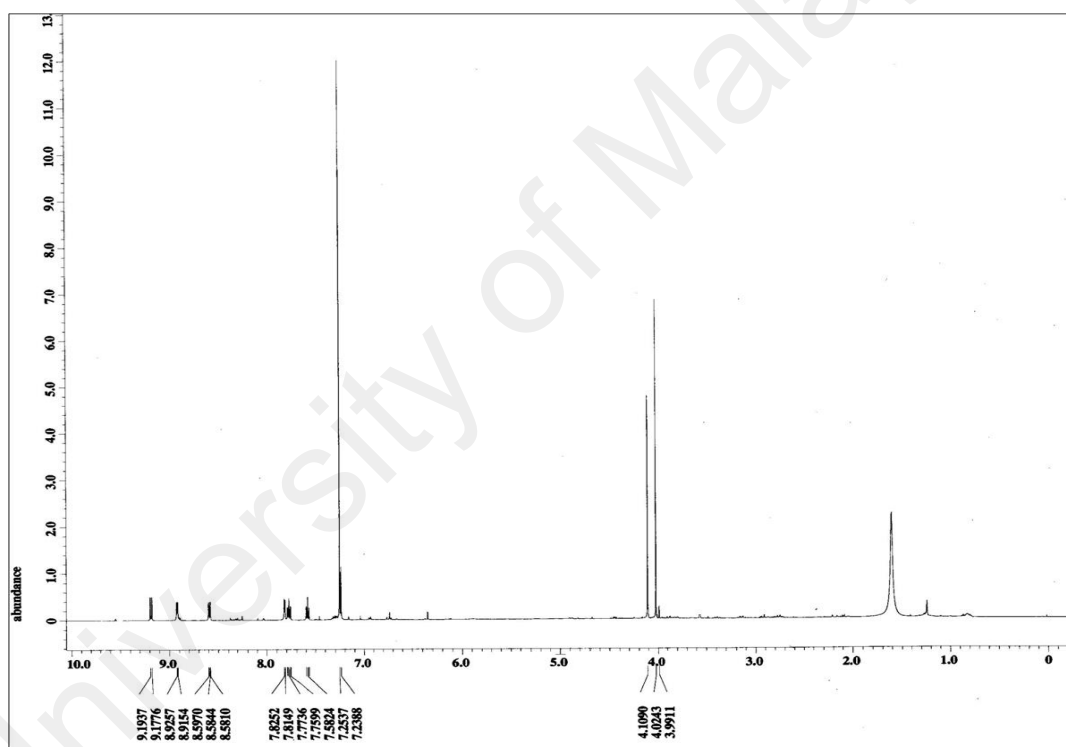
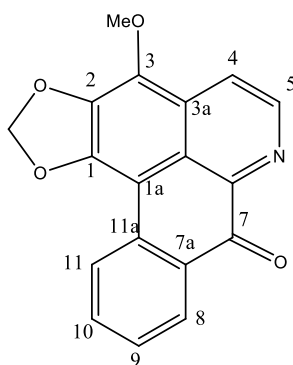


Fig. 4.99: ¹H NMR spectrum of lysicamine (39)

Alkaloid lysicamine (39) was isolated as a yellow amorphous solid and gave positive result to Dragendorff's test. The ¹H NMR spectrum (Figure 4.99) resembled lysicamine (39) which was isolated from *P. monticola*.

4.3.3 Atherospermidine (10)



10

Alkaloid atherospermidine (**10**) was isolated as bright yellow amorphous solid and showed positive result with Dragendorff's spray reagent. The UV spectrum showed the absorption bands at λ_{\max} 247, 281, 312, 383 and 440 nm suggesting the existence of a highly unsaturated chromophore and characteristic of an oxoaporphine alkaloid.

The IR spectrum showed strong absorption peak at 1737 cm^{-1} attributed typically to a highly conjugated ketone function of a carbonyl group and two peaks at 1051 cm^{-1} and 948 cm^{-1} indicate C-O stretching vibration of a methylenedioxy function.

The HREIMS (Figure 4.100) showed a molecular ion peak at m/z 306.0761 $[M+H]^+$ corresponding to the molecular formula $C_{18}H_{11}NO_4$. The molecular weight indicates an additional mass of 31 dalton compared to that of liriodenine (**3**) which could be attributed to a methoxy group. This was further confirmed by a methoxy peak at δ 4.31 in the ^1H NMR spectrum.

The ^1H NMR spectrum (Figure 4.101) showed six signals for six aromatic protons at δ 7.51 to 8.90 ppm and one methylenedioxy group (2H, δ 4.29). C-3 is substituted by the methoxy group in the absence of a proton singlet at δ 7.2.

In COSY spectrum (Figure 4.104), there are correlations between H-8 with H-9; H-9 with H-10 and H-8; H-10 with H-9 and H-11; and H-11 affirming that ring D is unsubstituted. Table 4.17 summarizes the ^1H - and ^{13}C NMR of the compound.

The ^{13}C and DEPT 135 NMR spectrum (Figure 4.102 and 4.103) showed signals for 18 carbons comprising of one methoxy, one methylenedioxy, one carbonyl, six methines and nine quaternary carbons. The low field chemical shift at δ 182.6 ppm showed the signal for carbonyl group. One methylenedioxy carbon and one methoxy carbon appeared at δ 102.3 and 60.3 ppm, respectively. HMQC spectrum (Figure 4.105 and 4.106) and HMBC spectrum (Scheme 4.8) confirmed all the assigned protons and carbons in the structure.

Finally, the compound was established as atherospermidine (**10**) which was previously isolated from *Pseuduvaria indochinensis* (Shou-Ming *et al.*, 1988).

Table 4.17: ^1H NMR (500 MHz) and ^{13}C NMR (125 MHz) spectral data of atherospermidine (**10**) in CDCl_3 (δ in ppm, J in Hz)

Position	^1H -NMR (δ ppm)	^{13}C -NMR (δ ppm)	^{13}C -NMR (δ ppm) (Emmanoel et al., 2011)
1	-	151.7	150.0
1a	-	102.5	102.6
1b	-	127.5	126.9
2	-	135.5	136.3
3	-	136.3	136.1
3a	-	129.2	130.6
3b	-	123.2	122.8
4	8.18 (1H, <i>d</i> , $J=5.7$)	119.3	119.5
5	8.90 (1H, <i>d</i> , $J=5.3$)	144.5	144.3
6a	-	146.7	144.9
7	-	182.5	182.6
7a	-	130.8	130.6
8	8.58 (1H, <i>d</i> , $J=8.0$)	127.5	128.5
9	7.60 (1H, <i>dt</i> , 7.5, 1.6)	126.5	127.4
10	7.77 (1H, <i>dt</i> , 7.6, 1.7)	134.0	134.1
11	8.67 (1H, <i>d</i> , $J=7.8$)	128.5	126.7
11a	-	133.0	133.1
$-\text{CH}_2\text{O}_2-$	6.33 (2H, <i>s</i>)	103.3	102.3
OCH_3	4.31 (3H, <i>s</i>)	60.2	60.2

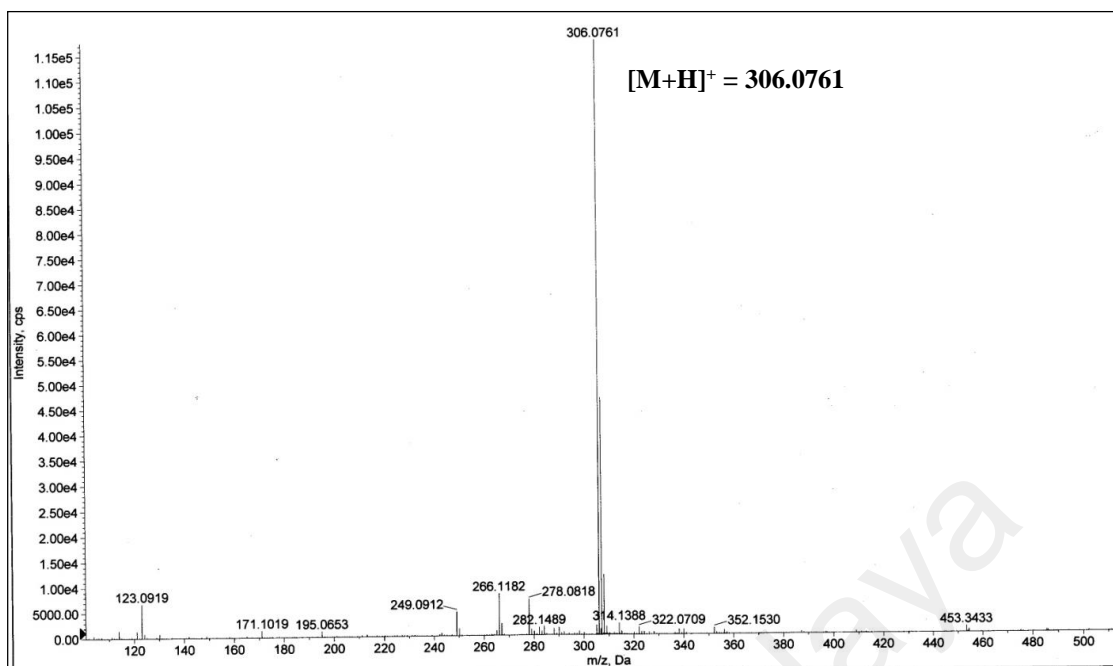


Figure 4.100: LC-MS spectrum of atherospermidine (10)

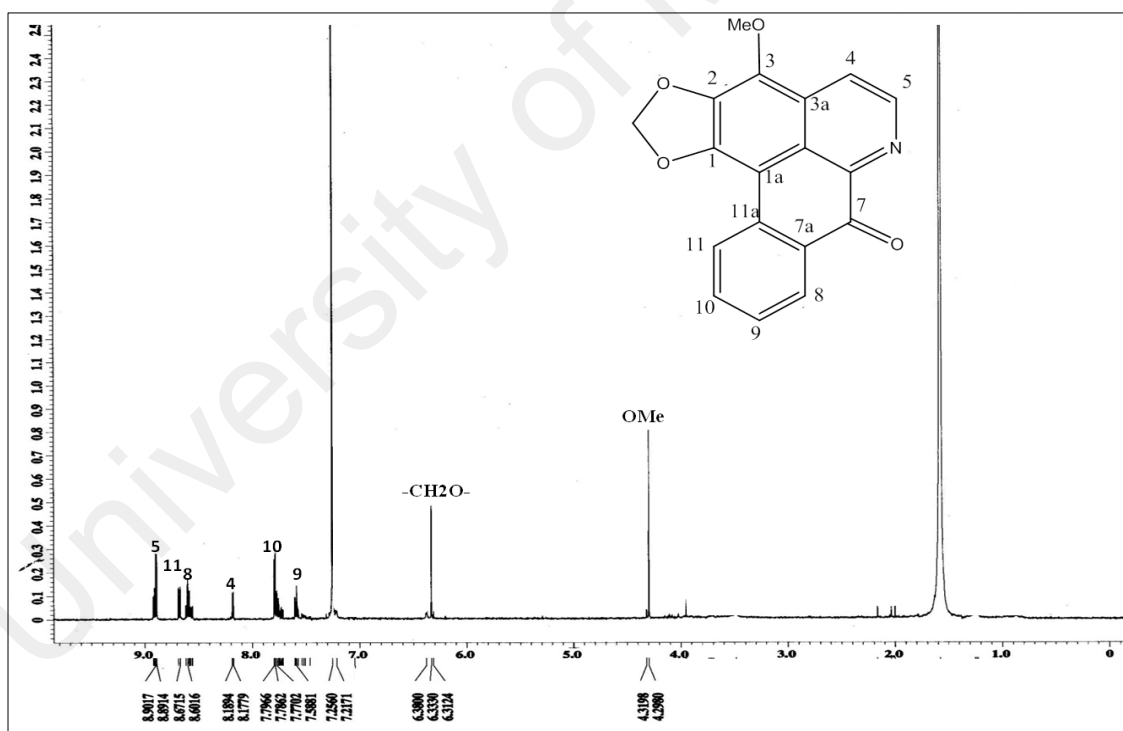


Fig. 4.101: ¹H NMR spectrum of atherospermidine (10)

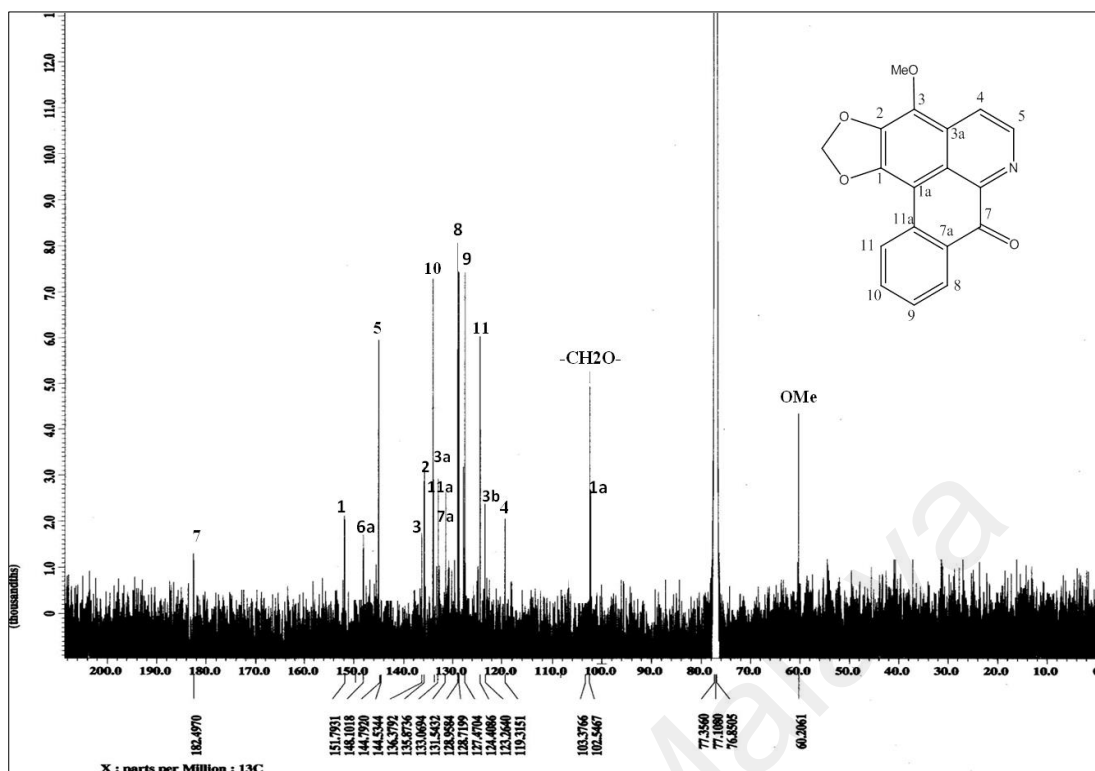


Fig. 4.102: ^{13}C NMR spectrum of atherospermidine (10)

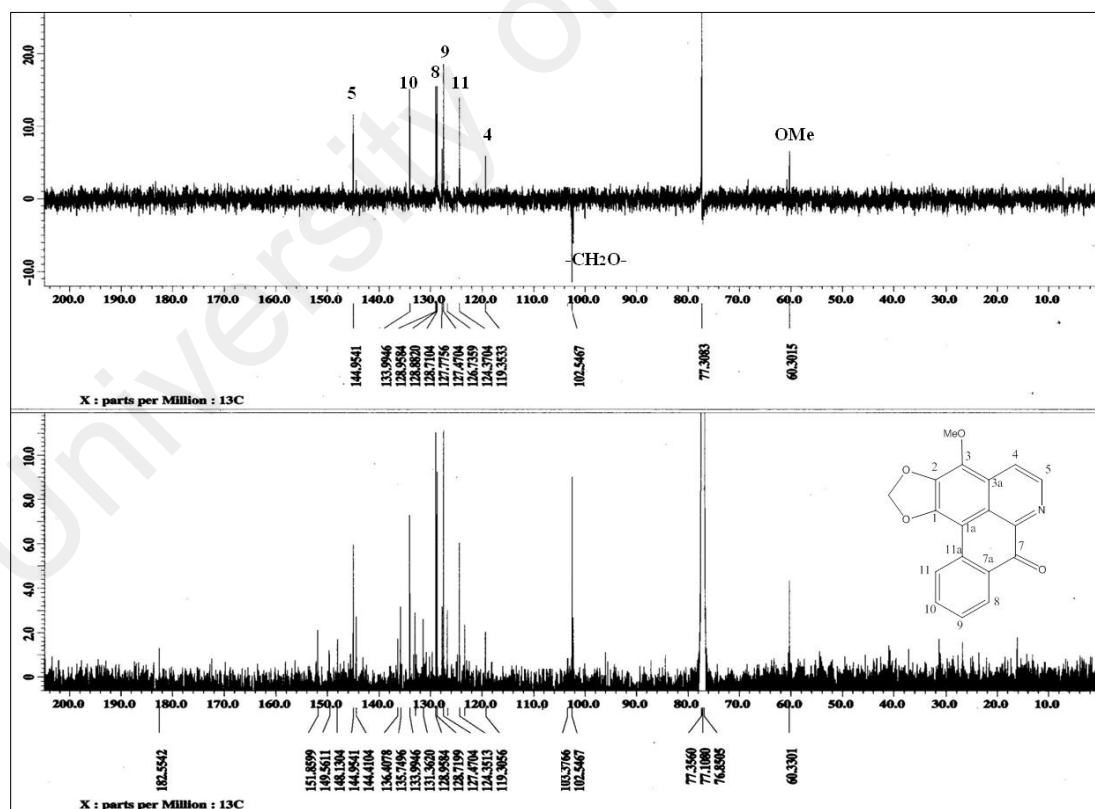


Fig. 4.103: DEPT 135 and ^{13}C NMR spectrum of atherospermidine (10)

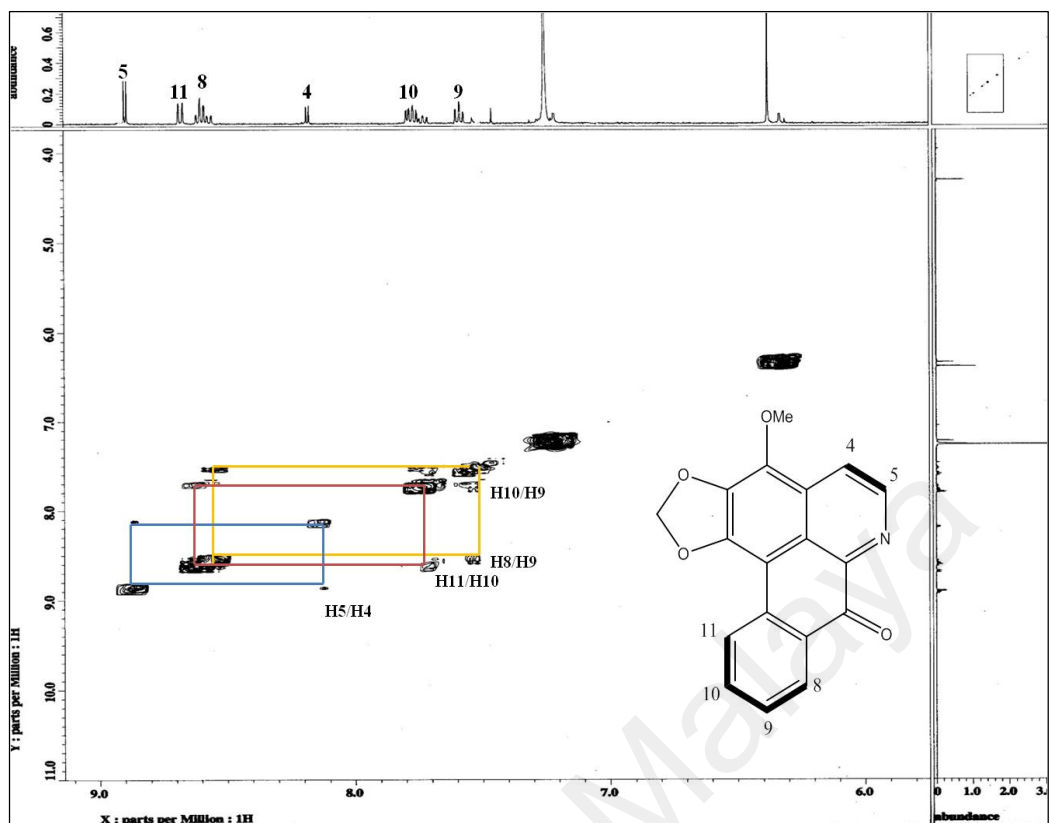


Fig. 4.104: Expanded COSY spectrum of atherospermidine (10)

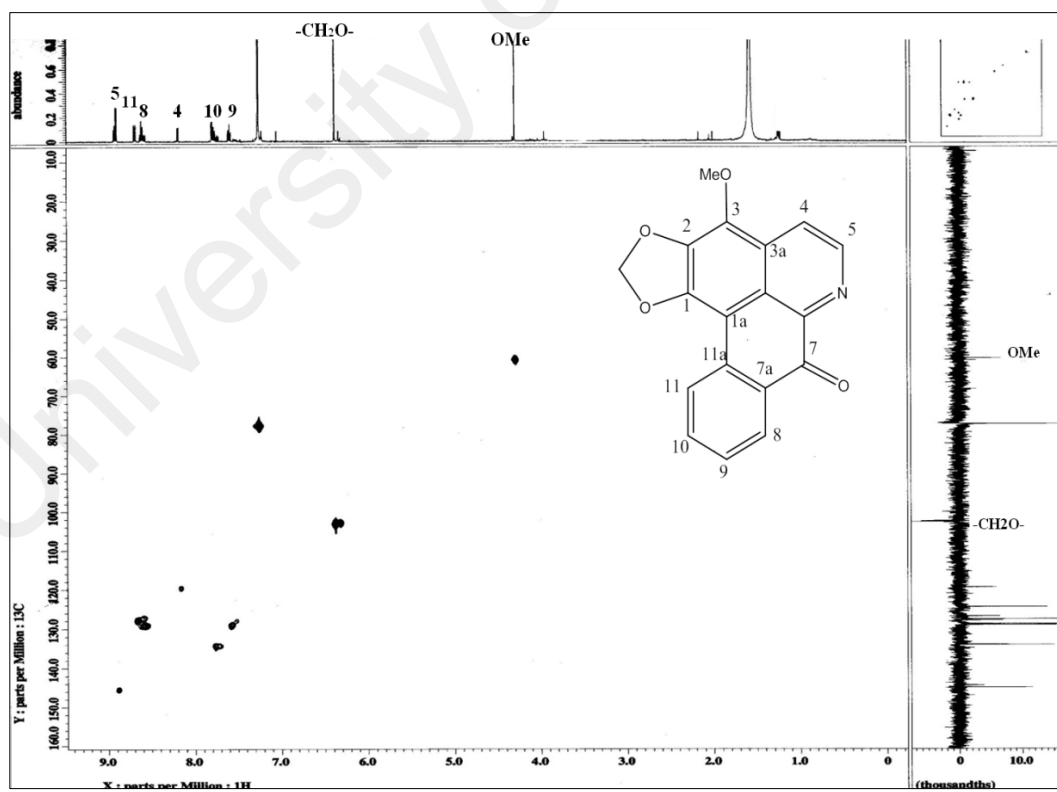


Fig. 4.105: HMBC spectrum of atherospermidine (10)

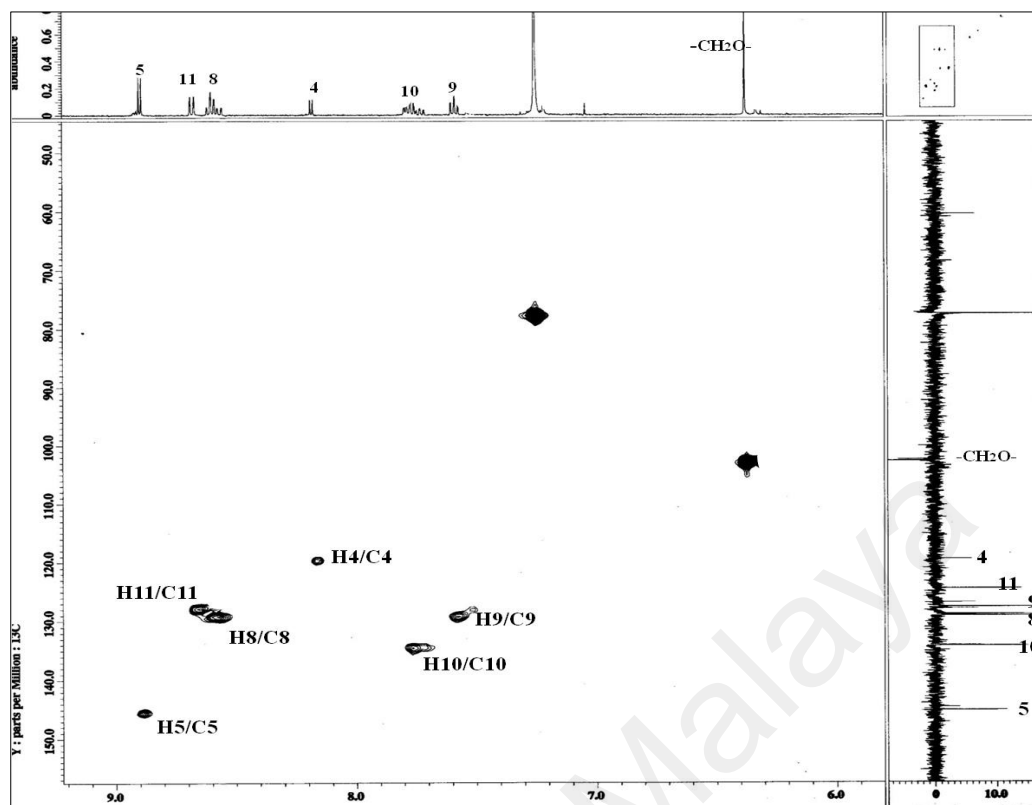
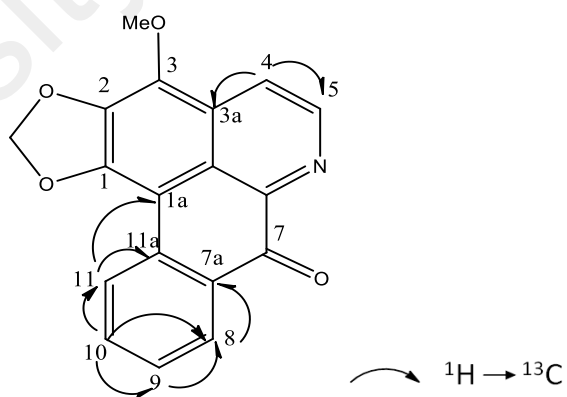
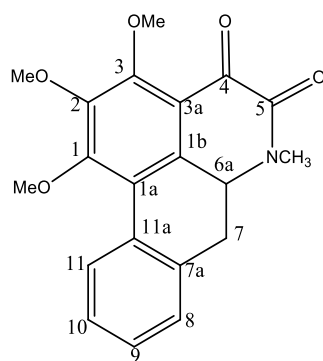


Fig. 4.106: Expanded HMQC spectrum of atherospermidine (**10**)



Scheme 4.8: The HMBC correlations of atherospermidine (**10**)

4.3.4 *N*-methylouregidione (5)



5

Alkaloid *N*-methylouregidione (**5**) was isolated as orange amorphous solid which gave a positive result with Dragendorff's test. On acidification, the compound turned red indicating the characteristic of an oxoaporphine. The UV spectrum showed absorption bands at λ_{\max} 212, 242, 275, 306, and 416 nm. The IR spectrum revealed an absorption peak at 1715 cm^{-1} which corresponds to the presence of two carbonyl functional groups in ring B.

The HREIMS (Figure 4.107) exhibited a molecular ion peak at m/z 352.1185 $[M+H]^+$ corresponding to the molecular formula of $C_{20}H_{17}NO_5$. Another fragment ion at m/z 337 $[M-CH_3]^+$ corresponded to the loss of methyl group attached to the nitrogen atom at position C-7. This confirmed the presence of *N*-methyl group in the structure.

The ^1H NMR spectrum (Figure 4.108) of this compound showed similar spectrum to that of ouregidione (**4**) except an additional of *N*-methyl signal at δ 3.44 ppm. Three methoxyl signals at δ 4.18, 4.09 and 4.01 assigned to C-3, C-2 and C-1, respectively, were observed. The presence of five aromatic protons were observed at δ 7.96 (*d*, $J= 8.0$ Hz), δ 7.62 (*t*, $J= 8.0$ Hz), δ 7.56 (*t*, $J= 8.0$ Hz) corresponding to H-8, H-9 and H-10 respectively. The proton signal for H-11 appeared at very lower field at δ 9.41 as doublet. Another aromatic

proton signal at C-7 appeared at δ 7.88 as one proton singlet. Again, the correlations of vicinal protons at H-8/H-9, H-9/H-10 and H-10/H-11 were fully supported by the cross peaks in the COSY spectrum (Figure 4.111 and 4.112) confirming that ring D is not substituted. Table 4.19 summarizes the ^1H - and ^{13}C NMR of the compound. Table 4.18 summarizes the ^1H - and ^{13}C NMR of the compound.

The ^{13}C NMR and DEPT 135 spectra (Figure 4.109 and 4.110) revealed a total of 20 carbons consisting of five methines, three methoxy and twelve quaternary carbons. The two carbonyl groups resonated at δ 160.1 and δ 170.2 belong to C-5 and C-4, respectively. An *N*-methyl carbon signal was observed at δ 31.0. The presence of *N*-methyl function was further confirmed by the cross peak in the HMQC spectrum (Figure 4.113). The HMBC correlation is shown in Scheme 4.9.

Finally, based on spectroscopic data and comparison with literature values, the compound was established as *N*-methyl ouregidione (**5**) which was also discovered in *Pseuduvaria rugosa* (Taha *et al.*, 2011).

Table 4.18: ^1H NMR (500 MHz) and ^{13}C NMR (125 MHz) spectral data of *N*-methyl ouregidione (**5**) in CDCl_3 (δ in ppm, *J* in Hz)

Position	^1H -NMR (δ ppm)	^{13}C -NMR(δ ppm)	^{13}C -NMR(δ ppm) (Mahmood <i>et al.</i> , 1986)
1	-	156.4	156.4
1a	-	115.7	115.6
1b	-	122.8	122.7
2	-	147.3	147.3
3	-	148.4	148.8
3a	-	131.1	131.1
4	-	157.2	158.0
5	-	179.2	179.1
6a	-	145.5	145.3
7	7.86 (1H, <i>s</i>)	114.5	114.3
7a	-	131.5	131.4
8	8.55-8.57 (1H, <i>d</i> , <i>J</i> =8.0)	128.7	128.9
9	7.52-7.55 (1H, <i>m</i>)	127.0	128.1
10	7.71-7.76 (1H, <i>m</i>)	126.3	126.4
11	9.10-9.12 (1H, <i>d</i> , <i>J</i> =8.6)	125.6	127.6
11a	-	134.5	134.4
1-OCH ₃	4.09 (3H, <i>s</i>)	60.9	60.9
2-OCH ₃	4.11 (3H, <i>s</i>)	61.4	61.4
3-OCH ₃	4.16 (3H, <i>s</i>)	61.8	61.7
<i>N</i> -CH ₃	4.00 (3H, <i>s</i>)	31.1	31.1
C=O	-	157.2	158.0
C=O	-	179.2	179.1

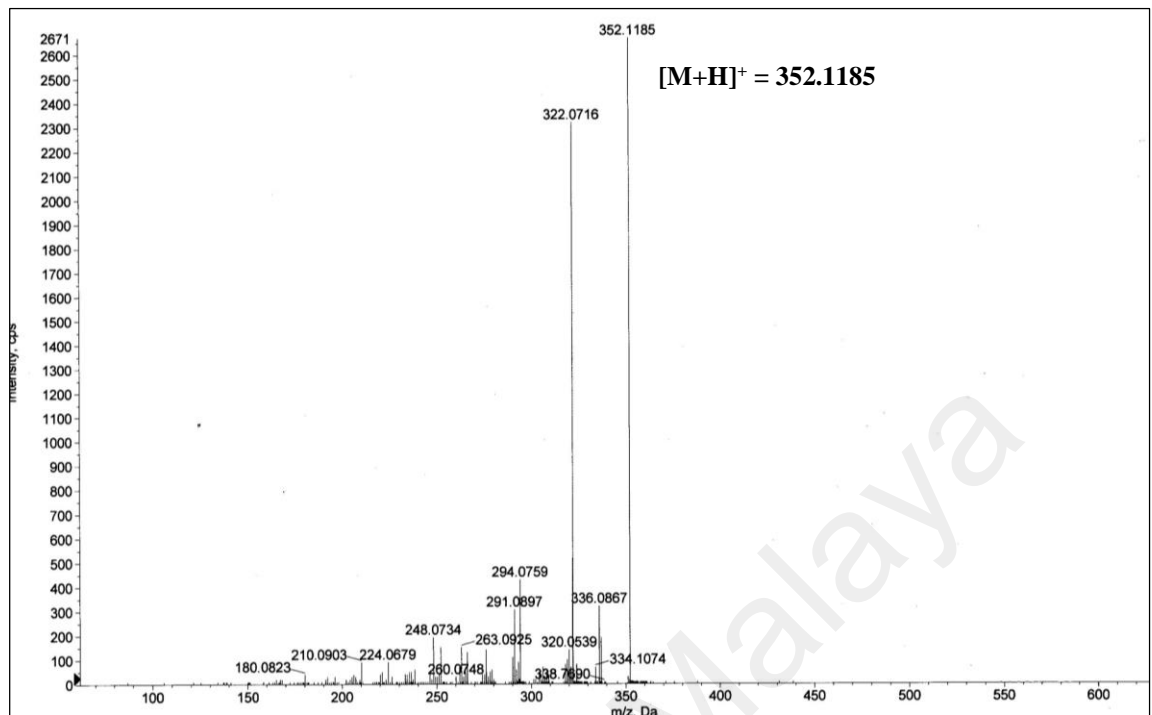


Fig. 4.107: LC-MS spectrum of *N*-methylouregidione (**5**)

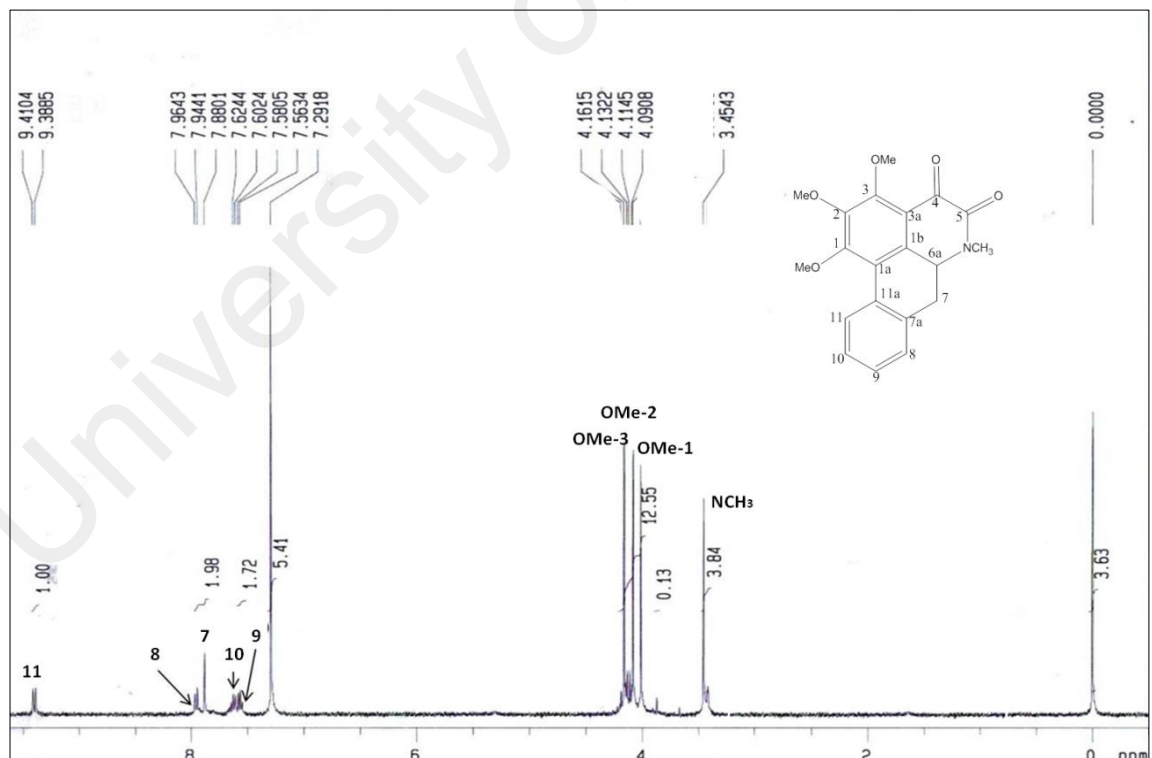


Fig. 4.108: ¹H NMR spectrum of *N*-methylouregidione (**5**)

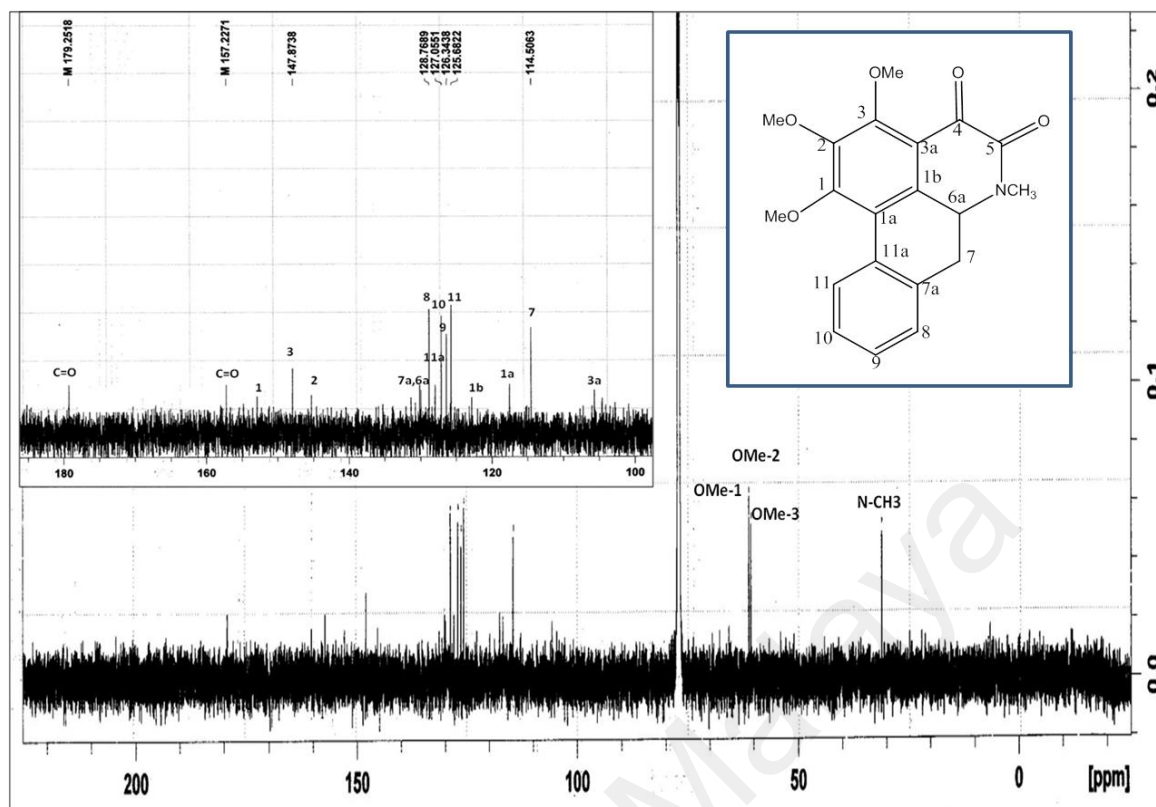


Fig. 4.109: ^{13}C NMR spectrum of *N*-methylouregidione (5)

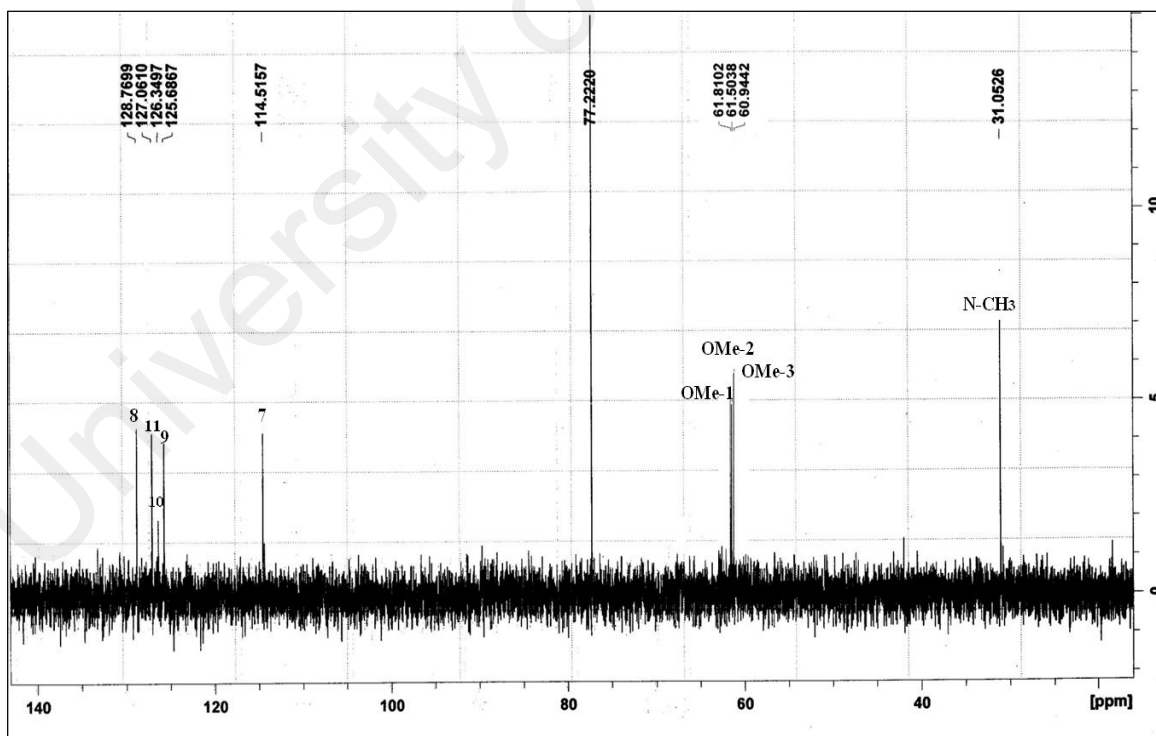


Fig. 4.110: DEPT 135 NMR spectrum of *N*-methylouregidione (5)

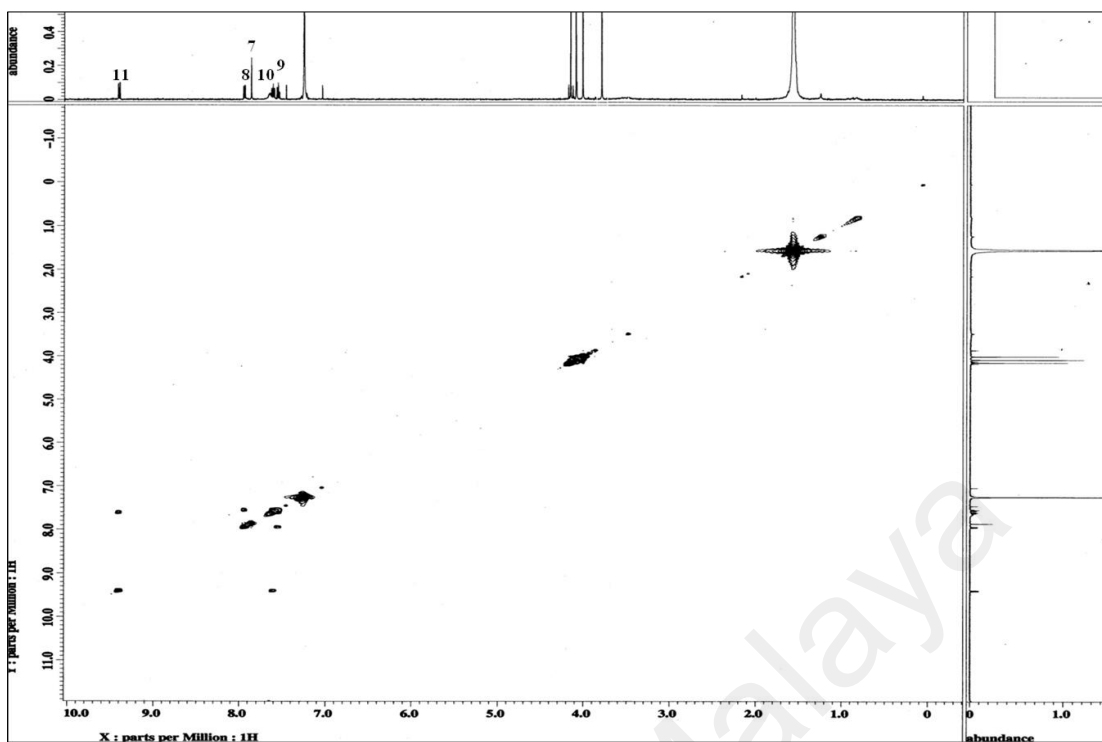


Fig. 4.111: COSY spectrum of *N*-methylouregidione (5)

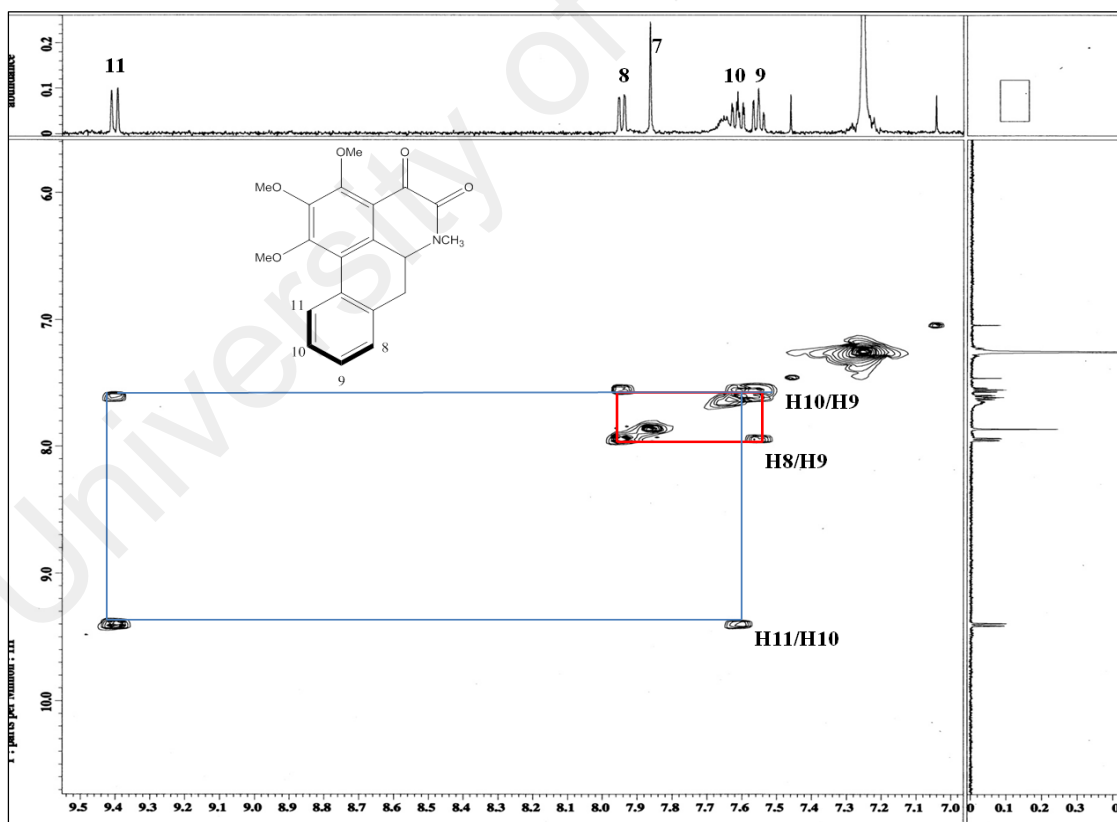


Fig. 4.112: Expanded COSY spectrum of *N*-methylouregidione (5)

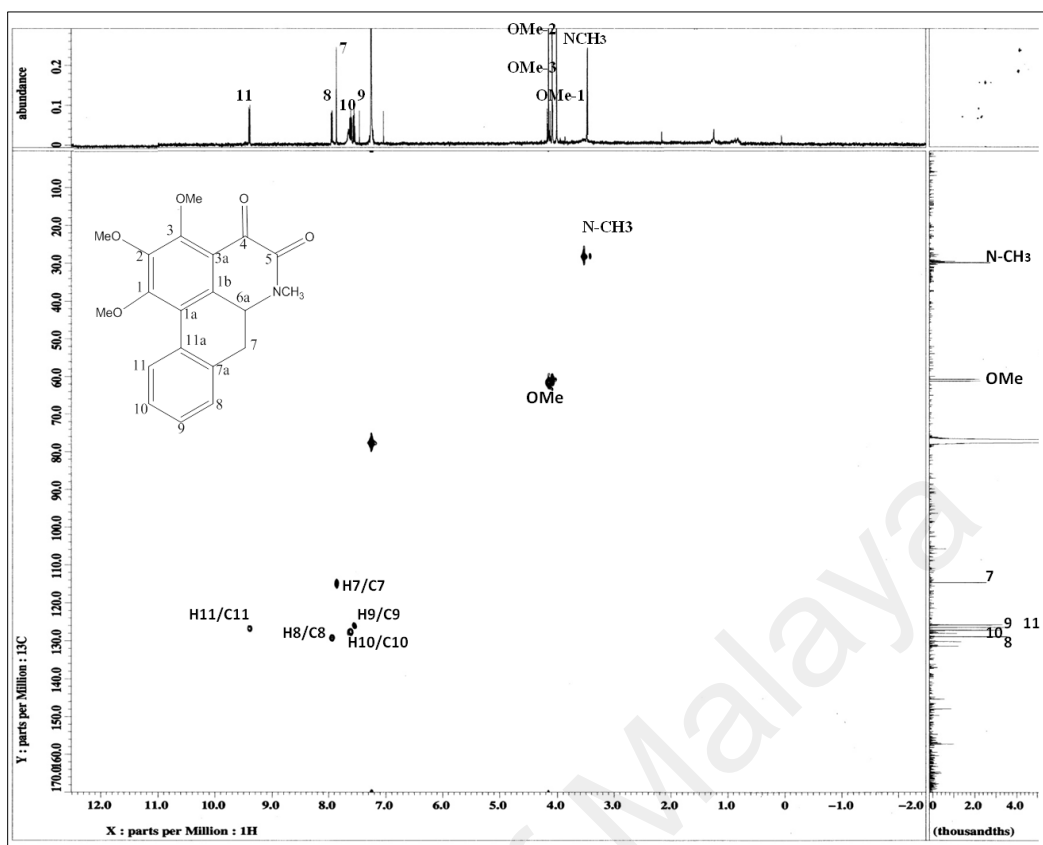
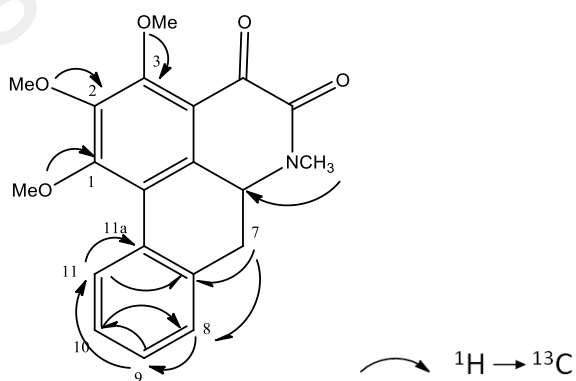
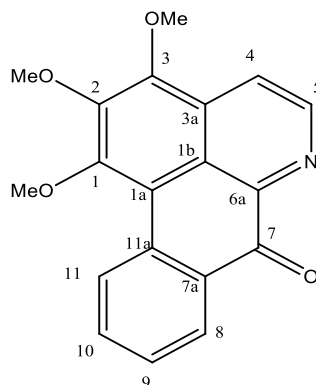


Fig. 4.113: HMOC spectrum of *N*-methylouregidione (5)



Scheme 4.9: The HMBC correlations of *N*-methylouregidione (5)

4.3.5 O-Methlymoschatoline (7)



7

O-methlymoschatoline (7), an alkaloid was isolated as yellow amorphous solid. The UV spectrum showed absorption peaks at λ_{max} at 270, 316 and 430 nm indicating a highly conjugated chromophore. The IR spectrum showed a strong absorption at 1665 cm^{-1} indicating the presence of a highly conjugated carbonyl group. The HREIMS (Figure 4.114) showed molecular ion peak at m/z 322.1073 $[\text{M}+\text{H}]^+$ corresponding to a molecular formula $\text{C}_{19}\text{H}_{15}\text{NO}_4$. The fragment ion peak at m/z 306 represents the loss of a methyl $[\text{M}-\text{CH}_3]^+$ from the methoxyl substituent in the structure.

The ^1H NMR spectrum (Figure 4.115 and 4.116) displayed the characteristic AB doublet of doublet aromatic at δ 8.96 (1H, $J=5.2$ Hz, H-5) and δ 8.22 (1H, $J=5.2$ Hz, H-4). The other four aromatic protons at δ 7.52 and 7.71 (1H, *dt*, $J=8.0, 1.5$ Hz) assigned for H-9 and H-10, and proton doublets at δ 8.57 and δ 9.10 (1H, *d*, $J= 8.0$ Hz) assigned for H-8 and H-11, respectively, indicate that ring D is unsubstituted. The spectrum also showed three distinctive methoxy peaks at δ 4.08, 4.11 and 4.18 attached to C-1, C-2 and C-3 indicating that ring A is substituted. The proton signal of H-11 is more downfield due to the deshielding effect of the methoxy group.

The COSY spectrum (Figure 4.120 and 4.121) showed proton-proton correlations between H-4 and H-5, H-8 and H-9, H-9 and H-10 indicating ring D were not substituted. Table 4.19 summarizes the ^1H - and ^{13}C NMR of the compound.

The ^{13}C NMR (Figure 4.117 and 4.118) and DEPT 135 spectrum (Figure 4.119) showed a total of 19 carbon signals comprising of three methoxyls, six methines and ten quaternary carbons. Three methoxy carbon signals were observed at δ 61.10, 61.57 and 61.91. Carbon peaks for C-4 and C-5 appeared at δ 119.3 and 144.7 respectively where C-5 resonated at lower field due to the adjacent nitrogen atom. The carbonyl peak resonated at δ 182 ppm. The HMQC spectrum (Figure 4.122 and 4.123) showed all the correlations of carbon to proton peaks.

Comparison with literature values and combined 2D spectra, COSY, HMQC and HMBC (Scheme 4.10) confirmed the compound as O-methylmoschatoline (**7**) which was isolated previously from *Pseuduvaria macrophylla* (Mahmood *et al.*, 1986).

Table 4.19: ^1H NMR (500 MHz) and ^{13}C NMR (125 MHz) spectral data of O-methylmoschatoline (**7**) in CDCl_3

Position	^1H -NMR (δ ppm)	^{13}C -NMR(δ ppm)	^{13}C -NMR(δ ppm) (Emmanoel <i>et al.</i> , 2011)
1	-	156.4	156.4
1a	-	115.7	115.6
1b	-	122.8	122.8
2	-	147.3	147.3
3	-	148.4	148.4
3a	-	131.1	131.1
4	8.22(1H, <i>d</i> , $J=5.15$)	119.3	119.1
5	8.96 (1H, <i>d</i> , $J=5.15$)	144.7	144.5
6a	-	145.5	145.4
7	-	182.6	182.6
7a	-	131.5	131.4
8	8.57 (1H, <i>d</i> , $J=8.0$)	128.9	128.9
9	7.52 (1H, <i>dt</i> , $J=8.0, 1.5$)	128.1	128.1
10	7.71 (1H, <i>dt</i> , $J=8.0, 1.5$)	134.3	134.3
11	9.12 (1H, <i>d</i> , $J=8.0$)	127.6	127.6
11a	-	134.5	134.5
OMe-1	4.08 (3H, <i>s</i>)	60.9	61.0
OMe-2	4.10 (3H, <i>s</i>)	61.4	61.4
OMe-3	4.16 (3H, <i>s</i>)	61.8	61.8

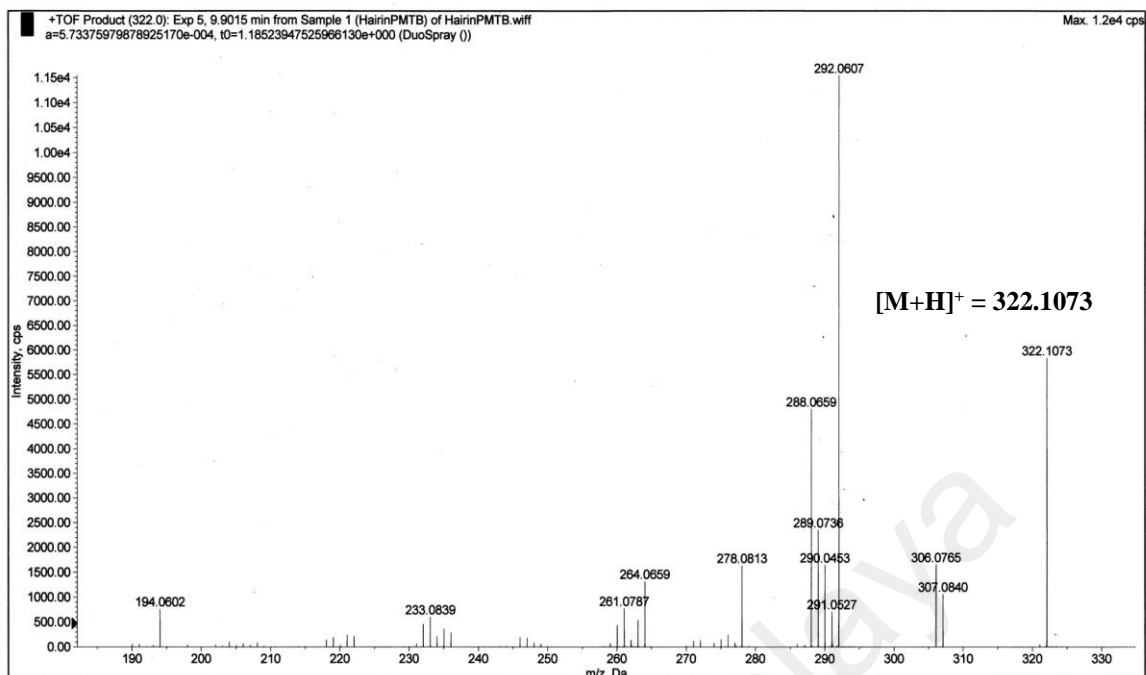


Fig. 4.114: LC-MS spectrum of O-methylmoschatoline (7)

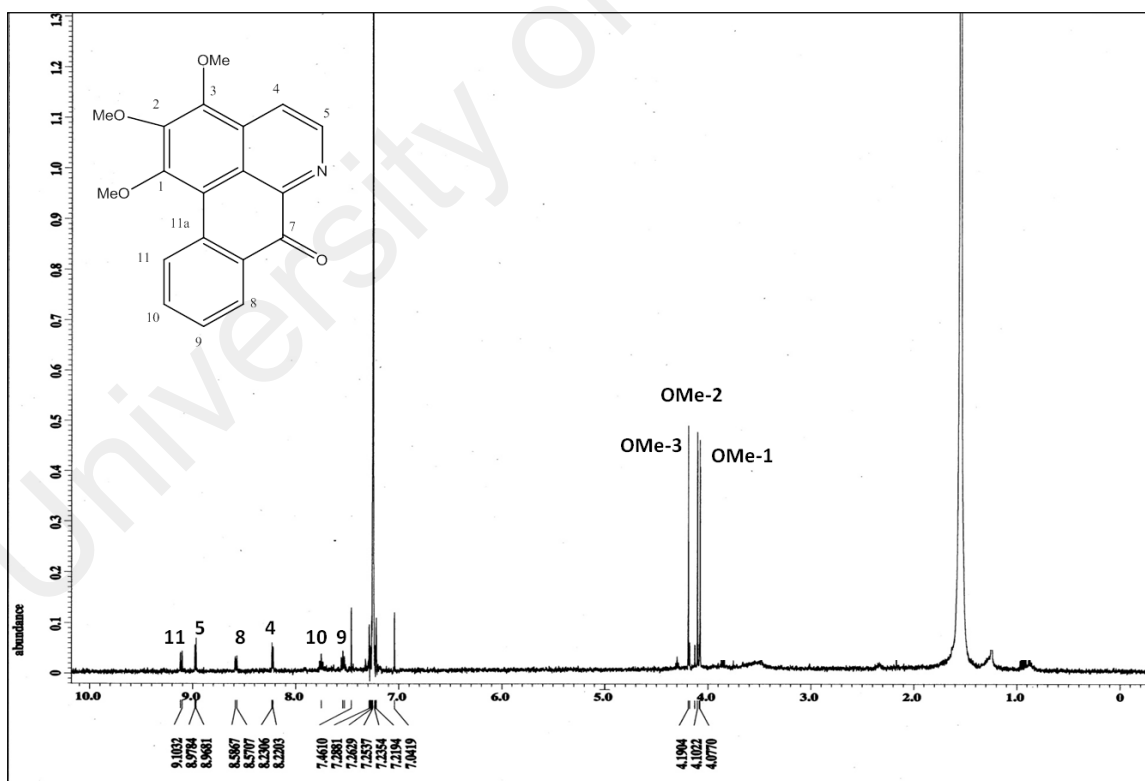


Fig. 4.115: ^1H NMR spectrum of O-methylmoschatoline (7)

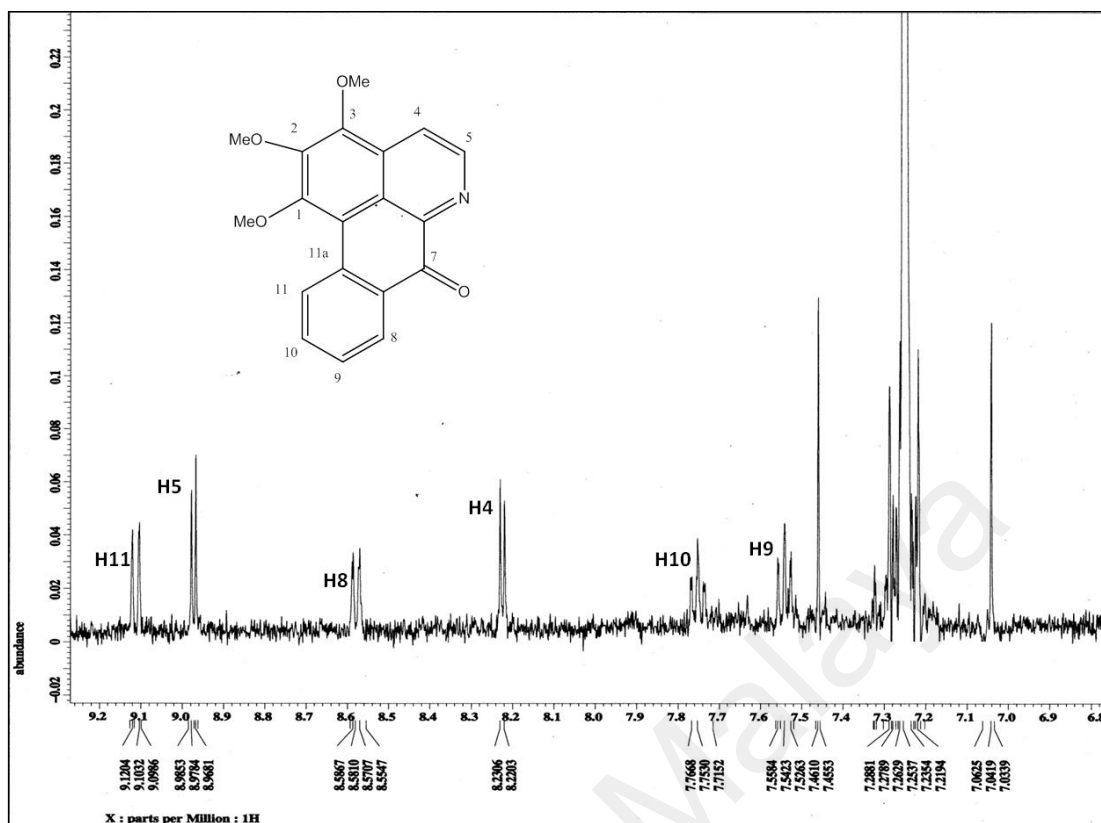


Fig. 4.116: Expanded ¹H NMR spectrum of O-methylmoschatoline (7)

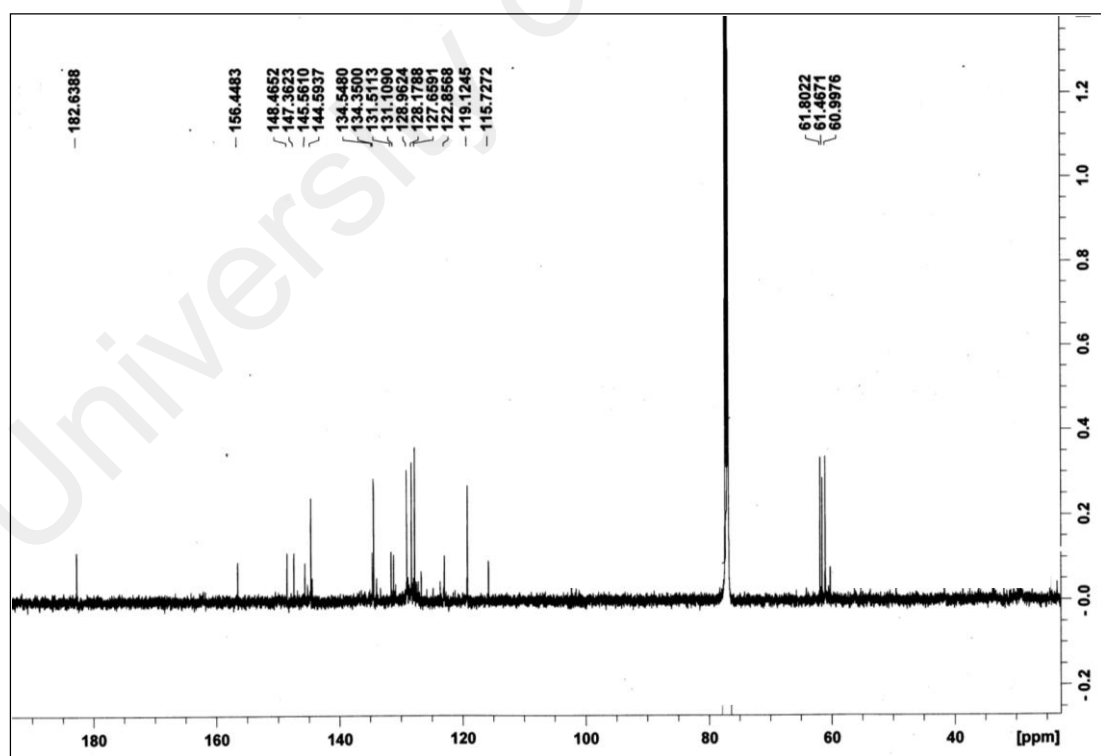


Fig. 4.117: ¹³C NMR spectrum of O-methylmoschatoline (7)

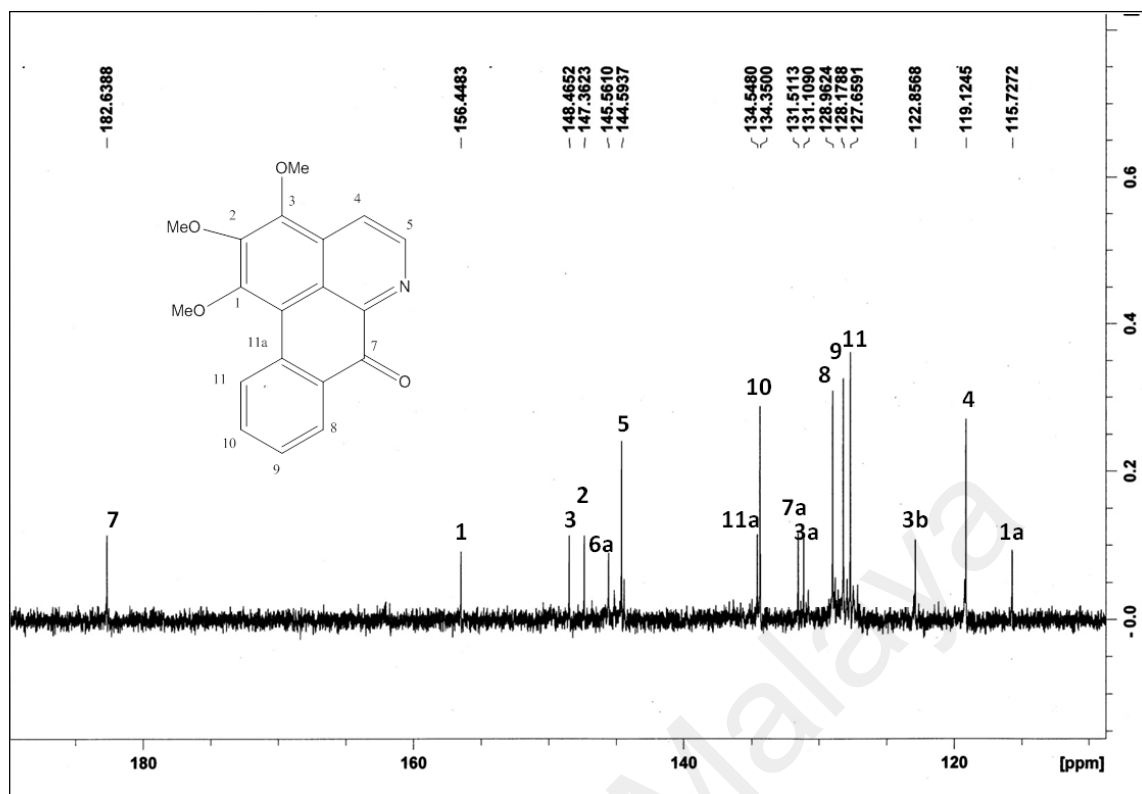


Fig. 4.118: Expanded ^{13}C NMR spectrum of O-methylmoschatoline (7)

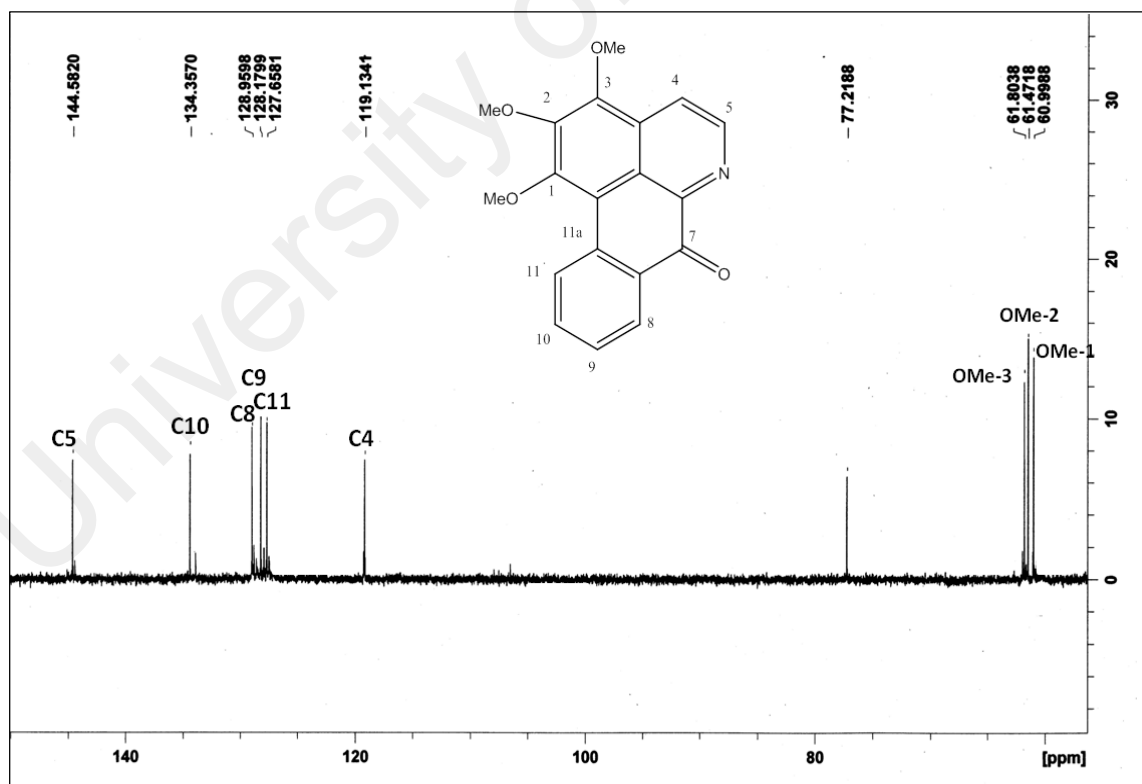


Fig. 4.119: DEPT 135 spectrum of O-methylmoschatoline (7)

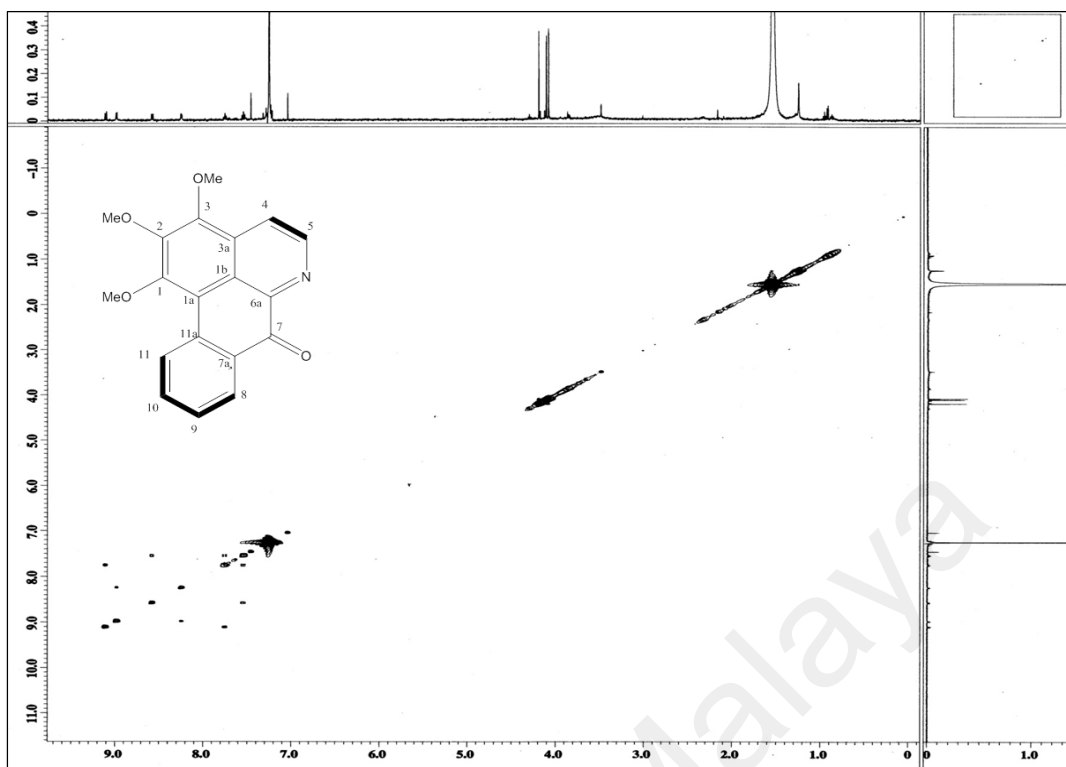


Fig 4.120: COSY spectrum of O-methylmoschatoline (7)

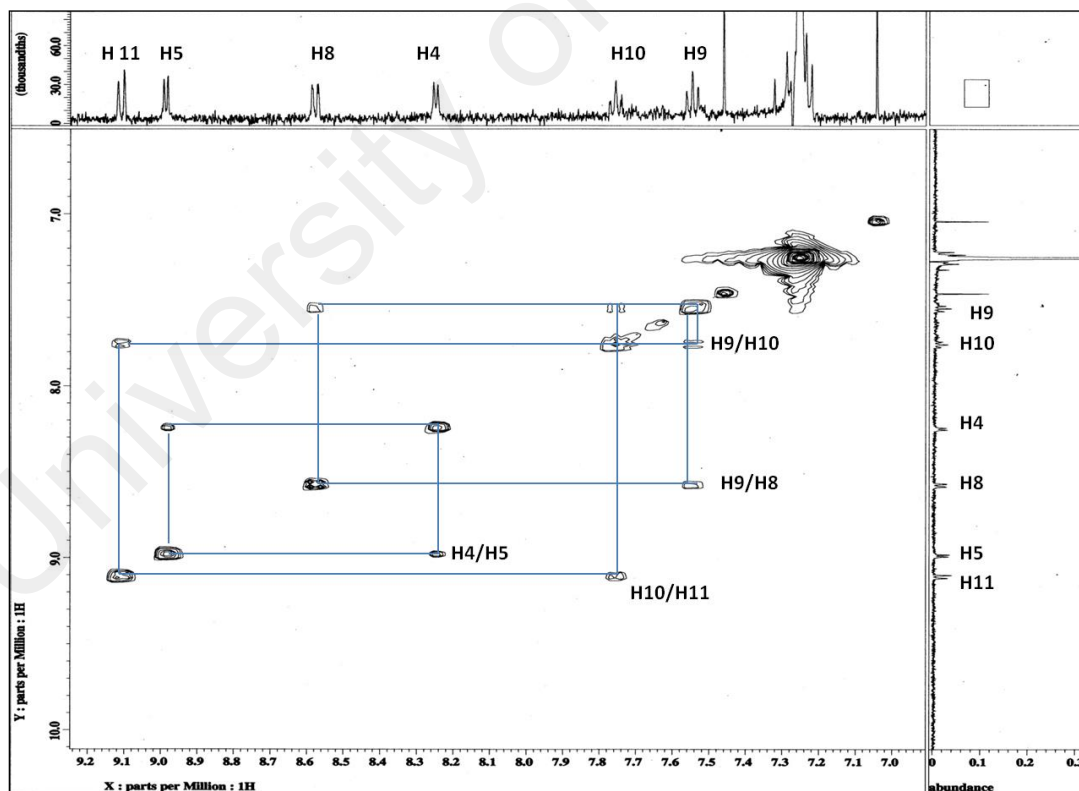


Fig 4.121: Expanded COSY spectrum of O-methylmoschatoline (7)

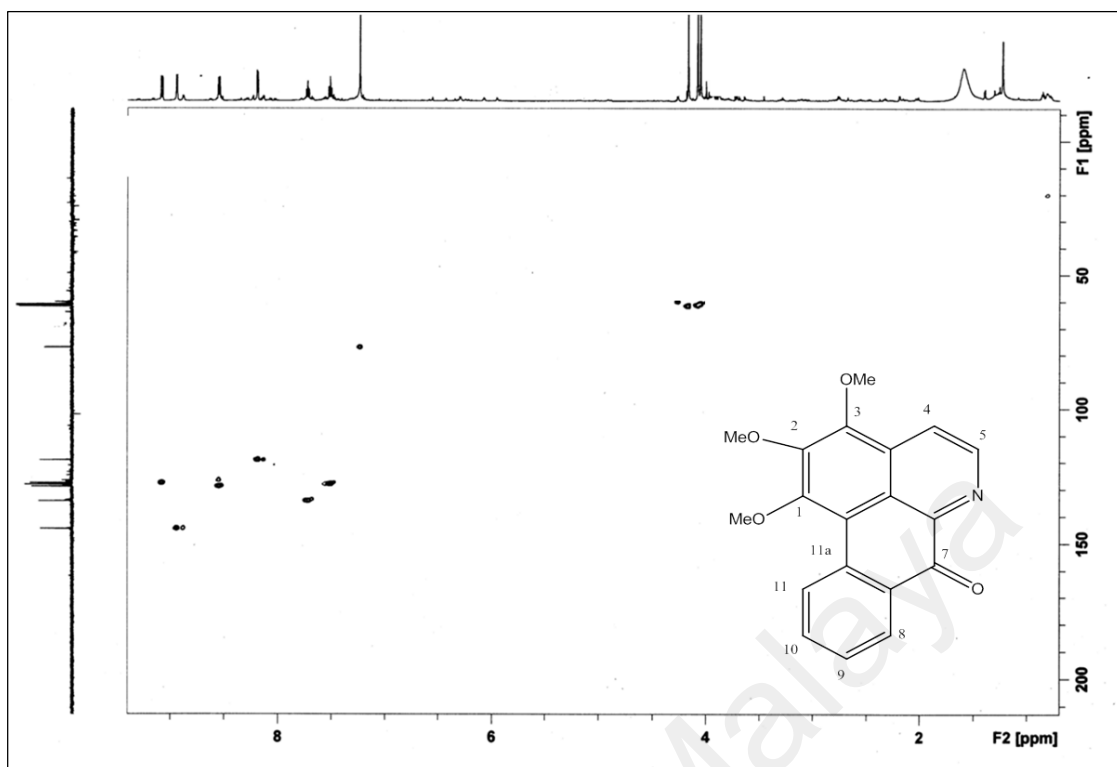


Fig 4.122: HMQC spectrum of O-methylmoschatoline (7)

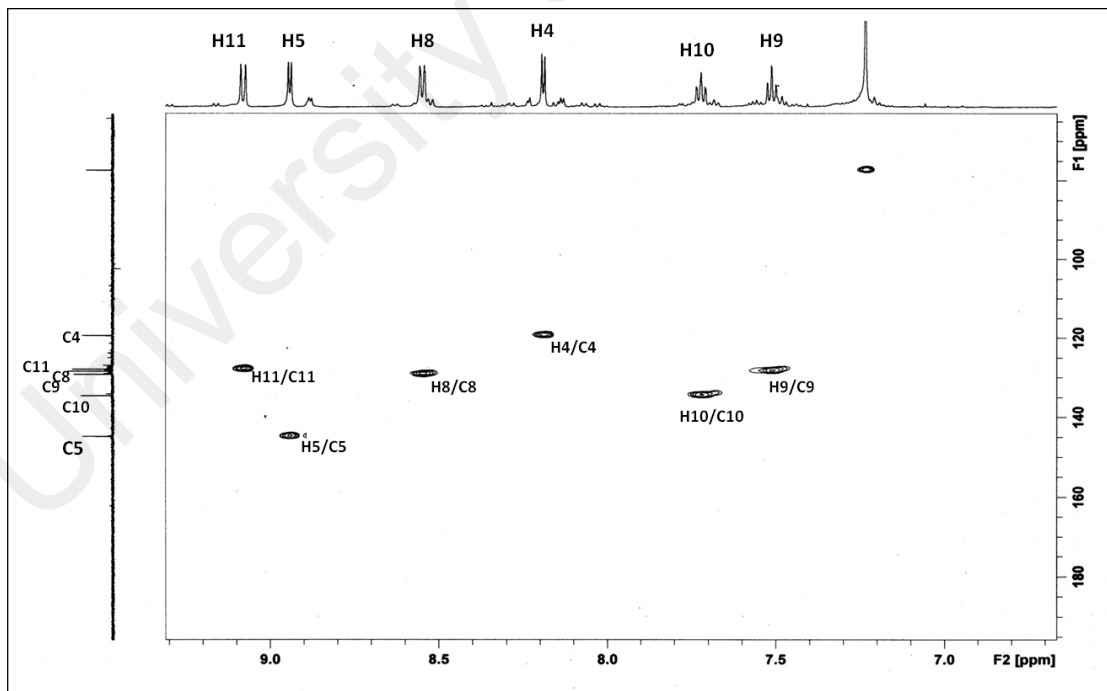
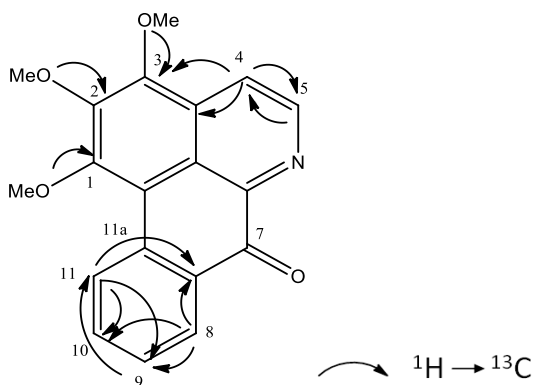


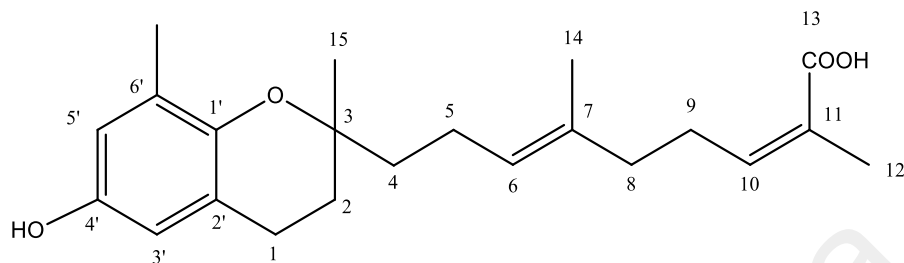
Fig 4.123: Expanded HMQC spectrum of O-methylmoschatoline (7)



Scheme 4.10: The HMBC correlations of O-methylmoschatoline (7)

University of Malaya

4.3.6 Polycerasoidol (16)



16

Polycerasoidol (**16**), a benzopyran derivative was afforded as yellow oil and showed $[\alpha]_D^{25}$ MeOH - 12.11° (*c* 0.5). The UV spectrum showed absorption bands at 230 nm and 298 nm indicating the presence of conjugated unsaturated aromatic system. In the IR spectrum, OH stretching vibration was observed at 3371 cm^{-1} . The presence of conjugated carbonyl was evidenced from the intense peak at 1692 cm^{-1} .

The HREIMS (Figure 4.124) revealed a molecular ion peak at m/z 359.2227 $[\text{M}+\text{H}]^+$ corresponding to the molecular formula $\text{C}_{22}\text{H}_{30}\text{O}_4$. The fragment ion peak at m/z 177 indicates partial subunit of the benzopyran with the hydroxyl group ($\text{C}_{11}\text{H}_{13}\text{O}_2$).

The ^1H NMR spectrum (Figure 4.125) showed four tertiary methyls at δ 2.12, 1.89, 1.58 and 1.25 (3H). In the aromatic region, two doublets were observed at δ 6.43 and δ 6.55, assigned to H-3' and H-5' respectively, that was meta coupled to each other, shown by coupling constant, $J=2.8$ Hz. The broad triplets at δ 6.03 and 5.14 ($J_1=7.5$ Hz and $J_2=1.2$ Hz) could be assigned to olefinic protons of H-10 and H-6, respectively. H-10 is more deshielded due to the electronegativity of the carboxylic group. The structure was further analysed by COSY spectrum (Figure 4.128) which showed crosspeaks between H-1 and

H-2, H-4, H-5 and H-6, and H-8, H-9 and H-10. Table 4.20 summarizes the ^1H - and ^{13}C NMR of the compound.

The ^{13}C NMR and DEPT 135 spectra (Figure 4.126 and 4.127) displayed twenty two carbon signals altogether, comprising of four methyls, four methines, six methylenes and eight quaternary carbons. The most downfield peak at δ 172.3 corresponds to the carbonyl function of the carboxylic acid at C-13. One oxygenated quaternary carbon assigned to C-3 was observed at δ 76.8. The quaternary carbon bonded to the hydroxy group resonated at δ 147.9. Two aromatic carbons assigned to C-3' and C-5' resonated at δ 112.7 and 115.7, respectively.

The HMQC spectrum (Figure 4.129, 4.130 and 4.131) showed the correlations of the specific protons to their carbons. The HMBC spectrum (Figure 4.132 and Scheme 4.11) showed correlations from H-10 to C-13 and H-12 to C-13, confirming the location of the carboxylic acid at C-13 as the terminal group of the chain.

Finally, based on the spectral evidence and comparison with reported data, the compound is identified as polycerasoidol (**16**). A recent report also mentioned the presence of polycerasoidol (**16**) from *Pseuduvaria indochinensis* Merr. thus confirming the common existence of benzopyran derivatives in this genus (Zhao *et al.*, 2014).

Table 4.20: ^1H NMR (500 MHz) and ^{13}C NMR (125 Hz) spectral data of polycerasoidol (**16**) in CDCl_3 (δ in ppm, J in Hz)

Position	^1H -NMR(δ ppm)	^{13}C -NMR (δ ppm)	^{13}C -NMR (δ ppm) (Gonzalez <i>et al.</i> , 1995)
1	2.69, <i>m</i>	22.5	22.4
2	1.74, <i>m</i>	31.5	31.4
3	-	76.8	75.2
4	1.59-1.89, <i>m</i>	39.5	39.4
5	2.06-2.12, <i>m</i>	22.2	22.1
6	5.14 (1H, <i>t</i> , $J=7.5, 1.2$)	125.1	125.0
7	-	134.4	134.1
8	2.04-2.10, <i>m</i>	39.1	38.9
9	2.56, <i>m</i>	28.2	28.1
10	6.03 (1H, <i>t</i> , $J=7.5, 1.2$)	146.1	146.1
11	-	127.4	126.2
CH ₃ -12	1.89, <i>s</i>	20.6	20.4
COOH-13	-	172.7	173.5
CH ₃ -14	1.58 (3H, <i>s</i>)	15.8	15.7
CH ₃ -15	1.25 (3H, <i>s</i>)	24.0	24.0
1'	-	145.9	
2'	-	121.2	121.0
3'	6.43 (1H, <i>d</i> , $J=2.8$)	112.7	112.5
4'	-	147.9	147.5
5'	6.55(1H, <i>d</i> , $J= 2.8$)	115.7	115.5
6'	-	126.6	127.3
CH ₃ -6'	2.12 (3H, <i>s</i>)	16.1	16.1

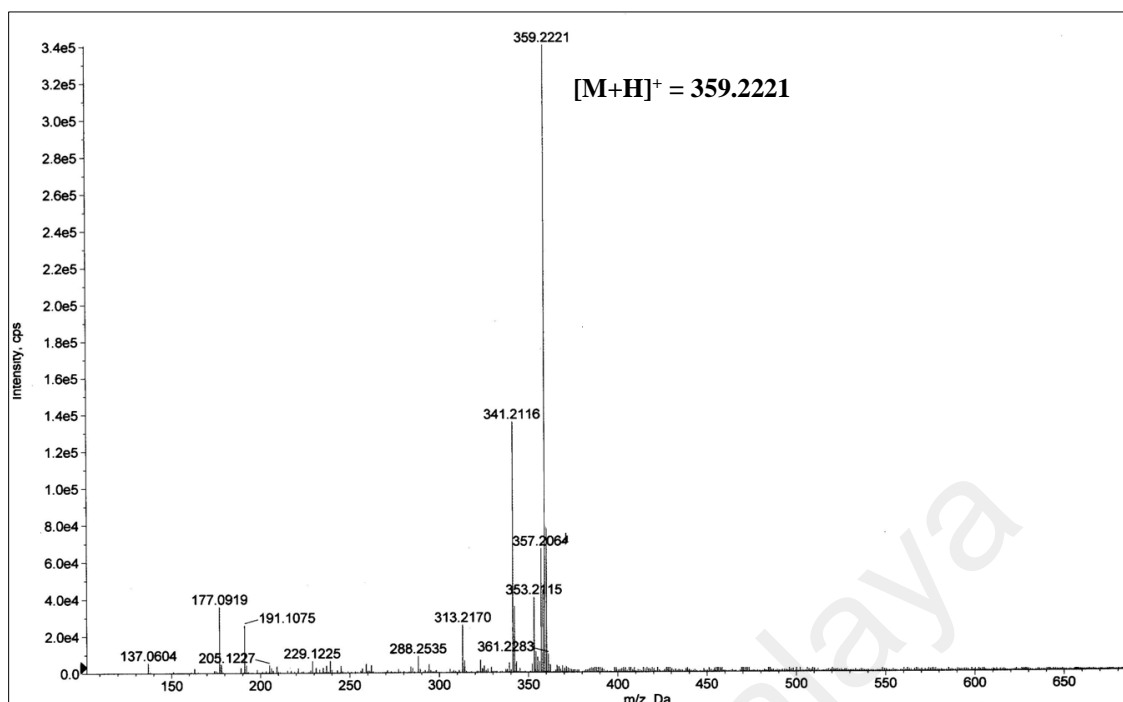


Fig 4.124: LC-MS spectrum of polycerasoidol (16)

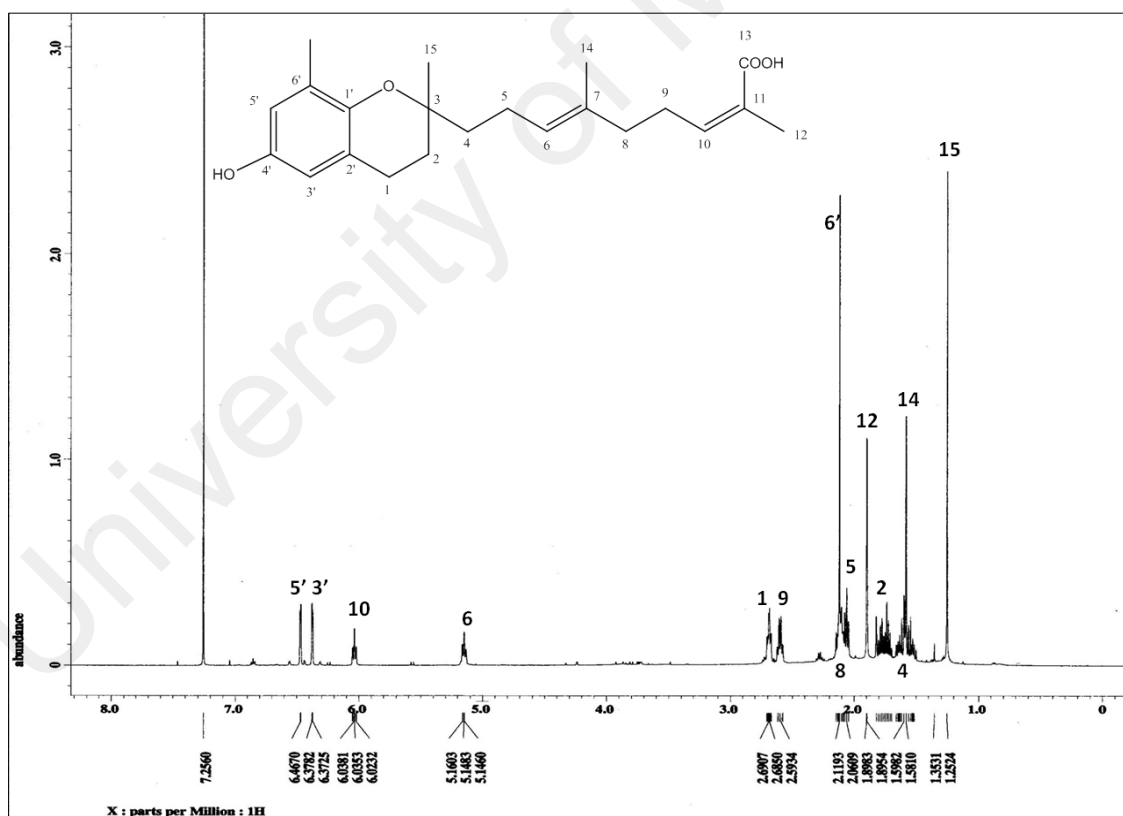


Fig 4.125: ^1H NMR spectrum of polycerasoidol (16)

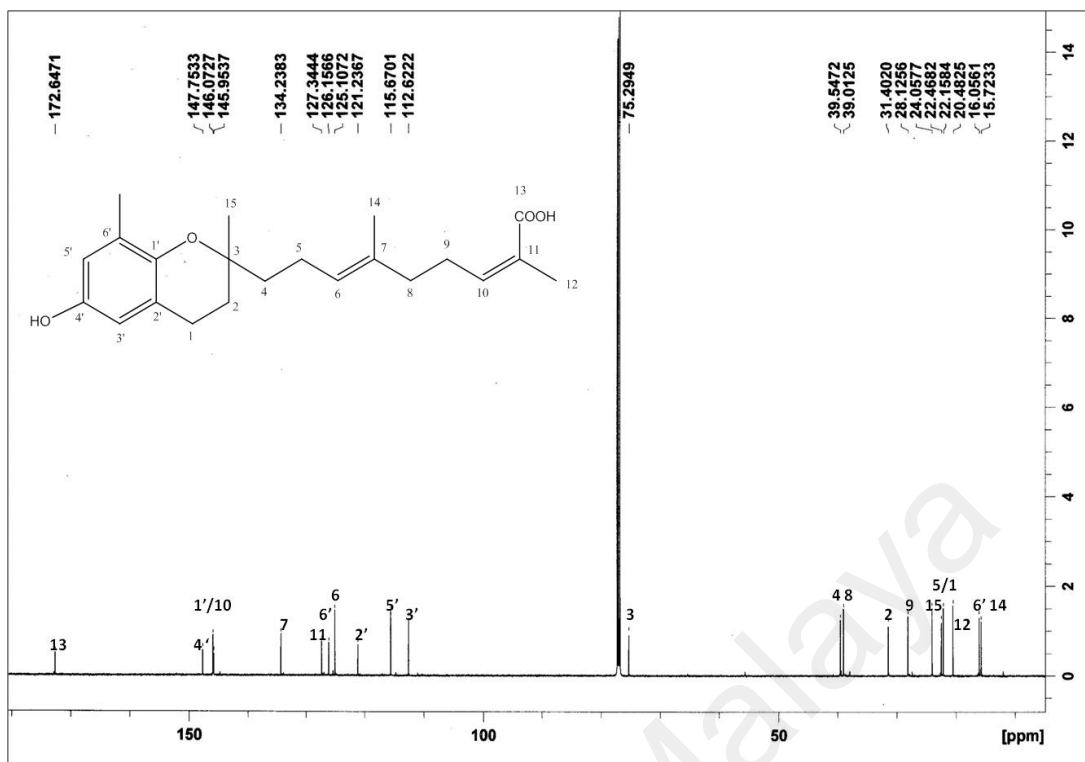


Fig. 4.126: ^{13}C NMR of polycerasoidol (16)

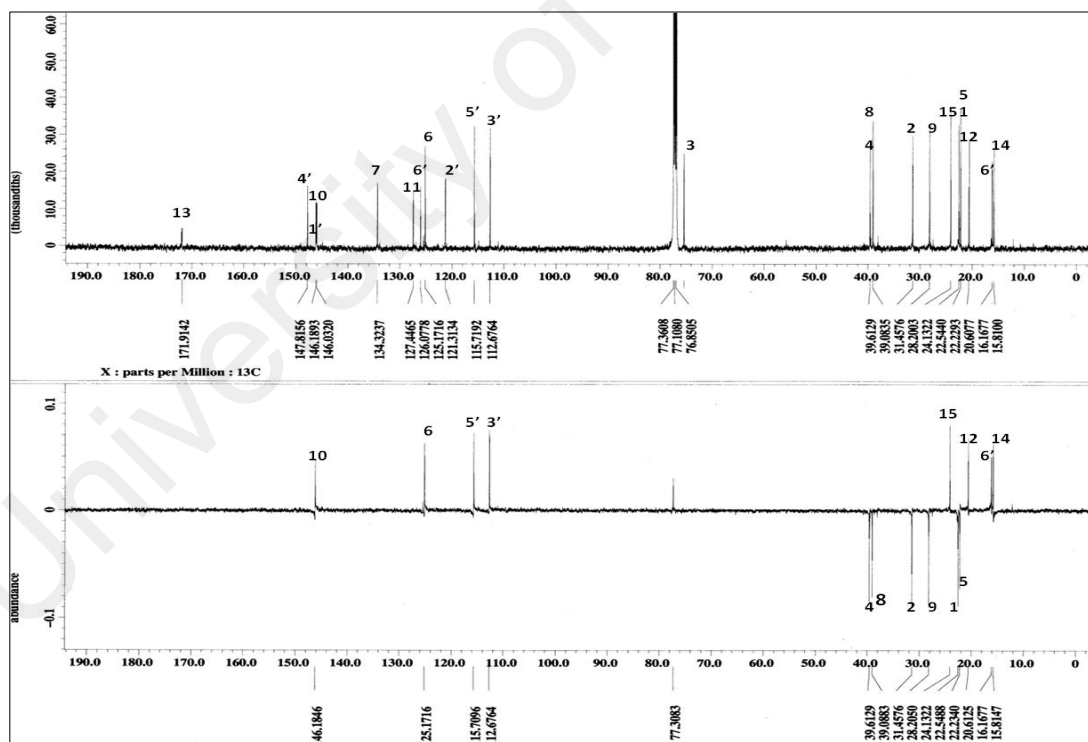


Fig. 4.127: DEPT 135 NMR spectrum of polycerasoidol (16)

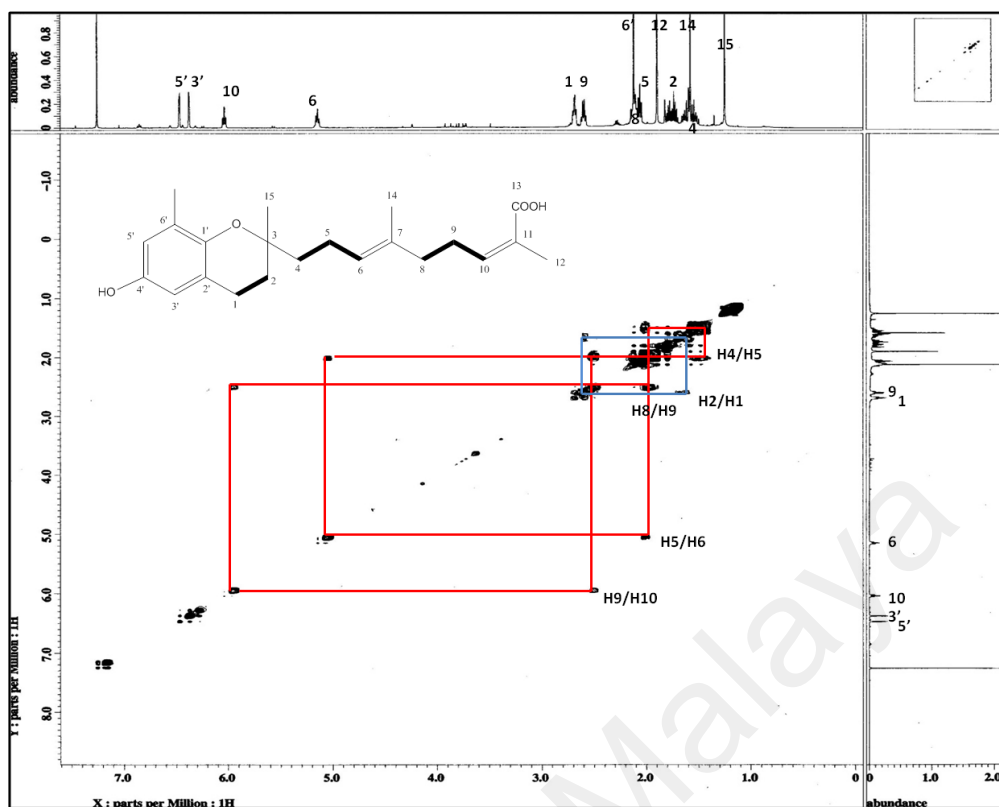


Fig. 4.128: COSY spectrum of polycerasoidol (16)

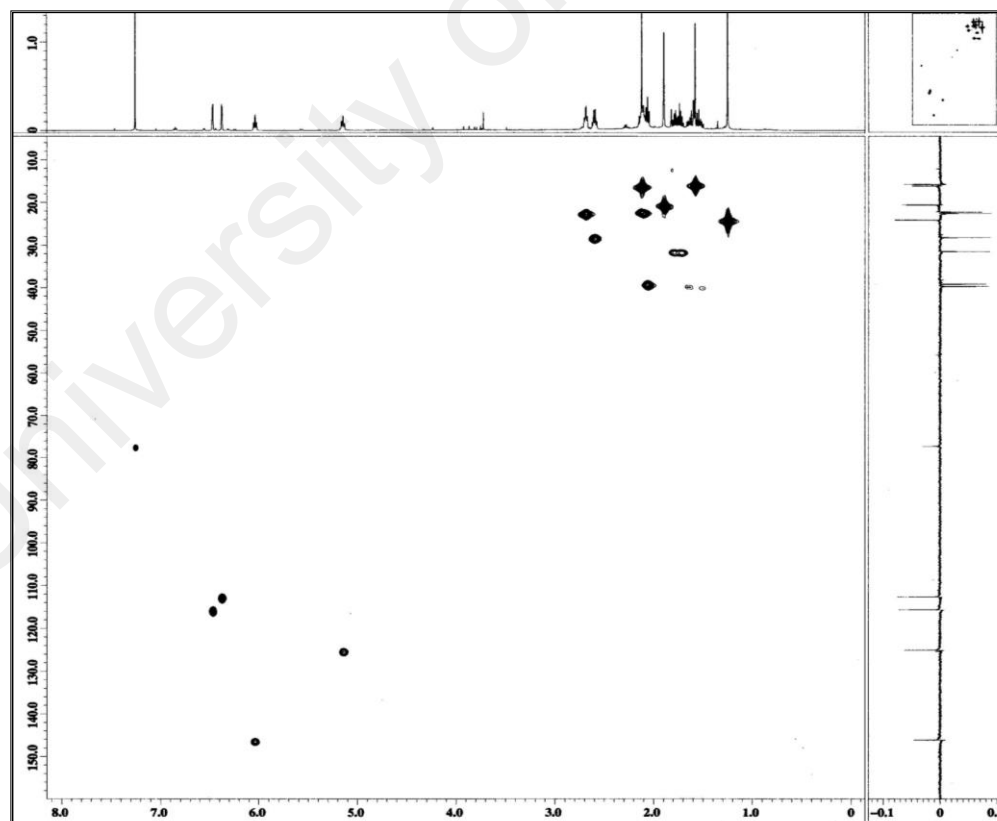


Fig. 4.129: HMBC spectrum of polycerasoidol (16)

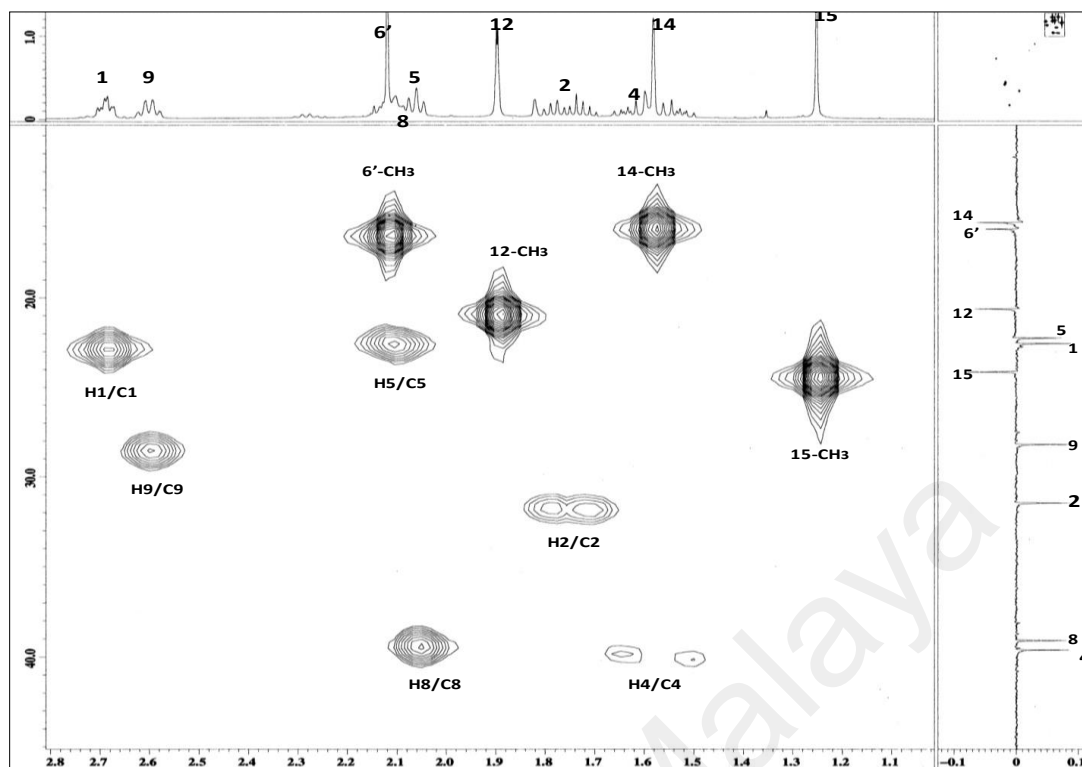


Fig. 4.130: Expanded HMQC spectrum in the aliphatic region

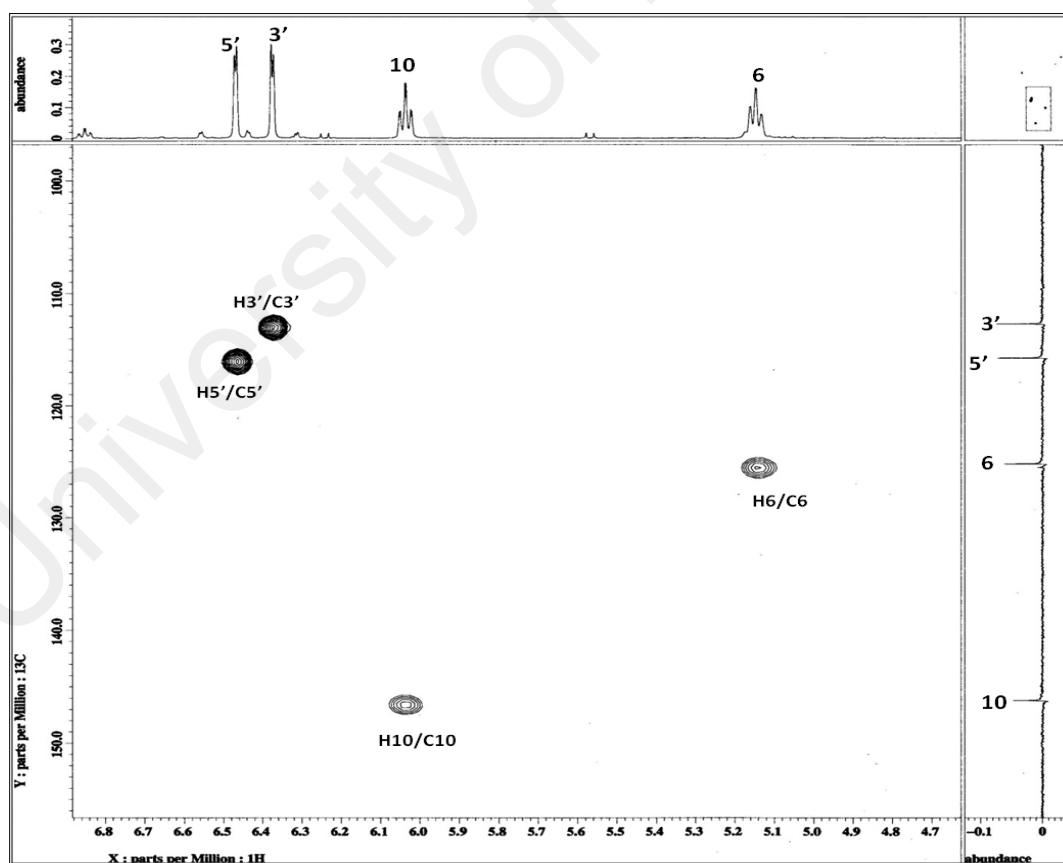


Fig. 4.131: Expanded HMQC spectrum in the aromatic region

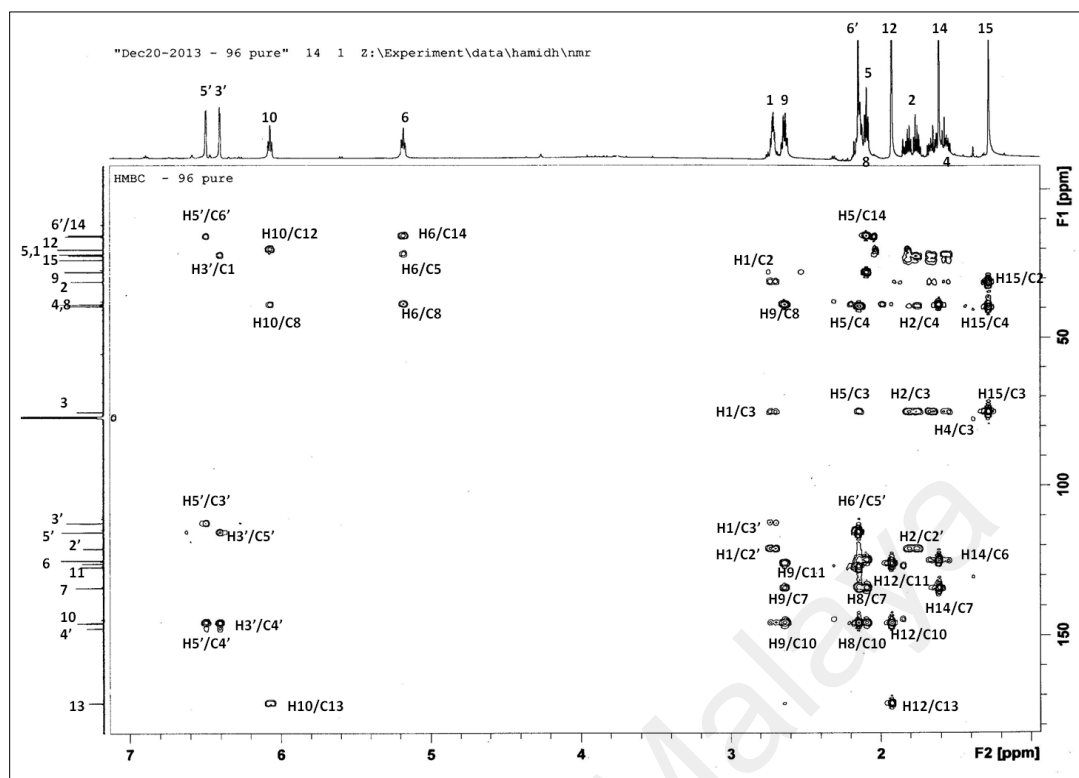
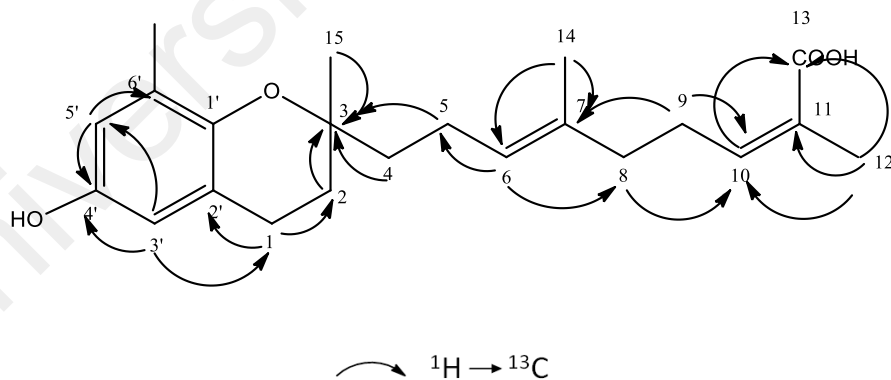
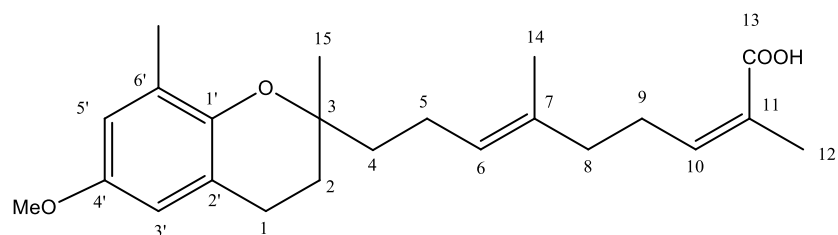


Fig. 4.132: HMBC spectrum of polycerasoidol (**16**)



Scheme 4.11: The HMBC correlations of polycerasoidol (**16**)

4.3.7 Polycerasoidin (49)



49

Polycerasoidin (**49**) was isolated as yellow oil and showed $[\alpha]_D^{25}$ MeOH - 13.10° (*c* 0.5). The UV absorption bands at 208 and 292 nm were consistent of a chromane skeleton. The IR spectrum showed an absorption band of a conjugated carbonyl function at 1689 cm^{-1} .

The HREIMS (Figure 4.133) showed molecular ion peak at m/z 373.2372 $[\text{M}+\text{H}]^+$ corresponding to the molecular formula $\text{C}_{23}\text{H}_{32}\text{O}_4$. The fragment ions at m/z 151 and 191 suggest a partial benzopyran structure with a methoxy group.

The chemical shifts in the ^1H -NMR spectrum (Figure 4.134) were similar to that of polycerasoidol (**16**) except for one proton signal of the methoxy group at δ 3.72 (3H). The COSY spectrum (Figure 4.137) showed all the ^1H - ^1H connectivity between H-1 and H-2, H-4, H-5 and H-6, and H-8, H-9 and H-10. Table 4.21 summarizes the ^1H - and ^{13}C NMR of the compound.

The ^{13}C -NMR and DEPT 135 spectrum (Figure 4.135 and 4.136) showed a total of 23 carbon atoms consisting of one methoxy, four methyls, four methines, six methylenes and eight quaternary carbons. A signal at δ 55.6 ppm corresponded to the methoxy group which was further confirmed by the crosspeaks in the HMQC spectrum (Figure 4.138).

In the HMBC spectrum (Figure 4.139 and Scheme 4.12), the three proton methoxy singlet correlates to C-4', thus assigning the methoxy group in the chroman nucleus.

Finally, comparison of all spectroscopic data with those of reported values, the compound was identified as polycerasoidin (**49**), a benzopyran derivative which was first isolated from *Pseuduvaria monticola*.

University of Malaya

Table 4.21: ^1H NMR (500 MHz) and ^{13}C NMR (125 MHz) spectral data of polycerasoidin (**49**) in CDCl_3 (δ in ppm, J in Hz)

Position	^1H -NMR(δ ppm)	^{13}C -NMR (δ ppm)	^{13}C -NMR (δ ppm) (Gonzalez <i>et al.</i> , 1995)
1	2.71 <i>m</i>	22.6	22.6
2	1.79 <i>m</i>	31.4	31.4
3	-	76.8	75.2
4	1.54-1.74 <i>m</i>	39.7	39.7
5	2.06-2.12 <i>m</i>	22.2	22.1
6	5.15 (1H, <i>t</i> , $J=7.0,1.2$)	125.1	125.3
7	-	134.2	134.2
8	2.06-2.12 <i>m</i>	39.0	39.0
9	2.62 <i>m</i>	28.1	28.1
10	6.04 (1H, <i>t</i> , $J=7.0,1.2$)	146.3	146.2
11	-	127.2	126.3
CH ₃ -12	1.89 (3H, <i>s</i>)	20.6	20.5
13	-	172.3	173.6
CH ₃ -14	1.59 (3H, <i>s</i>)	15.8	15.7
CH ₃ -15	1.25 (3H, <i>s</i>)	24.0	24.0
1'	-	146.0	146.2
2'	-	120.9	120.8
3'	6.43 (1H, <i>d</i> , $J=2.5$)	111.0	111.0
4'	-	152.1	152.1
5'	6.55 (1H, <i>d</i> , $J=2.5$)	114.8	114.8
6'	-	126.0	127.1
CH ₃ -6'	2.14, <i>s</i>	16.2	16.2
OCH ₃ -4'	3.72, <i>s</i>	55.6	55.5

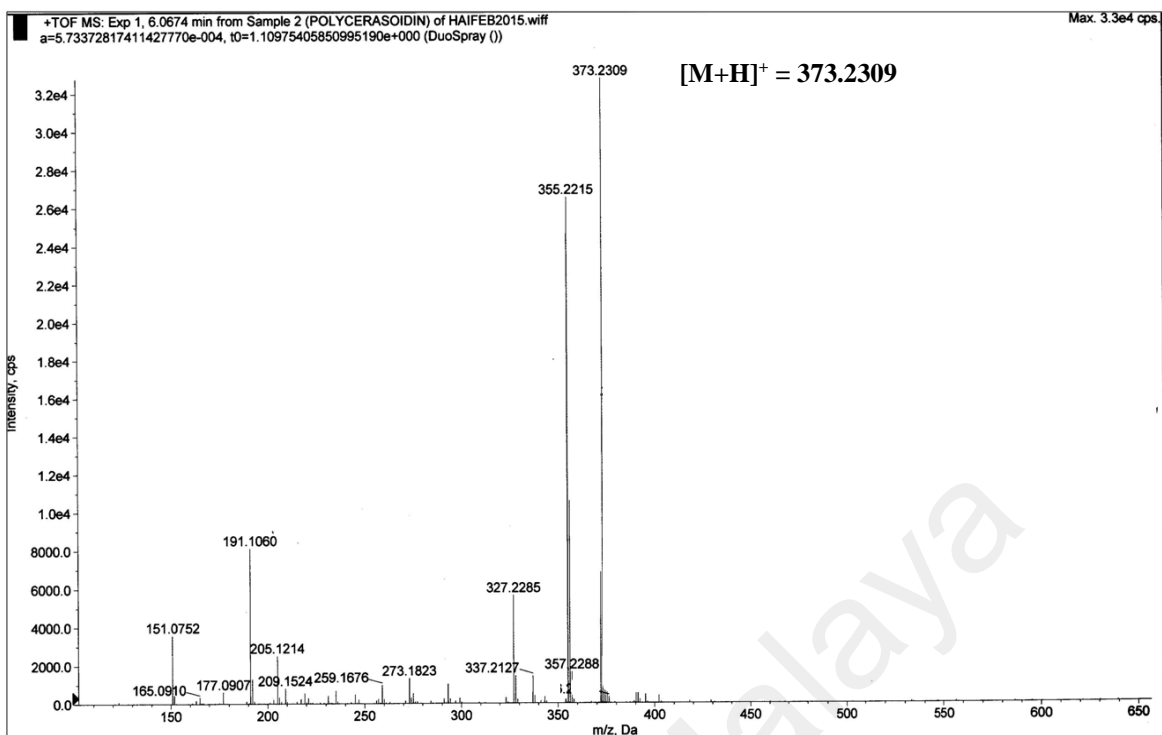


Fig 4.133: LC-MS spectrum of polycerasoidin (49)

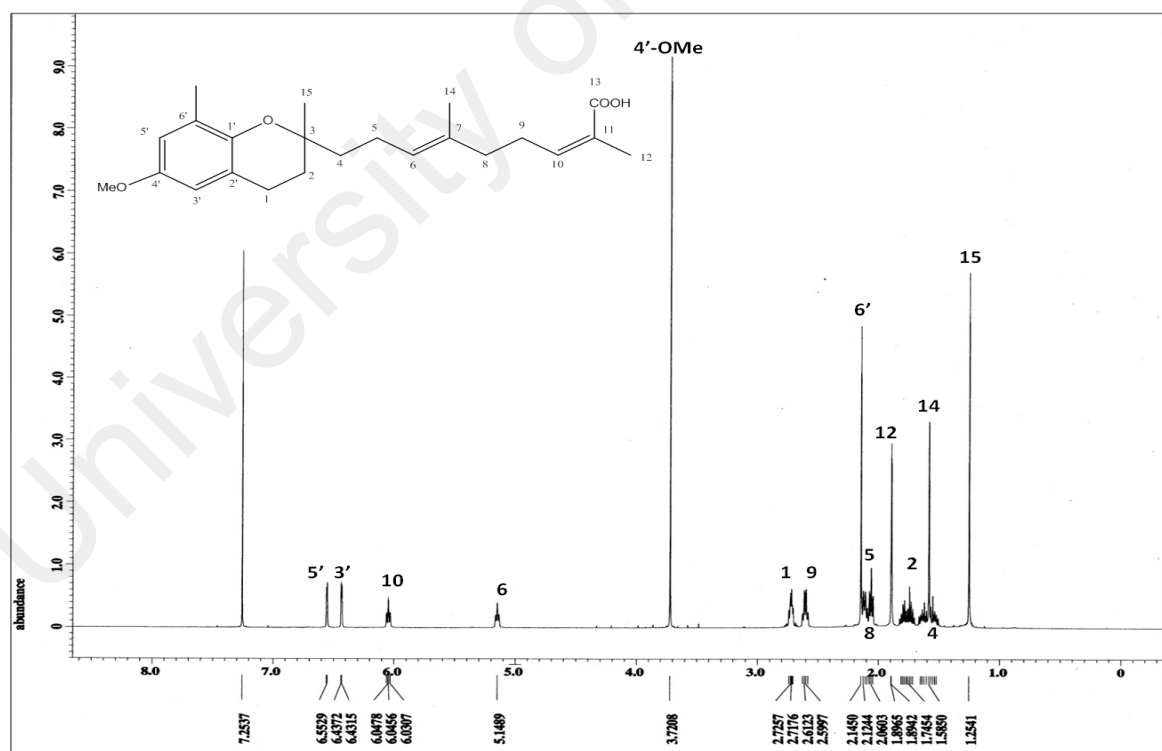


Fig 4.134: ^1H NMR spectrum of polycerasoidin (49)

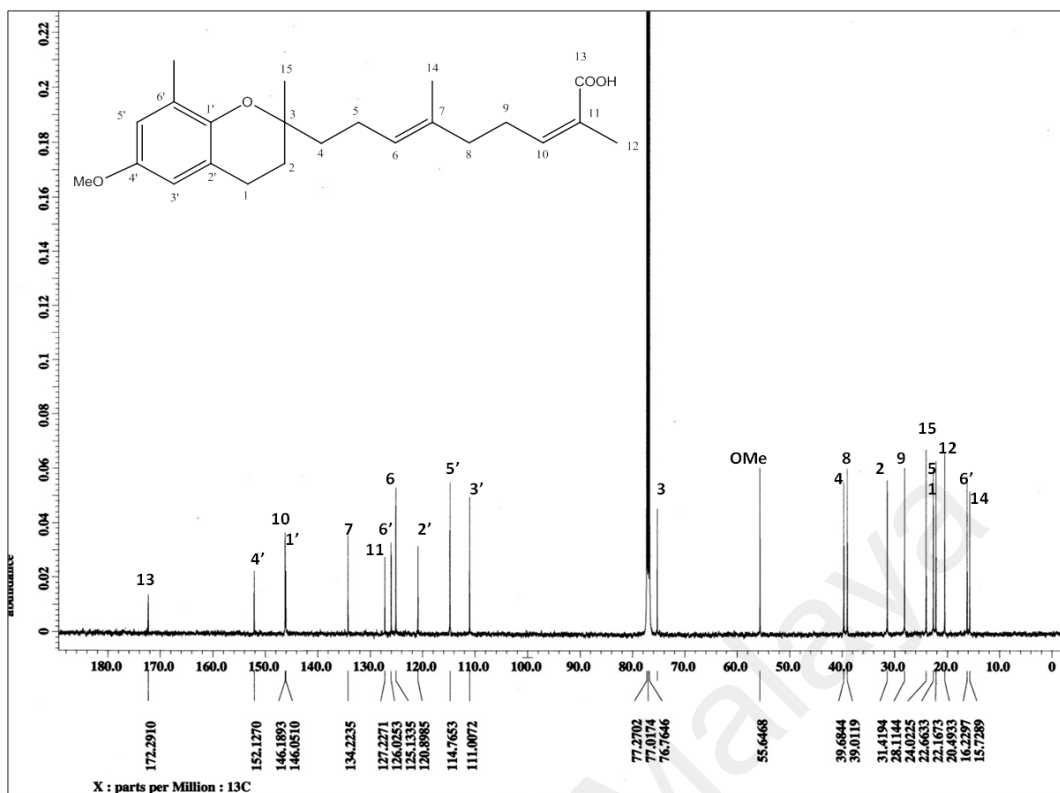


Fig. 4.135: ¹³C NMR spectrum of polycerasoidin (49)

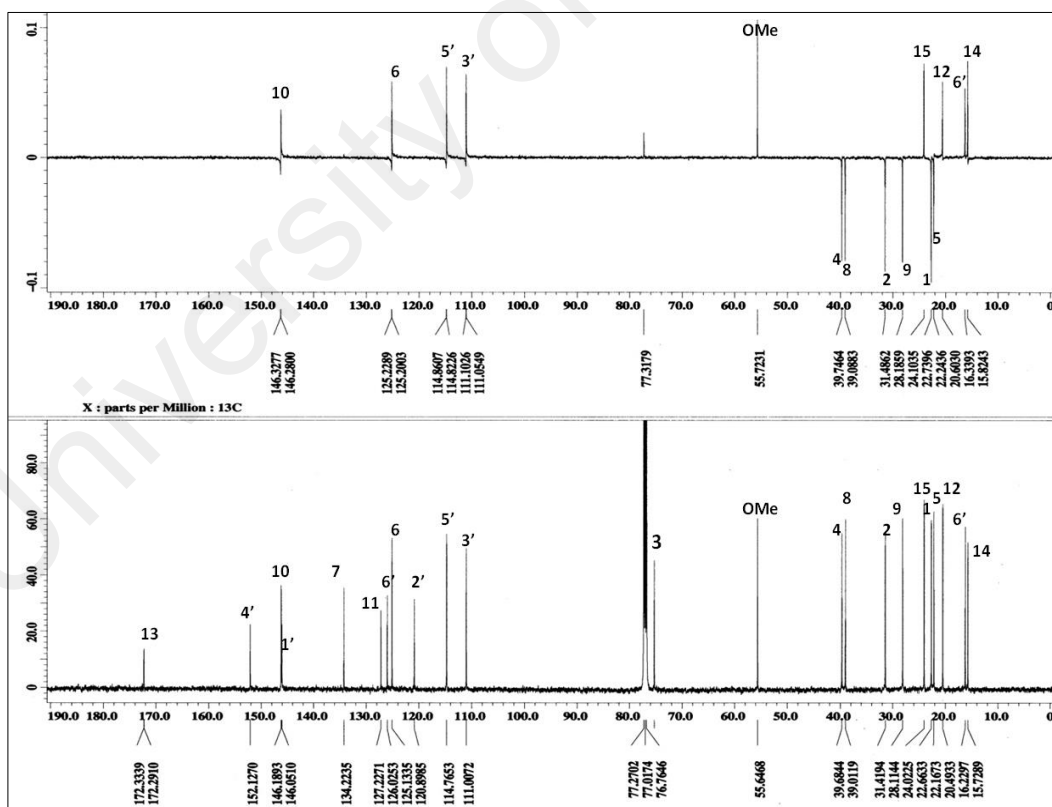


Fig. 4.136: DEPT 135 NMR spectrum of polycerasoidin (49)

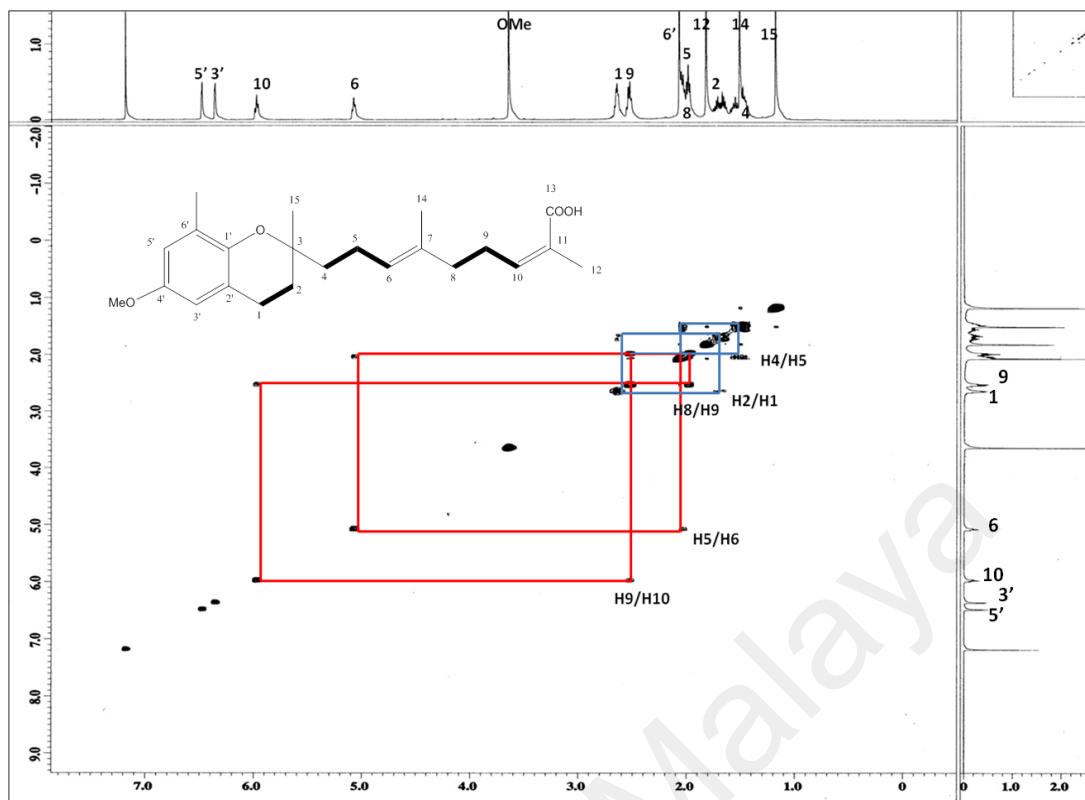


Fig. 4.137: COSY spectrum of polycerasoidin (49)

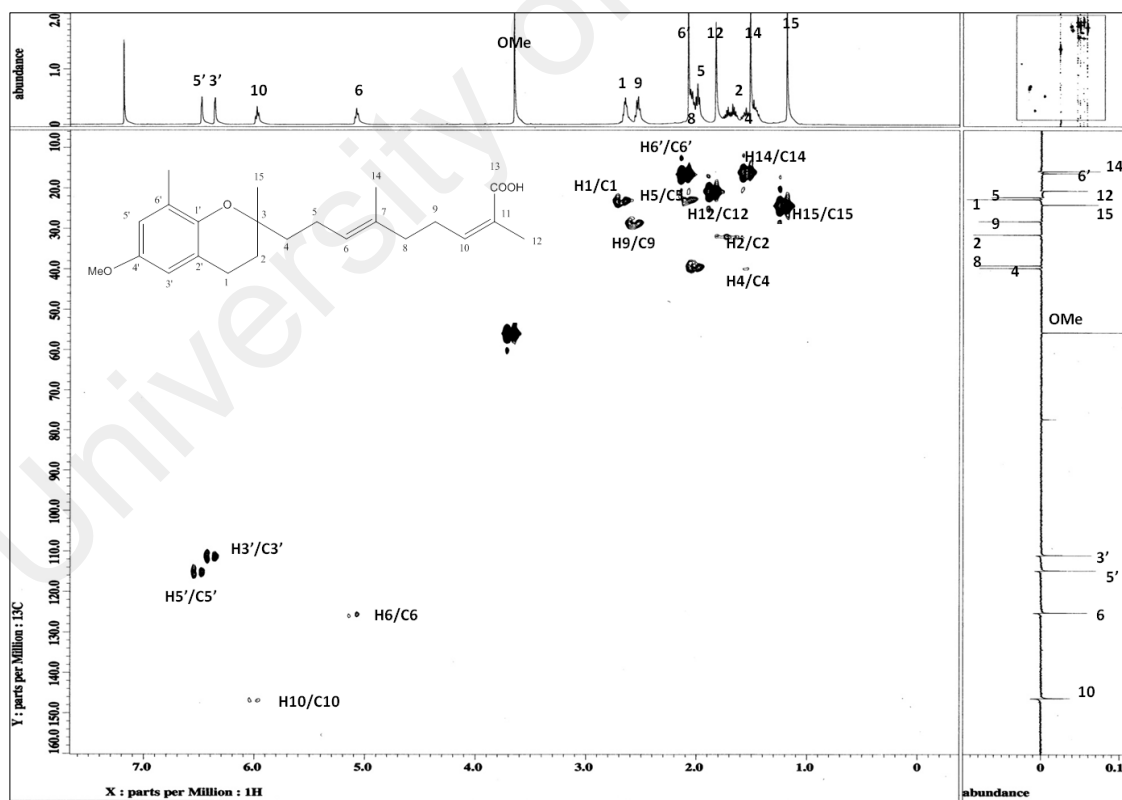


Fig. 4.138: HMQC spectrum of polycerasoidin (49)

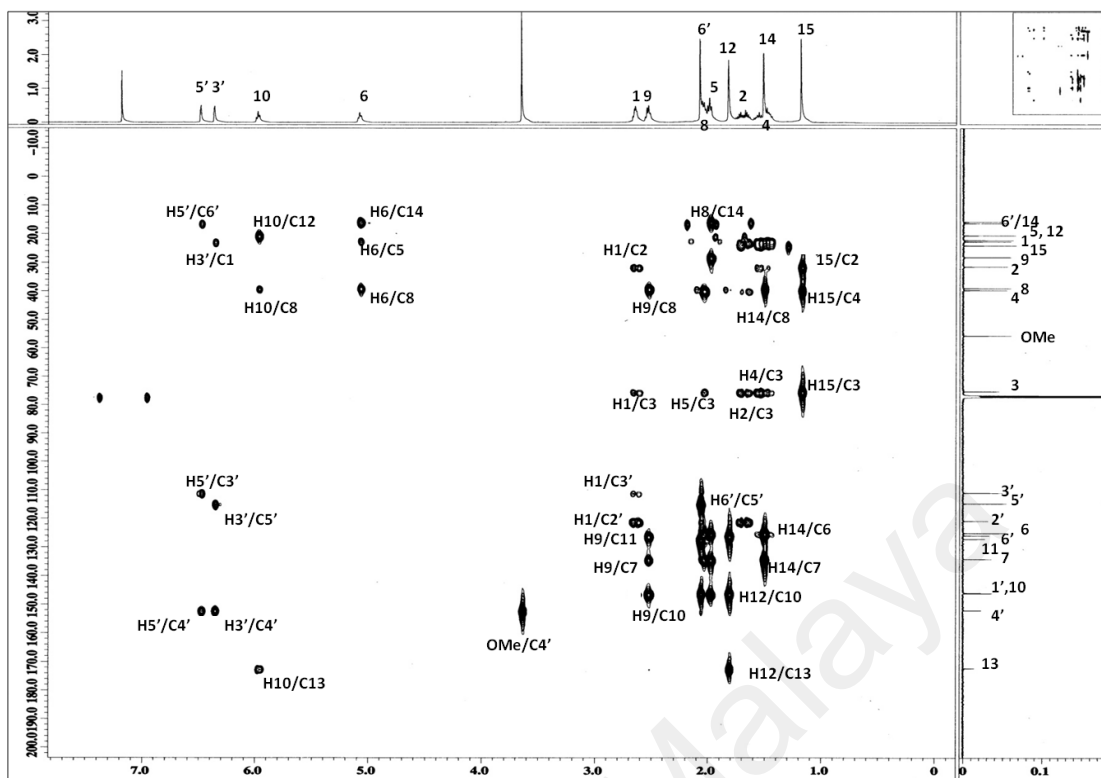
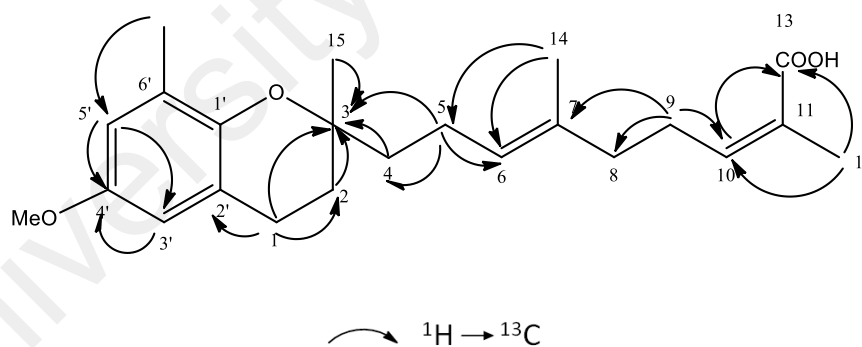
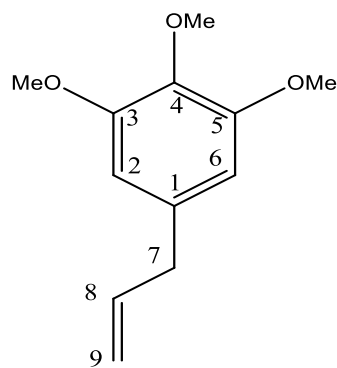


Fig. 4.139: HMBC spectrum of polycerasoidin (**49**)



Scheme 4.12: The HMBC correlations of polycerasoidin (**49**)

4.3.8 Elemicin (26)



26

Elimicin (**26**) was isolated as pale yellow oil. The UV spectrum exhibited absorption band at 265 nm indicating the presence of allylic group attached to the benzene ring. The IR spectrum displayed a peak at 1636 cm^{-1} indicating a double bond (an allyl group). Peaks at 3076 , 1612 and 1514 cm^{-1} represent C-H and C=C stretching in the aromatic ring.

The HREIMS (Figure 4.140) revealed a molecular ion peak at $m/z\ 209.1170\ [M+H]^+$ corresponding to a molecular formula $C_{12}H_{16}O_3$. Elemicin has been reported mostly from plant essential oils in a crude extract but rarely isolated as a pure compound.

The ^1H NMR spectrum (Figure 4.141) revealed two proton singlets at $\delta\ 6.40$ and 6.43 (1H,s) in the aromatic region that were assigned to positions H-2 and H-6. The rest of the positions in the aromatic ring are substituted by three methoxy groups at $\delta\ 3.84$ - 3.85 (3H). A proton doublet at $\delta\ 3.35$ indicates the presence of methylene proton on C-7, suggesting a CH_2 group attached to the aromatic ring. Two sets of multiplet protons signals at $\delta\ 5.12$ and 5.97 , assigned for H-9 and H-8 respectively suggest the presence of exocyclic double bond of allylic group. Table 4.22 summarizes the ^1H - and ^{13}C NMR of the compound.

The ^{13}C and DEPT 135 (Figure 4.142 and 4.143) showed a total of twelve carbon signals comprising of three methoxys, three methines, two methylenes and four quaternary carbons. Peaks at δ 40.7, 116.1 and 137.3 correspond to C-7, C-8 and C-9 respectively which further confirms the presence of allylic group. The presence of six aromatic carbons in the aromatic rings is indicated by the peaks at δ 136.0, 107.6, 153.2, 136.2, 153.2 and 105.4, assigned for C-1, C-2, C-3, C-4, C-5 and C-6, respectively.

The COSY spectrum (Figure 4.144) showed correlations between H-7 and H-8, and H-8 and H-9. The complete assignments of protons and carbons were shown in the HMQC spectrum (Figure 4.145) and the HMBC spectrum (Figure 4.146 and Scheme 4.13).

In view of the spectral data and comparison with reported values, the compound was established as elimicin (**26**) which was isolated for the first time from *Pseuduvaria macrophylla*. This is the first chemical report on the isolation and identification of phenylpropanoid derivatives from *Pseuduvaria* species.

Table 4.22: ^1H NMR (500 MHz) and ^{13}C NMR (125 MHz) spectral data of elimicin (**26**) in CDCl_3 (δ in ppm, J in Hz)

Position	^1H -NMR (δ ppm)	^{13}C -NMR (δ ppm)	^1H -NMR (δ ppm) (Sajjadi <i>et al.</i> , 2012)
1	-	136.0	
2	6.40 (1H, <i>s</i>)	107.6	6.44, <i>s</i>
3	-	153.2	3.86
4	-	136.2	3.85
5	-	153.2	3.86
6	6.43 (1H, <i>s</i>)	105.4	6.44, <i>s</i>
7	3.35 (2H, <i>d</i> , $J=7.0$)	40.7	3.36, <i>d</i>
8	5.97 (1H, <i>m</i>)	137.3	5.98, <i>m</i>
9	5.12, (1H, <i>m</i>)	116.1	5.14, <i>d</i>
OMe-1	3.85 (3H, <i>s</i>)	56.3	3.84 (3H, <i>s</i>)
OMe-2	3.84 (3H, <i>s</i>)	61.2	3.82 (3H, <i>s</i>)
OMe-3	3.85 (3H, <i>s</i>)	56.1	3.84 (3H, <i>s</i>)

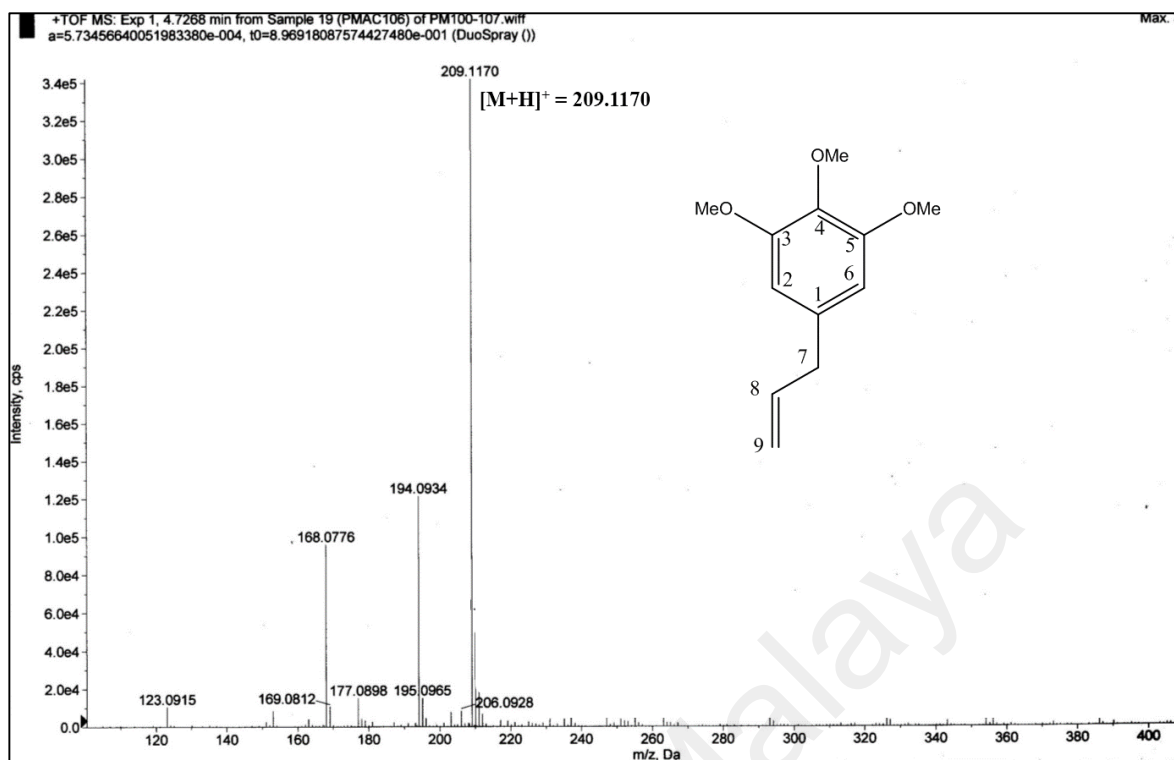


Fig. 4.140: LC-MS spectrum of elimicin (**26**)

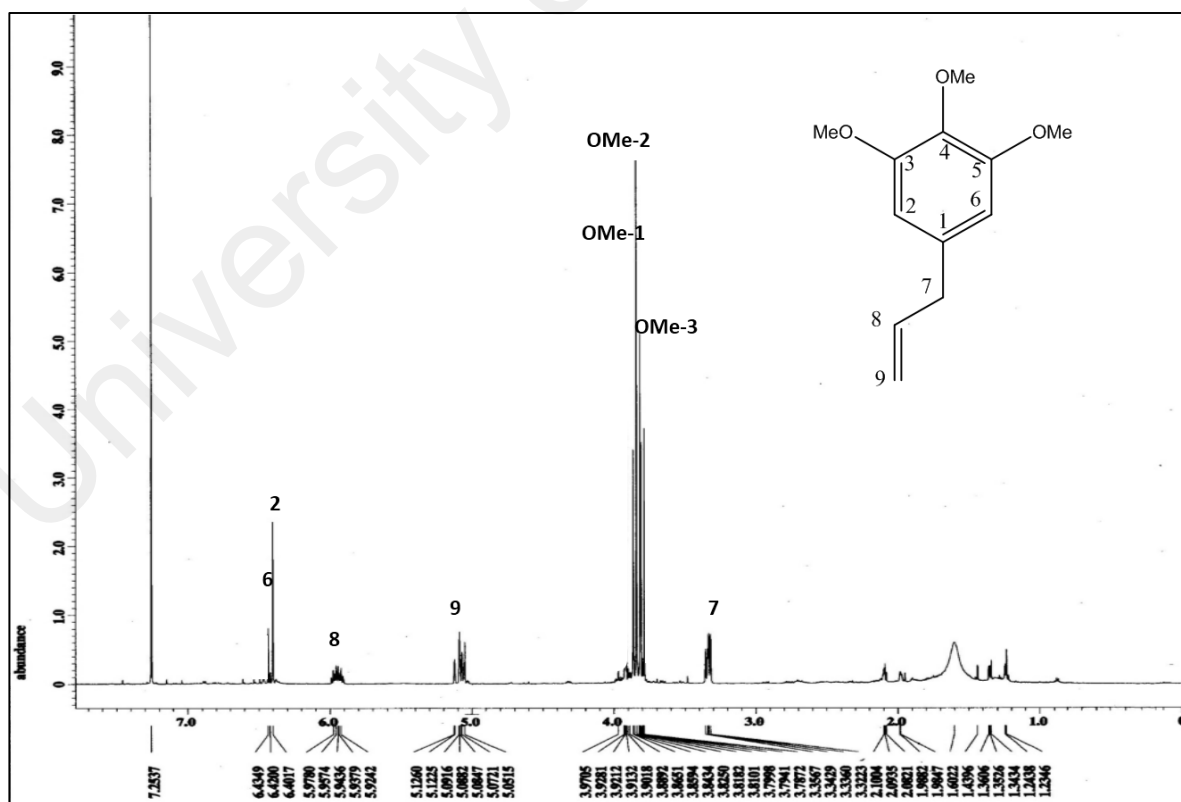


Fig. 4.141: ^1H NMR spectrum of elimicin (**26**)

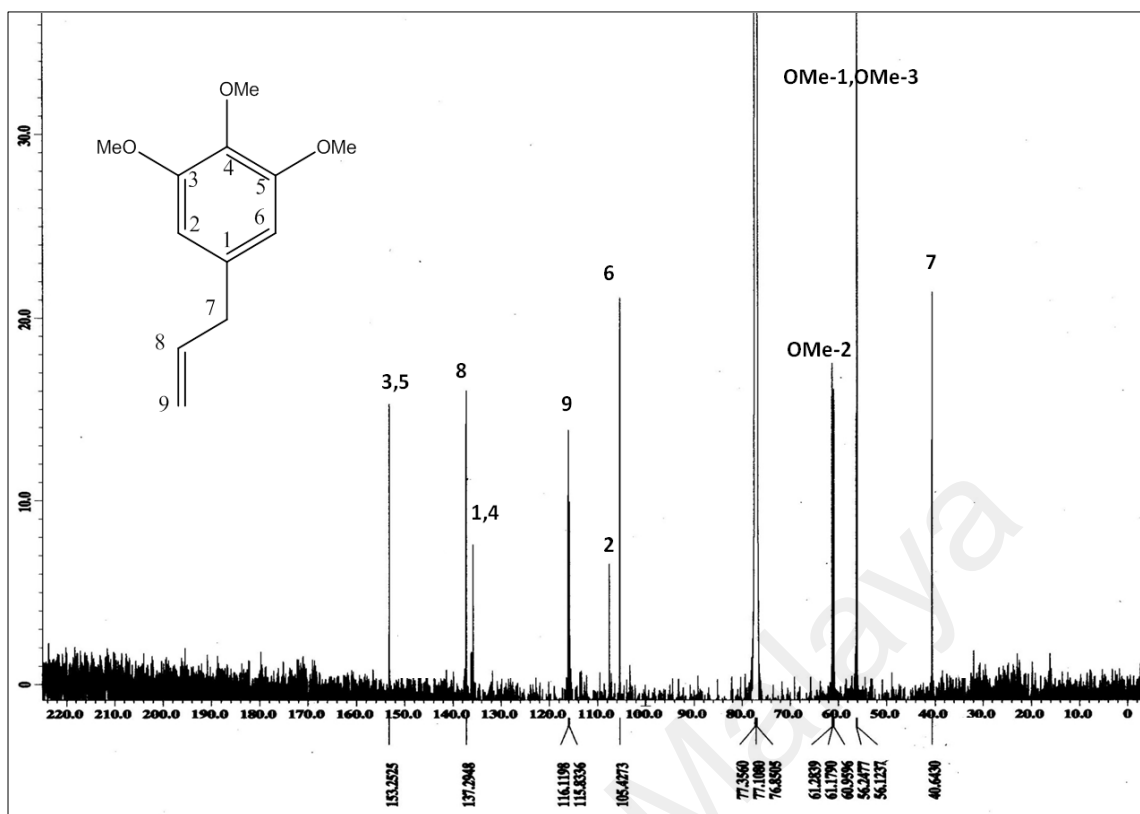


Fig. 4.142: ^{13}C NMR spectrum of elimicin (26)

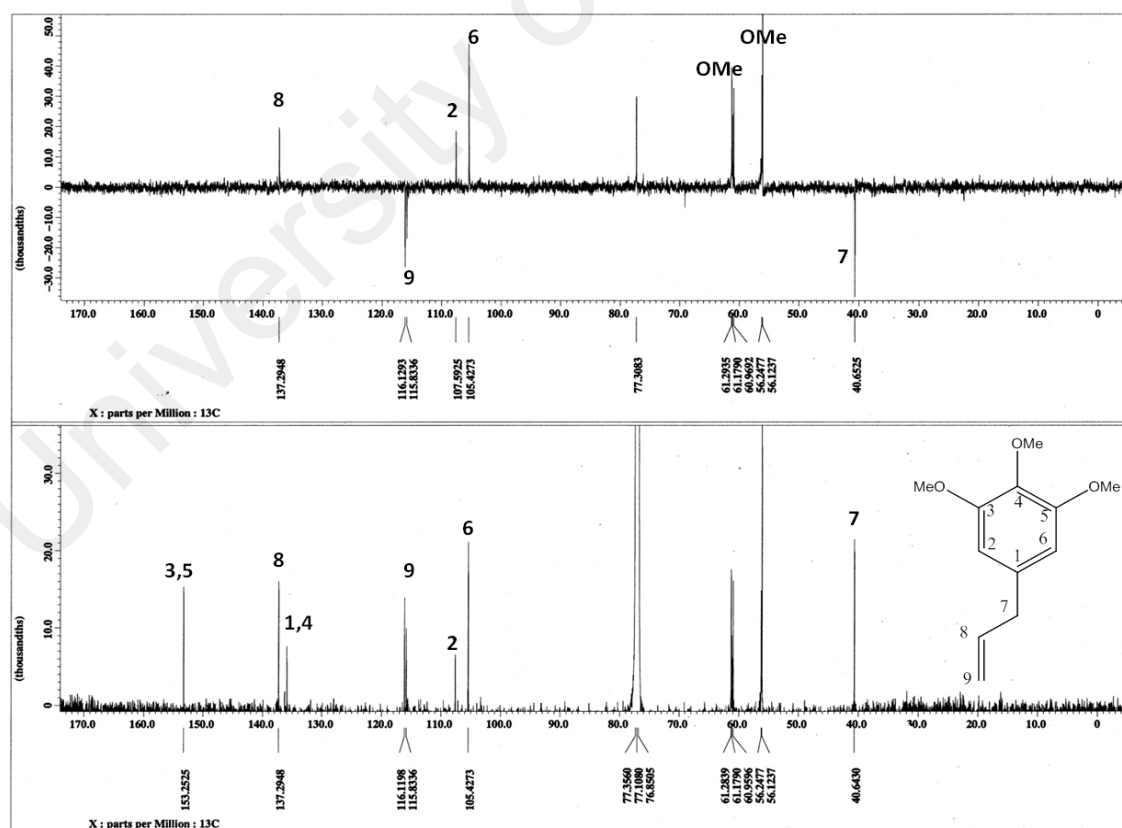


Fig. 4.143: DEPT 135 NMR spectrum of elimicin (26)

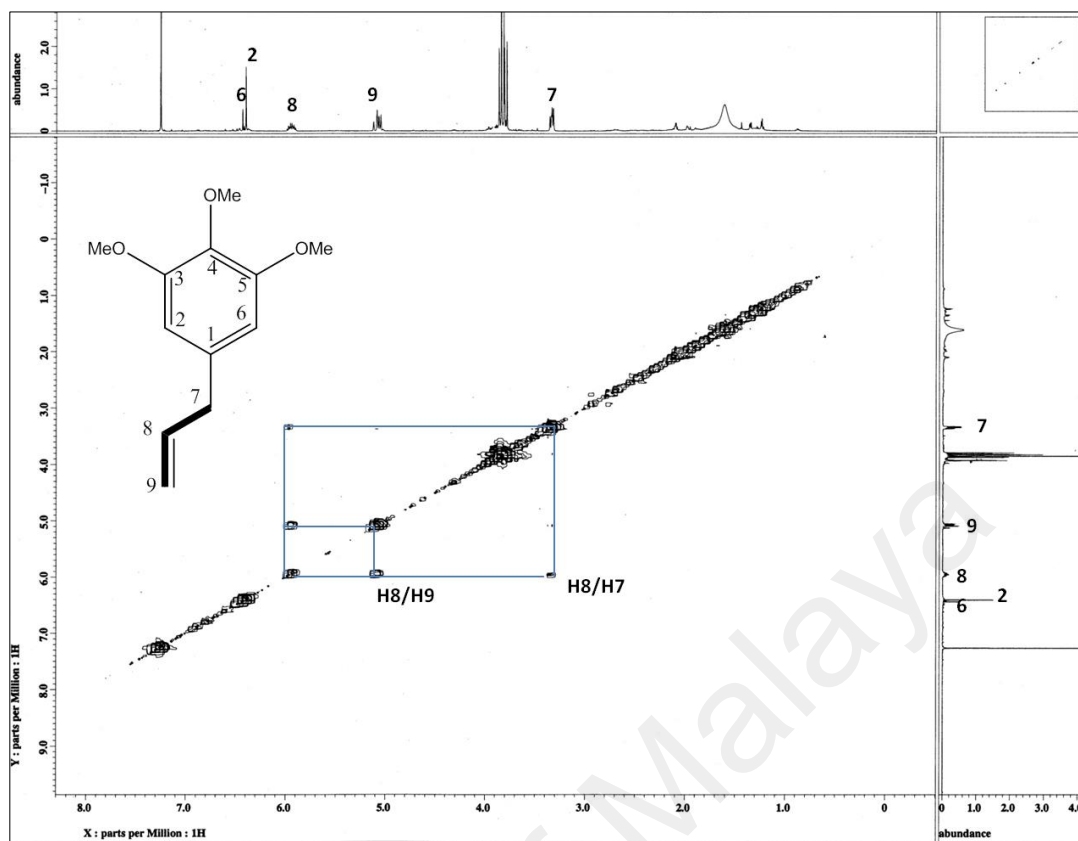


Fig. 4.144: COSY spectrum of elimicin (26)

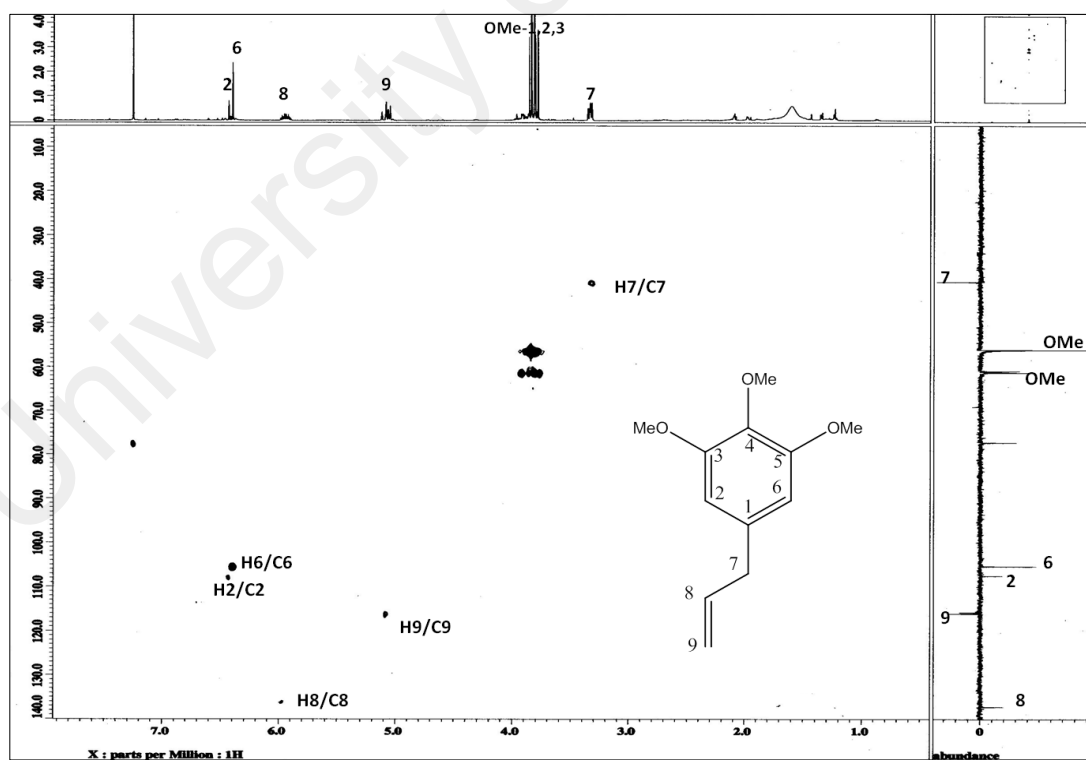


Fig. 4.145: HMQC spectrum of elimicin (26)

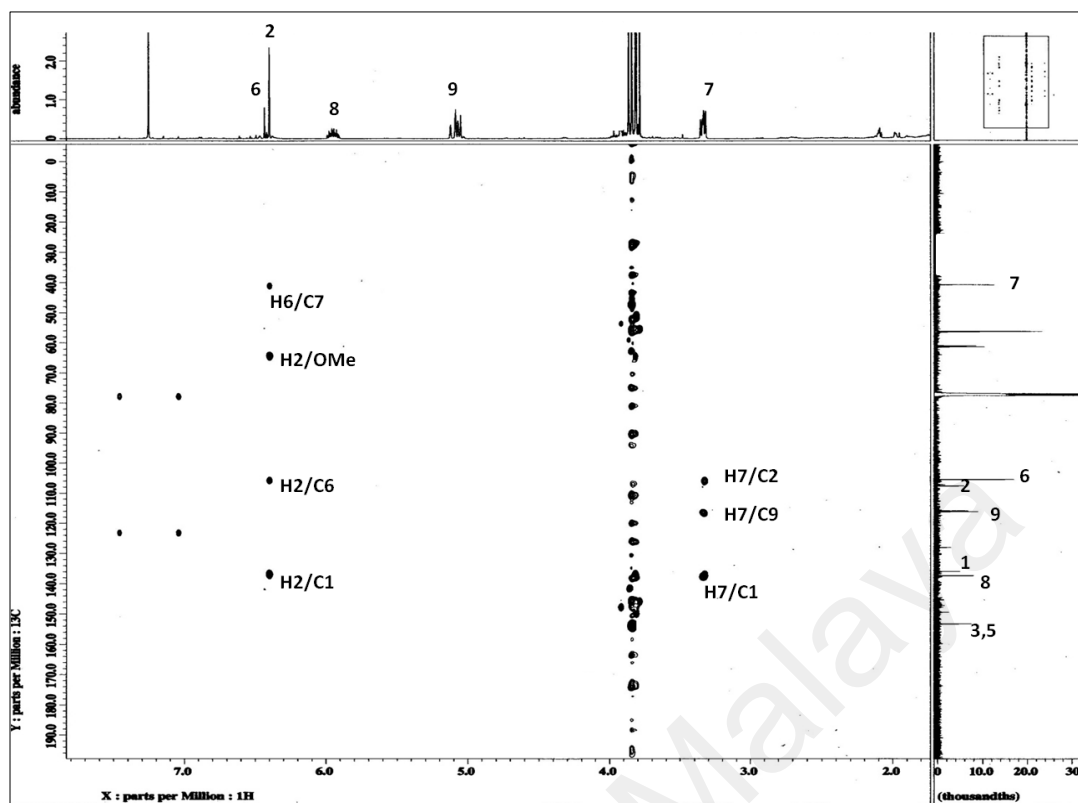
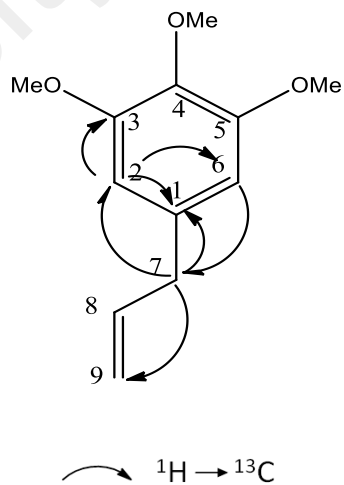
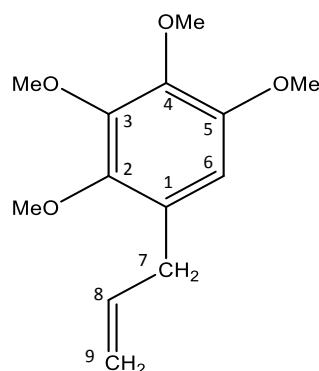


Fig. 4.146: HMBC spectrum of elimicin (26)



Scheme 4.13: The HMBC correlations of elimicin (26)

4.3.9 Elimicin 6-methoxy (50)



50

Elimicin-6-methoxy (**50**) was isolated as colorless oil. The UV spectrum showed absorption bands at 278 and 239 indicating the presence of unsaturated carbon-carbon bond. The IR spectrum showed absorption bands at 1592 cm⁻¹ and 1636 cm⁻¹ for aromatic ring and allyl group, respectively.

The HREIMS (Figure 4.147) revealed a molecular ion peak at *m/z* 239.1284 corresponding to a molecular formula C₁₃H₁₆O₃ and the GCMS spectrum (Figure 4.148) showed molecular ion peak at 238 [M]⁺.

The ¹H NMR spectrum (Figure 4.149) exhibited four methoxy groups resonated at δ 3.96, 3.90, 3.85 and 3.79 (3H, *s*) at positions C-2, C-3, C-4 and C-5 respectively. One proton singlet was observed at δ 6.42 assigned for H-6 in the aromatic ring. One proton doublet of sp³ methylene group was observed at δ 3.32 (C-7) and one proton doublet doublet of sp² methylene group resonated at δ 5.03 (C-9). The sp² methine was observed at δ 5.92 (C-8) as a multiplet.

In the COSY spectrum (Figure 4.152), the correlations between H7/H-8, H-8/H-9 confirm the presence of the allyl group. Table 4.23 summarizes the ^1H - and ^{13}C NMR of the compound.

The ^{13}C and DEPT 135 NMR spectra (Figure 4.150 and 4.151) showed thirteen carbons comprising of four methoxyls, two methines, two methylenes and five quaternary carbons. The peaks at δ 56.2, 56.3, 61.1 and 61.3 were assigned for methoxy groups at C-2, C-3, C-4 and C-5, respectively. Two methylenes resonated at δ 34.1 and δ 115.8 assigned for C-7 and C-9, respectively. One methine in the allyl group appeared at δ 137.3. Five quaternary carbons were observed at 127.9 (C-1), 149.4 (C-5), 147.1(C-3), 145.3 (C-2) and 141.4 (C-4), and one aromatic carbon at δ 107.6 (C-6). Combined analysis of HMQC spectrum (Figure 4.153) and HMBC spectrum (Figure 4.154) confirmed all the assigned protons and carbons in the structure.

Based on all spectroscopic data, the compound was established as elimicin 6-methoxy (**50**), a phenyl propanoid, which was isolated for the first time from *Pseuduvaria macrophylla*. To the author's knowledge, the compound has not been isolated as a pure compound but reported as part of essential oil extract identified by GC-MS. There was no reported NMR data on this compound.

Table 4.23: ^1H NMR (500 MHz) and ^{13}C NMR (125 MHz) spectral data of elimicin 6-methoxy (**50**) in CDCl_3 (δ in ppm, J in Hz)

Position	^1H -NMR (δ ppm)	^{13}C -NMR (δ ppm)
1	-	127.9
2	6.40, s,	145.3
3	-	147.1
4	-	141.4
5	-	149.4
6	6.42 (1H, <i>s</i>)	107.6
7	3.32 (2H, <i>d</i> , $J=6.9$)	34.1
8	5.92 (1H, <i>m</i>)	137.3
9	5.03 (2H, <i>m</i>)	115.8
OMe-1	3.96 (3H, <i>s</i>)	56.3
OMe-2	3.90 (3H, <i>s</i>)	61.1
OMe-3	3.85 (3H, <i>s</i>)	61.3
OMe-5	3.79 (3H, <i>s</i>)	61.3

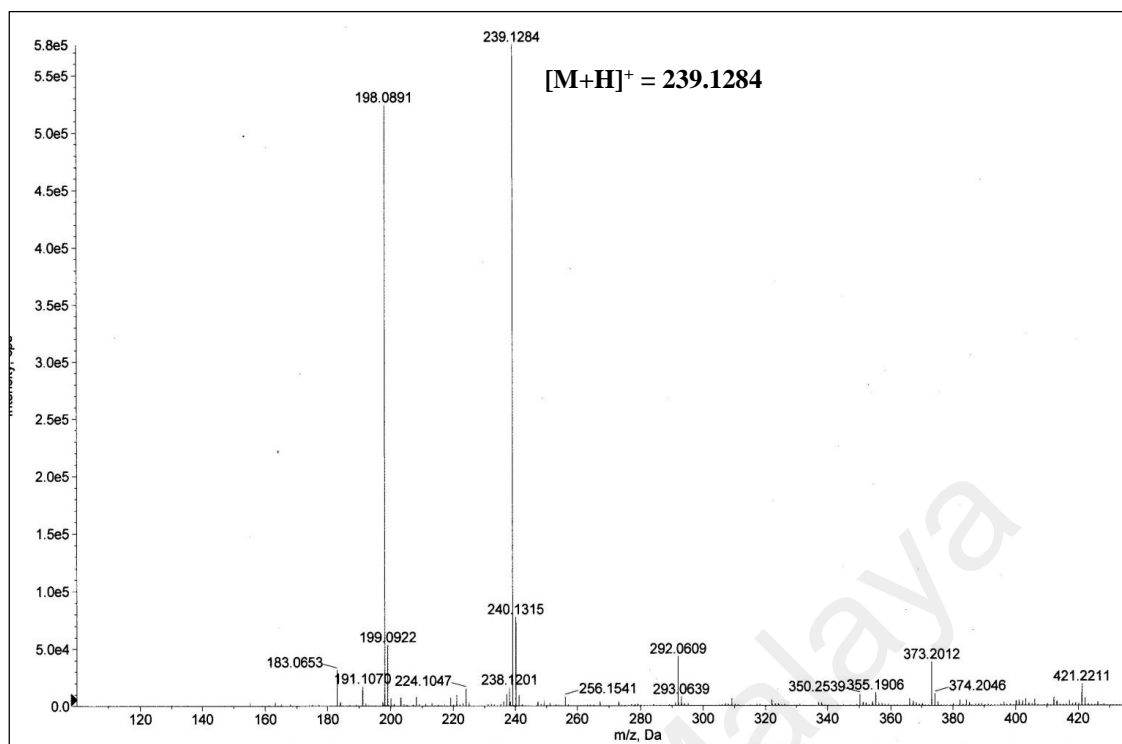


Fig. 4.147: LC-MS spectrum of elimicin-6-methoxy (50)

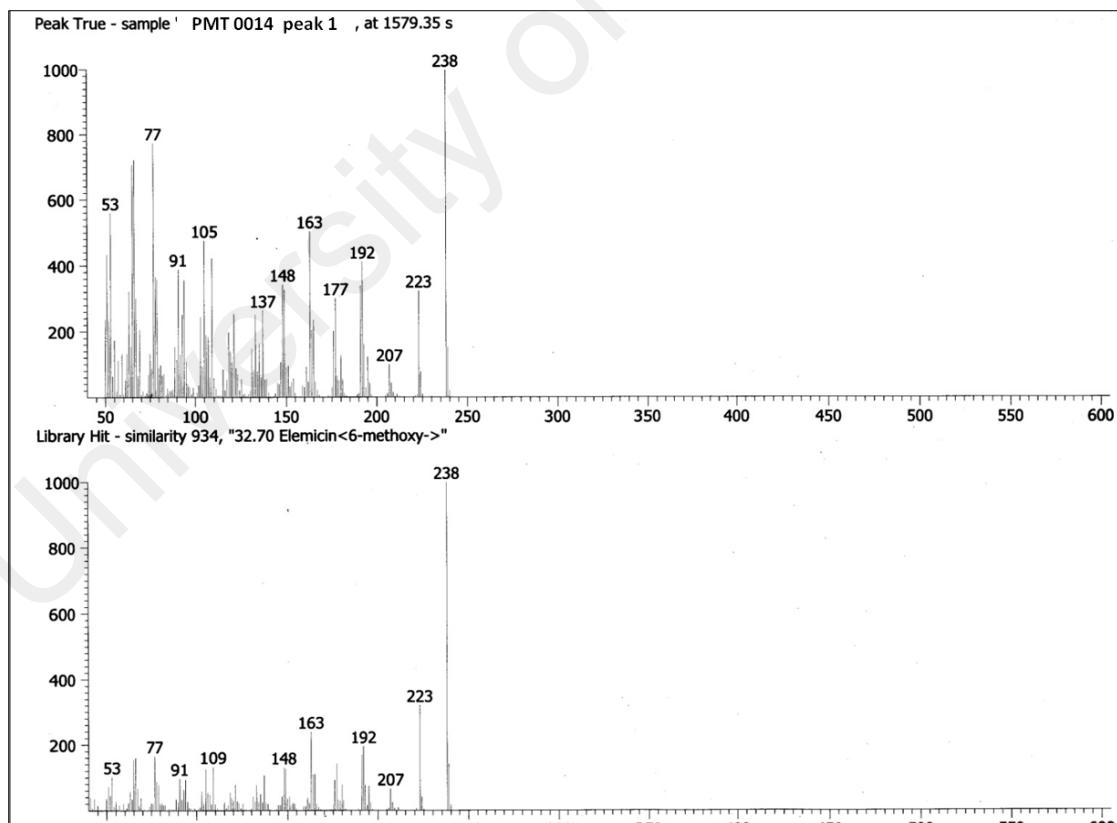


Fig. 4.148: GC-MS spectrum of elimicin-6-methoxy (50)

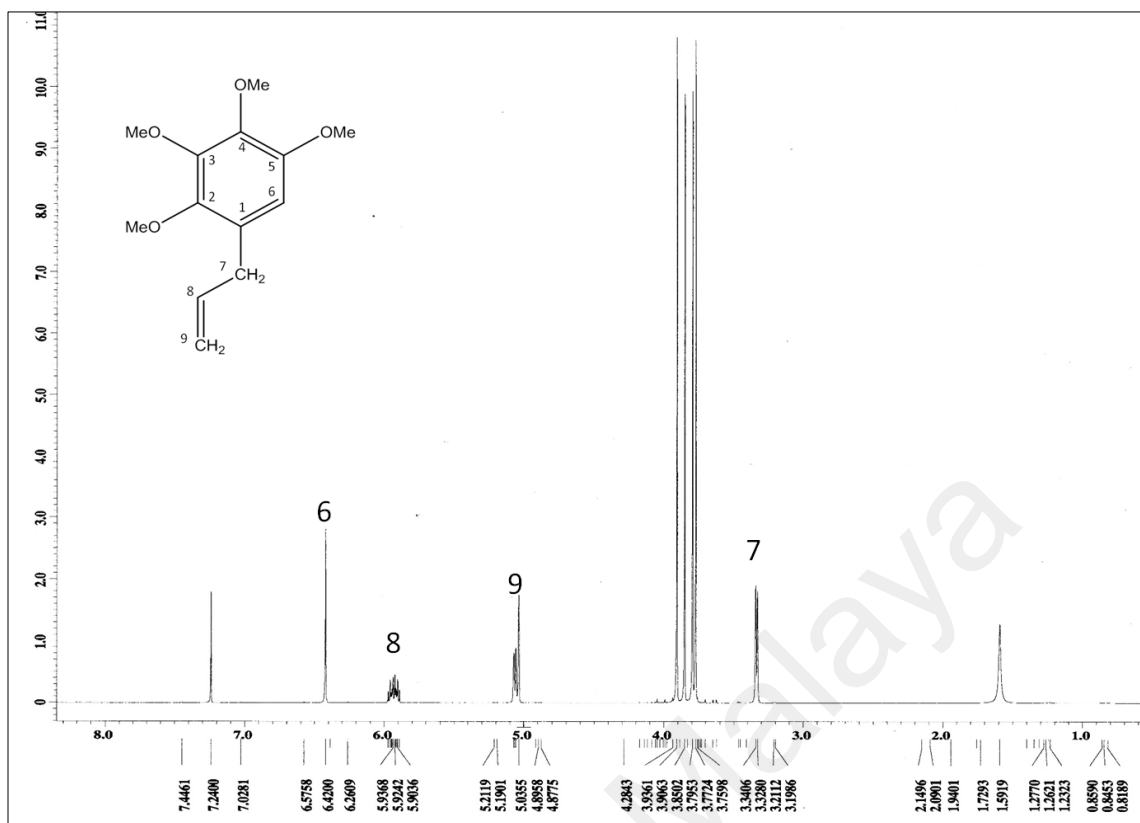


Fig. 4.149: $^1\text{H-NMR}$ spectrum of elimicin-6-methoxy (50)

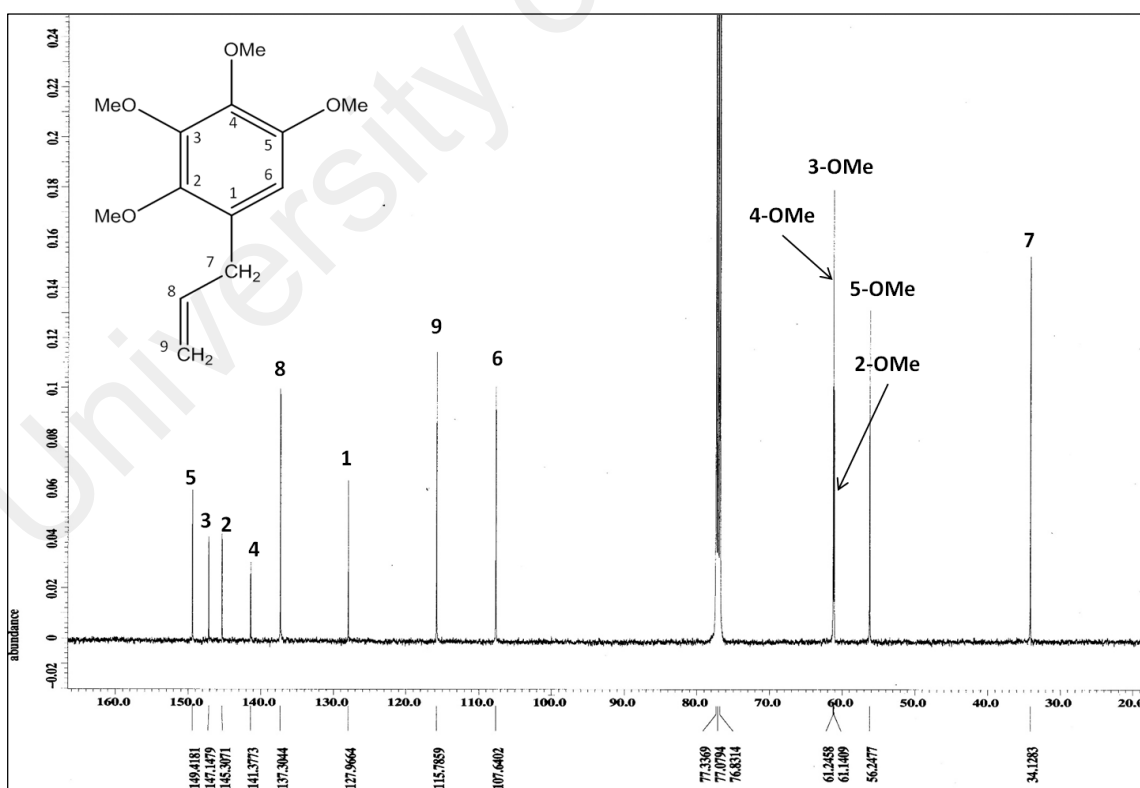


Fig. 4.150: $^{13}\text{C NMR}$ spectrum of elimicin-6-methoxy (50)

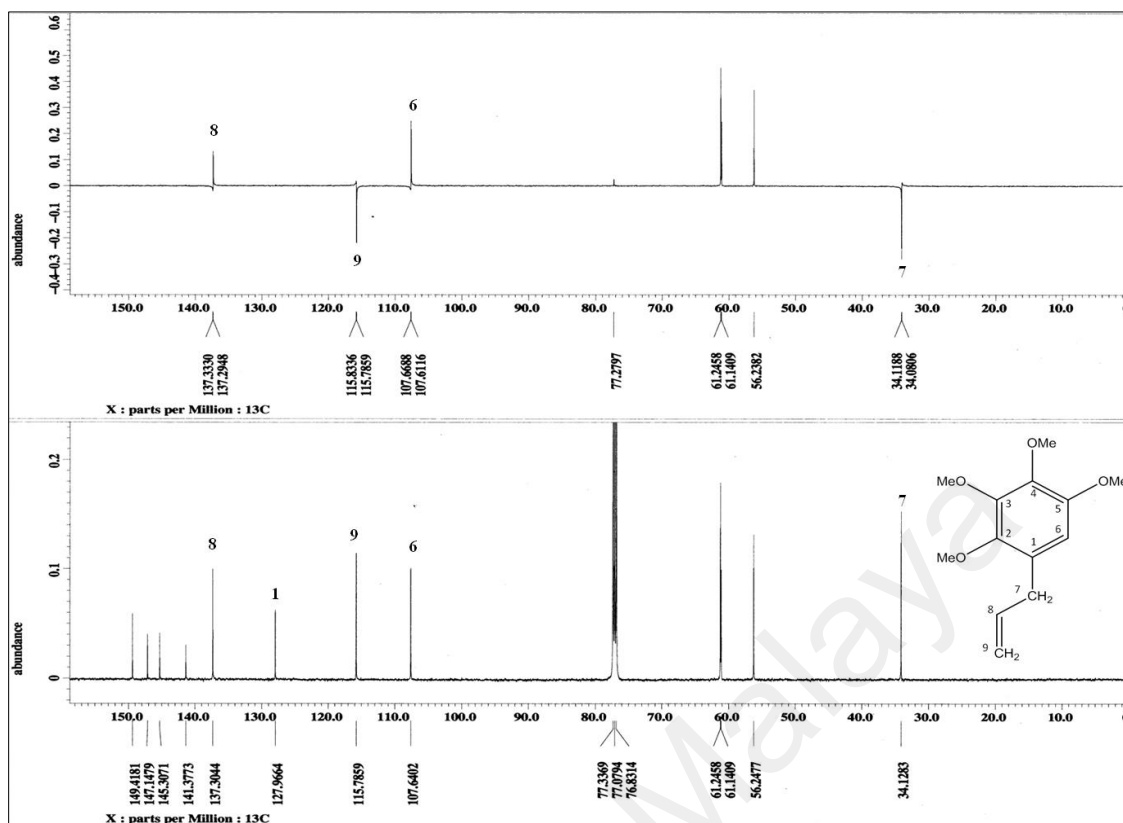


Fig. 4.151: DEPT 135 spectrum of elimicin-6-methoxy (50)

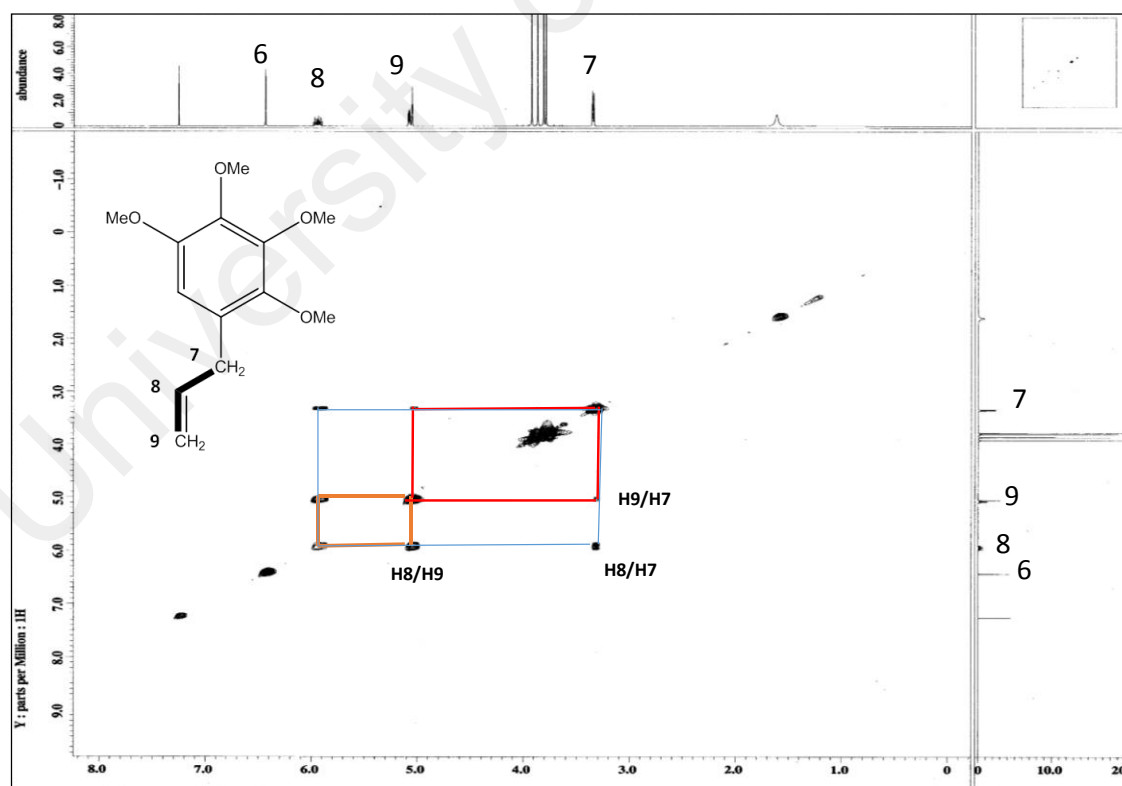


Fig. 4.152: COSY spectrum of elimicin-6-methoxy (50)

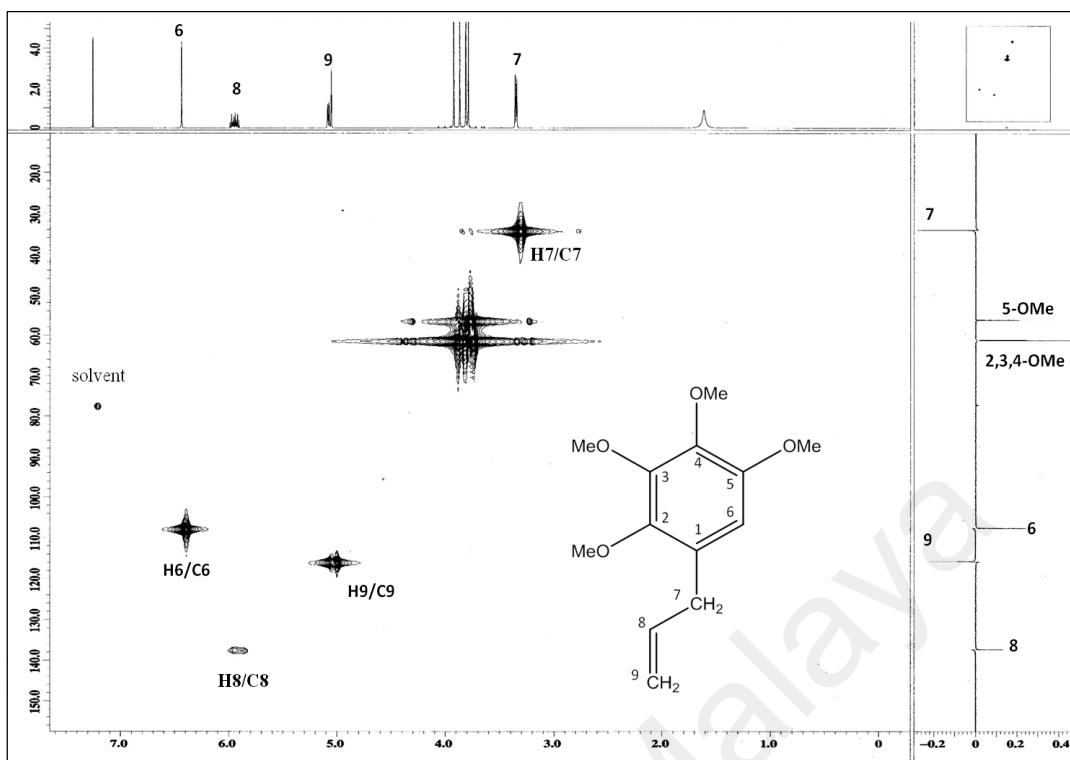


Fig. 4.153: HMQC spectrum of elimicin-6-methoxy (**50**)

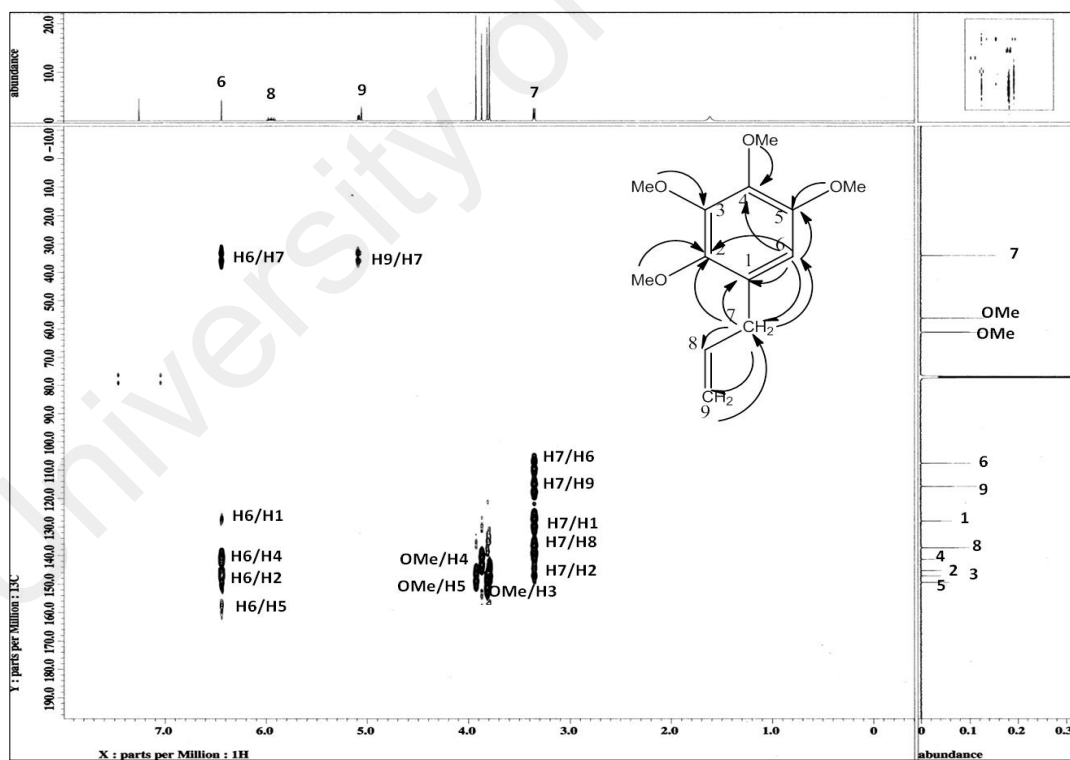
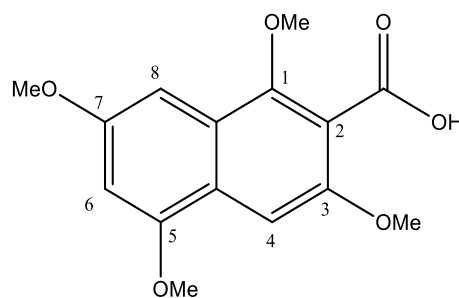


Fig. 4.154: HMBC spectrum of elimicin-6-methoxy (**50**)

4.3.10 1, 3, 5, 7-tetramethoxy-2-naphthoic acid (**51**)



51

1,3,5,7-tetramethoxy-2-naphthoic acid (**51**) was isolated as white amorphous solid. The UV spectrum showed absorption peaks at 250 and 300 nm. The IR spectra showed a carbonyl stretch C=O of a carboxylic acid at 1721 cm^{-1} .

The HREIMS (Figure 4.155) showed molecular ion peak at m/z 293.2478 corresponding to the molecular formula $\text{C}_{15}\text{H}_{16}\text{O}_6$.

The ^1H NMR spectrum (Figure 4.156) exhibited two doublets in meta position at δ 6.44 (1H, $J=1.2$ Hz) and 7.03(1H, $J= 1.2$ Hz) which most possibly belong to H-6 and H-8 in the aromatic ring and one proton singlet at δ 7.42(1H) that could be assigned to H-4. Four methoxy peaks were observed as singlet at δ 3.89, 3.87, 3.85 and 3.84.

In the ^{13}C NMR (Figure 4.157), the most downfield signal at δ 169.4 represents the carboxyl carbon atom. The rest of the signals in the upfield at δ 61.3, 61.2, 56.4 and 56.3 corresponded to the four methoxy carbon atoms. The remaining carbons belong to three methines and seven quaternary carbons.

The DEPT 135 spectrum (Figure 4.158) showed signal peaks for three methines and four methoxy groups and confirmed the absence of methylene carbons Table 4.24 summarizes

the ^1H - and ^{13}C NMR of the compound. There was no proton to proton correlation in the COSY spectrum (Figure 4.159).

The HMQC spectrum (Figure 4.160) clearly showed all the assigned protons and carbons. The HMBC experiment (Figure 4.161) showed correlations of H-8 to C-7, C-1, C-8a and C-4a, H-6 to C-5 and C-7, and H-4 to C-3 and C-5, thus confirming the structure of the compound.

Finally, based on spectroscopic data and comparison to the closest skeleton (Sharma & Gupta, 1985), the compound was established as 1,3,5,7-tetramethoxy-2-naphthoic acid (**51**) which is a new compound and a derivative from naphthoic acid. This is quite predictable since GC-MSTOF analysis on the non polar extracts of *Pseuduvaria macrophylla* did detect a considerable amount of naphthalene sources in the plant extracts.

Table 4.24: ^1H NMR (500 MHz) and ^{13}C NMR (125 MHz) spectral data of 1,3,5,7-tetramethoxy-2-naphthoic acid (**51**) in CDCl_3 (δ in ppm, J in Hz)

Position	^1H -NMR (δ ppm)	^{13}C -NMR (δ ppm)
1	-	157.9
2	-	100.8
3	-	149.7
4	7.42 (1H, <i>s</i>)	116.7
4a	-	125.6
5	-	153.2
6	6.44 (1H, <i>d</i> , $J=1.2$)	108.7
7	-	155.9
8	7.03(1H, <i>d</i> , $J= 1.2$)	104.9
8a	-	120.3
OMe-1	3.89 (3H, <i>s</i>)	61.3
OMe-3	3.87 (3H, <i>s</i>)	61.2
OMe-5	3.85 (3H, <i>s</i>)	56.4
OMe-7	3.84 (3H, <i>s</i>)	56.3

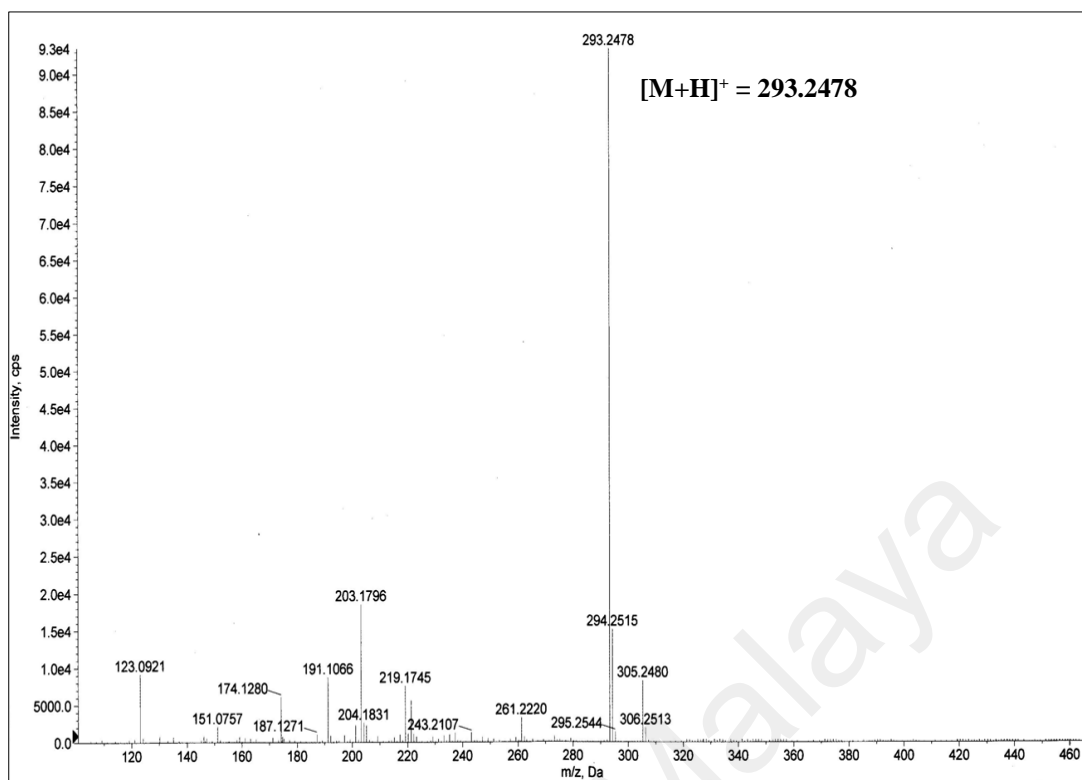


Fig. 4.155: LC-MS spectrum of 1,3,5,7-tetramethoxy-2-naphthoic acid (**51**)

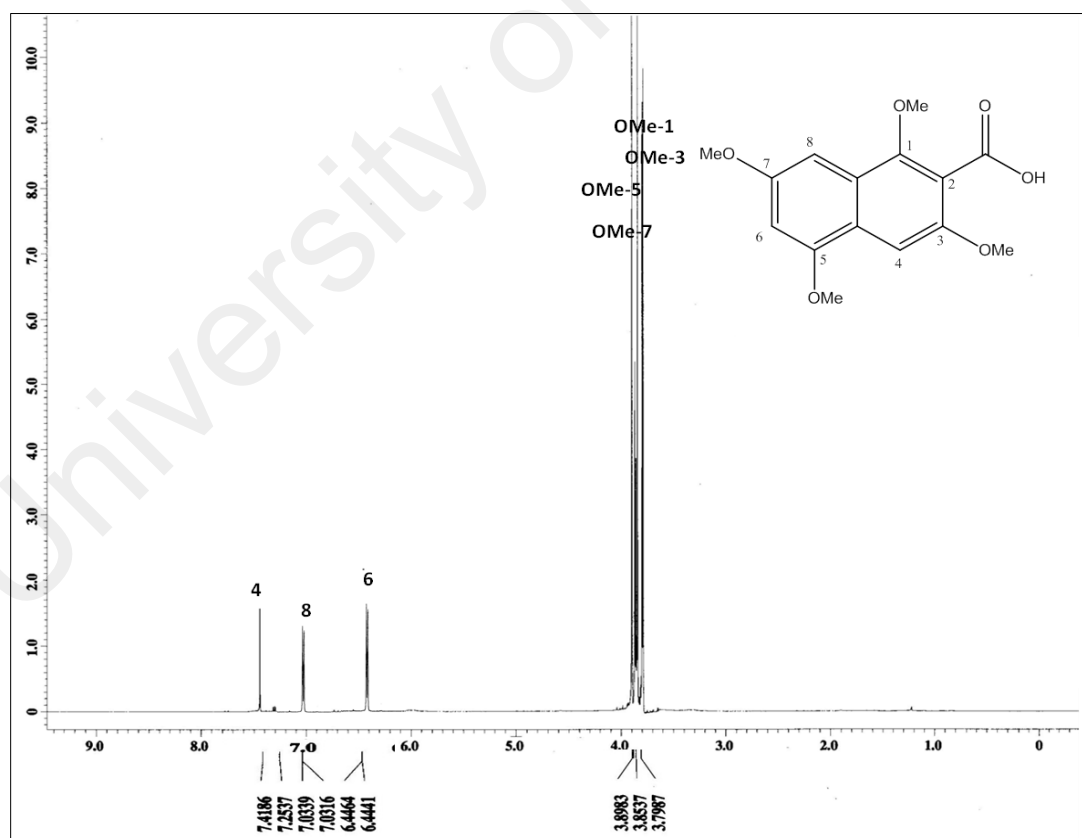


Fig. 4.156: ^1H NMR spectrum of 1,3,5,7-tetramethoxy-2-naphthoic acid (**51**)

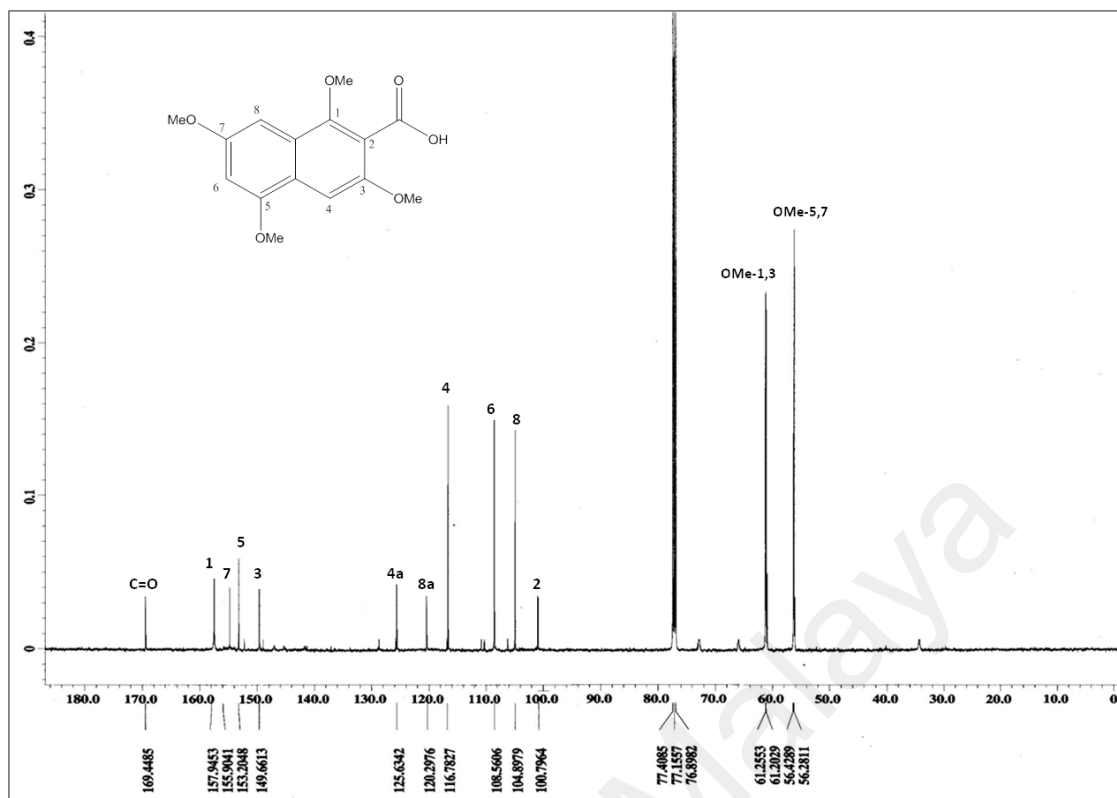


Fig. 4.157: ¹³C NMR spectrum of 1,3,5,7-tetramethoxy-2-naphthoic acid (**51**)

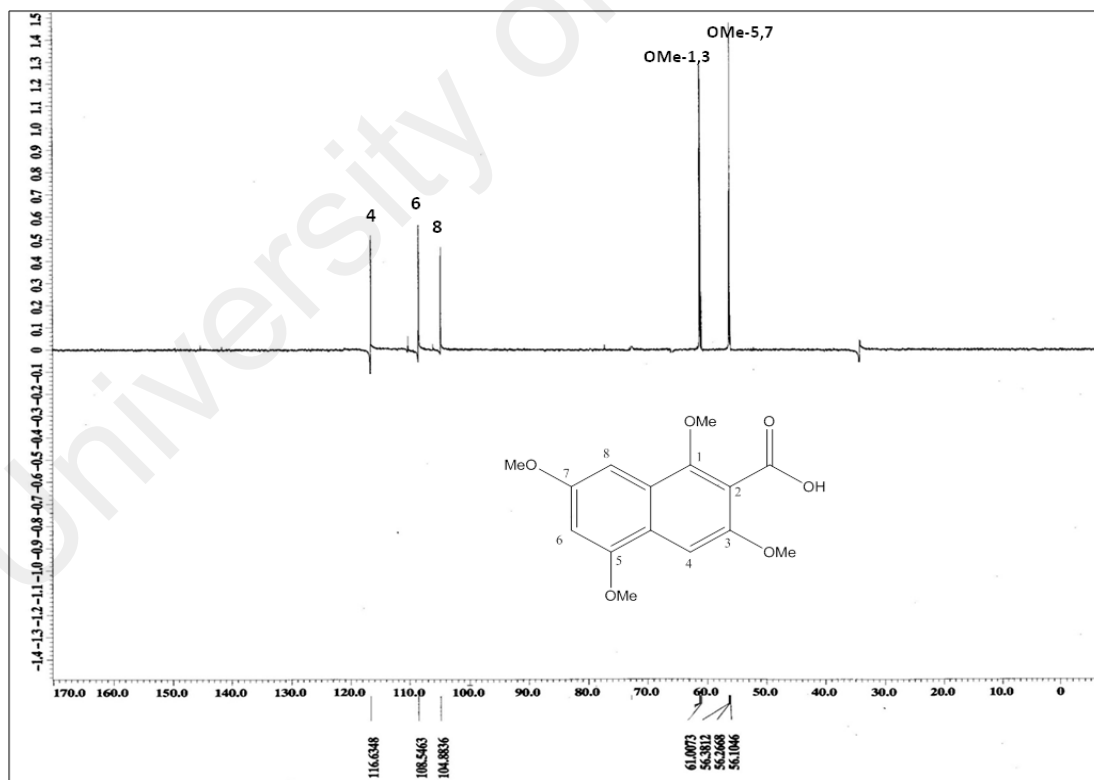


Fig. 4.158: DEPT 135 spectrum of 1,3,5,7-tetramethoxy-2-naphthoic acid (**51**)

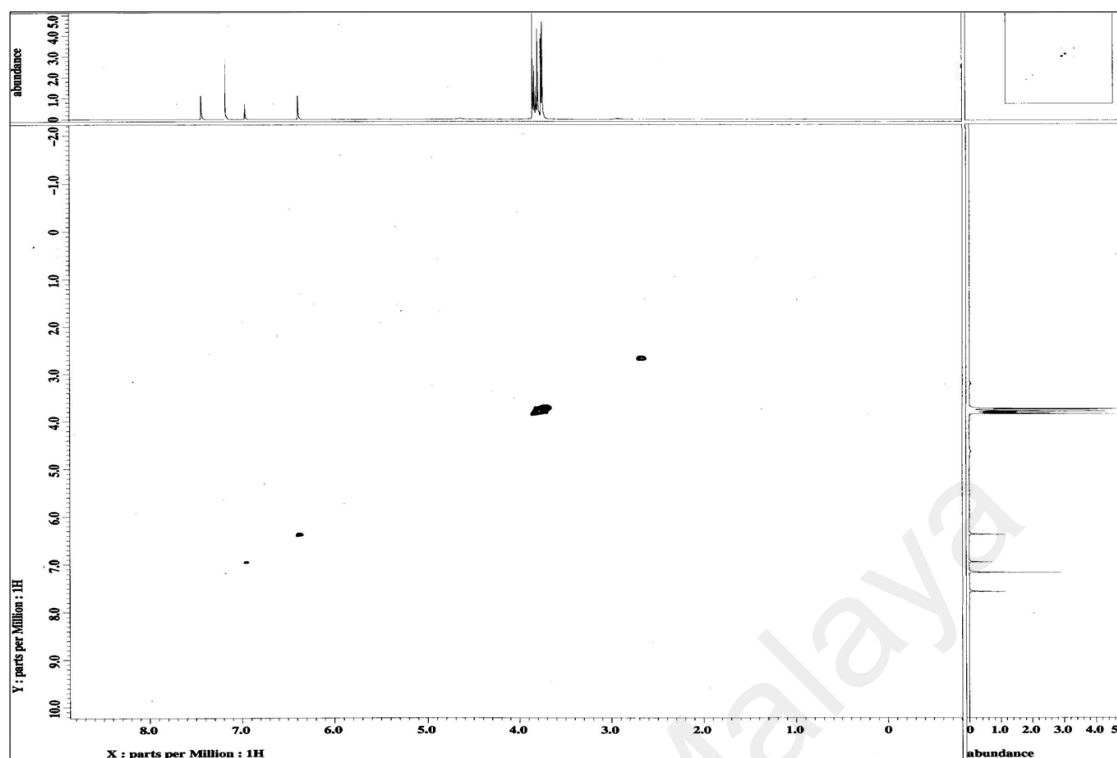


Fig. 4.159: COSY spectrum of 1,3,5,7-tetramethoxy-2-naphthoic acid (**51**)

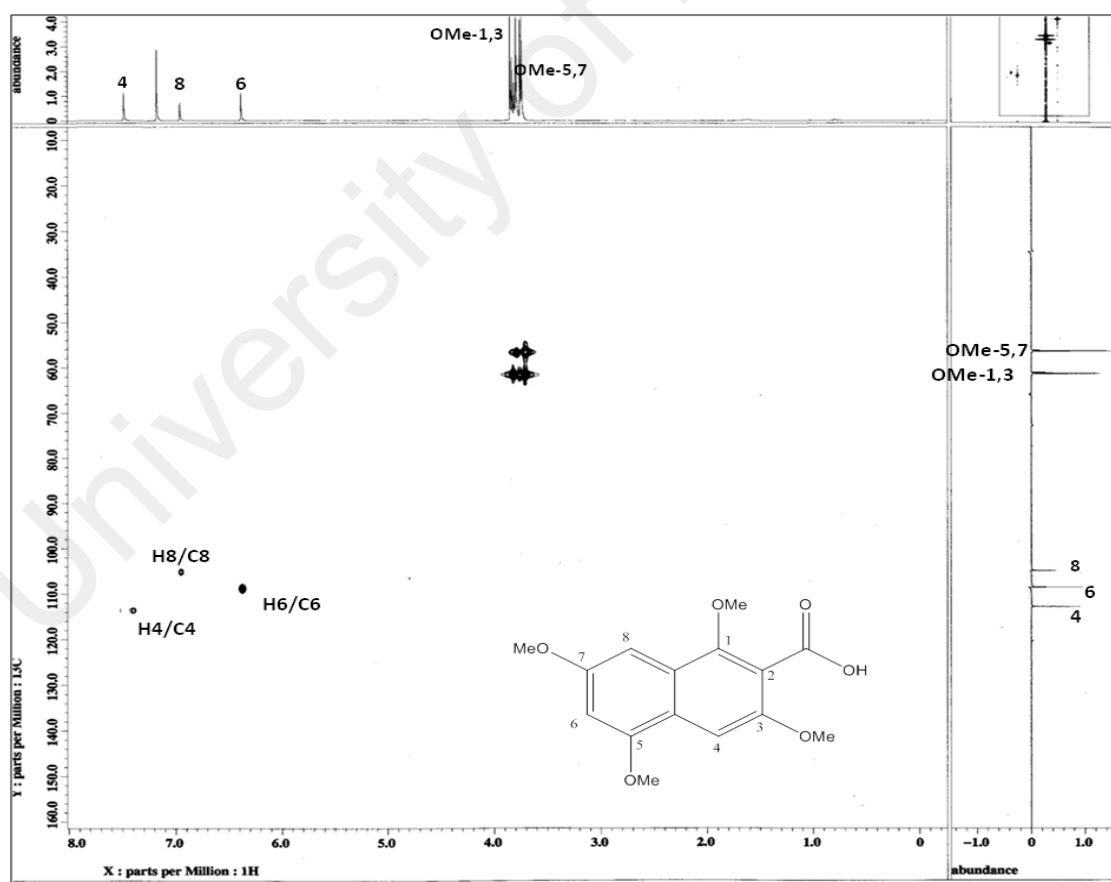


Fig. 4.160: HMBC spectrum of 1,3,5,7-tetramethoxy-2-naphthoic acid (**51**)

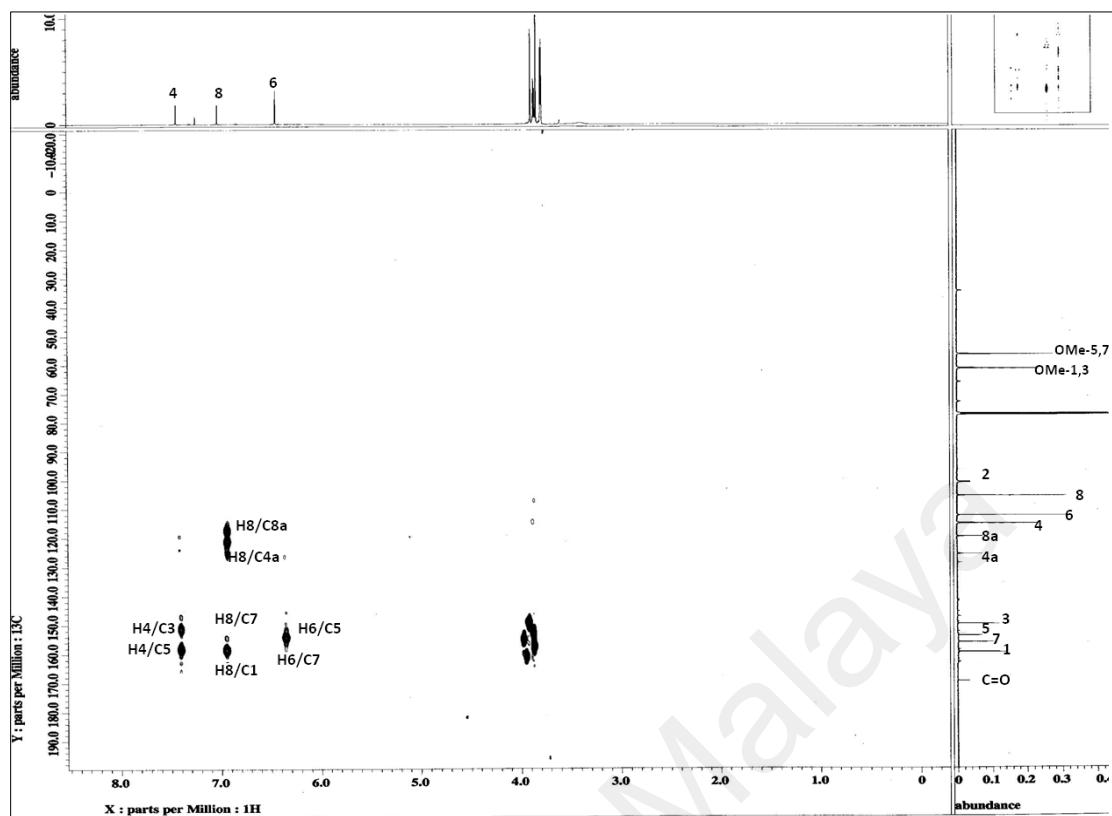
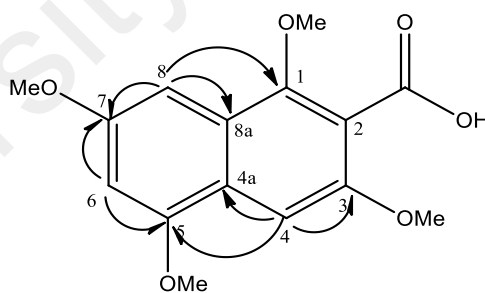
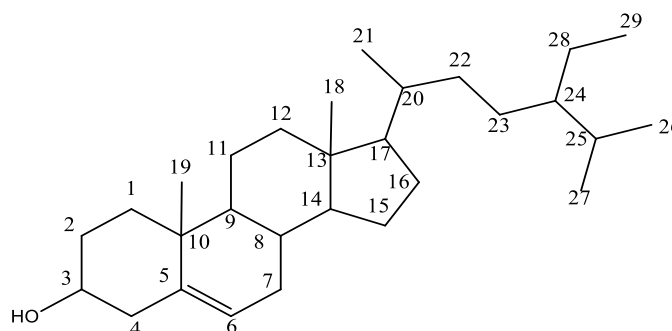


Fig. 4.161: HMBC spectrum of 1,3,5,7-tetramethoxy-2-naphthoic acid (**51**)



Scheme 4.14: The HMBC correlations of 1,3,5,7-tetramethoxy-2-naphthoic acid (**51**)

4.3.11 β -Sitosterol (**52**)



52

β -sitosterol (**52**) was isolated as a white amorphous solid. The UV spectrum showed absorption bands at 300 and 250 nm. The IR spectrum indicated the presence of hydroxyl group by the broad absorption band at 3400 cm^{-1} and peak at 1645 cm^{-1} represent a carbon-carbon double bond.

The GC-MS spectrum (Figure 4.162) revealed a molecular ion peaks at m/z 414 $[M]^+$ corresponding to the molecular formula of $C_{29}H_{50}O$ which matched the NIST library.

The ^1H NMR spectrum (Figure 4.163) showed a total of six methyl signals. Two methyl groups as proton singlets at δ 0.65 and 0.98 were assigned to H-8 and H-19. The rest of methyl groups resonated as a doublet at δ 0.77 ($J=6.60\text{ Hz}$), 0.81 ($J=7.56\text{ Hz}$), 0.79 ($J=7.08$) and 0.88 ($J=7.56\text{ Hz}$) were assigned to the protons H-21, H-26, H-27 and H-29 respectively. A very downfield peak resonated at δ 5.31-5.33 as a doublet was assigned to H-6 and a series of multiplet signals resonated between δ 0.83-2.26 were also observed. A multiplet peak at δ 3.52 indicates the presence of a hydromethine group (H-3). A doublet peak at δ 5.34 ($J=5.1\text{ Hz}$) belongs to an olefinic hydrogen (H-6). Table 4.25 summarizes the ^1H and ^{13}C NMR of the compound.

The ^{13}C and DEPT 135 NMR (Figure 4.164 and 4.165) showed the presence of 29 carbon signals consisting of six methyls, eleven methylenes, nine methines and two quaternary carbons. The signals at δ 140.7 and 121.7 showed the presence of olefinic carbon at C-5 and C-6 respectively. One significant carbon peak at δ 71.9 was assigned to the oxymethine proton C-3.

Finally, the compound was confirmed as β -sitosterol which is a plant sterol found in most plants (Mokbel & Hashinaga, 2006).

University of Malaya

Table 4.25: ^1H and ^{13}C NMR (500 MHz) spectral data of β -sitosterol (**52**) in CDCl_3 (δ in ppm, J in Hz)

Position	^1H -NMR (δ ppm)	^{13}C -NMR (δ ppm)	^{13}C -NMR (δ ppm) (Pateh <i>et al.</i> , 2009)
1	1.01-1.06, <i>m</i> 1.80-1.85, <i>m</i>	37.3	37.3
2	1.79-1.83, <i>m</i> 1.92-2.00, <i>m</i>	31.7	31.6
3	3.52 (1H, <i>m</i>)	71.9	71.8
4	1.90-2.00, <i>m</i>	42.3	42.2
5	-		
6	5.33 (1H, br s)	140.8	140.8
7	1.38-1.44, <i>m</i> 1.79-1.83, <i>m</i>	31.9	31.9
8	1.38-1.44, <i>m</i>	31.9	31.9
9	0.86-0.91, <i>m</i>	50.2	51.2
10	-	36.6	36.5
11	1.40-1.53, <i>m</i>	21.2	21.1
12	2.21-2.26, <i>m</i>	39.8	39.8
13	-	42.3	42.3
14	0.90-1.01, <i>m</i>	56.8	56.8
15	1.44-1.53, <i>m</i>	24.3	24.3
16	1.79-1.83, <i>m</i>	28.3	28.3
17	1.01-1.06, <i>m</i>	56.1	56.0
18	0.67 (3H, <i>s</i>)	11.9	11.9
19	1.00 (3H, <i>s</i>)	19.4	19.4
20	1.27-1.38, <i>m</i>	36.2	36.2
21	0.91 (3H, <i>d</i> , $J=6.60$)	18.8	18.8
22	0.95-1.01, <i>m</i> 120-126, <i>m</i>	34.0	33.9
23	1.01-1.10, <i>m</i>	26.1	26.1
24	0.83-0.88, <i>m</i>	45.9	45.9
25	1.61-1.66, <i>m</i>	29.2	29.2
26	0.81 (3H, <i>d</i> , $J=7.56$)	19.7	19.8
27	0.83 (3H, <i>d</i> , $J=7.08$)	19.2	19.3
28	1.20-1.28, <i>m</i>	23.1	23.1
29	0.85 (3H, <i>d</i> , $J=7.56$)	12.3	12.1

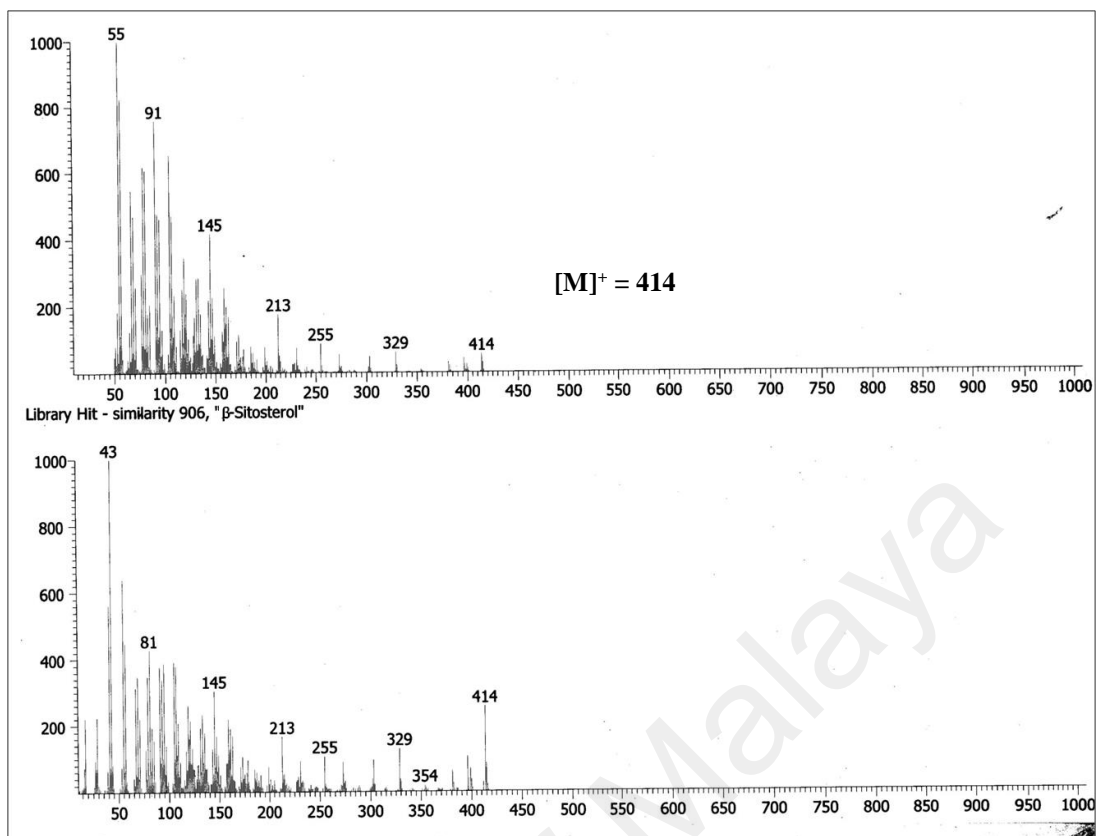


Fig. 4.162: GM-CS spectrum of β -sitosterol (**52**)

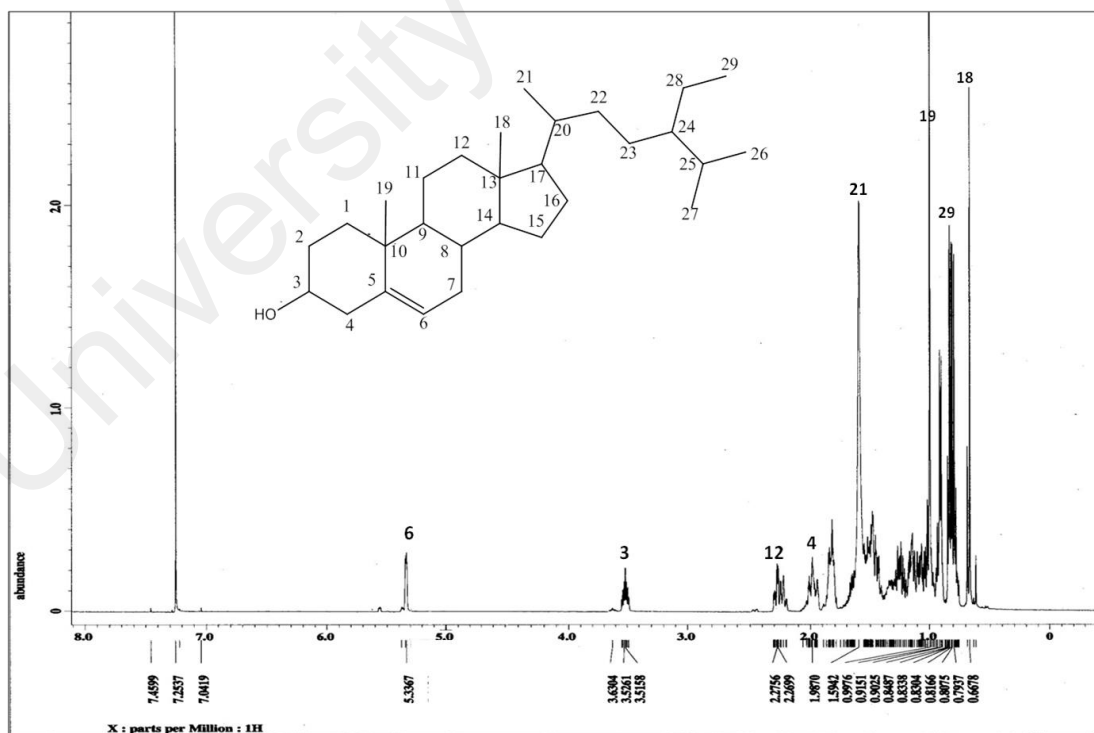


Fig. 4.163: ^1H NMR spectrum of β -sitosterol (**52**)

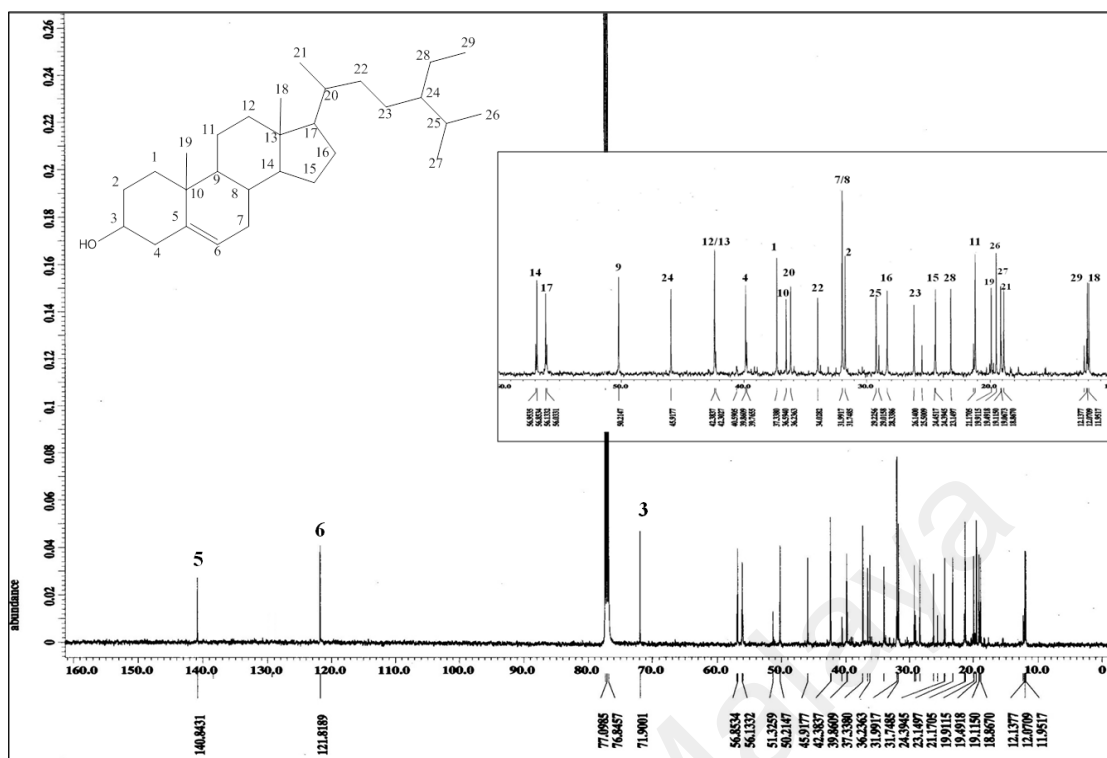


Fig. 4.164: ^{13}C -NMR spectrum of β -sitosterol (52)

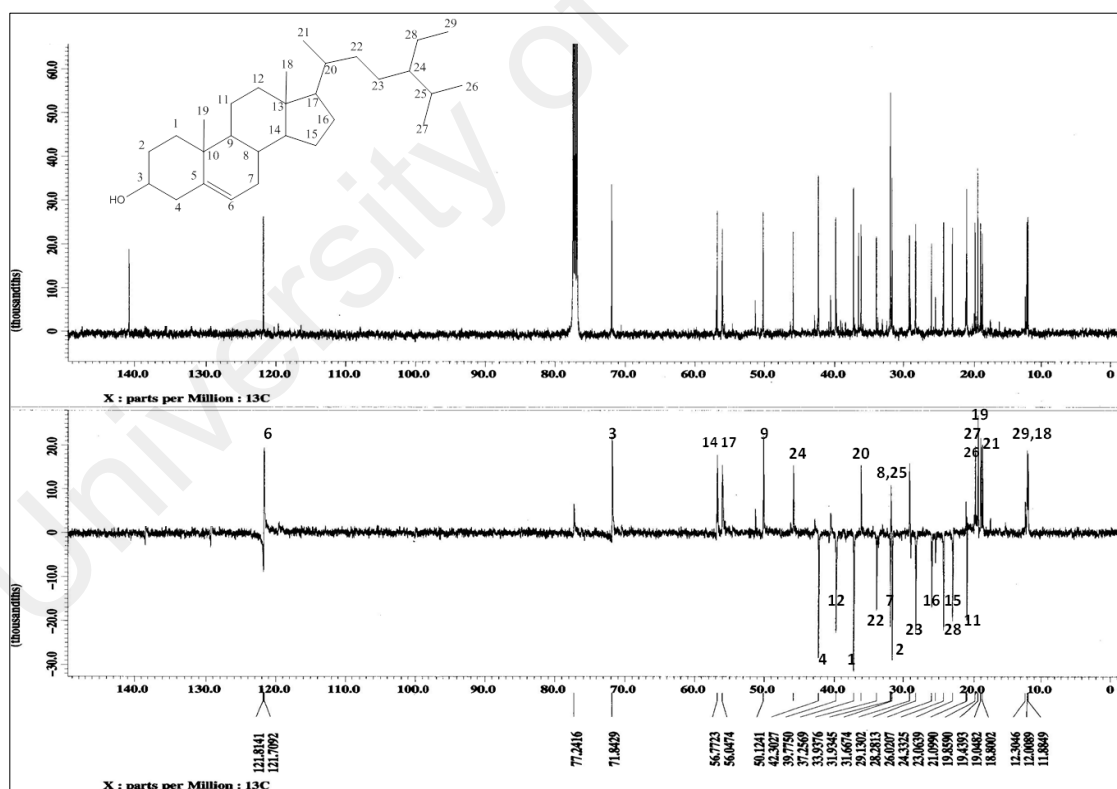
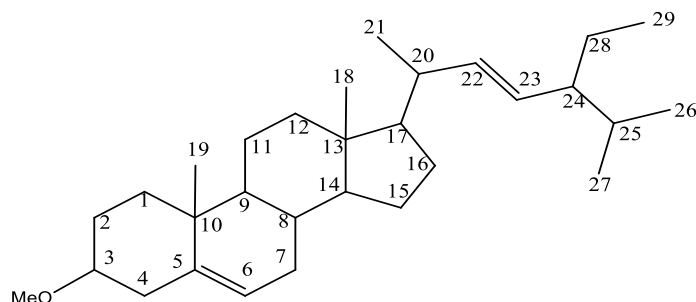


Fig. 4.165: DEPT 135 spectrum of β -sitosterol (52)

4.3.12 Stigmasta-5,22-diene, 3 methoxy (53)



53

Stigmasta-5,22-diene,3 methoxy (**53**), a steroid, was isolated as white amorphous solid. The UV spectrum showed absorption λ_{\max} at 282 nm. The IR spectrum indicated the presence of carbon-carbon double bond at 1618 cm^{-1} and 1676 cm^{-1} .

The GC-MSTOF spectrum (Figure 4.167) revealed a molecular ion peak $[M]^+$ at 426 (parent ion) corresponding to a molecular formula of $C_{30}H_{50}O$.

The ^1H NMR spectrum (Figure 4.168) of this compound was very similar to that of stigmasterol except for the presence of one sharp peak of three protons that represent a methoxy at δ 3.45 ppm. A multiplet proton signal observed at δ 3.05 belongs to H-3 (3H). Six methyl protons resonated as singlets, doublets and triplet at δ 0.78, 0.68, 0.82, 0.83, 0.80 and 0.70 assigned to H-18, H-19, H-21, H-26, H-27 and H-29 respectively. The eleven methylene protons resonated at δ 1.99, 2.24, 2.40, 1.80, 1.49, 2.02, 1.58, 1.82, 2.34, 1.23 and 1.23 were assigned to H-1, H-2, H-6, H-7, H-11, H-12, H-15, H-16, H-22, H-23 and H-28, respectively.

The other eight methine protons appeared at δ 1.41, 0.88, 1.00, 1.10, 1.64, 1.42 and 1.69 were assigned to H-8, H-9, H-14, H-17, H-20, H-24 and H-25, respectively. A characteristic proton doublet at δ 5.35 for H-6 indicates the presence of double bond

functionality between C-5 and C-6. Two doublet of a doublet signals at δ 5.1 and 5.0 were assigned to H-23 and H-22 indicating the presence of a double bond. Table 4.26 summarizes the ^1H - and ^{13}C NMR of the compound.

The ^{13}C NMR and DEPT 135 spectra (Figure 4.168 and 4.169) displayed 30 carbon signals comprising of one methoxy, six methyls, eleven methines, nine methylene and three quaternary carbons. The signals at δ 39.8, 139.9, 120.6 and 32.0 were assigned to the olefinic C-4, C-5, C-6 and C-7, respectively. The peak at δ 79.4 belongs to H-3 is more deshielded due to the methoxy moiety. A peak at δ 56.9 was assigned for methoxy. All the assignments of protons and carbons were confirmed by HMQC spectrum (Figure 4.170).

Combined analysis of spectroscopic data and reported data, the compound was identified as stigmasta-5,22-diene,3 methoxy which is a methyl ether derivative of stigmasterol (Rahman *et al.*, 2012).

Table 4.26: ^1H NMR (500 MHz) and ^{13}C NMR (125 MHz) spectral data of stigmasta-5, 22-diene, 3-methoxy (**53**) in CDCl_3 (δ in ppm, J in Hz)

Position	^1H -NMR (δ ppm)	^{13}C -NMR (δ ppm)
1	1.81	37.3
2	1.79	28.0
3	3.05, <i>m</i>	79.4
4	2.27	39.8
5	-	139.9
6	5.36, <i>m</i>	120.6
7	1.93	32.0
8	1.45	31.9
9	0.92	50.3
10	-	36.3
11	1.50	20.3
12	1.95	39.5
13	-	41.2
14	1.00	56.0
15	1.54	27.0
16	1.65	27.9
17	1.12	56.1
18	0.70	12.1
19	1.01, <i>s</i>	19.0
20	2.00	40.6
21	1.02, <i>d</i> , 7.5	20.2
22	5.09	138.4
23	4.96	129.3
24	1.52	51.3
25	1.53	31.9
26	0.79, <i>d</i> , 6.5	21.2
27	0.85, <i>d</i> , 6.5	19.0
28	1.43	25.4
29	0.804, <i>t</i> , 7.5	12.1
O-Me	3.34, <i>s</i>	56.9

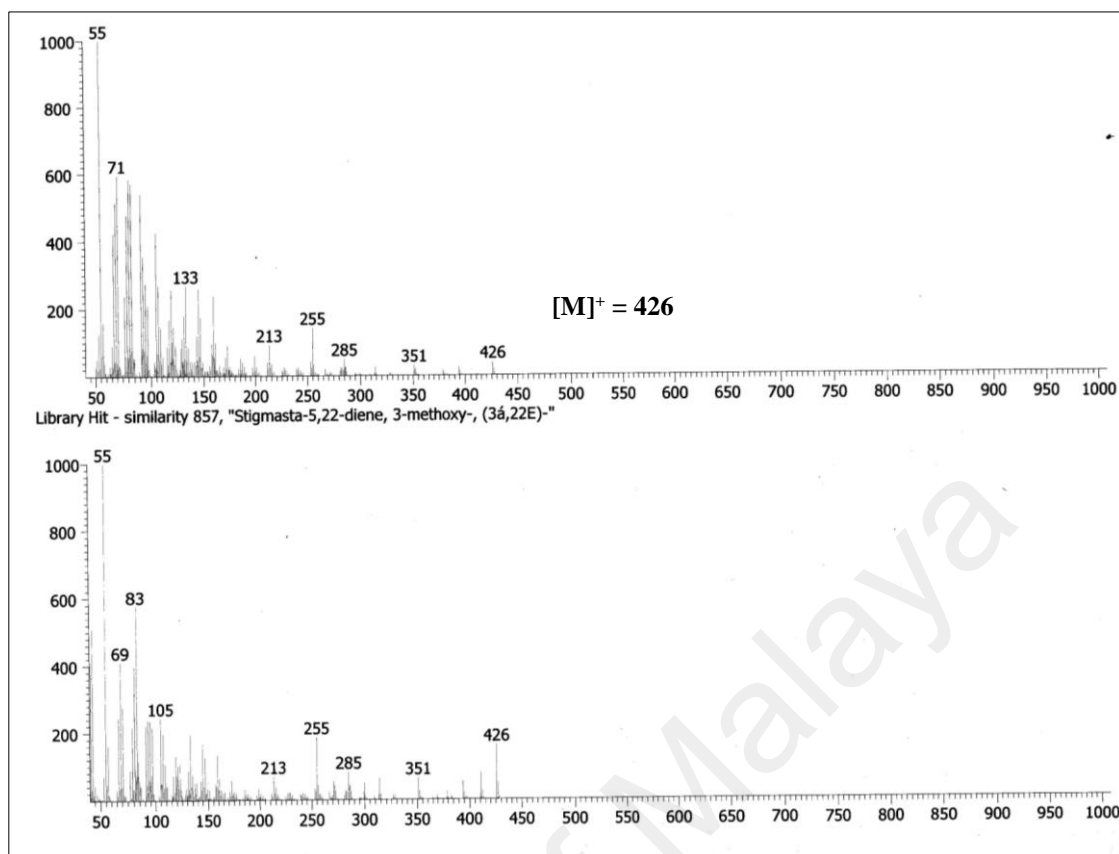


Fig. 4.166: GC-MS spectrum of stigmasta-5,22-diene,3 methoxy (**53**)

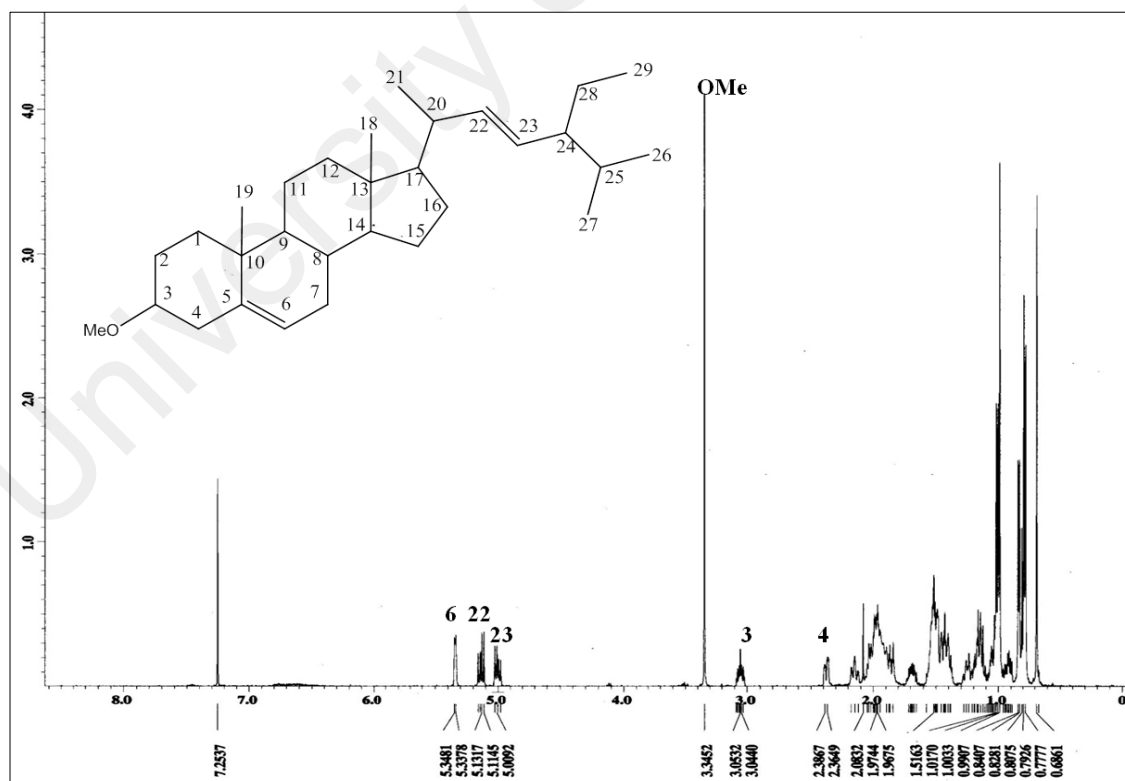


Fig. 4.167: ^1H NMR spectrum of stigmasta-5, 22-diene, 3 methoxy (**53**)

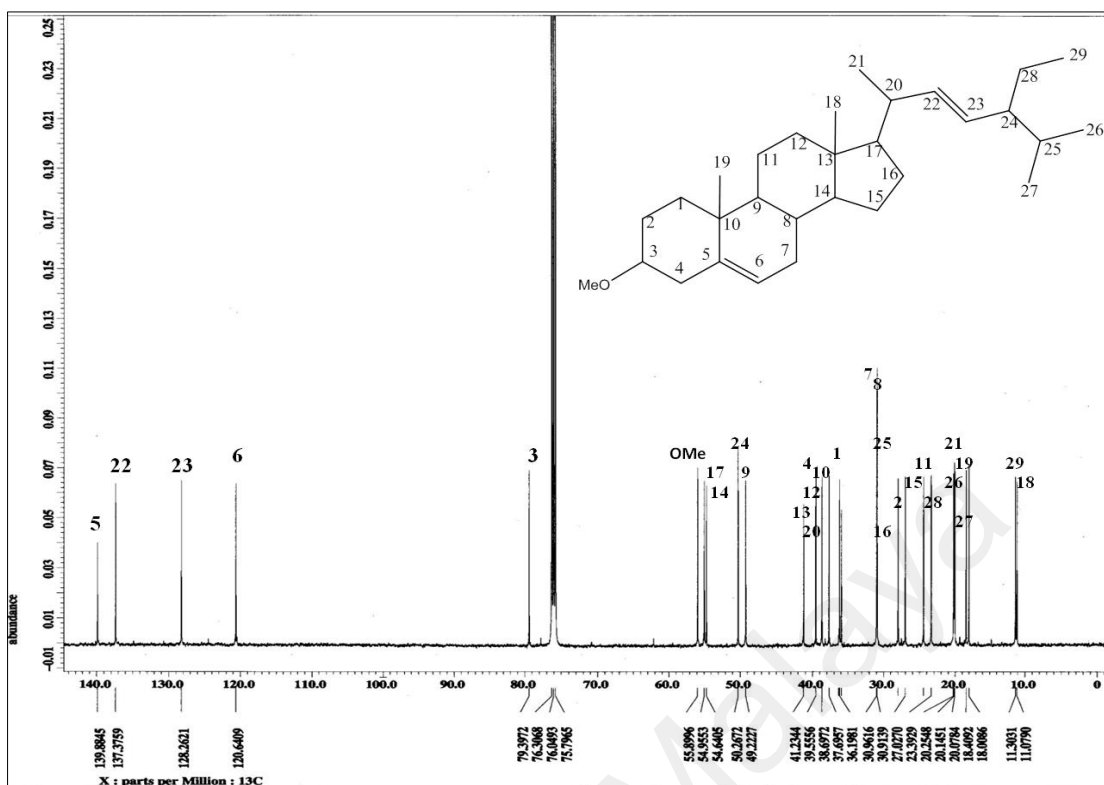


Fig. 4.168: ^{13}C NMR spectrum of stigmasta-5,22-diene,3 methoxy (53)

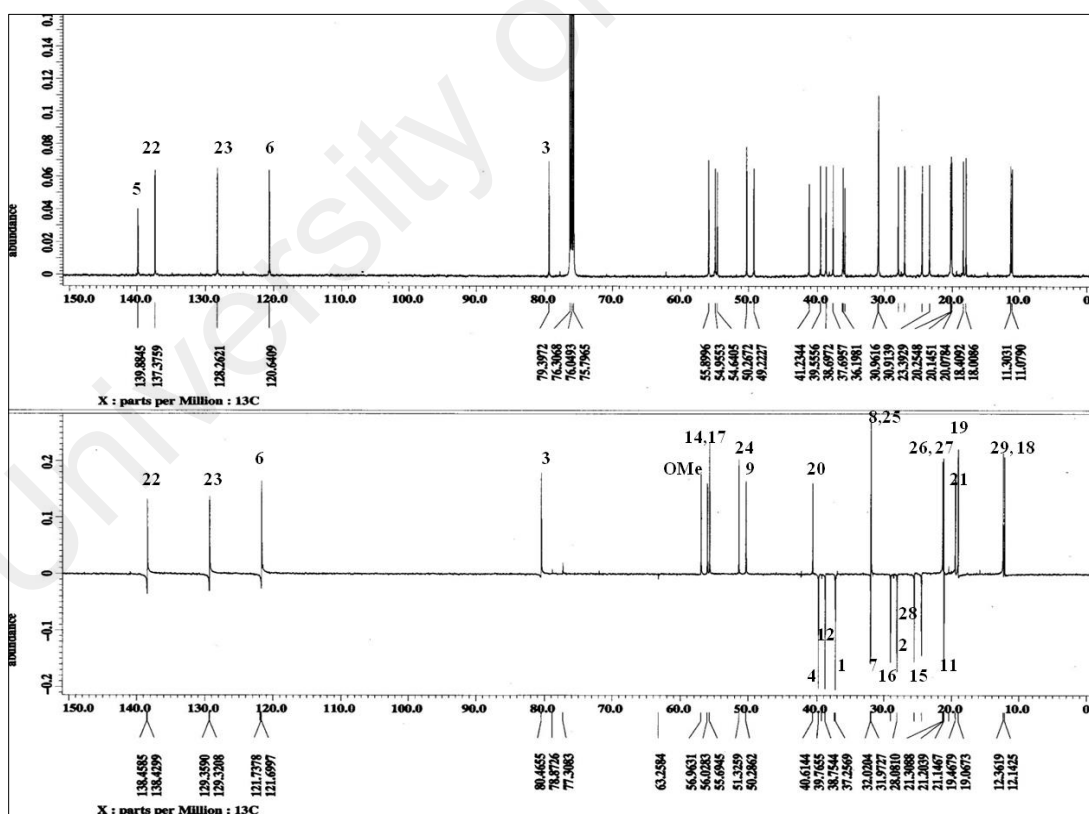


Fig. 4.169: DEPT 135 spectrum of of stigmasta-5,22-diene,3 methoxy (53)

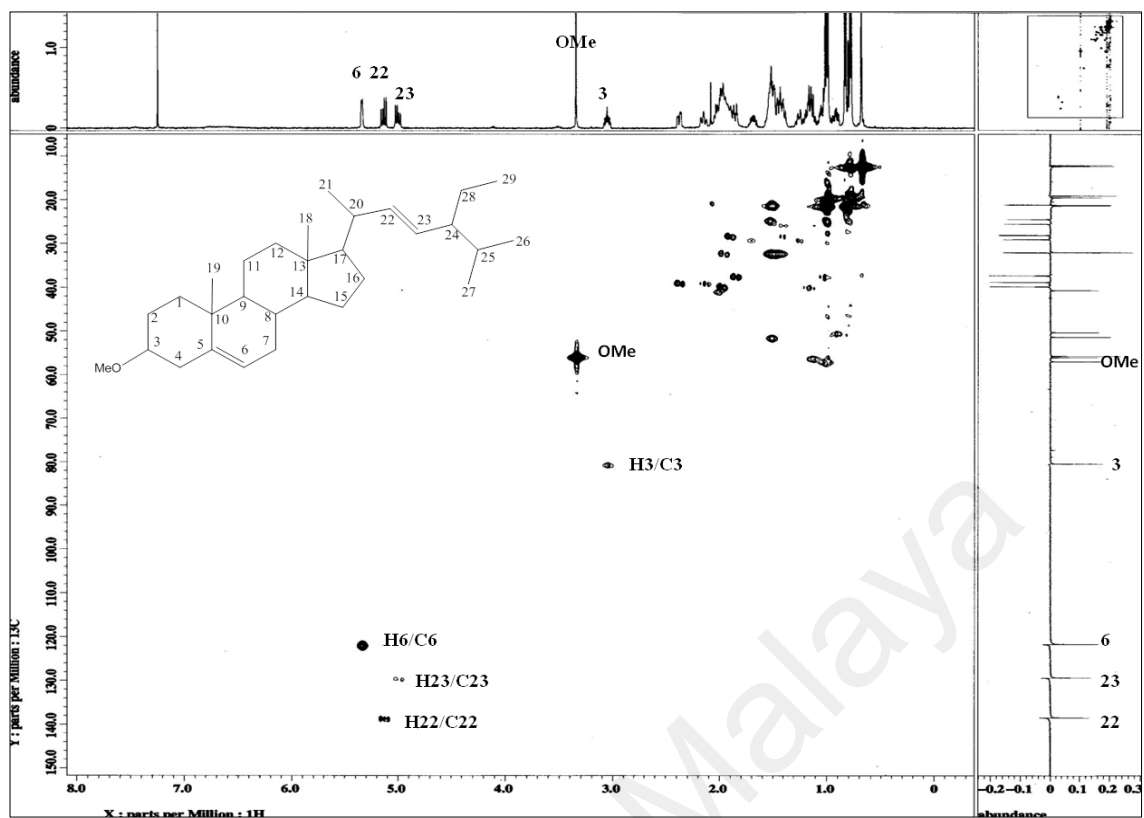
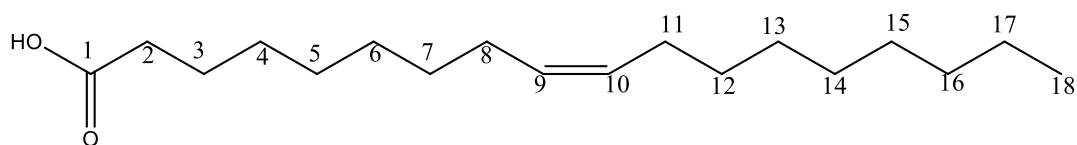


Fig. 4.170: HMQC spectrum of stigmasta-5,22-diene,3 methoxy (**53**)

4.3.13 Oleic acid (54)



54

Oleic acid (**54**) was obtained as pale yellow oil from the hexane extract. The UV spectrum showed absorption band at 280 nm. The IR spectrum showed broad OH stretching at 3432 cm^{-1} and a carbonyl function of carboxylic acid at 1704 cm^{-1} . The GC-MS spectrum (Figure 4.171) showed molecular ion peak at m/z 264 $[\text{M}-18]^+$, representing the loss of water ($-\text{H}_2\text{O}$) from the carboxyl group, corresponding to the formula $\text{C}_{18}\text{H}_{34}\text{O}_2$. The NIST library matched the compound with oleic acid (SI=93%).

The ^1H NMR spectrum (Figure 4.172) showed olefinic protons as multiplet at δ 5.34-5.35 assigned to H-9 and H-10, and CH_2 resonance together with a terminal methyl group in the aliphatic region. The ^{13}C and DEPT 135 spectra (Figure 4.173 and 4.174) showed a total of 18 carbon signals comprising of one methyl carbon peak at δ 14.2, two methine carbons at δ 130.3 and δ 130.1, a carbonyl group at δ 179.1 and the rest of fourteen methylene carbons. Table 4.27 summarizes the ^1H - and ^{13}C NMR of the compound.

Finally, based on spectroscopic data and matching NIST library (SI= 93%), the compound was identified as oleic acid (**54**).

Table 4.27: ^1H NMR (500 MHz) and ^{13}C NMR (125 MHz) spectral data of oleic acid (**54**) in CDCl_3 (δ in ppm, J in Hz)

Position	^1H -NMR (δ ppm)	^{13}C NMR (δ ppm)	^{13}C NMR(δ ppm) (Mafezoli <i>et al.</i> , 2003)
1	-	179.1	180.5
2	2.33 (2H, <i>t</i> , $J=7.3$)	34.0	34.1
3	1.63 (2H, <i>m</i>)	24.7	24.6
4-7	1.28 (2H, <i>m</i>)	29.1-29.7	29.0-29.7
8	2.04 (2H, <i>m</i>)	27.3	27.2
9	5.35 (2H, <i>m</i>)	130.3	130.0
10	5.33 (2H, <i>m</i>)	130.1	129.7
11	2.79 (2H, <i>t</i> , $J=6.5$)	24.6	24.5
12	1.28 (2H, <i>m</i>)	29.0-29.7	29.0-29.7
13	1.28 (2H, <i>m</i>)	29.0-29.7	29.0-29.7
14	2.05 (2H, <i>m</i>)	27.3	27.2
15	1.28 (2H, <i>m</i>)	29.0-29.7	29.0-29.7
16	1.28 (2H, <i>m</i>)	32.0	31.9
17	1.28 (2H, <i>m</i>)	22.8	22.7
18	0.87 (3H, <i>t</i> , $J=6.9$)	14.2	14.1

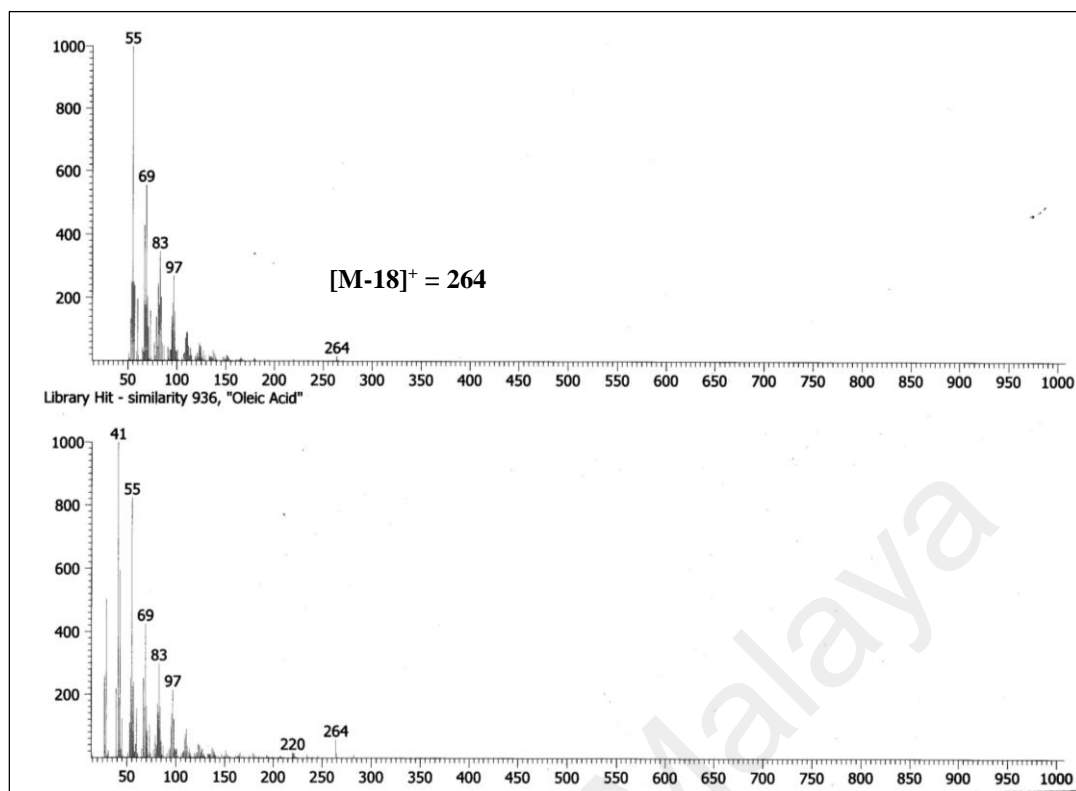


Fig. 4.171: GC-MS spectrum of oleic acid (54)

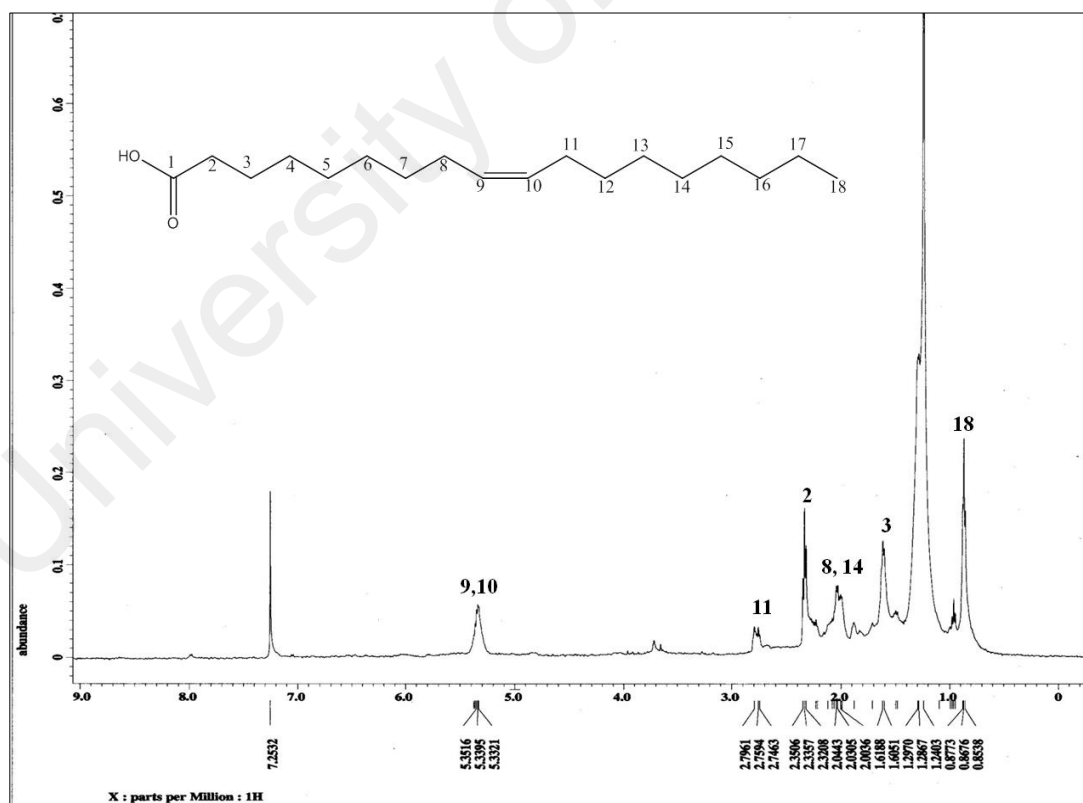


Fig. 4.172: ¹H NMR spectrum of oleic acid (54)

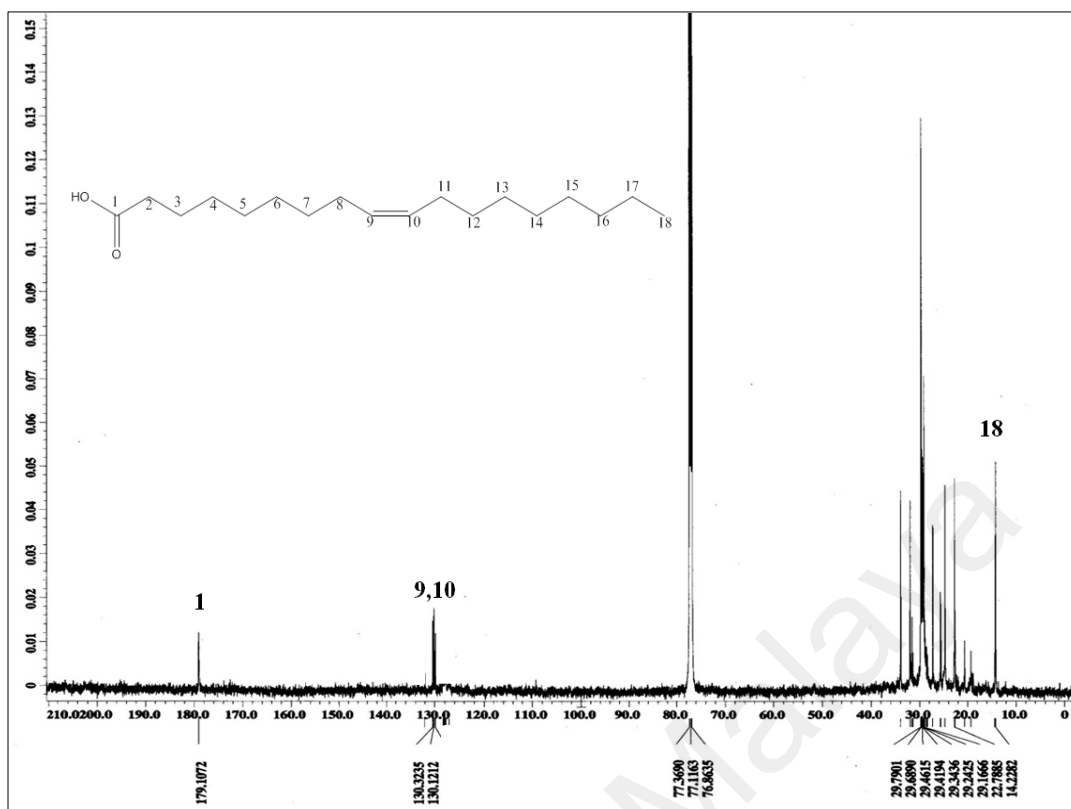


Fig. 4.173: ^{13}C NMR spectrum of oleic acid (54)

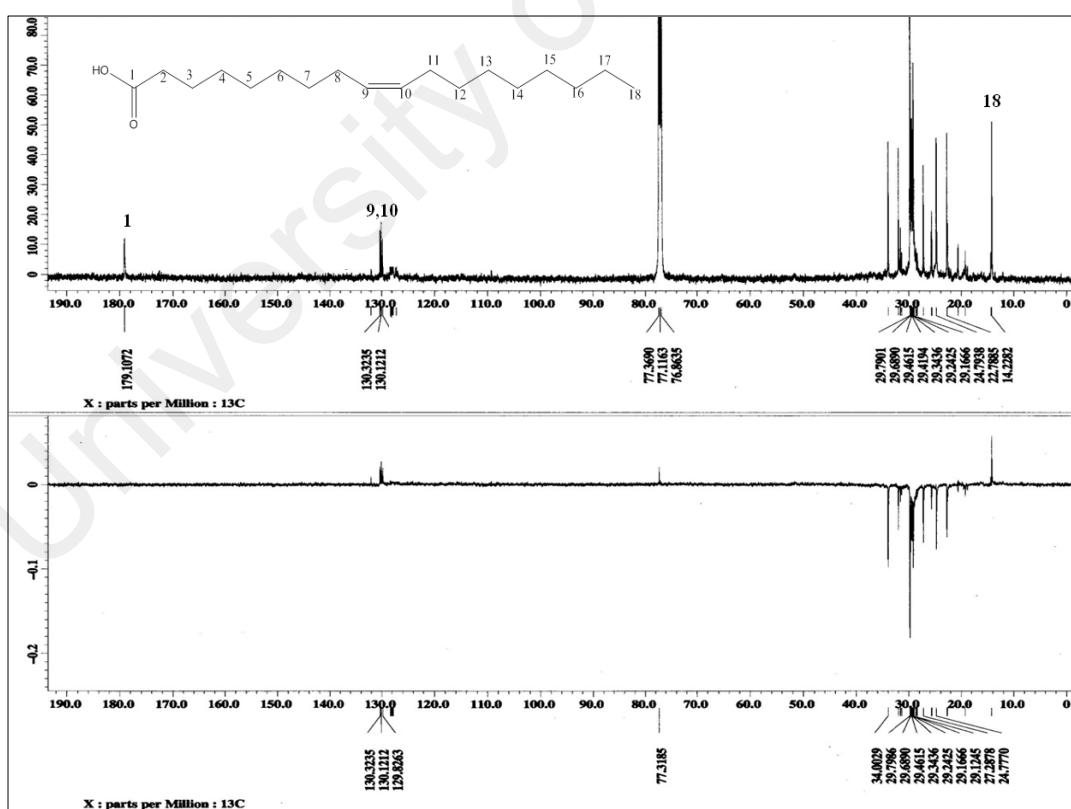
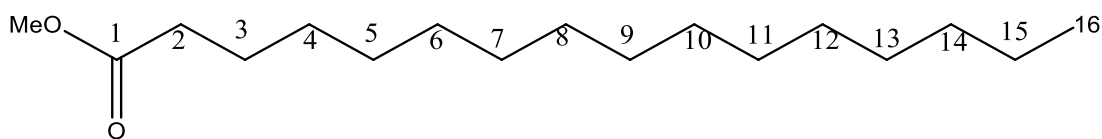


Fig. 4.174: DEPT 135 NMR spectrum of oleic acid (54)

4.3.14 Hexadecanoic acid methyl ester (**55**)



55

Hexadecanoic acid methyl ester (**55**) was isolated as yellow oil. The UV spectrum showed absorption peak at λ_{\max} 230 nm indicating there was no conjugation in the structure. The IR showed absorption bands at 1732 cm^{-1} indicated the presence of ester linkage of the carbonyl group. The GC-MS spectrum (Figure 4.175) gave a molecular ion peak at 270 $[M]^+$ corresponding to a molecular formula $C_{17}H_{34}O_2$, and this matched the NIST library for hexadecanoic acid methyl ester (SI=93%).

The ^1H NMR spectrum (Figure 4.176) showed signals between δ 0.87 and δ 2.80 suggesting the presence of terminal methyl proton and methylene groups in the aliphatic region. The presence of methylene proton next to carbonyl group was observed at 2.27-2.33(*m*) assigned for H-2. One signal at δ 3.67 (3H) indicate the presence of the methoxy group of a methyl ester.

In the ^{13}C and DEPT 135 NMR (Figure 4.177 and 4.178), sixteen carbon signals were observed, comprising of one ester carbonyl at δ 174.35, one methoxy signal at δ 51.53 ppm, one methyl signal at δ 14.20 ppm and the remaining of fourteen methylenes. Table 4.28 summarizes the ^1H and ^{13}C NMR of the compound.

Finally, based on spectroscopic data and matching NIST library (SI= 93%), the compound was identified as hexadecanoic acid methyl ester (**55**).

Table 4.28: ^1H NMR (500 MHz) and ^{13}C NMR (125 MHz) spectral data of hexadecanoic acid methyl ester (**55**) in CDCl_3 (δ in ppm, J in Hz)

Position	^1H -NMR (δ ppm)	^{13}C -NMR(δ ppm)	^{13}C -NMR(δ ppm) (Ajoku <i>et al.</i> ,2015)
1	-	174.3	174.6
2	2.28 (2H, <i>m</i>)	22.7	22.5
3	1.62 (2H, <i>m</i>)	29.2	29.2
4	1.29 (2H, <i>m</i>)	29.2	29.2
5	1.26 (2H, <i>m</i>)	29.3	29.3
6	1.26 (2H, <i>m</i>)	29.3	29.3
7	1.26 (2H, <i>m</i>)	29.4	29.4
8	1.26 (2H, <i>m</i>)	29.4	29.4
9	1.26 (2H, <i>m</i>)	29.4	29.4
10	1.26 (2H, <i>m</i>)	29.5	29.5
11	1.26 (2H, <i>m</i>)	29.5	29.5
12	1.26 (2H, <i>m</i>)	29.6	29.6
13	1.29 (2H, <i>m</i>)	29.6	29.6
14	1.29 (2H, <i>m</i>)	32.0	31.7
15	1.67 (2H, <i>m</i>)	34.2	33.9
16	0.86 (3H, <i>t</i>)	14.0	14.0
OMe	3.66 (3H, <i>s</i>)	51.5	51.7

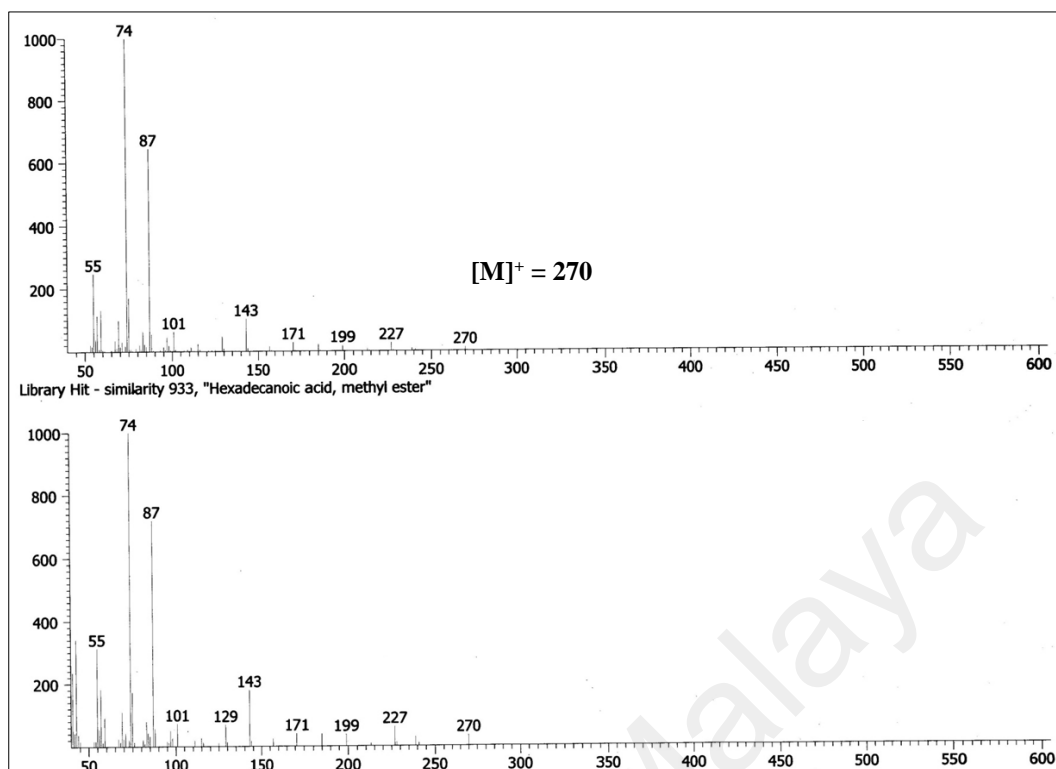


Fig. 4.175: GC-MS spectrum of hexadecanoic acid methyl ester (55)

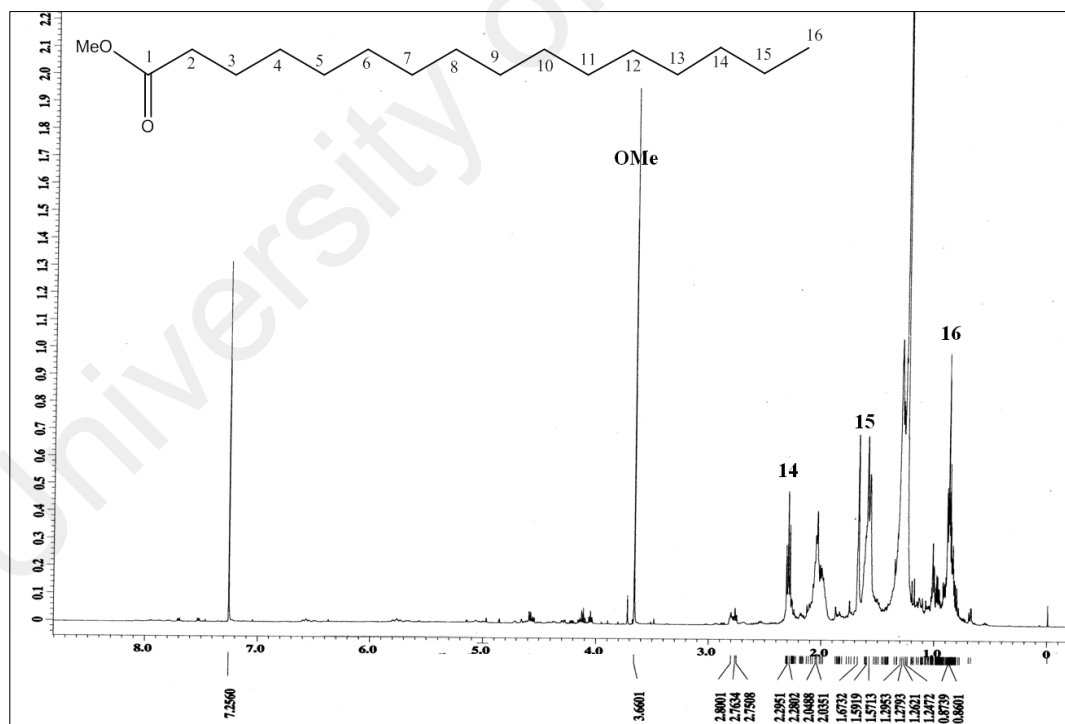


Fig. 4.176: ¹H NMR spectrum of hexadecanoic acid methyl ester (55)

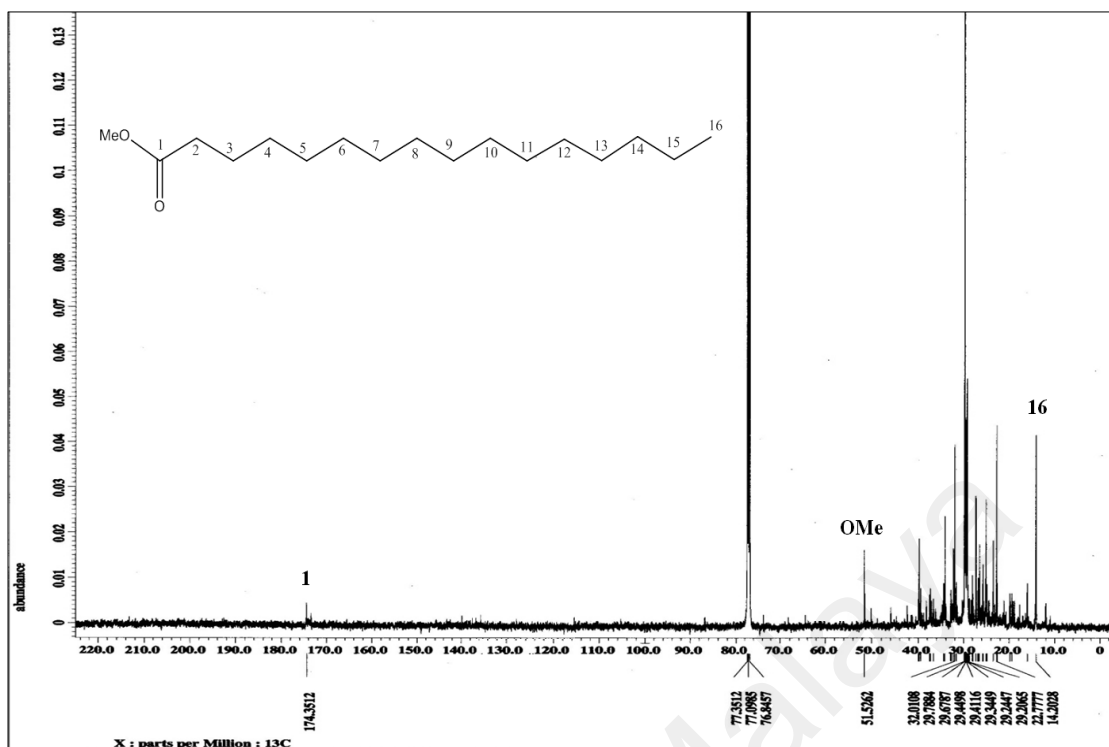


Fig. 4.177: ^{13}C NMR spectrum of hexadecanoic acid methyl ester (**55**)

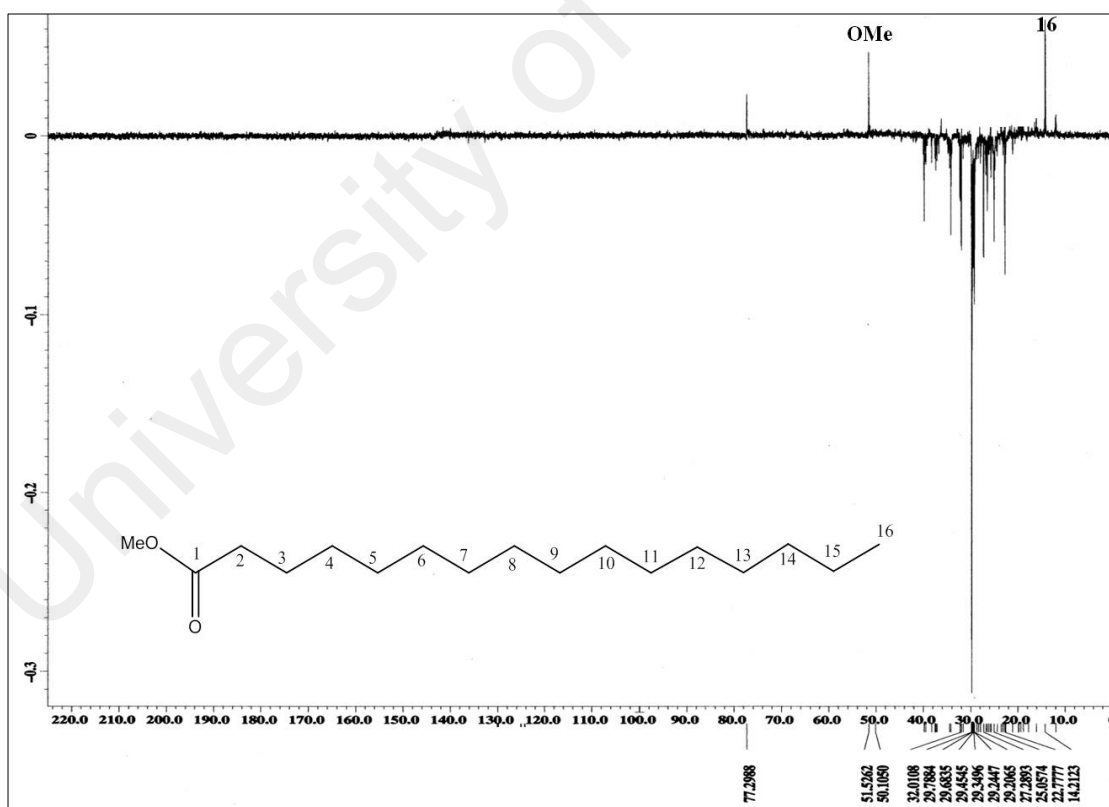


Fig. 4.178: DEPT 135 NMR spectrum of hexadecanoic acid methyl ester (**55**)

GC-MSTOF analysis of leaf essential oils

Plants species in this world still need to be investigated phytochemically and biologically especially plants from the tropical forests. A majority of compounds extracted from medicinal plants have demonstrated important biological activities including essential oils. Essential oils are variable mixtures composed of volatile and aromatic compounds such as terpenoids that give the plant its fragrance and flavour. The essential oils from plants contain secondary metabolites that may exhibit biological properties such as antioxidant, antimicrobial and anti-inflammatory (Baratta *et al.*, 1998).

Essential oils are aromatic that represent a small fraction of plant's composition and generally used as odorants, flavourings and pharmaceutical ingredients for the commercial industries (Miguel, 2010). Many parts of plants have been investigated for antioxidant activity including essential oils. Natural antioxidants protect organisms and cells from damage caused by oxidative stress which is considered as a cause of degenerative diseases and ageing (Bagchi *et al.*, 2000). The antioxidant capacity of plants is commonly associated with the activity of free radical scavenging enzymes and the contents of antioxidant substances.

Gas chromatography with flame ionization detection (GC-FID) is commonly used to characterize essential oil extracts. However, these analyses consume lengthy several hours per essential oil to allow complete chromatographic resolution of the individual components for compound identification. On the other hand, these same analyses can be completed in less than five minutes when analyzed with GC-Time of Flight Mass Spectrometry (TOFMS). The mass spectra are used to identify individual components. In addition, the MS information coupled with a fast spectral acquisition (up to 500/second) allows for unique automated deconvolution of overlapping chromatographic peaks.

4.4 Chemical compounds identified from *Pseuduvaria monticola* leaf essential oil

Figure 4.179 shows the TIC chromatogram of *Pseuduvaria monticola* leaf essential oil showing 46 peaks representing about 92.0 % of the essential oils that were characterized. Table 4.29 listed all the chemical constituents in leaf essential oil of *Pseuduvaria monticola* that were identified by GC-MSTOF. A total of 46 constituents have been identified which are dominated by alpha cadinol (**56**) (13.0%), cis calamenene (**57**) (6.9%) and alpha copaene (**25**) (4%).

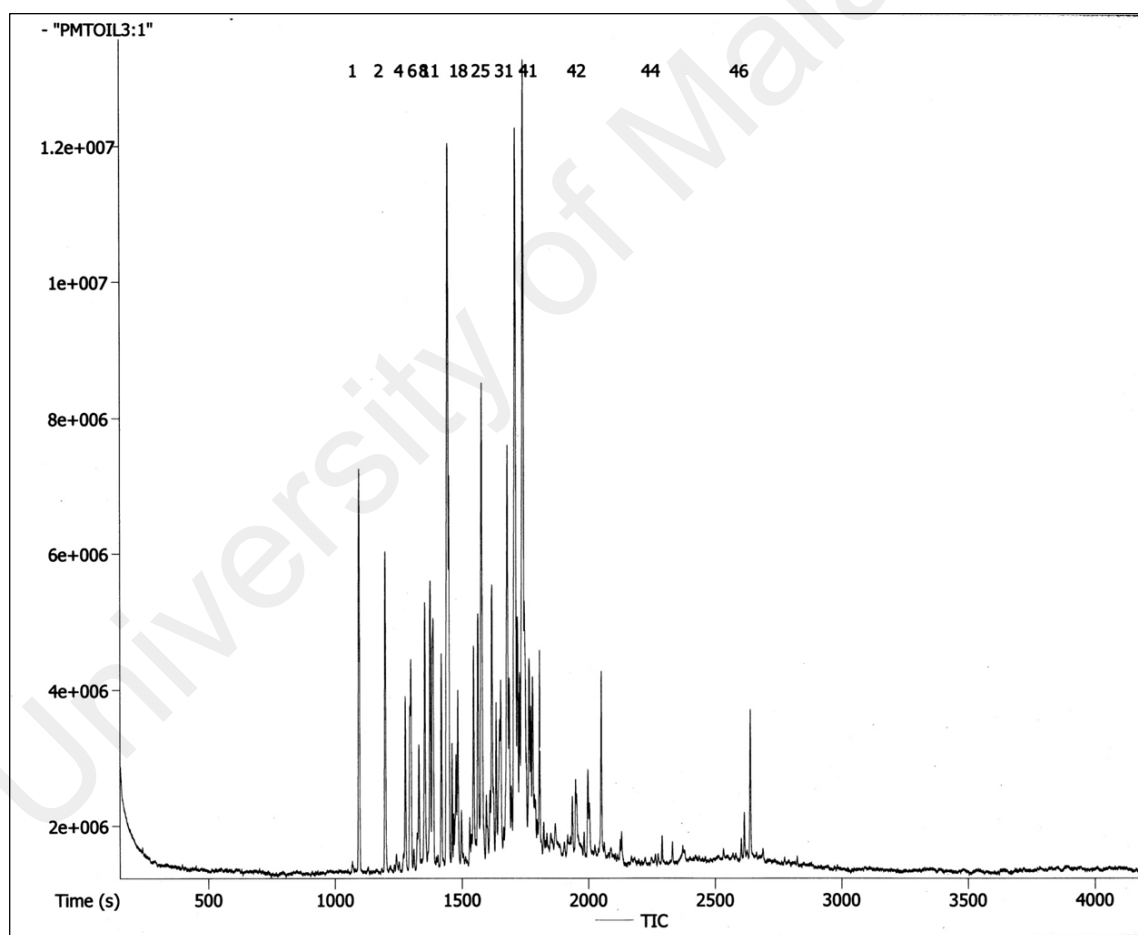


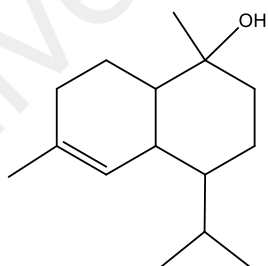
Fig 4.179: TIC chromatogram of *Pseuduvaria monticola* leaf essential oil by GC-MSTOF

Table 4.29: Chemical compounds identified from the leaf essential oil of *Pseuduvaria monticola* by GC-MSTOF.

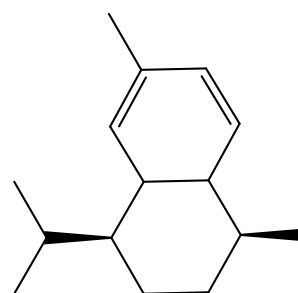
Peak	Name of compound	SI	RT (s)	Area %	MW	Molecular formula
1	Alpha copaene	91	1093.2	4.8	204	C ₁₅ H ₂₄
2	Caryophyllene	90	1196.3	2.8	204	C ₁₅ H ₂₄
3	Bourbonanone	66	1196.7	0.1	218	C ₁₅ H ₂₂ O
4	Humulene	91	1275.7	0.1	204	C ₁₅ H ₂₄
5	Ishwarane	89	1297.8	0.8	204	C ₁₅ H ₂₄
6	c-Muurolene	89	1329.6	1.6	204	C ₁₅ H ₂₄
7	Naphthalene derivative	93	1352.9	2.7	204	C ₁₅ H ₂₄
8	Azulene	88	1374.0	1.2	204	C ₁₅ H ₂₄
9	Epizonarene	85	1381.9	3.8	204	C ₁₅ H ₂₄
10	Alpha-muurolene	85	1385.5	0.5	204	C ₁₅ H ₂₄
11	Alpha-copaene	89	1417.5	2.2	204	C ₁₅ H ₂₄
12	Calamene-cis	89	1440.2	7.9	202	C ₁₅ H ₂₂
13	Naphthalene derivative	90	1443.8	4.0	204	C ₁₅ H ₂₄
14	Epizonarene	93	1447.5	0.3	204	C ₁₅ H ₂₄
15	Naphthalene	89	1459.4	0.4	204	C ₁₅ H ₂₄
16	Isolongifolene	76	1475.0	1.7	200	C ₁₅ H ₂₀
17	Calacorene -alpha	88	1482.7	3.0	200	C ₁₅ H ₂₀
18	Calacorene-beta	79	1528.9	1.2	200	C ₁₅ H ₂₀
19	Caryolan-8-ol	91	1544.6	3.5	222	C ₁₅ H ₂₆ O
20	Selina-6-en-4-ol	78	1561.5	0.7	222	C ₁₅ H ₂₆ O
21	Azulene-7-ol	84	1562.2	2.1	220	C ₁₅ H ₂₄ O
22	Caryophyllene oxide	75	1576.2	1.5	220	C ₁₅ H ₂₄ O
23	Eudesm	83	1576.5	1.2	222	C ₁₅ H ₂₆ O
24	Gleenol	59	1579.1	2.5	222	C ₁₅ H ₂₆ O
25	Cycloundecadien	85	1616.7	3.1	222	C ₁₅ H ₂₆ O
26	12-Oxabicyclo	85	1633.3	1.1	220	C ₁₅ H ₂₄ O
27	Cubenol	85	1646.8	0.1	222	C ₁₅ H ₂₆ O
28	Cis-a-Farnesene	81	1651.7	1.5	204	C ₁₅ H ₂₄
29	Muurola	84	1678.0	1.4	220	C ₁₅ H ₂₄ O
30	Alloaromadendrene	81	1685.2	0.3	204	C ₁₅ H ₂₄

31	Alpha-copaene	84	1709.6	4.2	204	C ₁₅ H ₂₄
32	Alpha-cadinol	60	1710.8	6.5	222	C ₁₅ H ₂₆ O
33	Naphthalenol	91	1718.0	0.1	222	C ₁₅ H ₂₆ O
34	Naphthalenemethanol	89	1726.3	0.2	222	C ₁₅ H ₂₆ O
35	Allo-hedycaryol	78	1731.7	2.5	222	C ₁₅ H ₂₆ O
36	Alpha-cadinol	89	1741.3	13.0	222	C ₁₅ H ₂₆ O
37	Calacorene -alpha	79	1747.1	2.8	200	C ₁₅ H ₂₀
38	Pyrazolo	61	1748.6	0.1	308	C ₁₈ H ₂₀ N ₄ O
39	Alpha-Calacorene	81	1763.7	0.4	200	C ₁₅ H ₂₀
40	Naphthalene,1,6-dimethyl	92	1777.9	2.5	198	C ₁₅ H ₁₈
41	Epiglobulol	83	1805.5	0.7	222	C ₁₅ H ₂₆ O
42	Calamenene-5-hydroxy-cis	86	1996.9	1.9		C ₁₅ H ₂₂ O
43	Calamenene-5-hydroxy-cis	87	2049.1	5.7	218	C ₁₅ H ₂₂ O
44	Hexadecanoic methyl ester	90	2289.1	1.0	218	C ₁₈ H ₃₆ O ₂
45	Isophytol	92	2329.9	0.1	296	C ₂₀ H ₄₀ O
46	Phytol	92	2636.8	0.2	296	C ₂₀ H ₄₀ O

SI=similarity index; RT= retention time; MW=molecular weight



(56)



(57)

4.4.1 Chemical compounds identified from *P. macrophylla* leaf essential oil

Figure 4.180 shows the TIC chromatogram of *Pseuduvaria macrophylla* leaf essential oil showing 11 peaks corresponding to the identification of chemical constituents accounting for 99.9% of total essential oils (Table 4.30). GC-MSTOF analysis showed the presence of 11 compounds dominated by caryophyllene oxide (**29**) (29.7%) and elimicin (**26**) (28%). It was observed that the amounts of compounds were quite small compared to that of *P. monticola*. This was probably due to the dry sample kept for a long time in the herbarium that could result in the evaporation of most of the volatile compounds.

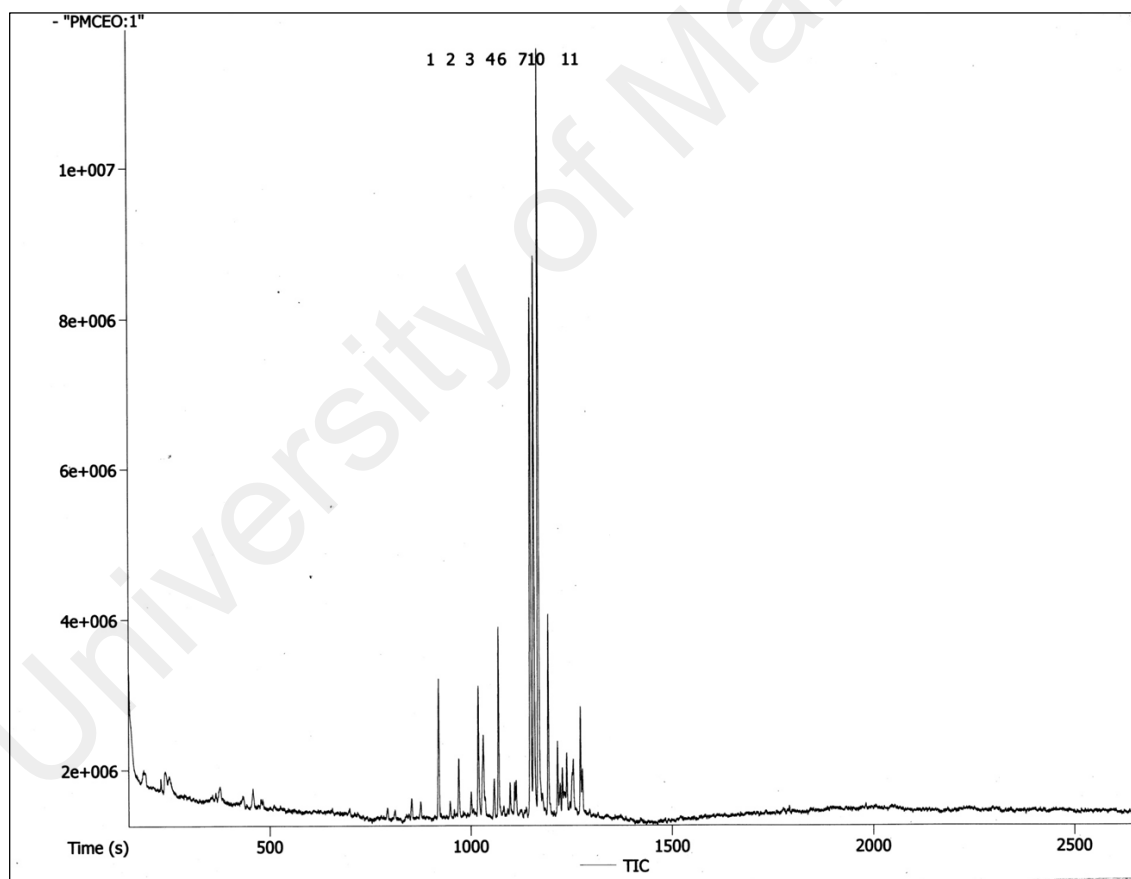


Fig 4.180: TIC chromatogram from GC-TOFMS analysis of *Pseuduvaria macrophylla* leaf essential oil.

Table 4.30: Chemical compounds of *Pseuduvaria macrophylla* leaf essential oil

Peak	Name of compound	SI	RT (s)	Area %	MW	Molecular formula
1	Caryophyllene	91	919.9	4.3	204	C ₁₅ H ₂₄
2	Humulene	91	969.8	5.2	204	C ₁₅ H ₂₄
3	Naphthalene derivative	93	1017.95	1.4	218	C ₁₅ H ₂₂ O
4	Naphthalene derivative	89	1067.8	5.7	204	C ₁₅ H ₂₄
5	Trans-calamenene	90	1068.0	7.5	202	C ₁₅ H ₂₂
6	Alpha calacorene	87	1096.5	2.9	200	C ₁₅ H ₂₀
7	Spathulenol	88	1148.15	3.8	220	C ₁₅ H ₂₄ O
8	Caryophyllene oxide	88	1156.8	29.7	220	C ₁₅ H ₂₄ O
9	Elimicin	93	1168.5	28.0	208	C ₁₂ H ₁₆ O ₃
10	Oxabicyclo	83	1191.7	8.9	204	C ₁₅ H ₂₄
11	Naphthalene derivative	92	1276.9	2.5	204	C ₁₅ H ₂₄

SI=similarity index; RT= retention time

The results from both GC-MSTOF analyses on both *Pseuduvaria* species show differences in chemical composition of the leaf essential oils. *Pseuduvaria monticola* contained the highest percentage of alpha cadinol (**56**) (13%) and *Pseuduvaria macrophylla* contained the highest percentage of caryophyllene oxide (**29**) (29.7) and elimicin (**26**) (28%).

4.5 Biological Activities

4.5.1 Antioxidant Activity

Introduction

Antioxidant plays an important in neutralising the effects of free radicals that harm the cells as part of the body's defence mechanism against oxidative damage. Excessive free radicals and reactive oxygen species (ROS) have been associated with cellular injury implicated in the cause of many chronic diseases such as diabetes, cancer, atherosclerosis, cardiovascular disease and neurodegenerative diseases. This condition is known as oxidative stress where there is an imbalance between the amount of antioxidants and the level of free radicals (Moylean & Reid, 2007).

4.5.2 Antioxidant activity of leaf essential oils by DPPH assay

This is the first report on the radical scavenging activity measured by DPPH assay method on the leaf essential oils of *Pseuduvaria monticola* and *Pseuduvaria macrophylla*. The scavenging activity of the leaf essential oils of *Pseuduvaria monticola* and *Pseuduvaria macrophylla* were tested at different concentrations (20 µg/mL, 40 µg/mL, 60µg/mL, 80 µg/mL and 100 µg/mL). The results are presented in Figure 4.181. Both the leaf essential oils were able to reduce the stable, purple -coloured radical DPPH to the yellow coloured DPPH-H in dose depending manner. Leaf essential oil of *Pseuduvaria macrophylla* exhibited slightly greater antioxidant activity than that of *Pseuduvaria monticola*.

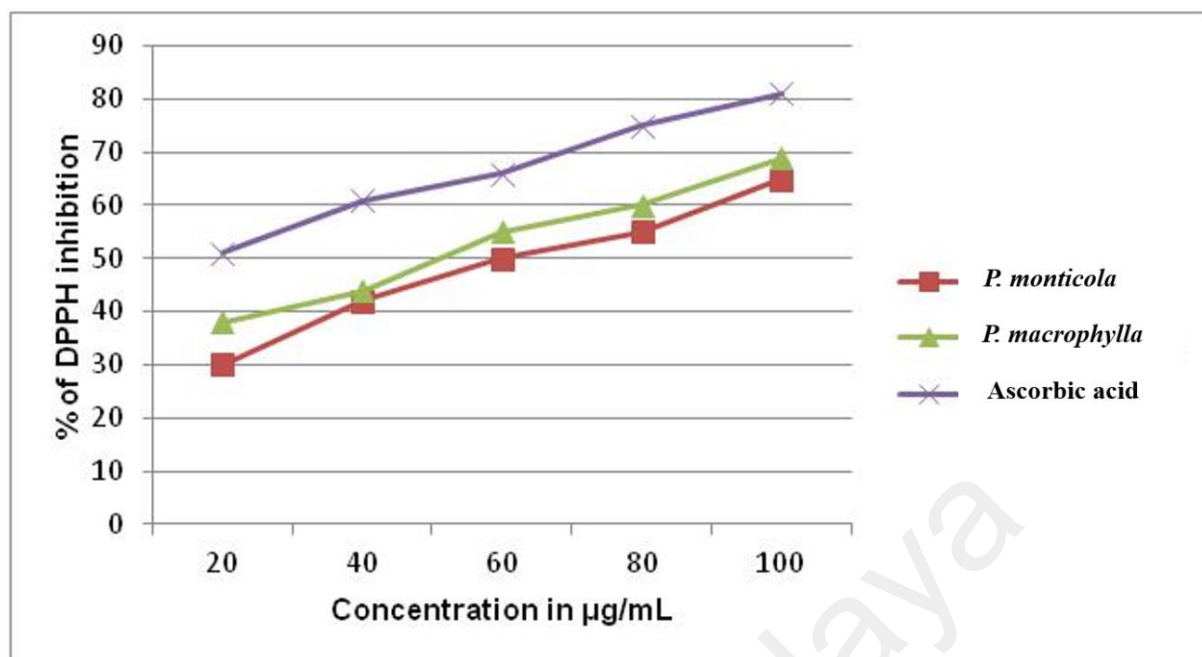


Fig. 4.181: Percentage inhibition of *P. monticola* and *P. macrophylla* leaf essential oils at varying concentrations

4.5.3 Antioxidant activity of crude extracts and isolated compounds by DPPH and ORAC assays

The antioxidant activity of the crude extracts of *P. monticola* and *P. macrophylla* were evaluated by DPPH and ORAC assays. Table 4.31 showed that methanol extracts were more active than the hexane extracts which is possibly due to the phenolic acid content in the extract.

From the methanol extract of *P. monticola*, caffeic acid (**44**) was the most active in DPPH radical scavenging activity; IC_{50} 15.64 µg/mL, followed by chlorogenic acid (**45**) (IC_{50} 16.41 µg/mL) and (6*E*,10*E*) isopolycerasoidol (**15**) (IC_{50} 22.56 µg/mL) when compared to quercetin standard (IC_{50} 6.89 µg/mL). The ORAC assay reflects the antioxidant capacity of the compounds which are relevant to their scavenging activities (Table 4.32).

Table 4.31: DPPH radical scavenging activity of *P. monticola* and *P. macrophylla* extracts.

DPPH radical scavenging activity (%)	
<i>P. monticola</i> extracts	
Hexane	5.3 ± 0.21
MeOH	72.1 ± 0.32
<i>P. macrophylla</i> extracts	
Hexane	6.5 ± 0.21
MeOH	80.5 ± 0.26

All measured values are means ± SD of three replicates

Table 4.32: DPPH and ORAC assays of isolated compounds from *Pseuduvaria monticola*.

Compound	DPPH IC ₅₀ (µg/mL) ± SD	ORAC* µM
Liriodenine (3)	NA	NA
Oxoputerine (40)	NA	NA
Lysicamine (39)	NA	NA
Ouregidione (4)	NA	NA
Chlorogenic acid (45)	16.41 ± 0.21	61.36 ± 0.46
Caffeic acid (44)	15.64 ± 0.24	68.54 ± 0.65
(6E,10E) Isopolycerasoidol (15)	22.56 ± 0.16	85.76 ± 0.21
(6E,10E) Isopolycerasoidol methyl ester (32)	75.83 ± 0.19	56.85 ± 0.35
Quercetin	6.89 ± 0.15	12.17 ± 0.56**

*Data expressed as µM of Trolox Equivalents (TE) per 100 µg/mL of sample. **ORAC value for quercetin (positive control) was expressed as µM TE per 1.25 µg/mL. All measured values are means ± SD of three replicates. NA= non active

Table 4.33: DPPH and ORAC assays of isolated compounds from *Pseuduvaria macrophylla*

Compound	DPPH IC ₅₀ (µg/mL) ± SD	ORAC* µM
Liriodenine (3)	NA	NA
<i>N</i> -methyl ouregidione (5)	NA	NA
<i>O</i> -methymoschatoline (7)	NA	NA
1,3,5,7-tetramethoxy-2-naphthoic acid (51)	25.54± 0.25	70.11± 0.22
Polycerasoidol (16)	18.89 ± 0.21	96.76 ± 0.21
Polycerasoidin (49)	71.65 ± 0.18	50.84 ± 0.35
Elemicin (26)	23.32 ± 0.23	79.76 ± 0.26
Elemicin 6-methoxy (50)	28.89 ± 0.21	61.76 ± 0.19
Quercetin**	7.01± 0.36	11.45 ± 0.13**

*Data expressed as µM of Trolox Equivalents (TE) per 100 µg/mL of sample. **ORAC value for quercetin (positive control) was expressed as µM TE per 1.25 µg/mL. All measured values are means ± SD of three replicates. NA= non active

Results from methanol extract of *Pseuduvaria macrophylla* showed that polycerasoidol (**16**) gave the highest antioxidant activity with an IC₅₀ of 18.89 µg/mL compared to quercetin standard (IC₅₀ 7.01 µg/mL) followed by elemicin (**26**) (IC₅₀ 23.32 µg/mL), 1,3,5,7-tetramethoxy-2-naphthoic acid (**51**) (IC₅₀ 25.54 µg/mL) and elemicin 6-methoxy (**50**) (IC₅₀ 28.89 µg/mL). Again, the ORAC assays reflect the antioxidant capacity of the compounds which are relevant to their scavenging activities (Table 4.33).

Polycerasoidol (**16**) was found to be active in antioxidant due to the presence of hydroxyl group in the aromatic ring, and its close similarity to the structure of tocopherol (Hostettmann *et al.*, 2001). The presence of high content of elemicin and its derivatives may also explain the antioxidant activity in the leaf essential oil of *P. macrophylla*.

In both extracts, the alkaloids showed poor activity in DPPH and ORAC assay probably due to the absence of electron-donating hydroxyl group in the structures (Emmanoel *et al.*, 2013). The high antioxidant effect of the compounds in the methanol extracts may be attributed to the hydroxyl moieties attached to the structures that may contribute the radical scavenging activity of the compounds due to its electron donating capacity.

From the results, the antioxidant activity of the methanol extract could be contributed by the phenolic acids, benzopyran derivatives and elemicin derivatives content. Compounds bind to electronegative group demonstrated higher radical scavenging activity.

Phenolic acids are widely distributed in plant kingdom and constitute one of the most important classes of natural antioxidant. The number and position of the OH functional group has a strong impact on the degree of antioxidant activity (Soobrattee *et al.*, 2005).

4.5.2 Anticancer Activity

Introduction

Cancer is a disease that affects the cells which is characterized by uncontrolled cell proliferation and differentiation resulting in cell death. Plants provide the source for anti cancer drugs. 50% of the anticancer drugs on trial were derived from natural products and approximately 25% of prescribed anti tumour drugs originate from plants (Pezzuto, 1997). Many *in vitro* studies have demonstrated the potential of plant extract and the isolated compounds as promising anticancer agent (Shoemaker, 2006).

4.5.2.1 Cytotoxic effects and apoptosis induction of (6E, 10E) isopolycerasoidol (15) and (6E, 10E) isopolycerasoidol methyl ester (32)

The cytotoxic effects of two benzopyran derivatives from *P. monticola*, (6E,10E) isopolycerasoidol (15) and (6E,10E) isopolycerasoidol methyl ester (32) were evaluated on MCF-7 and MDA-MB-231 human breast cancer cells and MCF-10A, a human normal breast epithelial cell-line using MTT assays. After 48 hour of treatment, the results showed that relatively high cell viability inhibitory effect was observed in both breast cancer cell lines compared to normal breast cell-line. The IC₅₀ values are shown in Table 4.34.

Table 4.34: Cytotoxic effects of (6E,10E) isopolycerasoidol and (6E,10E) isopolycerasoidol methyl ester on MCF-7, MDA-MB-231 and MCF-10A breast cell lines (IC₅₀).

Cell lines	(6E,10E) isopolycerasoidol (IC ₅₀ μM)	(6E,10E) isopolycerasoidol methyl ester (IC ₅₀ μM)
MCF-7	59 ± 5.1	43 ± 2.4
MDA-MB-231	76 ± 8.5	58 ± 2.6
MCF-10A	94 ± 5.9	90 ± 4.7

To confirm that reduced cell viability is due to the induction of apoptosis in MCF-7 and MDA-MB-231 cells, the cells were stained with Annexin V/propidium iodide (PI) and subjected to flow cytometric analysis. Figure 4.182 (A and B) illustrated the induction of apoptosis in MCF-7, MDA-MB-231 and MCF-10A cells confirmed by Annexin V/propidium iodide (PI) assay and flow cytometry analysis. Cells in early stages of apoptosis were positively stained with Annexin V, whereas cells in late apoptosis were positively stained with both Annexin V and PI. The lower left quadrant of the cytograms shows the viable cells, which excluded PI and were negative for Annexin V binding. The

upper right quadrant represents the non-viable, necrotic cells, positive for Annexin V binding and showing PI uptake. The lower right quadrant represents the apoptotic cells, Annexin V positive and PI negative, demonstrating Annexin V binding and cytoplasmic membrane integrity. Values shown were percentages of each quadrant. *P<0.05, in comparison to control.

Results showed an increase in the percentage of early and late apoptosis in the lower and upper right quadrant respectively. Annexin V+/PI—apoptotic cell population increased in a dose-dependent manner (approximately 10% to 30%) in both MCF-7 and MDA-MB-231 cells treated with (6E,10E) isopolycerasoidol (**15**) and (6E,10E) isopolycerasoidol methyl ester (**32**) compared to control at 12 hrs post treatment. In contrast, neither of the compounds much affect the MCF-10A cells with apoptotic cells constituting <10%.

Cellular senescence is an important mechanism for preventing the proliferation of potential cancer cells. To examine if (6E,10E) isopolycerasoidol (**15**) and (6E,10E) isopolycerasoidol methyl ester (**32**) could induce replicative senescence in cancer cells, treated MCF-7 and MDA-MB-231 cells were analyzed for senescence-associated β -gal activity *in situ* by incubation with X-gal at pH 6.0. Figure 4.182 (C) showed cell morphology of MCF-7 and MDA-MB-231 cells that were treated with DMSO (solvent), (6E,10E) isopolycerasoidol and (6E,10E) isopolycerasoidol methyl ester for 24 hours before subjected to *in situ* senescence-associated β -gal staining at pH 6. The development of blue color was examined by bright field microscopy. (Magnification 200X). The result showed that MCF-7 and MDA-MB-231 cells treated with (6E,10E) isopolycerasoidol (**15**) and (6E,10E) isopolycerasoidol methyl ester (**32**) demonstrated very low β -galactosidase activity, indicating that neither compound caused cellular senescence.

Therefore, it can be concluded that (6E,10E) isopolycerasoidol (**15**) and (6E,10E) isopolycerasoidol methyl ester (**32**) reduce cell viability and induce apoptosis but do not cause cellular senescence.

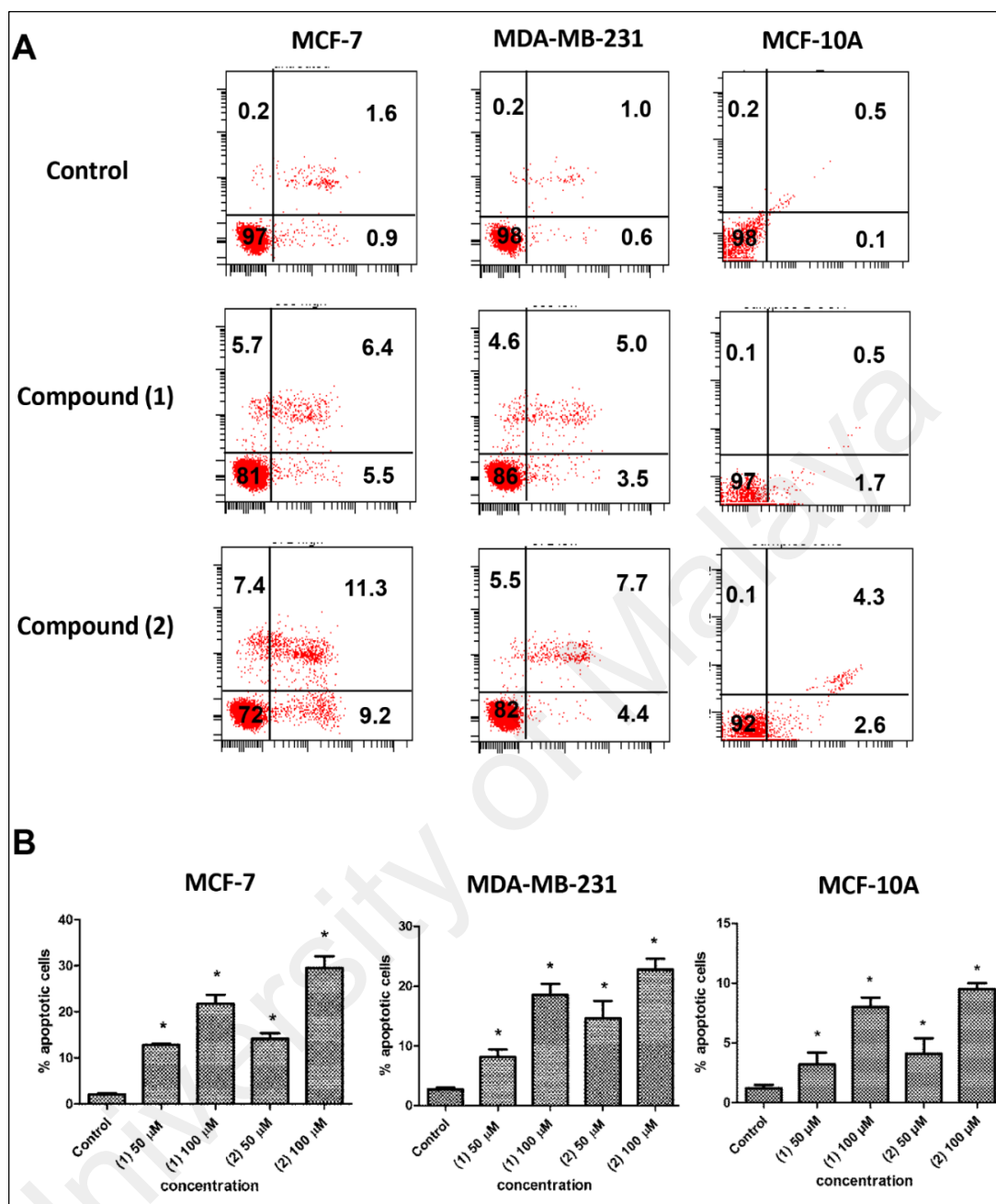


Figure 4.182 (A) (B): (A) Flow cytometric analysis of MCF-7, MDA-MB-231 and MCF-10A cells stained with Annexin-V-FITC/PI.

Note: Compound (1) = (6*E*,10*E*) isopolycerasoidol (15)

Compound (2) = (6*E*,10*E*) isopolycerasoidol methyl ester (32)

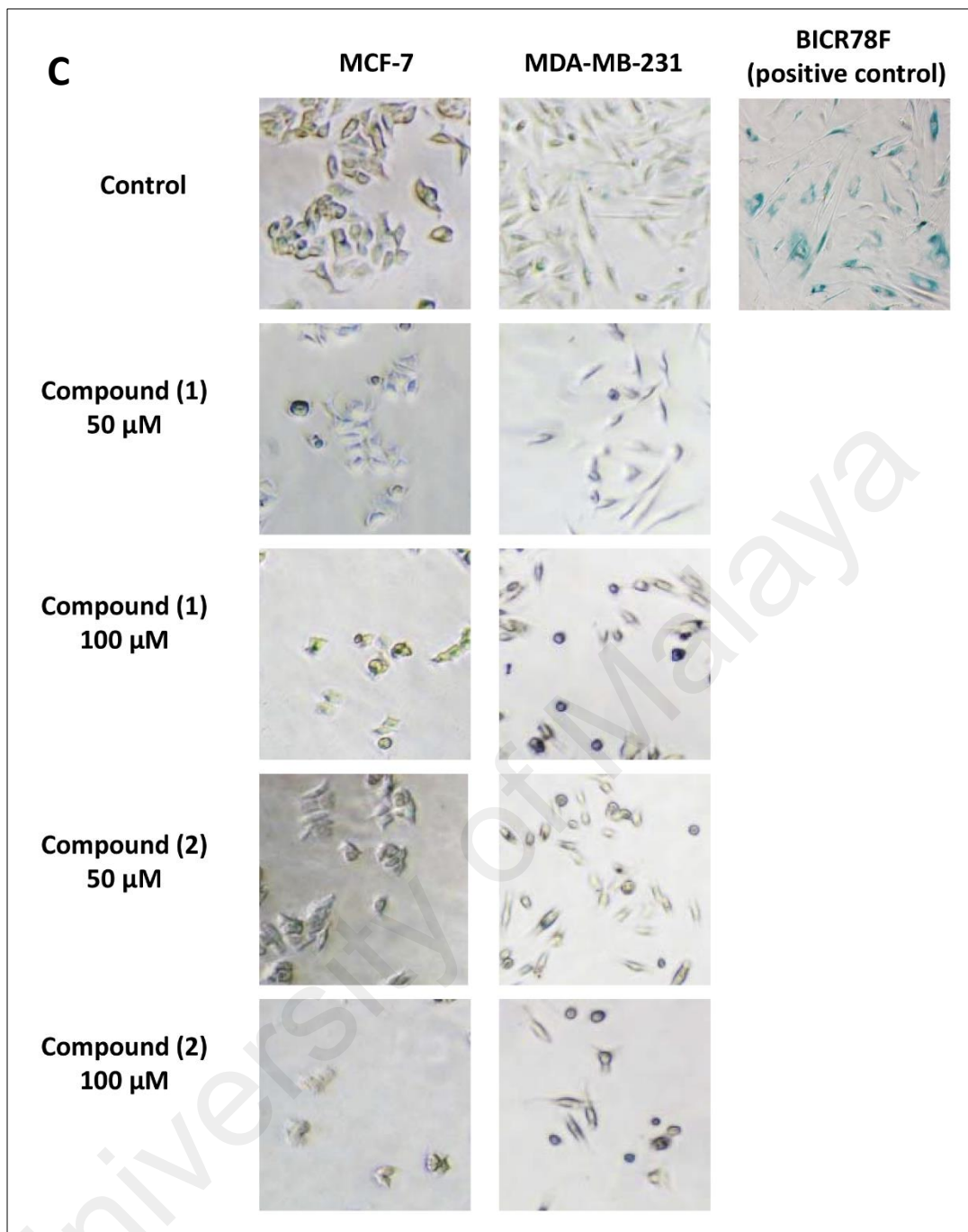


Figure 4.182 (C): Representative micrograph of MCF-7, MDA-MB-231 and MCF-10A cells stained with senescence-associated β -gal.

4.5.3 Antidiabetic activity

Introduction

Diabetes mellitus is a common endocrine malfunction characterized by abnormally high levels of glucose in the blood due to the inability of pancreas to secrete insulin (Kahn et al., 2003). About 25% of the world population has been affected by the disease. DM is categorized into Type 1 and Type 2 diabetes.

Type 1 diabetes mellitus (T1DM) is caused by inefficient insulin secretion from pancreatic β -cells whereas Type 2 diabetes mellitus (T2DM) is characterized by carbohydrate, lipid and protein disorders, and defects in insulin signalling involving insulin resistance.

T2DM's prevalence is closely related to obesity due to the practice of unhealthy dietary lifestyle (Crawford *et al.*, 2010). It was purported by the International Diabetes Federation (IDF) that the number of diabetic cases will increase from 194 million in 2003 to 333 million by the year 2025 (Zimmet, 2003).

Modern synthetic diabetic drugs such as glybenclamide and metformin have been associated with serious side effects such as hypoglycaemia; skin problems and stomach ailments over prolong use (Hussein *et al.*, 2004). On that note, safer antidiabetic agents from natural resources may provide other alternative.

A variety of plants were known to demonstrate antidiabetic properties which were traditionally used in the treatment and management of diabetes mellitus in the folk medicine (Jung *et al.*, 2006). The active chemical constituents isolated from these plants that exhibited hypoglycaemic properties include glycosides, flavonoids, phenolics, steroids, alkaloids and terpenoids (Chung *et al.*, 2011; Sharma *et al.*, 2010).

Many researchers now are focusing their interest into natural resources for potential antidiabetic agents in the management of diabetes mellitus (DM).

The present study was designed to evaluate the potential hypoglycaemic and anti-diabetic effect of the bark methanolic fraction of *P. monticola* and *P. macrophylla* using *in vitro* and *in vivo* models, with a view to establish the pharmacological basis for its usage as an anti-diabetic agent.

Pseuduvaria monticola

4.5.3.1 *In vitro* study

In vitro screening in this study showed that the bark methanolic extract of *Pseuduvaria monticola* (Pmt) drastically induced the glucose uptake and insulin secretion of mouse pancreatic β -cell line (NIT-1).

4.5.3.2 MTT cell viability assay

The cytotoxic effect of *P. monticola* extract on NIT-1 cell viability was determined by MTT assay. No significant cytotoxicity and cell inhibitory effect was observed in the NIT-1 cells after 48 h of treatment with *P. monticola* concentrations of up to 100 μ g/mL. Figure 4.183 showed (a) MTT assay growth curve of mouse NIT-1 cells treated with different concentrations of PMt. (b) Dynamic monitoring of proliferation of NIT-1 cells treated with different concentrations of PMt compared to the untreated cells using RTCA. The cells were seeded in a 16X E-plate device and monitored continuously up to 72 h after treatment. CI values were normalized to the time point of treatment, indicated by the vertical black line.

4.5.3.3 Effect of the Pmt extract on 2-NBDG glucose uptake

The uptake of the fluorescent hexose 2-NBDG, a glucose analog, was assayed on NIT-1 cells. Fluorescence appeared to increase markedly in the treated cells compared to

negative control. However, the fluorescence was restricted to the cytoplasm, which indicates that the cells retained their heterogeneous glucose uptake activity. Figure 4.184 showed (a) fluorescence images of PMt-treated and untreated mouse NIT-1 cells exposed to 1 mM of the fluorescent hexose, 2-NBDG, for 30 min revealing heterogeneous 2-NBDG uptake and metabolic activity, and (b) glucose uptake in PMt-treated and untreated NIT-1 cells after 30 min exposure to 1 mM 2-NBDG. Significant differences compared to negative control (* $P < 0.001$).

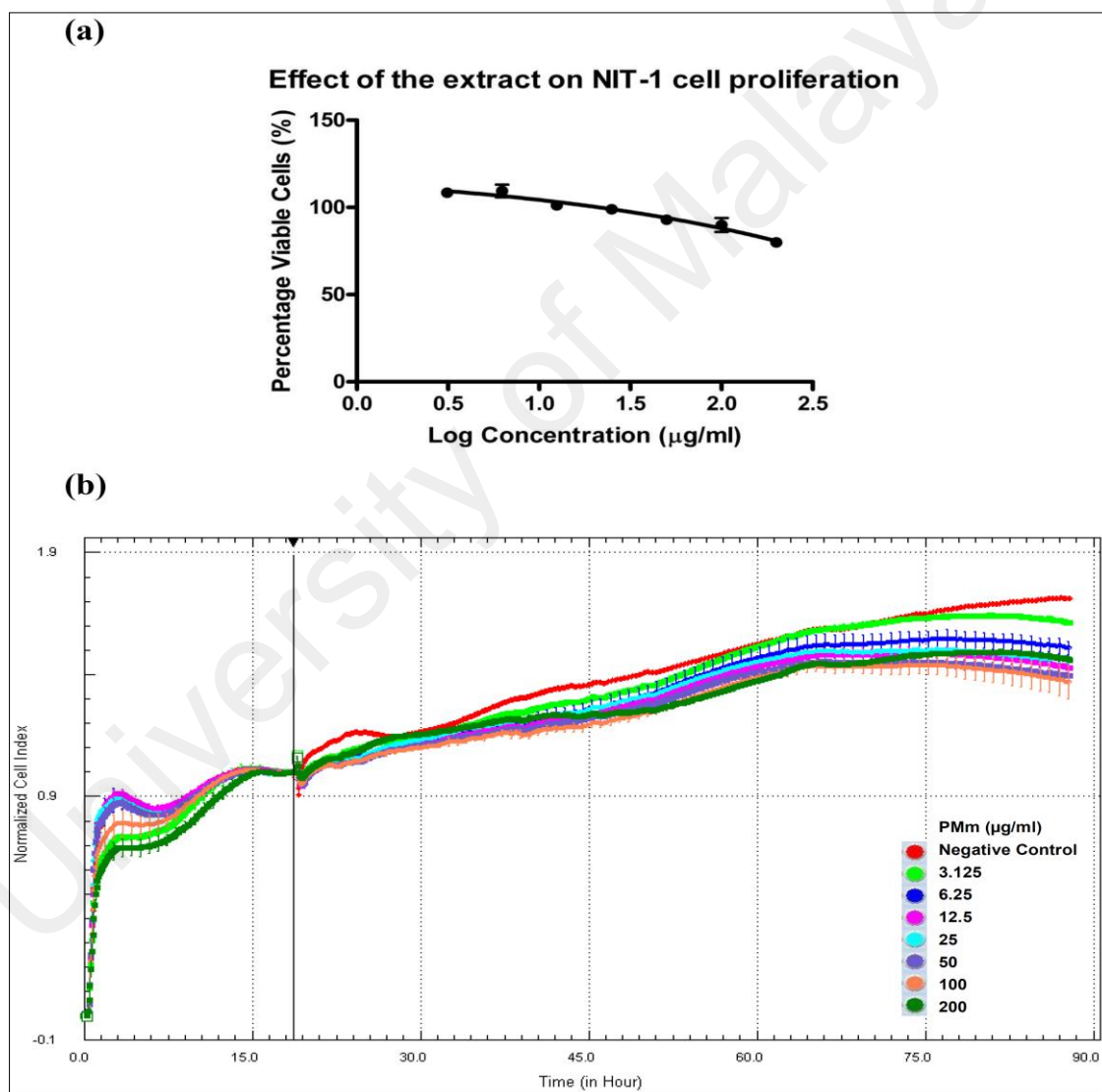


Fig. 4.183: Effect of PMt extract on NIT-1 cells

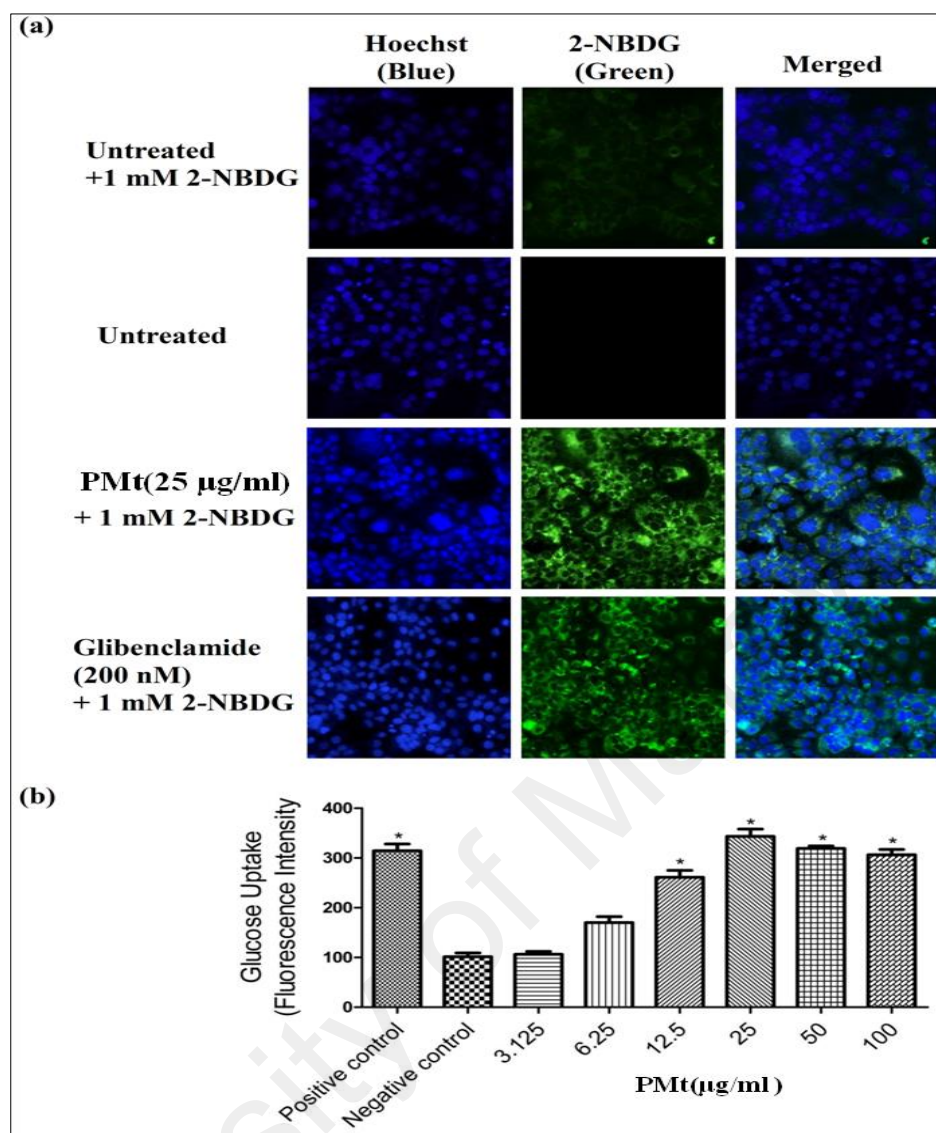


Fig. 4.184: Fluorescence images and glucose uptake of PMt-treated and untreated mouse NIT-1 cells

4.5.3.4 Effect of the Pmt extract on insulin secretion

The PMt methanol extract drastically increased insulin secretion in a dose-dependent manner at glucose concentrations of 6.25, 12.5 and 25 µg/ml. Significant induction of insulin secretion was observed in NIT-1 cells treated with PMt concentration as low as 12.5 µg/ml and the induction level of higher concentrations remained unchanged compared to 12.5 µg/ml (Figure 4.185). The PMt-treated and untreated cells were incubated in Krebs/HEPES buffer (pH 7.4) containing no glucose or 6.25, 12.5, or 25 mM glucose for 60 min at 37 °C.

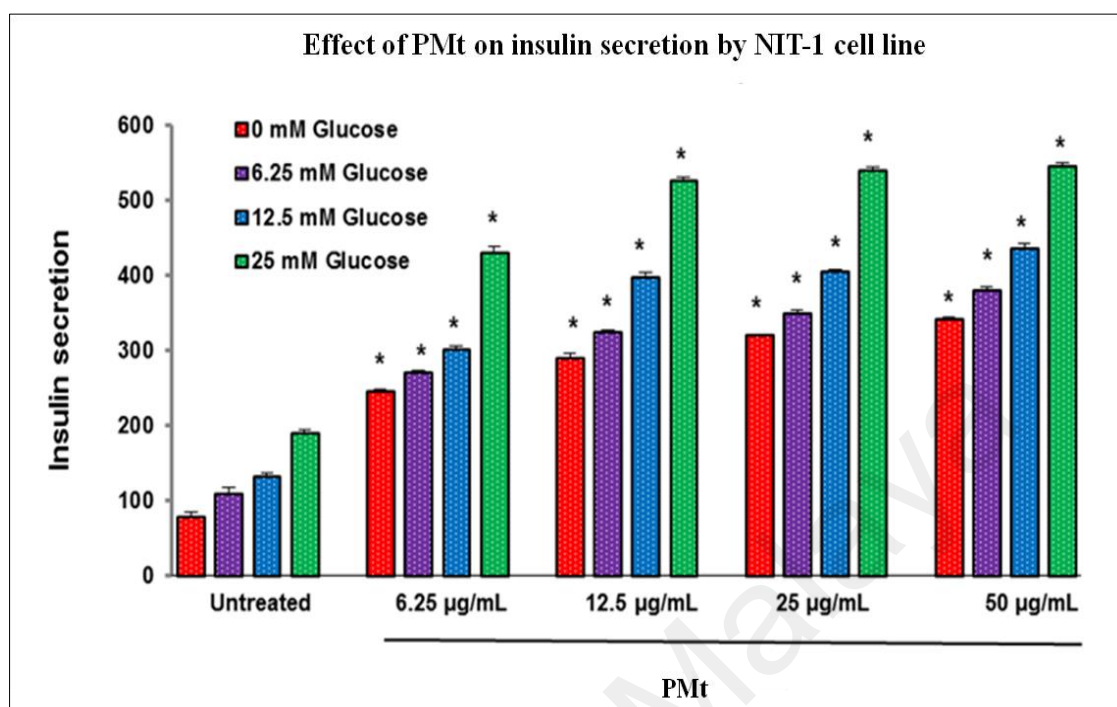


Fig. 4.185: Effect of PMt on insulin secretion by NIT-1 cell line.

4.5.3.5 Acute toxicity study

The acute oral toxicity studies revealed PMt is of non-toxic nature; no lethality or toxic reactions were observed at any of the doses tested. Based on these findings, 200 mg/kg and 400 mg/kg doses were selected for the type 1 and type 2 diabetic studies model, respectively.

4.5.3.6 Effect of PMt extract on blood glucose levels of type 1 and type 2 diabetic rats

Fasting blood glucose levels of all the groups were measured in type 1 and type 2 diabetic rat model segments, on every eleventh day up until the end of the 45 days treatment period.

The result of type 2 diabetic model segments revealed a significant reduction in the elevated blood glucose levels of type 2 diabetic rats treated with PMt (500 and 250 mg/kg) compared to that of untreated diabetic rats (Table 4.35).

On the other hand, in the type 1 diabetic model segments, diabetic rats did not show any significant reduction in elevated blood glucose level upon treatment with PMt at different doses level (500 and 250 mg/kg), compared to untreated diabetic rats.

At the end of the study period, the percentage inhibition in rats treated with a higher concentration of PMt was greater than that in glibenclamide-treated rats, the percentage inhibition effected by 500 and 200 mg/kg bw PMt was 69.82%, and 65.08%, respectively, compared to that of glibenclamide (68.53%) in type 2 diabetic model segments (Table 4.36).

Table 4.35: Effects of PMt on fasting blood glucose level of type 1 diabetic rats

Group	Fasting Blood Glucose Level (mmol/L)				
	No treatment	Treatment Days			
	Day 0	Day 11	Day 22	Day 33	Day 44
Normal control	5.1 ± 0.23	4.9 ± 0.33	5.3 ± 0.27	5.0 ± 0.31	5.6 ± 0.44
Diabetic control	19.4 ± 2.06	22.8 ± 2.47	23.5 ± 1.92	24.1 ± 2.10	25.7 ± 1.32
Insulin (6 U/kg)	20.3 ± 0.93	6.9 ± 0.64 ^a (71.05)	5.9 ± 0.26 ^a (74.89)	7.1 ± 1.57 ^a (70.53)	5.3 ± 0.81 ^a (79.37)
PMt (500 mg/kg)	21.4 ± 0.76	18.5 ± 1.32 (18.85)	17.2 ± 0.89 (26.80)	16.7 ± 1.66 ^a (30.70)	17.6 ± 0.54 (31.51)
PMt (250 mg/kg)	19.7 ± 1.13	20.3 ± 1.43 (10.96)	19.2 ± 1.25 (18.29)	18.8 ± 0.98 (21.99)	19.5 ± 1.67 (24.12)

Mean values ± SD, n = 6.

^a Significant compared to diabetic control ($P < 0.05$).

Parenthesis values shows, percentage decrease of blood glucose level in the treatment groups, compared to diabetic control within same day.

Table 4.36: Effects of PMt on fasting blood glucose level of type 2 diabetic rats

Group	Fasting Blood Glucose Level (mmol/L)				
	No treatment	Treatment Days			
	Day 0	Day 11	Day 22	Day 33	Day 44
Normal control	5.6 ± 0.65	5.3 ± 0.71	5.9 ± 0.54	6.2 ± 0.81	5.1 ± 0.25
Diabetic control	10.4 ± 0.97	11.9 ± 0.76	12.6 ± 0.39	12.9 ± 0.71	13.7 ± 0.66
Glibenclamide (50 mg/kg)	9.9 ± 0.65	6.4 ± 0.54 ^a (46.21)	5.7 ± 0.32 ^a (54.76)	5.5 ± 0.87 ^a (57.36)	5.2 ± 0.54 ^a (62.04)
PMt (500 mg/kg)	11.8 ± 0.88	7.4 ± 0.33 ^(37.81)	6.5 ± 0.39 ^a (48.41)	5.9 ± 0.76 ^a (54.26)	6.1 ± 0.55 ^a (55.47)
PMt (250 mg/kg)	10.8 ± 1.03	9.5 ± 0.76 ^(20.16)	9.4 ± 0.43 ^(25.39)	8.8 ± 0.67 ^(31.78)	8.7 ± 0.44 ^a (36.49)

Mean values ± SD, n = 6.

^a Significant compared to diabetic control ($P < 0.05$).

Parenthesis values shows, percentage decrease of blood glucose level in the treatment groups, compared to diabetic control within same day.

4.5.3.7 Oral glucose tolerance test on type 2 diabetic rats

Table 4.37 displays result of oral glucose tolerance test on type 2 diabetic rats. Diabetic rats upon treatment with PMt at 500 and 200 mg/kg showed significant decrease in blood glucose levels after 60-min of glucose load, when compared to untreated diabetic rats.

Similarly, after 90 min the blood glucose levels were constantly reduced to 66.31% and 52.94% after PMt treatment, whereas the glibenclamide-treated group caused (60.96%) reduction, respectively. This was followed by a reduction as great as 67.59% and 54.74% following the respective PMt doses at 120 min, whereas glibenclamide displayed 62.01% reduction in the blood glucose levels.

Table 4.37: Effects of PMt on fasting blood glucose level of type 2 diabetic rats after glucose load

Group	0 min	30 min	60 min	90 min	120 min
Normal control	5.7 ± 0.45	6.5 ± 0.76	6.1 ± 0.81	5.2 ± 0.55	5.5 ± 0.66
Diabetic control	14.1 ± 0.76	18.9 ± 0.73	19.9 ± 0.82	17.3 ± 0.49	18.3 ± 0.97
Glibenclamide (50 mg/kg)	5.8 ± 0.65	8.9 ± 0.38 ^a (52.91)	7.6 ± 0.61 ^a (61.80)	6.7 ± 0.77 ^a (61.27)	5.5 ± 0.28 ^a (69.94)
PMt (500 mg/kg)	6.5 ± 0.75	9.1 ± 0.57 ^a (51.85)	8.3 ± 0.68 ^a (58.29)	7.5 ± 0.92 ^a (56.64)	6.2 ± 0.85 ^a (66.12)
PMt (250 mg/kg)	8.9 ± 1.08	10.7 ± 0.78 ^a (43.38)	9.9 ± 0.67 ^a (50.25)	9.2 ± 0.37 ^a (46.82)	7.9 ± 0.92 ^a (56.83)

Mean values ± SD, n = 6.

^a Significant compared to diabetic control ($P < 0.05$).

Parenthesis values shows, percentage decrease of blood glucose level in the treatment groups, compared to diabetic control within same time period.

4.5.3.8 Effect of PMt extract on insulin and C-peptide level of type 1 and type 2 diabetic rats

Figure 4.186 showed the insulin and C-peptide levels in the type 1 and type 2 diabetic segment groups. Diabetic untreated rats in both the segments exhibited significant reduction of insulin and C-peptide in the serum, compared to normal control rats.

Upon daily treatment of standard positive and 500 or 200 mg/kg bw of PMt to diabetic rats for 45 days, showed significant improvement in insulin and C-peptide levels of type 2 diabetic rats as compared to untreated diabetic rats, whereas type 1 diabetic rats did not produce any significant sign of improvement in insulin and C-peptide levels.

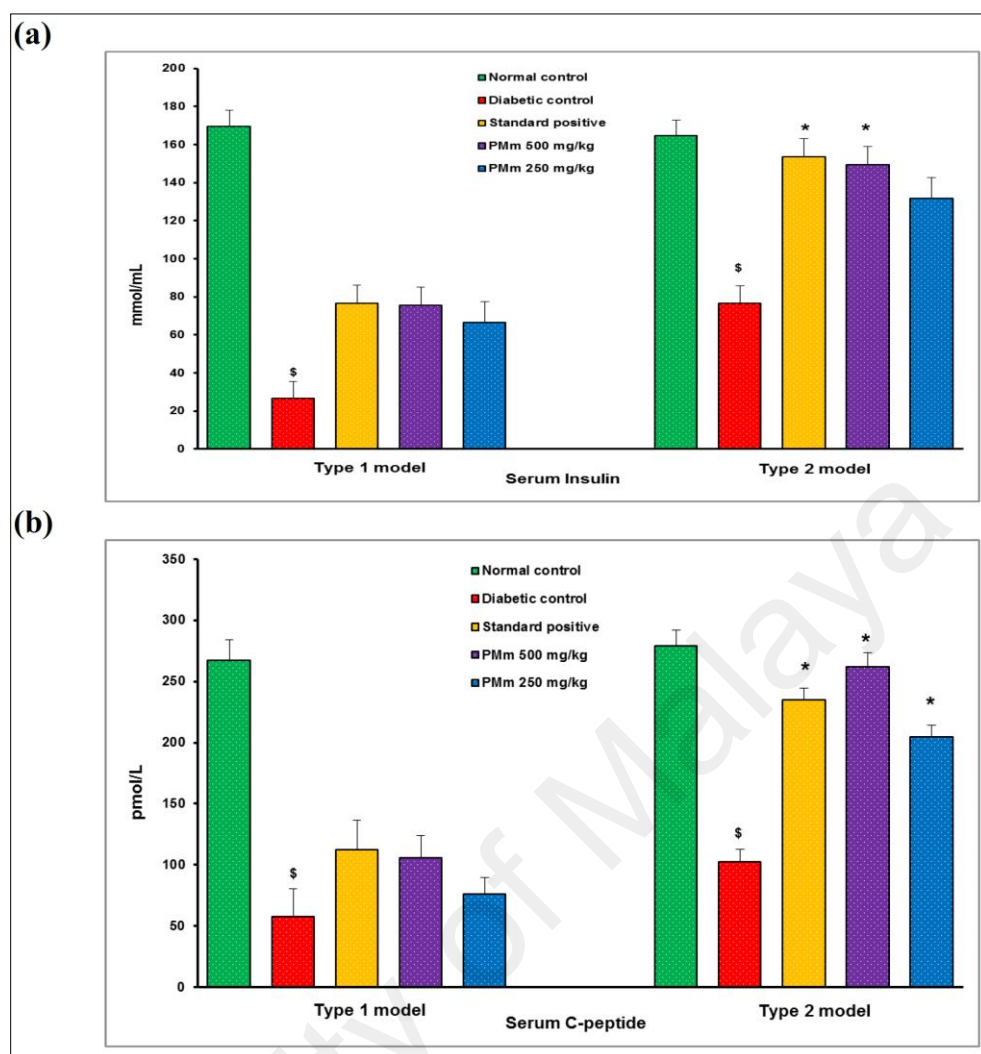


Fig. 4.186: Serum insulin and C-peptide levels in type 1 and type 2 diabetic rats

4.5.3.9 Effect of PMt extract on oxidative stress markers of type 1 and type 2 diabetic rats

In both the segment groups, serum GSH levels were reduced while MDA levels were significantly elevated in untreated diabetic rats compared to that of normal control rats (Figure 4.187). Upon administration of PMt at 500 mg/kg doses, demonstrated significant increase in serum GSH levels of type 2 diabetic rats, compared to untreated diabetic rats, whereas, type 1 diabetic rats treated with different doses of PMt did not produce any significant increase in GSH levels. In contrast, PMt at 500 mg/kg doses showed significant decrease in serum MDA levels of type 1 and type 2 diabetic rats.

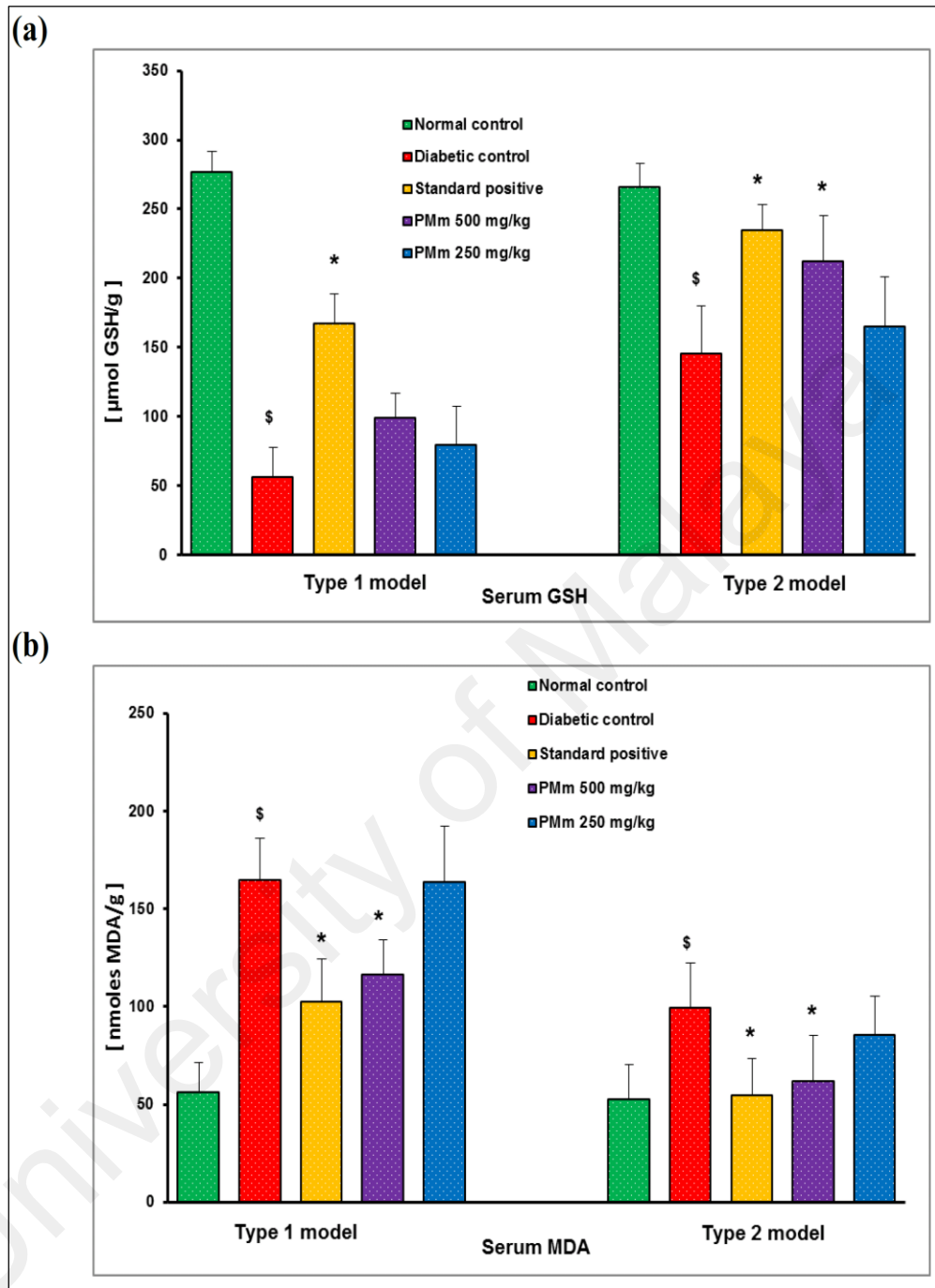


Fig. 4.187: Serum GSH (a) and MDA (b) levels in type 1 and type 2 diabetic rats

4.5.3.10 *In vivo* antidiabetic study of *Pseuduvaria macrophylla* methanol extract on streptozotocin-nicotinamide (STZ) induced type 2 diabetic rats

In this part of study, the antidiabetic potential of *Pseuduvaria macrophylla* was investigated through the evaluation of blood glucose level, serum insulin & C-peptide levels and oxidative stress markers (GSH and LPO levels).

Results showed that the body weights of treated rats with extracts showed significant increase compared to that of diabetic control (DC) (Figure 4.188). Blood glucose levels of treated groups (PMa and PMb) had significantly decreased over the testing period compared to that of diabetic control (DC) (Figure 4.189).

Insulin and C-peptide levels were enhanced in treated groups (Figure 4.190) indicating the reduction of blood glucose level. C- peptide is a chemical compound generated by beta cells in the pancreas at the same time as insulin, and C-peptide is used as bio marker of insulin production. The increase in glutathione (GSH) and decrease in lipid peroxidation (LPO) levels showed that the extract has antioxidant property (Figure 4.191).

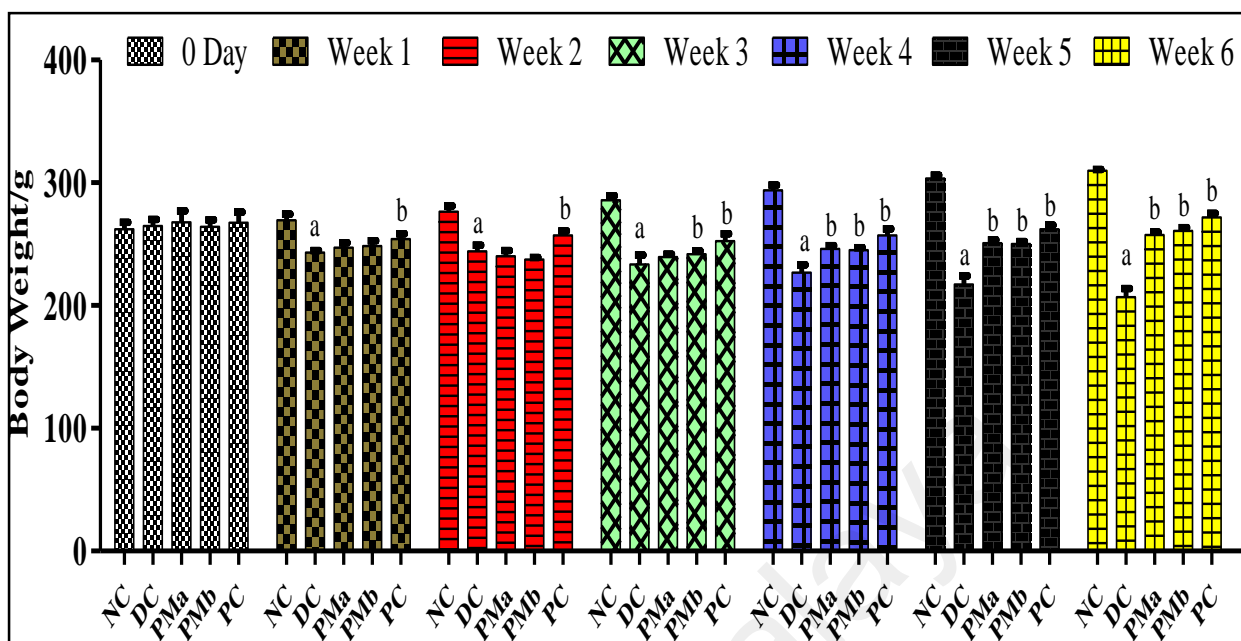


Fig.4.188: Effects of *P. macrophylla* extract on body weight in normal and diabetic rats.

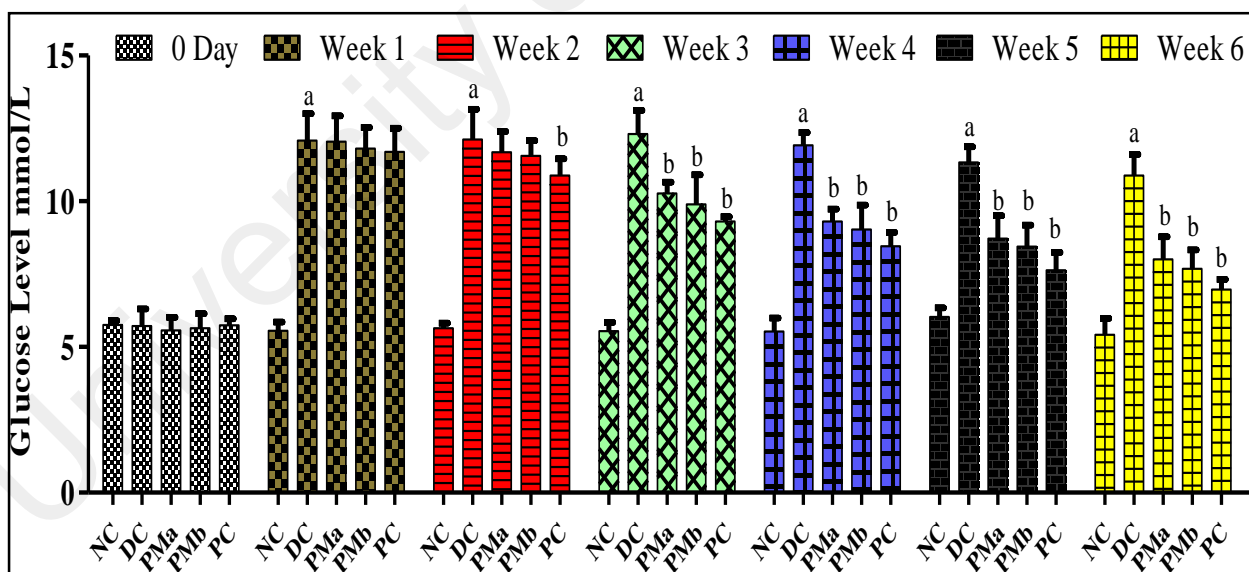


Fig.4.189: Effects of *P. macrophylla* extract on glucose level in normal and diabetic rats

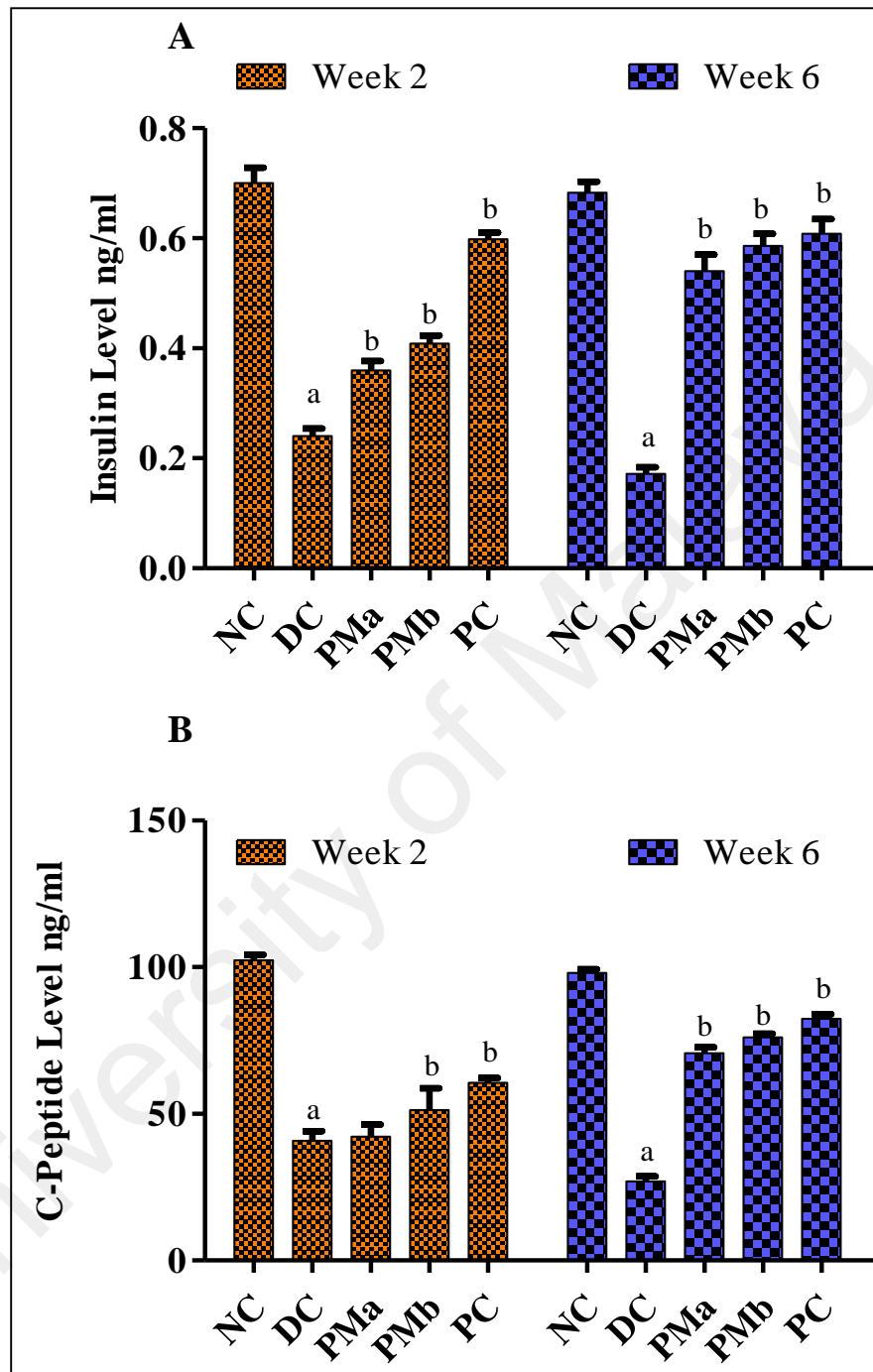


Fig.4.190: Effects of *P. macrophylla* extract on Insulin (A) and C-peptide (B) levels

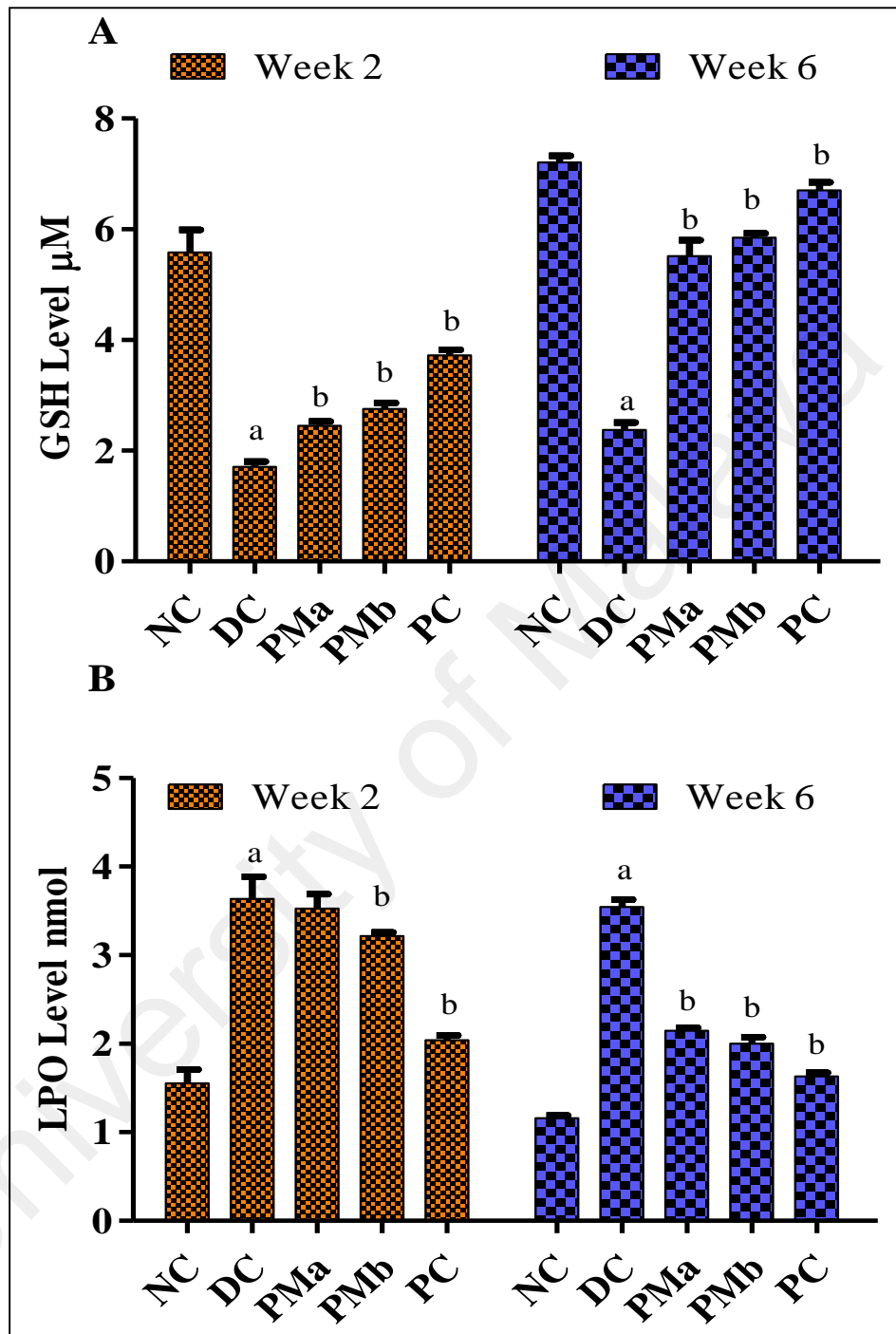


Fig. 4.191: Effects of *P. macrophylla* extract on GSH (A) and LPO (B) levels

4.5.3.11 Overall result

In the past years, *Pseuduvaria species* were specifically studied for their anticancer properties but no research work was conducted to investigate the antidiabetic property of the plants.

This is the first report that demonstrated the antidiabetic potential of *Pseuduvaria monticola* bark methanol extract on pancreatic NIT-1 cells and *in vivo* animal models. *Pseuduvaria monticola* was proven non-toxic even at high dosages and possesses positive effect on type 2 diabetic rats by down-regulating hyperglycemia and oxidative stress. This test has proven that the plant is non toxic and safe for consumption in addition to its traditional medicinal use.

The results also revealed that the extract dose-dependently stimulates glucose uptake and enhances insulin secretion in NIT-1 cells. In *in vivo* experiments, type 2 diabetic rats responded well to the extract by up-regulating insulin and C-peptide levels and down-regulate hyperglycemia and oxidative stress. The measurement of both C-peptide and insulin levels have been reported to be a valuable index of insulin secretion rather than insulin alone (Doda, 1996).

The outcomes of the result from the *Pseuduvaria macrophylla* extract is in agreement with the result from the antidiabetic study of *Pseuduvaria monticola* which showed a significant blood glucose reduction in type 2 diabetic rats and increased serum insulin and C-peptide levels. Oxidative stress conditions were also reduced. The overall results of both analyses are depicted in Figure 4.192 and 4.193.

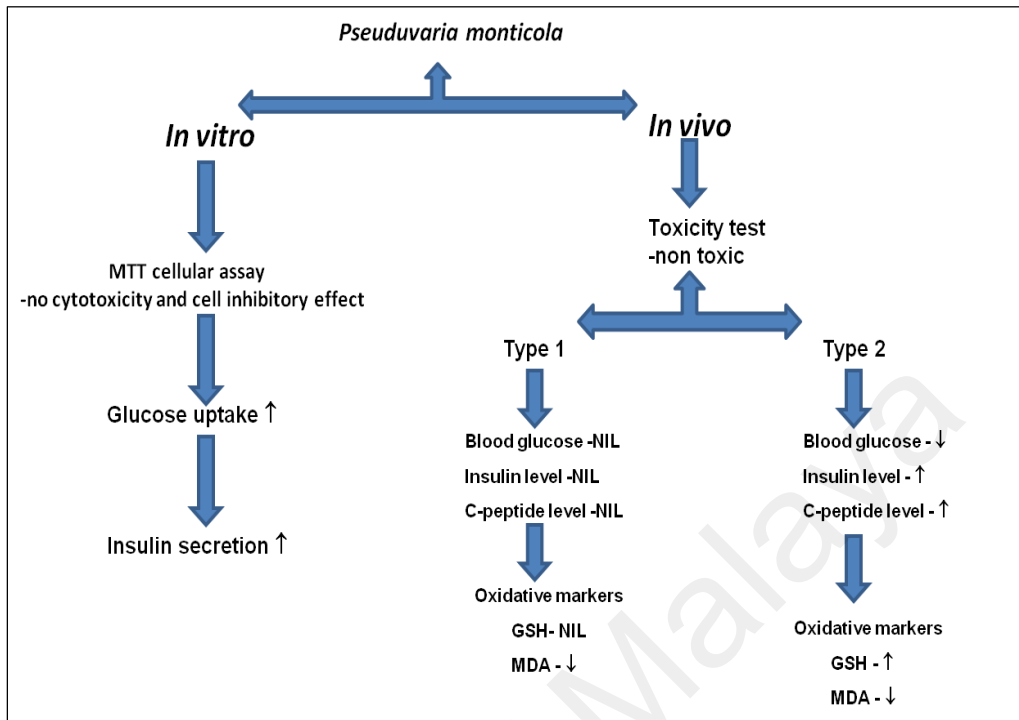


Fig. 4.192: Summary of antidiabetic results of *P. monticola*

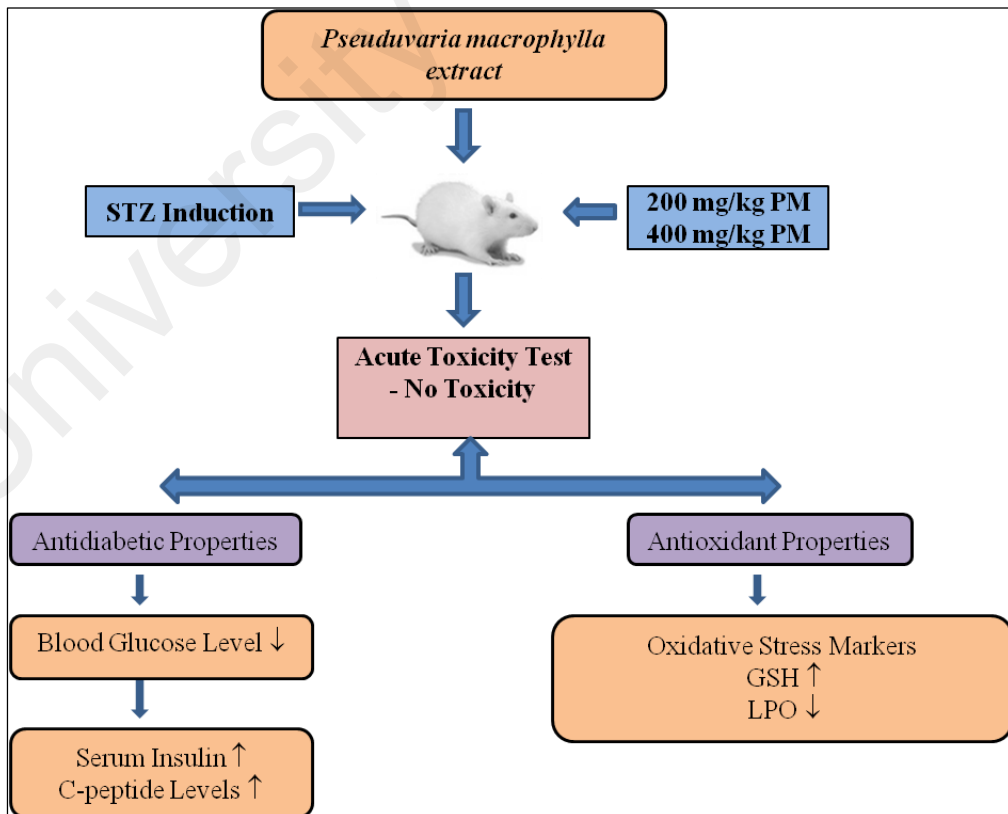


Fig. 4.193: Summary of antidiabetic results of *P. macrophylla*

CONCLUSION

Two species from the genus of *Pseuduvaria* were studied for their chemical constituents which are *P. monticola* and *P. macrophylla*. These two species were classified in the same division in plant phylogeny (evolutionary history of how plant evolves). This is the first phytochemical report for *Pseuduvaria monticola* and a comprehensive study, chemically and biologically, of both species. Previous studies mostly concentrated on the alkaloid contents of the plant species and their anticancer activities. Chemical constituents in the methanol extracts (polar fractions) have never been investigated.

Structural elucidation of the isolated compounds was established through numerous spectroscopic methods such as 1D and 2D NMR (^1H and ^{13}C NMR, COSY DEPT, HMQC, HMBC), UV, IR and MS (LC-MS and GC-MS). The leaf essential oils of both species were extracted by hydrodistillation method using the Clavenger's type apparatus and analysed by GC-MSTOF.

In this study, a total of 29 chemical constituents including 2 new compounds were isolated and elucidated from the bark and leaves of *Pseuduvaria monticola* and *Pseuduvaria macrophylla*. From *Pseuduvaria monticola*, 15 chemical compounds were isolated. They are four oxoaporphine alkaloids; liriodenine (**3**), lysicamine (**39**), oxoputerine (**40**), ouregidione (**4**), two phenanthrene alkaloids; atherosperminine (**41**) and argentinine (**42**), one sesquiterpene; T-cadinol (**43**), three benzopyran derivatives; oligandrol (**14**), (6*E*,10*E*) isopolycerasoidol (**15**), (6*E*,10*E*) isopolycerasoidol methyl ester (a new compound) (**32**), two phenolic acids; caffeic acid (**44**) and chlorogenic acid (**45**), two fatty acids; n-hexadecanoic acid (**46**), methyl oleate (**47**) and one sterol; stigmasterol (**48**).

Isolation and characterization of chemical compounds from the leaves and bark *Pseuduvaria macrophylla* afforded 14 compounds. They are one new compound of naphthoic acid derivative; 1,3,5,7-tetramethoxy-2-naphthoic acid (**51**), five oxoaporphine alkaloids; liriodenine (**3**), lysicamine (**39**) atherospermidine (**10**), *N*-methyl ouregidione (**5**) and *O*-methylmoschatoline (**7**), two benzopyran derivatives; polycerasoidol (**16**) and polycerasoidin (**49**), two phenyl propanoids; elimicin (**26**) and elimicin 6-methoxy (**50**), two sterols; β -sitosterol (**52**) and stigmasta-5,22-diene, 3 methoxy (**53**) and two fatty acids; oleic acid (**54**) and *n*-hexadecanoic acid methyl ester (**55**).

Liriodenine (**3**) and lysicamine (**39**) were discovered in both *Pseuduvaria monticola* and *Pseuduvaria macrophylla* which could confirm that both species indeed share the same phylogeny. Liriodenine (**3**) can be considered as the biomarker for *Pseuduvaria* genus due to its presence as one of the major compounds in *P. monticola* and *P. macrophylla*, including other *Pseuduvaria* species that were reported as well.

The chemical constituents in the leaf essential oils of *Pseuduvaria monticola* were mainly sesquiterpenes and the major compounds were α -cadinol (**56**) (13.0%), *cis* calamenene (**57**) (6.9%) and α -copaene (**25**) (4%). The major compounds in the leaf essential oils of *Pseuduvaria macrophylla* were caryophyllene oxide (**29**) (29.7%) and elimicin (**26**) (28%). Both essential oils showed good DPPH antioxidant activity.

In DPPH scavenging activity assay, polycerasoidol (**16**) and (6*E*,10*E*) isopolycerasoidol (**15**) demonstrated significant activity with an IC₅₀ of 18.89 μ g/mL and 22.56 μ g/mL, respectively, compared to quercetin (IC₅₀ 7.01 \pm 0.36). Leaf essential oil of *Pseuduvaria macrophylla* exhibited slightly greater antioxidant activity than that of *Pseuduvaria monticola*.

In anticancer activity, (6*E*, 10*E*) isopolycerasoidol (**16**) and (6*E*, 10*E*) isopolycerasoidol methyl ester (**32**) demonstrated cytotoxic effects on MCF-7 and MDA-MB-231 human

breast cancer cells (IC_{50} 59 ± 5.1 , 43 ± 2.4 and 76 ± 8.5 , 58 ± 2.6 respectively) and induced apoptosis.

In antidiabetic study, *in vitro* and *in vivo* experiment showed that the bark methanolic extract of *Pseuduvaria monticola* significantly induced the glucose uptake and insulin secretion of mouse pancreatic β -cell line (NIT-1) and upregulated insulin secretion and downregulated oxidative stress and hyperglycemia in STZ-nicotinamide-induced type 2 diabetic rats whereas the methanol extract of *Pseuduvaria macrophylla* upregulated insulin and C-peptide levels and down-regulated hyperglycemia and oxidative stress in STZ-nicotinamide-induced type 2 diabetic rats.

In conclusion, chemical compounds in both species not only contain alkaloids but also benzopyran derivatives, naphtholic phenolic acids and phenyl propanoids. Some isolated compounds from *Pseuduvaria monticola* and *Pseuduvaria macrophylla* showed good antioxidant and anticancer activity. For the first time, this study has also revealed that both species demonstrated antidiabetic potential against Type 2 diabetes rat (*in vivo* experiments). Thus, the prospect of *Pseuduvaria* species as antidiabetic source for antidiabetic agents in the future can be further explored and investigated.

REFERENCES

- A. Loaiza, O. H. P., Porras, L.F. Barros. (2003). Glutamate triggers rapid glucose transport stimulation in astrocytes as evidenced by real-time confocal microscopy. *The Journal of Neuroscience*, 23 7337-7342.
- Abbott, A. (2005). Avian flu special What's in the medicine cabinet? *Nature*, 435(7041), 407-409.
- Adibatti, N., Thirugnanasambantham, P., Kulothungan, C., Viswanathan, S., Kameswaran, L., Balakrishna, K., & Sukumar, E. (1991). A pyridine alkaloid from *Ceropegia juncea*. *Phytochemistry*, 30(7), 2449-2450.
- Aditya Arya, C. Y. L., Shiau Chuen Cheah, Mohd Rais Mustafa and Mustafa Ali Mohd. (2012). Anti-diabetic effects of *Centratherum anthelminticum* seeds methanolic fraction on pancreatic cells, β -TC6 and its alleviating role in type 2 diabetic rats. *Journal of Ethnopharmacology*, 144(1), 22–32.
- Ajoku, G., Okwute, S., & Okogun, J. (2015). Isolation of Hexadecanoic Acid Methyl Ester and 1, 1, 2-Ethanetricarboxylic Acid-1-Hydroxy-1, 1-Dimethyl Ester from the Calyx of Green Hibiscus Sabdariffa (Linn). *Natural Product Chemical Research*, 3(169), 2.
- Al-Khalil, S., Alkofahi, A., El-Eisawi, D., & Al-Shibib, A. (1998). Transtorine, a new quinoline alkaloid from *Ephedra transitoria*. *Journal of Natural Products*, 61(2), 262-263.
- Aminimoghadamfarouj, N., Nematollahi, A., & Wiart, C. (2011). Annonaceae: bio-resource for tomorrow's drug discovery. *Journal of Asian natural products research*, 13(05), 465-476.
- Arya, A., Achoui, M., Cheah, S.-C., Abdelwahab, S. I., Narrima, P., Mohan, Mohd, M. A. (2012). Chloroform fraction of *Centratherum anthelminticum* (L.) seed inhibits tumor necrosis factor alpha and exhibits pleotropic bioactivities: inhibitory role in human tumor cells. *Evidence-Based Complementary and Alternative Medicine*, 2012.
- Arya, A., Taha, H., Khan, A. K., Shahid, N., Ali, H. M., & Mohd, M. A. (2014). In vivo Antidiabetic and Antioxidant Potential of *Pseudovaria macrophylla* Extract. *In vivo*, 1, 12490.

- Asano, N., Kuroi, H., Ikeda, K., Kizu, H., Kameda, Y., Kato, A., Fleet, G. W. (2000). New polyhydroxylated pyrrolizidine alkaloids from *Muscari armeniacum*: structural determination and biological activity. *Tetrahedron: Asymmetry*, 11(1), 1-8.
- Ashihara, H., & Crozier, A. (2001). Caffeine: a well known but little mentioned compound in plant science. *Trends in plant science*, 6(9), 407-413.
- Aslan, M., Orhan, D. D., Orhan, N., Sezik, E., & Yesilada, E. (2007). In vivo antidiabetic and antioxidant potential of *Helichrysum plicatum* ssp. *plicatum capitulum* in streptozotocin-induced-diabetic rats. *Journal of ethnopharmacology*, 109(1), 54-59.
- Asres, Kaleab, & Bucar, Franz. (2005). Anti-HIV activity against immunodeficiency virus type 1 (HIV-I) and type II (HIV-II) of compounds isolated from the stem bark of *Combretum molle*. *Ethiopian Medical Journal*, 43(1), 15-20.
- Bagchi, D., Bagchi, M., Stohs, S. J., Das, D. K., Ray, S. D., Kuszynski, C. A., Pruess, H. G. (2000). Free radicals and grape seed proanthocyanidin extract: importance in human health and disease prevention. *Toxicology*, 148(2), 187-197.
- Bakkali, F., Averbeck, S., Averbeck, D., & Idaomar, M. (2008). Biological effects of essential oils – A review. *Food and Chemical Toxicology*, 46(2), 446-475.
- Balaabirami & Patharajan (2012). In vitro antimicrobial and antifungal activity of *Catharthus roseus* leaves extract against important pathogenic organisms. *International Journal of Pharmaceutical Sciences*, 4(3), 487-490.
- Balandrin Manuel, F., Kinghorn, A. D., & Farnsworth Norman, R. (1993). Plant-Derived Natural Products in Drug Discovery and Development *Human Medicinal Agents from Plants* (Vol. 534, pp. 2-12).
- Banfield, J. E., Black, D., Collins, D. J., Hyland, B. P., Lee, J. J., & Pranowo, S. R. (1994). Constituents of some species of *Beilschmiedia* and *Endiandra* (Lauraceae): New endiandric acid and benzopyran derivatives isolated from *B. oligandra*. *Australian Journal of Chemistry*, 47(4), 587-607.
- Baratta, M. T., Dorman, H., Deans, S. G., Figueiredo, A. C., Barroso, J. G., & Ruberto, G. (1998). Antimicrobial and antioxidant properties of some commercial essential oils. *Flavour and fragrance journal*, 13(4), 235-244.

- Barreca, D., Laganà, G., Ficarra, S., Tellone, E., Leuzzi, U., Galtieri, A., & Bellocco, E. (2011). Evaluation of the antioxidant and cytoprotective properties of the exotic fruit *Annona cherimola* Mill. (Annonaceae). *Food Research International*, 44(7), 2302-2310.
- Brophy, J. J., Goldsack, R. J., Hook, J. M., Fookes, C. J. R., & Forster, P. I. (2007). The leaf essential oils of the Australian species of *Pseuduvaria* (Annonaceae). *Journal of Essential Oil Research*, 362-366.
- Buchanan, M., & Dickey, E. (1960). Liriodenine, A Nitrogen-Containing Pigment of Yellow Poplar Heartwood (*Liriodendron tulipifera*, L.). *The Journal of Organic Chemistry*, 25(8), 1389-1391.
- Buchbauer, G. (2004). Evaluation of the harmonizing effect of ylang-ylang oil on humans after inhalation. *Planta Med*, 70, 632-636.
- Castedo, L., Granja, J. A., de Lera, A. R., & Villaverde, M. C. (1991). Alkaloids from *Guatteria goudotiana*. *Phytochemistry*, 30(8), 2781-2783.
- Catarino, M. D., Silva, A. M., Saraiva, S. C., Sobral, A. J., & Cardoso, S. M. (2015). Characterization of phenolic constituents and evaluation of antioxidant properties of leaves and stems of *Eriocephalus africanus*. *Arabian Journal of Chemistry*.
- Christophersen, Carsten. (1995). Theory of the origin, function, and evolution secondary metabolites. In R. Atta ur (Ed.), *Studies in Natural Products Chemistry* (Vol. Volume 18, Part 11, pp. 677-737)
- Chu, J. H.-Y. (2014). *Investigating in vitro anticancer properties of Malaysian rainforest plants: Acalypha wilkesiana Müll, Arg. Archidendron ellipticum (Blume) Hassk. Duabanga grandiflora Walp. Pseuduvaria macrophylla (Oliv.) Merr.* (Doctoral dissertation, University of Nottingham).
- Chung, I.-M., Kim, E.-H., Yeo, M.-A., Kim, S.-J., Seo, M. C., & Moon, H.-I. (2011). Antidiabetic effects of three Korean sorghum phenolic extracts in normal and streptozotocin-induced diabetic rats. *Food Research International*, 44(1), 127-132.
- Claeson, P., Andersson, R., & Samuelsson, G. (1991). T-cadinol: a pharmacologically active constituent of scented myrrh: introductory pharmacological characterization and high field ¹H- and ¹³C-NMR data. *Planta medica*, 57(4), 352-356.

- Costa, E. V., da Cruz, P. E. O., de Lourenco, C. C., de Souza Moraes, V. R., de Lima Nogueira, P. C., & Salvador, M. J. (2013). Antioxidant and antimicrobial activities of aporphinoids and other alkaloids from the bark of *Annona salzmannii* A. DC.(Annonaceae). *Natural Product Research*, 27(11), 1002-1006.
- Costa, E. V., Pinheiro, M. L. B., Souza, A. D. L. d., Barison, A., Campos, F. R., Valdez, R. H., Nakamura, C. V. (2011). Trypanocidal activity of oxoaporphine and pyrimidine- β -carboline alkaloids from the branches of *Annona foetida* Mart.(Annonaceae). *Molecules*, 16(11), 9714-9720.
- Couvreur, T. L. P., Pirie, M. D., Chatrou, L. W., Saunders, R. M. K., Su, Y. C. F., Richardson, J. E., & Erkens, R. H. J. (2011). Early evolutionary history of the flowering plant family Annonaceae: steady diversification and boreotropical geodispersal. *Journal of Biogeography*, 38(4), 664-680.
- Crawford, A. G., Cote, C., Couto, J., Daskiran, M., Gunnarsson, C., Haas, K., Schuette, R. (2010). Prevalence of obesity, type II diabetes mellitus, hyperlipidemia, and hypertension in the United States: findings from the GE Centricity Electronic Medical Record database. *Population health management*, 13(3), 151-161.
- Crozier, A., Jaganath, I. B., & Clifford, M. N. (2009). Dietary phenolics: chemistry, bioavailability and effects on health. *Natural product reports*, 26(8), 1001-1043.
- Dai, D., Huong, L. T., Hung, N. H., Thang, T. D., & Ogunwande, I. A. (2014). Chemical Compositions of Essential Oils of Selected Medicinal Plants from Thừa Thiên-Huế Province, Vietnam. *Journal of Herbs, Spices & Medicinal Plants*, 20(3), 269-281.
- De Araujo-Junior, J. X., Da-Cunha, E. V., Chaves, M. C. D. O., & Gray, A. I. (1997). Piperdardine, a piperidine alkaloid from *Piper tuberculatum*. *Phytochemistry*, 44(3), 559-561.
- De Fátima Costa Santos, M., Dutra, L. M., Regina de Souza Moraes, V., Barison, A., & Costa, E. V. (2015). Aporphine alkaloids from the stem bark of *Guatteria pogonopus* (Annonaceae). *Biochemical Systematics and Ecology*, 60(0), 106-109.
- De Lima, M. R. F., de Souza Luna, J., Dos Santos, A. F., De Andrade, M. C. C., Sant'Ana, A. E. G., Genet, J.-P., Moreau, N. (2006). Anti-bacterial activity of some Brazilian medicinal plants. *Journal of Ethnopharmacology*, 105(1), 137-147.
- Demain, Arnold, & Fang, Aiqi. (2000). The Natural Functions of Secondary Metabolites. In A. Fiechter (Ed.), *History of Modern Biotechnology I* (Vol. 69, pp. 1-39).

- Doda, R. F. (1996). Diabetes mellitus. In A. J. Kaplan LA (Ed.), *Clinical Chemistry* (pp. 613-641).
- Estévez, J. C., Villaverde, M. C., Estévez, R. J., Suas, J. A., & Castedo, L. (1990). New total synthesis of phenanthrene alkaloids. *Canadian Journal of Chemistry*, 68(6), 964-968.
- Figueiredo, A. C., Barroso, J. G., Pedro, L. G., & Scheffer, J. J. C. (2008). Factors affecting secondary metabolite production in plants: volatile components and essential oils. *Flavour and Fragrance Journal*, 23(4), 213-226.
- Frugier, F., Kosuta, S., Murray, J. D., Crespi, M., & Szczyglowski, K. (2008). Cytokinin: secret agent of symbiosis. *Trends in Plant Science*, 13(3), 115-120.
- Fryer, M. (1992). The antioxidant effects of thylakoid Vitamin E (α -tocopherol). *Plant, Cell & Environment*, 15(4), 381-392.
- González, M. C., Sentandreu, M. A., Rao, K. S., Zafra-Polo, M. C., & Cortes, D. (1996). Prenylated benzopyran derivatives from two *Polyalthia* species. *Phytochemistry*, 43(6), 1361-1364.
- Gonzalez, M. C., Serrano, A., Zafra-Polo, M. C., Cortes, D., & Rao, K. S. (1995). Polycerasoidin and polycerasoidol, two new prenylated benzopyran derivatives from *Polyalthia cerasoides*. *Journal of Natural Products*, 58(8), 1278-1284.
- Guerrero-Analco, J. A., Martineau, L., Saleem, A., Madiraju, P., Muhammad, A., Durst, T., Arnason, J. T. (2010). Bioassay-Guided Isolation of the Antidiabetic Principle from *Sorbus decora* (Rosaceae) Used Traditionally by the Eeyou Istchee Cree First Nations. *Journal of Natural Products*, 73(9), 1519-1523.
- Gyllenhaal, C., Kadushin, M. R., Southavong, B., Sydara, K., Bouamanivong, S., Xaiveu, M., Soejarto, D. D. (2012). Ethnobotanical approach versus random approach in the search for new bioactive compounds: Support of a hypothesis. *Pharmaceutical biology*, 50(1), 30-41.
- Habib, M., Nikkon, F., Rahman, M., Haque, Z., & Karim, M. (2007). Isolation of stigmaterol and β -sitosterol from methanolic extract of root. *Pakistan Journal of Biological Sciences*, 10(22), 4174-4176.
- Harvey, A. L. (2010). Plant natural products in anti-diabetic drug discovery. *Current Organic Chemistry*, 1670-1677.

- Harvey, A. L., Clark, R. L., Mackay, S. P., & Johnston, B. F. (2010). Current strategies for drug discovery through natural products. *Expert Opinion on Drug Discovery*, 559-568.
- Heinrichs, J., Anton, H., Gradstein, S. R., & Mues, R. (2000). Systematics of *Plagiochila* sect. *Glaucescentes* Carl (Hepaticae) from tropical America: a morphological and chemotaxonomical approach. *Plant Systematic and Evolution*, 220 (1-2), 115-138.
- Holley, R. A., & Patel, D. (2005). Improvement in shelf-life and safety of perishable foods by plant essential oils and smoke antimicrobials. *Food Microbiology*, 22(4), 273-292.
- Hoong, Y. B., Paridah, M. T., Loh, Y. F., Jalaluddin, H., & Chuah, L. A. (2011). A new source of natural adhesive: *Acacia mangium* bark extracts co-polymerized with phenol-formaldehyde (PF) for bonding *Mempisang* (Annonaceae spp.) veneers. *International Journal of Adhesion and Adhesives*, 31(3), 164-167.
- Hostettmann, K., & Marston, A. (2002). Twenty years of research into medicinal plants: results and perspectives. *Phytochemistry Reviews*, 1(3), 275-285.
- Hostettmann, K., Wolfender, J.-L., & Terreaux, C. (2001). Modern screening techniques for plant extracts. *Pharmaceutical Biology*, 39(s1), 18-32.
- Hsieh, T. J., Wu, Y. C., Chen, S. C., Huang, C. S., & Chen, C. Y. (2004). Chemical constituents from *Annona glabra*. *Journal of the Chinese Chemical Society*, 51(4), 869-876.
- Hussein, Z., Wentworth, J. M., Nankervis, A. J., Proietto, J., & Colman, P. G. (2004). Effectiveness and side effects of thiazolidinediones for type 2 diabetes: real-life experience from a tertiary hospital. *Medical Journal of Australia*, 181(10), 536-539.
- Hyun, S. K., Min, B. S., & Choi, J. S. (2010). Articles: Isolation of Phenolics, Nucleosides, Saccharides and an Alkaloid from the root of *Aralia cordata*. *Natural Product Sciences*, 16(1), 20-25.
- Jantan, I. (2004). Medicinal plant research in Malaysia: scientific interests and advances. *Jurnal Kesihatan Malaysia*, 2(2), 27-46.

- J.Sinclair. (1955). A Revision of the Malayan Annonaceae. *Garden Bulletin Singapore*, 14, 49-51.
- Jessup, L. W. (1987). The genus *Pseuduvaria* Miq.(Annonaceae) in Australia. *Austrobaileya*, 2, 307-313.
- Johns, S., Lamberton, J., Li, C., & Sioumis, A. (1970). Alkaloids from *Pseuduvaria* species, *Schefferomitra subaequalis*, and *Polyalthia nitidissima* (Annonaceae): isolation of a new alkaloid shown to be 1, 2, 9, 10-Tetramethoxynoraporphine (norglaucine). *Australian Journal of Chemistry*, 23(2), 423-426.
- Joshi, H., Joshi, A. B., Sati, H., Gururaja, M., Shetty, P. R., Subrahmanyam, E., & Satyanaryana, D. (2009). Fatty acids from *Memecylon umbellatum* (Burm.). *Asian Journal of Research in Chemistry*, 2(2), 178-180.
- Jung, M., Park, M., Lee, H. C., Kang, Y.-H., Kang, E. S., & Kim, S. K. (2006). Antidiabetic agents from medicinal plants. *Current medicinal chemistry*, 13(10), 1203-1218.
- Kamboj, A., & Saluja, A. K. (2011). Isolation of stigmasterol and β -sitosterol from petroleum ether extract of aerial parts of *Ageratum conyzoides* (Asteraceae). *Int J Pharm Pharm Sci*, 3(1), 94-96.
- Kaou, A. M., Mahiou-Leddet, V., Hutter, S., Aïnouddine, S., Hassani, S., Yahaya, Ollivier, E. (2008). Antimalarial activity of crude extracts from nine African medicinal plants. *Journal of Ethnopharmacology*, 116(1), 74-83.
- Keri, R. S., Budagumpi, S., Pai, R. K., & Balakrishna, R. G. (2014). Chromones as a privileged scaffold in drug discovery: A review. *European Journal of Medicinal Chemistry*, 340-374.
- Kahn, R. (2003). Follow-up report on the diagnosis of diabetes mellitus: The expert committee on the diagnosis and classifications of diabetes mellitus*. *Diabetes care*, 26(11), 3160.
- Koehn, F. E., & Carter, G. T. (2005). The evolving role of natural products in drug discovery. *Nature reviews Drug discovery*, 4(3), 206-220.
- Kuete, V., Ngameni, B., Wiench, B., Krusche, B., Horwedel, C., Ngadjui, B. T., & Efferth, T. (2011). Cytotoxicity and mode of action of four naturally occurring flavonoids from the genus *Dorstenia*: gancaonin Q, 4-hydroxyonchocarpin, 6-prenylapigenin, and 6,8-diprenyleriodytyol. *Planta Medica*, 77(18), 1984-1989.

- Kusurkar, R. S., Goswami, S. K., & Vyas, S. M. (2003). Efficient one-pot synthesis of anti HIV and antitumor compounds: harman and substituted harmans. *Tetrahedron letters*, 44(25), 4761-4763.
- Lahlou, M. (2004). Methods to study the phytochemistry and bioactivity of essential oils. *Phytotherapy Research*, 18(6), 435-448.
- Lang, G., Mayhudin, N. A., Mitova, M. I., Sun, L., van der Sar, S., Blunt, J. W., Munro, M. H. G. (2008). Evolving Trends in the Dereplication of Natural Product Extracts: New Methodology for Rapid, Small-Scale Investigation of Natural Product Extracts. *Journal of Natural Products*, 71(9), 1595-1599.
- Latiff, A. (2015). On the Annonaceae of Taman Negara, Peninsular Malaysia*. *The Malayan Nature Journal*, 65(4), 27.
- Leboeuf, M., Cavé, A., Bhaumik, P., Mukherjee, B., & Mukherjee, R. (1980). The phytochemistry of the Annonaceae. *Phytochemistry*, 21(12), 2783-2813.
- Lee, N. H., Xu, Y.-J., & Goh, S. (1999). 5-Oxonoraporphines from *Mitrephora* cf. *m* *aingayi*. *Journal of Natural Products*, 62(8), 1158-1159.
- Lee, S.-J., Umamo, K., Shibamoto, T., & Lee, K.-G. (2005). Identification of volatile components in basil (*Ocimum basilicum* L.) and thyme leaves (*Thymus vulgaris* L.) and their antioxidant properties. *Food Chemistry*, 91(1), 131-137.
- Lee, T., & Gong, Y.-D. (2012). Solid-phase parallel synthesis of drug-like artificial 2H-benzopyran libraries. *Molecules*, 17(5), 5467-5496.
- Liu, R. H. (2003). Health benefits of fruit and vegetables are from additive and synergistic combinations of phytochemicals. *The American Journal of Clinical Nutrition*, 78(3), 517S-520S.
- Looi CY, I. M., Takaki S, Sato M, Chiba N, Sasahara Y, Futaki S, Tshuchiya S, Kumaki S. (2011). Octa-arginine mediated delivery of wild-type Lnk protein inhibits TPO-induced M-MOK megakaryoblastic leukemic cell growth by promoting apoptosis. *PLoS ONE*, 6(8), e23640.
- Lucchesi, M. E., Chemat, F., & Smadja, J. (2004). Solvent-free microwave extraction of essential oil from aromatic herbs: comparison with conventional hydro-distillation. *Journal of Chromatography A*, 1043(2), 323-327.

- Mafezoli, J., Santos, R. H. A., Gambardela, M. T. P., & Silveira, E. R. (2003). Fatty acids and terpenoids from *Trigonia fasciculata*. *Journal of the Brazilian Chemical Society*, *14*, 406-410.
- Mahmood, K., Chan, K. C., Park, M. H., Han, Y. N., & Han, B. H. (1986). An aporphinoid alkaloid from *Pseuduvaria macrophylla*. *Phytochemistry*, *25*(6), 1509-1510.
- Massotte, D., & Kieffer, B. (1998). A molecular basis for opiate action. *Essays Biochem*, *33*, 65-77.
- McNeil, J., & Delisle, J. (1989). Are host plants important in pheromone-mediated mating systems of Lepidoptera? *Experientia*, *45*(3), 236-240.
- Miguel, M. G. (2010). Antioxidant and anti-inflammatory activities of essential oils: a short review. *Molecules*, *15*(12), 9252-9287.
- Mithöfer, A., & Boland, W. (2012). Plant defense against herbivores: chemical aspects. *Annual Review of Plant Biology*, *63*, 431-450.
- Mohammadjavad Paydar, Y. L. W., Bushra Abdulkarim Moharam, Won Fen Wong, Chung Yeng Looi. (2013). In vitro Anti-oxidant and Anti-cancer Activity of Methanolic Extract from *Sanchezia speciosa* Leaves. *Pakistan Journal of Biological Sciences*, *16*, 1212-1215.
- Mokbel, M. S., & Hashinaga, F. (2006). Evaluation of the antioxidant activity of extracts from buntan (*Citrus grandis* Osbeck) fruit tissues. *Food Chemistry*, *94*(4), 529-534.
- Montenegro, H., Gutierrez, M., Romero, L. I., Ortega-Barría, E., Capson, T. L., & Rios, L. C. (2003). Aporphine alkaloids from *Guatteria* spp. with leishmanicidal activity. *Planta medica*, *69*(7), 677-678.
- Moylan, J. S., & Reid, M. B. (2007). Oxidative stress, chronic disease, and muscle wasting. *Muscle & nerve*, *35*(4), 411-429.
- Newman, D. J., & Cragg, G. M. (2014). Making Sense of Structures by Utilizing Mother Nature's Chemical Libraries as Leads to Potential Drugs. *Natural Products: Discourse, Diversity, and Design*, 397-411.

- Nicolaou, K., Pfefferkorn, J., Roecker, A., Cao, G.-Q., Barluenga, S., & Mitchell, H. (2000). Natural product-like combinatorial libraries based on privileged structures. 1. General principles and solid-phase synthesis of benzopyrans. *Journal of the American Chemical Society*, 122(41), 9939-9953.
- Nishiyama, Y., Moriyasu, M., Ichimaru, M., Iwasa, K., Kato, A., Mathenge, S. G., Juma, F. D. (2004). Quaternary isoquinoline alkaloids from *Xylopia parviflora*. *Phytochemistry*, 939-944.
- Nordin, N., Majid, N. A., Hashim, N. M., Rahman, M. A., Hassan, Z., & Ali, H. M. (2015). Liriodenine, an aporphine alkaloid from *Enicosanthellum pulchrum*, inhibits proliferation of human ovarian cancer cells through induction of apoptosis via the mitochondrial signaling pathway and blocking cell cycle progression. *Drug Design, Development and Therapy*, 9, 1437-1448.
- Omar, H., Hashim, N. M., Zajmi, A., Nordin, N., Abdelwahab, S. I., A. H. A., Ali, H. M. (2013). Aporphine alkaloids from the leaves of *Phoebe grandis* (Nees) Mer.(Lauraceae) and their cytotoxic and antibacterial activities. *Molecules*, 18(8), 8994-9009.
- Othman, M., Genapathy, S., Liew, P. S., Ch'ng, Q. T., Loh, H. S., Khoo, T. J, Ting, K. N. (2011). Search for antibacterial agents from Malaysian rainforest and tropical plants. *Natural product research*, 25(19), 1857-1864.
- Pandey, K. B., & Rizvi, S. I. (2009). Plant polyphenols as dietary antioxidants in human health and disease. *Oxidative Medicine and Cellular Longevity*, 2(5), 270-278.
- Pateh, U., Haruna, A., Garba, M., Iliya, I., Sule, I., Abubakar, M., & Ambi, A. (2009). Isolation of stigmasterol, β -sitosterol and 2-hydroxyhexadecanoic acid methyl ester from the rhizomes of *Stylochiton lancifolius* Pyer and Kotchy (Araceae). *Nigerian Journal of Pharmaceutical Sciences*, 7(1), 19-25.
- Patel, D., Prasad, S., Kumar, R., & Hemalatha, S. (2012). An overview on antidiabetic medicinal plants having insulin mimetic property. *Asian Pacific Journal of Tropical Biomedicine*, 2(4), 320-330.
- Pezzuto, J. M. (1997). Plant-derived anticancer agents. *Biochemical pharmacology*, 53(2), 121-133.
- Phillipson, D. W., Milgram, K. E., Yanovsky, A. I., Rusnak, L. S., Haggerty, D. A., Farrell, W. P., Proefke, M. L. (2002). High-Throughput Bioassay-Guided Fractionation: A Technique for Rapidly Assigning Observed Activity to

Individual Components of Combinatorial Libraries, Screened in HTS Bioassays. *Journal of Combinatorial Chemistry*, 4(6), 591-599.

Pinheiro, M. L. B., Xavier, C. M., Souza, A. D. L. d., Rabelo, D. d. M., Batista, C. L., Batista, R. L., Nakamura, C. V. (2009). Acanthoic acid and other constituents from the stem of *Annona amazonica* (Annonaceae). *Journal of the Brazilian Chemical Society*, 20, 1095-1102.

Prachayasittikul, S., Manam, P., Chinworrungsee, M., Isarankura-Na-Ayudhya, C., Ruchirawat, S., & Prachayasittikul, V. (2009). Bioactive Azafluorenone Alkaloids from *Polyalthia debilis* (Pierre) Finet & Gagnep. *Molecules*, 14(11), 4414-4424.

Prajna, J., Richa, J., & Dipjyoti, C. (2013). HPLC Quantification of Phenolic Acids from *Vetiveria zizanioides* (L.) Nash and Its Antioxidant and Antimicrobial Activity. *Journal of Pharmaceutics*, 2013, 6.

Rahman, N. N. N. A., Zhari, S., Sarker, M. Z. I., Ferdosh, S., Yunus, M. A. C., & Kadir, M. O. A. (2012). Profile of *Parkia speciosa* Hassk Metabolites Extracted with SFE using FTIR-PCA Method. *Journal of the Chinese Chemical Society*, 59(4), 507-514.

Rasamizafy, S., Hocquemiller, R., Cave, A., & Fournet, A. (1987). Alkaloids of the Annonaceae. Part 78. Bark alkaloids of Bolivian *Duguetia spixiana*. *Journal of Natural Products*, 674-679.

Rates, S.M.K. (2001). Plants as source of drugs. *Toxicon*, 39(5), 603-613.

Rieser, M. J., Kozlowski, J. F., Wood, K. V., & McLaughlin, J. L. (1991). Muricatacin: a simple biologically active acetogenin derivative from the seeds of *Annona muricata* (Annonaceae). *Tetrahedron letters*, 32(9), 1137-1140.

Robert Hodgkinson, S. T. B., Akbar Zubaid, Thomas H. Knz. (2004). Temporal Variation in the Relative Abundance of Fruit Bats (Megachiroptera: Pteropodidae) in Relation to the Availability of Food in a Lowland Malaysian Rain Forest. *Biotropica*, 36(4), 522-553.

Saifah, E., Jongbunprasert, V., & Kelley, C. J. (1988). Piriferine, a new pyrrolidine alkaloid from *Aglaia pirifera* leaves. *Journal of Natural Products*, 51(1), 80-82.

Sajjadi, S. E., Shokoohinia, Y., & Hemmati, S. (2012). Isolation and identification of furanocoumarins and a phenylpropanoid from the acetone extract and

identification of volatile constituents from the essential oil of *Peucedanum pastinacifolium*. *Chemistry of Natural Compounds*, 48(4), 668-671.

- Santoyo, S., Cavero, S., Jaime, L., Ibanez, E., Senorans, F., & Reglero, G. (2005). Chemical composition and antimicrobial activity of *Rosmarinus officinalis* L. essential oil obtained via supercritical fluid extraction. *Journal of Food Protection*, 68(4), 790-795.
- Satoh, A., Utamura, H., Ishizuka, M., Endo, N., Tsuji, M., & Nishimura, H. (1996). Antimicrobial Benzopyrans from the Receptacle of Sunflower. *Bioscience, Biotechnology, and Biochemistry*, 60(4), 664-665.
- Savithamma, N., Rao, M. L., & Suhrulatha, D. (2011). Screening of medicinal plants for secondary metabolites. *Middle-East Journal of Scientific Research*, 8(3), 579-584.
- Sesang, W., Punyanitya, S., Pitchuanom, S., Udomputtimekakul, P., Nuntasaeen, N., Banjerdpongchai, Pompimon, W. (2014). Cytotoxic aporphine alkaloids from leaves and twigs of *Pseuduvaria trimera* (Craib). *Molecules*, 19(7), 8762-8772.
- Sesang, W., Punyanitya, S., Pitchuanom, S., Udomputtimekakul, P., Nuntasaeen, N., Banjerdpongchai, Pompimon, W. (2014). Cytotoxic aporphine alkaloids from leaves and twigs of *pseuduvaria trimera* (Craib). *Molecules*, 19(7), 8762-8772.
- Sharma, B., Salunke, R., Balomajumder, C., Daniel, S., & Roy, P. (2010). Anti-diabetic potential of alkaloid rich fraction from *Capparis decidua* on diabetic mice. *Journal of Ethnopharmacology*, 127(2), 457-462.
- Sharma, K., & Gupta, R. (1985). Constituents of *Diospyros ebenum* stem bark. *Fitoterapia*, 56(6), 366-367.
- Shoemaker, R. H. (2006). The NCI60 human tumour cell line anticancer drug screen. *Nature Reviews Cancer*, 6(10), 813-823.
- Shou-Ming, Z., Shou-Shun, Z., & Ning, X. (1988). Alkaloids from *Pseuduvaria indochinensis*. *Phytochemistry*, 27(12), 4004-4005.
- Soobrattee, M. A., Neergheen, V. S., Luximon-Ramma, A., Aruoma, O. I., & Bahorun, T. (2005). Phenolics as potential antioxidant therapeutic agents: mechanism and actions. *Mutation Research/Fundamental and Molecular Mechanisms of Mutagenesis*, 579(1), 200-213.

- Stein, A. C., Viana, A. F., Müller, L. G., Nunes, J. M., Stolz, E. D., Do Rego, J.-C., Rates, S. M. (2012). Uliginosin B, a phloroglucinol derivative from *Hypericum polyanthemum*: a promising new molecular pattern for the development of antidepressant drugs. *Behavioural Brain Research*, 228(1), 66-73.
- Stevigny, C., Block, S., De Pauw-Gillet, M., de Hoffmann, E., Llabrès, G., Adjakidje, V., & Quetin-Leclercq, J. (2002). Cytotoxic aporphine alkaloids from *Cassytha filiformis*. *Planta medica*, 68(11), 1042-1044.
- Stolz, E. D., Hasse, D. R., von Poser, G. L., & Rates, S. M. (2014). Uliginosin B, a natural phloroglucinol derivative, presents a multimediated antinociceptive effect in mice. *J Pharm Pharmacol*, 66(12), 1774-1785.
- Su, Y. C., & Saunders, R. M. (2009). Evolutionary divergence times in the Annonaceae: evidence of a late Miocene origin of *Pseuduvaria* in Sundaland with subsequent diversification in New Guinea. *BMC Evolutionary Biology*, 9(1), 153.
- Su, Y. C., Smith, G. J., & Saunders, R. M. (2008). Phylogeny of the basal angiosperm genus *Pseuduvaria* (Annonaceae) inferred from five chloroplast DNA regions, with interpretation of morphological character evolution. *Molecular Phylogenetics and Evolution*, 48(1), 188-206.
- Suleiman, M. M., Dzenda, T., & Sani, C. A. (2008). Antidiarrhoeal activity of the methanol stem-bark extract of *Annona senegalensis* Pers. (Annonaceae). *Journal of Ethnopharmacology*, 116(1), 125-130.
- Taha, H., Mohd, M. A., & Hamid, A. A. H. (2013). Bioactive Compounds of Some Malaysian Annonaceae Species. In *4th International Conference on Advances in Biotechnology and Pharmaceutical Science Singapore* (pp. 5-7).
- Taha, H., Arya, A., Paydar, M., Looi, C. Y., Wong, W. F., Murthy, C. V., Hadi, A. H. A. (2014). Upregulation of insulin secretion and downregulation of pro-inflammatory cytokines, oxidative stress and hyperglycemia in STZ-nicotinamide-induced type 2 diabetic rats by *Pseuduvaria monticola* bark extract. *Food and Chemical Toxicology*, 66, 295-306.
- Taha, H., Hadi, A. H. A., Nordin, N., Najmuldeen, I. A., Mohamad, K., Shirota, O., Morita, H. (2011). Pseuduvarines A and B, two new cytotoxic dioxoaporphine alkaloids from *Pseuduvaria rugosa*. *Chemical and Pharmaceutical Bulletin*, 59(7), 896-897.

- Taha, H., Looi, C. Y., Arya, A., Wong, W. F., Yap, L. F., Hasanpourghadi, M., . Mohd Ali, H. (2015). (6E,10E) Isopolycerasoidol and (6E,10E) Isopolycerasoidol Methyl Ester, Prenylated Benzopyran Derivatives from *Pseuduvaria monticola* Induce Mitochondrial-Mediated Apoptosis in Human Breast Adenocarcinoma Cells. *PLoS One*, *10*(5), e0126126. doi:10.1371/journal.pone.0126126
- Tan, A. C., Konczak, I., Sze, D. M. Y., & Ramzan, I. (2010). Towards the discovery of novel phytochemicals for disease prevention from native Australian plants: an ethnobotanical approach. *Asia Pacific Journal of Clinical Nutrition*, 330-334.
- Topliss, J. G., Clark, A. M., Ernst, E., Hufford, C. D., Johnston, G. A. R., Rimoldi, J. M., & Weimann, B. J. (2002). Natural and synthetic substances related to human health (IUPAC technical report). *Pure and Applied Chemistry*, *74*(10), 1957-1985.
- Uadkla, O., Yodkeeree, S., Buayairaksa, M., Meepowpan, P., Nuntasaeen, N., Limtrakul, P., & Pompimon, W. (2013). Antiproliferative effect of alkaloids via cell cycle arrest from *Pseuduvaria rugosa*. *Pharmaceutical Biology*, *51*(3), 400-404.
- Van Heusden, E. C. H. (1994). Revision of *Meiogyne* (Annonaceae). *Blumea-Biodiversity, Evolution and Biogeography of Plants*, *38*(2), 487-511.
- Vimala, S., Norhanom, A. W., & Yadav, M. (1999). Anti-tumour promoter activity in Malaysian ginger rhizobia used in traditional medicine. *British Journal of Cancer*, *80*(1-2), 110-116.
- Wang, R., Wang, R., & Yang, B. (2009). Extraction of essential oils from five cinnamon leaves and identification of their volatile compound compositions. *Innovative Food Science & Emerging Technologies*, *10*(2), 289-292.
- Wirasathien, L., Boonarkart, C., Pengsuparp, T., & Suttisri, R. (2006). Biological Activities of Alkaloids from *Pseuduvaria setosa*. *Pharmaceutical biology*, *44*(4), 274-278.
- Wolfender, J.-L., Marti, G., & Queiroz, E. F. (2010). Advances in techniques for profiling crude extracts and for the rapid identification of natural products: dereplication, quality control and metabolomics. *Current Organic Chemistry*, *14* (16), 1808-1832.
- Wu, Y.-C., Kao, S.-C., Huang, J.-F., Duh, C.-Y., & Lu, S.-T. (1990). Two phenanthrene alkaloids from *Fissistigma glaucescens*. *Phytochemistry*, *29*(7), 2387-2388.

- Xing, Y., Peng, H.-y., Zhang, M.-x., Li, X., Zeng, W.-w., & Yang, X.-e. (2012). Caffeic acid product from the highly copper-tolerant plant *Elsholtzia splendens* post-phytoremediation: its extraction, purification, and identification. *Journal of Zhejiang University Science B*, 13(6), 487-493.
- Xu, F., & Ronse, D. C. L. (2010). Floral ontogeny of Annonaceae: evidence for high variability in floral form. *Annals of Botany*, 106(4), 591-605.
- Young, J. E., Zhao, X., Carey, E. E., Welti, R., Yang, S.-S., & Wang, W. (2005). Phytochemical phenolics in organically grown vegetables. *Molecular Nutrition and Food Research*, 49 (12), 1136-1142.
- Zhang, Q., Tu, G., Zhao, Y., & Cheng, T. (2002). Novel bioactive isoquinoline alkaloids from *Carduus crispus*. *Tetrahedron*, 58(34), 6795-6798.
- Zhao, C.-G., Yao, M.-J., Yang, J.-W., Chai, Y.-L., Sun, X.-D., & Yuan, C.-S. (2014). A new benzopyran derivative from *Pseuduvaria indochinensis* Merr. *Natural product research*, 28(3), 169-173.

LIST OF PUBLICATIONS AND PAPERS PRESENTED

1. Taha, Hairin, *et al.* "Upregulation of insulin secretion and downregulation of pro-inflammatory cytokines, oxidative stress and hyperglycemia in STZ-nicotinamide-induced type 2 diabetic rats by *Pseuduvaria monticola* bark extract." *Food and Chemical Toxicology* 66 (2014): 295-306.
2. Taha, Hairin, *et al.* "(6E, 10E) Isopolycerasoidol and (6E, 10E) Isopolycerasoidol Methyl Ester, Prenylated Benzopyran Derivatives from *Pseuduvaria monticola* Induce Mitochondrial-Mediated Apoptosis in Human Breast Adenocarcinoma Cells." *Plos One* (2015): e0126126.
3. Taha, Hairin, Aditya Arya, Mustafa Ali Mohd, and A. Hamid A. Hadi. "Bioactive Compounds of Some Malaysian Annonaceae Species." (ICABPS 2013, Singapore)
4. Arya, Aditya, Hairin Taha, Ataul Karim Khan, Nayiar Shahid, Hapipah Mohd Ali, and Mustafa Ali Mohd. "In vivo Antidiabetic and Antioxidant Potential of *Pseuduvaria Macrophylla* Extract." *Int. Journal of Medical Health, Biomedical, bioengineering and Pharmaceutical Engineering* Vol: 8, 2014.
5. Hairin Taha, *et al.* "A Brief Review on Bioactive Compounds from *Pseuduvaria* Species." *The Open Conference Proceedings Journal*. Volume 6, 2015.
6. Hairin Taha *et al.* "Antidiabetic Potential of *Pseuduvaria Monticola* Bark Extract on the Pancreatic Cells, NIT-1 and Type 2 Diabetic Rat Model. (ICPP 2014, London).
7. Hairin Taha *et al.* "Antioxidant Activity and Chemical Constituents of Leaf Essential Oils of *Pseuduvaria Monticola* and *Pseuduvaria Macrophylla*. (ICMPNP 2015, Dubai).

APPENDIX

University of Malaya